

UC Berkeley

UC Berkeley Electronic Theses and Dissertations

Title

Development and Mechanistic Investigations of Gold-Catalyzed Reactions

Permalink

<https://escholarship.org/uc/item/2379q6b9>

Author

Shapiro, Nathan David

Publication Date

2010

Peer reviewed|Thesis/dissertation

Development and Mechanistic Investigations of Gold-Catalyzed Reactions

by

Nathan David Shapiro

A dissertation submitted in partial satisfaction of the

requirements for the degree of

Doctor of Philosophy

in

Chemistry

in the

Graduate Division

of the

University of California, Berkeley

Committee in charge:

Professor F. Dean Toste, Chair
Professor Richmond Sarpong
Professor Benito O. de Lumen

Spring 2010

Development and Mechanistic Investigations of Gold-Catalyzed Reactions

Copyright 2010

by Nathan David Shapiro

Abstract

Development and Mechanistic Investigations of Gold-Catalyzed Reactions

by

Nathan David Shapiro

Doctor of Philosophy in Chemistry

University of California, Berkeley

Professor F. Dean Toste, Chair

Historically, chemists have been motivated by problems in total synthesis or by a desire to develop reactions of broad utility. In answer to these challenges, several approaches to fundamental research have been developed. In chapter 1, we describe how our reactivity-driven approach has led to the discovery of numerous synthetic tools.

The development of new synthetically useful methodology often rests on an understanding of the mechanistic underpinnings of the desired transformation. This is particularly true when this knowledge forms the basis for subsequent mechanistic proposals. The coordination of an alkyne to a cationic Au(I) complex represents the prototypical mechanistic starting place for many Au(I)-catalyzed reactions. In chapter two, we describe the isolation and characterization of a gold(I)-coordinated alkyne. The crystal structure of this compound is compared to related Ag(I) and Cu(I) compounds. With these structures in hand, we can begin to understand the unique ability of Au(I) complexes to serve as effective π -activation catalysts, especially in understanding why gold is often more effective than copper or silver.

In addition to being able to activate π -bonds toward nucleophilic attack, it has been proposed that gold is also capable of stabilizing adjacent carbocations. Such species (i.e. $[L-Au-CR_2]^+$) have been referred to as gold-carbenoids or gold-stabilized carbocations. In chapter 3, we describe a bonding model for these intermediates that suggests that while the gold-carbon bond order is generally less than or equal to one, this bond includes both σ - and π -type bonding. Furthermore, the position of a given Au-stabilized intermediate on a continuum ranging from gold-stabilized singlet carbene to gold-coordinated carbocation is dictated by both the carbene substituents and the ancillary ligand. This model provides an explanation for observed ancillary ligand effects and should enable more efficient reaction optimization.

In chapter 4, a series of gold(I)-catalyzed rearrangement reactions of alkynyl sulfoxides, sulfimides and sulfur ylides are reported. Homopropargyl sulfoxides are rearranged to benzothiepinones or benzothiopynes, while α -thioenones are formed in the reaction of propargyl sulfoxides. It is proposed that these reactions proceed via an α -carbonyl gold-carbenoid intermediate formed through gold-promoted oxygen atom transfer from sulfoxide to alkyne.

In chapter 5, the development of a convenient gold(III)-catalyzed synthesis of azepines from the intermolecular annulation of propargyl esters and α,β -unsaturated imines is discussed. Mechanistic experiments suggest that this formal [4 + 3]-cycloaddition reaction proceeds via a stepwise process involving intermolecular trapping of a gold-carbenoid intermediate and subsequent intramolecular trapping of the resulting allyl-gold intermediate.

In chapter 6, we discuss the gold(III)-catalyzed [3+3]-cycloaddition reaction of propargyl esters and azomethine imines. This reaction provides a rapid entry into a wide range of substituted tetrahydropyridazine derivatives from simple starting materials. A mechanism similar to that proposed in chapter 5 is discussed, along with a detailed description of the consequences of this mechanism on the diastereoselectivity of the annulation reaction. In addition, a strategy for rendering this reaction asymmetric is presented.

Several future directions are presented in the appendices, along with additional supporting information.

Table of Contents

Chapter 1. *A Reactivity-Driven Approach to the Discovery and Development of Gold-Catalyzed Organic Reactions*

Introduction	2
Addition Reactions	3
Reactions Involving Carbenoid Intermediates	11
Further Insights into Reactivity from Au-Catalyzed Cycloisomerization Reactions	17
Intermolecular Annulation Reactions	21
Tandem Reactions	24
Conclusions	25
References	26

Chapter 2. *Understanding Gold Catalysis, Part 1: π -Activation*

Introduction	33
Results and Discussion	
(i) Synthesis of π -complexes	33
(ii) Description of π -complexes	35
Analysis	36
Conclusions	39
Supporting Information	40
References	47

Chapter 3. *Understanding Gold Catalysis, Part 2: Au-Carbene Complexes*

Introduction	50
Results and Discussion	
(i) Barrier to bond rotation energy	50
(ii) Impact of the carbene	51
(iii) Impact of the ligand	53
(iv) Charge Distribution	54
(v) Bonding and reactivity	54
Conclusions	55
Supporting Information	56
References	58
Additional Supporting Information	146

Chapter 4. *Rearrangements of Alkynyl Sulfoxides, Sulfimides, and Sulfur Ylides*

Introduction	62
Results and Discussion	
(i) Rearrangements of Homopropargyl Sulfoxides	62
(ii) Rearrangements of Propargyl Sulfoxides	66
(iii) Intermolecular Addition of Sulfoxides to Alkynes	69
(iv) Intermolecular Trapping of Gold Carbenoids	70

Conclusions	71
Supporting Information	72
References	92
Additional Supporting Information	149
Chapter 5. <i>Synthesis of Azepines by a Gold-Catalyzed Intermolecular [4+3] Annulation</i>	
Introduction	95
Results and Discussion	
(i) Optimization	95
(ii) Substrate Scope	96
(iii) Mechanistic Proposal	98
(iv) Annulation of Heteroaromatic Imines	100
Conclusions	101
Supporting Information	102
References	112
Additional Supporting Information	206
Chapter 6. <i>Gold-Catalyzed [3+3]-Annulation of Azomethine Imines with Propargyl Esters</i>	
Introduction	115
Results and Discussion	
(i) Optimization	115
(ii) Reaction Scope	116
(iii) Diastereoselectivity	118
(iv) Further Extensions	119
(v) Comparison to the [4+3] Annulation	121
Conclusions	122
Supporting Information	122
References	135
Additional Supporting Information	245
Appendices 1 – 7.	
1. Asymmetric Gold(I)-Catalyzed Alkynylation of Glyoxylate Imines	137
2. Brønsted Acid-Catalyzed Asymmetric Hydroamination of Dienes	142
3. Addition Supporting Information for Chapter 3 (NMR Spectra).....	146
4. Addition Supporting Information for Chapter 4	149
5. Addition Supporting Information for Chapter 5	206
6. Addition Supporting Information for Chapter 6	245

Acknowledgments

In retrospect, the past four and half years were nearly exactly as I expected: full of hard work, yet incredibly rewarding. What was less expected was how much fun I would have along the way. With regards to creating this rewarding and enjoyable atmosphere, I am extremely grateful to Dean for the intellectual freedom that he fosters in all of his students. Even though my ideas have frequently led to dead ends, this approach has been invaluable in my development as a scientist and future independent researcher. That being said, I would also like to thank Dean for the numerous times when he did offer guidance, especially with regards to the interpretation, design, and presentation of critical experiments.

When I came to Berkeley, my laboratory skills could be compared those of a headless chicken: frantic and doomed to fail. Things rapidly improved under the mentorship of the Toste group. These days I would like to think that even the most complicated laboratory procedures are no match for my deft nitrile-sheathed fingers. For this I give thanks.

Of course, I am also extremely grateful to all of the members of the Toste group, and to the Berkeley chemistry community at large. I've been able to come to work every day knowing I'll be entering a congenial and collaborative environment. Special thanks go to the members of 611, past and present, for putting up with my occasionally smelly chemistry, my often terrible taste in music, and my frequently ridiculous antics.

Finally, I'd like to thank my family for being the best that one could possibly hope for. It seems almost impossible how lucky I am. Thank you all for your support and patience. Most of all, I'd like to thank Katrien. I can't even begin to imagine what these years would have been like without you. From chemistry to cooking, from climbing to foraging, from laundry to DDR, and from arguments to jokes, I wouldn't give up a minute of it. Thank you for your endless encouragement and support. *muah*

Chapter 1 – A Reactivity-Driven Approach to the Discovery and Development of Gold-Catalyzed Organic Reactions.

Approaches to research in organic chemistry are as numerous as the reactions they describe. In this account, we describe our reactivity-based approach. Using our work in the area of gold-catalysis as a background, we discuss how a focus on reaction mechanism and reactivity paradigms can lead to the rapid discovery of new synthetic tools.

1.1 Introduction

“Our scientific theories do not, as a rule, spring full-armed from the brow of their creator. They are subject to slow and gradual growth...”

– Professor Gilbert N. Lewis writing in *Science* in 1901.¹

At the time Lewis was speaking of ionic theory, but his words resonate throughout chemistry. To an organic chemist, his words speak to the difficulty associated with the prediction of reactivity. In answer to this challenge, numerous approaches to chemical research have been devised. We have categorized these research styles into the four methods that we perceive to be most prevalent (Table 1).

Historically, chemists have been motivated by problems in total synthesis or by a desire to develop reactions of broad utility. With total synthesis of natural or unnatural compounds as the driving force, methods development is typically focused on the efficient synthesis of a certain chemical motif (Table 1).² In contrast, bond-based methodology programs focus on transformations of specific chemical bonds.³ A third approach employs high-throughput screening to identify reaction conditions that will allow a more general type of transformation.⁴ We have undertaken an alternative approach, one that we describe as reactivity-based. Instead of focusing on specific reactions, we concentrate our efforts on understanding and expanding specific reactivity paradigms.⁵

Table 1. Approaches to methodology research in organic chemistry.

<i>Approach</i>	<i>Hypothesis</i>
Motif-based	New methods for the synthesis of a specific chemical motif are needed.
Bond-based	The transformation of one specific set of chemical bonds into another would be a useful synthetic transformation.
High-throughput screening (HTS)	HTS of reaction conditions will lead to the discovery of new reactions.
Reactivity-based	Understanding and expanding reactivity paradigms will lead to the discovery of new reactions.

We do not argue that one of the approaches to reaction discovery described above is superior to the others. On the contrary, we would claim that each approach is important in and of itself, and that each complements the next. Nonetheless, this account will highlight our reactivity-based approach, using gold catalysis as a backdrop for this discussion.

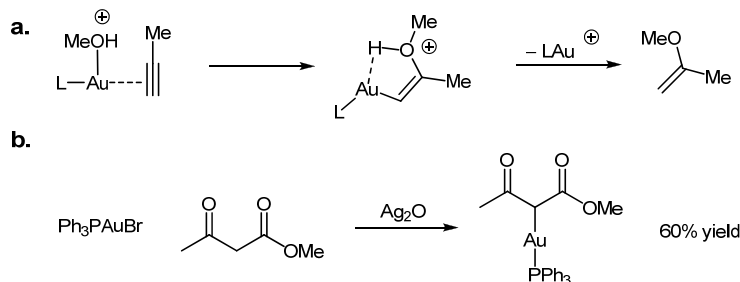
We typically begin our research with a fragment of theoretical knowledge, commonly a proposed reaction mechanism or intermediate. Initially, this background was derived from the literature; although, as our research program has developed, we have frequently been able to utilize our own proposed mechanisms. From this theoretical knowledge we seek to extract a hypothesis that can be subsequently tested in the laboratory. After designing and executing the appropriate test, conclusions are drawn that can either contradict, support, or expand the initial

theory. While it is not always the case, progress through this cycle frequently results in the discovery of new reactivity paradigms.

1.2 Addition reactions

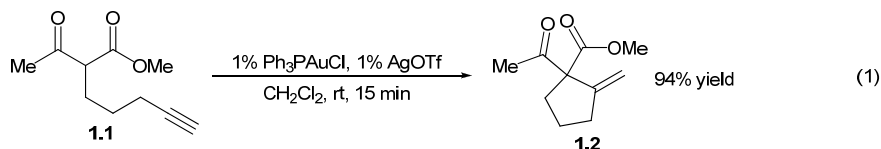
1.2.1 The Conia-Ene Reaction

We were initially attracted to the area of gold-catalysis by the pioneering report of Teles and coworkers showing that cationic gold(I) complexes can activate alkynes towards nucleophilic attack by alcohol nucleophiles.⁶ Based on a series of calculations, Teles proposed a *cis*-addition mechanism, in which the gold(I) catalyst is coordinated to both the alcohol and the alkyne (Scheme 1a). A subsequent survey of the literature led us to a report from 1974 describing the stoichiometric auration of β -ketoesters (Scheme 1b).⁷ Combining this report with Teles' mechanistic hypothesis led to the simple hypothesis that gold(I) complexes might be employed as catalysts for the addition of β -ketoesters to alkynes.



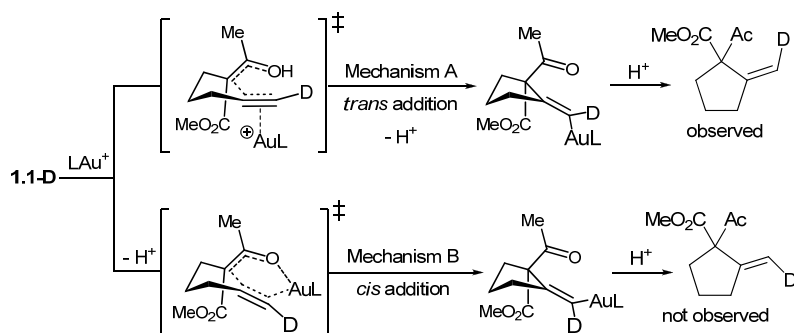
Scheme 1. (a) The mechanism, which has subsequently been disproved, originally proposed by Teles and coworkers for the addition of alcohols to alkynes mediated by Au(I) complexes. (b) A reaction reported in 1974 showing the carboauration of β -ketoesters. These reports prompted us to investigate the Au-catalyzed addition of β -ketoesters to alkynes.

To test this hypothesis, we designed a simple substrate (**1.1**) containing a β -ketoester-tethered alkyne (Equation 1).⁸ To our delight, $\text{Ph}_3\text{PAu}^+\text{TfO}^-$ (formed *in situ* from Ph_3PAuCl and AgOTf) catalyzed the desired C-C bond forming event rapidly at room temperature. Thus, by testing a simple hypothesis we had discovered a mild method for affecting C-C bond formation.^{9,10} Furthermore, we were able to contribute to the database of knowledge surrounding gold-catalysis.¹¹



This discovery also allowed us to postulate additional hypotheses. One of the simplest was that this reaction should be applicable to internal alkynes. To our surprise, these substrates were mostly unreactive even under more forcing conditions. This contradiction to our hypothesis, prompted us to test the validity of the *cis*-addition mechanism that had been proposed by Teles.

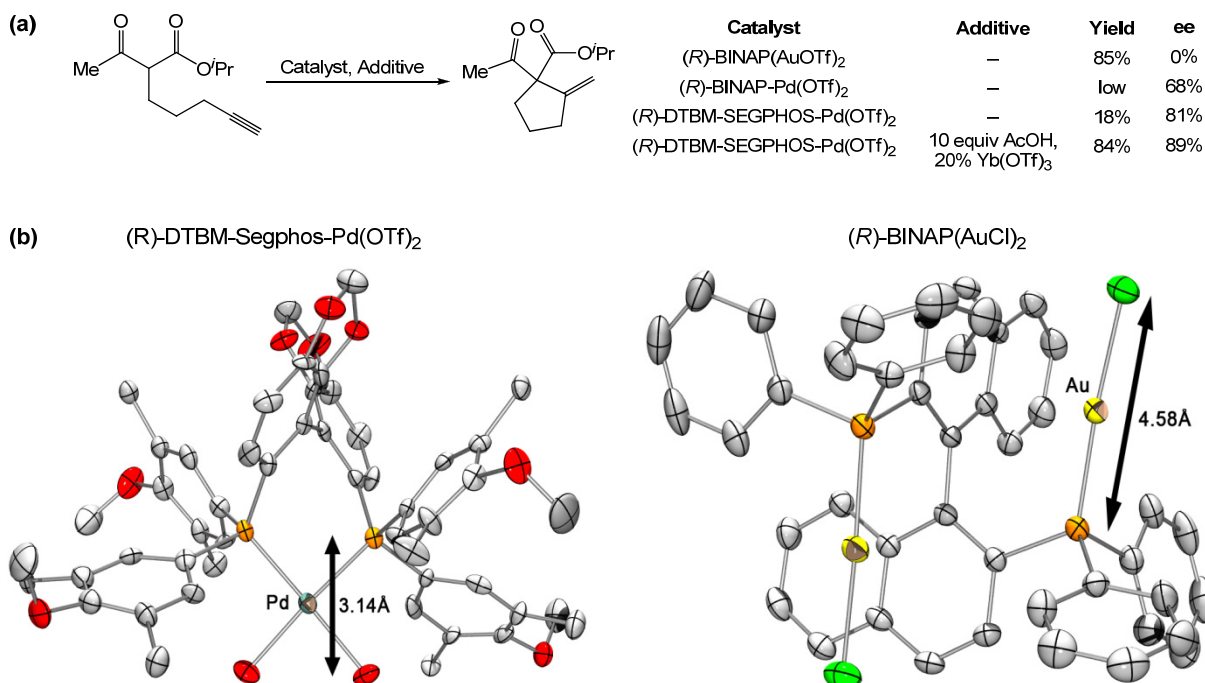
When deuterium-labeled alkyne **1.1-D** was subjected to the reaction conditions, the deuterium was selectively incorporated *syn* to the ketoester (Scheme 2). This result supports a mechanism involving *trans* addition of the ketoester to a pendant Au-activated alkyne.¹² Furthermore, this mechanism also provides an explanation for the poor reactivity of internal alkynes, which would experience severe 1,3-allylic strain in the cyclization transition state. Further support for this mechanism, including the isolation and characterization of related vinyl-gold intermediates, has accumulated.¹³



Scheme 2. Mechanistic proposals in the gold(I)-catalyzed Conia-ene reaction. Experimental results support a mechanism involving *trans* addition.

Our initial attempts to render this reaction enantioselective were frustrated by the consequences of a *trans*-addition mechanism. Employing chiral phosphinegold(I) complexes in the Conia-ene reaction induced very little enantioselectivity (Scheme 3a). This is not too surprising; gold(I) complexes typically adopt a two coordinate, linear geometry, which places the prochiral nucleophile more than 5 Å from the chiral phosphine in the cyclization transition state. This can be seen in x-ray crystal structure of (*R*)-BINAP(AuCl)₂ (Scheme 3b), where the distance between the phosphine and the chloride ligands is 4.58 Å. In the catalytic reaction, the alkyne of the substrate would replace the chloride, and the prochiral ketoester would approach the alkyne from a position *trans* to gold (as in Scheme 2, mechanism A).

In order to render the Conia-ene reaction enantioselective, we surveyed other π -acidic metal complexes that are not confined to a linear geometry. While chiral Cu(II), Ni(II), and Pt(II) complexes gave poor selectivity, we were satisfied to find that the square planar BINAP-Pd(OTf)₂ complex provided the desired product with moderate enantiomeric excess (68% ee), albeit in low yield (Scheme 3a). Further investigation revealed that the yield could be increased through the addition of Brønsted and Lewis acids¹⁴, while the enantioselectivity was improved by replacing (*R*)-BINAP with (*R*)-DTBM-SEGPHOS (89% ee). For comparison, the X-ray crystal structure of (*R*)-DTBM-SEGPHOS-Pd(OTf)₂ is illustrated in Scheme 3b. In this case, the distance between phosphine and substrate-binding sites is decreased to 3.14 Å (versus 4.58 Å for the Au(I) catalyst). We subsequently applied the principles we had learned in developing the Au(I)- and Pd(II)-catalyzed Conia-ene reactions to include transformations employing silyl enol ethers as nucleophiles.¹⁵ This methodology was subsequently applied to total synthesis of (+)-lycpladine A and (+)-fawcettimine.¹⁶



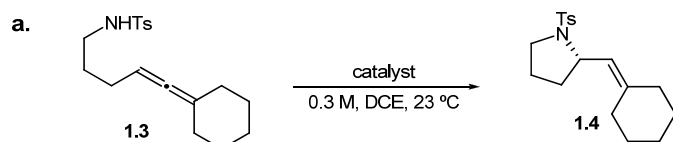
Scheme 3 Transition metal catalyzed enantioselective Conia-ene reaction. (a) Effect of transition metal and ligand on enantioselectivity. (b) A comparison of (*R*)-DTBM-SEGPHOS-Pd(OTf)₂ and (*R*)-BINAP(AuCl)₂ complexes showing the effect of metal geometry on the proximity of the ligand and substrate. (*tert*-butyl groups and OTf counteranions in the Pd complex have been removed for clarity).

1.2.2 Asymmetric Hydroamination

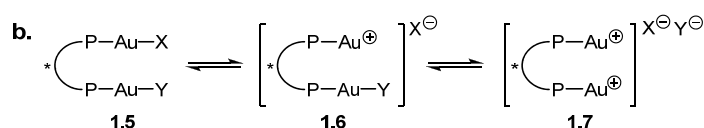
Despite our success using Pd(II)-catalysts to render the Conia-ene reaction enantioselective, we soon returned to the challenge of asymmetric gold catalysis. We quickly realized that the requirement for a prochiral nucleophile in enantioselective additions to alkynes greatly limits the scope of possible transformations. To overcome this problem, we have subsequently employed a number of strategies.

The first of these strategies involved gold-catalyzed addition of various nucleophiles to achiral allenes (which are prochiral electrophiles).¹⁷ In the hydroamination of allene **1.3**, we were initially frustrated by variable enantioselectivities (1-51% ee) when (*R*)-xylyl-BINAP(AuCl)₂ was employed as the precatalyst (Scheme 4a).¹⁸ After some experimentation, we found that the amount of AgBF₄ was crucial in determining the enantioselectivity of the transformation, with lower equivalents of Ag relative to Au providing higher ee. This suggested that the monocationic species **1.6** was providing enantioenriched product, while the dicationic species **1.7** was providing the product with lower enantiocontrol (Scheme 4b). ³¹P-NMR of a solution containing a 2:1 mixture of (*R*)-xylyl-BINAP(AuCl)₂ and AgBF₄ revealed that all three species **1.5-1.7** are present. By replacing the non-coordinating tetrafluoroborate counteranion with a more coordinating benzoate anion (OBz), we were able to shift the equilibrium towards **1.5** and **1.6**, resulting in a large increase in enantioselectivity (98% ee, Scheme 41, entry 3). Ultimately, the benzoate anion proved to be too coordinating, providing only low yields of the product even after extended reaction times. Fortunately, reactivity could be increased, without any decrease in selectivity, by switching to the *p*-nitrobenzoate (OPNB) counteranion (entry 4). The resulting

gold-OPNB complexes proved to be bench-stable white solids, the use of which further improved the yield of the reaction (entry 5).



Entry	Catalyst	Time (hrs)	Yield	ee
1	3% (<i>R</i>)-xylyl-BINAP(AuCl) ₂ + 6% AgBF ₄	0.5	82%	1%
2	3% (<i>R</i>)-xylyl-BINAP(AuCl) ₂ + 3% AgBF ₄	0.5	81%	51%
3	3% (<i>R</i>)-xylyl-BINAP(AuCl) ₂ + 6% AgOBz	24	27%	98%
4	3% (<i>R</i>)-xylyl-BINAP(AuCl) ₂ + 6% AgOPNB	24	76%	98%
5	3% (<i>R</i>)-xylyl-BINAP(AuOPNB) ₂	17	88%	98%



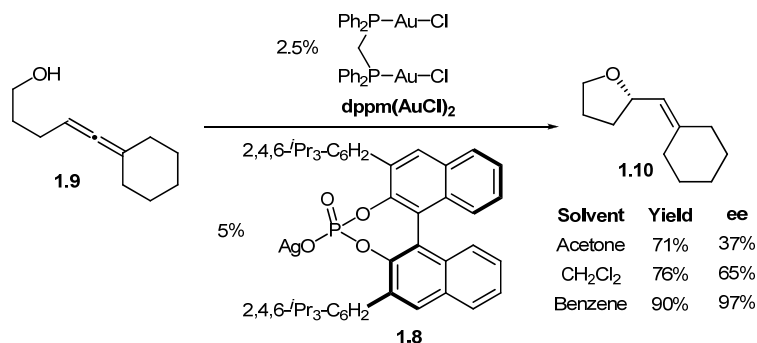
Scheme 4. (a) Development of a gold(I)-catalyzed asymmetric hydroamination reaction. (b) A possible rationale for the observed counteranion effects.

1.2.2 Chiral Counteranions

We initially hypothesized that gold(I) benzoates provide increased enantioselectivity in the formation of **1.4** by preventing the formation of the dicationic complex **1.7** and also by increasing the size of the remaining coordinated anion in the active catalyst (Y^- in **1.6**). Another possible explanation is that the counteranion (X^- in **1.6**) influences the relative rate of cyclization of the diastereomeric gold(I)-coordinated allene complexes. We predicted that if this were true, it should also be the case that chiral counteranions should be able to influence the relative rate of cyclization onto enantiomeric gold(I)-coordinated allene complexes.¹⁹ To test this third hypothesis, we prepared a set of chiral silver phosphates.

Treatment of $dppm(AuCl)_2$, an achiral gold(I) complex, with silver phosphate **1.8** provided a complex, which catalyzed the enantioselective hydroalkoxylation of allene **1.9** (Scheme 5).²⁰ Further optimization revealed that less polar solvents provided higher enantioselectivity, a result which is consistent with an ion-pair model for enantioinduction. This result is particularly remarkable in light of the fact that we were never able to achieve even moderate enantioselectivities for this transformation when chiral phosphines were employed. We have subsequently expanded the scope of these transformations to include both N- and O-linked hydroxylamine nucleophiles.²¹ As a group, these reactions provide access to a diverse range of enantioenriched heterocycles, including pyrazolidines, isoxazolidines, tetrahydrooxazines, tetrahydrofurans, tetrahydropyrans, pyrrolidines, and butyrolactones.

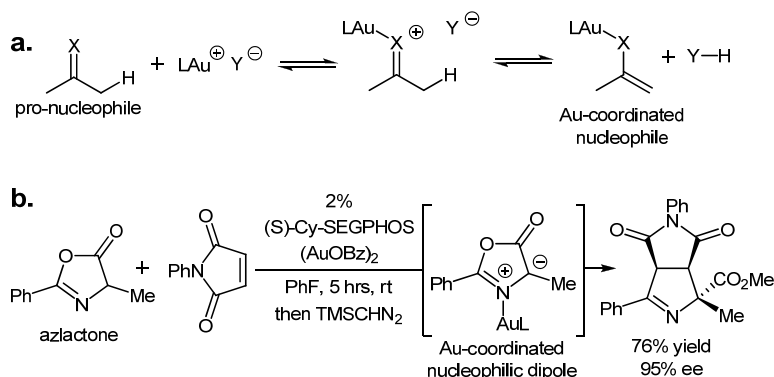
As an approach to asymmetric transition-metal catalysis, the use of chiral counteranions is complementary to the use of chiral ligands.^{22,23} It therefore has the potential to significantly expand the scope of reactions that can be rendered asymmetric.



Scheme 5. The first report of a highly enantioselective, chiral counteranion-controlled asymmetric reaction.

1.2.4 Exploiting Basic Counteranions

The observation that the reactivity of cationic gold(I)-complexes can be modulated through the basicity of the counteranion prompted us to investigate the potential of these catalysts to activate pronucleophiles. In this scenario, more basic counteranions should favor the formation of the Au-coordinated nucleophile and the conjugate acid of the counteranion (Scheme 6a).²⁴ We employed this strategy to activate azlactones for cycloaddition with electron deficient olefins (Scheme 6b).²⁵ Employing (*S*)-Cy-SEGPHOS(AuOBz)₂ as the catalyst, this reaction provides an attractive route to enantioenriched proline derivatives.²⁶

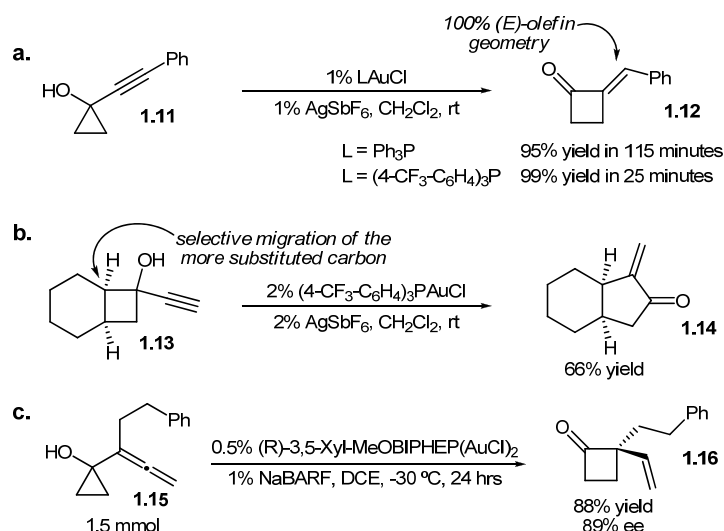


Scheme 6. (a) A potential mechanism for pro-nucleophile activation by Au(I). (b) Au(I)-catalyzed enantioselective 1,3-dipolar cycloaddition initiated by formation of a Au-coordinated Münchnone.

1.2.5 Ring Expansion Reactions

In the addition reactions described above, Au(I)-coordination to a C-C unsaturation is proposed to induce *trans* addition of a tethered nucleophile. This stands in contrast to nucleophile-activation-based mechanisms that have been proposed for early transition-metals, lanthanides, and actinides.²⁷ Based on this precedence, we hypothesized that Au(I) should also catalyze the addition of nucleophiles that lack metal-coordination sites (i.e. a C-C σ -bond). Thus,

treatment of alkynylcyclopropanol **1.11** with 1% of a cationic phosphine-Au(I) complex provided cyclobutanone **1.12** as a single olefin isomer (Scheme 7a).²⁸ Higher yields and shorter reaction times were obtained when electron-deficient arylphosphines were employed as ligands.²⁹ Alkynyl cyclobutanols, such as **1.13**, were also found to be viable substrates for gold(I)-catalyzed ring expansion (Scheme 7b). The formation of the (*E*)-olefin and the selective migration of the more substituted cycloalkanol carbons is consistent with a mechanism in which coordination of the gold(I) catalyst to the alkyne induces a 1,2-alkyl shift.^{30,31} A vinylogous variant of this reaction was applied to the total synthesis of ventricosene.³²



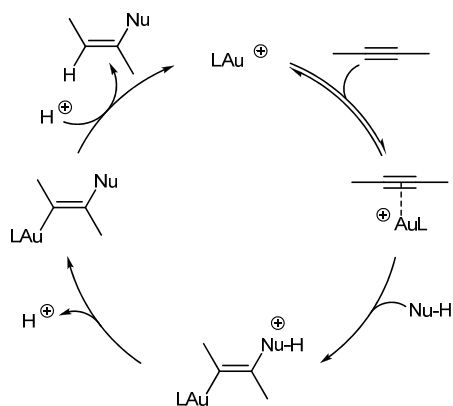
Scheme 7. Au(I)-catalyzed cyclopropanol ring expansion reactions.

Ring-expansion of allenylcyclopropanols (i.e. **1.15**) provides access to cyclobutanones possessing a vinyl-substituted quaternary center. This reaction could be rendered enantioselective by employing (*R*)-3,5-Xyl-MeOBIPHEP as the ancillary ligand (Scheme 7c).^{33,34}

1.2.6 Intramolecular carboalkoxylation

The research described in the previous sections illustrates that gold(I)-mediated electrophilic activation of C-C multiple-bonds provides an opportunity for mild C-C and C-X bond formation. In addition, through scrupulous choice of chiral ligand and/or chiral counteranion, many of these reactions can be rendered enantioselective. Nevertheless, these reactions fall under the reactivity paradigm encompassed by Markovnikov's rule.³⁵ An important expansion beyond these transformations would be to trap the proposed vinyl gold intermediates with electrophiles other than a proton. This would allow for the formation of additional bonds and the rapid generation of molecular complexity. Towards this goal, we envisioned that protonation of the vinyl gold intermediate could be avoided via *in situ* generation of an alternate electrophile. Thus, addition of a neutral, aprotic nucleophile to a gold-coordinated alkyne leads to an increase in positive charge on the nucleophile (Scheme 8a, 8b). Fragmentation of a single bond attached to this

In order to further understand these differences, we considered a prototypical catalytic cycle for the addition of a protic nucleophile to an alkyne (Scheme 9). In doing this, we made the assumption that coordination of the cationic Au(I)-catalyst to the alkyne is reversible and that nucleophilic addition is therefore rate determining. Thus, we reasoned that further study of Au(I)-coordinated π -bonds would lead to a better understanding of Au(I)-catalysis.⁴⁰



Scheme 9. A typical catalytic cycle for the Au(I)-catalyzed addition of protic nucleophiles to alkynes.

We noted that there was minimal literature presence for the isolation and characterization of cationic phosphineAu(I)- π -complexes. We hypothesized that these difficulties might be overcome by tethering a coordinatively stable phosphine ligand to the more labile alkyne.⁴¹ Using this strategy, we were able to obtain x-ray quality crystals of analogous cationic Au(I) and Ag(I)-coordinated alkynes. These structures allowed a comparative analysis, which was further augmented with DFT calculations. Second-order perturbative analysis revealed that σ -donation from the alkyne π -bond to the metal center is the most important bonding interaction for both Au and Ag (Table 2).⁴² However, the magnitude of this interaction is significantly larger for Au (56.6 kcal/mol versus 38.5 kcal/mol for Ag). This interaction is primarily responsible for augmenting the electrophilicity of the coordinated alkyne. Interestingly, back-donation from Au to the π^* of the coordinated alkyne is also larger in magnitude (13.3 kcal/mol versus 6.4 kcal/mol for Ag). While this interaction is expected to decrease the electrophilicity of the coordinated alkyne, it suggests that back-donation from Au may be important for other aspects of Au(I)-catalysis, as described below.

Table 2. Natural Bond Order Orbital Interaction Energies (kcal/mol)

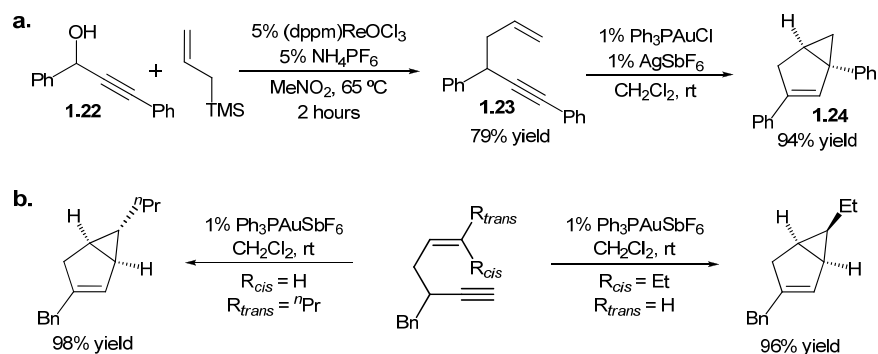
Parameter	20 (M = Au)	21 (M = Ag)	
$\pi \rightarrow M$	56.6	38.5	
$M \rightarrow \pi^*$	13.3	6.4	
Difference	43.3	32.1	

1.3 Reactions Involving Carbenoid Intermediates

A reactivity-based approach to organic synthesis requires that reaction mechanisms are constantly proposed and tested. As described throughout section 2, even in our forays in enantioselective catalysis, the testing of mechanistic proposals has frequently produced the most important advances. This testing process plays an even more pivotal role in the development of new, mechanistically distinct, reactions. In this section, we describe a series of reactions that are linked by a stream of mechanistic proposals.

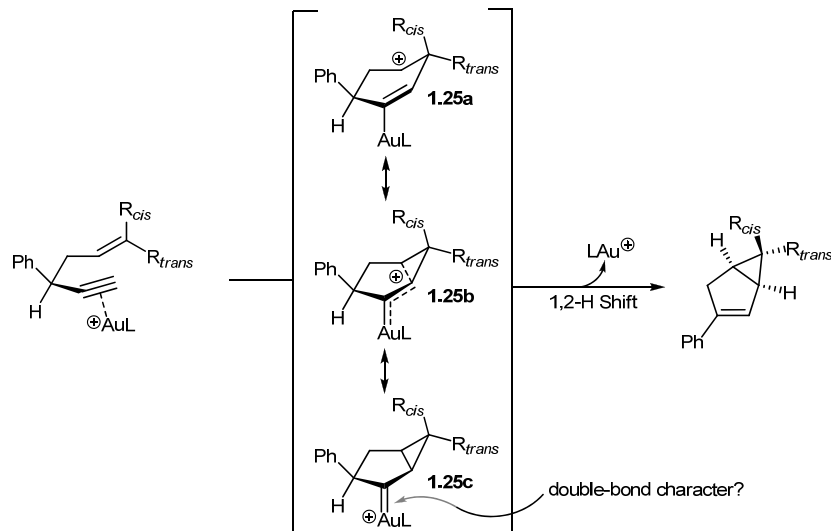
1.3.1 1,5-Enyne Cycloisomerization

Following our success with the Au(I)-catalyzed Conia-ene reaction we decided to explore the intramolecular addition of less-activated carbon nucleophiles to alkynes. A simple mono-substituted olefin constitutes the simplest of these nucleophiles. Coincidentally, we had recently developed a Re-catalyzed synthesis of 1,5-enynes from propargyl alcohols.⁴³ Thus, treatment of propargyl alcohol **1.22** with allylsilane and catalytic (dppm)ReOCl₃ produced 1,5-enyne **1.23** in 79% yield (Scheme 10a). Subsequent gold(I)-catalyzed cycloisomerization affected clean conversion to bicyclo[3.1.0]hexene **1.24**.^{44,45,46}



Scheme 10. (a) Re-catalyzed synthesis of 1,5-enynes and subsequent Au-catalyzed cycloisomerization. (b) Stereospecific cycloisomerizations.

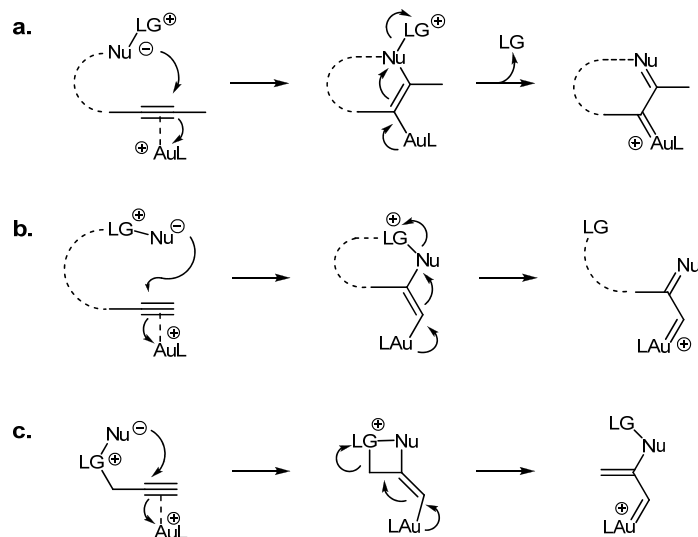
The formation of **1.24** suggested a new mode of reactivity in gold catalysis. This prompted us to further investigate the reaction mechanism. As illustrated in Scheme 10b, Reaction of substrates containing 1,2-disubstituted olefins proceeded stereospecifically. We also found that a propargyl deuterium label is selectively incorporated in the vinyl position of the product. On the basis of these observations, we proposed the mechanism that is partially illustrated in Scheme 11. Initial coordination of the alkyne by the cationic gold(I) catalyst induces cyclization of the pendant olefin, producing cationic intermediate **1.25**. The electronic structure of this intermediate can be represented by a number of resonance forms ranging from carbocation **1.25a** to gold carbenoid **1.25c**. The degree of bonding from gold to carbon will be further discussed in section 3.5. A 1,2-hydrogen shift produces the desired product and liberates the gold catalyst.



Scheme 11 Proposed 1,5-enyne cycloisomerization mechanism.

1.3.2 Intramolecular Addition of Dipolar Nucleophiles to Alkynes

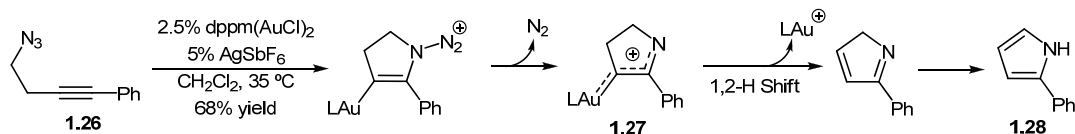
The postulate that gold can stabilize the positive charge in **1.25** was initially the matter of some debate. Nevertheless, the concept that gold can act as both a π -acid and as an electron donor has been useful in predicting new reactivity. We hypothesized that we could exploit this behavior in the gold-catalyzed addition of ylide-like nucleophiles to alkynes (Scheme 12).



Scheme 12. A few possible routes to gold-carbenoids from ylide-tethered alkynes. Nu = nucleophile, LG = leaving group.

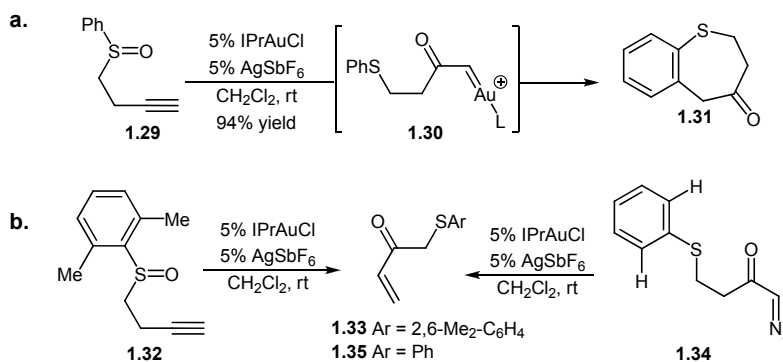
For example, following gold-catalyzed nucleophilic addition of the azide in **1.26** to the pendant alkyne, back-donation from gold is sufficient to affect the loss of dinitrogen (Scheme

13).⁴⁷ The resulting intermediate (**1.27**) is similar to **1.25** in appearance and again raises questions as to the nature of the Au-C bond in these types of intermediates. The observed pyrrole product **1.28** is produced following a 1,2-hydrogen migration and subsequent tautomerization.



Scheme 13. Gold(I)-catalyzed intramolecular acetylenic Schmidt reaction.

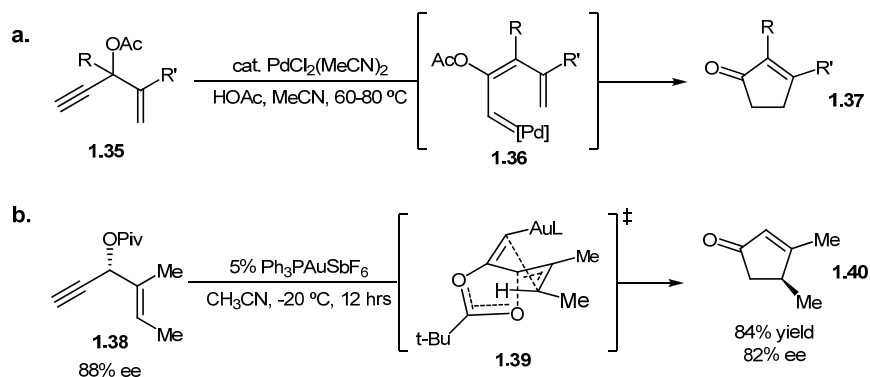
This concept was further expanded in the reaction of alkynyl sulfoxides (Scheme 14).⁴⁸ Gold(I)-catalyzed rearrangement of **1.29** provides an alternative route to a carbenoid intermediate (**1.30**) that would traditionally be accessed via transition metal catalyzed decomposition of α -diazocarbonyl compounds.^{49,50} In this particular case, the proposed carbenoid intermediate undergoes a formal intramolecular C-H insertion to provide benzothiepinone **1.31**. An internal competition inverse kinetic isotope effect suggests that the formal C-H insertion proceeds via a Friedel-Crafts type mechanism. When the ortho-positions of the aromatic ring are blocked (as in **1.32**), sluggish conversion to enone **1.33** is observed. Surprisingly, when *S*-phenyl, α -diazoketone **1.34** is subjected to the same reaction conditions, enone **1.35** is produced instead of benzothiepinone **1.31**. This suggests that the gold-catalyzed rearrangement of alkynyl sulfoxides provides a route to intermediates that are actually inaccessible from the corresponding α -diazocarbonyl compounds. An explanation of this divergent reactivity remains an area for future exploration.



Scheme 14. Gold(I)-catalyzed sulfoxide rearrangements.

In 1984, Rautenstrauch reported the palladium(II) catalyzed isomerization of propargyl acetates **1.35** to cyclopentenones **1.37** (Scheme 15a).⁵¹ This reaction is proposed to proceed via Pd-carbenoid **1.36**. Based on the similarity of this reaction mechanism to those discussed above, we postulated that propargyl ester rearrangement could provide a third route to gold-carbenoid intermediates. To our delight, gold(I)-catalysis allowed the substrate scope of this transformation to be significantly expanded.⁵² In order to confirm the proposed reaction mechanism, we subjected enantioenriched propargyl ester **1.38** to our gold-catalysis conditions (Scheme 15b). To our surprise, we observed excellent chirality transfer. This suggests that an achiral gold-

carbenoid intermediate is not present in the catalytic cycle. As an alternative mechanistic proposal, we suggested that a cyclic transition state (**1.39**) would account for chirality transfer. Subsequent calculations supported a similar hypothesis, in which a helical intermediate allows for efficient chirality transfer.⁵³ However, as will be discussed below, these results do not imply that carbene-like behavior cannot be accessed from propargyl esters.



Scheme 15. (a) Pd-catalyzed Rautenstrauch rearrangement. (b) The gold-catalyzed variant allows for efficient chirality transfer. In order to account for this observation, we proposed a cyclic transition state. Calculations later showed that the C-O breaking and C-C bond forming events occur separately, while the chirality is retained in a helically chiral intermediate.

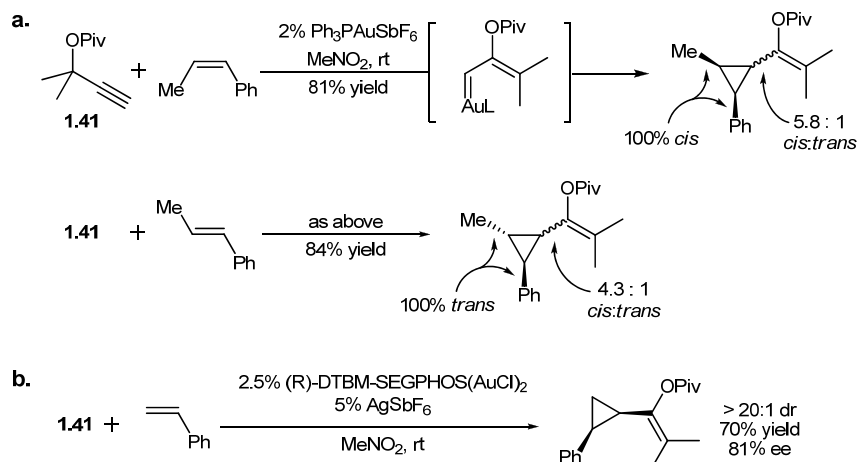
1.3.3 Stereospecific Cyclopropanation

The term ‘carbenoid’ is defined as a “description of intermediates which exhibit reactions qualitatively similar to those of carbenes without necessarily being free divalent carbon species.”⁵⁴ Therefore, in order for carbenoid to be apt descriptor of gold-stabilized cationic intermediates, such as **1.25**, these intermediates must exhibit reactivity that is similar to that of a free carbene.

Of the reactions that typify free singlet carbenes, the stereospecific cyclopropanation of olefins is one of the most indicative.⁵⁵ We therefore sought to test the ability of the proposed gold-carbenoid intermediates to cyclopropanate olefins.^{50,56} For this task we employed propargyl esters, which had been previously reported to be convenient precursors to carbenoid intermediates.⁵⁷ Accordingly, we found that cyclopropanation of *cis*- and *trans*- β -methyl styrenes with propargyl ester **1.41** occurs stereospecifically in the presence of a catalytic amount of a gold(I) catalyst (Scheme 16a). In addition, and in contrast to the Rautenstrauch rearrangements discussed above, we found that chirality was not transferred from enantioenriched propargyl esters to the cyclopropane products.

Encouraged by these results, we sought to develop an enantioselective variant of this reaction. Successful transmission of chiral information from the ancillary ligand on gold to the cyclopropane product would provide further evidence for the participation of the gold catalyst in the cyclopropanation step. In the event, (*R*)-DTBM-SEGPHOS(AuCl)₂ catalyzed the asymmetric cyclopropanation of styrene to provide the product with 81% ee (Scheme 16b).⁵⁸ This concept

was subsequently applied to the asymmetric synthesis of 7- and 8-membered rings via intramolecular Au(I)-catalyzed cyclopropanation.⁵⁹



Scheme 16. (a) Demonstrating that Au(I)-catalyzed cyclopropanation is stereospecific. (b) An enantioselective variant.

1.3.4 Au-C Bonding in Cationic Intermediates and Relativistic Effects

We were initially hesitant to define the exact nature of bonding between gold and carbon in intermediate **1.25**. We wrote: “cyclopropylcarbinyl cation [**1.25b**] may have some gold(I)-carbene character ([**1.25c**]). The bicyclo[3.1.0] hexene product is generated by a 1,2-hydrogen shift onto a cation or gold(I) carbene.” Even the boldness of this statement was based on literature precedence.⁶⁰ However, as evidence for gold-carbenoid reactivity accumulated (*vide supra*), we sought to provide a theoretical explanation for this behavior.

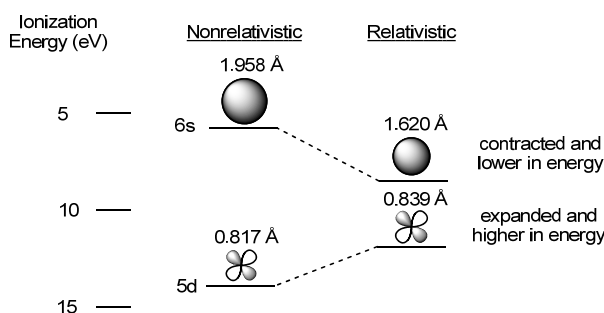


Figure 1. A comparison of calculated sizes and energies of Au 6s and 5d orbitals with and without consideration of relativistic effects.⁶²

Previous experimental and theoretical reports⁶¹ suggested that gold carbenoid behavior is indeed plausible and can be ascribed to the relativistic expansion of the 5d-orbitals on Au (Figure 1).⁶² This expansion allows delocalization of the electrons in these orbitals into carbon-based orbitals of sufficiently low energy (in particular an unoccupied p-orbital of a carbocation). This

provides an explanation for why Au-carbenes display behavior that is reminiscent of the reactivity of other transitional metal carbene complexes. On the other hand, the relativistic contraction of the 6s-orbital provides an explanation for the increased π -acidity of gold, as this orbital is the primary acceptor of electron-density from ligands and substrates.⁶³ Thus, cationic gold complexes are typically stronger π -acids when compared to Ag and Cu, yet also retain the ability to stabilize adjacent carbocations *via* back-donation.

1.3.5 A Bonding Model for Au(I)-Carbene Complexes

Consideration of relativistic effects allows carbenoid reactivity in Au-catalysis to be rationalized; however, we postulated that a more specific description of the bonding in Au-carbene complexes would allow improved prediction and explanation of reactivity.⁶⁴ With this in mind, in collaboration with the Goddard group, density functional theory calculations were used to determine the effect of both carbene substituents (R, R') and the ancillary ligand (L) on bonding in Au-carbene complexes **1.42**. In agreement with previous calculations, we found that the Au-C bond in complexes **1.43-1.45** is composed mainly of π -type bonding (Figure 2).⁶⁵ Furthermore, the degree of π -back donation from Au to the carbene is largely dictated by the carbene substituents. For example, π -bonding between Au and the carbene fragment is decreased relative to σ -bonding in **1.45**, a species which is stabilized by two oxygen-atoms.

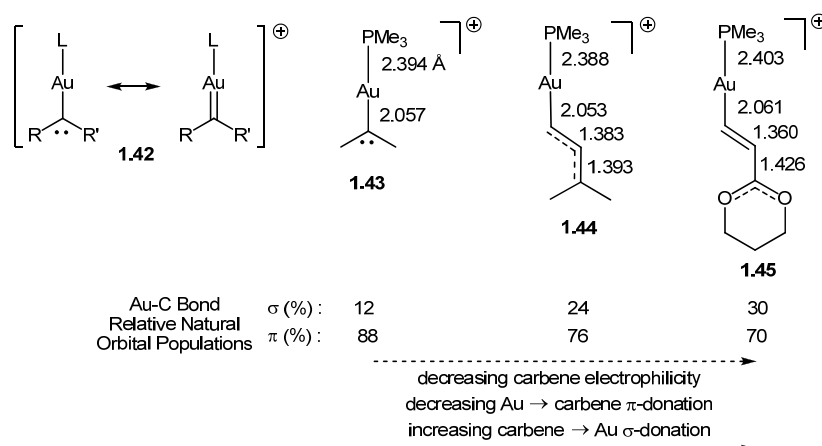


Figure 2. Calculated bond-distances and relative natural orbital populations for three cationic Au(I)-carbene complexes.

The ligand-Au-carbene bonding triad can be divided into three components (Figure 3). The σ -bonding is mainly composed of a 3 center – 4 electron hyperbond⁶⁶ (where hyperbond refers to bonding beyond the reduced 12-electron valence space and can be represented by the resonance forms: $L:Au-C \leftrightarrow P-Au:C$). As a result, strongly σ -donating ligands decrease the Au-C bond order (*trans* influence). The π -bonding is comprised of electron donation of two orthogonal d-orbitals on Au into π -acceptor orbitals on the ligand and the carbene. These two π -bonds compete for electron density and therefore have an indirect effect on each other. Overall, this bonding model suggests that formation of a Au-carbene complex from a vinyl Au-intermediate occurs with an increase in Au → C π -bonding and a decrease in C → Au σ -bonding. Thus, the depiction

of a gold-carbon double bond should be understood to mean that both π and σ components to the bond are present, but not that the Au-C bond has a bond order of two.⁶⁷ Indeed, the calculated natural bond orders for **1.43** (1.14), **1.44** (0.91), and **1.45** (0.53) are all significantly less than two.

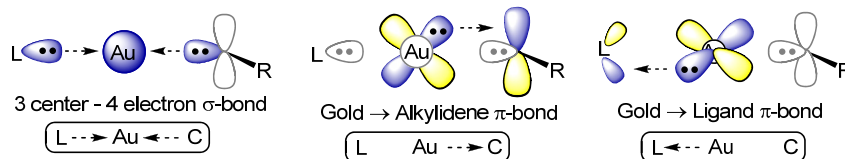
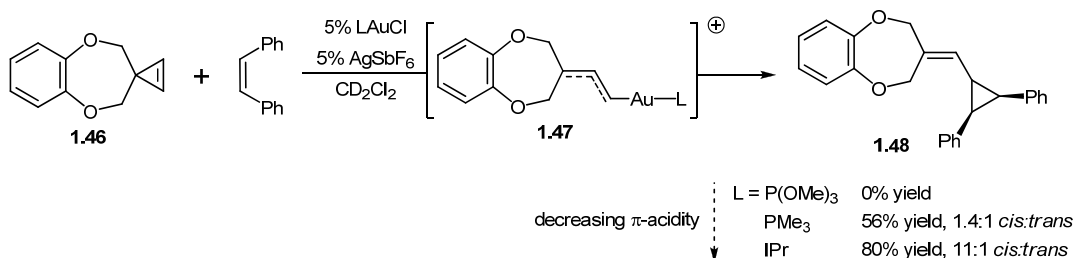


Figure 3. A bonding-model for Au-carbene complexes.

This bonding model can be used to predict the effect of ancillary ligands on reactivity.²⁹ Strongly σ -donating ligands increase the Au-C bond length, thereby increasing ‘free-carbene’ like behavior. In contrast, π -acidic ligands are expected to decrease σ -donation from Au to carbene, thereby increasing carbocation-type reactivity. As a result, carbene-like reactivity is favored for ancillary ligands that are π -donating or π -neutral and strongly σ -donating. This trend is demonstrated in the yield of cyclopropanation product **1.48** obtained from Au-catalyzed decomposition of cyclopropene **1.46** (Scheme 17). This reaction is expected to proceed via a Au-carbene intermediate (**1.47**) that is similar to **1.44**. The highest yield was obtained when the N-heterocyclic carbene (NHC) ligand IPr (1,3-bis(2,6-diisopropyl-phenyl)imidazol-2-ylidene) was employed (NHC ligands are strongly σ -donating and only weakly π -acidic). In contrast, trimethylphosphite, a strongly π -acidic ligand, provided none of the desired product.

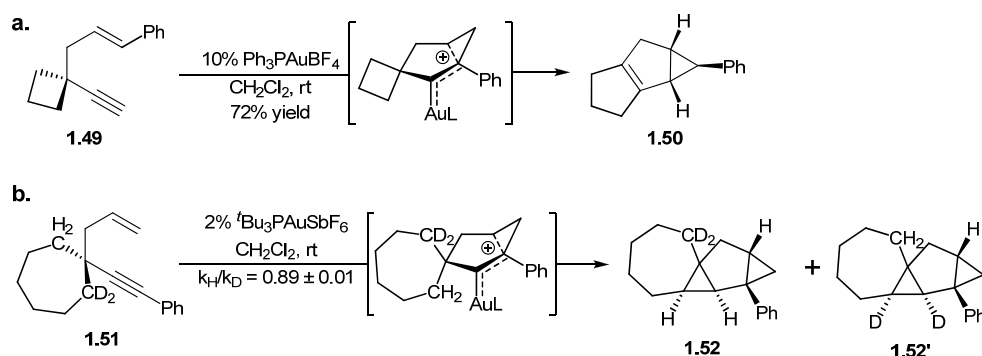


Scheme 17. The effect of the ancillary ligand (L) on the reactivity of Au(I)-carbene complexes.

1.4 Further Insights into Reactivity from Au-Catalyzed Cycloisomerization Reactions

1.4.1 Intramolecular Rearrangements of 1,5-Enynes

In the absence of an available hydrogen for a 1,2-hydride shift, a given gold carbenoid intermediate can undergo several other types of rearrangement. For example, a gold-carbene intermediate related to **1.25** will also undergo an intramolecular 1,2-alkyl shift/ring-expansion to produce tricycle **1.50** (Scheme 18a)⁴⁴ Interestingly, gold-catalyzed cycloisomerization of the related enyne **1.51** produces tetracycle **1.52** via an intramolecular C-H bond insertion (Scheme 18b).⁶⁸ In this case, we hypothesize that the adjacent 7-membered ring allows the adjacent C-H bonds to adopt an optimal position for insertion.^{69,70}



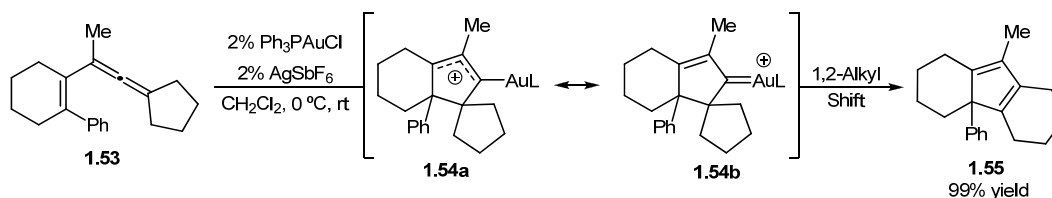
Scheme 18. Observed products resulting from intramolecular rearrangement of cationic intermediates.

We performed several kinetic isotope effect experiments in order to gain further insight into the mechanism of this C-H insertion. The results suggest that a mechanism involving simple hydride transfer to the carbenoid intermediate is unlikely.⁷¹

1.4.2 Ligand- and Substrate-Controlled Access to [2 + 2], [3 + 2], [4 + 2], and [4 + 3] Cycloadditions in Au-Catalyzed Reactions of Allene-Enes

We had developed a number of reactions suggesting that Au-containing cationic intermediates of type **1.42** can display either carbene-like or carbocation like reactivity. In order to further understand this divergence in reactivity, we sought to quantify the degree of carbocation stabilization in Au(I)-carbene complexes.

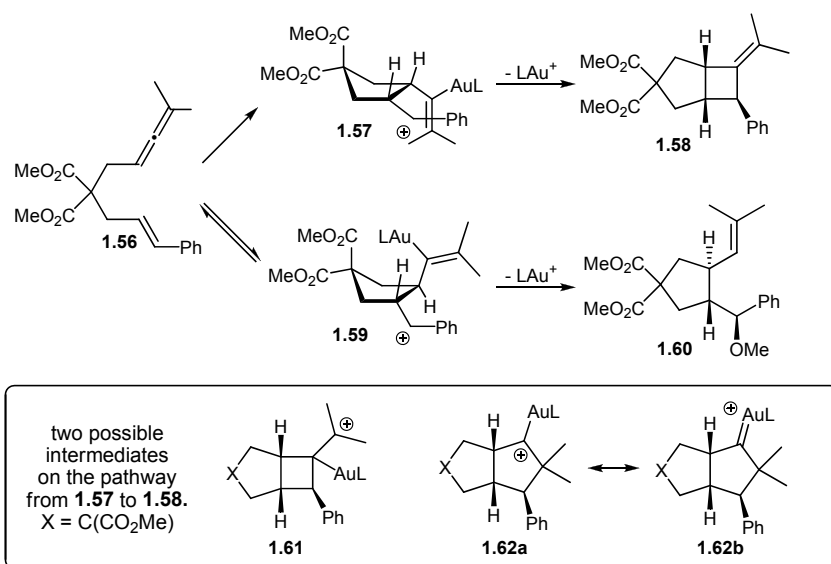
To identify a platform for these investigations, we considered the reactivity of 1,3-allenenes, such as **1.53** (Scheme 19).⁷² Our investigations suggest that gold(I)-catalyzed cycloisomerization to cyclopentadiene **1.55** proceeds via allyl-cation/Au-carbene **1.54**.⁷³ While we could not devise a method to quantify the degree of carbocation stabilization from gold in this particular reaction, we reasoned that the analogous 1,6-allene **1.56** might provide a path towards this type of insight.



Scheme 19. Gold(I)-catalyzed 1,3-allene cycloisomerization.

Initial coordination of a cationic Au(I) catalyst to the allene moiety of **1.56**, induces addition of the pendant olefin (Scheme 20).⁷⁴ The resulting carbocation can subsequently be trapped in one of two ways. In the absence of an external nucleophile, *cis*-bicycle **1.58** is produced.⁷⁵ While *trans*-cyclopentane **1.60** is produced in the presence of methanol. Furthermore, when these reactions are catalyzed by (*R*)-DTBM-SEGPHOS(AuCl)₂ **1.58** is produced in 92% yield and with 95% ee, while **1.60** is produced in 75% yield, but as a racemic mixture. Based on these

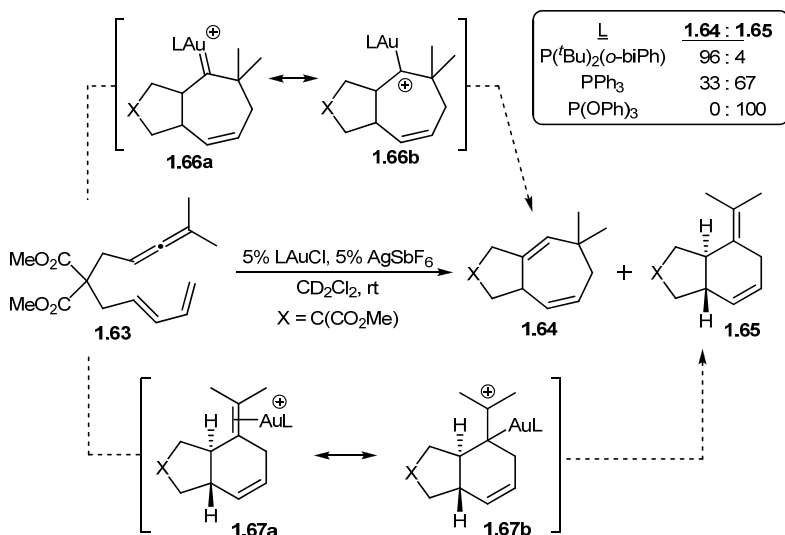
results, we proposed that initial addition of the olefin to produce **1.59** is fast and reversible. When an external nucleophile is present, **1.59** is trapped; however, in the absence of such a nucleophile, the reaction funnels through **1.57**. The formation of **1.57** from **1.56** may or may not be reversible. The exact mechanism of conversion of **1.57** to **1.58** has remained somewhat unclear. We initially hypothesized that the reaction most likely proceeds *via* trapping of the carbocation in **1.57** either by the pendant olefin to produce intermediate **1.61**, or by the Au-C bond to directly produce **1.58**. However, as the results below suggest, ring-contraction of gold-carbene intermediate **1.62** may be more likely.



Scheme 20. Observed reaction products and possible reactive intermediates in the Au-catalyzed reactions of allene **1.56**.

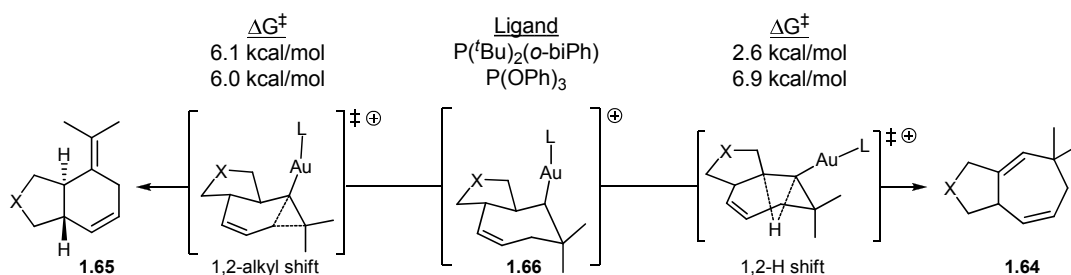
In light of these results, we were intrigued to find that Ph_3PAu^+ catalyzed cycloisomerization of allene-diene **1.63** produced a 33:67 mixture of [4 + 3] and [4 + 2] cycloadducts **1.64** and **1.65** (Scheme 21).^{76,77} We considered that this ratio might be altered by varying the ancillary ligand on Au. To our delight, electron-rich phosphines, including di-*tert*-butyl-*o*-biphenylphosphine provided the [4 + 3] product in high yield, while π -acidic ligands including triphenylphosphite provided exclusively the [4 + 2] adduct. This is one of the few examples of ligand-controlled divergent reactivity in Au-catalysis.^{29,78} Furthermore, by employing chiral, nonracemic phosphites and phosphoramidites it is possible to fully control the chemo-, diastereo- and enantioselectivity of this reaction.⁷⁹

Based on the results from the [2 + 2] cycloadditions described above, we initially assumed that this reaction would also proceed via a stepwise addition/trapping mechanism. This would indeed explain the observed ligand effect, with electron-rich ligands stabilizing Au-carbene **1.66** and π -acidic ligands disfavoring this pathway.



Scheme 21. Initial experimental observations and mechanistic hypothesis in ligand-directed, Au-catalyzed [4 + 3] and [4 + 2] cycloadditions.

In collaboration with the Goddard group, we initiated a theoretical study of this reaction in order to further elucidate the differences in bonding that lead to this divergent reactivity.⁸⁰ These calculations suggest that both **1.64** and **1.65** are actually formed through initial concerted [4 + 3] cycloaddition, producing Au-carbene intermediate **1.66** (Scheme 22). A subsequent 1,2-alkyl shift (ring contraction) or 1,2-hydride shift produces the observed products. Elucidating how the ancillary ligand controls product selectivity has led to some interesting insights.

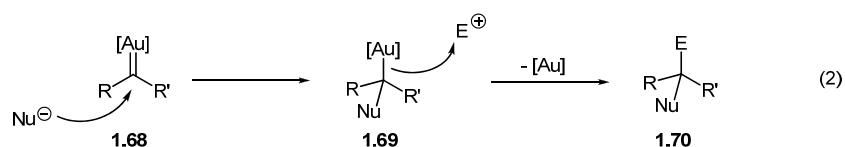


Scheme 22. Calculated structures and transition state energies for intermediates in Au-catalyzed [4 + 3] and [4 + 2] cycloadditions.

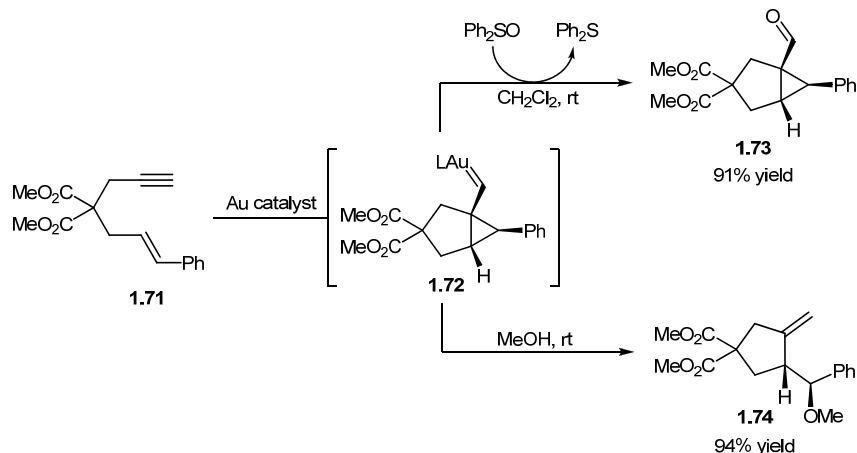
Due to steric interactions, the Au-moiety in **1.66** is puckered out of the plane of the bicycle. In addition, larger ligands cause the phosphine-Au-carbon bond to distort from 180° (169° for P(^tBu)₂(*o*-biPh) versus 178° for P(OPh)₃). As a result, π-donation from gold to carbon is actually reduced for the bulky, electron-rich P(^tBu)₂(*o*-biPh) and suggests that it is also important to consider sterics when attempting to predict the ability of a Au(I)-complex to stabilize an adjacent carbocation. In this reaction, increased occupation of the p-orbital on carbon in intermediate **1.66** disfavors the 1,2-H shift. As a result the 1,2-alkyl shift prevails with P(OPh)₃ as the ancillary ligand, while the 1,2-H shift is faster with P(^tBu)₂(*o*-biPh).

1.5 Intermolecular Annulation Reactions

Several additional experiments aimed at trapping proposed gold carbenoid intermediates were successful. Nucleophilic addition to gold-carbenoid intermediate **1.68** generates a gold-carbon sigma bond. In the case of protic nucleophiles, the Au catalyst is typically regenerated by protodeauration (Equation 2, $E^+ = H^+$).⁸¹ As an example, when the reaction of enyne **1.71** is conducted in methanol, the cationic intermediate **1.72** is trapped, producing methyl ether **1.74** (Scheme 23).⁸²



In the case of aprotic nucleophiles the Au-C bond may be trapped by electrophiles other than a proton. Thus, trapping of the intermediate carbenoid with diphenylsulfide produces ketone **1.73** after release of diphenylsulfide.⁸³ In addition to these reactions, Echavarren has also reported these intermediates can be trapped with olefins to produce cyclopropanation products.⁸⁴ Considering these results, we hypothesized that tethering the nucleophile and electrophile in Equation 2 would allow for an intermolecular annulation reaction.⁸⁵

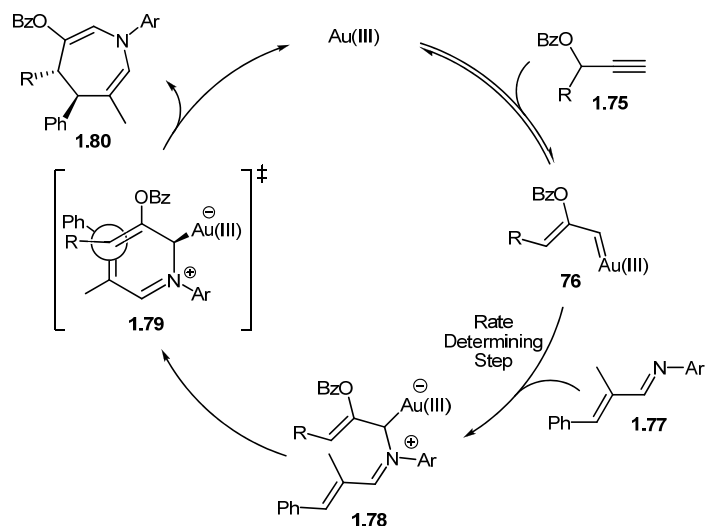


Scheme 23. Observed products resulting from intermolecular trapping of intermediate **1.72**.

1.5.1 A [4 + 3] Annulation Approach to Azepines

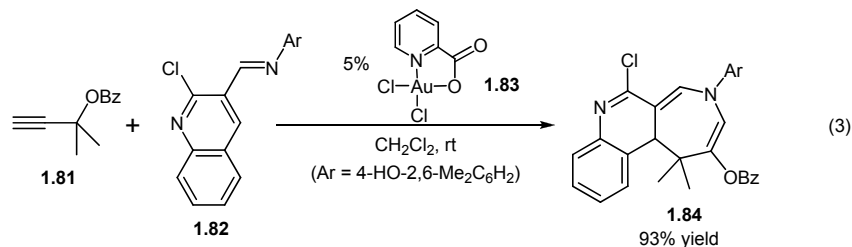
In analogy to related reactions of rhodium-stabilized carbenoids,⁸⁶ we reasoned that α,β -unsaturated imines could serve as appropriate coupling partners. On the basis of this hypothesis, we were pleased to find that Au(III) catalysts⁸⁷ efficiently promote the formation of azepine **1.80** from carbenoid precursor **1.75** and imine **1.77** (Scheme 24).⁸⁸ Based on the observed *trans* diastereoselectivity observed with secondary propargyl esters, we proposed that the cyclization occurs via transition state **1.79**. Overall, this transformation constitutes an example of the

reactivity paradigm that we had initially set out to observe (trapping of a Au-carbenoid with a tethered nucleophile-electrophile pair).



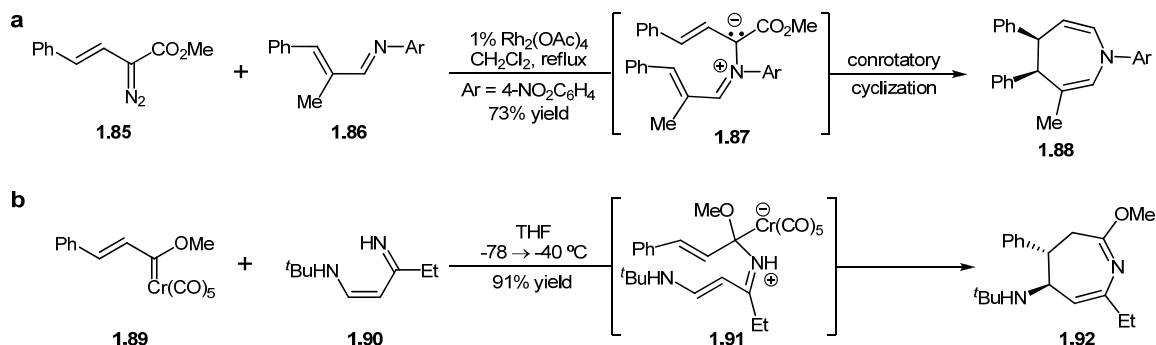
Scheme 24. Proposed mechanism of Au(III)-catalyzed azepine synthesis.

Further insight into this reaction was acquired through a Hammett analysis, which showed that the rate of the reaction is enhanced by electron-donating substituents on the N-Aryl and β -Aryl groups.⁸⁹ This supports our stepwise mechanism, and suggests that formation of **1.78** from carbenoid intermediate **1.76** is rate determining. In addition, this result implies that nucleophilic addition of C-aryl imines to **1.76** should occur despite the absence of a double bond for subsequent 7-membered ring formation. We were therefore curious to investigate potential dearomatization/annulation reactions. To our delight, heteroaromatic imines (i.e. **1.82**) could indeed be dearomatized *via* this methodology (Equation 3).



The proposed reaction mechanism for this transformation is particularly interesting in comparison to those that have been previously proposed for related reactions of rhodium-carbenoids and Fischer carbenes (Scheme 25). The $\text{Rh}_2(\text{OAc})_4$ -catalyzed decomposition of vinyl diazoester **1.85** in the presence of imine **1.86** is proposed to generate free ylide **1.87**, which undergoes a thermally allowed 8-electron electrocyclicization to produce *cis*-substituted azepine **1.88**.^{86a} In contrast, the stoichiometric reaction of 4-amino-1-aza-butadiene **1.90** with Fischer carbene **1.89** is proposed to produce *trans*-substituted azepine **1.92** via a transition state (**1.91**) that is quite similar to that proposed for the gold(III)-catalyzed reaction (**1.79**).^{86d} In this respect, the gold-catalyzed reaction can be considered a valuable alternative to the use of stoichiometric

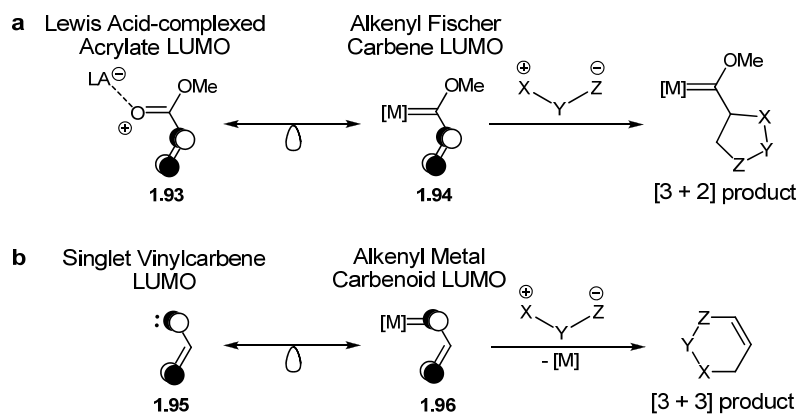
amounts of chromium reagents. On the other hand, it should be noted that these three reactions (Rh-catalyzed, Au-catalyzed, and Cr-mediated) provide access to azepines with complementary substitution patterns.



Scheme 25. Transition-metal catalyzed (a), and mediated (b) annulations of α,β -unsaturated imines.

1.5.2 Orbital Considerations in [3 + 3] Annulations

In light of these comparisons, we were curious to investigate gold-catalyzed annulation reactions of 1,3-dipoles, a type of transformation that is well known for alkenyl Fischer carbenes⁹⁰, but remains unprecedented for both free and metal-coordinated electrophilic alkenyl carbenes.⁹¹

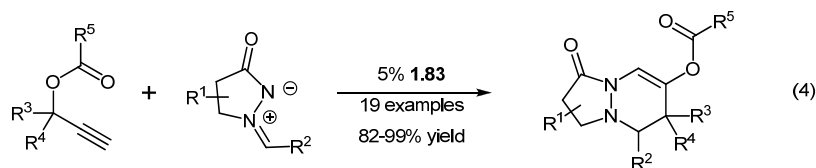


Scheme 26. Isolobal analogies of (a) alkenyl Fischer carbenes and (b) alkenyl metal carbenoids lead to predictions of distinct regioselectivity in the reaction of these species with 1,3-dipoles.

Reaction of alkenyl Fischer carbenes with 1,3-dipoles typically proceeds via concerted-asynchronous [3 + 2] cycloaddition. The regioselectivity of this cycloaddition can be rationalized by considering the molecular orbitals involved (Scheme 26). The LUMO of Fischer carbene **1.94** is isolobal with that of Lewis acid complexed acrylate **1.93**.⁹² As such, cycloaddition with 1,3-dipoles proceeds via [3 + 2] cycloaddition with the alkenyl fragment. In contrast, the LUMO of

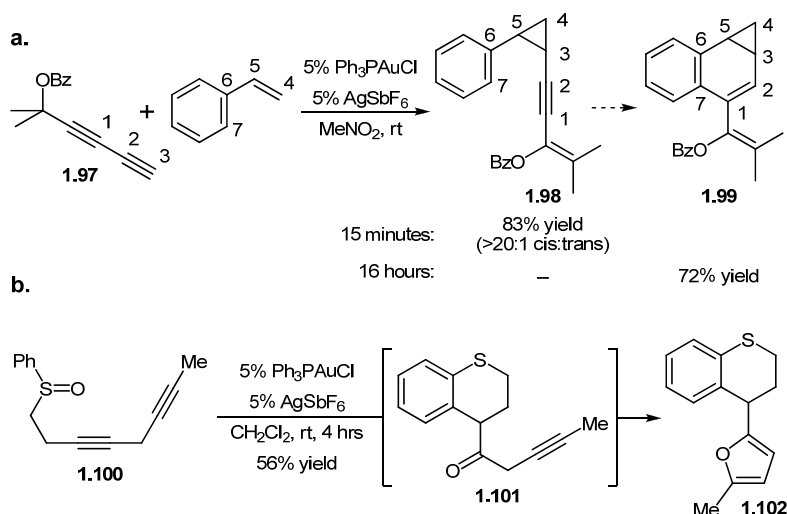
alkenyl metal carbenoid **1.96** can be approximated by free singlet vinylcarbene **1.95**.⁹³ Given this analogy, a [3 + 3]-cycloaddition between 1,3-dipoles and carbenoid **1.96** would be predicted. However, as mentioned previously, this type of reactivity had not been reported at the time we began our investigations.

We were therefore delighted to find that the picolinic acid derived Au(III) complex **1.83** efficiently catalyses the [3 + 3] annulation of azomethine imines and propargyl esters (Equation 4).⁹⁴ Mechanistic investigations suggest a stepwise mechanism similar to that proposed for the Au-catalyzed [4 + 3] annulation of imines and propargyl esters (*vide supra*).⁸⁸ In addition, this reaction serves to highlight the differences in the reactivity of alkenyl Fischer carbenes and the alkenyl Au-carbenoids.



1.6 Tandem Reactions

The ability to affect multiple, mechanistically distinct, bond-forming events into a single reaction sequence allows the rapid and efficient construction of complex molecular structures.⁹⁵ The design of tandem reactions requires an intricate understanding of reactivity. Each reaction must occur in the proper order and with high fidelity in order to ensure a high yield of the product. In our own research, we have developed several tandem reactions, and in doing so, have utilized several general strategies to ensure that these requirements are met.



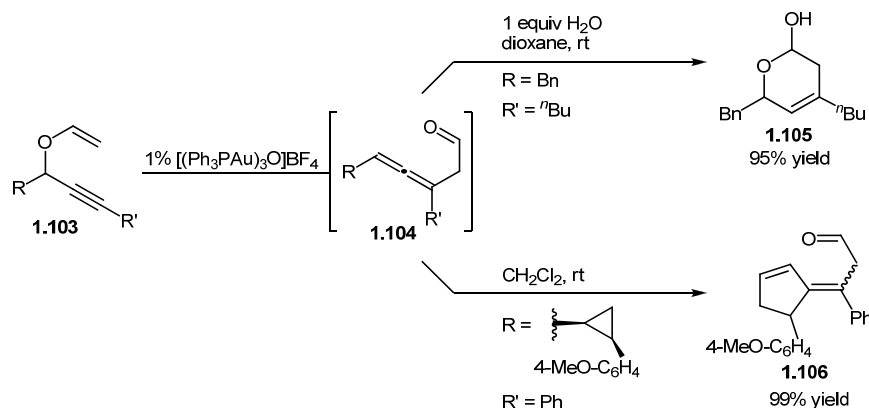
Scheme 27. Gold(I)-catalyzed tandem cyclization reactions.

One strategy is to employ sequential intramolecular/ intermolecular reactions. As an example, in what is overall a [4C + 3C] annulation, the intermolecular cyclopropanation of styrene with propargyl-ester containing diyne **1.97** can be coupled to an intramolecular hydroarylation (Scheme 27a).⁹⁶ This sequence utilizes the knowledge that the gold(I)-catalyzed

intermolecular cyclopropanation reaction occurs rapidly at room temperature (in this case, within 15 minutes).⁵⁶ This allows substrate-controlled regioselectivity in the subsequent intramolecular hydroarylation. If the rate of intermolecular hydroarylation was faster than or similar to the rate of cyclopropanation, then controlling the regioselectivity of the hydroarylation could become problematic.⁹⁷ A similar strategy is employed in the annulation of enynes or propargyl esters to form fluorenes or styrenes.^{78b}

An alternative strategy for the design of tandem reactions employs reactions that create functional groups that can undergo a second metal-catalyzed transformation. This strategy was employed in the bis-cyclization of diyne sulfoxide **1.100**: the ketone created in the first cyclization is subsequently transformed into the furan moiety of **1.102** (Scheme 27b).

Similarly, propargyl Claisen rearrangement of vinyl ether **1.103** forms allenyl aldehyde **1.104**.⁹⁸ In the presence of water, the aldehyde moiety will undergo further cyclization onto the allene, forming dihydropyran **1.105** (Scheme 28).⁹⁹ By excluding water from this reaction, cyclopropane-substituted allene **1.104** undergoes ring expansion to form cyclopentene **1.106**.¹⁰⁰



Scheme 28. Tandem propargyl-Claisen/cyclization reactions.

1.7 Conclusions

In this account¹⁰¹, we have attempted to illustrate the thought process and experimental testing that occurs throughout a reactivity-based approach to reaction discovery.⁵ In practice, this ‘method’ of organic chemistry research frequently involves close inspection of reaction mechanism, as well as the ability to identify and creatively expand upon reactivity paradigms. On a personal level, we have enjoyed the freedom to investigate new reactions that is afforded by this research method. But above all else, it is potential impact of discovering new reactivity, mechanisms and reactions that provides the driving force for this research program:

The goal is always finding something new, hopefully unimagined and, better still, hitherto unimaginable.

– Professor K. Barry Sharpless^{5a}

References

- (1) Lewis, G. N. *Science* **1909**, *30*, 1.
- (2) For recent discussions relevant to this approach see: (a) Nicolaou, K. C.; Snyder, S. A. *Proc. Natl. Acad. Sci. USA* **2004**, *101*, 11929. (b) Mohr, J. T.; Krout, M. R.; Stoltz, B. M. *Nature* **2008**, *455*, 323. (c) Shenvi, R. A.; O'Malley, D. P.; Baran, P. S. *Acc. Chem. Res.* **2009**, *42*, 530. (d) Wender, P. A.; Verma, V. A.; Paxton, T. J.; Pillow, T. H. *Acc. Chem. Res.* **2008**, *41*, 40. (e) Young, I. S.; Baran, P. S. *Nature. Chem.* **2009**, *1*, 193. (f) Morten, C. J.; Byers, J. A.; Van Dyke, A. R.; Vilotijevic, I.; Jamison, T. F. *Chem. Soc. Rev.* **2009**, *38*, 3175.
- (3) (a) Grubbs, R. H.; Chang, S. *Tetrahedron*, **1998**, *54*, 4413. (b) Dick, A. R.; Sanford, M. S. *Tetrahedron* **2006**, *62*, 2439. (c) Hartwig, J. F. *Nature* **2008**, *455*, 314. (d) Buchwald, S. L. *Acc. Chem. Res.* **2008**, *41*, 1439. (e) Sherry, B. D.; Fürstner, A. *Acc. Chem. Res.* **2008**, *41*, 1500. (f) Fu, G. C. *Acc. Chem. Res.* **2008**, *41*, 1555. (g) Afagh, N. A.; Yudin, A. K. *Angew. Chem., Int. Ed.* **2010**, *49*, 262.
- (4) (a) Francis, M. B.; Jamison T. F.; Jacobsen E. N. *Curr. Opin. Chem. Biol.* **1998**, *2*, 422. (b) Weber, L.; Illgen, K.; Almstetter, M. *Synlett* **1999**, 366. (c) Kanan, M. W.; Rozenman, M. M.; Sakurai, K.; Snyder, T. M., Liu, D. R. *Nature* **2004**, *431*, 545. (d) Beeler, A. B.; Su, S.; Singleton, C. A.; Porco, J. A. Jr. *J. Am. Chem. Soc.* **2007**, *129*, 1413. (e) Rozenman, M. M.; Kanan, M. W.; Liu, D. R. *J. Am. Chem. Soc.* **2007**, *129*, 14933. (f) Gorin, D. J.; Kamlet, A. S.; Liu, D. R. *J. Am. Chem. Soc.* **2009**, *131*, 9189.
- (5) For selected examples that highlight this approach, see: (a) Sharpless, K. B. *Angew. Chem. Int. Ed.* **2002**, *41*, 2024. (b) Johnson, J. S.; Evans, D. A. *Acc. Chem. Res.* **2000**, *33*, 325. (c) Fu, G. C. *Acc. Chem. Res.* **2000**, *33*, 412. (d) Fulton, J. R., Holland, A. W., Fox, D. J. and Bergman, R. G. *Acc. Chem. Res.* **2002**, *35*, 44. (e) Trost, B. M. *Acc. Chem. Res.* **2002**, *35*, 695. (f) Saito, S.; Yamamoto, H. *Acc. Chem. Res.* **2004**, *37*, 570. (g) Enders, D.; Neimeier, O.; Henseler, A.; *Chem. Rev.* **2007**, *107*, 5606. (h) MacMillan, D. W. C. *Nature* **2008**, *455*, 304. (i) Doyle, A. G.; Jacobsen, E. N. *Chem. Rev.* **2007**, *107*, 5713.
- (6) Teles, J. H.; Brode, S.; Chabanas, M. *Angew. Chem., Int. Ed.* **1998**, *37*, 1415.
- (7) Nesymanov, A. N.; Grandberg, K. I.; Dyadchenko, V. P.; Lemenovskii, D. A.; Perevalova, E. G. *Izv. Akad. Nauk SSSR, Ser. Khim.* **1974**, 1206.
- (8) Kennedy-Smith, J. J.; Staben, S. T.; Toste, F. D. *J. Am. Chem. Soc.* **2004**, *126*, 4526.
- (9) The thermally promoted Conia-ene reaction typically proceeds at temperatures above 200 °C. For a review, see: Conia, J. M.; Le Perche, P. *Synthesis* **1975**, 1.
- (10) For additional metal promoted Conia-ene reactions, see: (a) Pd-catalyzed: Balme, G.; Bouyssi, D.; Faure, R.; Gore, J.; Van Hemelryck, B. *Tetrahedron* **1992**, *48*, 3891. (b) Mo-catalyzed: McDonald, F. E.; Olson, T. C. *Tetrahedron Lett.* **1997**, *38*, 7691. (c) Cu-catalyzed: Bouyssi, D.; Monteiro, N.; Balme, G. *Tetrahedron Lett.* **1999**, *40*, 1297. (d) Ti-mediated: Kitagawa, O.; Suzuki, T.; Inoue, T.; Watanabe, Y.; Taguchi, T. *J. Org. Chem.* **1998**, *63*, 9470. (e) Hg/H⁺-catalyzed: Boaventura, M. A.; Drouin, J.; Conia, J. M. *Synthesis* **1983**, 801. (f) Co/hv-catalyzed: Renaud, J.-L.; Aubert, C.; Malacria, M. *Tetrahedron* **1999**, *55*, 5113. (g) Ni-catalyzed: Gao, Q.; Zheng, B.-F.; Li, J.-H.; Yang, D. *Org. Lett.*, **2005**, *7*, 2185. (h) Re-catalyzed: Kuninobu, Y.; Kawata, A.; Takai, K. *Org. Lett.*, **2005**, *7*, 4823.

-
- (11) A 5-endo-dig variant of this reaction is also viable, see: Staben, S. T.; Kennedy-Smith, J. J.; Toste, F. D. *Angew. Chem., Int. Ed.* **2005**, *43*, 5350.
- (12) For a similar study, see: Hashmi, A. S. K.; Weyrauch, J. P.; Frey, W.; Bats, J. W. *Org. Lett.* **2004**, *6*, 4391.
- (13) (a) Akana, J. A.; Bhattacharyya, K. X.; Müller, P.; Sadighi, J. P. *J. Am. Chem. Soc.* **2007**, *129*, 7736. (b) Liu, L.-P.; Xu, B.; Mashuta, M. S.; Hammond, G. B. *J. Am. Chem. Soc.* **2008**, *130*, 17642. (c) Hashmi, A. S. K.; Schuster, A. M.; Rominger, F. *Angew. Chem. Int. Ed.* **2009**, *48*, 8247.
- (14) We hypothesize that the Brønsted acid suppresses alkyne dimerization, while the Lewis acid increases the enolic character of the ketoester, see also: Trost, B. M.; Sorum, M. T.; Chan, C.; Harms, A. E.; Rühler, G. *J. Am. Chem. Soc.* **1997**, *119*, 698.
- (15) (a) Staben, S. T.; Kennedy-Smith, J. J.; Huang, D.; Corkey, B. K.; LaLonde, R. L.; Toste, F. D. *Angew. Chem., Int. Ed.* **2006**, *45*, 5991. (b) Corkey, B. K.; Toste, F. D. *J. Am. Chem. Soc.* **2007**, *129*, 2764.
- (16) Linghu, X.; Kennedy-Smith, J. J.; Toste, F. D. *Angew. Chem., Int. Ed.* **2007**, *46*, 7671.
- (17) For reviews of enantioselective hydroamination, see: (a) Hultsch, K. C. *Org. Biomol. Chem.* **2005**, *3*, 1819. (b) Hultsch, K. C. *Adv. Synth. Catal.* **2005**, *347*, 367.
- (18) LaLonde, R. L.; Sherry, B. D.; Kang, E. J.; Toste, F. D. *J. Am. Chem. Soc.* **2007**, *129*, 2452.
- (19) Hamilton, G. L.; Kang, E. J.; Mba, M.; Toste, F. D. *Science* **2007**, *317*, 496.
- (20) For another study on the Au(I)-catalyzed asymmetric hydroalkoxylation of allenes, see: Zhang, Z.; Widenhoefer, R. A. *Angew. Chem., Int. Ed.* **2007**, *46*, 283.
- (21) LaLonde, R. L.; Wang, Z. J.; Mba, M.; Lackner, A. D.; Toste, F. D. *Angew. Chem., Int. Ed.* **2009**, *49*, 598.
- (22) For a review of chiral anion mediated asymmetric chemistry, see: Lacour, J.; Hebbeviton, V. *Chem. Soc. Rev.*, **2003**, *32*, 373.
- (23) For other metal-catalyzed chiral-anion mediated asymmetric reactions, see: (a) Llewellyn, D. B.; Adamson, D.; Arndtsen, B. A. *Org. Lett.* **2000**, *2*, 4165. (b) Llewellyn, D. B.; Arndtsen, B. A. *Tetrahedron-Asymmetry* **2005**, *16*, 1789. (c) Dorta, R.; Shimon, L.; Milstein, D. *J. Organomet. Chem.* **2004**, *689*, 751. (d) Mukherjee, S.; List, B. *J. Am. Chem. Soc.* **2007**, *129*, 11336. (e) Hu, W.-H.; Xu, X.-F.; Zhou, J.; Liu, W.-J.; Huang, H.-X.; Hu, J.; Yang, L.-P.; Gong, L.-Z. *J. Am. Chem. Soc.* **2008**, *130*, 7782. (f) Li, C.; Wang, C.; Villa-Marcos, B.; Xiao, J. *J. Am. Chem. Soc.* **2008**, *130*, 14450. (g) Li, C.; Villa-Marcos, B.; Xiao, J. *J. Am. Chem. Soc.* **2009**, *131*, 6967. (h) Lu, Y.; Johnstone, T. C.; Arndtsen, B. A. *J. Am. Chem. Soc.* **2009**, *131*, 11284.
- (24) Ito, Y.; Sawamura, M.; Hayashi, T. *J. Am. Chem. Soc.* **1986**, *108*, 6405.
- (25) Melhado, A. D.; Luparia, M.; Toste, F. D. *J. Am. Chem. Soc.* **2007**, *129*, 12638.
- (26) For a racemic, Ag-catalyzed variant of this reaction, see: Peddibhotla, S.; Tepe, J. *J. Am. Chem. Soc.* **2004**, *126*, 12776.
- (27) Müller, T. E.; Beller, M. *Chem. Rev.* **1998**, *98*, 675.
- (28) Markham, J. P.; Staben, S. T.; Toste, F. D. *J. Am. Chem. Soc.* **2005**, *127*, 9708.
- (29) For a review of ligand effects in gold catalysis, see: Gorin, D. J.; Sherry, B. D.; Toste, F. D. *Chem. Rev.* **2008**, *108*, 3351.

-
- (30) Theoretical calculations support this mechanism, see: Sordo, T. L.; Ardura, D. *Eur. J. Org. Chem.* **2008**, 3004.
- (31) For a review of 1,2-alkyl migrations catalyzed by π acids, see: Crone, B.; Kirsch, S. F. *Chem.-Eur. J.* **2008**, *14*, 3514.
- (32) Sethofer, S. G.; Staben, S. T.; Hung, O. Y.; Toste, F. D. *Org. Lett.* **2008**, *10*, 4315.
- (33) Kleinbeck, F.; Toste, F. D. *J. Am. Chem. Soc.* **2009**, *131*, 9178.
- (34) For other reports of catalytic asymmetric ring expansion, see: (a) Trost, B. M.; Yasukata, T. *J. Am. Chem. Soc.* **2001**, *123*, 7162. (b) Trost, B. M.; Xie, J. *J. Am. Chem. Soc.* **2006**, *128*, 6044. (c) Trost, B. M.; Xie, J.; Maulide, N. *J. Am. Chem. Soc.* **2008**, *130*, 17258.
- (35) Markownikoff, W. *Liebigs Ann.* **1870**, *153*, 228.
- (36) For related reactions, see: (a) Cacchi, S.; Fabrizi, G.; Pace, P. *J. Org. Chem.* **1998**, *63*, 1001. (b) Fürstner, A.; Szillat, H.; Stelzer, F. *J. Am. Chem. Soc.* **2000**, *122*, 6785. (c) Shimada, T.; Nakamura, I.; Yamamoto, Y. *J. Am. Chem. Soc.* **2004**, *126*, 10546. (d) Nakamura, I.; Mizushima, Y.; Yamamoto, Y. *J. Am. Chem. Soc.* **2005**, *127*, 15022. (e) Nakamura, I.; Sato, T.; Yamamoto, Y. *Angew. Chem., Int. Ed.* **2006**, *45*, 4473. (f) Istrate, F. M.; Gagosz, F. *Org. Lett.* **2007**, *9*, 3181. (g) Nakamura, I.; Yamagishi, U.; Song, D.; Konta, S.; Yamamoto, Y. *Angew. Chem., Int. Ed.* **2007**, *46*, 2284. (h) Nakamura, I.; Sato, T.; Terada, M.; Yamamoto, Y. *Org. Lett.* **2007**, *9*, 4081. (i) Nakamura, I.; Sato, T.; Terada, M.; Yamamoto, Y. *Org. Lett.* **2008**, *10*, 2649. (j) Uemura, M.; Watson, I. D. G.; Katsukawa, M.; Toste, F. D. *J. Am. Chem. Soc.* **2009**, *131*, 3464.
- (37) Dubé, P.; Toste, F. D. *J. Am. Chem. Soc.* **2006**, *128*, 12062.
- (38) For a review of “memory of chirality”, see: (a) Zhao, H.; Hsu, D. C.; Carlier, P. R. *Synthesis* **2005**, 1.
- (39) For studies on the Ag/Cu catalyzed Conia-ene reaction, see: Deng, C.-L.; Zou, T.; Wang, Z.-Q.; Song, R.-J.; Li, J.-H. *J. Org. Chem.* **2009**, *74*, 412.
- (40) Shapiro, N. D.; Toste, F. D. *Proc. Natl. Acad. Sci. U.S.A.* **2008**, *105*, 2779.
- (41) For other reports of Au-alkyne complexes, see reference 13a, and: (a) Schulte, P.; Behrens, U. *Chem. Commun.*, **1998**, 1633. (b) Flügge, S.; Anoop, A.; Goddard, R.; Thiel, W.; Fürstner, A. *Chem.-Eur. J.* **2009**, *15*, 8558. For a review, see: (c) Schmidbaur, H.; Schier, A. *Organometallics* **2010**, *29*, 2.
- (42) For similar studies, see: (a) Nechaev, M. S.; Rayón, V. M.; Frenking, G. *J. Phys. Chem. A* **2004**, *108*, 3134. (b) Ziegler, T.; Rauk, A. *Inorg. Chem.* **1979**, *18*, 1558. (c) Hertwig, R. H.; Koch, W.; Schröder, D.; Schwarz, H.; Hrušák, J.; Schwerdtfeger, P. *J. Phys. Chem.* **1996**, *100*, 12253. (d) Kim, C. K.; Lee, K. A.; Kim, C. K.; Lee, B.; Lee, H.W. *Chem. Phys. Lett.* **2004**, *391*, 321. (e) Tai, H.-C.; Krossing, I.; Seth, M.; Deubel, D. V. *Organometallics* **2004**, *23*, 2343.
- (43) Luzung, M. R.; Toste, F. D. *J. Am. Chem. Soc.* **2003**, *125*, 15760.
- (44) Luzung, M. R.; Markham, J. P.; Toste, F. D. *J. Am. Chem. Soc.* **2004**, *126*, 10858.
- (45) For related reports, see: (a) Mamane, V.; Gress, T.; Krause, H.; Fürstner, A. *J. Am. Chem. Soc.* **2004**, *126*, 8654. (b) Harrak, Y.; Blaszykowski, C.; Bernard, M.; Cariou, K.; Mainetti, E.; Mouriés, V.; Dhimane, A.-L.; Fensterbank, L.; Malacria, M. *J. Am. Chem. Soc.* **2004**, *126*, 8656. (c) Horino, Y.; Luzung, M. R.; Toste, F. D. *J. Am. Chem. Soc.* **2006**, *128*, 11364.

- (46) For reviews on cycloisomerizations, see: (a) Aubert, C.; Buisine, O.; Malacria, M. *Chem. Rev.* **2002**, *102*, 813. (b) Trost, B. M.; Krische, M. J. *Synlett* **1998**, 1. (c) Ojima, I.; Tzamarioudaki, M.; Li, Z.; Donovan, R. J. *Chem. Rev.* **1996**, *96*, 635.
- (47) Gorin, D. J.; Davis, N. R.; Toste, F. D. *J. Am. Chem. Soc.* **2005**, *127*, 11260.
- (48) Shapiro, N. D.; Toste, F. D. *J. Am. Chem. Soc.* **2007**, *129*, 4160.
- (49) For reviews, see: (a) Wee, A. G. H. *Curr. Org. Synth.* **2006**, *3*, 499. (b) Davies, H. M. L.; Beckwith, R. E. J. *Chem. Rev.* **2003**, *103*, 2861. (c) Davies, H. M. L.; Antoulinakis, E. G. *Org. React.* **2001**, *57*, 1. (d) Ye, T.; McKervey, M. A. *Chem. Rev.* **1994**, *94*, 1091. (e) *Modern Catalytic Methods for Organic Synthesis with Diazo Compounds*; Doyle M. P., McKervey, M. A., Ye, T., Eds.; Wiley: New York, 1998. (f) *Metal-Carbenes in Organic Synthesis*; Zaragoza-Dorwald, F., Ed.; Wiley-VCH: Weinheim, Germany, 1998.
- (50) For gold-catalyzed reaction of α -diazoesters, see: (a) Fructos, M. R.; Belderrain, T. R.; de Frémont, P.; Scott, N. M.; Nolan, S. P.; Díaz-Requejo, M. M.; Pérez, P. J. *Angew. Chem., Int. Ed.* **2005**, *44*, 5284. (b) Fructos, M. R.; de Frémont, P.; Nolan, S. P.; Díaz-Requejo, M. M.; Pérez, P. J. *Organometallics* **2006**, *25*, 2237.
- (51) Rautenstrauch, V. *J. Org. Chem.* **1984**, *49*, 950.
- (52) Shi, X.; Gorin, D. J.; Toste, F. D. *J. Am. Chem. Soc.* **2005**, *127*, 5802.
- (53) Faza, O. N.; López, C. S.; Álvarez, R.; de Lera, A. R. *J. Am. Chem. Soc.* **2006**, *128*, 2434.
- (54) Closs, G. L.; Moss, R. A. *J. Am. Chem. Soc.* **1964**, *86*, 4042.
- (55) Skell, P. S.; Woodworth, R. C. *J. Am. Chem. Soc.* **1956**, *78*, 4496.
- (56) Johansson, M. J.; Gorin, D. J.; Staben, S. T.; Toste, F. D. *J. Am. Chem. Soc.* **2005**, *127*, 18002.
- (57) (a) Miki, K.; Ohe, K.; Uemura, S. *Tetrahedron Lett.* **2003**, *44*, 2019. (b) Miki, K.; Ohe, K.; Uemura, S. *J. Org. Chem.* **2003**, *68*, 8505. (c) Miki, K.; Uemura, S.; Ohe, K. *Chem. Lett.* **2005**, *34*, 1068. For a related gold(III)-catalyzed intramolecular cyclopropanation, see: (d) Fürstner, A.; Hannen, P. *Chem. Commun.* **2004**, 2546.
- (58) For a review of enantioselective cyclopropanation, see: Lebel, H.; Marcoux, J.-F.; Molinaro, C.; Charette, A. B. *Chem. Rev.* **2003**, *103*, 977.
- (59) Watson, I. D. G.; Ritter, S.; Toste, F. D. *J. Am. Chem. Soc.* **2009**, *131*, 2056.
- (60) (a) Fürstner, A.; Szillat, H.; Gabor, B.; Mynott, R. *J. Am. Chem. Soc.* **1998**, *120*, 8305. (b) Fürstner, A.; Stelzer, F.; Szillat, H. *J. Am. Chem. Soc.* **2001**, *123*, 11863. (c) Nieto-Oberhuber, C.; Muñoz, M. P.; Buñuel, E.; Nevado, C.; Cárdenas, D. J.; Echavarren, A. M. *Angew. Chem., Int. Ed.* **2004**, *43*, 2402. (d) Chatani, N.; Kataoka, K.; Murai, S.; Furukawa, N.; Seki, Y. *J. Am. Chem. Soc.* **1998**, *120*, 9104.
- (61) Gorin, D. J.; Toste, F. D. *Nature* **2007**, *446*, 395.
- (62) Pitzer, K. S. *Acc. Chem. Res.* **1979**, *12*, 271.
- (63) Schwerdtfeger, P.; Boyd, P. D. W.; Burrell, A. K.; Robinson, W. T.; Taylor, M. J. *Inorg. Chem.* **1990**, *29*, 3593.
- (64) Benitez, D.; Shapiro, N. D.; Tkatchouk, E.; Wang, Y.; Goddard, W. A. III; Toste, F. D. *Nature Chem.* **2009**, *1*, 482.
- (65) Irikura, K. K.; Goddard III, W. A. *J. Am. Chem. Soc.* **1994**, *116*, 8733.
- (66) Landis, C. R.; Weinhold, F. *J. Comput. Chem.* **2007**, *28*, 198.
- (67) This model is highly reminiscent of the double 'half-bond' model proposed for rhodium carbenoid intermediates, see: (a) Snyder, J. P.; Padwa, A.; Stengel, T.; Arduengo III, A. J.;

- Jockisch, A.; Kim, H.-L. *J. Am. Chem. Soc.* **2001**, *123*, 11318. (b) Costantino, G.; Rovito, R.; Macchiarulo, A.; Pellicciari, R. *J. Mol. Struct. Theochem*, **2002**, *581*, 111.
- (68) Horino, Y.; Yamamoto, T.; Ueda, K.; Kuroda, S.; Toste, F. D. *J. Am. Chem. Soc.* **2009**, *131*, 2809.
- (69) For a related study, see: Lemière, G.; Gandon, V.; Cariou, K.; Hours, A.; Fukuyama, T.; Dhimane, A.-L.; Fensterbank, L.; Malacria, M. *J. Am. Chem. Soc.* **2009**, *131*, 2993.
- (70) For related metal-catalyzed C(sp³)-H bond insertions, see ref 50b, and: (a) Bhunia, S.; Liu, R.-S. *J. Am. Chem. Soc.* **2008**, *130*, 16488. (b) Lee, S. J.; Oh, C. H.; Lee, J. H.; Kim, J. I.; Hong, C. S. *Angew. Chem., Int. Ed.* **2008**, *47*, 7505. (c) Cui, L.; Peng, Y.; Zhang, L. *J. Am. Chem. Soc.* **2009**, *131*, 8394.
- (71) Jones, W. D. *Acc. Chem. Res.* **2003**, *36*, 140.
- (72) Lee, J. H.; Toste, F. D. *Angew. Chem., Int. Ed.* **2007**, *46*, 912.
- (73) For related transformations, see: (a) Zhang, L.; Wang, S. *J. Am. Chem. Soc.* **2006**, *128*, 1442. (b) Funami, H.; Kusama, H.; Iwasawa, N. *Angew. Chem., Int. Ed.* **2007**, *46*, 909. (c) Lemière, G.; Gandon, V.; Cariou, K.; Fukuyama, T.; Dhimane, A.-L.; Fensterbank, L.; Malacria, M. *Org. Lett.* **2007**, *9*, 2207.
- (74) Luzung, M. P.; Mauleón, P.; Toste, F. D. *J. Am. Chem. Soc.* **2007**, *129*, 12402.
- (75) For a related mechanism, see: Zhang, L. *J. Am. Chem. Soc.* **2005**, *127*, 16804.
- (76) Mauleón, P.; Zeldin, R. M.; González, A. Z.; Toste, F. D. *J. Am. Chem. Soc.* **2009**, *131*, 6348.
- (77) For related studies, see: (a) Trillo, B.; López, F.; Montserrat, S.; Ujaque, G.; Castedo, L.; Lledós, A.; Mascareñas, J. L. *Chem.-Eur. J.* **2009**, *15*, 3336. (b) Alonso, I.; Trillo, B.; López, F.; Montserrat, S.; Ujaque, G.; Castedo, L.; Lledós, A.; Mascareñas, J. L. *J. Am. Chem. Soc.* **2009**, *131*, 13020.
- (78) See also: (a) Lemière, G.; Gandon, V.; Agenet, N.; Goddard, J.-P.; de Kozak, A.; Aubert, C.; Fensterbank, L.; Malacria, M. *Angew. Chem., Int. Ed.* **2006**, *45*, 7596. (b) Gorin, D. J.; Watson, I. D. G.; Toste, F. D. *J. Am. Chem. Soc.* **2008**, *130*, 3736. (c) Xia, Y.; Dudnik, A. S.; Gevorgyan, V.; Li, Y. *J. Am. Chem. Soc.* **2008**, *130*, 6940.
- (79) González, A.; Toste, F. D. *Org. Lett.* **2010**, *12*, 200.
- (80) Benitez, D.; Tkatchouk, E.; Gonzalez, A.; Goddard, W. A. III; Toste, F. D. *Org. Lett.* **2009**, *11*, 4798.
- (81) (a) Amijs, C. H. M., López-Carrillo, V., and Echavarren, A. M. *Org. Lett.* **2007**, *9*, 4021. (b) Leseurre, L.; Toullec, P. Y.; Genêt, J.-P.; Michelet, V. *Org. Lett.* **2007**, *9*, 4049.
- (82) Nieto-Oberhuber, C.; López, S.; Echavarren, A. M. *J. Am. Chem. Soc.* **2005**, *127*, 6178.
- (83) Witham, C. A.; Mauleón, P.; Shapiro, N. D.; Sherry, B. D.; Toste, F. D. *J. Am. Chem. Soc.* **2007**, *129*, 5838.
- (84) (a) Nieto-Oberhuber, C.; Paz Muñoz, M.; López, S.; Jiménez-Núñez, E.; Nevado, C.; Herrero-Gómez, E.; Raducan, M.; Echavarren, A. M. *Chem.-Eur. J.* **2006**, *12*, 1677. (b) Nieto-Oberhuber, C.; López, S.; Paz Muñoz, M.; Jiménez-Núñez, E.; Bunuel, E.; Cárdenas, D. J.; Echavarren, A. M. *Chem.-Eur. J.* **2006**, *12*, 1694. (c) López, S.; Herrero-Gómez, E.; Pérez-Galán, P.; Nieto-Oberhuber, C.; Echavarren, A. M. *Angew. Chem., Int. Ed.* **2006**, *45*, 6029.
- (85) For related Au-catalyzed intermolecular annulations, see: (a) Asao, N.; Takahashi, K.; Lee, S.; Kasahara, T.; Yamamoto, Y. *J. Am. Chem. Soc.* **2002**, *124*, 12650. (b) Kusama,

-
- H.; Miyashita, Y.; Takaya, J.; Iwasawa, N. *Org. Lett.* **2006**, *8*, 289. (c) Zhang, G.; Huang, X.; Li, G.; Zhang, L. *J. Am. Chem. Soc.* **2008**, *130*, 1814. (d) Zhang, G.; Zhang, L. *J. Am. Chem. Soc.* **2008**, *130*, 12598.
- (86) (a) Doyle, M. P.; Hu, W.; Timmons, D. *J. Org. Lett.* **2001**, *3*, 3741. (b) Doyle, M. P.; Yan, M.; Hu, W.; Gronenberg, L. S. *J. Am. Chem. Soc.* **2003**, *125*, 4692. (c) Davies, H. M. L.; Hu, B.; Saikali, E.; Bruzinski, P. R. *J. Org. Chem.* **1994**, *59*, 4535. For related reactions of Fischer carbenes, see: (d) Barluenga, J.; Tomás, M.; Ballesteros, A.; Santamaria, J.; Carbajo, R. J.; López-Ortiz, F.; Garcia-Granda, S.; Pertierra, P. *Chem.-Eur. J.* **1996**, *2*, 88. (e) Barluenga, J.; Tomás, M.; Rubio, E.; López-Pelegrín, J. A.; García-Granda, S.; Priede, M. P. *J. Am. Chem. Soc.* **1999**, *121*, 3065.
- (87) (a) Hashmi, A. S. K.; Weyrauch, J. P.; Rudolph, M.; Kurpejović, E. *Angew. Chem., Int. Ed.* **2004**, *43*, 6545. (b) Hashmi, A. S. K.; Kurpejović, E.; Wölflé, M.; Frey, W.; Bats, J. W. *Adv. Synth. Catal.* **2007**, *349*, 1743.
- (88) Shapiro, N. D.; Toste, F. D. *J. Am. Chem. Soc.* **2008**, *130*, 9244.
- (89) Hansch, C.; Leo, A.; Taft, R. W. *Chem. Rev.* **1991**, *91*, 165.
- (90) (a) Barluenga, J.; Rodrigues, F.; Fañanás, F. J.; Flórez, J. *Top. Organomet. Chem.* **2004**, *13*, 59. (b) Barluenga, J.; Santamaria, J.; Tomás, M. *Chem. Rev.* **2004**, *104*, 2259. (c) Sierra, M. A.; Fernández, I.; Cossío, F. P. *Chem. Commun.* **2008**, 4671.
- (91) (a) Bertrand, G. Ed.; *Carbene Chemistry: From Fleeting Intermediates to Powerful Reagents*; FontisMedia: Lausanne, Dekker, New York, 2002. (b) Moss, R. A., Platz, M. S., Jones, M., Jr., Eds.; *Reactive Intermediate Chemistry*; Wiley-Interscience: Hoboken, NJ, 2004. (c) Nucleophilic singlet vinylcarbenes react as 3-carbon units in cycloadditions with olefins; see: Boger, D. L.; Wysocki, R. J., Jr. *J. Org. Chem.* **1988**, *53*, 3408.
- (92) Sierra, M. A.; Fernández, I.; Cossío, F. P. *Chem. Commun.* **2008**, 4671.
- (93) (a) Hoffmann, R.; Zeiss, G. D.; Van Dine, G. W. *J. Am. Chem. Soc.* **1968**, *90*, 1485. (b) Davis, J. H.; Goddard, W. A., III; Bergman, R. G. *J. Am. Chem. Soc.* **1977**, *99*, 2427. (c) Sevin, A.; Arnaud-Danon, L. *J. Org. Chem.* **1981**, *46*, 2346. (d) Yoshimine, M.; Pacansky, J.; Honjou, N. *J. Am. Chem. Soc.* **1989**, *111*, 2785.
- (94) Shapiro, N. D.; Shi, Y. Toste, F. D. *J. Am. Chem. Soc.* **2009**, *131*, 11654.
- (95) Walji, A. M.; MacMillan, D. W. C. *Synlett* **2007**, 1477.
- (96) Gorin, D. J.; Dubé, P.; Toste, F. D. *J. Am. Chem. Soc.* **2006**, *128*, 14480.
- (97) (a) Reetz, M. T.; Sommer, K. *Eur. J. Org. Chem.* **2003**, 3485. (b) Shi, Z.; He, C. *J. Org. Chem.* **2004**, *69*, 3669. (c) Tarselli, M.A.; Liu, A.; Gagne, M. R. *Tetrahedron* **2009**, *65*, 1785.
- (98) Sherry, B. D.; Toste, F. D. *J. Am. Chem. Soc.* **2004**, *126*, 15978.
- (99) Sherry, B. D.; Maus, L.; Laforteza, B. N.; Toste, F. D. *J. Am. Chem. Soc.* **2006**, *128*, 8132.
- (100) Mauleón, P.; Krinsky, J. L.; Toste, F. D. *J. Am. Chem. Soc.* **2009**, *131*, 4513.
- (101) A version of this review has been published, see: Shapiro, N. D.; Toste, F. D. *Synlett* **2010**, DOI: 10.1055/s-0029-1219369.

Chapter 2 – Understanding Gold Catalysis, Part 1: π -Activation

The chemical community has recently witnessed a dramatic increase in the application of well-defined gold(I) and gold(III) complexes as homogeneous catalysts for organic synthesis. A majority of the reactions affected by these catalysts rely on nucleophilic addition to carbon-carbon multiple bonds. It has been proposed that coordination of a gold-catalyst to a C-C π -bond activates that bond towards subsequent nucleophilic attack. However, when the research reported in this chapter was initiated, structural evidence for coordination of gold complexes to alkenes and alkynes was limited. In addition, a detailed understanding of the way in which these π -bonds become activated, with regards to the orbitals involved, was somewhat devoid from the literature. We hypothesized that such an understanding could allow for improved design of new catalysts and reactions.

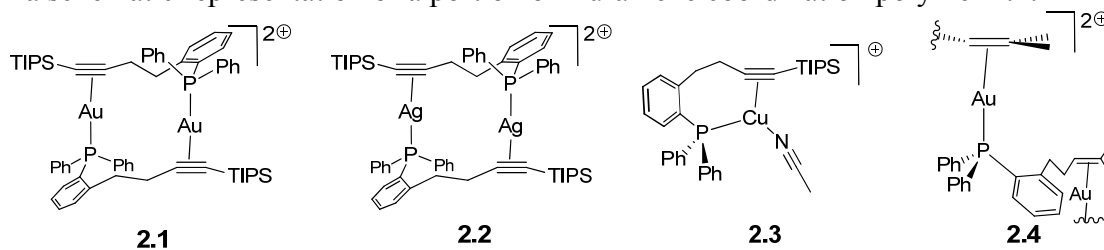
Here, we report the crystal structure of a gold(I)-phosphine η^2 -coordinated alkyne. Related Ag(I) and Cu(I) complexes have been synthesized for comparison. The crystallization of these complexes was enabled by tethering a labile alkyne ligand to a strongly coordinating triarylphosphine. This approach also proved applicable to crystallization of the first gold(I)-phosphine η^2 -coordinated alkene. A portion of the work discussed in this chapter has been published.¹

Introduction

The development of new synthetically useful methodology often rests on an understanding of the mechanistic underpinnings of the desired transformation. For example, the isolation and characterization of Zeise's salt, $K[PtCl_3(C_2H_4)]$, provided direct evidence for the ability of Pt(II) to remove electron density from ethylene, thereby rendering it susceptible to nucleophilic attack.² This insight provided the impetus for the development of numerous platinum and palladium catalyzed reactions. In contrast, homogeneous Au(I) and Au(III) complexes have only recently emerged as highly competent and selective catalysts for the activation of π -bonds.³ In light of the recent synthetic advances concerning Au(I) catalysis, a thorough understanding of the mechanistic and structural basis for these reactions has lagged behind.^{4,5}

The coordination of an alkyne to a cationic Au(I)-phosphine complex represents the prototypical mechanistic starting place for Au(I)-catalyzed reactions, despite the fact that little structural evidence exists for this assertion. In fact, prior to our investigations, there were no reported crystal structures of linear-phosphine-Au(η^2 -alkyne) complexes.⁶ Previously reported examples of Au(η^2 -alkyne)-containing compounds that have been characterized by x-ray crystallography include a gold(I)-[2]catenane containing a linear (η^1 -alkyne)-Au(η^2 -alkyne) moiety,⁷ several trigonal planar Au(I) complexes coordinated to organometallic 1,4-diyne,⁸ two trigonal planar strained cycloheptyne-Au(I) complexes,⁹ and a supramolecular complex containing a linear (η^2 -alkyne)-Au(η^2 -alkyne) moiety.¹⁰ Finally, a linear N-heterocyclic carbene-Au(η^2 -alkyne) had been characterized by NMR and IR spectroscopy.⁴ Here, we report the characterization of the 14-electron Au(I)-phosphine-(η^2 -alkyne) complex **2.1**, as well as its silver(I) and copper(I) analogues (**2.2** and **2.3**), and the cationic phosphine Au(I)-alkene complex (**2.4**) for comparison (Figure 1).^{11,12} With these structures in hand, we can begin to understand the unique ability of Au(I) complexes to serve as effective π -activation catalysts, especially in understanding why gold is often more effective than copper or silver.¹³

Figure 1. Schematic representations of the coinage metal-alkyne complexes **2.1-2.3**, together with a schematic representation of a portion of Au-alkene coordination polymer **2.4**.



Results and Discussion

Although Au(I)- π -complexes have traditionally been difficult to isolate and characterize, we hypothesized that these difficulties might be overcome by employing a tethered phosphine-alkyne ligand. To this end, reaction of alkynyl phosphine **2.5** with (dimethylsulfide) gold(I) chloride afforded the phosphinegold(I) chloride complex in 93% yield (Figure 2). This complex was converted into cationic phosphine gold(I) complex **2.1** in 98% yield by abstraction of the chloride with silver hexafluoroantimonate. Crystals of complex **2.1** were obtained when a layered CH_2Cl_2 /hexanes solution of **2.1** was allowed to stand at 0°C. The corresponding Ag(I) and Cu(I) complexes were obtained in quantitative yields by the reaction of ligand **2.5** directly

with cationic metal precursors. The structures of the complexes **2.1**–**2.3** were firmly established by x-ray crystallographic analysis (Figs. 3 and 4). In all cases, solvent molecules and counterions are completely separated from the cationic metal centers. The Au(I) and Ag(I) complexes **2.1** and **2.2** are structurally analogous dimers, both displaying pseudo-linear geometry about the metal.¹⁴ Although, the dimeric structure of **2.1** and **2.2** was unexpected, it is not surprising considering the structure of the ligand and the preferred linear Au(I)-coordination geometry. In contrast, the Cu(I) complex **3** is monomeric, with pseudo-trigonal planar geometry about copper.

Finally, a crystal structure of the first (η^2 -alkene)-Au(I)-phosphine complex **2.4** was obtained using an analogous alkene tethered phosphine ligand (Figure 5). In agreement with previous calculations, the Au(I)-alkene bond is longer than the Au(I)-alkyne bond, despite the fact that the former is calculated to be stronger.¹⁵

Figure 2. Synthesis of coinage metal alkyne complexes **2.1**–**2.3**, from alkynyl phosphine **2.5**.

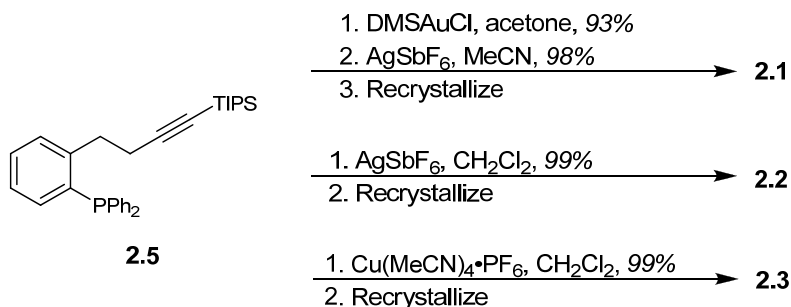


Figure 3. ORTEP-drawings of the Au- and Ag-alkyne complexes **2.1** and **2.2**, respectively, shown as 50% ellipsoids. Hydrogens, solvent, and counterions (SbF_6) omitted for clarity. For selected bond lengths and angles see Table 1.

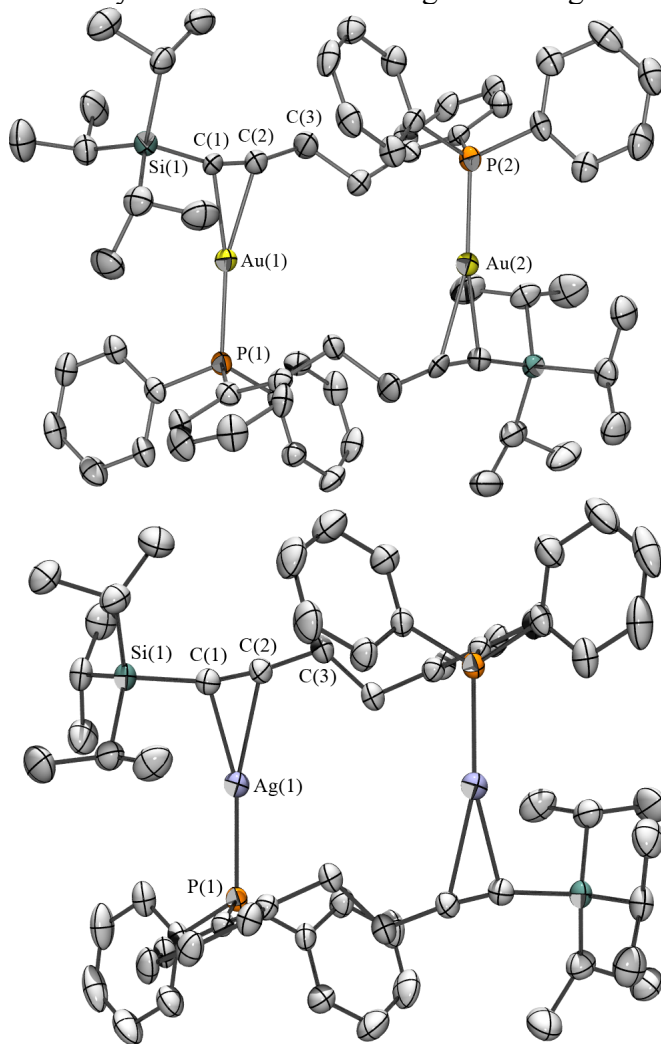


Figure 4. ORTEP-drawing of the Cu-alkyne complex **2.3**, shown as 50% ellipsoids. Hydrogens, solvent, and counterion (PF₆) omitted for clarity. For selected bond lengths and angles see Table 1.

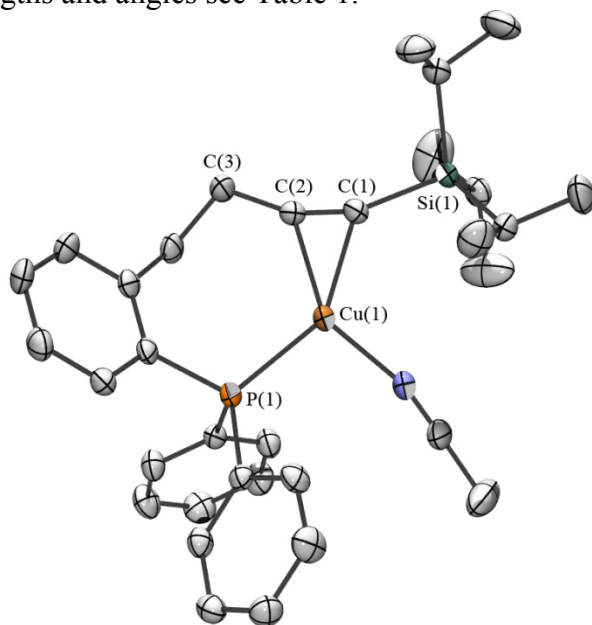
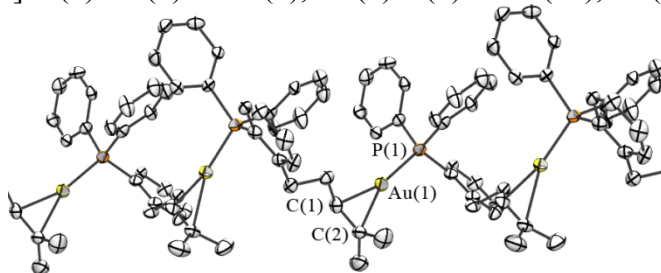


Figure 5. ORTEP-drawing of the Au-alkene complex **2.4**, shown as 50% ellipsoids. Hydrogens, solvent, and counterions (SbF₆) omitted for clarity. Selected bond lengths [Å]: P(1)-Au(1) 2.272(3), Au(1)-C(1) 2.250(10), Au(1)-C(2) 2.34(1).



A comparison of the some relevant structural features of **2.1–2.3** is given in Table 1. The Cu(I)-bound alkyne has the smallest C(1)-C(2)-C(3) and C(2)-C(1)-Si(1) angles [159.8(3)° and 159.5(2)°] and the lowest stretching frequency (2,020 cm⁻¹). In contrast, the Au(I)- and Ag(I)-bound alkynes exhibit significantly less distortion from linearity [C(1)-C(2)-C(3) angles of 167.2(6)° and 172.9(3)°, respectively]. The observed deviations of the alkyne from linearity correspond well to a decrease in the bond's stretching frequency. It is also important to note that in both the Au(I) and Ag(I) complexes (**2.1** and **2.2**), the metal center is significantly “slipped” to one side of the π -bond. Previous research suggests that such $\eta^2 \rightarrow \eta^1$ migration should accompany an increase in ligand electrophilicity.¹⁶ In contrast, the Cu-alkyne complex is highly symmetrical [2.029(2) vs. 2.024(2) Å], although this may be a result of the altered geometry and electron count of this complex.

Table 1. Selected bond lengths (Å), bond angles (°), and IR stretching frequencies (cm⁻¹) – experimental and calculated.

Entry ^a	Parameter	2.1 (M = Au) ^b	2.2 (M = Ag)	2.3 (M = Cu)
1a	d C(1)-C(2)	1.221(8)	1.211(4)	1.229(4)
1b		1.258	1.252	1.265
2a	∠C(1)-C(2)-C(3)	167.2(6)	172.9(3)	159.8(3)
2b		171.0	173.6	158.9
3a	∠Si(1)-C(1)-C(2)	164.4(5)	165.3(3)	159.5(2)
3b		160.0	160.8	161.3
4a	νC(1)≡C(2) ^c	2053	2095	2020
4b		2068	2100	2014
5a	d M(1)-C(1)	2.197(5)	2.294(3)	2.029(2)
5b		2.249	2.292	2.077
6a	d M(1)-C(2)	2.270(5)	2.445(3)	2.024(2)
6b		2.386	2.493	2.070
7a	d P(1)-M(1)	2.271(1)	2.3934(8)	2.2571(7)
7b		2.337	2.431	2.338

^a Experimental values (a), calculated values (b). ^b Data from one half of the unsymmetrical Au-dimer is shown. ^c The ν_{C(1)≡C(2)} of the free ligand is 2171 cm⁻¹.

Experimentally, we have observed that Au(I) complexes are generally superior π-activation catalysts, especially when compared with analogous Cu(I) and Ag(I) complexes. Intuitively, the superior catalytic activity of Au(I) in these reactions suggests that Au(I)-coordinated π-bonds are more activated toward nucleophilic attack than π-bonds that are coordinated to Ag(I) or Cu(I). Under the Dewar–Chatt–Duncanson bonding model, this further suggests increased π-to-metal σ-donation to gold and/or decreased metal-to-π* back-donation from gold.¹⁷ Therefore, we sought to compare the relative importance of these two types of bonding for complexes **2.1–2.3**. The situation is complicated by the fact that both π-to-metal σ-donation and metal-to-π* back-bonding elongate and distort a coordinated π-bond. As a result, one cannot directly correlate the degree of alkyne distortion with the degree of metal-to-π* back-donation. To circumvent this problem, we turned to DFT calculations.¹⁸

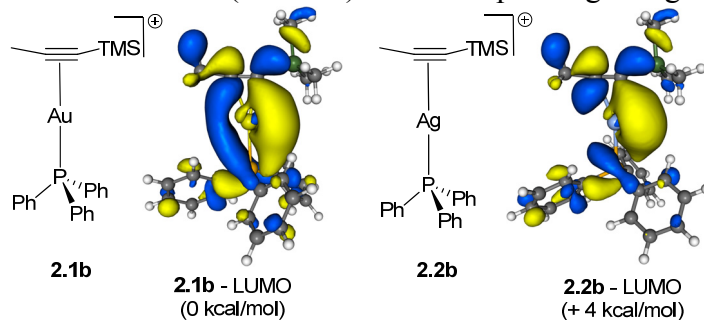
Table 2. Natural Bond Order orbital interaction energies (kcal/mol).

Parameter	2.1b (M = Au)	2.2b (M = Ag)	2.3b (M = Cu)
π → M	56.6	38.5	46.9
M → π*	13.3	6.4	12.0
difference	43.3	32.1	34.9

Beginning with the crystal structure of Au(I) complex **2.1**, we initially simplified the structure to monomeric triphenylphosphine-metal-alkyne complex **2.1b** (Figure 6). The experimental geometric features were well produced with the B3PW91 / LANL2DZ(Au), LANL2DZdp(Si,P), ccpVDZ(C,H) level of theory (Table 1). Importantly, this indicates that the geometry of the metal center in **2.1** is not significantly influenced by the constraints of crystallization. The structures of **2.2** and **2.3** were trimmed and optimized similarly; the experimental and calculated values are compared in Table 1. The same structural trends were

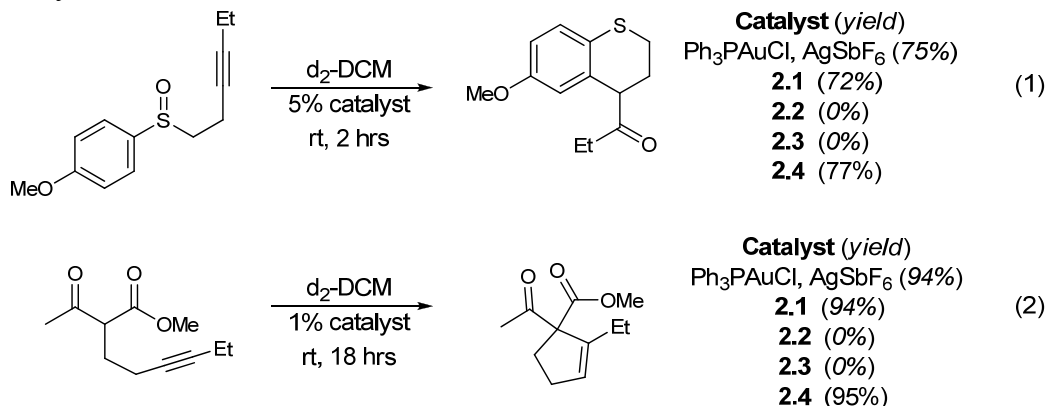
observed in both the calculated and experimental geometries. With these optimized geometries in hand, we turned to natural bond order calculations to investigate the nature of the metal-alkyne bond (Table 2).^{15a,18} Second-order perturbative analysis revealed that π -to-metal σ -donation is of the largest magnitude for Au (56.6 kcal/mol), as is metal-to- π^* back-donation (13.3 kcal/mol). For all three metals, σ -donation to the metal dominates, augmenting the electrophilicity of the alkyne, although the difference of the two bonding interactions is the largest for Au. These calculations also provide further insight into the observed distortion of the Cu(I)-bound alkyne. Noting that the calculated Cu-alkyne orbital interaction energies underestimate the degree of distortion suggests that some of the distortion of the Cu-bound alkyne may be due to geometrical constraints of that system.

Figure 6. Structures of **2.1b** and **2.2b** along with the calculated lowest unoccupied molecular orbitals (LUMOs) and corresponding energies.



In addition to NBO analysis, we also examined the frontier molecular orbitals of **2.1b** and **2.2b** (Figure 6).¹⁹ As expected, the lowest unoccupied molecular orbitals (LUMOs) contain the π^* -metal interaction. Furthermore, the LUMO of **2.1b** was calculated to be 4 kcal/mol lower in energy than the LUMO of **2.2b**. Although the energies of unoccupied orbitals must be considered with caution, this result is again qualitatively in agreement with Au(I) being a superior π -activation catalyst.

Figure 7. Reactivity of coinage metal complexes **2.1-2.4** in typical gold(I)-catalyzed reactions.

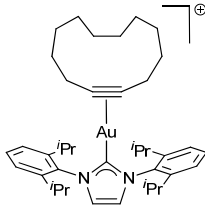
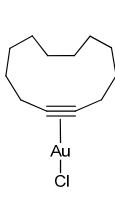
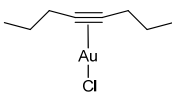
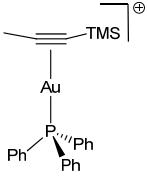


In agreement with the above claims, we have also found that complexes **2.1** and **2.4** are active in typical gold(I)-catalyzed reactions, whereas **2.2** and **2.3** are not (Figure 7).²⁰ It is worth mentioning that phosphine-Au(I)-chloride complexes (16-electron complexes upon alkyne coordination) are typically much less catalytically active than their cationic congeners. Thus,

Ph₃PAuCl is typically activated by addition of a silver salt (such as AgSbF₆), which serves to remove the chloride ligand and replace it with a less coordinating counteranion. Complexes **2.1** and **2.2** represent 14-electron Au(I) and Ag(I) complexes, whereas similar crystallization conditions result in 16-electron Cu(I) complex **2.3**. Furthermore, the observation that the alkene complex **2.4** is also catalytically active supports the assumption that coordination of cationic gold(I) complexes to π -bonds is reversible and that the observed selectivity for alkynes in many gold-catalyzed reactions does not arise as a result of preferred bonding to the alkyne.

Since our report, several other researchers have published similar reports and a comparison is of some interest.⁶ Fürstner and coworkers have reported cationic and neutral cyclododecyne complexes **2.6** and **2.7**, and Dias has reported neutral 3-hexyne complex **2.8** (Table 3).²¹ In addition, several Au-alkene complexes have been isolated.²²

Table 3. Calculated Natural Bond Order orbital interaction energies (kcal/mol) and Au-alkyne bond lengths (Å) from this and other reports.²¹

				
	2.6	2.7	2.8	2.1b
$\pi \rightarrow M$	77.4	100.1	76.2	56.6
$M \rightarrow \pi^*$	19.8	27.2	26.5	13.3
Difference	57.6	72.9	49.7	43.3
Au – alkyne (centroid) bond length	2.142	2.062	2.129	2.231

In comparison to complex **2.1b**, all three complexes **2.6-2.8** have noticeably shorter Au-alkyne bond distances. A comparison of **2.1b** and **2.6** is particularly telling. *N*-heterocyclic carbene ligands are considered to be strong σ -donors and weak π -acceptors, while phosphines are moderate σ -donors and moderate π -acceptors (in other words, NHCs are higher trans effect ligands than PR₃).²³ Thus, for a given set of alkyne-gold-ligand complexes, one would expect a decrease in the alkyne-gold bond distance in going from an NHC to a phosphine ligand. The fact that this trend is not observed on going from **2.1b** (Au-alkyne bond length of 2.231 Å) to **2.6** (2.142 Å) suggests that TMS-propyne is a weaker ligand than cyclododecyne. This is reflected in the lower calculated natural bond order interaction energies for complex **2.1b**.

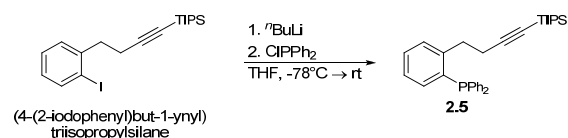
Conclusions

In summary, we have isolated and characterized, by x-ray crystallography, linear (η^2 -alkyne)- and (η^2 -alkene)-Au(I)-phosphine complexes. The isolation of these complexes was enabled by covalently linking kinetically labile alkenes and alkynes to triphenylphosphine. The success of this approach suggests that a similar approach could enable the isolation of other important reactive intermediates. Furthermore, the comparison of complexes **2.1-2.4** has provided an explanation for the superior activity of gold(I)-complexes in reactions that involve electrophilic π -activation.

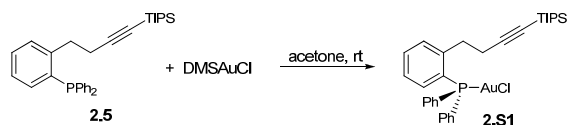
Supporting Information

General Information. Unless otherwise noted, all reagents were obtained commercially and used without further purification. Glassware was dried in an oven at 130 °C prior to use. Dichloromethane (CH₂Cl₂) was obtained from EMD. Silver hexafluoroantimonate (AgSbF₆) was obtained from the Aldrich Chemical Company. Triphenylphosphine-gold(I)chloride (Ph₃PAuCl) was prepared according to the method of Bruce.²⁴ Organic extracts were dried with anhydrous MgSO₄ and solvents were removed with a rotary evaporator. TLC analysis was carried out on Merck silica gel 60 F₂₅₄ TLC plates. Column chromatography was performed using Merck 60 silica gel (32-63 μm). ¹H and ¹³C NMR spectra were recorded with Bruker DRX-500, AVB-400, AVQ-400, and AV-300 spectrometers and referenced to CDCl₃, CD₃CN, or CD₂Cl₂. FT-IR spectra were recorded on NaCl plates with a Nicolet MAGNA-IR 850 spectrometer. Mass spectra and analytical data were obtained from the Micro-Mass/Analytical Facility operated by the College of Chemistry, University of California, Berkeley. X-ray structure acquisition and analysis were performed by Dr. Frederick J. Hollander of the University of California, Berkeley College of Chemistry X-ray crystallographic facility with the exception of compound **2.4**, for which the data was acquired by Henry S. La Pierre. Density functional calculations were performed by using the B3PW91 functional as implemented in Gaussian 03.²⁵ For Cu, Ag, and Au we used the LANL2DZ basis set, for P and Si we used the LANL2DZdp basis set, for all other atoms we used the cc-pVDZ basis set.²⁶ Optimized structures were further analyzed using the Natural Bond Order (NBO) technique.²⁷

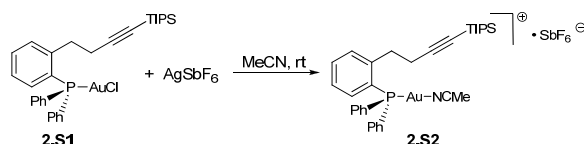
Experimental details and spectroscopic data



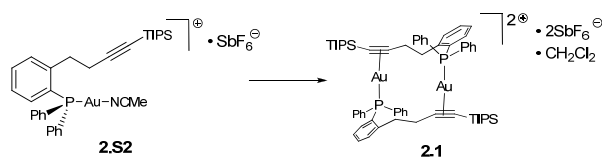
To a stirred solution of (4-(2-iodophenyl)but-1-ynyl)triisopropylsilane²⁸ (1.43 g, 3.47 mmol) in THF at -78°C, was slowly added ⁿBuLi (2.5 M in hexanes, 1.39 mL, 3.47 mmol). The resulting solution was stirred for 30 minutes at -78°C, followed by dropwise addition of chlorodiphenylphosphine (0.68 ml, 3.8 mmol). After stirring for 20 minutes, the solution was slowly warmed to room temperature and quenched with saturated aqueous NH₄Cl. The aqueous layer was extracted twice with Et₂O, dried, filtered and concentrated. Flash column chromatography (5% DCM in hexanes) of the resulting oil provided **2.5** as a white solid (880 mg, 54% yield), mp 60 - 62°C. IR: 2171, 1587, 1465, 1434, 883 cm⁻¹. ¹H NMR (400 MHz, CDCl₃) δ 7.42-7.32 (m, 12H), 7.16 (t, 1H, *J* = 7.4 Hz), 6.96-6.92 (m, 1H), 3.16 (t, 2H, *J* = 7.0 Hz), 2.53 (t, 2H, *J* = 7.0 Hz), 1.13-1.02 (m, 21H). ¹³C NMR (100 MHz, CDCl₃) δ 145.2 (d, *J* = 26 Hz), 137.0 (d, *J* = 11 Hz), 135.7 (d, *J* = 13 Hz), 134.1 (d, *J* = 20 Hz), 133.8, 130.0 (d, *J* = 5 Hz), 129.1, 128.9, 128.7 (d, *J* = 7 Hz), 126.8, 108.4, 81.2, 34.0 (d, *J* = 21 Hz), 21.5 (d, *J* = 4 Hz), 18.8, 11.5. ³¹P NMR (162 MHz, CDCl₃) δ -15.71. HRMS (FAB) calc. for [C₃₁H₃₉PSi + H]⁺ 471.2637, found 471.2639.



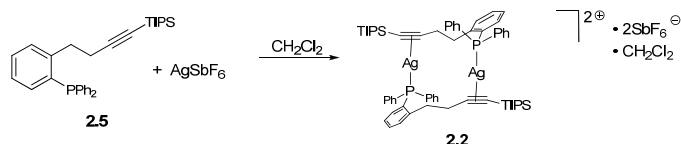
To a vigorously stirred suspension of Me_2SAuCl (99 mg, 0.34 mmol) in acetone (0.5 mL) at room temperature, was slowly added a solution of **2.5** (158 mg, 0.34 mmol) in 2 mL acetone. After stirring for 10 minutes, the solution was concentrated to 0.5 mL, filtered through celite, eluting with an addition 0.5 mL acetone. Subsequent concentration *in vacuo* provided **2.S1** as white solid (220 mg, 93% yield). IR: 2172, 1464, 1437, 1102, 883 cm^{-1} . ^1H NMR (400 MHz, d_3 -MeCN) δ 7.63-7.53 (m, 12H), 7.26-7.22 (m, 1H), 6.83-6.77 (m, 1H), 3.13 (t, 2H, $J = 7.4$ Hz), 2.44 (t, 2H, $J = 7.4$ Hz), 1.10-0.90 (m, 21H). ^{13}C NMR (100 MHz, d_3 -MeCN) δ 144.7 (d, $J = 12$ Hz), 135.4 (d, $J = 14$ Hz), 134.2 (d, $J = 8$ Hz), 133.3, 132.9, 132.0 (d, $J = 9$ Hz), 130.6 (d, $J = 12$ Hz), 129.2 (d, $J = 63$ Hz), 128.0 (d, $J = 11$ Hz), 127.5 (d, $J = 60$ Hz), 108.5, 82.6, 34.4 (d, $J = 12$ Hz), 21.0, 19.0, 12.0. ^{31}P NMR (162 MHz, d_3 -MeCN) δ 25.74. HRMS (FAB) calc. for $[\text{C}_{31}\text{H}_{39}\text{PSiAu}]^+$ 667.2224, found 667.2211.



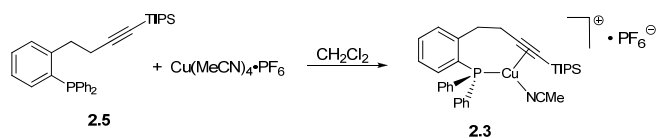
To a solution of **2.S1** (37 mg, 0.053 mmol) in d_3 -acetonitrile (0.4 mL) was added AgSbF_6 (18 mg, 0.053 mmol). Silver chloride precipitated immediately, providing a solution of **2.S2**. ^1H NMR (400 MHz, d_3 -MeCN) δ 7.64-7.51 (m, 12H), 7.27-7.22 (m, 1H), 6.80 (dd, 1H, $J = 13.4, 7.8$ Hz), 3.12 (t, 2H, $J = 7.3$ Hz), 2.51 (t, 2H, $J = 7.3$ Hz), 1.08-0.92 (m, 21H). ^{13}C NMR (100 MHz, d_3 -MeCN) δ 144.5 (d, $J = 12$ Hz), 135.3 (d, $J = 14$ Hz), 134.2 (d, $J = 9$ Hz), 133.5 (d, $J = 2$ Hz), 133.2, 131.8 (d, $J = 9$ Hz), 130.6 (d, $J = 12$ Hz), 128.4 (d, $J = 67$ Hz), 128.1 (d, $J = 10$ Hz), 126.8 (d, $J = 62$ Hz), 108.9, 82.5, 34.3 (d, $J = 12$ Hz), 21.1, 19.0, 11.9. ^{31}P NMR (162 MHz, d_3 -MeCN) δ 24.44.



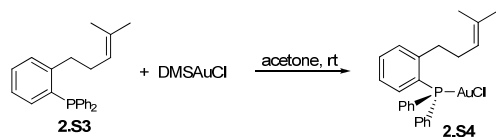
The solution of **2.S2** was filtered through celite and concentrated. The resulting solid (49mg, 98% yield) was dissolved in DCM, and again filtered through celite. X-ray quality crystals were grown by layering the resulting solution with hexanes. IR: 2053, 1472, 1439, 1102, 883, cm^{-1} . Attempted NMR analysis of the crystals was hampered by broad signals and instability of the sample to disproportionation. ^1H NMR (400 MHz, CDCl_3) δ 7.64-7.50 (m, 12H), 7.32 (m, 1H), 6.89 (m, 1H), 3.4-3.1 (m, 4H), 1.20-0.90 (m, 21H). ^{31}P NMR (162 MHz, CDCl_3) δ 29.3. HRMS (FAB) calc. for $[\text{C}_{31}\text{H}_{39}\text{PSiAu}]^+$ 667.2224, found 667.2218. X-ray data: $\text{C}_{31.5}\text{H}_{40}\text{F}_6\text{SiP}_2\text{ClSbAu}$, $M_r = 945.88$, triclinic, space group P1 (#2); $a = 13.963(2)$, $b = 14.920(2)$, $c = 18.703(2)$ Å, $\alpha = 69.422(1)$, $\beta = 77.264(2)$, $\gamma = 75.161(2)^\circ$, $V = 3489.2(7)$ Å³, $Z = 4$; $\rho_{\text{calcd}} = 1.80$ g/cm³, μ (Mo-K α) = 51.97 cm^{-1} , Mo-K α radiation ($\lambda = 0.71069$ Å), 153 K, $2\theta_{\text{max}} = 52.0^\circ$, 9559 unique reflections of 31450 measured, $R_{\text{int}} = 0.028$, $R = 0.032$, $R_w = 0.035$. Crystal dimensions: 0.08 x 0.08 x 0.17 mm.



A vial was charged with **2.5** (23 mg, 0.049 mmol), AgSbF₆ (17 mg, 0.049 mmol), and CH₂Cl₂ (0.5 mL). After stirring for 10 minutes, the solution was concentrated to yield a white solid (42 mg, *quantitative*). ¹H NMR (400 MHz) δ 7.63-7.40 (m, 12H), 7.32 (t, 1H, *J* = 7.4 Hz), 6.92 (m, 1H), 3.06 (m, 2H), 2.99 (m, 2H), 1.15-0.85 (m, 21H). ³¹P NMR (162 MHz) δ 7.54 (major peak). X-ray quality crystals were grown by layering the DCM solution successively with diethyl ether and hexanes. IR: 2095, 1468, 1438, 1099, 883 cm⁻¹. HRMS (FAB) calc. for [C₃₁H₃₉PSiAg]⁺ 577.1610, found 577.1601. X-ray data: C_{31.5}H₄₀F₆SiP₂ClSbAg, *M_r* = 856.78, triclinic, space group P1 (#2); *a* = 11.677(1), *b* = 11.787(1), *c* = 13.811(2) Å, α = 80.684(1), β = 71.843(1), γ = 83.029(1)°, *V* = 1777.2(3) Å³, *Z* = 2; ρ_{calcd} = 1.60 g/cm³, μ (Mo-Kα) = 15.14 cm⁻¹, Mo-Kα radiation (λ = 0.71069 Å), 175 K, 2θ_{max} = 49.4°, 4830 unique reflections of 12872 measured, *R_{int}* = 0.011, *R* = 0.027, *R_w* = 0.037. Crystal dimensions: 0.25 x 0.26 x 0.30 mm.

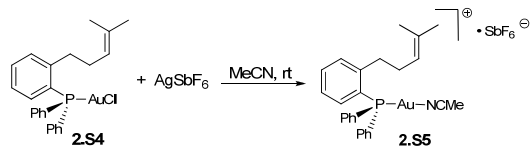


In a N₂ glove box, a vial was charged with **2.5** (30 mg, 0.064 mmol), (MeCN)₄CuPF₆ (24mg, 0.064 mmol), and CH₂Cl₂ (0.6 mL). The solution was stirred for one hour, after which point it was concentrated to provide **2.3** as a white solid (53 mg, *quantitative*). ¹H NMR (500 MHz, CD₂Cl₂) δ 7.62-7.48 (m, 7H), 7.38-7.32 (m, 5H), 7.26 (t, 1H, *J* = 7.5 Hz), 6.84 (t, 1H, *J* = 8.8 Hz), 3.11-3.07 (m, 2H), 2.90-2.87 (m, 2H), 2.06 (s, 3H), 1.23 (septet, 3H, *J* = 7.5 Hz), 1.09 (d, 18H, *J* = 7.5 Hz). ¹³C NMR (125 MHz, CD₂Cl₂) δ 145.2 (d, *J* = 18 Hz), 134.2 (d, *J* = 14 Hz), 133.6 (d, *J* = 4 Hz), 132.7, 132.1 (d, *J* = 3 Hz), 131.9 (d, *J* = 9 Hz), 130.2 (d, *J* = 10 Hz), 128.9 (d, *J* = 18 Hz), 128.7 (d, *J* = 40 Hz), 128.3 (d, *J* = 6 Hz), 120.3, 117.0, 89.9 (d, *J* = 4Hz), 33.3 (d, *J* = 10 Hz), 23.2 (d, *J* = 5 Hz), 19.0, 12.2, 2.5. ³¹P NMR (202 MHz, CD₂Cl₂) δ -4.73 (bs). HRMS (FAB) calc. for [C₃₁H₃₉PSiCu]⁺ 533.1855, found 533.1853. X-ray quality crystals were grown from a solution of **3** in toluene/CH₂Cl₂ layered with hexanes at 0°C. IR: 2020, 1465, 1436, 841. X-ray data: C₃₃H₄₂F₆SiP₂Cu, *M_r* = 720.27, triclinic, space group P1 (#2); *a* = 12.057(1), *b* = 12.899(1), *c* = 13.157(1) Å, α = 70.502(1), β = 67.822(1), γ = 69.927(1)°, *V* = 1729.8(3) Å³, *Z* = 2; ρ_{calcd} = 1.38 g/cm³, μ (Mo-Kα) = 8.14 cm⁻¹, Mo-Kα radiation (λ = 0.71069 Å), 168 K, 2θ_{max} = 52.7°, 5225 unique reflections of 15938 measured, *R_{int}* = 0.021, *R* = 0.036, *R_w* = 0.046. Crystal dimensions: 0.27 x 0.26 x 0.08 mm.

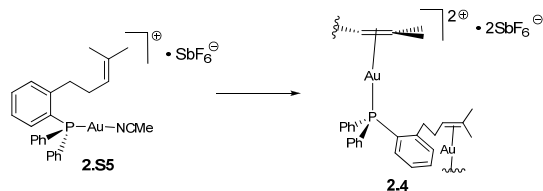


To a vigorously stirred suspension of Me₂SAuCl (58 mg, 0.20 mmol) in acetone (0.5 mL) at room temperature, was slowly added a solution of **2.53** (66 mg, 0.20 mmol) in 1 mL acetone. After stirring for 10 minutes, the solution was concentrated to 0.5 mL, filtered through celite, eluting with an addition 0.5 mL acetone. Subsequent concentration *in vacuo* provided **2.54** as white solid (105 mg, 94% yield), IR: 3054, 1589, 1480, 1437, 1102, 749 cm⁻¹. ¹H NMR (500 MHz, d₃-MeCN) δ 7.60-7.46 (m, 12H), 7.21 (t, 1H, *J* = 7.5 Hz), 6.78-6.73 (m, 1H), 5.02 (t, 1H, *J* = 6.8 Hz), 2.91 (t, 2H, *J* = 7.8 Hz), 2.24-2.17 (m, 2H), 1.58 (s, 3H), 1.43 (s, 3H). ¹³C NMR (125

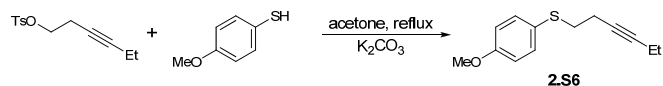
MHz, d_3 -MeCN) δ 147.2 (d, $J = 13$ Hz), 135.8 (d, $J = 14$ Hz), 135.4 (d, $J = 14$ Hz), 134.5 (d, $J = 9$ Hz), 134.1, 133.7 (d, $J = 3$ Hz), 132.3 (d, $J = 9$ Hz), 131.0 (d, $J = 13$ Hz), 129.9 (d, $J = 63$ Hz), 128.0 (d, $J = 10$ Hz), 127.5 (d, $J = 60$ Hz), 124.3, 35.9 (d, $J = 13$ Hz), 30.6, 26.2, 18.4. ^{31}P NMR (162 MHz, d_3 -MeCN) δ 24.40.



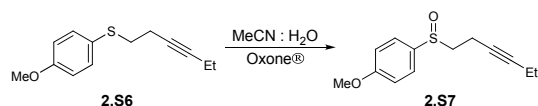
To a solution of **2.S4** (37 mg, 0.053 mmol) in d_3 -acetonitrile (0.4 mL) was added AgSbF_6 (18 mg, 0.053 mmol). Silver chloride precipitated immediately, providing a solution of **2.S5**. ^1H NMR (500 MHz, d_3 -MeCN) δ 7.62-7.48 (m, 12H), 7.23 (t, 1H, $J = 7.3$ Hz), 6.80-6.75 (m, 1H), 5.03 (t, 1H, $J = 6.8$ Hz), 2.91 (t, 2H, $J = 7.9$ Hz), 2.23-2.17 (m, 2H), 1.60 (s, 3H), 1.45 (s, 3H). ^{13}C NMR (125 MHz, d_3 -MeCN) δ 147.3 (d, $J = 11$ Hz), 135.8 (d, $J = 15$ Hz), 135.4 (d, $J = 13$ Hz), 134.6 (d, $J = 9$ Hz), 134.2, 133.9, 132.3 (d, $J = 10$ Hz), 131.0 (d, $J = 11$ Hz), 129.4 (d, $J = 65$ Hz), 128.1 (d, $J = 10$ Hz), 124.0, 35.9 (d, $J = 13$ Hz), 30.5, 26.2, 18.4 (1 carbon missing). ^{31}P NMR (162 MHz, d_3 -MeCN) δ 23.17.



The solution of **2.S5** was filtered through celite and concentrated. The resulting solid was dissolved in DCM, and again filtered through celite. X-ray quality crystals of **2.4** were grown by layering the resulting solution with diethyl ether and hexanes. IR: 1489, 1436, 1206, 1100 cm^{-1} . HRMS (FAB) calc. for $[\text{C}_{24}\text{H}_{25}\text{PAu}]^+$ 541.1359, found 541.1362. X-ray data: $\text{C}_{24}\text{H}_{25}\text{F}_6\text{PSbAu}$, $M_r = 777.14$, triclinic, centric space group $\text{P}2_1/c$; $a = 15.049(4)$, $b = 14.392(4)$, $c = 13.211(4)$ Å, $\beta = 112.718(4)^\circ$, $V = 2639(1)$ Å³, $Z = 4$; $\rho_{\text{calcd}} = 1.956$ g/cm^3 , μ (Mo- $\text{K}\alpha$) = 67.06 cm^{-1} , Mo- $\text{K}\alpha$ radiation ($\lambda = 0.71069$ Å), 112 K, $2\theta_{\text{max}} = 49.4^\circ$, 2439 unique reflections of 11804 measured, $R_{\text{int}} = 0.034$, $R = 0.040$, $R_w = 0.038$. Crystal dimensions: 0.03 x 0.05 x 0.12 mm.

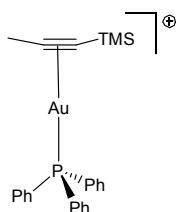


A solution of hex-3-ynyl *p*-toluenesulfonate (1.47 g, 6.21 mmol), 4-methoxybenzenethiol (802 μL , 6.51 mmol), and potassium carbonate (1.03 g, 7.45 mmol) in 25 mL acetone was refluxed for 3 hours. The resulting solution was filtered through celite and concentrated to yield **S6** as faint yellow oil, which was carried on without further purification (1.37 g, quantitative). ^1H NMR (400 MHz) δ 7.40-7.35 (m, 2H), 6.86-6.82 (m, 2H), 3.79 (s, 3H), 2.91 (t, 2H, $J = 7.6$ Hz), 2.38 (td, 2H, $J = 7.6, 2.4$ Hz), 2.14 (qt, 2H, $J = 7.6, 2.4$ Hz), 1.10 (t, 3H, $J = 7.6$ Hz). ^{13}C NMR (100 MHz) δ 159.3, 134.0, 132.8, 125.8, 114.7, 83.1, 77.6, 55.5, 35.5, 20.0, 14.3, 12.6. HRMS (EI) calc. for $[\text{C}_{13}\text{H}_{16}\text{OS}]^+$ 220.0922, found 220.0923.



To a solution of crude **2.S6** (1.2 g, 5.4 mmol) in 15 mL 1 : 1 acetonitrile : water at 0 °C was added Oxone® (2.3 g, 3.8 mmol). After stirring for 20 minutes, the reaction was warmed to room temperature and stirred until complete consumption of starting material, determined by TLC analysis (2 hours). The reaction was quenched with 50 mL brine and extracted with ether (3 x 50 mL). The combined etherous layers were dried and concentrated. Flash column chromatography (30% ethyl acetate in hexanes) provided **2.S7** as a colorless oil (1.1 g, 89% yield). IR: 2974, 1595, 1497, 1252, 1088 cm⁻¹. ¹H NMR (400 MHz) δ 7.55 (d, 2H, *J* = 8.8 Hz), 7.01 (d, 2H, *J* = 8.8 Hz), 3.83 (s, 3H), 2.94-2.84 (m, 2H), 2.63-2.55 (m, 1H), 2.39-2.32 (m, 1H), 2.11 (qt, 2H, *J* = 7.4, 2.4 Hz), 1.07 (t, 3H, *J* = 7.4 Hz). ¹³C NMR (100 MHz) δ 162.2, 134.3, 126.2, 115.0, 84.2, 75.9, 56.4, 55.7, 14.2, 12.8, 12.6. Anal Calcd. For C₁₃H₁₆O₂S: C, 66.07. H, 6.82. Found: C, 65.72. H, 7.02.

Computational results

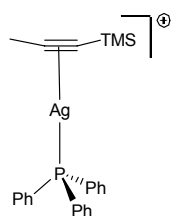


Complex 2.1b

E(RB-PW91) = -1076.54875174

Au	0.931342	0.618188	0.014273	H	-1.547697	2.658194	0.871514
P	-1.285852	-0.119212	0.002741	H	4.186012	-0.844239	2.538664
Si	4.286851	-0.649035	0.045138	H	2.776542	-2.080634	-1.349480
C	-1.856141	-0.671170	1.664580	H	6.750947	-0.813984	-0.085406
C	-0.957516	-1.358955	2.508812	H	6.175508	0.588394	-1.040245
C	-1.385841	-1.814278	3.763682	H	6.277612	0.697881	0.750891
C	-2.705764	-1.579649	4.184501	H	4.481096	-2.619071	-1.444601
C	-3.599587	-0.891817	3.348342	H	3.947737	-1.184630	-2.374779
C	-3.181617	-0.436634	2.087965	H	4.695673	-2.379260	1.769340
C	-2.421971	1.232035	-0.532459	H	2.968833	-1.912931	1.762082
C	-2.308992	2.492768	0.095562	H	2.055326	3.843463	-0.964889
C	-3.176827	3.532732	-0.263673	H	2.109401	3.905767	0.834172
C	-4.152976	3.325734	-1.254000	H	3.625756	4.012524	-0.116396
C	-4.262909	2.075558	-1.881615	H	-0.269861	-0.577976	-2.704259
C	-3.402080	1.024503	-1.524283	H	-0.574345	-2.431071	-4.345402
C	-1.499957	-1.525478	-1.168486	H	-1.957556	-4.431741	-3.741469
C	-2.279023	-2.650589	-0.828413	H	-3.043093	-4.568467	-1.488553
C	-2.438734	-3.691830	-1.757113	H	-2.755836	-2.718981	0.158049
C	-1.830092	-3.614145	-3.019522	H	0.078095	-1.535347	2.185624
C	-1.053513	-2.492976	-3.359288	H	-0.683700	-2.346852	4.418703

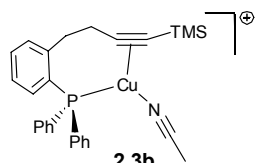
C	-0.881636	-1.451544	-2.436798	H	-3.036748	-1.929833	5.171284
C	2.627021	3.533049	-0.069967	H	-4.630053	-0.703684	3.677902
C	2.812868	2.084334	-0.025082	H	-3.883336	0.107089	1.441859
C	3.165293	0.876787	0.009006	H	-3.495331	0.049614	-2.020235
C	3.823722	-1.726425	-1.416930	H	-5.024379	1.911278	-2.655602
C	4.000771	-1.519550	1.680883	H	-4.828553	4.143742	-1.537360
C	6.030012	0.028948	-0.095937	H	-3.089245	4.510102	0.229362



Complex 2.2b **2.2b**

E(RB-PW91) = -1086.82644978

P	1.194166	-0.046553	-0.004791	H	4.176247	-1.758395	-3.660793
Ag	-1.130961	0.658409	-0.066176	H	2.576109	-3.555534	-4.356498
Si	-4.453975	-0.563513	-0.032818	H	0.386971	-3.811068	-3.164245
C	3.216762	-1.874263	-3.139265	H	-2.368026	3.996308	-0.998075
C	2.320136	-2.881827	-3.527958	H	-6.539449	0.701754	-0.592659
C	1.091687	-3.025442	-2.860742	H	-6.323580	0.569487	1.186042
C	1.661243	-1.148474	-1.412082	H	-6.897785	-0.842464	0.243047
C	2.893996	-1.007268	-2.082810	H	-3.853473	4.162596	-0.012182
C	0.758573	-2.159098	-1.810122	H	-4.523836	-0.745057	-2.527563
C	2.345734	1.399048	-0.066540	H	-3.187550	-1.736192	-1.858009
C	3.423650	1.525786	0.832947	H	-4.876444	-2.313378	-1.737982
C	4.278094	2.637301	0.746667	H	-3.937316	-1.104601	2.356042
C	4.066201	3.618836	-0.233651	H	-4.492038	-2.547427	1.454273
C	2.992480	3.494384	-1.132355	H	-2.812870	-1.968606	1.255414
C	2.128802	2.393438	-1.046743	H	0.880807	-0.797089	4.906544
C	1.577245	-0.969505	1.549571	H	2.343231	-2.832340	4.902562
C	2.401023	-2.114382	1.549006	H	3.310734	-3.672428	2.750279
C	2.671612	-2.779373	2.755935	H	2.826055	-2.491282	0.609430
C	2.129800	-2.307506	3.961861	H	0.378232	0.386568	2.771607
C	1.308918	-1.166915	3.965296	H	3.595641	0.761255	1.601666
C	1.026253	-0.502512	2.763592	H	5.115374	2.732299	1.450912
C	-2.866748	3.659925	-0.069133	H	4.737078	4.485873	-0.297536
C	-3.078828	2.214777	-0.061151	H	2.824183	4.260688	-1.900897
C	-3.397210	1.004183	-0.054504	H	1.289918	2.302503	-1.752644
C	-6.213639	0.030399	0.225243	H	-2.266796	3.992860	0.799125
C	-3.861927	-1.637208	1.387912	H	3.598787	-0.218889	-1.787582
C	-4.233275	-1.411123	-1.691919	H	-0.205362	-2.274294	-1.293020



Complex 2.3b

E(RB-PW91) = -1308.14828879

Cu	1.147527	0.105302	0.206278	H	1.671509	-3.618348	1.272701
P	-1.179490	-0.978600	0.010542	H	-0.192479	1.165238	-2.464855
Si	4.641085	-0.394414	-0.011335	H	5.466838	-2.521898	-1.047962
N	1.601710	2.062846	0.299839	H	4.386882	1.462938	1.659566
C	-1.804064	1.405773	-1.011607	H	5.641425	-2.565641	0.738329
C	-1.082933	1.744669	-2.179212	H	6.791445	-1.613662	-0.252758
C	-1.506403	2.808809	-2.988366	H	4.953958	-0.045244	2.445154
C	-2.641278	3.557121	-2.635100	H	6.095215	0.949292	1.489238
C	-3.352354	3.233854	-1.463797	H	5.789960	1.030129	-1.692927
C	-2.940296	2.160536	-0.655717	H	4.085782	1.548337	-1.513600
C	-2.134675	0.041092	1.595078	H	4.477166	0.085600	-2.460786
C	-1.582133	0.742291	2.689188	H	2.839937	4.968860	-0.053539
C	-2.279478	0.817730	3.904046	H	1.890307	4.997880	1.476581
C	-3.526736	0.185812	4.038898	H	1.047744	5.161907	-0.107807
C	-4.076289	-0.521359	2.956918	H	-0.947907	3.055149	-3.901730
C	-3.386142	-0.596545	1.736679	H	-2.971427	4.392330	-3.262324
C	-1.728101	-1.541360	-0.883466	H	-4.239707	3.815712	-1.179826
C	-2.574596	-1.446503	-2.926400	H	-3.505099	1.913439	0.252875
C	-2.947758	-2.592713	-2.725885	H	-3.818302	-1.158848	0.897703
C	-2.478881	-3.848831	-2.316739	H	-5.048765	-1.021032	3.061958
C	-1.647770	-3.948114	-1.191874	H	-4.069033	0.239042	4.992404
C	-1.251423	-2.811676	-0.457248	H	-1.843352	1.363979	4.751236
C	-0.353966	-3.012373	0.753254	H	-0.601119	1.228767	2.589547
C	1.162564	-3.092670	0.437452	H	-2.944522	-0.464954	-2.331952
C	1.977100	-1.822214	0.255318	H	-3.608025	-2.520100	-3.598303
C	2.883600	-1.033924	0.147300	H	-2.767098	-4.755052	-2.865943
C	5.049269	0.584211	1.538723	H	-1.301028	-4.939317	-0.864664
C	4.751394	0.665723	-1.557838	H	-0.633030	-3.973299	1.226557
C	5.729532	-1.919447	-0.156678	H	-0.527600	-2.236970	1.524140
C	1.729139	3.225585	0.353930	H	1.325446	-3.714880	-0.467176
C	1.885967	4.668795	0.421200				

References

- (1) Shapiro, N. D.; Toste, F. D. *Proc. Natl. Acad. Sci. U.S.A.* **2008**, *105*, 2779.
- (2) (a) Zeise, W. C. *Poggendorff's Ann. Phys.* **1827**, *9*, 632. (b) Wunderlich, J. A.; Mellor, D. P. *Acta Crystallogr.* **1954**, *7*, 130. (c) Jarvis, J. A. J.; Kilbourn, B. T.; Owsten, P. G. *Acta Crystallogr. B* **1971**, *27*, 366. (d) Love, R. A.; Koetzle, T. F.; Williams, G. J. B.; Andrews, L. C.; Bau, R. *Inorg. Chem.* **1975**, *14*, 2653.
- (3) (a) Gorin, D. J.; Toste, F. D. *Nature* **2007**, *446*, 395. (b) Jiménez-Núñez, E.; Echavarren, A. M. *Chem. Commun.* **2007**, 333. (c) Fürstner, A.; Davies, P. W. *Angew. Chem., Int. Ed.* **2007**, *46*, 3410 (d) Hashmi, A.S.K. *Chem. Rev.* **2007**, *107*, 3180.
- (4) Most previous mechanistic investigations of Au(I)-catalyzed reactions have not involved the isolation of Au-containing intermediates; for an exception, see: Akana, J. A.; Bhattacharyya, K. X.; Müller, P.; Sadighi, J. P. *J. Am. Chem. Soc.* **2007**, *129*, 7736.
- (5) Since this work was published, several Au-containing intermediates have been characterized, see: (a) Liu, L.-P.; Xu, B.; Mashuta, M. S.; Hammond, G. B. *J. Am. Chem. Soc.* **2008**, *130*, 17642. (b) Weber, D.; Tarselli, M. A.; Gagné, M. R. *Angew. Chem., Int. Ed.* **2009**, *48*, 5733. (c) Weber, D.; Gagné, M. R. *Org. Lett.* **2009**, *11*, 4962. (d) Hashmi, A. S. K.; Schuster, A. M.; Rominger, F. *Angew. Chem. Int. Ed.* **2009**, *48*, 8247.
- (6) Since our results were published, several similar gold π -complexes have been isolated and characterized, for a review see: Schmidbaur, H.; Schier, A. *Organometallics* **2010**, *29*, 2.
- (7) Mingos, D. M. P.; Yau, J.; Menzer, S.; Williams, D. J. *Angew. Chem., Int. Ed.* **1995**, *34*, 1894.
- (8) (a) Lang, H.; Köhler, K.; Zsolnai, L. *Chem. Commun.* **1996**, 2043. (b) Köhler, K.; Silverio, S. J.; Hyla-Krypsin, I.; Gleiter, R.; Zsolnai, L.; Driess, A.; Huttner, G.; Lang, H. *Organometallics* **1997**, *16*, 4970.
- (9) Schulte, P.; Behrens, U. *Chem. Commun.*, **1998**, 1633.
- (10) Yip, S.; Cheng, E. C.; Yuan, L.; Zhu, N.; Yam, V. W. *Angew. Chem., Int. Ed.* **2004**, *43*, 4954.
- (11) For a review of η^2 -alkyne Cu(I) and Ag(I) compounds, see: Lang, H.; Köhler, K.; Blau, S. *Coord. Chem. Rev.* **1995**, *143*, 113.
- (12) For linear phosphine-Au(I)-(η^2 -arene) complexes, see: Herrero-Gómez, E.; Nieto-Oberhuber, C.; López, S.; Benet-Buchholz, J.; Echavarren, A. M. *Angew. Chem., Int. Ed.* **2006**, *45*, 5455.
- (13) Reactions involving Cu-catalyzed electrophilic π -bond activation are rare; for examples, see: (a) Bouyssi, D.; Monteiro, N.; Balme, G. *Tetrahedron Lett.* **1999**, *40*, 1297. (b) Asao, N.; Nogami, T.; Lee, S.; Yamamoto, Y. *J. Am. Chem. Soc.* **2003**, *125*, 10921. (c) Asao, N.; Kasahara, T.; Yamamoto, Y. *Angew. Chem., Int. Ed.* **2003**, *42*, 3504. (d) Patil, N. T.; Wu, H.; Yamamoto, Y. *J. Org. Chem.* **2005**, *70*, 4531. (e) Fehr, C.; Farris, I.; Sommer, H. *Org. Lett.* **2006**, *8*, 1839.
- (14) In the case of the Ag(I) dimer there is a center of inversion, whereas the two halves of the Au(I) complex are pseudo-symmetric.
- (15) (a) Nechaev, M. S.; Rayón, V. M.; Frenking, G. *J. Phys. Chem. A* **2004**, *108*, 3134. (b) Yamamoto, Y. *J. Org. Chem.* **2007**, *72*, 7817.
- (16) Eisenstein, O.; Hoffmann, R. *J. Am. Chem. Soc.* **1981**, *103*, 4308. (b) Wright, L. L.; Wing, R. M.; Rettig, M. F. *J. Am. Chem. Soc.* **1982**, *104*, 610–612.

-
- (17) Dewar, M. *Bull. Soc. Chim. Fr.* **1951**, *18*, C71. (b) Chatt, J.; Duncanson, L. A. *J. Chem. Soc.* **1953**, 2939.
- (18) (a) Cinellu, M. A.; Minghetti, G.; Cocco, F.; Stoccoro, S.; Zucca, A.; Manassero, M.; Arca, M. *J. Chem. Soc. Dalton Trans.* **2006**, 5703. (b) Ziegler, T.; Rauk, A. *Inorg. Chem.* **1979**, *18*, 1558. (c) Hertwig, R. H.; Koch, W.; Schröder, D.; Schwarz, H.; Hrušák, J.; Schwerdtfeger, P. *J. PhysChem* **1996**, *100*, 12253. (d) Kim, C. K.; Lee, K. A.; Kim, C. K.; Lee, B.; Lee, H. W. *Chem. Phys. Lett.* **2004**, *391*, 321. (e) Tai, H.-C.; Krossing, I.; Seth, M.; Deubel, D. V. *Organometallics* **2004**, *23*, 2343. (f) Nakanishi, W.; Yamanaka, M.; Nakamura, E. *J. Am. Chem. Soc.* **2005**, *127*, 1446.
- (19) The frontier molecular orbitals of **2.3b** are similar. However, a comparison of **2.3b** with **2.1b** and **2.2b** is less informative because of the altered electron count and geometry about the Cu(I) center.
- (20) (a) Shapiro, N. D.; Toste, F. D. *J. Am. Chem. Soc.* **2007**, *129*, 4160. (b) Kennedy-Smith, J. J.; Staben, S. T.; Toste, F. D. *J. Am. Chem. Soc.* **2004**, *126*, 4526. (c) Staben, S. T.; Kennedy-Smith, J. J.; Toste, F. D. *Angew. Chem., Int. Ed.* **2005**, *43*, 5350.
- (21) (a) Flügge, S.; Anoop, A.; Goddard, R.; Thiel, W.; Fürstner, A. *Chem.–Eur. J.* **2009**, *15*, 8558. (b) Wu, J.; Kroll, P.; Dias, H. V. R. *Inorg. Chem.* **2009**, *48*, 423.
- (22) (a) Brown, T. J.; Dickens, M. G.; Widenhofer, R. A. *J. Am. Chem. Soc.* **2009**, *131*, 6350. (b) Hooper, T. N.; Green, M.; McGrady, J. E.; Patel, J. R.; Russell, C. A. *Chem. Commun.* **2009**, 3877. (c) Fianchini, M.; Dai, H.; Dias, H. V. R. *Chem. Commun.* **2009**, 6373. (d) Brown, T. J.; Dickens, M. G.; Widenhofer, R. A. *Chem. Commun.* **2009**, 6451.
- (23) Crabtree, R. H. *J. Organomet. Chem.* **2005**, *690*, 5451.
- (24) Bruce, M. I.; Nicholson, B. K.; Shawkataly, O. B. *Inorg. Syn.* **1989**, *26*, 324.
- (25) (a) Becke, A. D. *J. Chem. Phys.* **1993** *98*, 5648. (b) Burke, K.; Perdew, J. P.; Yang, W. in *Electronic Density Functional Theory: Recent Progress and New Directions*, **1998**, eds. Dobson, J. F.; Vignale, G.; Das, M. P. (c) Gaussian 03, Revision D.01, Frisch, M. J.; *et. al.* Gaussian, Inc., Wallingford, CT, **2004**.
- (26) (a) Hay, P. J.; Wadt, W. R. *J. Chem. Phys.* **1985**, *82*, 270. (b) Wadt, W. R.; Hay, P. J. (1985) *J. Chem. Phys.* **1985**, *82*, 284. (c) Hay, P. J.; Wadt, W. R. *J. Chem. Phys.* **1985**, *82*, 299. (d) Check, C. E.; Faust, T. O.; Bailey, J. M.; Wright, B. J.; Gilbert, T. M.; Sunderlin, L. S. *J. Phys. Chem. A* **2001**, *105*, 8111. (e) Dunning Jr., T. H. *J. Chem. Phys.* **1989**, *90*, 1007.
- (27) Reed, A. E.; Curtiss, L. A.; Weinhold, F. *Chem. Rev.* **1988**, *88*, 899.
- (28) Teplý, F.; Stará, I. G.; Starý, I.; Kollárovič, A.; Šaman, D.; Fiedler, P. *Tetrahedron* **2002**, *58*, 9007.

Chapter 3 – Understanding Gold Catalysis, Part 2: Au-carbene complexes.

In addition to being able to activate π -bonds toward nucleophilic attack, it has been proposed that gold is also capable of stabilizing adjacent carbocations. Such species (i.e. $[L-Au-CR_2]^+$) have been referred to as gold-carbenoids or gold-stabilized carbocations. This dichotomous nomenclature alludes to the controversy concerning the nature of bonding between gold and carbon in these species. In light of this debate, and in collaboration with the Goddard group, we initiated a joint computational and experimental study with the aim of fully describing this bonding interaction. Herein, we propose that the carbon–gold bond in these intermediates is comprised of, to varying degrees, both σ - and π -bonding; however, the overall bond order is generally less than or equal to one. The bonding in a given gold-stabilized intermediate, and the position of this intermediate on a continuum ranging from gold-stabilized singlet carbene to gold-coordinated carbocation is dictated by the carbene substituents and the ancillary ligand. Experiments show that the correlation between bonding and reactivity is reflected in the yield of gold-catalyzed cyclopropanation reactions. A portion of the work discussed in this chapter has been published.¹

Introduction

The unique reactivity of organogold intermediates² has recently enabled a wide variety of new carbon–carbon bond-forming reactions to be developed³. On the basis of the reactivity patterns that have emerged⁴, several mechanistic pathways⁵ and bonding models⁶ for key intermediates have been proposed, including intermediates ranging from gold carbenes to gold-stabilized carbocations.⁷ In the last year, theoretical investigations⁸ and experimental observations⁹ have further polarized the discussion surrounding the carbenoid or cationic character of organogold species, mostly in support of their carbocationic character.¹⁰ However, gold catalysis has been applied successfully to perform reactions that are traditionally carried out with carbenic systems.¹¹ Given this apparent lack of a consistent and clear understanding of the Au–CR₂⁺ bond, we have performed a broad theoretical analysis on key intermediates relevant to gold(I) catalysis. Experimental results in support of our analysis are also presented.

The study of carbon–metal multiple bonds has been an area of intense discussion since their discovery. For example, after the detection of rhodium carbenoids, debate ensued as to the nature of the rhodium–carbon bond.¹² Although certain calculations and experiments showed that the rhodium–carbon bond order was close to one, eventually it was accepted, on the basis of reactivity, that a metal–carbon double bond was a more useful and convenient descriptor.¹³ A similar discussion has recently emerged concerning the nature of the gold–carbon bond. Although partially semantic, the correct description is useful for both predicting and explaining reactivity.

Results and Discussion

Barrier to bond rotation energy. The magnitude of rotational barriers is a practical way of estimating the strength of π -bonds. Fürstner and co-workers devised a clever experiment to evaluate the carbenic/carbocationic character of (Z)-AuO^{PPh} and (Z)-AuOMe^{PMe} (see Figure 1 for explanation of notation) by measuring the rotational barrier of bonds adjacent to gold.¹⁰ They concluded that the contribution of the ‘carbene’ resonance was marginal. We used Fürstner’s experiments to validate our theoretical methodology based on the M06 functional of density functional theory.¹⁴

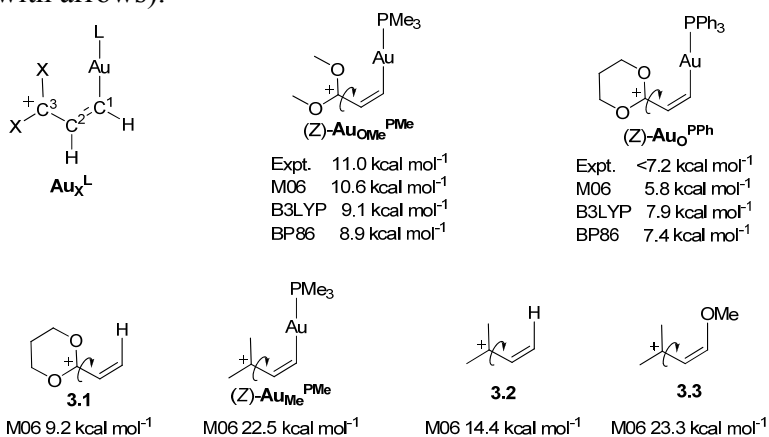
Recently, the M06 functional has been shown to accurately describe transition-metal-catalyzed organic transformations.¹⁵ To confirm this, we calculated rotational barriers for (Z)-AuO^{PPh} and (Z)-AuOMe^{PMe} (Figure 1) and obtained $\Delta G^\ddagger = 10.6 \text{ kcal mol}^{-1}$ for (Z)-AuO^{PPh}, which is in excellent agreement with experiment ($\Delta G^\ddagger = 11.0 \text{ kcal mol}^{-1}$), and $\Delta G^\ddagger = 5.8 \text{ kcal mol}^{-1}$ for (Z)-AuOMe^{PMe}, also consistent with experiment ($<7.2 \text{ kcal mol}^{-1}$). Previous density functional theory studies⁸ used either B3LYP or BP86 functionals. Although these methods have proven valuable for many organometallic studies, we find that they are insufficient to resolve the issues of interest here. For example, B3LYP predicts rotational barriers of $\Delta G^\ddagger = 9.1$ and $7.9 \text{ kcal mol}^{-1}$, whereas BP86 predicts $\Delta G^\ddagger = 8.9$ and $7.4 \text{ kcal mol}^{-1}$ for (Z)-AuO^{PPh} and (Z)-AuOMe^{PMe}, respectively. This suggests that both B3LYP and BP86 cannot resolve the effects of the more electron-donating PMe₃ from the less electron-donating PPh₃.

Using our validated computational method, we calculated the barriers to bond rotation for metal-free allyl cations **3.1**, **3.2**, and **3.3**, as well as the gold species (Z)-Au_M^{PMe}. The results confirm the conclusion of Fürstner and co-workers¹⁰ that the gold moiety has little effect on the barrier to rotation in (Z)-AuO^{PPh} (a difference of $\sim 1.4 \text{ kcal mol}^{-1}$ between (Z)-AuO^{PPh} and **3.1**);

however, this conclusion is only valid in the presence of the highly carbocation-stabilizing oxygen atoms. When these heteroatoms are absent, the effect of the gold moiety is quite large (a difference of ~ 8.1 kcal mol⁻¹ between (Z)-AuMe^{PMe} and **3.2**). For comparison, the highly stabilizing methoxy group in **3.3** increases the barrier to rotation to 8.9 kcal mol⁻¹ higher than that of **2**.

These results suggest that the reactivity of a given gold-stabilized carbene is highly dependent upon the carbene substituents. To gain further insight into the nature of the gold-carbon bond, we examined the structures of these types of intermediates, while varying both the carbene and ancillary ligand substituents.

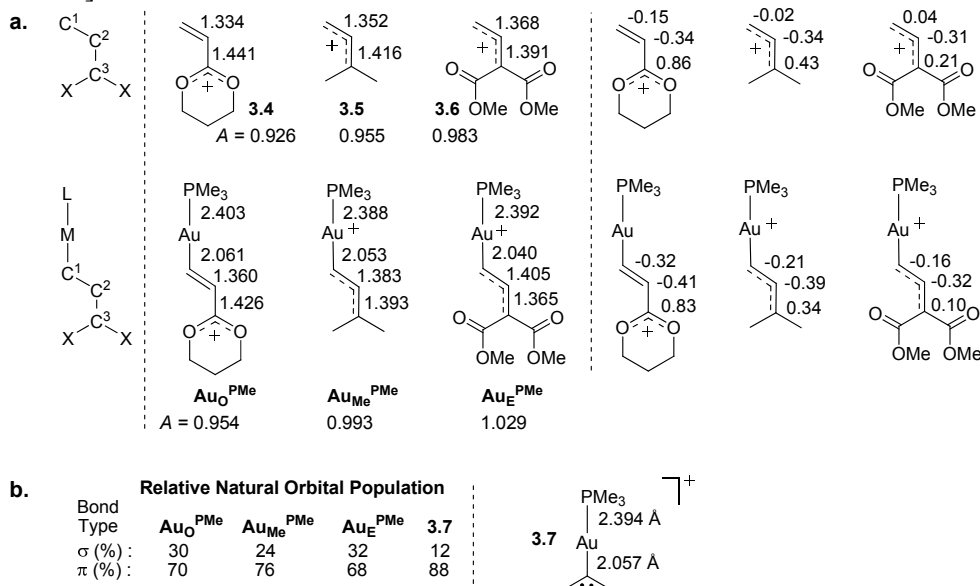
Figure 1. Calculated and experimental activation energies to bond rotation (indicated with arrows).



C3–C2 bond rotation barriers are decreased when C3 is substituted with carbocation-stabilizing oxygen atoms. Throughout this article, gold complexes will be referred to according to the Au_X^L notation, where **L** indicates the ancillary ligand on gold and **X** indicates the C3 substituents (Me = methyl, O = 1,3-dioxanyl, OMe = methoxy, E = methyl ester). M06, B3LYP and BP86 refer to the specific functional used in density functional theory calculations.

Impact of the carbene. As a basis for comparison, we began by calculating the structures and natural atomic charges¹⁶ of metal-free allyl cations **3.4**, **3.5**, and **3.6** (Figure 2a). We also defined parameter A as the ratio of the bond lengths: $A \equiv (C1-C2)/(C2-C3)$, so that A indicates roughly whether the partial positive charge on the substrate is more stabilized by its C1 or C3 substituents. The low value of A in **3.4** (0.926) is indicative of the stabilizing nature of the oxygen lone pairs. The magnitude of A increases with less σ -donating C3-methyl substituents ($A = 0.955$) and even further for ester-substituted substrate **6** ($A = 0.983$). The corresponding gold-coordinated structures Au_O^{PMe}, Au_{Me}^{PMe} and Au_E^{PMe} all show increased A values as a result of the ability of the gold moiety to stabilize positive charge at C1. In Au_{Me}^{PMe}, A is close to 1 (0.993), suggesting that a secondary gold-stabilized carbocation is as stabilized as a tertiary carbocation. For the diester-substituted allyl carbene Au_E^{PMe}, the π -system is now polarized towards the electron-deficient C3 leading to $A = 1.029$. Importantly, the magnitude of stabilization from the gold moiety grows with increasing electrophilicity of the allyl cation. This conclusion can also be reached by considering the natural atomic charge on C3. This charge is essentially unaffected in **3.4** (0.86) compared with Au_O^{PMe} (0.83), whereas it is significantly reduced in **5** (0.43) compared with Au_{Me}^{PMe} (0.34), and in **3.6** (0.21) compared with Au_E^{PMe} (0.10).

Figure 2. Structural and electronic comparison of cationic metal-free and $[\text{AuPMe}_3]^+$ substituted substrates.

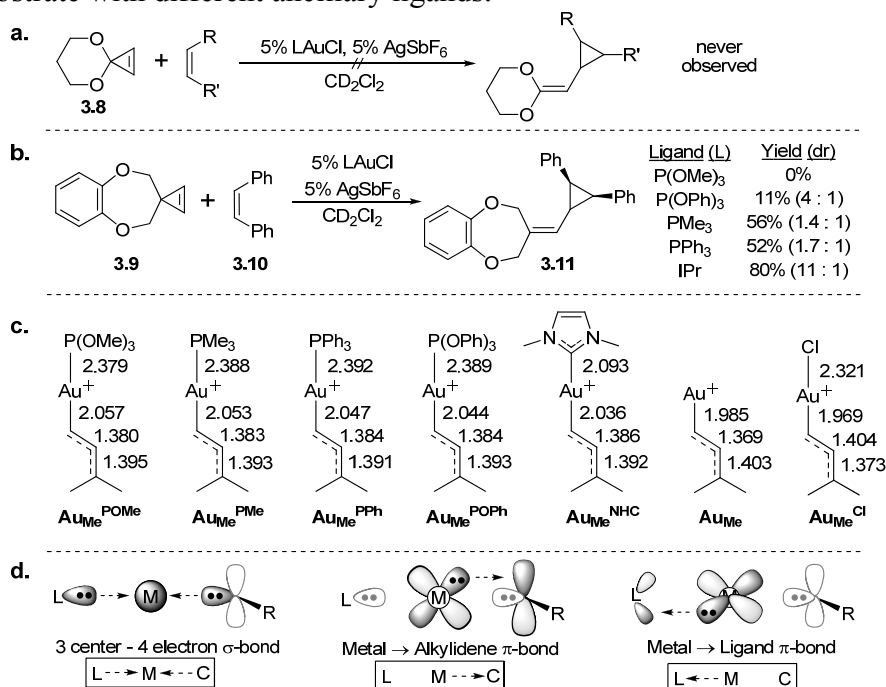


a. On the left, calculated bond distances (\AA), and on the right, natural charges for C1, C2, and C3. Parameter A is defined as the ratio of bond distances $(\text{C1-C2})/(\text{C2-C3})$ and correlates to the polarization of the π -electrons along the delocalized C1-C2-C3 system. **b.** A comparison with gold alkylidene **3.7** showing the relative natural orbital populations of σ and π contributions to the gold-carbon bond. Calculated bond distances (\AA) for **3.7** are shown on the right.

In order to examine the bonding and reactivity of non-vinylc gold(I) intermediates, we also examined gold alkylidene **7** and compared it to the gold vinylc carbene species (Figure 2b). Our results show that the gold-carbon bond distance (2.057 \AA) varies little from the vinyl carbenes. However, in the absence of a delocalized neighbouring vinyl group, the gold-carbon bond possesses more π -character, with decreased σ -donation from alkylidene to gold.¹⁷ This demonstrates the ability of the gold moiety to stabilize carbenes of varying electrophilicity by modulating the nature of the gold-carbon bond.

A direct consequence of the differences between $\text{Au}_\text{O}^{\text{PMe}}$ and $\text{Au}_\text{Me}^{\text{PMe}}$ is the increased barrier to C2-C3 bond rotation in $\text{Au}_\text{Me}^{\text{PMe}}$ (Figure 1). In addition, a difference in reactivity could be expected: $\text{Au}_\text{O}^{\text{PMe}}$ may react as a gold-stabilized carbocation, whereas $\text{Au}_\text{Me}^{\text{PMe}}$ may react more as a gold-stabilized carbene. We tested and confirmed this hypothesis experimentally. We were unable to observe productive cyclopropanation of intermediates resulting from the gold-catalyzed reaction of cyclopropene **3.8** (as a precursor to $\text{Au}_\text{O}^{\text{PMe}}$, Figure 3a). However, the gold-catalyzed reaction of cyclopropene **3.9** (which should decompose to an intermediate similar to $\text{Au}_\text{Me}^{\text{PMe}}$) with cis-stilbene provided the product of stereospecific olefin cyclopropanation (Figure 3b). As the yield of this reaction was highly dependent on the ancillary ligand, we next examined the effect of this ligand on the nature of the Au-C1 bond.

Figure 3. Experimental and theoretical comparison for the carbene reactivity of the substrate with different ancillary ligands.



a,b, Attempted (**a**) and observed (**b**) carbene-like reactivity, demonstrating the impact of the ancillary ligand on the yield of cyclopropanation product. **c,** Bond distances in AuMe^L complexes. **d,** A stylized depiction of the most important bonding interactions in L-Au(I)-CR_2^+ species. d.r., diastereomeric ratio.

Impact of the ligand.^{2,18} The computed structures of AuMe^L , for various ligands (L) are shown in Figure 3c. The L–Au–C1 bonding network can be partitioned into three components (Figure 3d).¹⁹ Because there is only one vacant valence orbital on gold (6s), the Pauli exclusion principle tells us that a three-centre–four-electron σ -hyperbond²⁰ (where hyperbond refers to bonding beyond the reduced 12-electron valence space) must be formed for the P–Au–C triad as $[\text{P}:\text{Au}-\text{C} \leftrightarrow \text{P}-\text{Au}:\text{C}]$ (or C–Au–C triad for the NHC ligand). As a result, the Au–C1 bond order decreases with increasing trans ligand σ -donation (trans influence). In the absence of a trans ligand, the Au–C bond in AuMe is notably shorter (1.985 Å), whereas, in $\text{AuMe}^{\text{PMe}_3}$, the electron-donating PMe_3 (strong trans influence) results in a correspondingly long Au–C1 bond length of 2.053 Å.

In addition, the metal centre is able to form two π -bonds by donation from perpendicular filled d-orbitals into empty π -acceptors on the ligand and C1. Although these two bonds are not mutually exclusive, they compete for electron density from gold. As a result, strongly π -acidic ligands decrease back-donation to the substrate, resulting in even longer Au–C1 bonds (2.057 Å for $\text{AuMe}^{\text{POMe}}$). In contrast, the π -donating chloride ligand in AuMe^{Cl} increases back-donation to C1 resulting in a very short gold2carbon bond (1.969 Å). In general, the strength of the back-donation to C1 is dependent on both ligand and (as demonstrated in the previous section) the electrophilicity of the π -acceptor on C1.

The impact of these changes on reactivity is directly apparent in the yield of the cyclopropanation product (Figure 3b). π -acidic ligands are expected to increase carbocation-like reactivity by decreasing gold-to-C1 π -donation. Accordingly, we found that strongly π -acidic

phosphite ligands provide only traces of the desired product and significant polymerization. Conversely, ligands that increase gold-to-C1 π -donation are expected to reduce carbocation-like reactivity, whereas those ligands that decrease C1-to-gold σ -donation should increase carbene-like reactivity. The N-heterocyclic ligand IPr (1,3-bis(2,6-diisopropylphenyl)imidazol-2-ylidene) should therefore affect both of these changes (it is strongly σ -donating and only weakly π -acidic). This was reflected by our results, in which IPrAu⁺ gave the product of stereospecific cyclopropanation in excellent yield and with high diastereoselectivity (80% yield, 11:1 cis:trans). Phosphine ligands fell in between these two extremes. Finally, AuCl was unreactive under these conditions.

Charge distribution. In order to provide a better and more general view of the bonding in gold vinyl carbene species, we calculated natural charge distributions for the ligand, gold and substrate using natural bond orbital analyses. Table 1 shows that the charge is relatively equally distributed between the substrate, gold and the ligand. Across the AuMe^L and AuO^L series, the charge on the ligand and the gold is well correlated: an increase in ligand charge is associated with a similar decrease in charge on the gold, but these changes have little effect on the charge on the substrate. However, changing the substrate from AuMe^L to AuO^L results in an increase in substrate charge. This correlates with a decrease in the charges on both the gold and the ligand. These results again demonstrate that both the ligand and the substrate play important roles in determining the overall electronic structure.

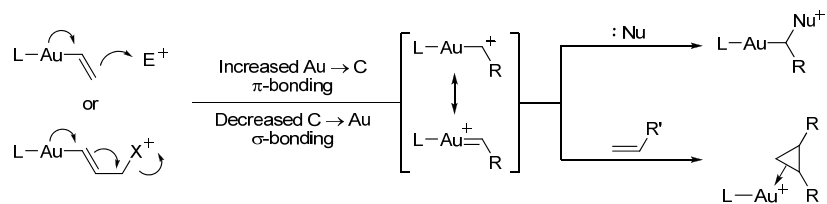
Table 1. Calculated natural populations (charge) for the ancillary ligand, gold atom, and substrate.

	AuMe ^{NHC}	AuMe ^{PMe}	AuMe ^{POMe}	AuO ^{NHC}	AuO ^{PMe}	AuO ^{POMe}
Ligand	0.32	0.40	0.45	0.31	0.37	0.42
Metal	0.39	0.30	0.25	0.36	0.27	0.23
Substrate	0.29	0.31	0.31	0.33	0.36	0.35

Bonding and reactivity. The model in Figure 3d for bonding in gold stabilized carbenes proposes that these intermediates possess highly electron-deficient α -carbons that are stabilized, to varying degrees, by back-donation from the metal to the vacant π^* -orbital of the singlet carbene. This electron deficiency reduces donation from the filled sp^2 s-orbital of the carbene to the metal, therefore minimizing gold-carbon σ -bonding. Thus, our model suggests that the conversion of a vinylgold intermediate into a gold stabilized carbene, which is commonly proposed in gold-catalyzed reactions,²¹ occurs with an increase in gold-carbon π -bonding and a decrease in the σ -bonding (Figure 4). The bonding situation in these carbene intermediates has often been depicted by two extreme resonance structures: a carbocation with a gold-carbon single bond or a carbene with a gold-carbon double bond. Much like the double ‘half-bond’ model proposed for rhodium carbenoid intermediates²², the depiction of a gold-stabilized carbene with a gold-carbon double bond should not be taken as an indication of a bond order of two, but rather a means to convey that both σ and π components to the bond are present. To illustrate this, we calculated gold-carbon natural bond orders for AuO^{PMe} (0.53), AuMe^{PMe} (0.91), and **7** (1.14). Nucleophilic attack on the now highly electrophilic π^* -orbital of the carbon adjacent to gold restores the gold-carbon σ -bond.²³ In this scenario, divergence towards carbocation-like or carbene-like reactivity may also be influenced by the potential of the nucleophile to intercept the developing positive charge. Alternatively, gold-stabilized carbene intermediates may react with concerted carbene-like reactivity (for example, as in cyclopropanation), especially when the gold

is coordinated to electron-donating ligands. Subsequent studies have shown that steric interactions can also have a strong influence on reactivity.²⁴ For example, steric interactions that force the L-Au-C1 bond angle to divert from 180° result in a decrease in Au-to-C1 π -donation. Under these circumstances, bulky, electron-rich ligands may actually favor carbocation-like reaction pathways.

Figure 4. Arrow pushing in the formation of gold-stabilized carbenes.



Such arrow pushing is a useful mnemonic for keeping track of electrons, but it can lead to misconceptions about bonding. Although the gold-carbon bond in the intermediate carbene has both σ and π components, the overall bond order is generally less than or equal to one.

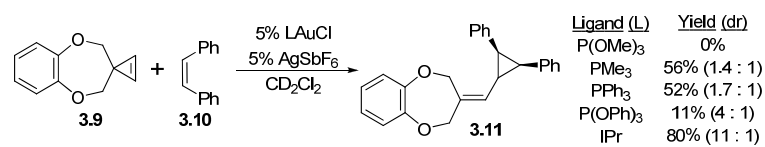
Conclusions

We suggest that the reactivity in gold(I)-coordinated carbenes is best accounted for by a continuum ranging from a metal-stabilized singlet carbene to a metal-coordinated carbocation. The position of a given gold species on this continuum is largely determined by the carbene substituents and the ancillary ligand. Consideration of the bonding description described herein provides insight into previously reported gold-catalyzed transformations and a basis for the *ab initio* prediction of reactivity, optimization of ligand effects and design of new gold-catalyzed reactions.

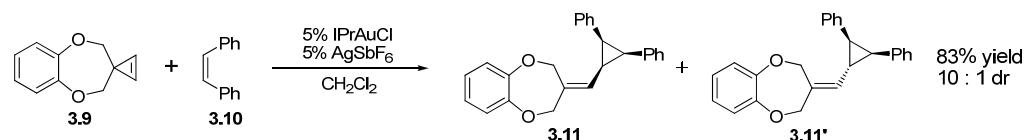
Supporting Information

Calculations were performed using density functional theory with the M06 functional, as implemented in Jaguar 7.6.²⁵ All calculations used the Hay and Wadt small core–valence relativistic effective core potential.²⁶ The LACVP** basis set was used for all geometry optimizations and LACV3P^{++**}(2f) for energies. LACV3P^{++**}(2f) uses the LACV3P^{++**} basis set as implemented in Jaguar plus a double-zeta f-shell with exponents from Martin and Sundermann.²⁷ All electrons were described for all other atoms using the 6-31G** or 6-311⁺⁺G** basis sets²⁸. For each optimized structure, the M06 analytic Hessian was calculated to obtain the vibrational frequencies, which in turn were used to obtain the zero-point energies and free energy corrections (without translational or rotational components). Solvent corrections were based on single-point self-consistent Poisson–Boltzmann continuum solvation calculations for CH₂Cl₂ ($\epsilon = 8.93$ and $R_0 = 2.33$ Å using the PBF module in Jaguar).²⁹

Unless otherwise noted, reagents were obtained commercially and used without further purification. HPLC grade dichloromethane (CH₂Cl₂), ACS grade hexanes, and ACS grade ethyl acetate (EtOAc) were obtained from Fischer Scientific. TLC analysis of reaction mixtures was performed on Merck silica gel 60 F254 TLC plates using UV light and ceric ammonium molybdate stain to visualize the reaction components. Flash chromatography was carried out on ICN SiliTech 32-63 D 60 Å silica gel. ¹H and ¹³C NMR spectra were recorded with a Bruker AV-600 spectrometer and referenced to CDCl₃ unless otherwise noted. Mass spectral and analytical data were obtained via the Micro-Mass/Analytical Facility operated by the College of Chemistry, University of California, Berkeley.

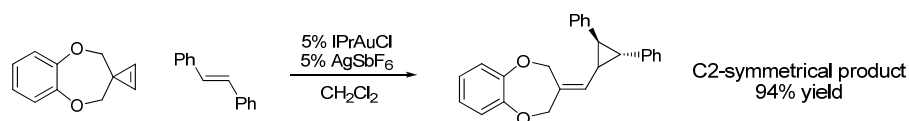


A one dram vial was charged with cyclopropene (5 x 1 equiv, 5 x 0.075 mmol, 65 mg), *cis*-stilbene (5 x 4 equiv, 5 x 0.3 mmol, 270 mg), dibenzyl ether (as an internal standard, approx 15 mg), and CD₂Cl₂ (0.4 mL). An small aliquot of this solution diluted with CDCl₃ and used to acquire a time zero ¹H-NMR. The remainder of the mixture was divided between 5 one dram vials. Subsequently, an additional 5 one dram vials were charged with gold catalyst (0.05 equiv, 0.0038 mmol), AgSbF₆ (0.05 equiv, 0.0038 mmol), and CD₂Cl₂ (0.1 mL). After 5 minutes the resulting heterogeneous mixtures were filtered through glass wool into the one dram vials containing the cyclopropene mixture. These five reactions were allowed to sit for 5 minutes after which point aliquots were removed and diluted for ¹H-NMR analysis. Yields and diastereoselectivity were determined by comparing these spectra to the time zero spectra. Except in the case of Me₃PAuCl, all starting material was consumed after 5 minutes. For low yielding reactions, significant polymerization was observed. In the case of Me₃PAuCl, the reaction was incomplete after 5 minutes, so an additional ¹H-NMR spectrum was acquired after 30 minutes.



A one dram vial was charged with [1,3-bis(2,6-diisopropylphenyl)imidazol-2-ylidene]gold(I) chloride (IPrAuCl, 0.05 equiv, 0.01 mmol, 6.2 mg), AgSbF₆ (0.05 equiv, 0.01 mmol, 3.4 mg),

and CH_2Cl_2 (0.3 mL). The resulting heterogeneous mixture was sonicated for 30 seconds and filtered through glass wool into a separate one dram vial containing a stirring mixture of the cyclopropene (1 equiv, 0.2 mmol, 35 mg) and *cis*-stilbene (4 equiv, 0.8 mmol, 144 mg) in CH_2Cl_2 (0.3 mL). After 20 minutes, the pale yellow reaction mixture was directly subjected to flash column chromatography on silica gel (10% CH_2Cl_2 in hexanes \rightarrow 5% EtOAc + 10% CH_2Cl_2 in hexanes). The desired product (**3.11**) was isolated as a clear oil (59mg, 83% yield, 10:1 *cis:trans*), containing 5% of the C2-symmetrical product (the *cis*-stilbene was contaminated with 2% *trans*-stilbene). ^1H NMR (600 MHz, CDCl_3) δ 7.25-7.10 (m, 6.6H), 6.98-6.87 (m, 8.8H), 5.48 (d, 1H, $J = 10.2$ Hz), 5.41 (d, 0.1H, $J = 8.4$ Hz), 5.09 (d, 0.2H, $J = 1.2$ Hz), 5.00 (d, 2H, $J = 1.2$ Hz), 4.81 (s, 0.2H), 4.68 (s, 2H), 2.82 (d, 2H, $J = 9$ Hz), 2.56 (d, 0.2H, $J = 5.4$ Hz), 2.37 (app q, 1H, $J = 9.2$ Hz), 2.31 (dt, 0.1H, $J = 8.4, 5.4$ Hz). ^{13}C NMR (150 MHz, CDCl_3) δ 149.8, 149.2, 136.0, 135.9, 130.9, 128.0, 126.3, 125.2, 123.8, 122.7, 121.8, 120.8, 74.8, 71.0, 28.5, 21.6. HRMS (ESI) calc. for $[\text{C}_{25}\text{H}_{22}\text{O}_2\text{Na}]^+$ 377.1512, found 377.1517.



An authentic sample of the C2-symmetrical isomer could be obtained by running the reaction described above with *trans*-stilbene in the place of *cis*-stilbene (94% yield). ^1H NMR (400 MHz, CDCl_3) δ 7.36-7.21 (m, 10H), 6.97-6.85 (m, 4H), 5.04 (d, 1H, $J = 9.6$ Hz), 4.97 (s, 2H), 4.63 (dd, 2H, $J = 16, 13.2$ Hz), 2.82 (dd, 1H, $J = 9.2, 6$ Hz), 2.49 (app t, 1H, $J = 5.6$ Hz), 2.13 (ddd, 1H, $J = 9.6, 9.2, 5.2$ Hz). ^{13}C NMR (100 MHz, CDCl_3) δ 149.8, 149.3, 141.2, 137.4, 135.5, 129.3, 128.8, 128.6, 127.2, 126.8, 126.5, 126.4, 123.8, 122.7, 121.8, 120.8, 74.6, 20.8, 33.3, 31.4, 28.5.

References

- (1) Benitez, D.; Shapiro, N. D.; Tkatchouk, E.; Wang, Y.; Goddard, W. A. III; Toste, F. D. A bonding model for gold(I) carbene complexes. *Nature Chem.* **1**, 482 (2009).
- (2) Gorin, D. J., Sherry, B. D.; Toste, F. D. Ligand effects in homogeneous Au catalysis. *Chem. Rev.* **108**, 3351–3378 (2008).
- (3) Hashmi, A. S. K. Gold-catalyzed organic reactions. *Chem. Rev.* **107**, 3180–3211 (2007).
- (4) Fürstner, A.; Davies, P. W. Catalytic carbophilic activation: catalysis by platinum and gold π acids. *Angew. Chem. Int. Ed.* **46**, 3410–3449 (2008).
- (5) Jiménez-Núñez, E.; Echavarren, A. M. Gold-catalyzed cycloisomerizations of enynes: a mechanistic perspective. *Chem. Rev.* **108**, 3326–3350 (2008).
- (6) Gorin, D. J.; Toste, F. D. Relativistic effects in homogeneous gold catalysis. *Nature* **446**, 395–403 (2007).
- (7) (a) Fedorov, A., Moret, M. E.; Chen, P. Gas-phase synthesis and reactivity of a gold carbene complex. *J. Am. Chem. Soc.* **130**, 8880–8881 (2008). (b) Hashmi, A. S. K. High noon in gold catalysis: Carbene versus carbocation intermediates. *Angew. Chem. Int. Ed.* **47**, 6754–6756 (2008).
- (8) Correa, A. *et al.* Golden carousel in catalysis: the cationic gold/propargylic ester cycle. *Angew. Chem. Int. Ed.* **47**, 718–721 (2008).
- (9) Fürstner, A.; Morency, L. On the nature of the reactive intermediates in goldcatalyzed isomerization reactions. *Angew. Chem. Int. Ed.* **47**, 5030–5033 (2008).
- (10) Seidel, G., Mynott, R.; Fürstner, A. Elementary steps of gold catalysis: NMR spectroscopy reveals the highly cationic character of a “gold carbenoid.” *Angew. Chem. Int. Ed.* **48**, 2510–2513 (2009).
- (11) (a) Johansson, M. J., Gorin, D. J., Staben, S. T.; Toste, F. D. Gold(I)-catalyzed stereoselective olefin cyclopropanation. *J. Am. Chem. Soc.* **127**, 18002–18003 (2005). (b) Horino, Y., Yamamoto, T., Ueda, K., Kuroda, S.; Toste, F. D. Au(I)-catalyzed cycloisomerizations terminated by sp^3 C–H bond insertion. *J. Am. Chem. Soc.* **131**, 2809–2811 (2009). (c) Lemière, G. *et al.* Generation and trapping of cyclopentenylidene gold species: four pathways to polycyclic compounds. *J. Am. Chem. Soc.* **131**, 2993–3006 (2009). (d) Frutos, M. R. *et al.* A gold catalyst for carbene-transfer reactions from ethyl diazoacetate. *Angew. Chem. Int. Ed.* **44**, 5284–5288 (2005). (e) López, S., Herrero-Gómez, E., Pérez-Galán, P., Nieto-Oberhuber, C.; Echavarren, A. M. Gold(I)-catalyzed intermolecular cyclopropanation of enynes with alkenes: trapping of two different gold carbenes. *Angew. Chem. Int. Ed.* **45**, 6029–6032 (2005). (f) Fedorov, A.; Chen, P. Electronic effects in the reactions of olefin-coordinated gold carbene complexes. *Organometallics* **28**, 1278–1281 (2009).
- (12) Sheehan, S. M., Padwa, A.; Snyder, J. P. Dirhodium(II) tetracarboxylate carbenoids as catalytic intermediates. *Tetrahedron Lett.* **39**, 949–952 (1998).
- (13) (a) Doyle, M. P. Electrophilic metal carbenes as reaction intermediates in catalytic reactions. *Acc. Chem. Res.* **19**, 348–356 (1986). (b) Nowlan, D. T., Gregg, T. M., Davies, H. M. L.; Singleton, D. A. Isotope effects and the nature of selectivity in rhodium-catalyzed cyclopropanations. *J. Am. Chem. Soc.* **125**, 15902–15911 (2004).
- (14) Zhao, Y.; Truhlar, D. G., Density functionals with broad applicability in chemistry. *Acc. Chem. Res.* **41**, 157–167 (2008).

-
- (15) (a) Truhlar, D. G. Molecular modeling of complex chemical systems. *J. Am. Chem. Soc.* **130**, 16824–16827 (2008). (b) Zhao, Y.; Truhlar, D. G. *J. Chem. Theory Comput.* **5**, 324–333 (2009).
- (16) Reed, A. E., Curtiss, L. A.; Weinhold, F. Intermolecular interactions from a natural bond orbital, donor-acceptor viewpoint. *Chem. Rev.* **88**, 899–926 (1988).
- (17) Irikura, K. K.; Goddard III, W. A. Energetics of third-row transition metal methylenes MCH_2^+ ($M = La, Hf, Ta, W, Re, Os, Ir, Pt, Au$). *J. Am. Chem. Soc.* **116**, 8733–8740 (1994).
- (18) Padwa, A.; Austin, D. J. Ligand effects on the chemoselectivity of transition metal catalyzed reactions of α -diazo carbonyl compounds. *Angew. Chem. Int. Ed. Engl.* **33**, 1797–1815 (1994).
- (19) (a) Dewar, M. A review of the π -complex theory. *Bull. Soc. Chim. Fr.* **18**, C71–C77 (1951). (b) Chatt, J.; Duncanson L. A. Olefin co-ordination compounds. Part III. Infra-red spectra and structure: attempted preparation of acetylene complexes. *J. Chem. Soc.* 2939–2947 (1953).
- (20) Landis, C. R.; Weinhold, F. Valence and extra-valence orbitals in main group and transition metal bonding. *J. Comput. Chem.* **28**, 198–203 (2007).
- (21) (a) Mamane, V., Gress, T., Krause, H.; Fürstner, A. Platinum- and gold-catalyzed cycloisomerization reactions of hydroxylated enynes. *J. Am. Chem. Soc.* **126**, 8654–8655 (2004). (b) Luzung, M. R., Markham, J. P.; Toste, F. D. Catalytic isomerization of 1,5-enynes to bicyclo[3.1.0]hexenes. *J. Am. Chem. Soc.* **126**, 10858–10859 (2004). (c) Gorin, D. J. Davis, N. R.; Toste, F. D. Gold(I)-catalyzed intramolecular acetylenic Schmidt reaction. *J. Am. Chem. Soc.* **127**, 1126–1127 (2005). (d) Nieto-Oberhuber, C., Muñoz, M. P., Buñuel, E., Nevado, C., Cárdenas, D. J.; Echavarren, A. M. Cationic gold(I) complexes: highly alkynophilic catalysts for the exo- and endo-cyclization of enynes. *Angew. Chem. Int. Ed.* **43**, 2402–2406 (2004). (e) Shapiro, N. D.; Toste, F. D. Rearrangement of alkynyl sulfoxides catalyzed by gold(I) complexes. *J. Am. Chem. Soc.* **129**, 4160–4161 (2007). (f) Zhang, G.; Zhang, L. Au-containing all-carbon 1,3-dipoles: generation and [3 + 2] cycloaddition reactions. *J. Am. Chem. Soc.* **130**, 12598–12599 (2008).
- (22) (a) Snyder, J. P. et al. A stable dirhodium tetracarboxylate carbenoid: crystal structure, bonding analysis, and catalysis. *J. Am. Chem. Soc.* **123**, 11318–11319 (2001). (b) Costantino, G., Rovito, R., Macchiarulo, A.; Pellicciari, R. Structure of metal carbenoid intermediates derived from the dirhodium(II)tetracarboxylate mediated decomposition of α -diazocarbonyl compounds: a DFT study. *J. Mol. Struct. Theochem.* **581**, 111 (2002).
- (23) (a) Amijs, C. H. M., López-Carrillo, V.; Echavarren, A. M. Gold-catalyzed addition of carbon nucleophiles to propargyl carboxylates. *Org. Lett.* **9**, 4021–4024 (2007). (b) Davies, P. W. Albrecht, S. J.-C. Alkynes as masked ylides: gold-catalyzed intermolecular reactions of propargylic carboxylates with sulfides. *Chem. Commun.* 238–240 (2008). (c) Nieto-Oberhuber, C. et al. Gold(I)-catalyzed cyclizations of 1,6-enynes: alkoxy cyclizations and exo/endo skeletal rearrangements. *Chem. Eur. J.* **12**, 1677–1693 (2006).
- (24) Benitez, D.; Tkatchouk, E.; Gonzalez, A.; Goddard, W. A. III; Toste, F. D. *Org. Lett.* **2009**, *11*, 4798.
- (25) Jaguar 7.6 (Schrodinger, New York, 2006).

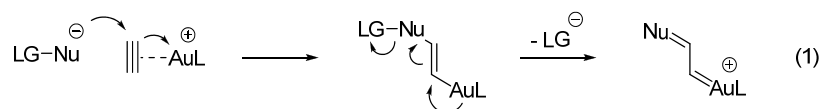
-
- (26) Hay, P. J.; Wadt, W. R. Ab initio effective core potentials for molecular calculations—potentials for K to Au including the outermost core orbitals. *J. Chem. Phys.* **82**, 299–310 (1985).
- (27) Martin, J. M. L.; Sundermann, A. Correlation consistent valence basis sets for use with the Stuttgart-Dresden-Bonn relativistic effective core potentials: The atoms Ga-Kr and In-Xe. *J. Chem. Phys.* **114**, 3408–3420 (2001).
- (28) (a) Krishnan, R., Binkley, J. S., Seeger, R.; Pople, J. A. Self-consistent molecular orbital methods. XX. A basis set for correlated wave-functions. *J. Chem. Phys.* **72**, 650–654 (1980). (b) Frisch, M. J., Pople, J. A.; Binkley, J. S. Self-consistent molecular-orbital methods 25. Supplementary functions for Gaussian-basis sets. *J. Chem. Phys.* **80**, 3265–3269 (1984).
- (29) Tannor, D. J. et al. Accurate first principles calculation of molecular charge distributions and solvation energies from ab-initio quantum-mechanics and continuum dielectric theory. *J. Am. Chem. Soc.* **116**, 11875–11882 (1994).

Chapter 4 – Rearrangements of Alkynyl Sulfoxides, Sulfimides, and Sulfur Ylides

A series of gold(I)-catalyzed rearrangement reactions of alkynyl sulfoxides, sulfimides and sulfur ylides are reported. Homopropargyl sulfoxides are rearranged to benzothiepinones or benzothiopynes, while α -thioenones are formed in the reaction of propargyl sulfoxides. It is proposed that these reactions proceed via an α -carbonyl gold–carbenoid intermediate formed through gold-promoted oxygen atom transfer from sulfoxide to alkyne. A portion of the work discussed in this chapter has been published.^{1,2}

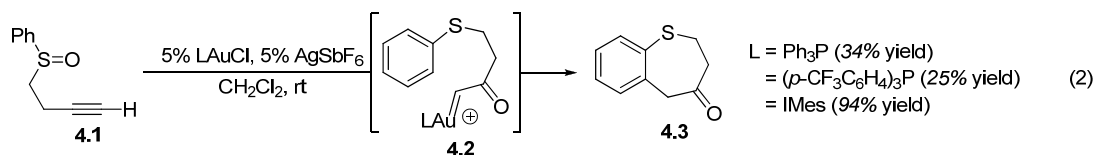
Introduction

Recently, gold-carbenoid species have been proposed as intermediates in gold-catalyzed enyne rearrangements.³ Additionally, the reaction of gold complexes with propargyl esters has been developed as an alternative approach to metal carbenoids capable of effecting olefin cyclopropanation,^{4,5} however, to date, the reaction of electrophilic metals with alkynes has not been amenable to the generation of α -carbonyl carbenoids analogous to those traditionally formed in situ from transition-metal-catalyzed decomposition of α -diazocarbonyl compounds.^{6,7} We recently described a rearrangement of homopropargyl azides to pyrroles in which gold(I) promotes addition of a leaving-group-bearing nucleophile (Nu = N) to an acetylene and subsequent loss of the leaving group (LG = N₂) (eq 1).⁸ On the basis of this reactivity principle, we envisioned that α -carbonyl metal carbenoids could be generated from alkynes via a gold(I)-catalyzed rearrangement in which sulfoxides serve the role of nucleophile (Nu = O) and latent leaving group (LG = R₂S).



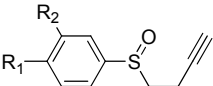
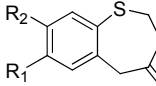
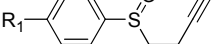
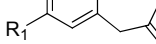
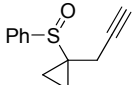
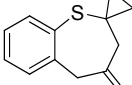
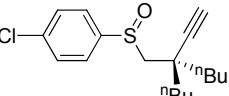
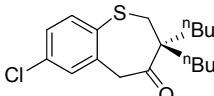
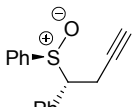
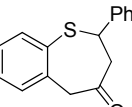
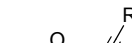
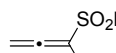
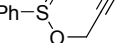
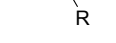
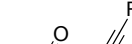
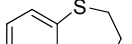
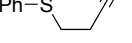
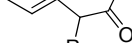
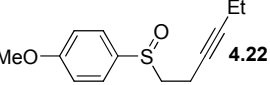
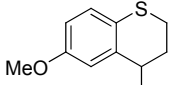
Rearrangements of Homopropargyl Sulfoxides

In order to explore this hypothesis, homopropargyl sulfoxide **4.1** was treated with 5 mol % of Ph₃PAuCl/AgSbF₆ in dichloromethane. Gratifyingly, this reaction produced 1-benzothiepin-4-one **4.3**, presumably via the desired α -carbonyl carbenoid intermediate **4.2**, albeit in only 34% yield (eq 2). While switching to an electron-deficient phosphine ligand resulted in a decreased yield, the use of an *N*-heterocyclic carbene (IMes) ligated gold(I) complex as catalyst dramatically improved the yield of ketone **3** to 94%.



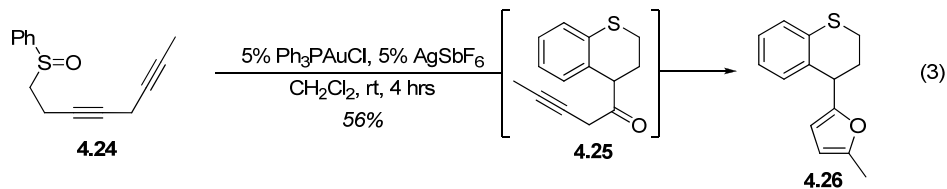
Under these conditions, a wide range of homopropargyl arylsulfoxides underwent the gold-catalyzed rearrangement to benzothiepinones (Table 1). The reaction proceeded smoothly when the aryl group of the sulfoxide was substituted with electron-withdrawing (entry 1) or electron-donating groups (entry 2), although the latter underwent the gold-catalyzed rearrangement with increased yield. Substitution at the homopropargyl (entry 3) and propargyl (entry 4) position of the sulfoxide is tolerated; however, the latter required slightly elevated temperatures to afford **4.11** in 76% yield. Notably, one diastereomer (illustrated) of phenyl-substituted propargyl sulfoxide (\pm)-**4.12** was significantly more reactive than the other in the gold(I)-catalyzed rearrangement, affording **4.13** in 94% yield (entry 5). The less reactive diastereomer of (\pm)-**12** (characterized by X-ray crystallography) proceeded to only 15% conversion after reaction at 35 °C for 24 hrs. If the linker is altered to include an oxygen atom, as in the case of propargyl sulfinates **4.14** and **4.16**, facile conversion to the corresponding allenyl sulfones is observed (entries 6-7).⁹

Table 1. Au(I)-Catalyzed Rearrangements of Homopropargyl Sulfoxides

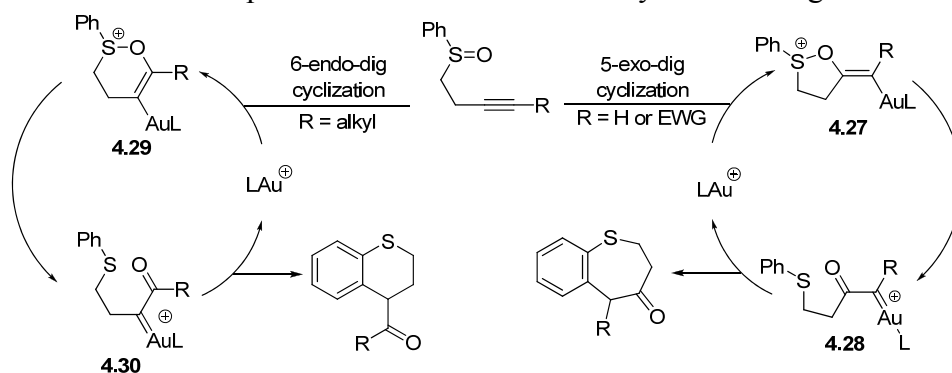
entry	sulfoxide	conditions ^a	product	yield
1		4.4 R ₁ =NO ₂ , R ₂ =H	A	 4.5 71%
2		4.6 R ₁ =R ₂ =OMe	A	 4.7 87%
3		4.8	A	 4.9 71%
4		4.10	B	 4.11 76% ^b
5		(±)- 4.12	A	 4.13 94%
6		4.14 R=H	B	 4.15 99%
7		4.16 R=Me	B	 4.17 98%
8		4.18 R=4-NO ₂ -C ₆ H ₄	B	 4.19 63%
9		4.20 R=CO ₂ Et	A	 4.21 91% ^c
10		4.22	B	 4.23 64%

^a Conditions: (A) Sulfoxide (0.2 M in CH₂Cl₂), 5% IMesAuCl, 5% AgSbF₆, rt; (B) Sulfoxide (0.2 M in CH₂Cl₂), 5% Ph₃PAuCl, 5% AgSbF₆, rt. ^b Reaction run at 60 °C. ^c 5 Å Sieves added.

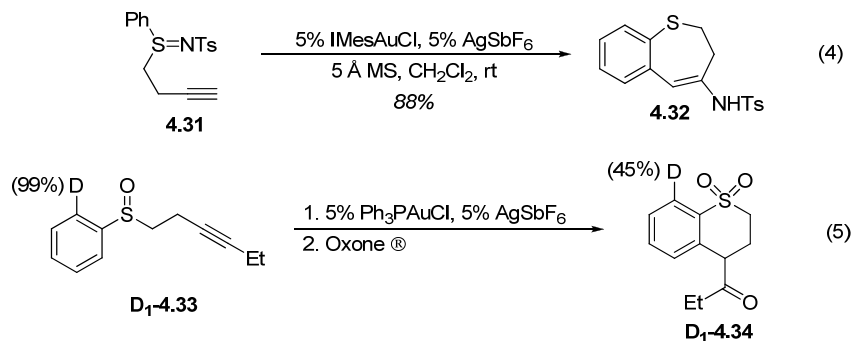
The triphenylphosphinegold(I)-catalyzed reaction of a sulfoxide containing an alkyne substituted with an electron-deficient aryl group¹⁰ (entry 8) or an ester (entry 9) produced the anticipated benzothiepinones **4.19** and **4.21** in 63 and 91% yield, respectively. In sharp contrast, the gold(I)-catalyzed reaction of alkyl-substituted alkyne **4.22** afforded benzothiepine **4.23** in 64% yield (entry 10).¹¹ On the basis of this reaction, 1,4-diyne **4.24** was converted to furan **4.26** in 56% yield by a gold(I)-catalyzed sulfoxide rearrangement and subsequent cycloisomerization of propargyl ketone **4.25** (eq 3).¹²



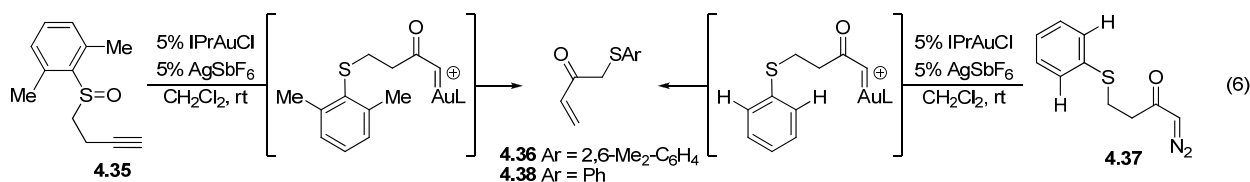
Scheme 1. Proposed Mechanism of Au-Catalyzed Rearrangements

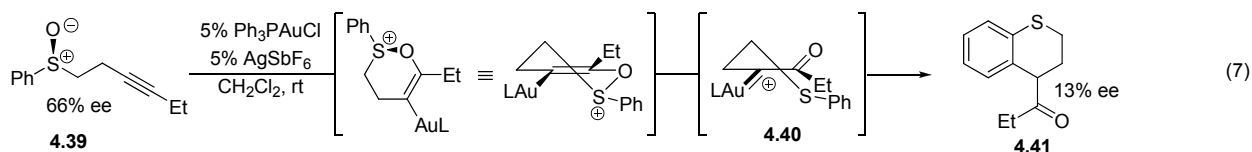


A proposed mechanism for the gold-catalyzed rearrangement of homopropargyl sulfoxides is detailed in Scheme 1. Coordination of cationic gold(I) to the alkyne induces nucleophilic addition of the sulfoxide oxygen. When the alkyne is terminal or substituted with an electron-withdrawing group, 5-*exo*-dig cyclization of the nucleophile onto the internal carbon of the alkyne is favored, yielding intermediate **4.27**. On the other hand, when the alkyne is substituted with an alkyl group, **4.29** is generated by a 6-*endo*-dig cyclization. After cyclization, gold(I)-assisted sulfide release produces gold-carbenoid intermediate **4.28** or **4.30**. The observation that gold(I)-catalyzed rearrangement of sulfimine **4.31** proceeded in 88% yield to furnish *N*-tosyl enamine **4.32** (eq 4) is consistent with the proposal that the carbonyl oxygen in the product is transferred from the sulfoxide. Finally, carbenoids **4.28** and **4.30** undergo intramolecular arylation to produce the observed products and liberate the cationic gold(I) catalyst.¹³ No kinetic isotope effect was observed in the cyclization of *o*-deuterophenyl **D₁-4.1**, while a slight inverse secondary kinetic isotope effect of 0.96 was observed for deuterated **D₁-4.33** (eq 5). These values are similar to those measured previously for electrophilic aromatic substitution reactions.¹⁴

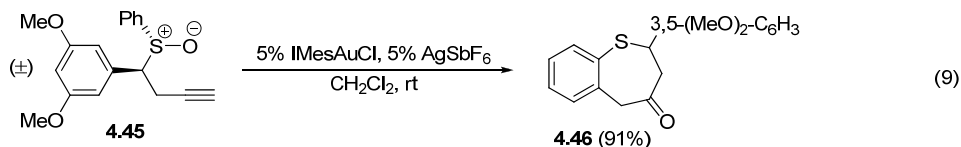
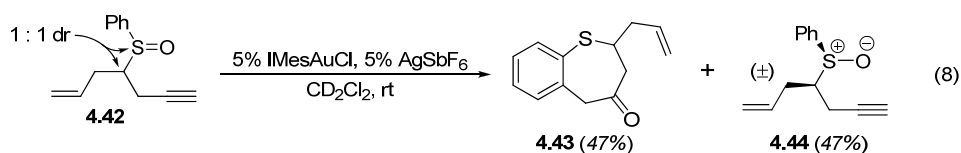


When the *ortho*-positions of the aromatic ring are blocked (as in **4.35**), sluggish conversion to enone **4.36** is observed (eq 6).¹⁵ Surprisingly, when *S*-phenyl, α -diazoketone **4.37** is subjected to the same reaction conditions, enone **4.38** is produced instead of benzothiepinone **4.3**. This suggests that the gold-catalyzed rearrangement of alkynyl sulfoxides provides a route to intermediates that are actually inaccessible from the corresponding α -diazocarbonyl compounds.

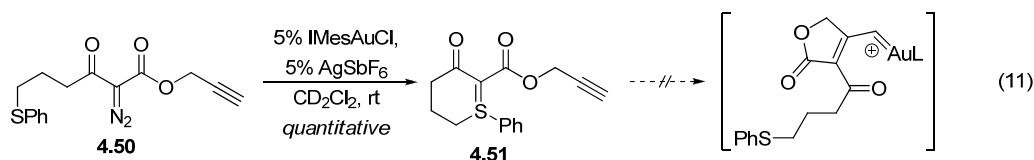
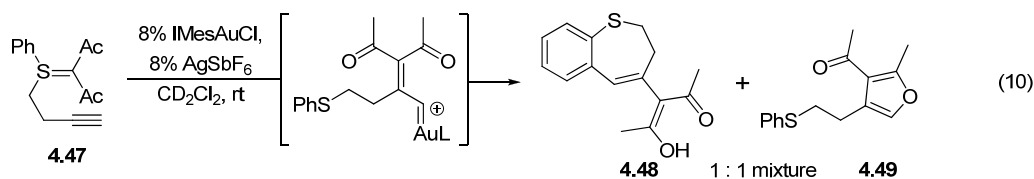




With this result in hand we devised several experiments aimed at probing the nature of the proposed gold-carbenoid intermediates. In an initial experiment, enantioenriched sulfoxide **4.39** was subjected to the standard reaction conditions (eq 7). Surprisingly, some chirality transfer was observed. When the reaction was stopped before completion, the remaining starting material was recovered without any racemization. These results suggest that trapping of the gold carbenoid occurs on the same time scale as racemization of planar chiral intermediate **4.40**.¹⁶ This result is in accord with the observation that the carbenoid intermediate was not trapped by pendant olefins (eq 8) or electron rich aromatic rings (eq 9).

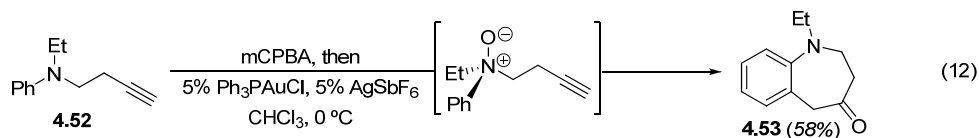


On the other hand, an alternative reaction pathway was provided in the rearrangement of ylide **4.47**; in this case, trapping with the aryl sulfide to form benzothiepine **4.48** was competitive with cyclization of the carbonyl to form furan **4.49** (eq 10). Based on this new mode of reactivity, we envisioned that diazo alkyne **4.50** could undergo a tandem biscyclization cascade (eq 11). While the first cyclization to form ylide **4.51** proceeded in excellent yield, no further reaction was observed. Additional investigation of such dual cyclization cascades is a promising area for future research. Zhang and coworkers have also demonstrated that Au-carbenoids generated from sulfoxides and alkynes can be trapped by pinacol-rearrangement.¹⁷



Having developed a number of reactions from the rearrangement of alkynyl sulfoxides, sulfimides, and sulfur ylides, we postulated that replacing sulfur with other heteroatoms might allow access to an even greater array of products. For example, we were pleased to find gold(I)-catalyzed rearrangement of amine oxide **4.52** provided benzoazepine **4.53** (eq 12). This mode of reactivity was subsequently reported by and expanded upon by Zhang and coworkers.¹⁸ Unfortunately, this reactivity could not be extended to include the analogous phosphine oxides or

phosphine sulfides; for both of these substrates no reaction was observed upon treatment with gold(I) or gold(III) catalysts.



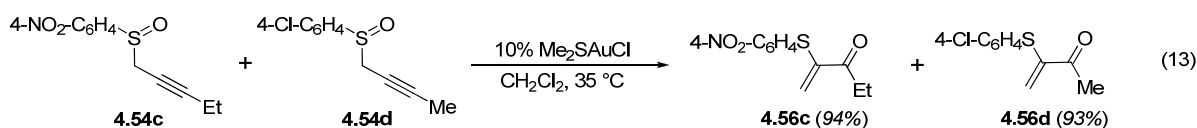
Part 2: Rearrangements of Propargyl Sulfoxides

Gold(I) complexes also catalyze the conversion of propargyl sulfoxides to α -thioenones in high yields.^{19,20} In this case, (dimethylsulfide)gold(I) chloride proved to be the optimal catalyst (*vide infra*), affording enones **4.56a-j** from propargyl sulfoxides **4.54a-j** with excellent tolerance for substitution on the alkyne and the sulfoxide (Table 2). Interestingly, a slight decrease in yield is observed with increasing electron density in the aromatic ring of the sulfoxide (entries 4-6). This decreased yield corresponds to both a slight increase in the observed rate and increased conversion to the dimerized products **4.67** (*vide infra*). In analogy to the mechanism described in Scheme 1, this rearrangement is postulated to proceed through gold(I)-promoted sequential 5-*endo-dig* cyclization/cleavage of the S–O bond leading to gold(I)-carbenoid intermediate **4.55** which undergoes a 1,2-sulfide shift.²¹ The lack of sulfide cross-over in the gold-catalyzed rearrangement of **4.54c** and **4.54d** is consistent with an intramolecular sulfide shift (eq 13).

Table 2. Au(I)-Catalyzed Propargyl Sulfoxide Rearrangements

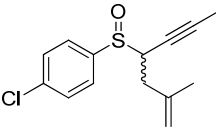
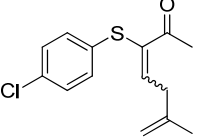
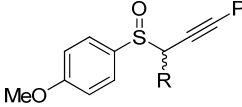
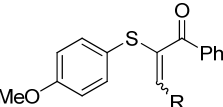
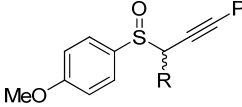
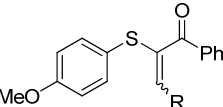
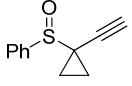
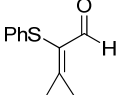
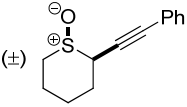
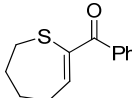
entry	sulfoxide	R ₁	R ₂	product	yield
1	4.54a	4-MeO-C ₆ H ₄	Ph	4.56a	67%
2	4.54b	2,6-Cl ₂ -C ₆ H ₃	Ph	4.56b	95%
3	4.54c	4-NO ₂ -C ₆ H ₄	Et	4.56c	91%
4	4.54d	4-Cl-C ₆ H ₄	Me	4.56d	94% ^a
5	4.54e	Ph	Me	4.56e	85% ^a
6	4.54f	4-MeO-C ₆ H ₄	Me	4.56f	81% ^a
7	4.54g	Ph		4.56g	85%
8	4.54h	Ph	H	4.56h	51%
9	4.54i	Et	H	4.56i	73% ^a
10	4.54j	4-MeO-C ₆ H ₄		4.56j	27%

^a Yield by ¹H-NMR vs an internal standard (1,3,5-trinitrobenzene).



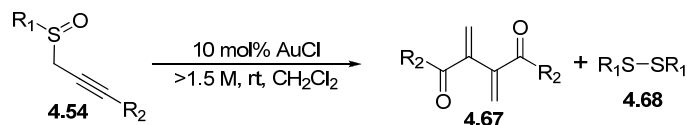
Additionally, secondary and tertiary propargyl sulfoxides react under these conditions to provide trisubstituted and tetrasubstituted alkenes (Table 3). For example, sulfoxide **4.57** underwent gold(I)-catalyzed rearrangement to enone **4.58** in preference to cycloisomerization of the 1,5-enyne (entry 1).^{3c} The rearrangement of **4.63** to strained methylene cyclopropane aldehyde **4.64**, illustrates the power of Au-catalysis to assemble structures that would otherwise be difficult to access. Finally, a single diastereomer of cyclic sulfoxide **4.65** (presumably the *cis* isomer) was slowly transformed to tetrahydrothiepine **4.66**.

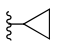
Table 3. Secondary and Tertiary Propargyl Sulfoxide Rearrangements.^a

entry	sulfoxide	product	yield (E : Z)
1	 4.57	 4.58	99% (1.6 : 1)
2 ^b	 4.59 (R = Bn)	 4.60	90% (2.5 : 1)
3	 4.61 (R = Me)	 4.62	73% (2.5 : 1)
3	 4.63	 4.64	86%
4	 4.65	 4.66	24%

^a Sulfoxide (0.2 M in CH₂Cl₂), 5% Me₂SAuCl, rt. ^b Both diastereomers of the starting sulfoxide produce the same E : Z ratio in the product.

Table 4. Scope of gold-catalyzed dimerization reaction.



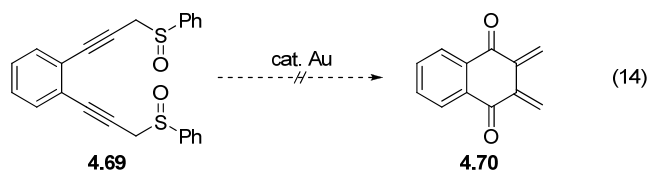
entry	sulfoxide	R ₁	R ₂	yield 4.67 ^a	yield 4.68 ^a
1	4.54a	4-MeO-C ₆ H ₄	Ph	81%	76%
2	4.54b	2,6-Cl ₂ -C ₆ H ₃	Ph	25% ^b	23% ^b
3	4.54k	Ph	2-MeO-C ₆ H ₄	58%	58%
4	4.54d	4-Cl-C ₆ H ₄	Me	63%	72%
5	4.54e	Ph	Me	70%	70%
6	4.54f	4-MeO-C ₆ H ₄	Me	59%	59%
7	4.54g	Ph		67%	74%
8	4.54h	Ph	H	0% ^d	65%

^a Isolated Yield. ^b Also isolated 74% of the α -thioenone **2c**. ^c Mostly decomposition by ¹H NMR. ^d Decomposed on silica gel.

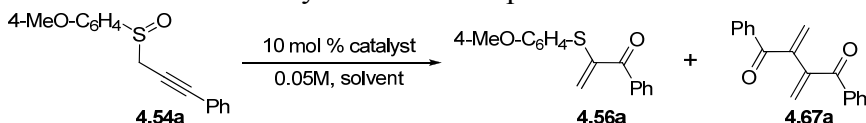
When the primary propargyl sulfoxides were subjected to catalytic AuCl at high concentrations, the formation of dienes **4.67**, along with the corresponding disulfides was favored. The scope of this reaction is illustrated in Table 4. Good to moderate yields were obtained for both aryl and alkyl substituted alkynes (entries 1-7). Terminal alkyne **4.54h** also underwent the desired transformation, although the bis-aldehyde product proved to be too unstable to isolate. Interestingly, formation of these dimeric products was significantly inhibited by ortho-substitution of the aryl sulfoxide **4.54b** (entry 2), which also explains the high yield obtained in Table 2, entry 2. Little or no dimerization was observed for secondary or tertiary propargyl sulfoxides.

Additional attempts were made to understand the mechanism of formation of the dimer products **4.67** and **4.68**. Subjecting the α -thioenone **4.56a** to 10 mol% AuCl did not generate any **4.67a**, thereby ruling the α -thioenone out as an intermediate. Initial attempts to intercept any ionic or radical pathways, through the addition of acetic acid or 1,4-cyclohexadiene, respectively had little or no effect. On the other hand, the addition of 1.5 equivalents of dimethyl sulfide to the reaction of **4.54a** with 10 mol% Me₂SAuCl, both significantly decreases the reaction rate and also completely inhibits the formation of dimer **4.67a**. This suggests that coordination of a semi labile ligand may play a critical role in directing the course of the reaction.

We postulated that any radical or ionic intermediates might be too short lived to be trapped intermolecularly, so we synthesized a new diyne substrate **4.69** (eq 14). We hypothesized that if radicals were being generated, the adjacent alkyne would serve as an effective trap. Furthermore, if the dimer products arise from a tail-to-tail dimerization, then we hoped **4.69** would increase the yield of dimerization, yielding **4.70**. Unfortunately, treatment of the diyne **4.69** with a variety of Au(I) species including AuCl led to complete degradation. Addition of 1,4-cyclohexadiene once again had little effect. Since this report similar dimerizations have been reported.²²



The effect of the catalyst structure and reaction conditions on the product distribution are demonstrated in Table 5. The highest yield of α -thioenone **4.56a** was obtained using Me₂SAuCl in dichloromethane (entries 1-2). Mild heating increased the reaction rate, such that most substrates were entirely consumed within 24 hours (entry 2, see also Table 2). In less polar solvents, significant dimerization was observed (entry 3), whereas more polar solvents led to decreased conversion or competitive decomposition (entries 4-5). When AuCl was employed at low concentration, the amount of dimerization was significantly reduced (entry 6, compare to Table 4). The neutral triphenylphosphine gold(I) chloride complex did not catalyze the formation of either product, even at elevated temperatures (entry 7). On the other hand, AgSbF₆ led to complete decomposition within 4 hours at room temperature (entry 8). Copper salts were unreactive at room temperature, and led to decomposition at elevated temperatures (entry 9). A Brønsted acid also failed to catalyze the reaction (entry 10). Interestingly, the cationic triphenylphosphine gold(I) complex provided a low yield of α -thioenone **4.56a**, whereas the dimeric 1,1'-bis(diphenylphosphino)methane gold(I) complex provided dimer **4.67a** (entries 11-12).

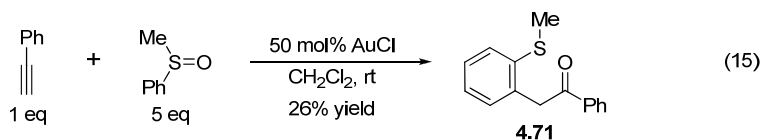
Table 5. Effect of catalyst structure on product distribution.


Entry	Catalyst	Yield 4.56a (%) ^a	Yield 4.67a (%) ^a	Conversion (%) ^a	Temp. (°C)	Time (hrs)	Solvent
1	Me ₂ SAuCl	80	9	95	rt	24	CD ₂ Cl ₂
2	Me ₂ SAuCl	78	5	100	35	8	CD ₂ Cl ₂
3	Me ₂ SAuCl	58	31	100	rt	24	C ₆ D ₆
4	Me ₂ SAuCl	18	7	34	rt	24	MeNO ₂
5	Me ₂ SAuCl	45	0	100	rt	24	MeOD
6	AuCl	41	29	100	rt	24	CD ₂ Cl ₂
7	PPh ₃ AuCl	0	0	20	65	5	C ₆ D ₆
8	AgSbF ₆	0	0	100	0	4	CD ₂ Cl ₂
9	CuI	0	0	100	65	5	C ₆ D ₆
10	TfOH	0	0	95	65	24	C ₆ D ₆
11	PPh ₃ AuCl, AgOTf	36	0	100	0	2	CD ₂ Cl ₂
12	dppm(AuCl) ₂ , AgOTf ^b	0	40	100	0	4	CD ₂ Cl ₂

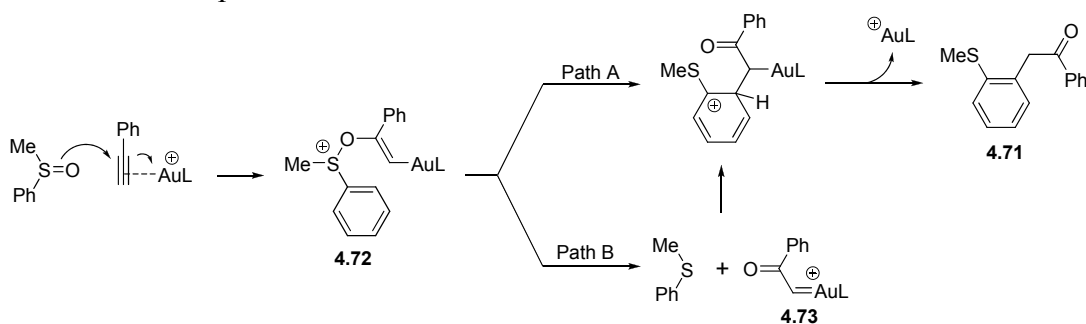
^aBy ¹H NMR against an internal standard (1,2,3-trinitrobenzene). ^bUsing 5 mol% AgOTf

Intermolecular addition of sulfoxides to alkynes

Homogeneous gold-catalyzed intermolecular addition of nucleophiles to alkynes has typically been limited to addition followed by protodemetalation.^{3, 30-32} Therefore, it was with much excitement that we discovered that AuCl catalyzes the intermolecular addition of aromatic sulfoxides to alkynes. Addition of phenylacetylene to a mixture of five equivalents of methylphenylsulfoxide and 50 mol% AuCl led to a 27% isolated yield of ketone **4.71** (eq 15).

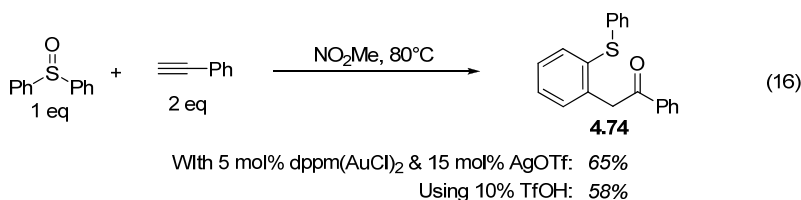


Two possible mechanisms for the formation of **4.71** were proposed (Scheme 2). Following path A, addition of the sulfoxide to the alkyne is followed by 3,3-sigmatropic rearrangement, rearomatization, and protonation of the Au-C bond. In pathway B, the addition complex **4.72** fragments to provide methylphenylsulfide and gold(I) carbenoid **4.73**. A subsequent Friedel-Crafts type alkylation reaction leads to the observed product.

Scheme 2. Two possible mechanisms for the formation of ketone **4.44**.

To distinguish these pathways, an excess of methyl(p-tolyl)sulfide was added to the reaction mixture. No crossover between sulfides was detected by $^1\text{H-NMR}$ or GC-MS. Furthermore, a methyl(p-tolylsulfide)-gold(I) complex was synthesized. This complex did catalyze the reaction; however, once again, no crossover between sulfides was observed by $^1\text{H-NMR}$ or GC-MS. To date, all experiments support path A. Subsequent to the completion of these experiments, a similar study was reported by Asensio and coworkers, which also supported a 3,3-sigmatropic pathway.²³

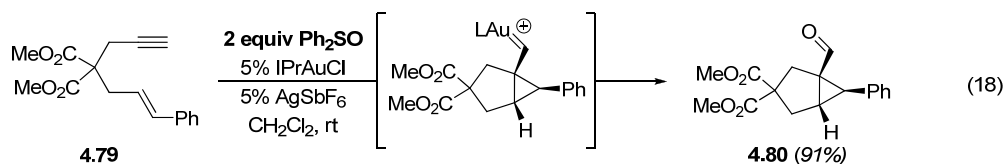
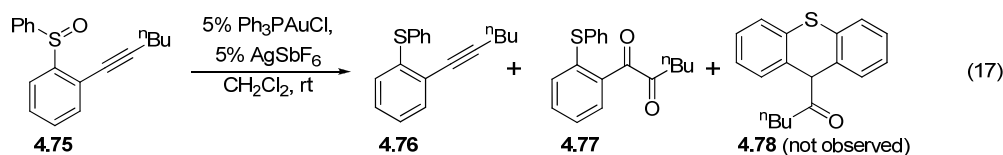
We then turned our focus to increasing the yield of the reaction. Numerous catalyst, solvent, and additive screens all led to disappointing results. Eventually, it was discovered that heating 5 mol% $\text{dppm}(\text{AuCl})_2$ and 15 mol% AgOTf with diphenylsulfoxide and two equivalents phenylacetylene in nitromethane overnight at 80°C led to a 65% isolated yield of ketone **4.74** (eq 16). Under these conditions, we observed that gold nanoparticles appeared after only 15 minutes. Therefore, we were skeptical that a cationic gold(I) species remained as the active catalyst. We subsequently discovered that 10 mol% triflic acid catalyzed the same reaction under identical conditions with nearly identical yield.



The acid-catalyzed reaction is of synthetic interest, and an attempt to identify its scope is in progress. The results are summarized in Table 6. So far, the reaction is limited to terminal alkynes with phenyl acetylene providing the best yields. Nonetheless, this reaction provides ortho-substituted aromatic sulfides in one pot from cheap, commercially available starting materials.

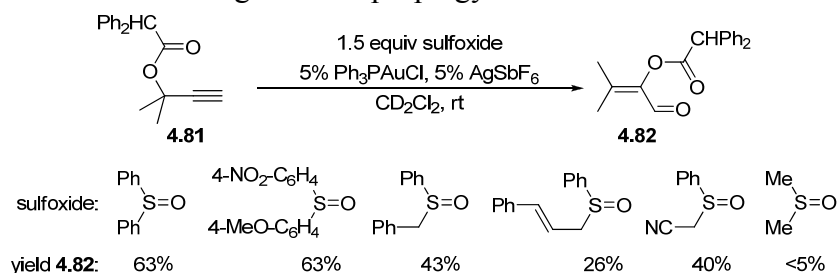
Intermolecular trapping of Au-carbenoids

During the course of further exploring the substrate scope, it was observed that exposure of sulfoxide **4.75** to a variety of cationic Au(I) catalysts produced a mixture of reduced sulfide **4.76** and diketone **4.77** (eq 17). Indeed, none of the expected cyclized product **4.78** was observed. This result suggested an *intermolecular* transfer of oxygen from sulfoxide to a Au-carbenoid intermediate.²⁴ This was borne out in subsequent experiments, and eventually these observations merged with an ongoing project in our lab aimed at the oxidation of Au-carbenoid intermediates (for example, eq 18).²

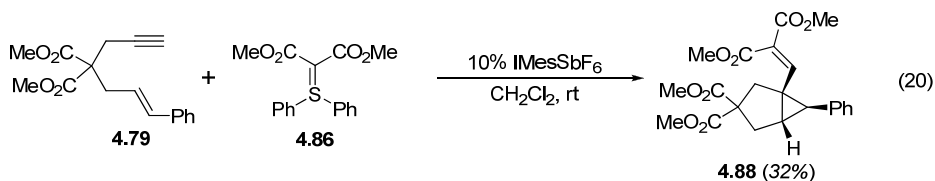
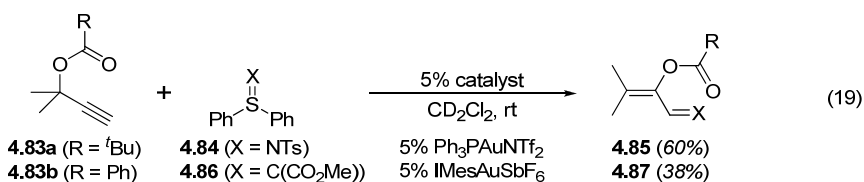


During the course of optimizing the oxidation of propargyl ester **4.81**, a number of sulfoxides were screened (Scheme 3). Ultimately, we found that diphenylsulfoxide (commercially available) provided the highest yield for this transformation.

Scheme 3. Screening of sulfoxides for the gold-catalyzed oxidative rearrangement of propargyl ester **4.54**.



We also found that this intermolecular transfer reactivity could be extended to include sulfimides and sulfur ylides (eqs 19-20). For example, amination of propargyl pivalate **4.83a** with sulfimide **4.84** was affected by triphenylphosphine-gold(I) bistriflimide. Similarly, sulfur ylide **4.86** successfully olefinated both pivalate **4.83b** and enyne **4.79** in the presence of catalytic IMes-gold(I) hexafluoroantimonate.²⁵



Conclusions

In conclusion, we have shown that alkynyl sulfoxides undergo gold-catalyzed rearrangements to provide a wide variety of products, including benzothiepinones, benzothiepinines, enones, furans, α -thioenones, and *ortho*-alkylated thiophenols. Many of these reactions are proposed to proceed via oxo-transfer from sulfoxide to gold-activated alkyne. We have explored the chemistry of the resulting gold-carbenoid intermediates, and shown that they can be trapped both inter- and intramolecularly. Importantly, the reactivity of these proposed intermediates is analogous to the reactivity that has been demonstrated for other metal-carbenoids (typically generated from the decomposition of α -diazocarbonyl compounds). In addition, we have shown that similar chemical transformations can be accessed from sulfimides and sulfur ylides. Finally, we have shown that all three of these functional groups (sulfoxides, sulfimides, and sulfur ylides) can trap gold-carbenoids intermolecularly, to provide aldehydes, imines, and olefins, respectively.

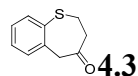
Supporting Information

General Information. Unless otherwise noted, all reagents were obtained commercially and used without further purification. Glassware and 5Å molecular sieves were dried in an oven at 130 °C prior to use. Dichloromethane (CH₂Cl₂) was obtained from EMD. Silver hexafluoroantimonate (AgSbF₆) and silver trifluoromethanesulfonate (AgOTf) were obtained from the Aldrich Chemical Company. Triphenylphosphinegold(I)chloride (Ph₃PAuCl) was prepared according to the method of Bruce.²⁶ Tris(*para*-trifluoromethylphenyl)phosphinegold(I)chloride [(*p*-CF₃-C₆H₄)₃PAuCl] was prepared according to the method of Onaka.²⁷ N,N'-bis(2,4,6-trimethylphenyl)imidazolyliidene-gold(I)chloride [IMesAuCl] was prepared according to the method of Echavarren.²⁸ Small scale reactions (< 2 mL) were carried out in disposable one dram vials unless otherwise noted. Organic extracts were dried with anhydrous MgSO₄ and solvents were removed with a rotary evaporator. TLC analysis was carried out on Merck silica gel 60 F₂₅₄ TLC plates. Column chromatography was performed using Merck 60 silica gel (32-63 μm). All melting points are uncorrected. ¹H and ¹³C NMR spectra were recorded with Bruker DRX-500, AVB-400, AVQ-400, and AV-300 spectrometers and referenced to CDCl₃ unless otherwise noted. FT-IR spectra were recorded on NaCl plates with a Nicolet MAGNA-IR 850 spectrometer. Mass spectra and analytical data were obtained from the Micro-Mass/Analytical Facility operated by the College of Chemistry, University of California, Berkeley.

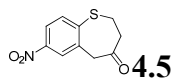
General procedures for the synthesis of benzothiepinones and benzothiopyrans from homopropargyl sulfoxides.

Method A: A one dram vial was charged with the appropriate sulfoxide (1 equiv), CH₂Cl₂ (0.2M based on sulfoxide), IMesAuCl (5 mol%), and AgSbF₆ (5 mol%). The reaction was stirred until TLC indicated full consumption of starting materials. Upon completion, the crude reaction mixture was loaded directly onto a silica gel column; elution with an appropriate ethyl acetate/hexanes mixture provided the desired benzothiepinone.

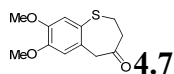
Method B: A one dram vial was charged with the appropriate sulfoxide (1 equiv), CH₂Cl₂ (0.2M based on sulfoxide), Ph₃PAuCl (5 mol%), and AgSbF₆ (5 mol%). The reaction mixture was stirred until TLC indicated full consumption of starting materials. Upon completion, the crude reaction mixture was loaded directly onto a silica gel column; elution with an appropriate ethyl acetate/hexanes mixture provided the desired product.



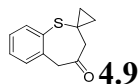
Method A (flash column chromatography with 5% EtOAc/hexanes) provided the desired product as a clear oil (44.8 mg, 94% yield). IR: 1712, 1467, 754 cm⁻¹. ¹H NMR (400 MHz) δ 7.53 (d, 1H, *J* = 7.4 Hz), 7.29-7.24 (m, 2H), 7.20 (td, 1H, *J* = 7.0, 2.0 Hz), 3.99 (s, 2H), 3.07-3.04 (m, 2H), 2.87-2.84 (m, 2H). ¹³C NMR (100 MHz) δ 206.5, 138.4, 135.2, 134.2, 130.5, 129.1, 128.0, 51.4, 45.3, 31.9. HRMS (EI) calc. for [C₁₀H₁₀OS]⁺ 178.0452, found 178.0448.



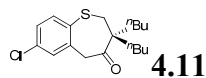
Method A (flash column chromatography with 5% EtOAc/hexanes) provided the desired product as a yellow solid (24.2 mg, 71% yield), mp 127 – 131 °C. IR: 1706, 1342, 742 cm^{-1} . ^1H NMR (500 MHz) δ 8.12 (d, 1H, $J = 2.3$ Hz), 8.03 (dd, 1H, $J = 8.5, 2.3$ Hz), 7.65 (d, 1H, $J = 8.5$ Hz), 4.07 (s, 2H), 3.19-3.16 (m, 2H), 2.95-2.92 (m, 2H). ^{13}C NMR (125 MHz) δ 204.0, 147.6, 144.2, 138.8, 134.0, 125.3, 122.7, 50.8, 44.9, 31.1. HRMS (EI) calc. for $[\text{C}_{10}\text{H}_9\text{NO}_3\text{S}]^+$ 223.0303, found 223.0303.



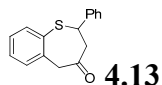
Method A (flash column chromatography with 25% EtOAc/hexanes) provided the desired product as a white solid (32.5 mg, 87% yield), mp 128 – 130 °C. IR: 1693, 1501, 1257 cm^{-1} . ^1H NMR (400 MHz) δ 7.03 (s, 1H), 6.78 (s, 1H), 3.90 (s, 2H), 3.86 (s, 3H), 3.85 (s, 3H), 3.05-3.00 (m, 2H), 2.85-2.81 (m, 2H). ^{13}C NMR (100 MHz) δ 206.9, 149.5, 148.0, 131.2, 126.0, 117.1, 113.3, 56.3, 56.2, 50.9, 45.6, 33.0. HRMS (EI) calc. for $[\text{C}_{12}\text{H}_{14}\text{O}_3\text{S}]^+$ 238.0664, found 238.0665.



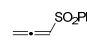
Method A (flash column chromatography with 3% EtOAc/hexanes) provided the desired product as a white solid (17.0 mg, 71% yield), mp 77 – 80 °C. IR: 3062, 1708, 752 cm^{-1} . ^1H NMR (400 MHz) δ 7.38 (dd, 1H, $J = 7.5, 1.2$ Hz), 7.32 (d, 1H, $J = 7.5$ Hz), 7.27 (td, 2H, $J = 7.5, 1.4$ Hz), 7.18 (td, 1H, $J = 7.5, 1.5$), 4.06 (s, 2H), 2.74 (s, 2H), 0.90 (dd, 2H, $J = 6.6, 5.0$ Hz), 0.72 (dd, 2H, $J = 6.6, 5.0$ Hz). ^{13}C NMR (100 MHz) δ 205.2, 137.8, 136.1, 133.9, 130.7, 129.1, 127.6, 56.6, 51.3, 26.2, 17.0. HRMS (EI) calc. for $[\text{C}_{12}\text{H}_{12}\text{OS}]^+$ 204.0609, found 204.0609.



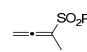
Method B (reaction performed in dichloroethane at 60 °C with 20 mg 5Å sieves; flash column chromatography with 3% EtOAc/hexanes) provided the desired product as a white solid (125 mg, 76% yield), mp 55 – 57 °C. IR: 2957, 2932, 2871, 1709, 1463, 1096, 816 cm^{-1} . ^1H NMR (500 MHz) δ 7.33 (dd, 1H, $J = 8.3, 2.8$ Hz), 7.26-7.22 (m, 1H), 7.09-7.05 (m, 1H), 3.92 (s, 2H), 2.84 (s, 2H), 1.99 (td, 2H, $J = 13.4, 4.2$ Hz), 1.53 (td, 2H, $J = 13.4, 4.2$ Hz), 1.32 (4H, sextet, $J = 7.5$ Hz), 1.23-1.14 (2H, m), 1.06-0.98 (2H, m), 0.90 (6H, t, $J = 7.3$ Hz). ^{13}C NMR (125 MHz) δ 208.7 (C), 139.6 (C), 135.4 (C), 134.0 (C), 133.5 (CH), 130.3 (CH), 127.3 (CH), 55.3 (C), 47.2 (CH₂), 42.9 (CH₂), 33.1 (CH₂), 26.1 (CH₂), 23.5 (CH₂), 14.1 (CH₃). HRMS (EI) calc. for $[\text{C}_{18}\text{H}_{25}\text{ClOS}]^+$ 324.1315, found 324.1310.



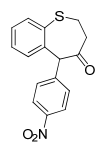
Method A (flash column chromatography with 5% EtOAc/hexanes) provided the desired product as a clear oil (19.0 mg, 94% yield). IR: 1710, 754, 697 cm^{-1} . ^1H NMR (400 MHz) δ 7.54 (d, 1H, $J = 7.2$ Hz), 7.36-7.30 (m, 4H), 7.29-7.23 (m, 4H), 4.36 (dd, 1H, $J = 11.2, 4.4$ Hz), 4.17 (d, 1H, $J = 14.8$ Hz), 3.97 (d, 1H, $J = 14.8$ Hz), 3.27 (dd, 1H, $J = 12.8, 11.2$ Hz), 2.87 (dd, 1H, $J = 12.8, 4.4$ Hz). ^{13}C NMR (100 MHz) δ 206.1, 142.0, 139.4, 135.3, 133.4, 130.3, 129.7, 129.1, 128.4, 128.0, 126.8, 51.1, 50.4, 49.7. HRMS (EI) calc. for $[\text{C}_{16}\text{H}_{14}\text{OS}]^+$ 254.0765, found 254.0766.

 **4.15**

Method B (flash column chromatography with 15% EtOAc/hexanes) provided the desired product as a clear oil (15.0 mg, 99% yield). ¹H NMR (400 MHz) δ 7.91 (d, 2H, *J* = 8 Hz), 7.63 (t, 1H, *J* = 7.3 Hz), 7.55 (t, 2H, *J* = 7.8 Hz), 6.24 (t, 1H, *J* = 6.5 Hz), 5.45 (d, 2H, *J* = 6.5 Hz). ¹³C NMR (100 MHz) δ 209.6, 141.3, 133.8, 129.4, 127.8, 101.1, 84.4.

 **4.17**

Method B (flash column chromatography with 15% EtOAc/hexanes) provided the desired product as a clear oil (23.0 mg, 98% yield). ¹H NMR (400 MHz, CD₂Cl₂) δ 7.88-7.85 (m, 2H), 7.67-7.63 (m, 1H), 7.58-7.54 (m, 2H), 5.32 (q, 2H, *J* = 3.2 Hz), 1.90 (t, 3H, *J* = 3.2 Hz). ¹³C NMR (100 MHz, CD₂Cl₂) δ 208.6, 140.4, 134.0, 129.7, 128.5, 108.6, 83.1, 13.9.



4.19

Method B (flash column chromatography with 2% EtOAc/hexanes) provided the desired product as a pale yellow solid (37.8 mg, 63% yield), mp 134 – 137 °C. IR: 1712, 1515, 1347, 759, 736 cm⁻¹. ¹H NMR (500 MHz) δ 8.18 (d, 2H, *J* = 8.5 Hz), 7.68-7.66 (m, 1H), 7.52 (d, 2H, *J* = 8.5 Hz), 7.33-7.27 (m, 1H), 7.12-7.09 (m, 1H), 5.41 (s, 1H), 3.28-3.21 (m, 1H), 3.13-3.05 (m, 2H), 2.86-2.79 (m, 1H). ¹³C NMR (125 MHz) δ 206.1, 147.3, 144.7, 142.0, 136.1, 132.6, 130.8, 130.5, 129.9, 129.0, 123.7, 64.4, 41.8, 31.9. HRMS (EI) calc. for [C₁₆H₁₃NO₃S]⁺ 299.0616, found 299.0618.



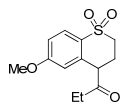
4.21

Following Method A, with the addition of 5 Å molecular sieves to the reaction mixture (flash column chromatography with 2% EtOAc/hexanes), provided the desired product as a clear oil (32.0 mg, 91% yield). ¹H NMR (400 MHz) δ 13.13 (s, 1H), 7.61 (d, 1H, *J* = 8.0 Hz), 7.38-7.32 (m, 2H), 7.20 (td, 1H, *J* = 7.0, 2.0 Hz), 3.77 (s, 3H), 3.54 (bs, 1H), 3.41 (bs, 1H), 2.44 (bs, 2H). ¹³C NMR (100 MHz) δ 177.3, 171.9, 139.8, 135.3, 132.5, 131.1, 128.3, 127.6, 102.5, 52.1, 38.6, 31.9. HRMS submitted.

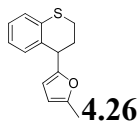
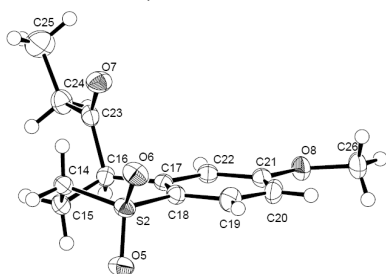


4.23

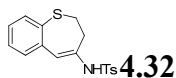
Method B (flash column chromatography with 5% EtOAc/hexanes) provided the desired product as a clear oil (42 mg, 64% yield). IR: 2936, 2360, 1710, 1598, 1478, 1235, 1032 cm⁻¹. ¹H NMR (500 MHz) δ 7.08 (d, 1H, *J* = 8.5 Hz), 6.75 (dd, 1H, *J* = 8.5, 2.5 Hz), 6.63 (d, 1H, *J* = 2.5 Hz), 3.77 (s, 3H), 3.69 (t, 1H, *J* = 4.8 Hz), 3.05-2.98 (m, 1H), 2.92-2.86 (m, 1H), 2.69-2.63 (m, 1H), 2.43 (dq, 1H, *J* = 18.5, 7.0 Hz), 2.34 (dq, 1H, *J* = 18.5, 7.0 Hz), 1.94 (octet, 1H, *J* = 5.0 Hz), 0.99 (t, 3H, *J* = 7.0 Hz). ¹³C NMR (125 MHz) δ 211.5 (C), 157.3 (C), 134.5 (C), 128.8 (CH), 124.6 (C), 116.3 (CH), 113.9 (CH), 55.6 (CH₃), 52.9 (CH), 34.5 (CH₂), 25.7 (CH₂), 24.6 (CH₂), 8.0 (CH₃). HRMS (EI) calc. for [C₁₃H₁₆O₂S]⁺ 236.0871, found 236.0875. Anal Calcd. For C₁₃H₁₆O₂S: C, 66.07. H, 6.82. Found: C, 65.05. H, 7.01.



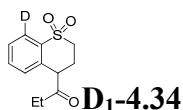
To a solution of sulfide **4.23** (26 mg, 0.11 mmol) in MeCN:H₂O 1:1 (5 mL) was added Oxone® (203 mg, 0.33 mmol) and the mixture was stirred for 3 hours. The reaction was diluted into 10 mL water and extracted with EtOAc (2 x 10 mL). The combined organic fractions were dried (MgSO₄), filtered and concentrated). Flash column chromatography (15% → 30% EtOAc/hexanes eluent) provided the desired sulfone (17.1 mg, 57% yield). X-ray quality crystals were grown from hexanes/ether. ¹H NMR (400 MHz) δ 7.90 (d, 1H, *J* = 8.6 Hz), 6.98 (dd, 1H, *J* = 8.6, 2.4 Hz), 7.62 (d, 2H, *J* = 2.4 Hz), 3.95 (t, 1H, *J* = 5.8 Hz), 3.83 (s, 3H), 3.46 (ddd, 1H, *J* = 14.0, 9.6, 4.6 Hz), 3.23 (ddd, 1H, *J* = 14.0, 7.0, 4.2 Hz), 2.73-2.60 (m, 2H), 2.59-2.46 (m, 2H), 1.06 (t, 3H, 7.4 Hz). ¹³C NMR (100 MHz) δ 209.1, 162.6, 136.3, 131.3, 126.6, 115.1, 114.3, 55.8, 50.8, 48.0, 34.7, 23.8, 8.0. X-ray structure (see Appendix for more information):



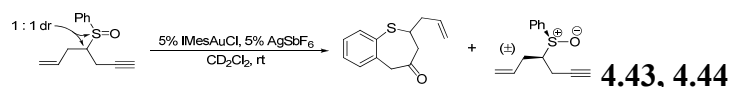
Method B, (flash column chromatography with 1% EtOAc/hexanes) provided the desired product as a clear oil (29.0 mg, 56% yield). ¹H NMR (400 MHz) δ 7.15-7.07 (m, 2H), 7.05-7.02 (m, 1H), 7.00-6.95 (m, 1H), 5.83 (d, 1H, *J* = 2.9 Hz), 5.61 (d, 1H, *J* = 2.9 Hz), 2.98 (td, 1H, *J* = 11.5, 3.1 Hz), 2.87-2.81 (m, 1H), 2.60-2.52 (m, 1H), 2.27 (s, 3H), 2.23-2.14 (m, 1H). ¹³C NMR (100 MHz) δ 155.3, 151.3, 133.4, 133.2, 131.3, 127.3, 126.7, 124.0, 109.0, 106.2, 38.4, 27.3, 23.8, 13.8. HRMS (EI) calc. for [C₁₄H₁₄OS]⁺ 230.0765, found 230.0766.



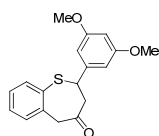
Following Method A, with the addition of 5Å molecular sieves to the reaction mixture, (flash column chromatography with 10% EtOAc/hexanes) provided the desired product as a clear oil (30.1 mg, 88% yield). IR: 3356, 1710, 1330, 1305, 1161 cm⁻¹. ¹H NMR (500 MHz) δ 7.82 (d, 2H, *J* = 8.0 Hz), 7.36 (d, 1H, *J* = 8.0 Hz), 7.31 (d, 2H, *J* = 8.0 Hz), 7.17 (t, 1H, *J* = 7.5 Hz), 7.10 (d, 1H, *J* = 7.5 Hz), 7.06 (t, 1H, *J* = 7.5 Hz), 6.48 (s, 1H), 6.37 (bs, 1H), 2.96 (t, 2H, *J* = 5.9 Hz), 2.59 (t, 2H, *J* = 5.9 Hz). ¹³C NMR (125 MHz) δ 144.3, 137.3, 137.2, 136.4, 136.3, 132.7, 132.4, 130.0, 127.7, 127.3, 126.8, 121.3, 37.1, 34.1, 21.8. HRMS (FAB) calc. for [C₁₇H₁₇NO₂S₂]⁺ 331.0701, found 331.0704.



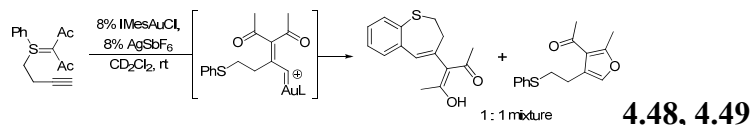
Method B (stirred at room temperature; flash column chromatography with 2% EtOAc/hexanes), provided the benzothiopyran contaminated with 15% of an inseparable impurity (20.0 mg). This mixture was dissolved in DCM (1 mL), cooled to 0°C, and treated with mCPBA (71 mg, 0.29 mmol). After stirring for 1 hour, the mixture was quenched with saturated Na₂SO₃. The organic layer was separated, dried (MgSO₄), and concentrated. Flash column chromatography (20% EtOAc/hexanes eluent) provided the desired sulfone **D₁-35** as a clear oil (14 mg, 43% yield over two steps). ¹H NMR (400 MHz) δ 7.98 (d, 0.47H, *J* = 9.2 Hz), 7.55-7.51 (m, 2H), 7.18 (d, 1H, *J* = 6.8 Hz) 4.02 (t, 1H, *J* = 5.4 Hz), 3.56-3.49 (m, 1H), 3.31-3.24 (m, 1H), 2.75-2.70 (m, 2H), 2.64-2.44 (m, 2H), 1.06 (t, 3H, *J* = 7.2 Hz). ¹³C NMR (100 MHz) δ 209.2, 134.1, 132.8, 130.0, 129.1, 129.0, 124.5, 50.5, 47.9, 34.9, 23.7, 8.0. HRMS (EI) calc. for [C₁₂H₁₃DO₃S]⁺ 239.0726, found 239.0746.



Reaction was monitored by ¹H-NMR versus an internal standard (Method A), after 15 minutes benzothiopyne **4.43** was formed in 47% yield, leaving 47% of sulfoxide **4.44** unreacted. Flash column chromatography first provided benzothiopyne **4.43**. ¹H NMR (500 MHz) δ 7.55 (d, 1H, *J* = 8 Hz), 7.32-7.22 (m, 3H), 5.78 (ddt, 1H, *J* = 17.5, 10.0, 7.5 Hz), 5.11 (d, 1H, *J* = 10 Hz), 5.07 (d, 1H, *J* = 17.5 Hz), 4.01 (d, 1H, *J* = 14.5 Hz), 3.84 (d, 1H, *J* = 14.5 Hz), 3.29-3.23 (m, 1H), 2.79 (dd, 1H, *J* = 12, 4.5 Hz), 2.65 (dd, 1H, *J* = 12, 8.5 Hz), 2.27 (app nonet, 2H, *J* = 7.5 Hz). Followed by diastereopure unreacted sulfoxide **4.44**. ¹H NMR (500 MHz) δ 7.67-7.64 (m, 2H), 7.59-7.52 (m, 3H), 5.71 (ddt, 1H, *J* = 16.5, 10.0, 7.5 Hz), 5.15 (d, 1H, *J* = 17.5 Hz), 5.12 (d, 1H, *J* = 10.0 Hz), 2.76 (app pentet, 1H, *J* = 6.7 Hz), 2.60 (ddd, 1H, *J* = 17.5, 6.5, 2.5 Hz), 2.49 (app t, 2H, *J* = 7.3 Hz), 2.29 (ddd, 1H, 17.5 6.0, 2.5 Hz), 2.09 (t, 1H, *J* = 2.5 Hz).



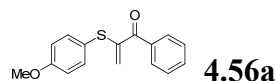
Method A (flash column chromatography with 10% EtOAc/hexanes) provided the desired product (32 mg, 91% yield). ¹H NMR (400 MHz) δ 7.49 (d, 1H, *J* = 7.6 Hz), 7.29-7.17 (m, 3H), 6.32 (d, 2H, *J* = 2.4 Hz), 6.29 (t, 1H, *J* = 2.4 Hz), 4.19 (dd, 1H, *J* = 11.2, 4 Hz), 4.06 (d, 1H, *J* = 14.8 Hz), 3.90 (d, 1H, *J* = 14.8 Hz), 3.69 (s, 6H), 3.16 (app t, 1H, *J* = 12 Hz), 2.77 (dd, 1H, *J* = 12.8 Hz). ¹³C NMR (100 MHz) δ 206.0, 161.2, 144.3, 139.5, 135.4, 133.3, 130.3, 129.8, 128.4, 104.8, 99.9, 55.5, 51.1, 50.3, 49.8.



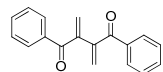
To a solution of sulfur ylide **4.47** (39 mg, 0.15 mmol) in CD₂Cl₂ (0.3 mL) was added a solution of IMeSAuCl (8 mol %) and AgSbF₆ (8 mol %) in CD₂Cl₂ (0.2 mL). The reaction was stirred overnight at room temperature. column chromatography provided benzothiopyne **4.48** (10 mg, 26% yield): ¹H NMR (400 MHz) δ 16.46 (s, 1H), 7.46 (d, 1H, *J* = 7.6 Hz), 7.24-7.19 (m, 2H), 7.15-7.11 (m, 1H), 6.53 (s, 1H), 3.18 (t, 2H, *J* = 6 Hz), 3.25 (t, 2H, *J* = 6 Hz), 2.19 (s, 6H). ¹³C

NMR (100 MHz) δ 190.5, 139.7, 138.3, 137.0, 134.5, 132.8, 132.3, 127.2, 127.1, 118.3, 39.7, 35.3, 23.5. HRMS (EI) calc. for $[\text{C}_{15}\text{H}_{16}\text{O}_2\text{S}]^+$ 260.0871, found 260.0872. Followed by furan **4.49** (10 mg, 26% yield), 7.35 (d, 2H, $J = 7.6$ Hz), 7.30-7.25 (m, 2H), 7.16 (t, 1H, $J = 7.2$ Hz), 7.09 (s, 1H), 3.15 (t, 2H, $J = 7.2$ Hz), 2.93 (t, 2H, $J = 7.2$ Hz), 2.56 (s, 3H), 2.41 (s, 3H). ^{13}C NMR (100 MHz) δ 194.5, 159.1, 138.7, 136.7, 129.3, 129.0, 126.0, 124.1, 122.2, 33.4, 31.0, 25.4, 15.9. HRMS (EI) calc. for $[\text{C}_{15}\text{H}_{16}\text{O}_2\text{S}]^+$ 260.0871, found 260.0868.

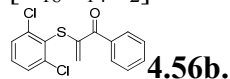
Representative procedure for the Me_2SAuCl catalyzed rearrangement of primary propargyl sulfoxides to α -thioenones.



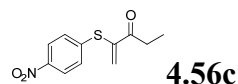
4.54a (72 mg, 0.27 mmol) was dissolved in 5.35 mL DCM (0.050 M). Me_2SAuCl (7.9 mg, 0.027 mmol) was added and the reaction was stirred at 35 °C and monitored periodically by TLC. Upon completion (22 hours), the reaction mixture was filtered through a short plug of silica gel, eluting with DCM, and concentrated. Column chromatography of the resulting oil (10% \rightarrow 40% DCM in hexanes) provided **4.56a** as a pale yellow oil (48 mg, 67% yield). IR: 2837, 1658, 1592, 1493, 1249 cm^{-1} . ^1H NMR (400 MHz) δ 7.78 (d, 2H, $J = 8.8$ Hz), 7.57-7.51 (m, 1H), 7.46-7.41 (m, 4H), 7.32 (d, 2H, $J = 8.8$ Hz), 5.74 (s, 1H), 5.41 (s, 1H), 3.82 (s, 3H). ^{13}C NMR (100 MHz) δ 194.2 (C), 160.7 (C), 147.9 (C), 137.1 (CH), 136.8 (C), 132.9 (CH), 129.7 (CH), 128.4 (CH), 121.6 (CH_2), 121.2 (C), 115.4 (CH), 55.5 (CH_3). HRMS (EI) calc. for $[\text{C}_{16}\text{H}_{14}\text{O}_2\text{S}]^+$ 270.0715, found 270.0715.



4.67a was also isolated as a small impurity (1.8 mg, 5% yield). Larger amounts can be obtained by running the reaction at higher concentrations (*vide infra*). **4.67a** was isolated as a white solid, mp 77 – 79 °C. IR: 3062, 1653, 1597, 1448 cm^{-1} . ^1H NMR (300 MHz) δ 7.92-7.89 (m, 4H), 7.57 (tt, 2H, $J = 7.4, 1.2$ Hz), 7.46 (t, 4H, $J = 7.4$ Hz), 6.15 (s, 2H), 5.77 (s, 2H). ^{13}C NMR (75 MHz) δ 196.7, 146.3, 137.2, 133.1, 130.0, 128.6, 126.1. HRMS (EI) calc. for $[\text{C}_{18}\text{H}_{14}\text{O}_2]^+$ 262.0994, found 262.0994.

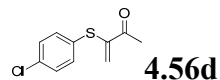


Analogous to the representative procedure, treating **4.54b** (27 mg, 0.086 mmol) with Me_2SAuCl (2.2 mg, 0.0075 mmol) yielded the title compound as a clear oil (26 mg, 95% yield). IR: 1655, 1587, 1555, 1425 cm^{-1} . ^1H NMR (500 MHz) δ 7.80 (d, 2H, $J = 7.5$ Hz), 7.64 (t, 1H, $J = 7.5$ Hz), 7.47-7.43 (m, 4H), 7.31-7.27 (m, 1H), 5.76 (d, 1H, $J = 1.5$ Hz), 5.34 (d, 1H, $J = 1.5$ Hz). ^{13}C NMR (125 MHz) δ 193.6 (C), 143.5 (C), 142.1 (C), 136.7 (C), 133.0 (CH), 131.4 (CH), 129.9 (C), 129.8 (CH), 129.2 (CH), 128.5 (CH), 122.0 (CH_2). HRMS (EI) calc. for $[\text{C}_{15}\text{H}_{10}\text{Cl}_2\text{OS}]^+$ 307.9829, found 307.9820.

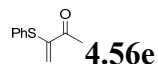


Analogous to the representative procedure, treating **4.54c** (70 mg, 0.30 mmol) with Me_2SAuCl (8.7 mg, 0.030 mmol) yielded the title compound as a white solid (64 mg, 91% yield), mp 44 – 46 °C. ^1H NMR (400 MHz) δ 8.17-8.14 (m, 2H), 7.44-7.41 (m, 2H), 6.51 (s, 1H), 5.94 (s, 1H), 2.76 (q, 2H, $J = 7.2$ Hz), 1.09 (t, 3H, $J = 7.2$ Hz). ^{13}C NMR (100 MHz) δ 198.4, 147.0, 143.4,

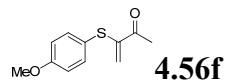
143.1, 130.8, 129.1, 124.5, 32.1, 8.3. HRMS (EI) calc. for $[C_{11}H_{11}NO_3S]^+$ 237.0460, found 237.0462.



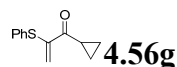
Analogous to the representative procedure, treating **4.54d** (65 mg, 0.31 mmol) with Me_2SAuCl (9.0 mg, 0.031 mmol) yielded the title compound as a white solid (58 mg, 89% yield), mp 70 – 72 °C. IR: 1679, 1580, 1476, 1092 cm^{-1} . 1H NMR (400 MHz) δ 7.40-7.35 (m, 4H), 6.16 (d, 1H, J = 1.4 Hz), 5.35 (d, 1H, J = 1.4 Hz), 2.41 (s, 3H). ^{13}C NMR (100 MHz) δ 195.9 (C), 147.8 (C), 137.6 (C), 135.9 (CH), 135.4 (C), 130.1 (CH), 122.2 (CH₂), 26.4 (CH₃). HRMS (EI) calc. for $[C_{16}H_{14}OS]^+$ 212.0063, found 212.0060.



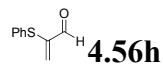
Analogous to the representative procedure, treating **4.54e** (76 mg, 0.43 mmol) with Me_2SAuCl (12.6 mg, 0.043 mmol) yielded the title compound as a yellow oil (55 mg, 72% yield). 1H NMR (400 MHz) δ 7.47-7.37 (m, 5H), 6.13 (d, 1H, J = 1.2 Hz), 5.32 (d, 1H, J = 1.2 Hz), 2.41 (s, 3H). ^{13}C NMR (75 MHz) δ 196.2, 148.2, 134.7, 131.5, 129.9, 129.1, 121.9, 26.5. Spectral data matches literature values.²⁹



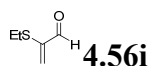
Analogous to the representative procedure, treating **4.54f** (73 mg, 0.35 mmol) with Me_2SAuCl (10.3 mg, 0.035 mmol) yielded the title compound as a clear oil (58 mg, 79% yield). IR: 1716, 1648, 1592, 1493 cm^{-1} . 1H NMR (400 MHz) δ 7.39-7.36 (m, 2H), 6.93-6.91 (m, 2H), 6.05 (d, 1H, J = 1.6 Hz), 5.16 (d, 1H, J = 1.6 Hz), 3.81 (s, 3H), 2.40 (s, 3H). ^{13}C NMR (100 MHz) δ 196.2 (C), 160.7 (C), 149.5 (C), 137.1 (CH), 121.3 (C), 120.1 (CH₂), 115.5 (CH), 55.5 (CH₃), 26.4 (CH₃). m/z 208 (M^+). HRMS (EI) calc. for $[C_{11}H_{12}O_2S]^+$ 208.0558, found 208.0555.



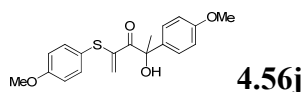
Analogous to the representative procedure, treating **4.54g** (40 mg, 0.20 mmol) with Me_2SAuCl (2.9 mg, 0.010 mmol) yielded the title compound as a clear oil (34 mg, 85% yield). 1H NMR (500 MHz) δ 7.46-7.44 (m, 2H), 7.40-7.33 (m, 3H), 6.26 (s, 1H), 5.40 (s, 1H), 2.48 (septet, 1H, J = 4.2 Hz), 1.11-1.08 (m, 2H), 0.94-0.90 (m, 2H). ^{13}C NMR (125 MHz) δ 198.5, 147.9, 134.1, 132.1, 129.8, 128.8, 121.5, 17.5, 12.3. HRMS (EI) calc. for $[C_{12}H_{12}OS]^+$ 204.0609, found 204.0609.



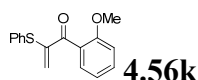
Analogous to the representative procedure, treating **4.54h** (69 mg, 0.42 mmol) with Me_2SAuCl (12 mg, 0.042 mmol) yielded the title compound as a yellow oil (35 mg, 51% yield). IR: 2825, 1732, 1694, 1581, 1475, 1147 cm^{-1} . 1H NMR (400 MHz) δ 9.57 (s, 1H), 7.51-7.48 (m, 2H), 7.43-7.39 (m, 3H), 6.13 (d, 1H, J = 0.8 Hz), 5.73 (d, 1H, J = 0.8 Hz). ^{13}C NMR (100 MHz) δ 189.9 (CH), 149.2 (C), 135.1 (CH), 130.0 (CH), 129.5 (C), 129.5 (CH), 128.8 (CH₂). HRMS (EI) calc. for $[C_9H_8OS]^+$ 164.0296, found 164.0291.



Sulfoxide **4.54i** (20 mg, 0.17 mmol) was dissolved in CD₂Cl₂ with 1,3,5-trinitrobenzene (~ 5 mg). After acquisition of a ¹H-NMR spectrum, Me₂SAuCl (2.5 mg, 0.0086 mmol) was added and the mixture was stirred for 3 hours at 35 °C. Acquisition of an additional ¹H-NMR spectrum revealed a 73% yield of the title compound (based on 1,3,5-trinitrobenzene internal standard). ¹H NMR (400 MHz, CD₂Cl₂) δ 9.58 (s, 1H), 6.80 (s, 1H), 6.33 (s, 1H), 2.70 (q, 2H, *J* = 7.2 Hz), 1.30 (t, 3H, *J* = 7.2 Hz).

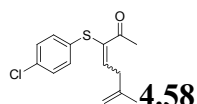


Analogous to the representative procedure, treating **4.54j** (75 mg, 0.22 mmol) with Me₂SAuCl (6.4 mg, 0.022 mmol) yielded the title compound as a yellow oil (20 mg, 27% yield). IR: 3448, 1654, 1592, 1508, 1494, 1249 cm⁻¹. ¹H NMR (300 MHz) δ 7.31-7.25 (m, 4H), 6.88-6.84 (m, 4H), 5.58 (d, 1H, *J* = 1.5 Hz), 5.12 (d, 1H, *J* = 1.5 Hz), 4.40 (s, 1H), 3.79 (s, 3H), 3.78 (s, 3H), 1.81 (s, 3H). ¹³C NMR (100 MHz) δ 200.6 (C), 160.9 (C), 159.7 (C), 144.5 (C), 137.2 (CH), 134.4 (C), 127.4 (CH), 123.2 (CH₂), 121.0 (C), 115.5 (CH), 114.4 (CH), 79.5 (C), 55.6 (CH₃), 55.5 (CH₃), 26.6 (CH₃). HRMS (FAB) calc. for [C₁₉H₂₀O₄S]⁺ 344.1082, found 344.1089.



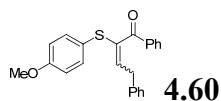
Analogous to the representative procedure, treating **4.54k** (21 mg, 0.075 mmol) with Me₂SAuCl (2.3 mg, 0.0075 mmol) yielded the title compound as a clear oil containing 5% of an unknown impurity (1.5 mg, 7% yield). ¹H NMR (500 MHz) δ 7.49-7.47 (m, 2H), 7.42-7.29 (m, 1H), 7.37-7.33 (m, 3H), 7.25-7.23 (m, 1H), 6.97-6.91 (m, 2H), 5.88 (d, 1H, *J* = 0.5 Hz), 5.48 (d, 1H, *J* = 0.5 Hz), 3.81 (s, 3H). ¹³C NMR (125 MHz) δ 194.1, 157.5, 148.2, 134.4, 132.3, 132.0, 129.7, 129.6, 128.7, 128.1, 125.4, 120.4, 111.6, 55.9. HRMS (EI) calc. for [C₁₆H₁₄O₂S]⁺ 270.0715, found 270.0710.

Representative Procedure for the Me₂SAuCl catalyzed rearrangement of secondary and tertiary propargyl sulfoxides to α-thioenones.

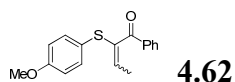


Sulfoxide **4.57** (46 mg, 0.17 mmol) was dissolved in DCM (0.1 M). Me₂SAuCl (2.5 mg, 0.05 equiv) was added and the reaction was stirred at room temperature for 15 minutes. The reaction mixture was filtered through a short plug of silica gel, eluting with DCM, and concentrated. Flash column chromatography (10% → 40% DCM in hexanes) yielded first the less polar, major (*E*)-**4.58** isomer as a clear oil (28 mg, 61% yield). ¹H NMR (500 MHz) δ 7.26-7.23 (m, 2H), 7.17-7.14 (m, 2H), 6.44 (t, 1H, *J* = 7.6 Hz), 4.81 (s, 1H), 4.74 (s, 1H), 3.11 (d, 2H, *J* = 7.6 Hz), 2.24 (s, 3H), 1.76 (s, 3H). ¹³C NMR (125 MHz) δ 200.0, 145.8, 143.0, 133.9, 133.8, 132.9, 129.9, 129.7, 112.2, 38.6, 29.6, 23.0. HRMS (EI) calc. for [C₁₄H₁₅O₂SCl]⁺ 266.0532, found 266.0533. Followed by the more polar, minor (*Z*)-**4.58** isomer as a clear oil (18 mg, 39% yield). ¹H NMR (500 MHz) δ 7.26 (t, 1H, *J* = 7.5 Hz), 7.22 (dd, 2H, *J* = 6.8, 2.0 Hz), 7.09 (dd, 2H, *J* = 6.8, 2.0 Hz), 4.83 (s, 1H), 4.73 (s, 1H), 3.22 (d, 2H, *J* = 7.5 Hz), 2.29 (s, 3H), 1.77 (s, 3H). ¹³C

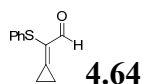
NMR (125 MHz) δ 197.2, 149.2, 142.1, 135.7, 134.3, 132.4, 129.6, 129.3, 112.7, 39.1, 27.7, 23.2. HRMS (EI) calc. for $[C_{23}H_{20}O_2S]^+$ 360.1184, found 360.1188.



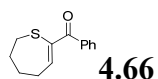
Analogous to the representative procedure, treating sulfoxide **4.59** (40 mg, 0.11 mmol) with Me_2SAuCl (1.6 mg, 0.05 equiv) yielded a 2.5 : 1 mixture of E and Z isomers. Flash column chromatography of the crude reaction mixture (20% \rightarrow 40% DCM in hexanes) provided an inseparable mixture of E and Z isomers as a faint yellow oil (36 mg, 90%). Major isomer 1H NMR (500 MHz) δ 7.67 (d, 2H, $J = 7.5$ Hz), 7.50 (t, 1H, $J = 7.5$ Hz), 7.38-7.22 (m, 9H), 6.72 (d, 2H, $J = 8.7$ Hz), 6.63 (t, 1H, $J = 7.5$ Hz), 3.93 (d, 2H, $J = 7.5$ Hz), 3.74 (s, 3H). Minor isomer 1H NMR (500 MHz) δ 7.88 (d, 2H, $J = 7.5$ Hz), 7.56 (t, 1H, $J = 7.5$ Hz), 7.43 (t, 2H, $J = 7.5$ Hz), 7.38-7.22 (m, 5H), 7.14 (d, 2H, $J = 7.5$ Hz), 6.76 (d, 2H, $J = 8.5$ Hz), 6.30 (t, 1H, $J = 7.8$ Hz), 3.76 (s, 3H), 3.41 (d, 2H, $J = 7.8$ Hz). ^{13}C NMR (125 MHz) δ 194.4, 194.2, 160.0, 159.6, 143.0, 139.0, 138.8, 138.1, 137.5, 135.6, 135.1, 134.0, 133.7, 132.7, 129.8, 129.6, 129.0, 128.8, 128.7, 128.7, 128.3, 126.8, 126.7, 123.7, 114.9, 114.8, 55.5, 36.8, 36.6. HRMS (EI) calc. for $[C_{23}H_{20}O_2S]^+$ 360.1184, found 360.1188.



Analogous to the representative procedure, treating sulfoxide **4.61** (37 mg, 0.14 mmol) with Me_2SAuCl (4.1 mg, 0.1 equiv) yielded a 2.5 : 1 mixture of E and Z isomers. Flash column chromatography of the crude reaction mixture (20% \rightarrow 40% DCM in hexanes) provided an inseparable mixture of E and Z isomers as a faint yellow oil (27 mg, 73%). Major isomer 1H NMR (500 MHz) δ 7.67 (d, 2H, $J = 7.5$ Hz), 7.50 (t, 1H, $J = 7.5$ Hz), 7.38 (t, 2H, $J = 7.8$ Hz), 7.21-7.18 (m, 2H), 6.73-6.69 (m, 2H), 6.61 (q, 1H, $J = 6.8$ Hz), 3.73 (s, 3H), 2.14 (d, 3H, $J = 6.8$ Hz). Minor isomer 1H NMR (500 MHz) δ 7.83 (d, 2H, $J = 7.5$ Hz), 7.54 (t, 1H, $J = 7.5$ Hz), 7.42 (t, 2H, $J = 7.8$ Hz), 7.26-7.23 (m, 2H), 6.77-6.75 (m, 2H), 6.27 (q, 1H, $J = 7.3$ Hz), 3.76 (s, 3H), 1.72 (d, 3H, $J = 7.3$ Hz). ^{13}C NMR (125 MHz) δ 194.8, 194.4, 159.9, 159.3, 141.3, 138.6, 137.7, 136.2, 134.8, 134.7, 133.6, 133.5, 133.3, 132.5, 129.6, 129.6, 128.7, 124.2, 123.1, 114.8, 114.8, 55.5, 55.5, 16.4, 16.3.



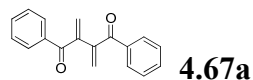
Analogous to the representative procedure, treating sulfoxide **4.63** (19.0 mg, 0.100 mmol) with Me_2SAuCl (1.5 mg, 0.05 equiv) followed by flash column chromatography (5% EtOAc/hexanes) yielded the title compound as a clear oil (16.4 mg, 86% yield). 1H NMR (400 MHz) δ 9.14 (s, 1H), 7.58-7.54 (m, 2H), 7.42-7.40 (m, 3H), 2.64 (t, 1H, $J = 3.4$ Hz), 2.55 (t, 1H, $J = 3.4$ Hz). ^{13}C NMR (100 MHz) δ 184.1, 158.7, 137.2, 134.3, 130.0, 129.9, 129.6, 31.7, 25.1. HRMS (EI) calc. for $[C_{11}H_{10}OS]^+$ 190.0452, found 190.0454.



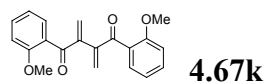
A solution of sulfoxide **4.55** (54 mg, 0.25 mmol) and $AuCl$ (5.8 mg, 0.1 equiv) in CH_2Cl_2 (0.2 mL) was stirred overnight at room temperature. Purification on silica gel provided the desired ring-expansion product (12.8 mg, 24% yield). 1H NMR (500 MHz) δ 7.70 (d, 1H, $J = 7.5$ Hz),

7.53 (t, 1H, $J = 7.5$ Hz), 7.43 (t, 2H, $J = 7.5$ Hz), 6.89 (t, 1H, $J = 13.5$ Hz), 2.84-2.81 (m, 2H), 2.59-2.55 (m, 2H), 2.10-2.04 (m, 2H), 1.75 (app pentet, 2H, $J = 5.8$ Hz). ^{13}C NMR (125 MHz) δ 195.6, 146.8, 142.1, 137.2, 132.4, 129.5, 128.4, 34.2, 32.1, 29.8, 23.9.

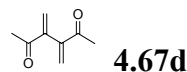
Representative Procedure for the AuCl catalyzed rearrangement and dimerization of propargyl sulfoxides.



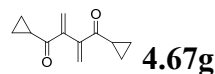
4.54a (76 mg, 0.28 mmol) was placed in a scintillation vial and dissolved in 150 μL DCM. AuCl (6.5 mg, 0.028 mmol) was added and the reaction was stirred at room temperature. Conversion was monitored by TLC. After reaction completion (3 hours), the crude reaction mixture was loaded onto a silica gel column and eluted with 10% \rightarrow 60% DCM in hexanes. **4.67a** was isolated as a white solid (30 mg, 81% yield), mp 77 – 79 $^{\circ}\text{C}$. IR: 3062, 1653, 1597, 1448 cm^{-1} . ^1H NMR (300 MHz) δ 7.92-7.89 (m, 4H), 7.57 (tt, 2H, $J = 7.4, 1.2$ Hz), 7.46 (t, 4H, $J = 7.4$ Hz), 6.15 (s, 2H), 5.77 (s, 2H). ^{13}C NMR (75 MHz) δ 196.7, 146.3, 137.2, 133.1, 130.0, 128.6, 126.1. HRMS (EI) calc. for $[\text{C}_{18}\text{H}_{14}\text{O}_2]^+$ 262.0994, found 262.0994.



Analogous to the representative procedure, treating **4.54k** (52 mg, 0.19 mmol) with AuCl (4.4 mg, 0.019 mmol) in 100 μL DCM for 3 hours yielded the title compound as a pale yellow solid slowly fading to green (18 mg, 59% yield), mp 120 – 123 $^{\circ}\text{C}$. IR: 2838, 1665, 1598, 1251 cm^{-1} . ^1H NMR (400 MHz) δ 7.42-7.37 (m, 4H), 6.97-6.91 (m, 4H), 6.07 (s, 2H), 5.83 (s, 2H), 3.79 (s, 6H). ^{13}C NMR (100 MHz) δ 196.0 (C), 157.7 (C), 147.5 (C), 132.2 (CH), 130.6 (CH), 128.7 (CH₂), 128.4 (C), 120.3 (CH), 111.6 (CH), 55.9 (CH₃). HRMS (EI) calc. for $[\text{C}_{20}\text{H}_{18}\text{O}_4]^+$ 322.1205, found 322.1205.

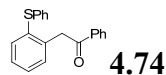


Analogous to the representative procedure, treating **4.54e** (89 mg, 0.50 mmol) with AuCl (11.6 mg, 0.050 mmol) in 250 μL DCM for 5 minutes yielded the title compound as a yellow solid fading to brown (24 mg, 70% yield from **4.54e**), mp 52-55 $^{\circ}\text{C}$. IR: 3002, 1920, 1673, 1365, 1106 cm^{-1} . ^1H NMR (400 MHz) δ 6.06 (s, 2H), 5.91 (s, 2H), 2.36 (s, 6H). ^{13}C NMR (100 MHz) δ 198.7, 148.2, 126.6, 26.4.

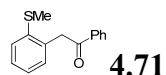


Analogous to the representative procedure, treating **4.54g** (50 mg, 0.25 mmol) with AuCl (5.7 mg, 0.025 mmol, 0.1 equiv) in 150 μL DCM for 5 minutes yielded the title compound as a clear oil (15.2 mg, 67%). ^1H NMR (500 MHz) δ 6.18 (s, 2H), 2.30 (app septet, 2H, $J = 4.1$ Hz), 1.09 (app pentet, 4H, $J = 3.9$ Hz), 0.95-0.91 (m, 4H). ^{13}C NMR (125 MHz) δ 200.9, 148.4, 125.2, 17.6, 11.9. HRMS (EI) calc. for $[\text{C}_{12}\text{H}_{14}\text{O}_2]^+$ 190.0994, found 190.0997.

Representative Procedure for the Gold(I) or Triflic Acid Catalyzed Alkylation of Aryl Sulfoxides with Alkynes



Diphenylsulfoxide (37 mg, 0.18 mmol) and phenyl acetylene (40 μ L, 0.37 mmol, 2 equiv) were dissolved in 0.4 mL nitromethane in a scintillation vial equipped with a stir bar. Triflic acid (5 mol%, 0.64 M in nitromethane, 14 μ L) (or 5 mol% dppm(AuCl)₂ and 10 mol% AgSbF₆) was added. The vial was sealed with Teflon tape, partially submerged in an 80 °C oil bath, and stirred overnight. The reaction mixture was then cooled, filtered through a short plug of silica with dichloromethane and concentrated. Purification on silica gel (15 : 4 : 1 hexanes : dichloromethane : ethyl acetate) provided the title compound as a yellow oil (32 mg, 58% yield). IR: 3059, 1686, 1581 cm^{-1} . ¹H NMR (300 MHz) δ 7.97 (d, 2H, J = 7.2 Hz), 7.58-7.52 (m, 1H), 7.48-7.41 (m, 3H), 7.33-7.14 (m, 8H), 4.49 (s, 2H). ¹³C NMR (75 MHz) δ 197.3, 137.8, 136.9, 136.9, 134.8, 134.2, 133.3, 131.5, 129.4, 129.3, 128.7, 128.7, 128.6, 128.3, 126.5, 44.0. HRMS (EI) calc. for [C₂₀H₁₆OS]⁺ 304.0922, found 304.0913.

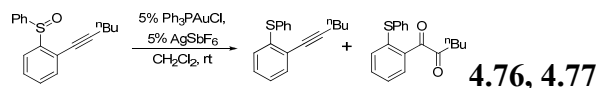


Analogous to the representative procedure, treating phenylmethylsulfoxide (27 mg, 0.45 mmol) and phenyl acetylene (99 μ L, 0.90 mmol) with triflic acid (5 mol%, 0.64 M in nitromethane, 35 μ L) yielded the title compound as a yellow oil (24 mg, 31%). IR: 2918, 1687, 1596, 1447, 1331, 1216 cm^{-1} . ¹H NMR (300 MHz) δ 8.06 (d, 2H, J = 7.2 Hz), 7.59-7.51 (m, 1H), 7.50-7.45 (m, 2H), 7.35-7.15 (m, 4H), 4.45 (s, 2H), 2.43 (s, 3H). ¹³C NMR (75 MHz) δ 197.4, 162.5, 138.0, 137.0, 134.2, 133.3, 130.7, 128.6, 128.1, 127.6, 125.8, 43.72, 16.89. HRMS (EI) calc. for [C₁₅H₁₄OS]⁺ 242.0765, found 242.0760.

Preparation of Methyl(*p*-tolyl)sulfide gold(I) chloride.

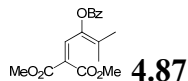


Synthesis was carried out as for the analogous dimethylsulfide gold(I) chloride complex.⁹ Methyl(*p*-tolyl)sulfide (2.13 mL, 15.8 mmol) was added drop wise to a solution of hydrogen tetrachloroaurate (1.08 g, 3.17 mmol) in 20 mL methanol. After addition, the mixture was stirred for one hour. The resulting white precipitate was filtered off and dried under vacuum to yield **14** as a fluffy white solid (1.17 g, 73% yield). ¹H NMR (500 MHz) δ 7.59 (d, 2H, J = 8.0 Hz), 7.26 (d, 2H, J = 8.0 Hz), 2.97 (s, 3H), 2.39 (s, 3H). Anal Calcd. For C₈H₁₀AuClS: C, 25.92. H, 2.72. Found: C, 25.87. H, 2.63.

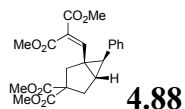


To a solution of sulfoxide **4.75** (16 mg, 0.057 mmol, 1 equiv) in CD₂Cl₂ was added a solution of Ph₃PAuCl (0.1 equiv) and AgOTf (0.1 equiv). After 2 hours at room temperature the crude reaction mixture was purified on silica gel. First to elute was sulfide **4.76** (3.6 mg, 24% yield): ¹H NMR (500 MHz, CD₂Cl₂) δ 7.44-7.31 (m, 6H), 7.15-7.09 (m, 2H), 6.98-6.95 (m, 1H), 2.43 (t, 2H, J = 7 Hz), 1.56 (app pentet, 2H, J = 7 Hz), 1.48 (app sextet, 2H, J = 7.5 Hz), 0.93 (t, 3H, J = 7.3 Hz). Followed by diketone **4.77** (7 mg, 41%): ¹H NMR (500 MHz, CD₂Cl₂) δ 7.69 (dd, 1H, J = 8, 1.5 Hz), 7.43 (td, 1H, J = 7.8, 1.5 Hz), 7.4-7.32 (m, 6H), 7.18 (d, 1H, J = 8 Hz), 2.93 (t, 2H,

$J = 7.5$ Hz), 1.64 (app pentet, 2H, $J = 7.5$ Hz), 1.38 (app sextet, 2H, $J = 7.5$ Hz), 0.92 (t, 3H, $J = 7.3$ Hz). ^{13}C NMR (125 MHz, CD_2Cl_2) δ 202.6, 194.9, 139.6, 135.0, 134.7, 133.8, 132.6, 132.1, 132.1, 130.1, 128.8, 127.2, 38.3, 25.6, 22.8, 14.2. The diketone is formed exclusively if two equivalents of diphenylsulfoxide are added to the reaction prior to addition of the catalyst mixture.



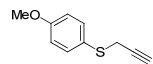
To a solution of sulfur ylide **4.86** (110 mg, 0.35 mmol, 1.75 equiv) and propargyl benzoate **4.83b** (37 mg, 0.20 mmol, 1 equiv) in CH_2Cl_2 (0.5 mL) was added a solution of IMesAuCl (5.3 mg, 0.01 mmol, 0.05 equiv) and AgSbF_6 (3.4 mg, 0.01 mmol, 0.05 equiv) in CH_2Cl_2 (0.3 mL). After 24 hours at room temperature, the crude reaction mixture was purified by flash column chromatography, yielding the desired olefinated product as a clear oil (24 mg, 38 % yield). ^1H NMR (400 MHz) δ 8.11 (d, 2H, $J = 7.6$ Hz), 7.69 (s, 1H), 7.62 (t, 1H, $J = 7.6$ Hz), 7.50 (t, 2H, $J = 7.6$ Hz), 3.75 (s, 3H), 3.15 (s, 3H), 2.09 (s, 3H), 1.76 (s, 3H). ^{13}C NMR (100 MHz) δ 166.7, 164.9, 164.0, 139.1, 138.3, 134.0, 132.4, 130.3, 129.0, 128.8, 122.3, 52.8, 52.4, 20.2, 19.9.



In an unoptimized procedure, the reaction of enyne **4.79** (25 mg, 0.086 mmol, 1 equiv) and ylide **4.86** (35 mg, 0.11 mmol, 1.3 equiv) in CD_2Cl_2 (0.3 mL) was monitored by ^1H -NMR using 1,3,5-trinitrobenzene as an internal standard. A solution of IMesAuCl and AgSbF_6 (5 mol % of each) in CD_2Cl_2 (0.2 mL) was filtered through glass wool into the reaction mixture. After 18 hours, another solution of IMesAuCl and AgSbF_6 (5 mol % of each) in CD_2Cl_2 (0.2 mL) was filtered through glass wool into the reaction mixture. After an additional 24 hours ^1H -NMR analysis indicated a 32% yield of the desired olefinated product. The crude reaction mixture was purified on silica to yield 11.3 mg of the desired product as a 2:1 mixture with the cycloisomerization/water-trapping product.³⁰ ^1H NMR (500 MHz) δ 7.33-7.27 (m, 2H), 7.18 (t, 1H, $J = 7.5$ Hz), 7.11 (d, 2H, $J = 7.0$ Hz), 6.54 (s, 1H), 3.88 (s, 3H), 3.76 (s, 3H), 3.72 (s, 3H), 3.66 (s, 3H), 2.88 (d, 1H, $J = 14$ Hz), 2.79-2.69 (m, 2H), 2.63 (d, 1H, $J = 14$ Hz), 2.35-2.25 (m, 2H).

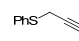
Substrate Synthesis

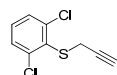
Representative Procedure for the Preparation of Propargyl Sulfides from Propargyl Bromides.



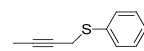
(4-Methoxyphenyl)(prop-2-ynyl)sulfide. To 100 mL THF at 0 °C was added propargyl bromide (80% by weight in toluene, 1.84 mL, 17.1 mmol) and triethylamine (2.70 mL, 19.5 mmol). 4-Methoxybenzenethiol (2.00 mL, 16.3 mmol) was added slowly, whereupon a white precipitate began to form. After addition, the reaction mixture was warmed to room temperature and stirred for 3 hours or until TLC analysis revealed complete consumption of the starting materials. The reaction mixture was then filtered through a plug of silica, eluting with DCM. Concentration of the resulting solution yielded the title compound as a faint yellow solid

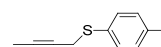
(2.85 g, 98% yield), which was carried on without need for further purification, mp 46 – 49 °C (lit. 51 °C).³¹ ¹H NMR (400 MHz) δ 7.49-7.45 (m, 2H), 6.89-6.85 (m, 2H), 3.80 (s, 3H), 3.49 (d, 2H, *J* = 2.6 Hz), 2.32 (t, 1H, *J* = 2.6 Hz). ¹³C NMR (100 MHz) δ 159.9, 134.5, 125.1, 114.7, 80.4, 71.8, 55.4, 24.7. HRMS (EI) calc. for [C₁₀H₁₀OS]⁺ 178.0452, found 178.0448.

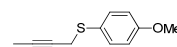
 **Phenyl(prop-2-ynyl)sulfide.** Purified by silica gel chromatography (hexanes). Analogous to the representative procedure, propargyl bromide (80% by weight in toluene, 18.8 mL, 126 mmol) treated with triethylamine (20 mL, 145 mmol) and benzenethiol (10.0 mL, 97.1 mmol) yielded the title compound as a colorless oil (8.60 g, 60% yield). ¹H NMR (300 MHz) 7.50-7.45 (m, 2H), 7.38-7.24 (m, 3H), 3.63 (d, 2H, *J* = 2.7 Hz), 2.26 (t, 1H, *J* = 2.7 Hz). Anal Calcd. For C₉H₈S: C, 72.93. H, 5.44. Found: C, 72.21. H, 5.42.



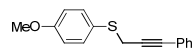
(2,6-Dichlorophenyl)(prop-2-ynyl)sulfide. Analogous to the representative procedure, propargyl bromide (80% by weight in toluene, 0.84 mL, 7.8 mmol) treated with triethylamine (1.6 mL, 12 mmol) and 2,6-dichlorobenzenethiol (1.37 g, 7.66 mmol) yielded the title compound as a yellow oil containing 5% of unknown impurities (1.61 g, 97% yield). ¹H NMR (400 MHz) δ 7.39-7.36 (m, 2H), 7.24-7.17 (m, 1H), 3.64 (d, 2H, *J* = 2.6 Hz), 2.13 (t, 1H, *J* = 2.6 Hz). ¹³C NMR (100 MHz) δ 141.9, 131.5, 130.7, 128.8, 78.8, 72.3, 22.9. HRMS (EI) calc. for [C₉H₆Cl₂S]⁺ 215.9567, found 215.9563.

 **Phenyl(but-2-ynyl)sulfide.** Analogous to the representative procedure, bromo-2-butyne (1.00 mL, 11.4 mmol) treated with triethylamine (2.4 mL, 17 mmol) and benzenethiol (1.53 mL, 14.9 mmol) yielded the title compound as a mixture with approx. 10% thiophenol (1.85 g, 99% yield), carried through to oxidation without further purification. ¹H NMR (400 MHz) δ 7.42 (d, 2H, *J* = 7.2 Hz), 7.32-7.21 (m, 3H), 3.61 (q, 2H, *J* = 2.4 Hz), 1.81 (t, 3H, *J* = 2.4 Hz).

 **(4-Chlorophenyl)(but-2-ynyl)sulfide.** Analogous to the representative procedure, bromo-2-butyne (0.87 mL, 10 mmol) treated with triethylamine (2.1 mL, 15 mmol) and 4-chlorobenzenethiol (1.44 g, 9.96 mmol) yielded the title compound as a colorless oil (1.93 g, 99%). ¹H NMR (500 MHz) δ 7.34 (d, 2H, *J* = 8.5 Hz), 7.27 (d, 2H, *J* = 8.5 Hz), 3.57 (q, 2H, *J* = 2.5 Hz), 1.80 (t, 3H, *J* = 2.5 Hz). ¹³C NMR (125 MHz) δ 134.3 (C), 132.8 (C), 131.2 (CH), 129.2 (CH), 80.0 (C), 74.5 (C), 23.4 (CH₂), 3.8 (CH₃). HRMS (EI) calc. for [C₁₀H₉ClS]⁺ 196.0114, found 196.0113.

 **(4-Methoxyphenyl)(but-2-ynyl)sulfide.** Analogous to the representative procedure, bromo-2-butyne (1.00 mL, 11.4 mmol) treated with triethylamine (2.4 mL, 17 mmol) and 4-methoxybenzenethiol (1.41 mL, 11.4 mmol) yielded the title compound as a colorless oil containing 5% of an unknown impurity (2.19 g, 99%). ¹H NMR (500 MHz) δ 7.44 (dd, 2H, *J* = 7.0, 2.0 Hz), 6.86 (dd, 2H, *J* = 7.0, 2.0 Hz), 3.78 (s, 3H), 3.48 (q, 2H, *J* = 2.5 Hz), 1.80 (t, 3H, *J* = 2.5 Hz). ¹³C NMR (125 MHz) δ 159.6 (C), 134.1 (CH), 125.8 (C), 114.6 (CH), 79.7 (C), 75.1 (C), 55.4 (CH₃), 25.3 (CH₂), 3.8 (CH₃). HRMS (EI) calc. for [C₁₁H₁₂OS]⁺ 192.0609, found 192.0606.

Representative procedure for the preparation of propargyl sulfides from propargyl alcohols.

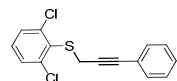


(4-Methoxyphenyl)(3-phenylprop-2-ynyl)sulfide. To a solution of carbon tetrabromide (11.6 g, 34.9 mmol), and triphenylphosphine (9.16 g, 34.9 mmol), in 75 mL benzene at 0 °C was added 3-phenyl-2-propyn-1-ol (4.57 g, 34.6 mmol). The reaction mixture was stirred at 0 °C for 3 hours, then filtered through silica, eluting with benzene. The eluent was concentrated and redissolved in 100 mL THF. Triethylamine (5.24 mL, 37.8 mmol) and 4-methoxythiophenol (4.22 mL, 34.4 mmol) were added, and the mixture was stirred for 30 minutes, during which time a white precipitate formed. Filtration of the reaction mixture through silica and concentration yielded the crude product, containing approximately 10% 4-methoxythiophenol, as a colorless oil (8.80 g), which was carried on without further purification. ¹H NMR (300 MHz) 7.64 (d, 2H, *J* = 7.2 Hz), 7.52-7.24 (m, 6 H), 6.91-6.81 (m, 3H), 3.79 (s, 3H), 3.73 (s, 2H). ¹³C NMR (75 MHz) δ 159.9, 135.0, 132.8, 131.7, 128.3, 128.2, 114.7, 114.6, 85.9, 83.9, 55.4, 25.9. HRMS (EI) calc. for [C₁₆H₁₄OS]⁺ 254.0765, found 254.0762.

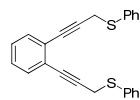


Phenyl(3-phenylprop-2-ynyl)sulfide. Analogous to the representative procedure, 3-phenyl-2-propyn-1-ol (2.02 g, 15.3 mmol) treated with carbon tetrabromide (5.31 g, 16.0 mmol) and triphenylphosphine (4.20 g, 16.0 mmol) followed by triethylamine (2.6 mL, 18 mmol) and benzenethiol (1.65 mL, 16.0 mmol). Isolated as a colorless oil containing approximately 30% diphenyldisulfide and other unknown impurities (3.59 g). ¹H NMR (300 MHz) 7.54-7.42 (m, 2H), 7.38-7.23 (m, 8H), 3.85 (s, 2H).

Representative Procedure for Sonogashira Coupling.

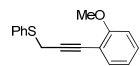


(2,6-Dichlorophenyl)(3-phenylprop-2-ynyl)sulfide. A mixture of (2,6-dichlorophenyl)(prop-2-ynyl)sulfide (2.10 mmol) and iodobenzene (2.31 mmol) in 1:3 triethylamine : acetonitrile (5 mL) was cooled to 0 °C and degassed three times, by successive vacuum/nitrogen purges. Copper iodide (0.21 mmol, 40 mg) was added, the solution was again degassed. Bis(triphenylphosphine) palladium(II) dichloride (0.11 mmol, 74 mg) was added and the reaction was degassed three times. The reaction was then warmed to 50 °C and stirred until consumption of the alkyne was determined by TLC. The reaction was quenched with saturated ammonium chloride (10 mL), extracted with ether (3 x 20 mL), dried, filtered through celite and concentrated. The mixture was purified by column chromatography (hexanes : ethyl acetate) to provide the title compound as a yellow oil (386 mg, 63% yield). ¹H NMR (300 MHz) δ 7.42 (d, 2H, *J* = 8.1 Hz), 7.25-7.19 (m, 6H), 3.90 (s, 2H). ¹³C NMR (125 MHz) δ 142.2, 131.8, 130.7, 129.3, 128.8, 128.4, 128.3, 123.1, 84.3, 84.2, 24.0. GC/MS: *m/z* 257 ([M - Cl]⁺). Anal Calcd. For C₁₅H₁₀Cl₂S: C, 61.44. H, 3.44. Found: C, 60.99. H, 3.44.



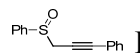
1,2-Bis(3-(phenylthio)prop-1-ynyl)benzene. Analogous to the representative procedure, treating phenyl(prop-2-ynyl)sulfide (734 mg, 4.96 mmol) and 1,2-diiodobenzene (243 μL, 1.91 mmol) with copper iodide (73 mg, 0.38 mmol) and bis(triphenylphosphine) palladium(II) dichloride (134 mg, 0.19 mmol) in 1:3 diisopropylamine : THF yielded the title

compound as a yellow oil (432 mg, 61% yield). ¹H NMR (300 MHz) 7.59-7.50 (m, 4H), 7.26-7.19 (m, 10H), 3.81 (s, 4H).

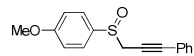


(3-(2-Methoxyphenyl)prop-2-ynyl)(phenyl)sulfide. Reaction required heating to 65 °C. Analogous to the representative procedure, treating phenyl(prop-2-ynyl)sulfide (1.18 g, 7.96 mmol) and *o*-iodoanisole (863 μL, 6.63 mmol) with copper iodide (76 mg, 0.40 mmol) and bis(triphenylphosphine) palladium(II) dichloride (140 mg, 0.20 mmol) yielded the title compound as a clear oil (1.44 g, 86% yield). ¹H NMR (300 MHz) δ 7.54-7.51 (m, 2H), 7.33-7.19 (m, 5H), 6.87-6.80 (m, 2H), 3.92 (s, 2H), 3.82 (s, 3H). ¹³C NMR (75 MHz) δ 160.3, 135.6, 133.9, 130.6, 129.8, 129.0, 127.0, 120.5, 112.3, 110.8, 89.5, 80.2, 55.9, 24.3. Anal Calcd. For C₁₆H₁₄OS: C, 75.55. H, 5.55. Found: C, 75.38. H, 5.55.

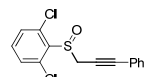
Representative Procedure for the Oxidation of Sulfides to Sulfoxides.



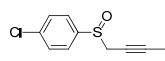
Phenyl(3-phenylprop-2-ynyl)sulfoxide. To a solution of crude phenyl(3-phenylprop-2-ynyl)sulfide (1.16 g, 5.19 mmol) in 15 mL 1 : 1 acetonitrile : water at 0 °C was added Oxone® (2.23 g, 3.63 mmol, 0.7 equiv). After stirring for 20 minutes, the reaction was warmed to room temperature and stirred until complete consumption of starting material, determined by TLC analysis (1 hour). The reaction was diluted with 50 mL water and 75 mL ether, and extracted with ether (3 x 50 mL). The combined etherous layers were dried and concentrated *in vacuo*. Flash chromatography on silica gel, eluting with 30% ethyl acetate in hexanes, provided the title compound as a colorless oil (440 mg, 35% yield from 3-phenyl-2-propyn-1-ol). ¹H NMR (400 MHz) δ 7.79-7.76 (m, 2H), 7.57-7.55 (m, 3H), 7.34-7.27 (m, 5H), 4.02 (d, 1H, *J* = 15.4 Hz), 3.76 (d, 1H, *J* = 15.4 Hz). ¹³C NMR (100 MHz) δ 142.9, 131.7, 131.6, 128.0, 128.7, 128.3, 124.5, 122.0, 88.1, 78.1, 48.8. Anal Calcd. For C₁₅H₁₂OS: C, 74.97. H, 5.03. Found: C, 74.65. H, 5.05.

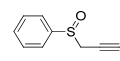


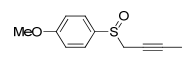
(4-Methoxyphenyl)(3-phenylprop-2-ynyl)sulfoxide (4.54a). Analogous to the representative procedure, treating crude (4-methoxyphenyl)(3-phenylprop-2-ynyl)sulfide (34 mmol) with Oxone® (10.7 g, 17.3 mmol, 0.5 equiv) provided the title compound as a white solid (6.20 g, 66% yield from 3-phenyl-2-propyn-1-ol), mp 75 – 78 °C. IR: 2360, 1593, 1495, 1254, 1287, 1052 cm⁻¹. ¹H NMR (400 MHz) δ 7.70 (d, 2H, *J* = 8.8 Hz), 7.34-7.30 (m, 5H), 7.05 (d, 2H, *J* = 8.8 Hz), 4.04 (d, 1H, *J* = 15.6 Hz), 3.87 (s, 3H), 3.68 (d, 1H, *J* = 15.6 Hz). ¹³C NMR (100 MHz) δ 162.5, 133.9, 131.7, 128.7, 128.3, 126.5, 122.1, 114.5, 87.9, 78.2, 55.5, 49.1. Anal Calcd. For C₁₆H₁₄O₂S: C, 71.08. H, 5.22. Found: C, 70.71. H, 5.10.

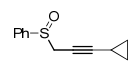


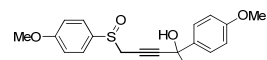
(2,6-Dichlorophenyl)(3-phenylprop-2-ynyl)sulfoxide (4.54b). Analogous to the representative procedure, treating (2,6-dichlorophenyl)(3-phenylprop-2-ynyl)sulfide (386 mg, 1.32 mmol) with Oxone® (811 mg, 1.32 mmol) yielded the title compound as a pale yellow solid (310 mg, 77% yield), mp 92 – 94 °C. IR: 2360, 1558, 1090, 1069 cm⁻¹. ¹H NMR (500 MHz) δ 7.37-7.32 (m, 3H), 7.30-7.21 (m, 5H), 4.65 (d, 1H, *J* = 15.5), 4.28 (d, 1H, *J* = 15.5). ¹³C NMR (100 MHz) δ 136.4, 136.2, 133.0, 131.7, 130.3, 128.8, 128.3, 121.9, 87.9, 77.7, 43.1. Anal Calcd. For C₁₅H₁₀Cl₂OS: C, 58.26. H, 3.26. Found: C, 58.01. H, 3.31.

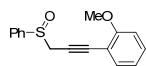
 **(4-Chlorophenyl)(but-2-ynyl)sulfoxide (4.54d)**. Analogous to the representative procedure, treating crude (4-chlorophenyl)(but-2-ynyl)sulfide (1.81 g, 9.21 mmol) with Oxone® (3.96 g, 6.45 mmol) yielded the title compound as a white solid (1.42 g, 71% yield over two steps from 1-bromo-but-2-yne), mp 71 – 73 °C. IR: 2237, 1573, 1476, 1089, 1053 cm⁻¹. ¹H NMR (400 MHz) δ 7.64-7.61 (m, 2H), 7.52-7.48 (m, 2H), 3.69 (dq, 1H, *J* = 15.6, 2.4 Hz), 3.68 (dq, 1H, *J* = 15.6, 2.4 Hz), 1.79 (t, 3H, *J* = 2.4 Hz). ¹³C NMR (100 MHz) δ 141.9, 138.0, 129.4, 126.1, 85.2, 67.6, 48.8, 3.9. Anal Calcd. For C₁₀H₉ClOS: C, 56.47. H, 4.26. Found: C, 56.58. H, 4.38.

 **Phenyl(but-2-ynyl)sulfoxide (4.54e)**. Analogous to the representative procedure, treating crude phenyl(but-2-ynyl)sulfide (1.85 g, 11.4 mmol) with Oxone® (4.92 g, 8.00 mmol) yielded the title compound as a colorless oil (1.69 g, 83% over two steps from 1-bromo-but-2-yne). ¹H NMR (400 MHz) δ 7.67-7.64 (m, 2H), 7.51-7.48 (m, 2H), 3.64 (dq, 1H, *J* = 15.2, 2.4 Hz), 3.46 (dq, 1H, *J* = 15.2, 2.4 Hz), 1.76 (t, 3H, *J* = 2.4 Hz). Anal Calcd. For C₁₀H₁₀OS: C, 67.38. H, 5.65. Found: C, 67.05. H, 5.86.

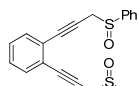
 **(4-Methoxyphenyl)(but-2-ynyl)sulfoxide (4.54f)**. Analogous to the representative procedure, treating crude (4-methoxyphenyl)(but-2-ynyl)sulfide (2.14 g, 10.3 mmol) with Oxone® (4.42 g, 7.18 mmol) yielded the title compound as a colorless oil (1.93 g, 83% yield over two steps from 1-bromo-but-2-yne). IR: 2236, 1595, 1088, 1027 cm⁻¹. ¹H NMR (400 MHz) δ 7.58-7.55 (m, 2H), 6.98-6.96 (m, 2H), 3.82 (s, 3H), 3.63 (dq, 1H, *J* = 15.4, 2.4 Hz), 3.39 (dq, 1H, *J* = 15.4, 2.4 Hz), 1.73 (t, 3H, *J* = 2.4 Hz). ¹³C NMR (100 MHz) δ 162.3 (C), 134.1 (C), 126.4 (CH), 114.5 (CH), 84.4 (C), 68.1 (C), 55.5 (CH₃), 48.7 (CH₂), 3.8 (CH₃). HRMS (EI) calc. for [C₁₁H₁₂O₂S]⁺ 208.0558, found 208.0556.

 **Phenyl(3-cyclopropyl-prop-2-ynyl)sulfoxide (4.54g)**. Analogous to the representative procedure, treating phenyl(3-cyclopropyl-prop-2-ynyl)sulfide (220 mg, 1.17 mmol) with Oxone® (503 mg, 0.82 mmol, 0.7 equiv) yielded the title compound as a colorless oil (215 mg, 90% yield). ¹H NMR (500 MHz) δ 7.69-7.66 (m, 2H), 7.52-7.50 (m, 3H), 3.64 (dd, 1H, *J* = 15.5, 2 Hz), 3.51 (dd, 1H, *J* = 15.5, 2 Hz), 1.21-1.15 (m, 1H), 0.74-0.70 (m, 2H), 0.57-0.55 (m, 2H). ¹³C NMR (125 MHz) δ 143.2, 131.7, 129.0, 124.7, 92.4, 64.0, 48.8, 8.4, -0.3. HRMS (EI) calc. for [C₁₂H₁₂OS]⁺ 204.0609, found 204.0606.

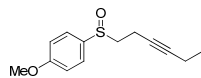
 **5-(4-methoxyphenylthio)-2-(4-methoxyphenyl)pent-3-yn-2-ol (4.54j)**. Analogous to the representative procedure, treating 5-(4-methoxyphenylthio)-2-(4-methoxyphenyl)pent-3-yn-2-ol (800 mg, 2.68 mmol) with Oxone® (1.15 g, 1.88 mmol) yielded the title compound as a highly viscous colorless oil (640 mg, 76% yield). IR: 3404, 2360, 1594, 1253, 1088, 1029 cm⁻¹. ¹H NMR (400 MHz) δ 7.64-7.59 (m, 2H), 7.41-7.37 (m, 2H), 7.00-6.96 (m, 2H), 6.85-6.82 (m, 2H), 3.84 (s, 3H), 3.81 (s, 3H), 3.78 (d, 1H, *J* = 15.6 Hz), 3.66 (d, 1H, *J* = 15.6 Hz), 2.72 (bs, 1H), 1.67 (d, 3H, *J* = 2.8 Hz). ¹³C NMR (100 MHz) δ 162.2, 158.6, 137.7, 132.9, 126.5, 126.1, 114.4, 113.2, 92.5, 72.7, 68.7, 55.3, 55.1, 47.7, 32.9. Anal Calcd. For C₁₉H₂₀O₄S: C, 66.26. H, 5.85. Found: C, 66.08. H, 6.10.



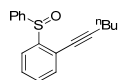
(3-(2-Methoxyphenyl)prop-2-ynyl)(phenyl)sulfoxide (4.54k). Analogous to the representative procedure, treating (3-(2-methoxyphenyl)prop-2-ynyl)(phenyl)sulfide (240 mg, 0.95 mmol) with Oxone® (466 mg, 0.76 mmol) yielded the title compound as a yellow oil (148 mg, 58% yield). ¹H NMR (300 MHz) δ 7.83-7.80 (m, 2H), 7.56-7.53 (m, 3H), 7.30-7.27 (m, 2H), 6.92-6.85 (m, 2H), 4.15 (d, 1H, *J* = 15.6 Hz), 3.85 (s, 3H), 3.77 (d, 1H, *J* = 15.6 Hz). ¹³C NMR (75 MHz) δ 160.4, 143.4, 133.9, 131.7, 130.4, 129.1, 124.8, 120.6, 111.4, 110.8, 84.7, 82.1, 55.8, 49.5. Anal Calcd. For C₁₆H₁₄O₂S: C, 71.08. H, 5.22. Found: C, 70.74. H, 5.38.



1,2-Bis(3-(phenylsulfinyl)prop-1-ynyl)benzene (4.68). Analogous to the representative procedure, treating 1,2-bis(3-(phenylthio)prop-1-ynyl)benzene (300 mg, 0.81 mmol) with Oxone® (950 mg, 1.55 mmol) yielded the title compound as a yellow oil (60 mg, 11% yield) along with recovered starting material (90 mg, 30%). IR: 2326, 1087, 1050 cm⁻¹. ¹H NMR (400 MHz) δ 7.76-7.73 (m, 4H), 7.50-7.48 (m, 6H), 7.32-7.24 (m, 4H), 3.92 (dd, 2H, *J* = 15.6, 1.9 Hz), 3.82 (dd, 2H, *J* = 15.6, 4.5 Hz). ¹³C NMR (100 MHz) δ 143.4, 132.3, 131.8, 129.2, 128.6, 125.1, 124.7, 86.4, 82.7, 49.4.

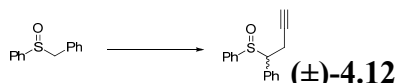


(4-Methoxyphenyl)(hex-3-ynyl)sulfoxide (4.22). Analogous to the representative procedure, treating crude (4-methoxyphenyl)(hex-3-ynyl)sulfide (1.2 g, 5.4 mmol) with Oxone® (2.3 g, 3.8 mmol) yielded the title compound as a colorless oil (1.1 g, 89% yield). IR: 2974, 1595, 1497, 1252, 1088 cm⁻¹. ¹H NMR (400 MHz) δ 7.55 (d, 2H, *J* = 8.8 Hz), 7.01 (d, 2H, *J* = 8.8 Hz), 3.83 (s, 3H), 2.94-2.84 (m, 2H), 2.63-2.55 (m, 1H), 2.39-2.32 (m, 1H), 2.11 (qt, 2H, *J* = 7.4, 2.4 Hz), 1.07 (t, 3H, *J* = 7.4 Hz). ¹³C NMR (100 MHz) δ 162.2 (C), 134.3 (C), 126.2 (CH), 115.0 (CH), 84.2 (C), 75.9 (C), 56.4 (CH₂), 55.7 (CH₃), 14.2 (CH₃), 12.8 (CH₂), 12.6 (CH₂). Anal Calcd. For C₁₃H₁₆O₂S: C, 66.07. H, 6.82. Found: C, 65.72. H, 7.02.



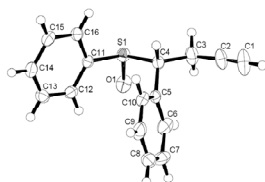
Phenyl(2-(1-hexynyl)-phenyl)sulfoxide (4.75) Analogous to the representative procedure, treating the sulfide (305 mg, 1.48 mmol, 1 equiv) with Oxone® (0.64 g, 1.0 mmol, 0.7 equiv) yielded the title compound as a colorless oil (207 mg, 50% yield). ¹H NMR (500 MHz) δ 7.98 (d, 1H, *J* = 8 Hz), 7.74-7.72 (m, 2H), 7.49-7.30 (m, 6H), 2.46 (t, 2H, *J* = 7 Hz), 1.62-1.55 (m, 2H), 1.47 (app sextet, 2H, *J* = 7.4 Hz), 0.94 (t, 3H, *J* = 7.3 Hz). ¹³C NMR (125 MHz) δ 146.7, 145.7, 133.0, 131.2, 130.6, 129.2, 128.9, 125.6, 123.8, 121.7, 99.6, 30.6, 22.2, 19.5, 13.8.

Additional Procedures

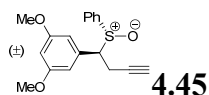


To a solution of benzylphenylsulfide (556 mg, 2.57 mmol) in tetrahydrofuran (25 mL) at -78 °C was added dropwise *n*-BuLi (2.4 M in hexanes, 1.23 mL, 2.96 mmol). The solution was stirred for 10 minutes and propargyl bromide (80% in toluene, 0.34 mL, 3.08 mmol) was added. The solution was allowed to slowly warm to room temperature, quenched with saturated ammonium chloride solution (10 mL) and extracted with ether (3 x 20 mL). The combined

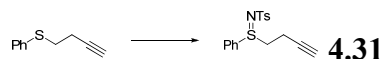
organic layers were dried (MgSO₄), concentrated, and purified by flash column chromatography (10% → 25 % EtOAc/hexanes). First to elute was the diastereomer which proved less reactive in the gold(I)-catalyzed rearrangement (101 mg, 15% yield). ¹H NMR (500 MHz) δ 7.37 (d, 1H, *J* = 7.5 Hz), 7.31-7.24 (m, 5H), 7.21-7.17 (m, 2H), 6.87 (d, 1H, *J* = 7.5 Hz) 3.95 (t, 1H, *J* = 7.8 Hz), 3.25 (ddd, 1H, *J* = 17.0, 7.8, 2.5 Hz), 2.73 (ddd, 1H, *J* = 17.0, 7.8, 2.5 Hz), 2.04 (t, 3H, *J* = 2.5 Hz). ¹³C NMR (100 MHz) δ 140.5, 131.3, 131.2, 129.2, 128.7, 128.6, 128.2, 124.9, 80.4, 71.4, 68.5, 18.2. X-ray quality crystals were grown from diethyl ether. X-ray structure (see Appendix for more information):



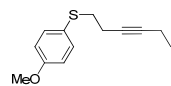
Next to elute was a mixture of both diastereomers (204 mg, 31% yield). This was followed by the more reactive diastereomer (54 mg, 8% yield). ¹H NMR (500 MHz) δ 7.41 (t, 1H, *J* = 7.3 Hz), 7.35-7.23 (m, 7H), 7.04 (d, 1H, *J* = 7.0 Hz) 3.85 (dd, 1H, *J* = 10.0, 5.0 Hz), 3.09-2.98 (m, 2H), 2.04 (t, 3H, *J* = 2.8 Hz). ¹³C NMR (100 MHz) δ 141.7, 133.1, 131.5, 129.3, 128.9, 128.8, 128.7, 125.1, 79.9, 71.5, 70.7.



Prepared as above. Column chromatography (10% EtOAc in hexanes) first provided the less reactive diastereomer, followed by the more reactive diastereomer (pictured above). ¹H NMR (500 MHz) δ 7.43 (t, 1H, *J* = 7 Hz), 7.37 (t, 2H, *J* = 7.5 Hz), (d, 2H, *J* = 7.5 Hz), 6.38 (s, 1H), 6.19 (s, 2H), 3.73-3.65 (m, 7H), 3.10-2.97 (m, 2H), 1.96 (s, 1H). ¹³C NMR (125 MHz) δ 160.9, 142.1, 135.3, 131.5, 128.9, 125.1, 107.3, 101.0, 80.0, 71.5, 71.2, 55.5, 19.4.



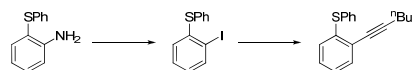
To a solution of 3-butynylphenylsulfide (415 mg, 2.56 mmol) in 10 mL acetonitrile was added Chloramine T trihydrate (864 mg, 3.07 mmol). This solution was stirred overnight at 50 °C. After cooling to room temperature, the solution was diluted with CH₂Cl₂ (20 mL), filtered through celite and concentrated. Flash column chromatography (30 % EtOAc/hexanes) provided the desired N-tosylsulfilimine as a clear oil (255 mg, 30% yield). IR: 3256, 1445, 1282, 1141, 1089 cm⁻¹. ¹H NMR (300 MHz) δ 7.77-7.67 (m, 4H), 7.53-7.45 (m, 3H), 7.15 (d, 2H, *J* = 8.1 Hz), 3.32-3.01 (m, 2H), 2.60-2.51 (m, 1H), 2.42-2.36 (m, 1H), 2.32 (s, 3H), 2.01 (t, 1H, *J* = 2.7 Hz). ¹³C NMR (75 MHz) δ 141.9, 141.2, 134.1, 132.7, 130.1, 129.4, 126.4, 126.3, 79.2, 71.8, 52.5, 21.5, 13.4. HRMS (FAB) calc. for [C₁₇H₁₇NO₂S₂]⁺ 331.0701, found 331.0706.



(4-Methoxyphenyl)(hex-3-ynyl)sulfide.

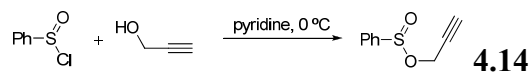
A solution of hex-3-ynyl 4-methylbenzenesulfonate (1.47 g, 6.21 mmol), 4-methoxybenzenethiol (802 μL, 6.51 mmol), and potassium carbonate (1.03 g, 7.45 mmol) in 25 mL acetone was refluxed for 3 hours. The resulting solution was filtered through celite and concentrated to yield

a faint yellow oil, which was carried on without further purification (1.37 g, quantitative). ^1H NMR (400 MHz) δ 7.40-7.35 (m, 2H), 6.86-6.82 (m, 2H), 3.79 (s, 3H), 2.91 (t, 2H, $J = 7.6$ Hz), 2.38 (td, 2H, $J = 7.6, 2.4$ Hz), 2.14 (qt, 2H, $J = 7.6, 2.4$ Hz), 1.10 (t, 3H, $J = 7.6$ Hz). ^{13}C NMR (100 MHz) δ 159.3, 134.0, 132.8, 125.8, 114.7, 83.1, 77.6, 55.5, 35.5, 20.0, 14.3, 12.6. HRMS (EI) calc. for $[\text{C}_{13}\text{H}_{16}\text{OS}]^+$ 220.0922, found 220.0923.

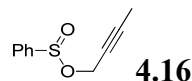


Phenyl(2-(1-hexynyl)-phenyl)sulfide (4.76).

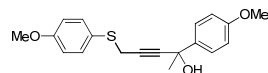
A solution of sodium nitrate (3.17 g, 45.9 mmol, 1.5 equiv) in water (5 mL) was added dropwise to a slurry of 2-(phenylthio)aniline (6.16 g, 30.6 mmol, 1 equiv) in water (20 mL) and concentrated hydrochloric acid (12 mL) at 0°C. After stirring for 45 minutes, potassium iodide (7.62 g, 45.9 mmol, 1.5 equiv) in water (5 mL) was added slowly. The reaction mixture was warmed to room temperature and stirred for an additional 45 minutes before being carefully diluted with aqueous sodium bisulfite and hexanes/ether (3:1). The organic fraction was separated, washed with additional aqueous sodium bisulfite, dried over MgSO_4 and filtered through a short plug of silica and concentrated *in vacuo* to yield white crystals of 2-iodophenyl(phenyl)sulfide (5.16 g, 54%). Sonogashira coupling with 1-hexyne under the standard conditions (*vide supra*) provided sulfide **4.76**. ^1H NMR (500 MHz, CD_2Cl_2) δ 7.44-7.31 (m, 6H), 7.15-7.09 (m, 2H), 6.98-6.95 (m, 1H), 2.43 (t, 2H, $J = 7$ Hz), 1.56 (app pentet, 2H, $J = 7$ Hz), 1.48 (app sextet, 2H, $J = 7.5$ Hz), 0.93 (t, 3H, $J = 7.3$ Hz).



Crude benzene sulfanyl chloride³² (9.7 mmol, 1.5 equiv), was slowly added to a solution of propargyl alcohol (0.38 mL, 6.5 mmol, 1 equiv) in pyridine (2 mL) at 0 °C. The solution was stirred for 30 minutes, poured into 1M HCl and extracted with ether (2 x 20 mL). The combined organic extracts were dried over anhydrous MgSO_4 , filtered and concentrated *in vacuo*. Flash column chromatography provided the desired sulfinate (0.94 g, 80% yield). ^1H NMR (400 MHz) δ 7.76-7.72 (m, 2H), 7.60-7.51 (m, 3H), 4.60 (dd, 1H, $J = 15.6, 2.4$ Hz), 4.31 (dd, 1H, $J = 15.6, 2.4$ Hz), 2.49 (t, 1H, $J = 2.4$ Hz). ^{13}C NMR (100 MHz) δ 144.1, 132.7, 129.3, 125.5, 77.6, 76.4, 51.9.



Prepared as above (1.0g, 79% yield). ^1H NMR (400 MHz) δ 7.74-7.71 (m, 2H), 7.55-7.51 (m, 3H), 4.58 (dq, 1H, $J = 15.2, 2.4$ Hz), 4.28 (dq, 1H, $J = 15.2, 2.4$ Hz), 1.80 (t, 1H, $J = 2.4$ Hz). ^{13}C NMR (100 MHz) δ 144.4, 132.5, 129.2, 125.5, 85.1, 73.2, 53.1, 3.9.



5-(4-Methoxyphenylthio)-2-(4-methoxyphenyl)pent-3-yn-2-ol. *n*-BuLi (2.45 M in hexanes, 1.17 mL, 2.86 mmol) was added drop wise to a solution of (4-methoxyphenyl)(but-2-ynyl)sulfide (535 mg, 3.00 mmol) in 20 mL THF at -78 °C. The solution was warmed to room temperature and stirred for ten minutes. The solution was then again

cooled to $-78\text{ }^{\circ}\text{C}$ and a solution of 4-methoxyacetophenone (429 mg, 2.86 mmol, in 15 mL THF at $-30\text{ }^{\circ}\text{C}$) was added. The resulting mixture was slowly warmed to room temperature and stirred for three hours. The reaction was quenched with saturated ammonium chloride (50 mL), extracted with ether (3 x 30 mL), dried and concentrated. Purification on silica gel (7:2:1 hexanes : dichloromethane : ethyl acetate) yielded the title compound as a white solid (800 mg, 95% yield). IR: 3451, 2350 cm^{-1} . ^1H NMR (500 MHz) δ 7.45 (d, 2H, $J = 8.5$ Hz), 7.41 (d, 2H, $J = 8.5$ Hz), 6.83 (t, 4H, $J = 8.5$ Hz), 3.79 (s, 3H), 3.78 (s, 3H), 3.57 (s, 2H), 2.74 (s, 1H), 1.69 (s, 3H). ^{13}C NMR (125 MHz) δ 159.8, 159.0, 137.9, 134.9, 126.4, 124.9, 114.6, 113.5, 87.4, 81.1, 69.6, 55.4, 55.3, 33.2, 25.0. HRMS (FAB) calc. for $[\text{C}_{19}\text{H}_{20}\text{O}_3\text{S}]^+$ 328.1133, found 328.1138.

References

- (1) Shapiro, N. D.; Toste, F. D. *J. Am. Chem. Soc.* **2007**, *129*, 4160.
- (2) Witham, C. A.; Mauleón, P.; Shapiro, N. D.; Sherry, B. D.; Toste, F. D. *J. Am. Chem. Soc.* **2007**, *129*, 5838.
- (3) For recent examples involving Au-carbenoid intermediates in the cycloisomerization of enynes, see: (a) Nieto-Oberhuber, C.; Muñoz, M. P.; Buñuel, E.; Nevado, C.; Cárdenas, D. J.; Echavarren, A. M. *Angew. Chem., Int. Ed.* **2004**, *43*, 2402. (b) Mamane, V.; Gress, T.; Krause, H.; Fürstner, A. *J. Am. Chem. Soc.* **2004**, *126*, 8654. (c) Luzung, M. R.; Markham, J. P.; Toste, F. D. *J. Am. Chem. Soc.* **2004**, *126*, 10858. (d) Zhang, L.; Wang, S. *J. Am. Chem. Soc.* **2006**, *128*, 1442. (e) López, S.; Herrero-Gómez, E.; Pérez-Galán, P.; Nieto-Oberhuber, C.; Echavarren, A. M. *Angew. Chem., Int. Ed.* **2006**, *45*, 6029. (f) Horino, Y.; Luzung, M. R.; Toste, F. D. *J. Am. Chem. Soc.* **2006**, *128*, 11364. (g) Lee, J. H.; Toste, F. D. *Angew. Chem., Int. Ed.* **2007**, *46*, 912. For a review, see: (h) Gorin, D. J.; Toste, F. D. *Nature* **2007**, *446*, 395.
- (4) For the reactions of Au-carbenoid intermediates generated from propargyl esters, see: (a) Miki, K.; Ohe, K.; Uemura, S. *J. Org. Chem.* **2003**, *68*, 8505. (b) Fürstner, A.; Hannen, P. *Chem. Commun.* **2004**, 2546. (c) Johansson, M. J.; Gorin, D. J.; Staben, S. T.; Toste, F. D. *J. Am. Chem. Soc.* **2005**, *127*, 18002. (d) Ohe, K.; Fujita, M.; Matsumoto, H.; Tai, Y.; Miki, K. *J. Am. Chem. Soc.* **2006**, *128*, 9270. (e) Gorin, D. J.; Dube, P.; Toste, F. D. *J. Am. Chem. Soc.* **2006**, *128*, 14480.
- (5) For generation and reactions of furylcarbenoid intermediates, see: (a) Miki, K.; Nishino, F.; Ohe, K.; Uemura, S. *J. Am. Chem. Soc.* **2002**, *124*, 5260. (b) Miki, K.; Yokoi, T.; Nishino, F.; Kato, Y.; Washitake, Y.; Ohe, K.; Uemura, S. *J. Org. Chem.* **2004**, *69*, 1557. For an excellent review, see: (c) Miki, K.; Uemura, S.; Ohe, K. *Chem. Lett.* **2005**, *34*, 1068.
- (6) For reviews, see: (a) Wee, A. G. H. *Curr. Org. Synth.* **2006**, *3*, 499. (b) Davies, H. M. L.; Beckwith, R. E. *J. Chem. Rev.* **2003**, *103*, 2861. (c) Davies, H. M. L.; Antoulinakis, E. G. *Org. React.* **2001**, *57*, 1. (d) Ye, T.; McKervey, M. A. *Chem. Rev.* **1994**, *94*, 1091. (e) *Modern Catalytic Methods for Organic Synthesis with Diazo Compounds*; Doyle M. P., McKervey, M. A., Ye, T., Eds.; Wiley: New York, 1998. (f) *Metal-Carbenes in Organic Synthesis*; Zaragoza-Dorwald, F., Ed.; Wiley-VCH: Weinheim, Germany, 1998.
- (7) For gold-catalyzed reaction of α -diazoesters, see: (a) Fructos, M. R.; Belderrain, T. R.; de Frémont, P.; Scott, N. M.; Nolan, S. P.; Díaz-Requejo, M. M.; Pérez, P. *J. Angew. Chem., Int. Ed.* **2005**, *44*, 5284. (b) Fructos, M. R.; de Frémont, P.; Nolan, S. P.; Díaz-Requejo, M. M.; Pérez, P. *J. Organometallics* **2006**, *25*, 2237.
- (8) Gorin, D. J.; Davis, N. R.; Toste, F. D. *J. Am. Chem. Soc.* **2005**, *127*, 11260.
- (9) (a) Harmata, M.; Huang, C. *Adv. Synth. Catal.* **2007**, *350*, 972. (b) Hiroi, D.; Kato, F. *Tetrahedron* **2001**, *57*, 1543. (c) Mukai, C.; Hirose, T.; Teramoto, S.; Kitagaki, S. *Tetrahedron* **2005**, *61*, 10983.
- (10) Under all conditions examined, the unsubstituted aryl derivative produced only a trace of the desired benzothiepinones.
- (11) The sulfone derivative of **4.23** was characterized by X-ray crystallography (see Supporting Information).
- (12) Hashmi, A. S. K.; Schwarz, L.; Choi, J.-H.; Frost, T. M. *Angew. Chem., Int. Ed.* **2000**, *39*, 2285.

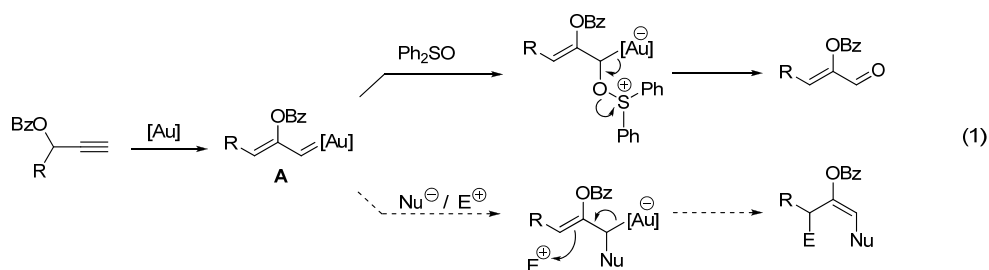
-
- (13) (a) Padwa, A.; Austin, D. J.; Price, A. T.; Semones, M. A.; Doyle, M. P.; Protopopova, M. N.; Winchester, W. R.; Tran, A. *J. Am. Chem. Soc.* **1993**, *115*, 8669. (b) Etkin, N.; Babu, S. D.; Fooks, C. J.; Durst, T. *J. Org. Chem.* **1990**, *55*, 1093.
- (14) Nakane, R.; Kurihara, O.; Takematsu, A. *J. Org. Chem.* **1971**, *36*, 2753.
- (15) A similar mode of reactivity was elegantly used to synthesize thiophenes and thiopyrans from alkynyl sulfoxides, see: Davies, P. W.; Albrecht, S. J.-C. *Angew. Chem., Int. Ed.* **2009**, *48*, 8372.
- (16) (a) Dubé, P.; Toste, F. D. *J. Am. Chem. Soc.* **2006**, *128*, 12062. (b) For a review of “memory of chirality”, see: (a) Zhao, H.; Hsu, D. C.; Carlier, P. R. *Synthesis* **2005**, 1.
- (17) Li, G.; Zhang, L. *Angew. Chem., Int. Ed.* **2007**, *46*, 5156.
- (18) For other gold(I)-catalyzed rearrangements of alkynyl N-oxides, see: (a) Cui, L.; Zhang, G.; Peng, Y.; Zhang, L. *Org. Lett.* **2009**, *11*, 1225. (b) Cui, L.; Peng, Y.; Zhang, L. *J. Am. Chem. Soc.* **2009**, *131*, 8394.
- (19) For the rearrangements of aryl propargylsulfoxides, see: (a) Majumdar, K. C.; Thyagarajan, B. S. *J. Chem. Soc., Chem. Commun.* **1972**, 83. (b) Baudin, J.-B.; Julia, S. A.; Lorne, R. *Synlett* **1991**, 509. (c) Majumdar, K. C.; Ghosh, S. K. *Tetrahedron Lett.* **2002**, *43*, 2123.
- (20) For a leading reference on the coinage metal-catalyzed rearrangement of other propargyl functional groups, see: Schwier, T.; Sromek, A. W.; Yap, D. M. L.; Chernyak, D.; Gevorgyan, V. *J. Am. Chem. Soc.* **2007**, *129*, 9868.
- (21) For 1,2-thio migration of Rh(II) carbenes, see: Xu, F.; Shi, W.; Wang, J. *J. Org. Chem.* **2005**, *70*, 4191.
- (22) Cui, L.; Zhang, G.; Zhang, L. *Bioorg. Med. Chem. Lett.* **2009**, *19*, 3884.
- (23) Cuenca, A. B.; Montserrat, S.; Hossain, K. M.; Mancha, G.; Lledós, A.; Medio-Simón, M.; Ujaque, G.; Asensio, G. *Org. Lett.* **2009**, *11*, 4906.
- (24) Attempted trapping of the proposed carbenoid intermediate with olefins was unsuccessful.
- (25) Iodonium ylides dimerized under similar reaction conditions.
- (26) Bruce, M. I.; Nicholson, B. K.; Bin Shawkataly, O. *Inorg. Syn.* **1989**, *26*, 324.
- (27) Nunokawa, K.; Onaka, S.; Tatematsu, T.; Ito, M.; Sakai, J. *Inorganica Chimica Acta* **2001**, *322*, 56.
- (28) Nieto-Oberhuber, C.; López, S.; Echavarren, A.M. *J. Am. Chem. Soc.* **2005**, *127*, 6178.
- (29) Takaki, K.; Okada, M.; Yamada, M.; Negoro, K. *J. Org. Chem.* **1982**, *47*, 1200.
- (30) Nieto-Oberhuber, C.; Paz Muñoz, M.; López, S.; Jiménez-Núñez, E.; Nevado, C.; Herrero-Gómez, E.; Raducan, M.; Echavarren, A. M. *Chem.-Eur. J.* **2006**, *12*, 1677.
- (31) Pourcelot, G.; Georgoulis, C. *J. Chim. Phys. Phys.-Chim. Biol.* **1974**, *71*, 1393.
- (32) Herrmann, R.; Youn, J.-H. *Synthesis* **1987**, 72.

Chapter 5 – Synthesis of Azepines by a Gold-Catalyzed Intermolecular [4 + 3]-Annulation

The development of a convenient gold(III)-catalyzed synthesis of azepines from the intermolecular annulation of propargyl esters and α,β -unsaturated imines is discussed. Mechanistic experiments suggest that this formal [4 + 3]-cycloaddition reaction proceeds via a stepwise process involving intermolecular trapping of a gold-carbene and subsequent intramolecular trapping of the resulting allyl-gold intermediate. A portion of this work has been published.¹

Introduction

Gold catalysis has recently generated a variety of valuable methods for the synthesis of complex structures from simple starting materials.² While the majority of efforts have focused on intramolecular rearrangement and addition reactions, a number of transformations that take advantage of the intermolecular reaction of the a gold-stabilized cationic intermediates generated from the 1,2-rearrangement of propargyl esters have been described.³ In these reactions, the cationic intermediate shows reactivity analogous to that reported for electrophilic metal-stabilized vinylcarbenoids.^{4,5,6} For example, we have shown that sulfoxides react with intermediate **A** to form carbonyl compounds (eq 1).⁶ On the basis of this reactivity, we postulated that allyl gold intermediate **B**, generated by reaction of **A** with a nucleophile, could be induced to react with electrophiles. Herein, we report the realization of this goal leading to a convenient method for the construction of azepines.



Results and Discussion

In analogy to related reactions of rhodium-stabilized vinylcarbenoids,⁷ we reasoned that generation of allyl gold intermediate **B** and a proximate electrophile could be accomplished by reaction of **A** with a nucleophilic diene, such as an α,β -unsaturated imine. On the basis of this hypothesis, we were pleased to find that subjecting propargyl ester **5.1** and *N*-phenyl imine **5.2a** to our typical conditions for cationic triphenylphosphine-gold(I)-catalyzed reactions afforded a trace amount of azepine **5.3a** (Table 1, entry 1). While changing the ligand from triphenylphosphine to an *N*-heterocyclic carbene only slightly improved the yield (entry 2), the use of 10 mol % of AuCl allowed for the formation of azepine **5.3a** in 44% yield (entry 3). On the basis of reports that suggest AuCl may form Au(III) species in situ,⁸ we subsequently examined Au(III) sources and were pleased to find that picolinic acid derived catalyst **5.4a** catalyzed the formation of the desired product with increased efficiency (65% yield, entry 5).⁹

Table 1. Optimization of the Au-Catalyzed [4 + 3]-Cycloaddition

Reaction scheme showing the [4 + 3]-cycloaddition of propargyl ester **5.1** (1.3 equiv) and *N*-phenyl imine **5.2a** to form azepine **5.3a**. The reaction conditions are 10% catalyst in CD₂Cl₂ at room temperature (rt).

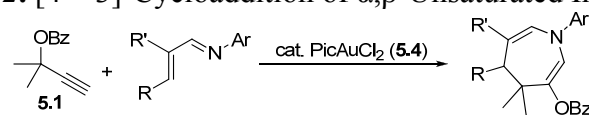
entry	catalyst	time (h)	yield (%) ^a
1	Ph ₃ PAuCl + AgSbF ₆	24	6
2	IMesAuCl + AgSbF ₆	24	17
3	AuCl	4	44
4	AuCl ₃	4	33
5	PicAuCl ₂ (5%)	2	65

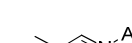
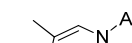
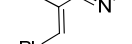
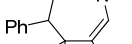

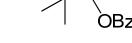

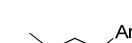
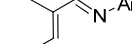
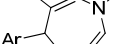
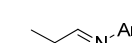
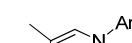
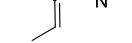
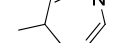
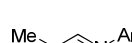
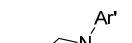


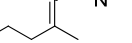
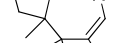
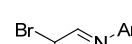
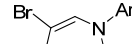
Structure of PicAuCl₂ (**5.4**):

^a By ¹H NMR versus an internal standard.

With optimized conditions in hand, we first examined the scope in imine of the gold-catalyzed [4 + 3]-cycloaddition (Table 2). In general, the highest yields were obtained with substrates containing electron-rich *N*-aryl groups on the imine nitrogen (entries 1-5). On the other hand, the reaction proved highly tolerant of variation at the other positions of the imine. Imines in conjugation with electron-rich and electron-deficient aryl groups both underwent the desired formal cycloaddition in good yield (entries 6 and 7). The olefin substituents can also be aliphatic (entries 8-10). For example, imine **5.9** underwent chemoselective [4 + 3]-cycloaddition to afford **5.10** in 62% yield without cyclopropanation of the isolated alkene.¹⁰ Notably, β -disubstituted imine **5.11** was converted to azepine **5.12**, a compound which contains two adjacent all quaternary carbon centers (entry 10). Additionally, gold-catalyzed cycloaddition of vinyl bromide **5.13** produced a 63% yield of bromoazepine **5.14**, a potential cross coupling partner (entry 10).

Table 2. [4 + 3]-Cycloaddition of α,β -Unsaturated Imines



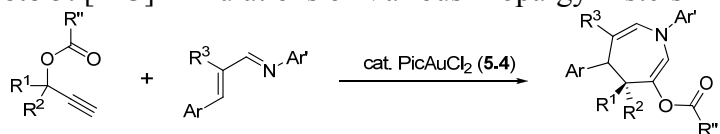
entry ^a	imine	azepine	yield
1	 5.2b	 5.3b	87% Ar = 4-HO-2,6-Me ₂ -C ₆ H ₂ ≡ Ar'
2	 5.2c	 5.3c	80% Ar = 2,6-Me ₂ -C ₆ H ₃
3	 5.2d	 5.3d	88% Ar = 2,3-Me ₂ -C ₆ H ₃
4	 5.2e	 5.3e	65% Ar = 4-MeO-C ₆ H ₄
5	 5.2f	 5.3f	55% Ar = 4-F-C ₆ H ₄
6	 5.5a	 5.6a	70% Ar = 4-NO ₂ -C ₆ H ₄
7	 5.5b	 5.6b	80% Ar = 4-MeOC ₆ H ₄
8	 5.7	 5.8	65%
9	 5.9	 5.10	62%
10	 5.11	 5.12	63%
11 ^b	 5.13	 5.14	30%

^a Conditions: 1.3 equiv **5.1**, 5% **5.4**, CH₂Cl₂, rt. ^b Conditions: 1.3 equiv **5.1**, 10% **5.4**, ClCH₂CH₂Cl, 60 °C. Ar' = 4-HO-2,6-Me₂-C₆H₂.

We next turned to examine the scope of the propargyl ester component of the cycloaddition (Table 3). With secondary benzylic propargyl esters **5.15** and **5.17**, the reactions provided azepine products **5.16** and **5.18** in good yields and as single diastereomers (entries 1 and 2).¹¹ Tertiary propargyl esters also participated in the cycloaddition, smoothly affording all-carbon quaternary centers in azepines **5.20** and **5.21**, albeit with diminished diastereocontrol (entries 3

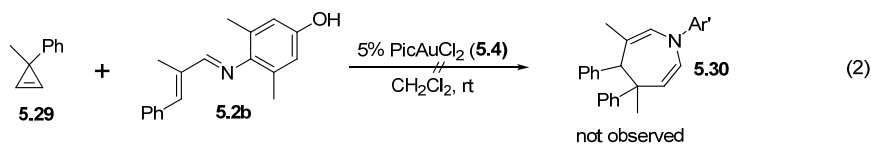
and 4). Similarly, *tert*-butylcyclohexanone derived ester **5.23** underwent the gold catalyzed cycloaddition to generate **5.24** with 2.5:1 *dr* with respect to the axial stereocenter (entry 5). Propargyl esters other than benzoate were also tolerated; when chiral racemic ester **5.25** was employed, a complete lack of diastereoselectivity in the formation of **5.26** was observed (entry 6). Substitution of the alkyne terminus was not tolerated: when diyne **5.27a** or alkynoate **5.27b** were employed, no desired product was observed (entries 7-8).¹² Cyclopropene **5.29** was also not a viable coupling partner (eq 2). On the other hand, Zhang and coworkers have reported that 2-(1-alkynyl)-2-alken-1-ones do provide [4 + 3] annulation products.¹³

Table 3. [4+3] Annulations of Various Propargyl Esters



entry ^a	propargyl ester or cyclopropene	imine	azepine	yield (<i>dr</i>)
1		5.15 5.5a		99% (>20:1)
2		5.17 5.11		73% (>20:1)
3		5.19 5.2b		73% (3.3:1)
4		5.21 5.2b		83% (1.4:1)
5 ^b		5.23 5.2b		58% ^b (2.5:1)
6		5.25 5.2b		80% (1:1)
7		5.27a 5.2b		0%
8		5.27b 5.2b		0%

^a Conditions: 1.3 equiv propargyl ester, 5% **5.4**, CH₂Cl₂, rt. ^b Conditions: 2 equiv propargyl ester, 10% **5.4**, ClCH₂CH₂Cl, 60 °C. Ar' = 4-HO-2,6-Me₂-C₆H₂.



A proposed mechanism that accounts for this diastereoselectivity is detailed in Scheme 1. Gold-promoted isomerization of the propargyl ester leads to gold-carbenoid intermediate **A**. Subsequent nucleophilic addition of the imine nitrogen generates allyl gold intermediate **5.31**, which undergoes intramolecular cyclization via transition state **5.32**.

Scheme 1. Mechanistic Hypothesis

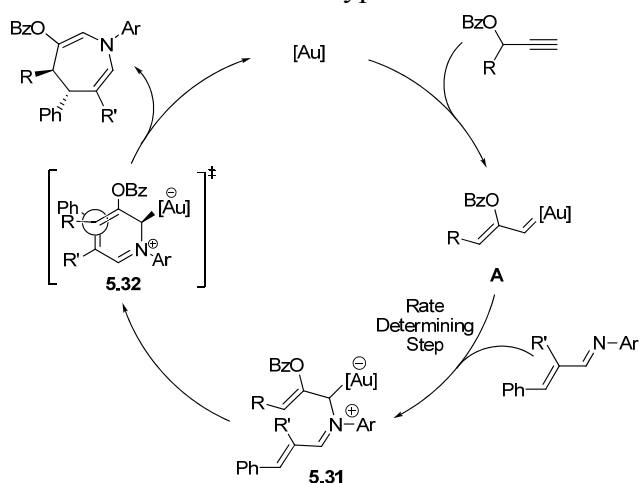
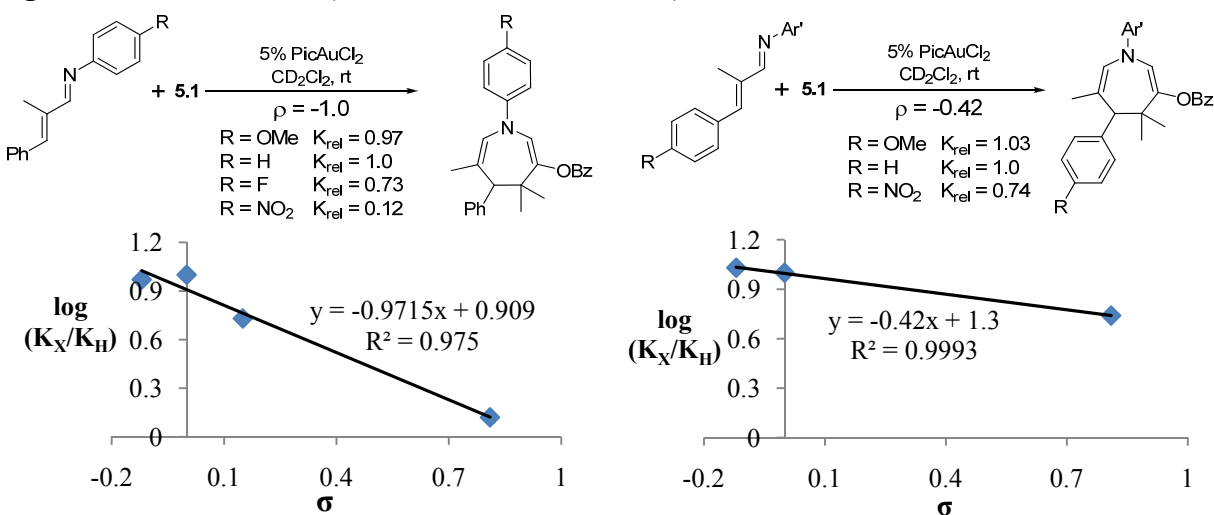
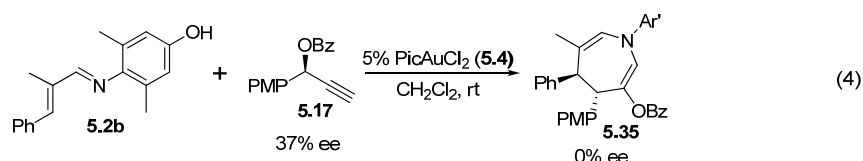
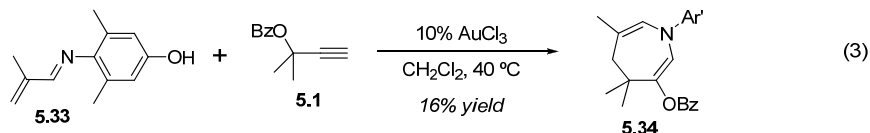


Figure 1. Hammett Plots ($\text{Ar}' = 4\text{-HO-2,6-Me}_2\text{-C}_6\text{H}_2$)



A brief Hammett plot was constructed to ascertain the effect varying the electronics of the N -aryl and β -aryl groups on the rate of the reaction (Figure 1). To obtain these plots, a competition experiment was performed by mixing an excess of two imines (3 equivalents each, one with $R = \text{H}$, the other with $R = \text{X}$), one equivalent of propargyl ester **5.1**, and an internal standard in deuterated methylene chloride. The reaction was initiated by addition of 10% catalyst (PicAuCl₂) and monitored by ¹H-NMR. Upon consumption of ester **5.1**, the ratio of the resulting two azepine products was assumed to be the same as the relative rates of reaction for each imine. These experiments revealed that electron-donating substituents on the N -aryl and β -aryl groups enhance the rate of the gold-catalyzed cycloaddition. This supports a stepwise mechanism in which

formation of iminium **5.31** is likely to be the rate-determining step. This is in agreement with literature precedence that suggests the formation of carbenoid **A** is reversible.¹⁴ In addition, these Hammett plots suggest that the poor reactivity of β -unsubstituted imine **5.33** may be a result of unfavorable electronics (eq 3).

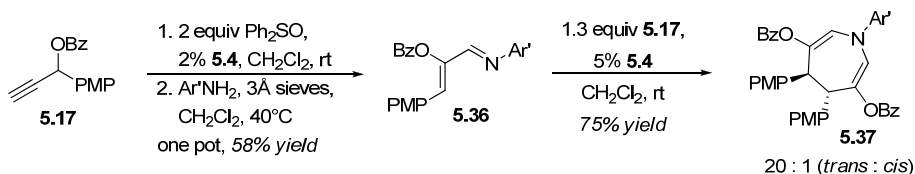


Additional evidence for the formation of carbenoid intermediate **A** was obtained from two additional experiments. Firstly, and as was observed in the intermolecular cyclopropanation of these intermediates,^{4b} chirality was not transferred in the cycloaddition of enantioenriched propargyl ester **5.17** with imine **5.2b** (eq 4). In addition, it was observed the *E/Z*-selectivities obtained by trapping intermediate **A** with diphenyl sulfoxide⁶ are not identical to the diastereoselectivities observed in the formation of azepines (Table 4). This suggests that **A** is formed reversibly^{3b} and reacts with nucleophile-dependent selectively. It is also notable that both components employed in the cycloaddition reaction to form azepine **5.37** can be generated from gold catalyzed rearrangements of propargyl ester **5.17** (eq 5).

Table 4. Comparison of Observed Diastereoselectivities

Ar' dr (yield) ^a	propargyl ester 	Z : E (yield) ^b
> 20 : 1 ^c (86%)		12 : 1 (73%)
1 : 3.3 (73%)		1 : 4.1 (90%)
1.4 : 1 (83%)		1.2 : 1 (75%)

^a Conditions: 1.3 equiv propargyl ester, 5% **5.4**, CH₂Cl₂, rt. ^b Conditions: 2 equiv Ph₂SO, 5% **5.4**, CH₂Cl₂, rt. ^c Only the *trans* diastereomer was observed. Ar' = 4-HO-2,6-Me₂-C₆H₂



On the basis of these mechanistic experiments, we envisioned that heteroaryl imines might also serve as heterodienes in the gold-catalyzed [4 + 3]-cycloaddition (Table 5). We were pleased to find that indole azepine **5.39** was formed from the gold-catalyzed cycloaddition of **5.1** with imine **5.38**, albeit at slightly elevated temperatures and increased catalyst loading (entry 1). On the other hand, quinoline imine **5.40** underwent gold-catalyzed coupling with propargyl ester **5.1** to furnish tricyclic azepine **5.41** in 93% yield at room temperature (entry 2). Unfortunately, no product was isolated in the reactions of pyridine imine **5.42**, pyridinium imine **5.44**, or benzothiophene imine **5.46**.

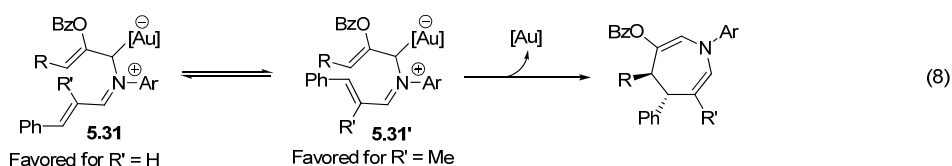
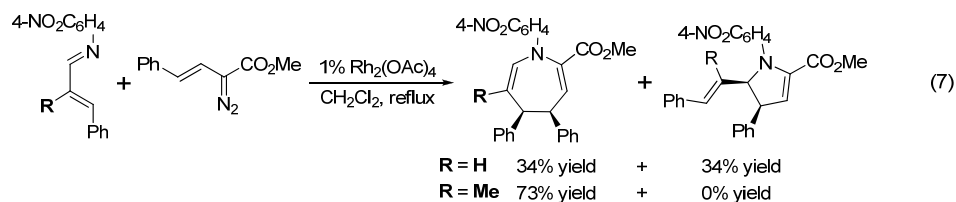
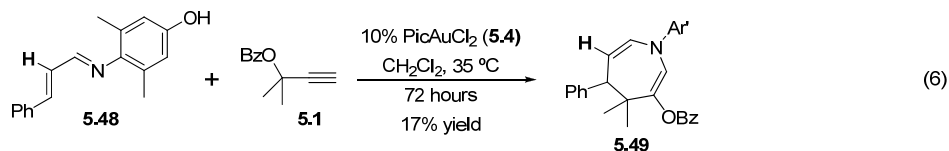
Table 5. Cyclization of heteroaromatic imines.

entry	imine	azepine	yield
1 ^a			61%
2 ^b			93%
3 ^b			0%
4 ^b			0%
5 ^b			0%

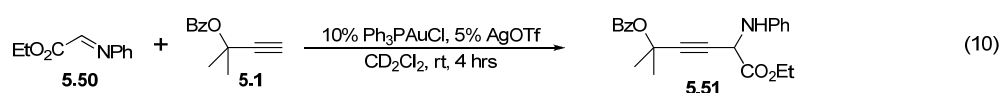
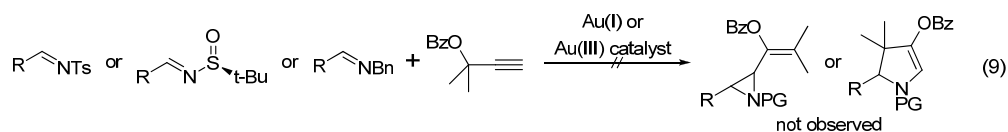
^a Conditions: 2 equiv **5.1**, 10% **5.4**, ClCH₂CH₂Cl, 60 °C. ^b Conditions: 1.3 equiv **5.1**, 5% **5.4**, CH₂Cl₂, rt. Ar' = 4-HO-2,6-Me₂-C₆H₂.

One limitation of this annulation reaction is the near requirement for the imine to have an α -substituent. For example, replacing the α -methyl substituent of imine **5.2b** with a hydrogen as in **5.48**, results in a dramatic decrease in yield (eq 6; an 87% yield was obtained with imine **5.2b**, see Table 2, entry 1). Doyle and coworkers observed a similar effect in their rhodium-catalyzed annulation of styryldiazoacetates and α,β -unsaturated imines (eq 7).^{7a} In their case, they observed competitive formation of a pyrrolidine product in the absence of an α -substituent. They hypothesized that this substituent controls the conformational dynamics of the product forming intermediates. A similar situation may exist in the Au(III)-catalyzed reaction, with the product-forming conformation of intermediate **5.31'** being favored for steric reasons when an α -substituent is present (eq 8). Curiously, and in stark contrast to the Rh-catalyzed reaction,

formation of pyrrolidine or aziridine products was never observed. Explaining this lack of reactivity remains an area for future research.



Several attempts were made to coax the system towards the formation of a five-membered ring. For example, several N-protected imines were subjected to standard annulation reaction conditions; however, in no case was any annulated product detected (eq 9). Another approach was to increase the electrophilicity of the imine by installing an adjacent electron withdrawing substituent. In this case, productive reactivity was observed, although neither of the expected products was formed. Instead, the acetylide addition product **5.51** was isolated (eq 10).^{15,16,17}

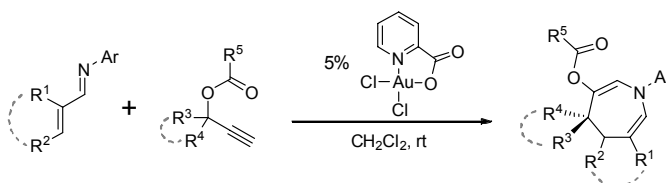


Conclusions

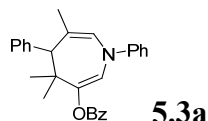
We have developed a Au(III)-catalyzed synthesis of azepines via the annulation of simple, readily available starting materials. In addition to representing a rare example of a Au-catalyzed intermolecular annulation reaction,¹⁸ the [4 + 3]-cycloaddition highlights the generation and subsequent electrophilic trapping of an allyl-gold intermediate from gold-stabilized vinyl carbenoid **A**. This mechanistic paradigm was subsequently utilized in the development of a gold(III)-catalyzed [3 + 3] annulation (see Chapter 6).

Supporting Information

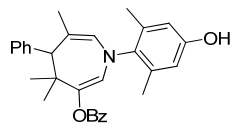
General Information. Unless otherwise noted, reagents were obtained commercially and used without further purification. Small scale reactions (< 3mL) were carried out in Fisher Scientific disposable scintillation vials. HPLC grade dichloromethane (CH_2Cl_2), ACS grade hexanes, and ACS grade ethyl acetate (EtOAc) were obtained from Fischer Scientific. TLC analysis of reaction mixtures was performed on Merck silica gel 60 F254 TLC plates using UV light and ceric ammonium molybdate stain to visualize the reaction components. Flash chromatography was carried out on ICN SiliTech 32-63 D 60 Å silica gel. ^1H and ^{13}C NMR spectra were recorded with Bruker AV-300, AVB-400, AVQ-400, DRX-500, and AV-500 spectrometers and referenced to CDCl_3 unless otherwise noted. Mass spectral and analytical data were obtained via the Micro-Mass/Analytical Facility operated by the College of Chemistry, University of California, Berkeley. X-ray structure acquisition and analysis were performed by Dr. Frederick J. Hollander of the University of California, Berkeley College of Chemistry X-ray crystallographic facility.



General procedure for the gold(III)-catalyzed [4+3] reaction. To a one dram vial equipped with a magnetic stir bar, was sequentially added N-aryl imine (~0.3 mmol, 1 equiv), propargyl ester (1.3 equiv), CH_2Cl_2 (0.3 M) and PicAuCl_2 (0.05 equiv). The resulting mixture was stirred at room temperature and monitored periodically by TLC. Upon consumption of the imine (2 – 6 hrs), the reaction mixture was directly subjected to silica gel chromatography (hexanes/ethyl acetate/dichloromethane) to give the desired azepine products.

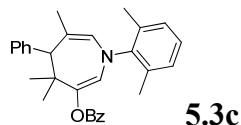


^1H NMR (400 MHz, CDCl_3) δ 7.91 (d, 2H, $J = 8.0$ Hz), 7.53 (t, 1H, $J = 7.4$ Hz), 7.41-7.24 (m, 11H), 7.09 (t, 1H, $J = 7.2$ Hz), 6.47 (s, 2H), 3.24 (s, 1H), 1.80 (s, 3H), 1.47 (s, 3H), 0.94 (s, 3H). ^{13}C NMR (100 MHz, CDCl_3) δ 166.5, 147.6, 143.8, 138.5, 133.3, 130.1, 130.0, 129.9, 129.4, 128.6, 127.9, 126.6, 124.1, 123.6, 120.9, 115.8, 62.5, 42.8, 30.1, 26.3, 25.7. HRMS (FAB) calc. for $[\text{C}_{28}\text{H}_{27}\text{NO}_2]^+$ 409.2042, found 409.2041.

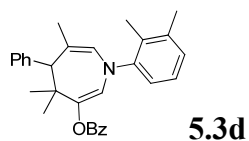


^1H NMR (500 MHz, CDCl_3) δ 7.93 (d, 2H, $J = 8.0$ Hz), 7.53-7.48 (m, 3H), 7.39-7.32 (m, 4H), 7.26 (t, 1H, $J = 7.3$ Hz), 6.56 (s, 1H), 6.53 (s, 1H), 5.99 (s, 1H), 5.72 (s, 1H), 5.71 (bs, 1H), 3.25

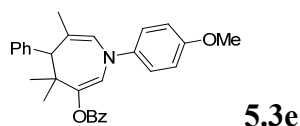
(s, 1H), 2.33 (s, 3H), 2.32 (s, 3H), 1.73 (s, 3H), 1.56 (s, 3H), 0.92 (s, 3H). ^{13}C NMR (125 MHz, CDCl_3) δ 167.3, 154.7, 145.3, 140.1, 139.0, 137.3, 133.7, 133.3, 130.1, 130.0, 130.0, 128.6, 127.8, 126.3, 126.0, 125.4, 115.1, 115.1, 112.2, 63.5, 43.0, 31.3, 26.9, 25.5, 18.7, 18.7. HRMS (FAB) calc. for $[\text{C}_{30}\text{H}_{31}\text{NO}_3]^+$ 453.2304, found 453.2306.



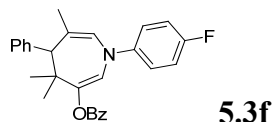
^1H NMR (400 MHz, CDCl_3) δ 7.91 (d, 2H, $J = 7.2$ Hz), 7.51-7.48 (m, 3H), 7.38-7.31 (m, 4H), 7.28-7.25 (m, 1H), 7.10 (s, 3H), 5.98 (s, 1H), 5.74 (s, 1H), 3.25 (s, 1H), 2.47 (s, 3H), 2.40 (s, 3H), 1.74 (s, 3H), 1.56 (s, 3H), 0.91 (s, 3H). ^{13}C NMR (75 MHz, CDCl_3) δ 166.9, 162.6, 146.8, 145.4, 137.7, 136.0, 130.3, 130.2, 130.1, 129.0, 129.0, 128.6, 127.9, 127.7, 126.5, 125.5, 124.9, 112.5, 63.6, 43.2, 31.4, 27.0, 25.6, 18.8. HRMS (FAB) calc. for $[\text{C}_{30}\text{H}_{31}\text{NO}_2]^+$ 437.2355, found 437.2362.



^1H NMR (400 MHz, CDCl_3) δ 7.91 (d, 2H, $J = 8.0$ Hz), 7.49 (t, 1H, $J = 7.6$ Hz), 7.47 (d, 2H, $J = 8.0$ Hz), 7.38-7.32 (m, 4H), 7.26 (t, 1H, $J = 7.2$ Hz), 7.19 (d, 1H, $J = 7.6$ Hz), 7.11 (t, 1H, $J = 7.2$ Hz), 7.06 (d, 1H, $J = 7.2$ Hz), 6.13 (s, 1H), 5.96 (s, 1H), 3.25 (s, 1H), 2.33 (s, 3H), 2.31 (s, 3H), 1.76 (s, 3H), 1.56 (s, 3H), 0.94 (s, 3H). ^{13}C NMR (100 MHz, CDCl_3) δ 166.8, 148.1, 144.9, 138.7, 134.2, 133.6, 133.1, 130.2, 130.0, 130.0, 128.5, 128.3, 127.9, 126.5, 126.4, 126.3, 125.6, 125.3, 112.5, 63.2, 43.0, 30.9, 26.7, 25.5, 20.8, 14.8. HRMS (FAB) calc. for $[\text{C}_{30}\text{H}_{31}\text{NO}_2]^+$ 437.2355, found 437.2346.

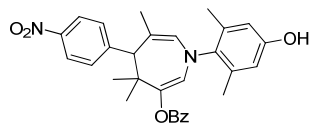


^1H NMR (500 MHz, CDCl_3) δ 7.92 (d, 2H, $J = 7.5$ Hz), 7.52 (t, 1H, $J = 7.5$ Hz), 7.41-7.36 (m, 4H), 7.32 (t, 2H, $J = 7.5$ Hz), 7.26 (t, 1H, $J = 7.5$ Hz), 7.21 (d, 2H, $J = 9.0$ Hz), 6.88 (d, 2H, $J = 9.0$ Hz), 6.38 (s, 1H), 6.34 (s, 1H), 3.81 (s, 3H), 3.24 (s, 1H), 1.80 (s, 3H), 1.48 (s, 3H), 0.94 (s, 3H). ^{13}C NMR (125 MHz, CDCl_3) δ 166.6, 156.4, 144.2, 141.8, 136.8, 133.2, 130.1, 129.9, 128.5, 127.9, 126.5, 125.0, 124.1, 123.2, 114.6, 114.5, 62.7, 55.8, 42.9, 30.5, 26.4, 25.7. HRMS (FAB) calc. for $[\text{C}_{29}\text{H}_{29}\text{NO}_3]^+$ 439.2147, found 439.2144.



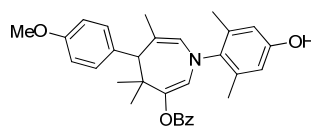
^1H NMR (500 MHz, CDCl_3) δ 7.91 (d, 2H, $J = 7.5$ Hz), 7.53 (t, 1H, $J = 7.0$ Hz), 7.40-7.35 (m, 4H), 7.31 (t, 2H, $J = 7.5$ Hz), 7.27-7.20 (m, 3H), 7.03 (t, 2H, $J = 8.5$ Hz), 6.38 (s, 1H), 6.36 (s, 1H), 3.23 (s, 1H), 1.79 (s, 3H), 1.46 (s, 3H), 0.94 (s, 3H). ^{13}C NMR (125 MHz, CDCl_3) δ 166.5, 159.5 (d, $J = 241$ Hz), 144.1 (d, $J = 4$ Hz), 143.8, 138.1, 133.3, 130.1, 129.9, 129.9, 128.6, 127.9,

126.6, 124.4, 123.7, 122.9 (d, $J = 8$ Hz), 116.0 (d, $J = 23$ Hz), 115.6, 62.5, 42.9, 30.2, 26.3, 25.7. HRMS (FAB) calc. for $[\text{C}_{28}\text{H}_{26}\text{NO}_2\text{F}]^+$ 427.1948, found 427.1954.



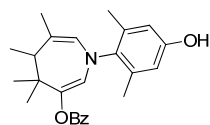
5.6a

^1H NMR (400 MHz, CDCl_3) δ 8.20 (d, 2H, $J = 8.8$ Hz), 7.92 (d, 2H, $J = 7.6$ Hz), 7.67 (d, 2H, $J = 8.8$ Hz), 7.53 (t, 1H, $J = 7.6$ Hz), 7.38 (t, 2H, $J = 7.6$ Hz), 6.57 (s, 1H), 6.55 (s, 1H), 6.02 (s, 1H), 5.77 (s, 1H), 5.77 (bs, 1H), 3.40 (s, 1H), 2.32 (s, 3H), 2.30 (s, 3H), 1.72 (s, 3H), 1.58 (s, 3H), 0.92 (s, 3H). ^{13}C NMR (100 MHz, CDCl_3) δ 167.2, 154.9, 153.1, 146.7, 139.8, 138.7, 137.0, 133.5, 133.0, 130.6, 130.0, 129.7, 128.7, 127.0, 125.8, 123.1, 115.3, 115.2, 110.8, 63.3, 43.1, 31.4, 26.7, 25.3, 18.7, 18.6. HRMS (FAB) calc. for $[\text{C}_{30}\text{H}_{30}\text{N}_2\text{O}_5]^+$ 498.2155, found 498.2156



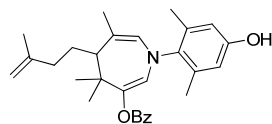
5.6b

^1H NMR (500 MHz, CDCl_3) δ 7.93 (d, 2H, $J = 7.5$ Hz), 7.52 (t, 1H, $J = 7.5$ Hz), 7.41 (d, 2H, $J = 8.5$ Hz), 7.38 (t, 2H, $J = 8.0$ Hz), 6.89 (d, 2H, $J = 8.5$ Hz), 6.55 (s, 1H), 6.53 (s, 1H), 5.97 (s, 1H), 5.69 (s, 1H), 5.68 (bs, 1H), 3.84 (s, 3H), 3.19 (s, 1H), 2.33 (s, 3H), 2.31 (s, 3H), 1.73 (s, 3H), 1.54 (s, 3H), 0.91 (s, 3H). ^{13}C NMR (125 MHz, CDCl_3) δ 167.3, 158.2, 154.7, 139.0, 140.1, 139.0, 137.6, 137.3, 133.7, 133.3, 130.8, 130.1, 128.6, 125.8, 125.4, 115.1, 115.1, 113.2, 112.6, 62.6, 55.4, 43.1, 31.2, 26.9, 25.5, 18.7, 18.7. HRMS (FAB) calc. for $[\text{C}_{31}\text{H}_{33}\text{NO}_4]^+$ 483.2410, found 483.2421.



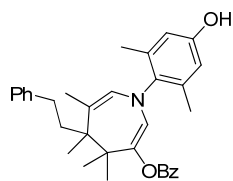
5.8

^1H NMR (400 MHz, CDCl_3) δ 8.10 (d, 2H, $J = 8.0$ Hz), 7.57 (t, 1H, $J = 7.4$ Hz), 7.45 (t, 2H, $J = 8.0$ Hz), 6.50 (s, 2H), 6.15 (bs, 1H), 5.77 (s, 1H), 5.52 (s, 1H), 2.23 (s, 3H), 2.16 (s, 3H), 2.13 (q, 1H, $J = 7.0$ Hz), 1.81 (s, 3H), 1.38 (s, 3H), 1.28 (d, 3H, $J = 7.0$ Hz), 1.15 (s, 3H). ^{13}C NMR (100 MHz, CDCl_3) δ 167.9, 154.7, 140.0, 138.3, 138.1, 133.3, 132.1, 130.3, 130.1, 128.6, 125.6, 125.1, 117.6, 115.0, 114.8, 50.2, 43.2, 31.5, 26.7, 25.1, 18.3, 18.2, 17.3. HRMS (FAB) calc. for $[\text{C}_{25}\text{H}_{29}\text{NO}_3]^+$ 391.2147, found 391.2153.



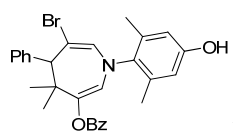
5.10

^1H NMR (400 MHz, CDCl_3) δ 8.08 (d, 2H, $J = 7.4$ Hz), 7.56 (t, 1H, $J = 7.4$ Hz), 7.42 (t, 2H, $J = 7.4$ Hz), 6.50 (d, 1H, $J = 3.0$ Hz), 6.48 (d, 1H, $J = 3.0$ Hz), 5.72 (s, 1H), 5.62 (s, 1H), 5.51 (bs, 1H), 4.75 (s, 1H), 4.74 (s, 1H), 2.32-2.26 (m, 1H), 2.26 (s, 3H), 2.16 (s, 3H), 2.12-2.02 (m, 2H), 1.99 (app t, 2H, $J = 7.8$ Hz), 1.83 (s, 3H), 1.77 (s, 3H), 1.36 (s, 3H), 1.19 (s, 3H). ^{13}C NMR (125 MHz, CDCl_3) δ 167.7, 154.5, 146.8, 140.2, 138.3, 138.1, 133.3, 132.1, 130.4, 130.1, 128.6, 126.4, 124.9, 117.0, 115.1, 114.7, 109.9, 55.8, 43.4, 36.4, 31.9, 29.9, 27.0, 26.9, 23.0, 18.4, 18.2. HRMS (FAB) calc. for $[\text{C}_{29}\text{H}_{35}\text{NO}_3]^+$ 445.2617, found 445.2619.



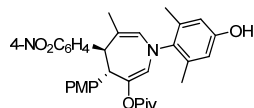
5.12

^1H NMR (500 MHz, CDCl_3) δ 8.05 (d, 2H, $J = 7.5$ Hz), 7.54 (t, 1H, $J = 7.3$ Hz), 7.42 (t, 2H, $J = 7.8$ Hz), 7.30 (t, 2H, $J = 7.5$ Hz), 7.23 (d, 2H, $J = 7.5$ Hz), 7.19 (t, 1H, $J = 7.3$ Hz), 6.50 (dd, 2H, $J = 12, 3$ Hz), 5.79 (s, 1H), 5.74 (s, 1H), 4.98 (s, 1H), 2.76-2.63 (m, 2H), 2.29 (s, 3H), 2.25 (td, 1H, $J = 12.5, 5$ Hz), 2.17 (s, 3H), 1.83 (s, 3H), 1.76 (dt, 1H, $J = 12.5, 5.5$ Hz), 1.29 (s, 3H), 1.27 (s, 3H), 1.10 (s, 3H). ^{13}C NMR (125 MHz, CDCl_3) δ 18.4, 18.6, 20.4, 21.3, 24.8, 27.6, 31.6, 41.0, 47.6, 47.9, 114.6, 115.1, 115.9, 124.4, 125.7, 127.3, 128.5, 128.6, 128.7, 130.1, 130.3, 133.2, 133.8, 137.9, 138.4, 140.4, 143.8, 154.3, 167.7. HRMS (FAB) calc. for $[\text{C}_{33}\text{H}_{37}\text{NO}_3]^+$ 495.2773, found 495.2773.



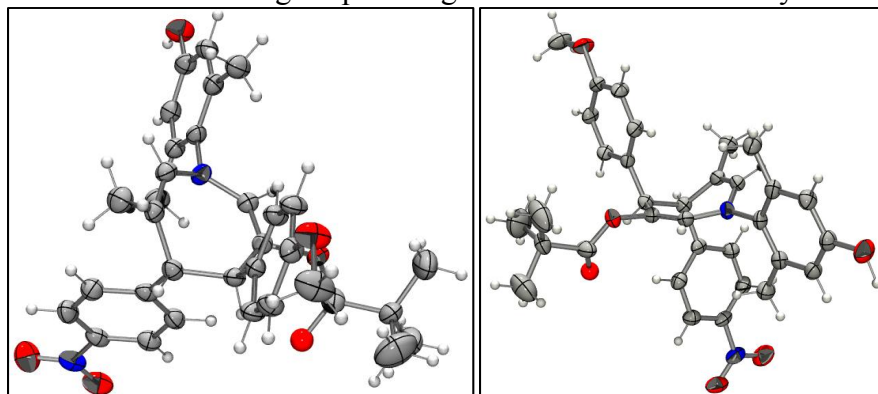
5.14

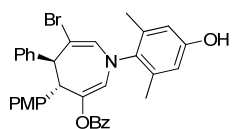
^1H NMR (400 MHz, CDCl_3) δ 7.90 (d, 2H, $J = 7.6$ Hz), 7.53 (t, 1H, $J = 7.4$ Hz), 7.47 (d, 2H, $J = 7.0$ Hz), 7.41-7.35 (m, 4H), 7.32 (t, 1H, $J = 7.0$ Hz), 6.56 (s, 1H), 6.53 (s, 1H), 6.40 (s, 1H), 6.01 (s, 1H), 5.60 (bs, 1H), 3.84 (s, 1H), 2.34 (s, 3H), 2.32 (s, 3H), 1.68 (s, 3H), 0.92 (s, 3H). ^{13}C NMR (100 MHz, CDCl_3) δ 166.9, 155.1, 143.2, 139.0, 138.8, 137.1, 135.5, 133.6, 131.4, 130.1, 129.8, 129.5, 128.7, 128.2, 127.1, 125.2, 115.3, 100.1, 67.6, 44.2, 30.7, 26.6, 18.7, 18.6. HRMS (FAB) calc. for $[\text{C}_{29}\text{H}_{28}\text{NO}_3\text{BrNa}]^+$ 540.1150, found 540.1147.



5.16

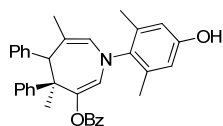
A single isomer was detected by ^1H NMR. ^1H NMR (500 MHz, CDCl_3) δ 8.20 (d, 2H, $J = 8.3$ Hz), 7.78 (d, 2H, $J = 8.3$ Hz), 7.39 (d, 2H, $J = 8.5$ Hz), 6.88 (d, 2H, $J = 8.5$ Hz), 6.54 (s, 1H), 6.47 (s, 1H), 5.98 (s, 1H), 5.84 (s, 1H), 5.40 (bs, 1H), 4.12 (d, 1H, $J = 3.0$ Hz), 3.82 (d, 1H, $J = 3.0$ Hz), 3.82 (s, 3H), 2.30 (s, 3H), 1.99 (s, 3H), 1.62 (s, 3H), 1.05 (s, 9H). ^{13}C NMR (125 MHz, CDCl_3) δ 178.4, 158.4, 154.7, 152.3, 146.5, 139.6, 137.9, 137.8, 136.4, 130.2, 129.3, 129.2, 128.4, 127.7, 123.6, 115.4, 115.0, 113.8, 113.1, 55.4, 54.7, 52.7, 38.9, 27.2, 25.7, 18.6, 18.4. HRMS (FAB) calc. for $[\text{C}_{33}\text{H}_{36}\text{N}_2\text{O}_6]^+$ 556.2573, found 556.2558. X-ray quality crystals were grown from ethanol. Views showing azepine ring and *trans* stereochemistry:





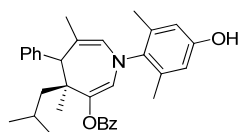
5.18

A single isomer was detected by ^1H NMR. ^1H NMR (400 MHz, CDCl_3) δ 7.86 (d, 2H, $J = 7.6$ Hz), 7.66 (d, 2H, $J = 7.6$ Hz), 7.54-7.48 (m, 3H), 7.43 (t, 2H, $J = 7.6$ Hz), 7.38-7.29 (m, 3H), 6.94 (d, 2H, $J = 8.4$ Hz), 6.50 (s, 2H), 6.48 (s, 1H), 6.20 (s, 1H), 5.28 (bs, 1H), 4.50 (d, 1H, $J = 2.8$ Hz), 4.25 (d, 1H, $J = 2.8$ Hz), 3.84 (s, 3H), 2.23 (s, 3H), 2.19 (s, 3H). ^{13}C NMR (100 MHz, CDCl_3) δ 165.8, 158.5, 154.9, 143.3, 138.9, 137.9, 137.8, 135.7, 134.0, 133.4, 131.3, 130.0, 129.9, 129.2, 128.6, 128.5, 128.3, 127.2, 127.0, 115.3, 115.2, 114.0, 99.7, 59.4, 55.5, 54.8, 18.5. HRMS (FAB) calc. for $[\text{C}_{34}\text{H}_{30}\text{NO}_4\text{Br}]^+$ 595.1358, found 595.1357.



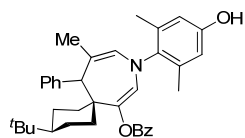
5.20

Obtained as an inseparable 3.3:1 mixture of diastereomers. ^1H NMR (400 MHz, CDCl_3) Major diastereomer: δ 7.60 (d, 2H, $J = 8.0$ Hz), 7.41-7.03 (m, 13H), 6.59 (s, 2H), 6.21 (s, 1H), 5.81 (s, 1H), 5.60 (bs, 1H), 3.49 (s, 1H), 2.47 (s, 3H), 2.44 (s, 3H), 1.96 (s, 3H), 1.68 (s, 3H). Minor diastereomer: δ 7.92 (d, 2H, $J = 8.0$ Hz), 7.75 (d, 2H, $J = 7.6$ Hz), 7.71 (d, 2H, $J = 7.6$ Hz), 7.50 (t, 1H, $J = 7.2$ Hz), 7.41-7.03 (m, 8H), 6.50 (s, 2H), 6.40 (s, 1H), 5.60 (bs, 1H), 5.51 (s, 1H), 3.98 (s, 1H), 2.28 (s, 3H), 2.03 (s, 3H), 1.58 (s, 3H), 1.29 (s, 3H). ^{13}C NMR (100 MHz, CDCl_3) δ 167.3, 155.0, 149.7, 144.4, 143.9, 143.4, 140.2, 139.9, 139.0, 138.3, 137.6, 137.2, 133.4, 133.1, 131.1, 130.8, 130.7, 130.0, 129.8, 129.2, 128.6, 128.3, 128.2, 128.0, 127.5, 127.4, 127.3, 127.0, 126.7, 126.6, 126.4, 126.0, 125.9, 116.1, 115.3, 115.1, 113.6, 63.9, 61.5, 52.2, 52.0, 29.0, 28.7, 25.3, 24.8, 19.0, 18.6, 18.4, 15.4. HRMS (FAB) calc. for $[\text{C}_{35}\text{H}_{33}\text{NO}_3]^+$ 515.2460, found 515.2463.



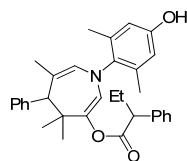
5.22

Obtained as an inseparable 1.4:1 mixture of diastereomers. ^1H NMR (400 MHz, CDCl_3) Major diastereomer: δ 7.99-7.90 (m, 2H), 7.59-7.22 (m, 8H), 6.58 (s, 1H), 6.54 (s, 1H), 6.17 (bs, 1H), 6.12 (s, 1H), 5.70 (s, 1H), 3.35 (s, 1H), 2.35 (s, 3H), 2.30 (s, 3H), 2.04 (app sept, 1H, $J = 6.0$ Hz), 1.97-1.92 (m, 1H), 1.76 (s, 3H), 1.11 (d, 3H, $J = 6.4$ Hz), 1.08 (d, 3H, $J = 6.4$ Hz), 0.96 (s, 3H). Minor diastereomer: δ 7.99-7.90 (m, 2H), 7.59-7.22 (m, 8H), 6.56 (s, 1H), 6.53 (s, 1H), 6.17 (bs, 1H), 5.99 (s, 1H), 5.70 (s, 1H), 3.53 (s, 1H), 2.33 (s, 3H), 2.26 (s, 3H), 1.87-1.79 (m, 1H), 1.78 (s, 3H), 1.33-1.27 (m, 1H), 1.22-1.77 (m, 1H), 0.81 (d, 3H, $J = 6.4$ Hz), 0.80 (d, 3H, $J = 6.4$ Hz). ^{13}C NMR (100 MHz, CDCl_3) δ 167.6, 166.7, 154.9, 145.0, 144.9, 140.2, 140.0, 138.7, 138.3, 137.6, 137.3, 134.8, 133.4, 133.3, 132.8, 130.5, 130.3, 130.2, 130.1, 130.0, 128.6, 128.2, 128.0, 127.9, 127.8, 126.3, 126.2, 126.0, 126.0, 125.8, 115.2, 115.1, 112.5, 112.3, 62.0, 60.6, 53.4, 46.7, 46.3, 45.6, 27.3, 26.1, 25.9, 25.8, 25.5, 25.4, 25.1, 25.0, 23.9, 23.6, 18.8, 18.8, 18.7, 18.6. HRMS (FAB) calc. for $[\text{C}_{33}\text{H}_{37}\text{NO}_3]^+$ 495.2773, found 495.2768.



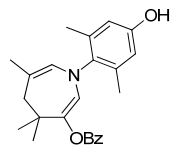
5.24

Prepared by slight modification the general procedure. Imine (1 eq), propargyl ester (2 eq) and PicAuCl₂ (10 mol %) were stirred in dichloroethane (0.3M) at 60°C overnight. NMR analysis of the crude reaction mixture indicated a 2.5:1 ratio of diastereomers. Chromatography (10% → 20% EtOAc in hexanes) provided the diastereomeric mixture as a pale yellow foam (68 mg, 58% yield). ¹H NMR (500 MHz, CDCl₃) Major diastereomer: δ 7.82 (d, 2H, *J* = 8.0 Hz), 7.59-7.26 (m, 8H), 6.58 (s, 2H), 6.19 (s, 1H), 5.96 (bs, 1H), 5.79 (s, 1H), 3.26 (s, 1H), 2.67 (app d, 1H, *J* = 11.5 Hz), 2.36 (s, 3H), 2.34 (s, 3H), 1.89-0.98 (m, 8H), 1.69 (s, 3H), 0.77 (s, 9H). Minor diastereomer: δ 7.93 (d, 2H, *J* = 7.5 Hz), 7.59-7.26 (m, 8H), 6.54 (s, 2H), 6.02 (s, 1H), 5.96 (bs, 1H), 5.77 (s, 1H), 3.99 (s, 1H), 2.42 (app d, 1H, *J* = 11.0 Hz), 2.33 (s, 3H), 2.32 (s, 3H), 1.89-0.98 (m, 8H), 1.79 (s, 3H), 0.92 (s, 9H). ¹³C NMR (100 MHz, CDCl₃) δ 167.5, 165.9, 154.8, 144.8, 144.4, 139.9, 139.9, 139.0, 138.8, 137.2, 137.1, 135.9, 133.4, 133.1, 130.6, 130.2, 130.2, 130.1, 130.0, 129.8, 128.6, 128.6, 127.9, 127.6, 126.8, 126.7, 126.4, 126.3, 126.2, 125.8, 115.2, 115.1, 110.8, 110.5, 65.2, 51.8, 48.0, 47.4, 46.3, 45.3, 38.1, 37.4, 36.3, 32.6, 32.5, 30.5, 27.7, 25.5, 25.4, 25.0, 23.8, 23.4, 21.6, 18.8, 18.8. HRMS (FAB) calc. for [C₃₇H₄₃NO₃]⁺ 549.3243, found 549.3227.



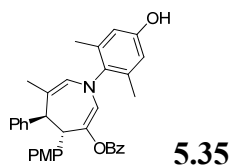
5.26

Obtained as an inseparable 1:1 mixture of diastereomers. ¹H NMR (400 MHz, CDCl₃) δ 7.43-7.14 (m, 10 H), 6.56-6.45 (m, 2H), 5.83 (s, 1H), 5.81 (s, 0.5 H), 5.70 (s, 0.5H), 5.66 (s, 1H), 3.41 (app t, 1H, *J* = 7.6 Hz), 3.17 (s, 0.5 H), 3.12 (s, 0.5 H), 2.29 (s, 1.5 H), 2.25 (s, 1.5H), 2.24 (s, 1.5H), 2.22 (s, 1.5 H), 2.08-1.98 (m, 1H), 1.82-1.71 (m, 1H), 1.64 (s, 3H), 1.46 (s, 1.5H), 1.38 (s, 1.5 H), 0.84 (t, 1.5 H, *J* = 7.8 Hz), 0.80 (t, 1.5 H, *J* = 7.8 Hz), 0.71 (s, 1.5H), 0.52 (s, 1.5H). ¹³C NMR (100 MHz, CDCl₃) δ 12.3, 12.4, 14.3, 18.6, 18.7, 22.9, 25.4, 25.5, 26.4, 26.6, 26.9, 31.1, 31.2, 31.8, 34.9, 42.7, 42.8, 53.4, 53.5, 63.4, 63.4, 112.1, 112.3, 115.1, 115.1, 125.0, 125.2, 125.9, 126.0, 126.2, 127.2, 127.3, 127.8, 128.2, 128.3, 128.7, 128.8, 129.9, 130.0, 133.5, 133.7, 137.3, 137.3, 138.7, 138.8, 138.9, 140.0, 140.1, 145.1, 145.2, 154.7, 154.9, 174.9, 175.1.



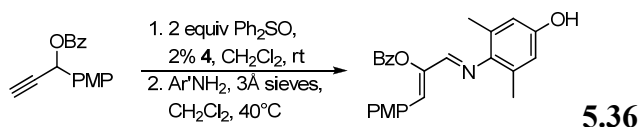
5.34

¹H NMR (500 MHz, CDCl₃) δ 8.07 (d, 2H, *J* = 7.3 Hz), 7.55 (t, 1H, *J* = 7.3 Hz), 7.44 (t, 2H, *J* = 7.3 Hz), 6.50 (s, 2H), 5.70 (s, 1H), 5.68 (s, 1H), 4.71 (bs, 1H), 2.31 (s, 2H), 2.26 (s, 3H), 1.78 (s, 3H), 1.26 (s, 6H).

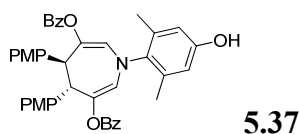


A single isomer was detected by ^1H NMR. Column chromatography provided the desired product as a white solid (18 mg, 86% yield). ^1H NMR (500 MHz, CDCl_3) δ 7.90 (d, 2H, $J = 8$ Hz), 7.66 (d, 2H, $J = 8$ Hz), 7.51-7.46 (m, 3H), 7.39 (t, 2H, $J = 7.8$ Hz), 7.35 (t, 2H, $J = 7.5$ Hz), 7.29-7.25 (m, 1H), 6.53 (s, 1H), 6.48 (s, 1H), 6.17 (s, 1H), 5.84 (s, 1H), 5.2 (bs, 1H), 4.33 (d, 1H, $J = 3$ Hz), 4.84 (d, 1H, $J = 3$ Hz), 3.82 (s, 3H), 2.37 (s, 3H), 2.07 (s, 3H), 1.63 (s, 3H), 1.27 (s, 3H).

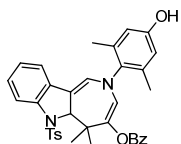
^{13}C NMR (125 MHz, CDCl_3) δ 18.5, 18.7, 26.0, 53.9, 55.2, 55.4, 113.6, 114.3, 115.0, 115.2, 126.4, 128.1, 128.3, 128.4, 128.4, 128.6, 129.0, 129.3, 130.0, 130.4, 133.1, 137.1, 138.0, 138.3, 140.0, 144.8, 154.5, 158.1, 166.3. HRMS (FAB) calc. for $[\text{C}_{35}\text{H}_{33}\text{NO}_4]^+$ 531.2410, found 531.2413. Enantiomeric excess was determined on a Shimadzu VP Series Chiral HPLC (Chiralcel AD-H column, 94:06 hexanes/2-propanol, 1 mL/min) tr 17.2 min, 21.3 min.



To a one dram vial equipped with a magnetic stir bar, was added propargyl ester (233mg, 0.875 mmol, 1 equiv), diphenylsulfoxide (353mg, 1.75 mmol, 2 equiv) and CH_2Cl_2 (2.9 mL). The mixture was cooled to 10°C and PicAuCl_2 (6.8 mg, 0.017 mmol, 2 mol %) was added. The cooling bath was subsequently removed and the mixture was stirred for 1 hour at which point TLC analysis indicated consumption of the propargyl ester. 3\AA molecular sieves (250 mg) and 4-hydroxy-2,6-dimethylaniline (132 mg, 0.962 mmol, 1.1 equiv) were added and the solution was stirred at 40°C overnight. After cooling to room temperature, the mixture was subjected twice to silica gel chromatography (first with 1% triethylamine in 10% \rightarrow 50% EtOAc in hexanes, and then with 20 \rightarrow 35% EtOAc in hexanes) to yield the desired imine as a yellow solid (204 mg, 58% yield). ^1H NMR (500 MHz, CDCl_3) δ 8.25 (d, 2H, $J = 7.5$ Hz), 7.82 (s, 1H), 7.64-7.60 (m, 3H), 7.50 (t, 2H, $J = 7.5$ Hz), 7.86 (d, 2H, $J = 8.0$ Hz), 6.67 (s, 1H), 6.43 (s, 2H), 5.25 (bs, 1H), 3.80 (s, 3H), 2.04 (s, 6H). ^{13}C NMR (125 MHz, CDCl_3) δ 164.4, 160.6, 157.4, 152.2, 144.2, 143.8, 133.7, 131.6, 130.6, 129.6, 129.5, 129.2, 128.8, 125.9, 114.9, 114.5, 55.5, 18.7, 14.4.

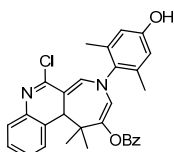


Obtained as an inseparable 20:1 mixture of diastereomers. ^1H NMR (500 MHz, CDCl_3) Major diastereomer: δ 7.88 (d, 4H, $J = 8.0$ Hz), 7.57 (d, 4H, $J = 8.5$ Hz), 7.50 (t, 2H, $J = 7.5$ Hz), 7.35 (t, 4H, $J = 7.5$ Hz), 6.94 (d, 4H, $J = 8.5$ Hz), 6.52 (s, 2H), 6.26 (s, 2H), 5.70 (bs, 1H), 4.16 (s, 2H), 3.81 (s, 6H), 2.35 (s, 6H). Additionally, the following peaks were assigned to the minor diastereomer: 8.11 (d, 4H, $J = 7.5$ Hz), 7.80 (d, 4H, $J = 7.5$ Hz), 6.67 (m, 6H), 6.18 (s, 2H), 4.52 (s, 2H), 3.72 (s, 6H), 2.44 (s, 6H). ^{13}C NMR (125 MHz, CDCl_3) δ 166.1, 158.4, 138.1, 136.1, 133.3, 131.1, 130.4, 130.1, 130.0, 129.6, 128.7, 128.5, 127.1, 115.2, 113.8, 55.4, 53.4, 18.6. HRMS (FAB) calc. for $[\text{C}_{42}\text{H}_{37}\text{NO}_7]^+$ 667.2570, found 667.2568.



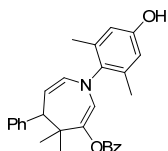
5.39

Prepared by slight modification the general procedure. Imine (1 eq), propargyl ester (2 eq) and PicAuCl₂ (10 mol %) were stirred in dichloroethane (0.3M) at 60°C overnight. Chromatography provided the desired compound as a yellow powder. ¹H NMR (400 MHz, CDCl₃) δ 8.10 (d, 2H, *J* = 7.2 Hz), 7.67 (d, 1H, *J* = 8.0 Hz), 7.59 (t, 1H, *J* = 7.4 Hz), 7.46 (t, 2H, *J* = 7.6 Hz), 7.36 (d, 2H, *J* = 8.0 Hz), 7.11 (td, 1H, *J* = 7.2, 1.6 Hz), 7.05 (d, 2H, *J* = 8.0 Hz), 7.02-6.95 (m, 2H), 6.55 (s, 1H), 6.53 (s, 1H), 6.22 (s, 1H), 5.87 (s, 1H), 5.40 (bs, 1H) 4.77 (s, 1H), 2.30 (s, 3H), 2.27 (s, 3H), 2.03 (s, 3H), 1.62 (s, 3H), 1.00 (s, 3H). ¹³C NMR (100 MHz, CDCl₃) δ 167.3, 155.3, 143.9, 142.2, 138.4, 138.0, 137.3, 134.5, 133.8, 133.6, 133.4, 130.2, 129.8, 129.3, 128.7, 128.0, 126.5, 125.9, 125.9, 122.7, 119.7, 118.0, 115.4, 115.0, 114.9, 71.2, 48.1, 24.5, 23.4, 21.7, 18.1, 17.8. HRMS (FAB) calc. for [C₃₆H₃₄N₂O₅S]⁺ 606.2188, found 606.2195.



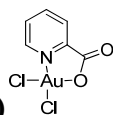
5.41

¹H NMR (500 MHz, CDCl₃) δ 8.08 (d, 2H, *J* = 8.0 Hz), 7.60 (t, 1H, *J* = 7.3 Hz), 7.47 (t, 2H, *J* = 7.5 Hz), 7.41 (d, 1H, *J* = 8.0 Hz), 7.31 (s, 1H), 7.30 (t, 1H, *J* = 7.5 Hz), 7.25 (d, 2H, *J* = 8.0 Hz), 7.18 (t, 1H, *J* = 7.3 Hz), 6.66 (s, 1H), 6.61 (s, 1H), 6.01 (s, 1H), 3.93 (s, 1H), 2.33 (s, 3H), 2.22 (s, 3H), 1.19 (s, 3H), 1.07 (s, 3H). ¹³C NMR (125 MHz, CDCl₃) δ 166.5, 155.1, 144.5, 144.1, 133.8, 132.0, 130.2, 129.5, 128.8, 128.5, 127.4, 126.0, 125.7, 125.6, 115.9, 115.3, 49.9, 48.5, 26.3, 24.5, 18.1, 18.0, 14.4. HRMS (FAB) calc. for [C₃₀H₂₇N₂O₃Cl]⁺ 498.1710, found 498.1712.



5.49

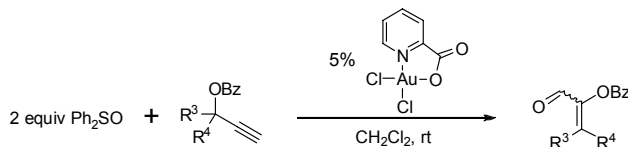
¹H NMR (500 MHz, CDCl₃) δ 7.98 (d, 2H, *J* = 7.5 Hz), 7.53 (t, 1H, *J* = 7.5 Hz), 7.41-7.38 (m, 4H), 7.32 (t, 2H, *J* = 7.5 Hz), 7.24 (t, 1H, *J* = 7.5 Hz), 6.55 (s, 1H), 6.53 (s, 1H), 5.98 (s, 1H), 5.84 (d, 1H, *J* = 9.5 Hz), 4.84 (dd, 1H, *J* = 9.5, 7 Hz), 3.57 (d, 1H, *J* = 7 Hz), 2.32 (s, 6H), 1.35 (s, 3H), 1.04 (s, 3H). ¹³C NMR (125 MHz, CDCl₃) δ 18.5, 18.6, 26.3, 44.3, 56.5, 105.7, 115.1, 125.7, 126.3, 127.9, 128.6, 129.9, 130.1, 130.6, 133.4, 136.0, 137.5, 138.8, 139.4, 145.6, 154.7, 167.3. HRMS (FAB) calc. for [C₂₉H₂₉NO₃]⁺ 439.2147, found 439.2142.



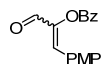
Synthesis of PicAuCl₂ (5.4)

Prepared according to Dar *et. al.*¹⁹ As such, 2-picolinic acid (175mg, 1.42 mmol) in water (14 mL) was added slowly to a stirred solution of sodium tetrachloroaurate (III) hydrate (283mg, 0.71 mmol) in 14 mL of water. After 3 hours, the resulting solution was filtered through celite. The yellow precipitate rinsed with water (15 mL) and eluted with acetone. Concentration *in vacuo* provided the desired dichloro(pyridine-2-carboxylato)gold(III) complex (PicAuCl₂, **5.4**) as

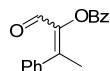
a yellow powder (190mg, 68% yield). ^1H NMR (400 MHz, acetone- d_6) δ 9.31 (d, 1H, $J = 6.0$ Hz), 8.69 (t, 1H, $J = 7.6$ Hz), 8.26 (app t, 1H, $J = 6.8$ Hz), 8.20 (d, 1H, $J = 7.6$ Hz).



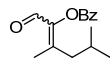
General procedure for the gold(III)-catalyzed oxidation of propargyl esters. To a one dram vial equipped with a magnetic stir bar, was sequentially added propargyl ester (1 equiv), diphenylsulfoxide (2 equiv), CH_2Cl_2 (0.3M) and PicAuCl_2 (5 mol %). The resulting mixture was stirred at room temperature and monitored periodically by TLC. Upon consumption of the propargyl ester (15-30 min), an aliquot was removed from the reaction mixture for ^1H -NMR analysis of the resulting diastereomeric ratio. The reaction mixture was subsequently subjected to silica gel chromatography to give the desired aldehydes.



NMR analysis of the crude reaction mixture indicated a 12:1 *Z*:*E* ratio. Chromatography (2% \rightarrow 20% EtOAc in Hexanes) provided the minor *E* diastereomer as a clear oil (38.1 mg, 7% yield). ^1H NMR (500 MHz, CDCl_3) δ 9.82 (s, 1H), 8.16 (d, 2H, $J = 7.5$ Hz), 7.63 (t, 1H, $J = 7.5$ Hz), 7.52-7.48 (m, 3H), 7.42 (d, 2H, $J = 8.5$ Hz), 6.97 (d, 2H, $J = 8.5$ Hz), 3.87 (s, 3H). ^{13}C NMR (125 MHz, CD_2Cl_2) δ 184.3, 165.0, 161.7, 145.8, 137.8, 134.2, 132.3, 130.8, 129.1, 129.0, 123.9, 114.8, 55.9. The major *Z* diastereomer was isolated as a mixture with diphenylsulfoxide, further silica gel chromatography (1% EtOAc in benzene) provided the major *Z* as a clear oil (350 mg, 66% yield). ^1H NMR (500 MHz, CD_2Cl_2) δ 9.47 (s, 1H), 8.23 (d, 2H, $J = 7.5$ Hz), 7.69-7.66 (m, 3H), 7.54 (t, 1H, $J = 7.5$ Hz), 7.08 (s, 1H), 6.90 (d, 2H, $J = 8.5$ Hz), 3.82 (s, 3H). ^{13}C NMR (125 MHz, CD_2Cl_2) δ 185.5, 163.6, 162.0, 144.8, 137.2, 134.2, 132.7, 130.7, 129.0, 128.8, 124.6, 114.8, 55.6. HRMS (EI) calc. for $[\text{C}_{17}\text{H}_{14}\text{O}_4]^+$ 282.0892, found 282.0889.



NMR analysis of the crude reaction mixture indicated a 4.1:1 *E*:*Z* ratio. Chromatography (2% \rightarrow 10% EtOAc in hexanes) provided first the major *E* diastereomer as a clear oil (37.5 mg, 72% yield). ^1H NMR (500 MHz, CD_2Cl_2) δ 9.39 (s, 1H), 8.18 (d, 2H, $J = 7.5$ Hz), 7.68 (t, 1H, $J = 7.5$ Hz), 7.55 (t, 2H, $J = 7.5$ Hz), 7.50-7.45 (m, 5H), 2.29 (s, 3H). ^{13}C NMR (125 MHz, CD_2Cl_2) δ 184.5, 164.4, 150.2, 144.8, 137.0, 134.3, 130.7, 129.9, 129.6, 129.4, 129.2, 129.1, 20.5. Followed by the major *Z* diastereomer as a clear oil (9.5 mg, 18% yield). ^1H NMR (500 MHz, CD_2Cl_2) δ 10.09 (s, 1H), 7.94 (d, 2H, $J = 7.5$ Hz), 7.58 (t, 1H, $J = 7.5$ Hz), 7.45-7.39 (m, 4H), 7.37-7.29 (m, 3H), 2.61 (s, 3H). ^{13}C NMR (125 MHz, CD_2Cl_2) δ 183.4, 165.0, 146.4, 142.6, 138.5, 134.1, 130.5, 129.5, 129.3, 129.1, 128.9, 127.7, 18.3. HRMS (EI) calc. for $[\text{C}_{17}\text{H}_{14}\text{O}_3]^+$ 266.0943, found 266.0943.



NMR analysis of the crude reaction mixture indicated a 1.2:1 *Z*:*E* ratio. Chromatography (2% \rightarrow 10% EtOAc in Hexanes) provided first the minor *E* diastereomer as a clear oil (17.4 mg, 35% yield). ^1H NMR (500 MHz, CD_2Cl_2) δ 9.89 (s, 1H), 8.12 (d, 2H, $J = 7.5$ Hz), 7.65 (t, 1H, $J = 7.5$ Hz), 7.51 (t, 2H, $J = 7.5$ Hz), 2.56 (d, 2H, $J = 7.5$ Hz), 1.98 (nonet, 1H, $J = 6.8$ Hz), 1.92 (s, 3H),

1.03 (d, 6H, $J = 6.5$ Hz). ^{13}C NMR (125 MHz, CD_2Cl_2) δ 182.0, 164.5, 150.3, 144.6, 134.1, 130.6, 129.6, 129.1, 40.9, 28.0, 22.6, 18.5. Followed by the major *Z* diastereomer as a clear oil (19.7 mg, 40% yield). ^1H NMR (500 MHz, CD_2Cl_2) δ 9.92 (s, 1H), 8.11 (d, 2H, $J = 7.5$ Hz), 7.65 (t, 1H, $J = 7.5$ Hz), 7.51 (t, 2H, $J = 7.5$ Hz), 2.27 (s, 3H), 2.18 (d, 2H, $J = 7.5$ Hz), 1.94 (nonet, 1H, $J = 6.5$ Hz), 0.93 (d, 6H, $J = 6.5$ Hz). ^{13}C NMR (125 MHz, CD_2Cl_2) δ 182.6, 164.6, 149.5, 143.8, 134.1, 130.5, 129.6, 129.2, 43.1, 27.4, 22.9, 16.7. HRMS (EI) calc. for $[\text{C}_{15}\text{H}_{18}\text{O}_3]^+$ 246.1256, found 246.1258.

Hammett Plots

A solution of 3 equivalents R = H imine, 3 equivalents R = X imine, 1 equivalent of propargyl ester, and 0.3 equivalents internal standard (1,3,5-trinitrobenzene) were dissolved in d_2 -DCM (0.1 M in propargyl ester). An initial ^1H -NMR spectrum was acquired followed by addition of 0.1 equiv PicAuCl₂. The reaction was monitored periodically by NMR. Upon completion, relative rates were obtained from NMR integrations of the products in the crude reaction mixture.

References

- (1) Shapiro, N. D.; Toste, F. D. *J. Am. Chem. Soc.* **2008**, *130*, 9244.
- (2) For recent reviews of gold-catalyzed reactions, see: (a) Jiménez-Núñez, E.; Echavarrén, A. M. *Chem. Commun.* **2007**, 333. (b) Gorin, D. J.; Toste, F. D. *Nature* **2007**, *446*, 395. (c) Furstner, A.; Davies, P. W. *Angew. Chem., Int. Ed.* **2007**, *46*, 3410. (d) Hashmi, A. S. K. *Chem. Rev.* **2007**, *107*, 3180. (e) Shen, H. C. *Tetrahedron* **2008**, *64*, 3885.
- (3) (a) Marion, N.; Nolan, S. P. *Angew. Chem., Int. Ed.* **2007**, *46*, 2750. (b) Correa, A.; Marion, N.; Fensterbank, L.; Malacria, M.; Nolan, S. P.; Cavallo, L. *Angew. Chem., Int. Ed.* **2008**, *47*, 718.
- (4) (a) Miki, K.; Ohe, K.; Uemura, S. *J. Org. Chem.* **2003**, *68*, 8505. (b) Johansson, M. J.; Gorin, D. J.; Staben, S. T.; Toste, F. D. *J. Am. Chem. Soc.* **2005**, *127*, 18002. (c) Gorin, D. J.; Dube, P.; Toste, F. D. *J. Am. Chem. Soc.* **2006**, *128*, 14480. (d) Gorin, D. J.; Watson, I. D. G.; Toste, F. D. *J. Am. Chem. Soc.* **2008**, *130*, 3736.
- (5) (a) Amijs, C. H. M.; López-Carrillo, V.; Echavarrén, A. M. *Org. Lett.* **2007**, *9*, 4021. (b) Davies, P. W.; Albrecht, S. J.-C. *Chem. Commun.* **2008**, 238.
- (6) Witham, C. A.; Mauleón, P.; Shapiro, N. D.; Sherry, B. D.; Toste, F. D. *J. Am. Chem. Soc.* **2007**, *129*, 5838.
- (7) (a) Doyle, M. P.; Hu, W.; Timmons, D. J. *Org. Lett.* **2001**, *3*, 3741. (b) Doyle, M. P.; Yan, M.; Hu, W.; Gronenberg, L. S. *J. Am. Chem. Soc.* **2003**, *125*, 4692. (c) Davies, H. M. L.; Hu, B.; Saikali, E.; Bruzinski, P. R. *J. Org. Chem.* **1994**, *59*, 4535. For a related reaction of Fischer carbenes, see: (d) Barluenga, J.; Tomás, M.; Ballesteros, A.; Santamaría, J.; Carbajo, R. J.; López-Ortiz, F.; García-Granda, S.; Pertierra, P. *Chem. Eur. J.* **1996**, *2*, 88. (e) Barluenga, J.; Tomás, M.; Rubio, E.; López-Pelegrin, J. A.; García-Granda, S.; Priede, M. P. *J. Am. Chem. Soc.* **1999**, *121*, 3065.
- (8) Lemiére, G.; Gandon, V.; Agenet, N.; Goddard, J. P.; de Kozak, A.; Aubert, C.; Fensterbank, L.; Malacria, M. *Angew. Chem., Int. Ed.* **2006**, *45*, 7596.
- (9) (a) Hashmi, A. S. K.; Weyrauch, J. P.; Rudolph, M.; Kurpejovic, E. *Angew. Chem., Int. Ed.* **2004**, *43*, 6545. (b) Hashmi, A. S. K.; Kurpejovic, E.; Wölflé, M.; Frey, W.; Bats, J. W. *Adv. Synth. Catal.* **2007**, *349*, 1743.
- (10) It should be noted that attempted cyclopropanation of this olefin using typical Au(I)-catalyzed reaction conditions also failed, when either the starting imine or the azepine product were employed.
- (11) The *trans*-diaryl stereochemistry, which is opposite to that produced in related rhodium-catalyzed cycloadditions,^{7a} was established by an X-ray crystal structure (see Supporting Information) of **5.16**.
- (12) Gorin, D. J.; Dubé, P.; Toste, F. D. *J. Am. Chem. Soc.* **2006**, *128*, 14480.
- (13) Gao, H.; Zhao, X.; Yu, Y.; Zhang, J. *Chem.-Eur. J.* **2010**, *16*, 456.
- (14) Watson, I. D. G.; Ritter, S.; Toste, F. D. *J. Am. Chem. Soc.* **2009**, *131*, 2056.
- (15) Ji, J.-X.; Au-Yeung, T. T.-L.; Wu, J.; Yip, C. W.; Chan, A. S. C. *Adv. Synth. Catal.* **2004**, *346*, 42.
- (16) (a) Wei, C.; Mague, J. T.; Li, C.-J. *Proc. Natl. Acad. Sci. U.S.A.* **2004**, *101*, 5749. (b) Rueping, M.; Antonchick, A. P.; Brinkmann, C. *Angew. Chem., Int. Ed.* **2007**, *46*, 6903. (c) Lu, Y.; Johnstone, T. C.; Arndtsen, B. A. *J. Am. Chem. Soc.* **2009**, *131*, 11284. For a general review covering enantioselective addition to imines, see: Kobayashi, S.; Ishitani, H. *Chem. Rev.* **1999**, *99*, 1069.

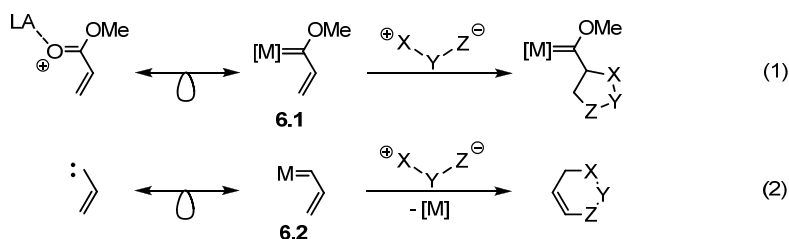
-
- (17) An enantioselective version of this reaction was subsequently developed in collaboration with Daniel Lloyd Gray. For further information, see his Master's Thesis.
- (18) For additional examples of intermolecular gold-catalyzed annulations, see: (a) Melhado, A. D.; Luparia, M.; Toste, F. D. *J. Am. Chem. Soc.* **2007**, *129*, 12638. (b) Hsu, Y.-C.; Datta, S.; Ting, C.-M.; Liu, R.-S. *Org. Lett.* **2008**, *10*, 521. (c) Zhang, G.; Huang, X.; Li, G.; Zhang, L. *J. Am. Chem. Soc.* **2008**, *130*, 1814. (d) Barluenga, J.; Fernández-Rodríguez, M. A.; García-García, P.; Aguilar, E. *J. Am. Chem. Soc.* **2008**, *130*, 2764.
- (19) Dar, A.; Moss, K.; Cottrill, S. M.; Parish, R. V.; McAuliffe, C. A.; Pritchard, R. G.; Beagley, B.; Sandbank, J. *J. Chem. Soc. Dalton Trans.* **1992**, 1907.

Chapter 6 – Gold-Catalyzed [3+3]-Annulation of Azomethine Imines with Propargyl Esters

The gold-catalyzed [3+3]-cycloaddition reaction of propargyl esters and azomethine imines has been developed. The reaction provides a rapid entry into a wide range of substituted tetrahydropyridazine derivatives from simple starting materials. A stepwise mechanism involving addition of the 1,3-dipole to a gold-carbenoid intermediate is proposed. In addition, a strategy for rendering this reaction asymmetric is presented. A portion of the work discussed in this chapter has been published.¹

Introduction

The reactions of alkenyl Fischer carbenes **6.1** with 1,3-dipoles typically proceed via a concerted-asynchronous [3+2] cycloaddition (eq 1). Considering the orbitals involved in these transformations, the isolobal analogy allows the comparison of the reactivity of **6.1** to that of Lewis acid complexed acrylates.² In contrast, the LUMO of alkenyl metal carbenoids of type **6.2** may be approximated as singlet vinylcarbenes (eq 2).^{3,4} Given this analogy, a [3+3]-cycloaddition between 1,3-dipoles and carbenoids of type **6.2** would be predicted. Unfortunately, free electrophilic vinylcarbenes undergo rapid rearrangement to cyclopropenes, and intermolecular cycloadditions of these species are typically low yielding.^{5,6} This problem has been circumvented through the use of alkenyl metal-carbenoids **6.2**, which are typically generated in situ from metal-catalyzed diazo decomposition;⁷ however, cycloaddition reactions of 1,3-dipoles with carbenoids⁸ of type **6.2** have yet to be reported. We report herein a gold(III)-catalyzed [3+3]-cycloaddition⁹ of propargyl esters and azomethine imines, which is proposed to proceed via stepwise cycloaddition with a gold(III)-carbenoid intermediate of type **6.2**.^{10,11,12}



Beginning with our previously optimized reaction conditions,^{10d} we were delighted to find that bicyclic [3+3] cycloadduct **6.5a** was formed in 90% yield and with 6:1 diastereoselectivity in the Au(III)-catalyzed reaction of ylide **6.4a** with propargyl ester **6.3a** (Table 1, entry 1). X-ray crystallography was used to assign the major isomer as *cis*.¹³ While varying the solvent failed to provide an increase in the diastereoselectivity (entries 2-4), lowering the temperature to 0 °C improved the ratio of *cis:trans* to 8:1 (entry 5).¹⁴ Other Au(III) chloride salts also catalyzed the reaction with only slightly diminished yields (entries 6-7); however, Au(III) bromide and various Au(I) catalysts failed to provide any of the desired product (entries 8-9).¹⁵

Table 1. Reaction optimization.

entry	catalyst	solvent	temp.	conversion	yield ^a	dr (<i>cis:trans</i>)
1	PicAuCl ₂ (6.6) ^b	CD ₂ Cl ₂	rt	100%	90%	(6 : 1)
2 ^c	6.6	MeCN	rt	48%	44%	(6 : 1)
3 ^c	6.6	NO ₂ Me	rt	71%	61%	(5 : 1)
4	6.6	C ₆ D ₆	rt	— ^d	49%	(3 : 1)
5 ^c	6.6	CD ₂ Cl ₂	0 °C	100%	89% (79% ^e)	(8 : 1)
6	NaAuCl ₄	CD ₂ Cl ₂	rt	100%	73%	(6 : 1)
7	AuCl ₃	CD ₂ Cl ₂	rt	100%	85%	(6 : 1)
8	AuBr ₃	CD ₂ Cl ₂	rt	20%	<5%	—
9	Ph ₃ PAuCl/AgSbF ₆	CD ₂ Cl ₂	rt	<5%	<5%	—

ORTEP drawing of *cis* **6.5a**.

^a Yield and diastereomeric ratio determined by ¹H NMR versus an internal standard. ^b Pic = 2-picolinate. ^c Reaction time was 4 h. ^d The starting ylide was partially insoluble in 0.3 M C₆D₆. ^e Isolated yield of analytically pure *cis* **6.5a**.

Reaction Scope in Azomethine imine

With optimal conditions in hand (Table 1, entry 5), the substrate scope of the gold-catalyzed [3+3]-cycloaddition reaction was examined. As demonstrated in the reaction of β -phenyl substituted azomethine imine **6.4a**, substitution of the β -position of the pyrazolidinone generally provides bicyclic product **6.5a** with high *cis* selectivity (*vide infra*). Alkyl substituents are also tolerated at this position (Table 2, entries 1-2), with larger substituents giving increased selectivity (20:1 for *tert*-butyl versus 8:1 for methyl). Remarkably, even an alkynyl substituent is sufficient to provide high selectivity (7:1, entry 3).

Table 2. Variation of the Azomethine Imine.

entry	product	yield (<i>cis:trans</i>)
1	6.5b R = Me	98% (8 : 1)
2	6.5c R = <i>t</i> Bu	92% (20 : 1)
3	6.5d R = C \equiv CTIPS	96% (7 : 1)
4	6.5e (R = H)	94% (1.3 : 1)
5	6.5f (R = Me)	83% (10 : 1)
6	6.5g	90% (>20:1)
7	6.5h R = R' = H	82% ^a
8	6.5i R = Me, R' = H	82% ^{a,b}
9	6.5j R = H, R' = Me	88% ^a
10	6.5k R = Ph, R' = 3,4,5-(MeO) ₃ -C ₆ H ₂	80% (6 : 1)
11	6.5l R = Ph, R' = 4-CN-C ₆ H ₄	94% (5 : 1)
12	6.5m R = Ph, R' = 3-pyridyl-2-Cl	98% (1.7 : 1)
13	6.5n R = Me, R' = 2-I-C ₆ H ₄	72% (1.8 : 1)
14	6.5o R = Me; R' = 2,6-Cl ₂ -C ₆ H ₃	<5% ^a

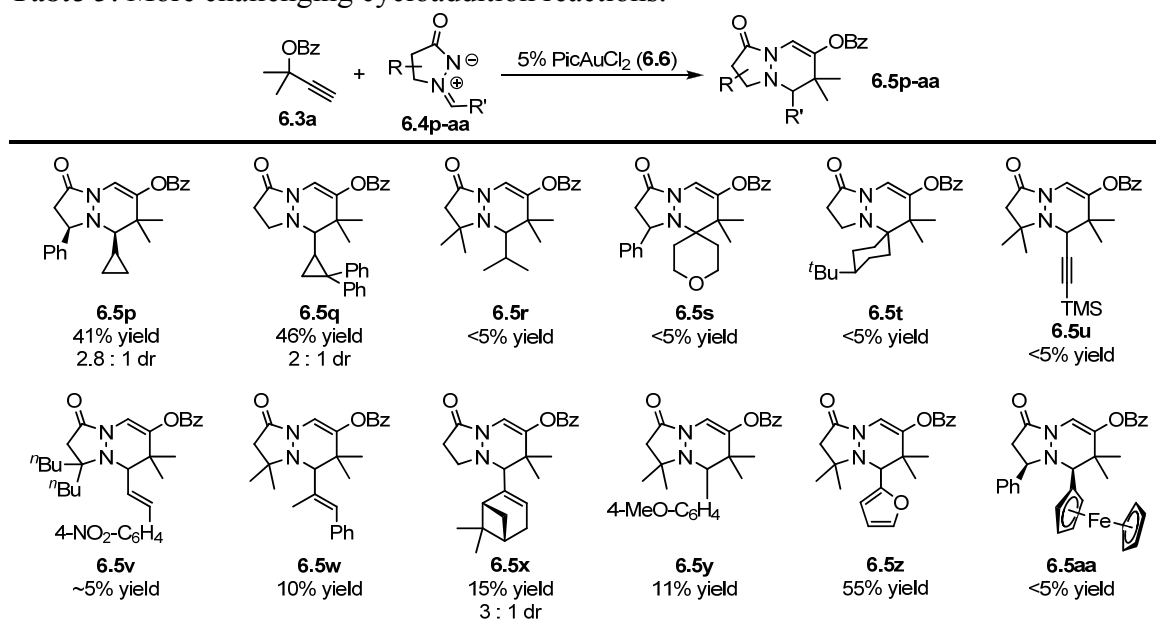
^a Reaction performed at room temperature. ^b 2 mmol scale.

The azomethine imine can also be substituted at the α -position, although in this case the product (**6.5e**) was formed with moderate 1.3:1 *cis:trans* diastereoselectivity (entry 4). On the other hand, the cycloaddition of azomethine imine **6.4f**, having both α - and β -substituents, remained highly selective (10:1, entry 5). Finally, the backbone need not be substituted (entry 7) but can also accommodate quaternary carbons in either position (entries 8-9).

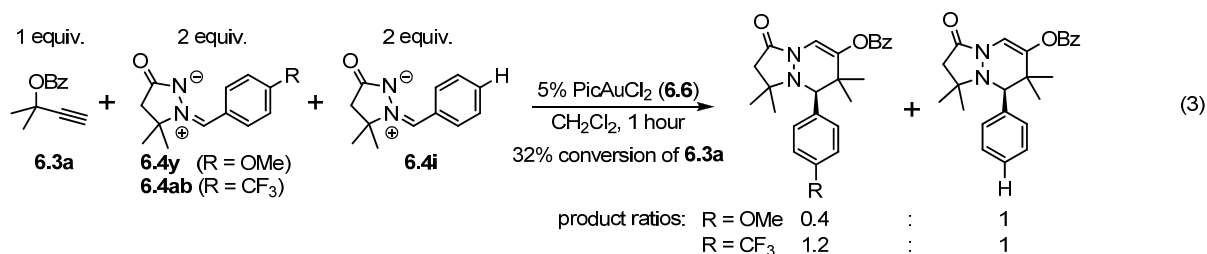
The aldehyde-derived substituent of the azomethine imine can also be varied. Both electron-rich and electron-deficient aryl groups are well tolerated in the gold(III)-catalyzed cycloaddition (entries 10-11). Ortho-substituted aryl groups are also accommodated but provide the cycloadducts with significantly lower diastereoselectivity (entries 12-13). On the other hand, only traces of the desired product were observed when the aryl ring was doubly ortho-substituted (entry 14).

Several other classes of azomethine imine also proceeded in moderate to poor yield (Table 3). For example, imines derived from cyclopropyl aldehydes provided bicycles **6.5p** and **6.5q** in moderate yield, while other aliphatic imines gave only trace quantities of the desired product (i.e. **6.5r**). Notably, the diphenyl substituted cyclopropane in **6.4q** did not ring open under the reaction conditions. Azomethine imines derived from aliphatic ketones (**6.5s,t**) were inert under the standard reaction conditions; running these reactions at elevated temperatures resulted in decomposition. Imines derived from alkynyl and α,β -unsaturated aldehydes were also poor substrates for this reaction. In one notable example, imine **6.4x**, synthesized from (-)-myrtenal, provided tricycle **6.5x** with 3:1 dr, albeit in poor yield (15%). Finally, azomethine imines derived from aldehydes with strongly electron-donating substituents proceeded sluggishly (**6.4y** and **6.4z**) or not at all (**6.4aa**).

Table 3. More challenging cycloaddition reactions.

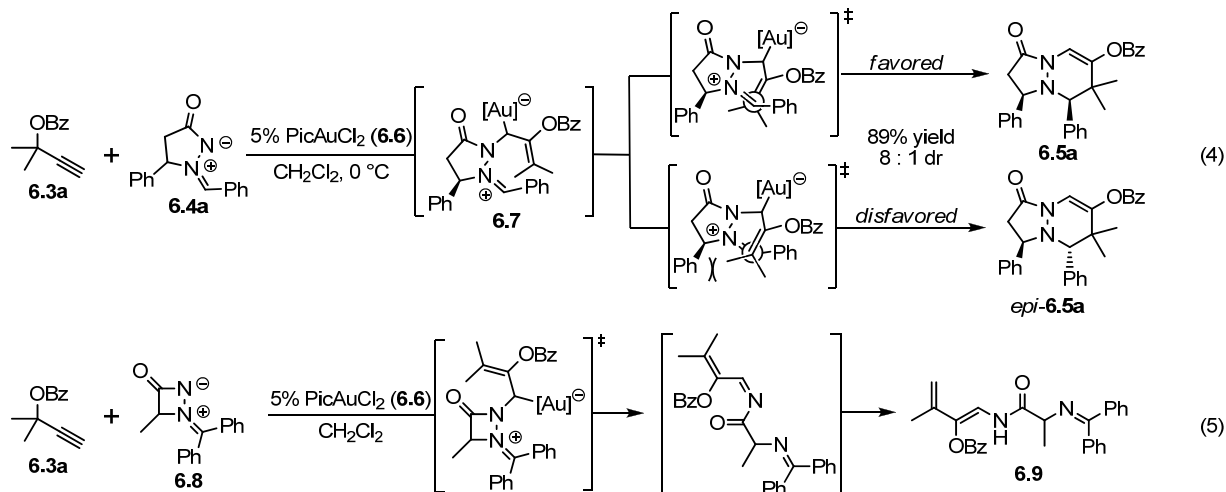


In order to gain further insight into the decreased yields obtained for these substrates, we performed a series of competition experiments (eq 3). Two equivalents of azomethine imine **6.4i** were combined with two equivalents of either methoxy-substituted imine **6.4y** or trifluoromethyl-substituted imine **6.4ab**. In both cases, after one hour under the standard reaction conditions, 32% of propargyl ester **6.3a** was consumed, with the less electron-rich imine consumed preferentially. This suggests both that competitive binding of the catalyst by the imine does not affect the overall rate of the reaction, and that ring-closing of intermediate **6.7** is rate-determining (*vide supra*).

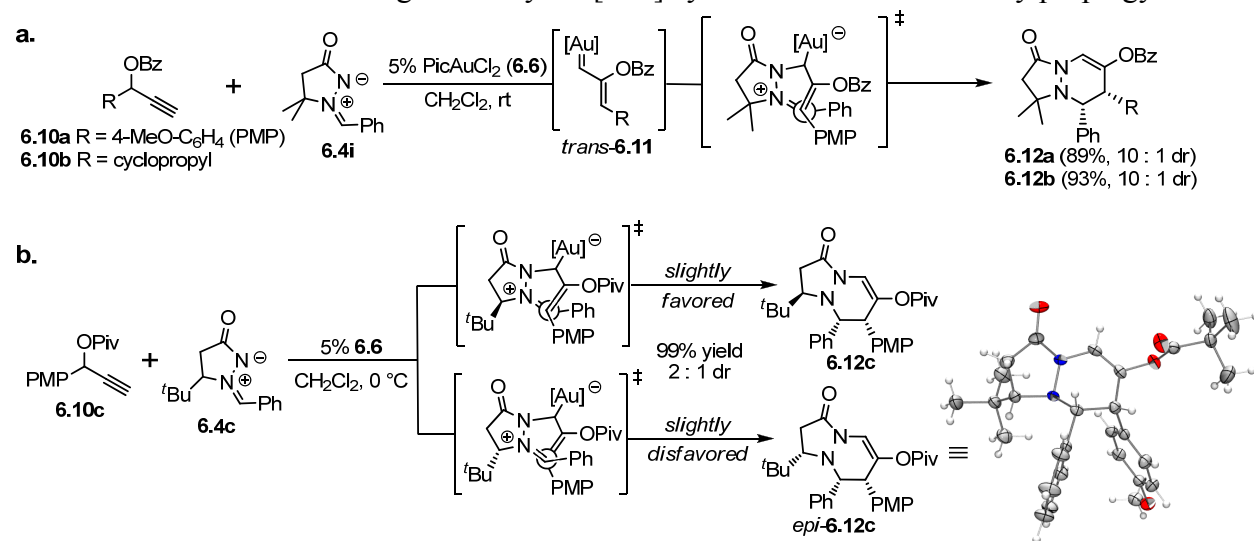


Diastereoselectivity

The high diastereoselectivity in the gold-catalyzed cycloaddition of **6.3a** and **6.4a** can be rationalized by a minimization of unfavorable steric interactions between the propargyl ester methyl groups and the β -substituent in the ring closing transition state (eq 4). Thus, we propose that the diastereoselectivity is determined during ring closing, rather than in the formation of allylgold intermediate **6.7**.¹³ Additional evidence for a stepwise mechanism was obtained in the reaction of azomethine imine **6.8**, which furnished enamine **6.9** after ring fragmentation and tautomerization (eq 5).



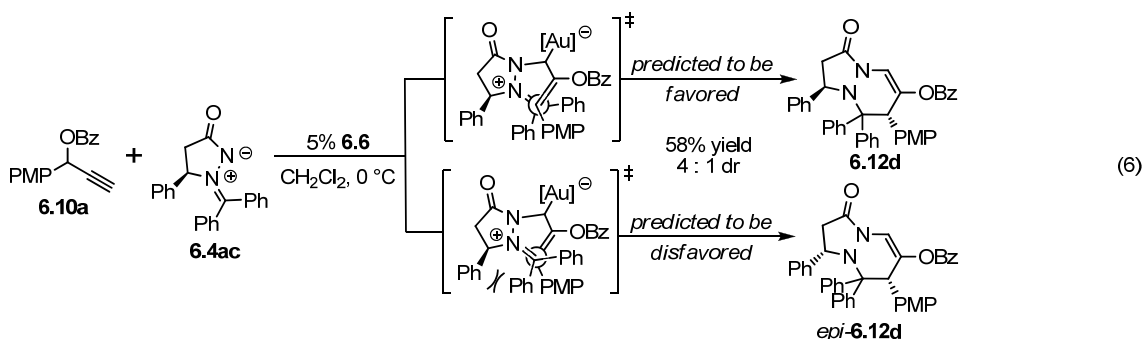
Scheme 1. Diastereoselective gold-catalyzed [3+3] cycloadditions of secondary propargyl esters.



An additional stereocenter is generated when secondary propargyl esters are employed (Scheme 1a). In this case, regardless of whether the cycloaddition is concerted or stepwise (as depicted), the high 1,2-*cis* diastereoselectivity can be rationalized as resulting from the *cis*-imine geometry and the preferred *trans* geometry of the proposed gold-carbenoid intermediate

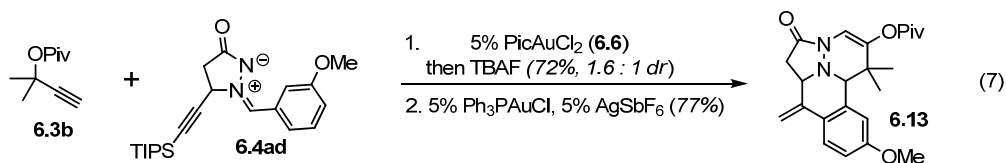
6.11.^{10d,16} To gain further insight into the origin of the 1,2-*cis* stereoselectivity, secondary propargyl ester **6.10c** was reacted with *tert*-butyl substituted azomethine imine **6.4c** (Scheme 1b).¹⁷ In this case, a 2:1 mixture of diastereomers with respect to the pyrazolidinone substituent, and favoring the 1,3-*trans* isomer of **6.12c**, was formed. The configuration of the minor isomer was confirmed by X-ray crystallography. Taken as a whole, these results support a mechanism in which the 1,3-selectivity is determined during cyclization (eq 4), whereas the 1,2-selectivity is determined by the geometry of the carbenoid intermediate **6.11** (Scheme 1a). Interestingly, the 1,3-selectivity increases with decreasing temperature (see Table 1), whereas the 1,2-selectivity shows no temperature dependence.

Based on these models for diastereoselection, we propose a model for 1,4-selectivity in the annulation of benzophenone derived azomethine imine **6.4ac** with benzoate **6.10a** (eq 6). The desired product **6.12d** was formed in 58% yield and as a 4:1 mixture of diastereomers. Unfortunately, we were unable to assign the geometries of the two isomers using NMR analyses.

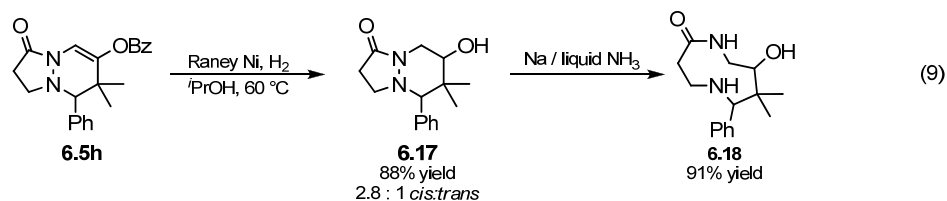
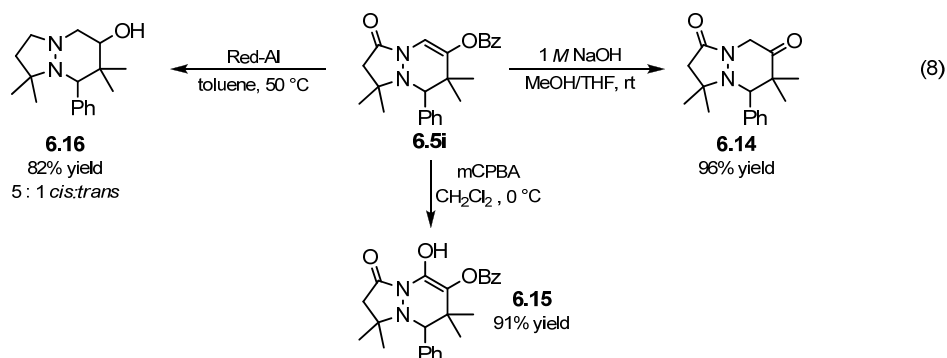


Further Extensions

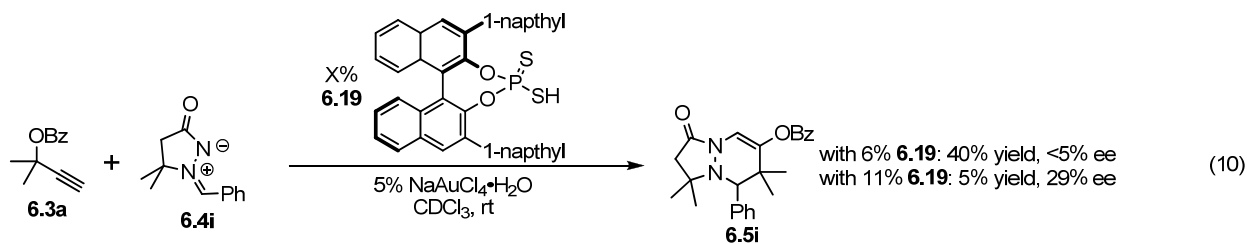
We envisioned that this reaction could be extended to the synthesis of tetracycles via sequential gold-catalyzed cyclization reactions (eq 7). Following initial [3+3] cycloaddition of azomethine imine **6.4ad**, the alkyne was deprotected with TBAF and subjected to Au(I)-catalyzed hydroarylation conditions to deliver **6.13**.¹⁸



We explored some further synthetic transformations of the diazabicycles. Hydrolysis of the propargyl ester of **6.5i** with NaOH in MeOH/THF provides ketone **6.14** (eq 8). Alternatively, the electron rich enol ether moiety can be oxidized with mCPBA to provide enol **6.15**. Simultaneous reduction of the amide and the enol ether moieties can be achieved with Red-Al, providing hydrazine-alcohol **6.16** as a 5:1 mixture of *cis* and *trans* isomers. Alternatively, the enol ether moiety can be reduced chemoselectively with Raney nickel and hydrogen (eq 9). Treatment of the resulting alcohol (**6.17**) with sodium in ammonia results in cleavage of N-N bond, providing macrocyclic amide **6.18**.

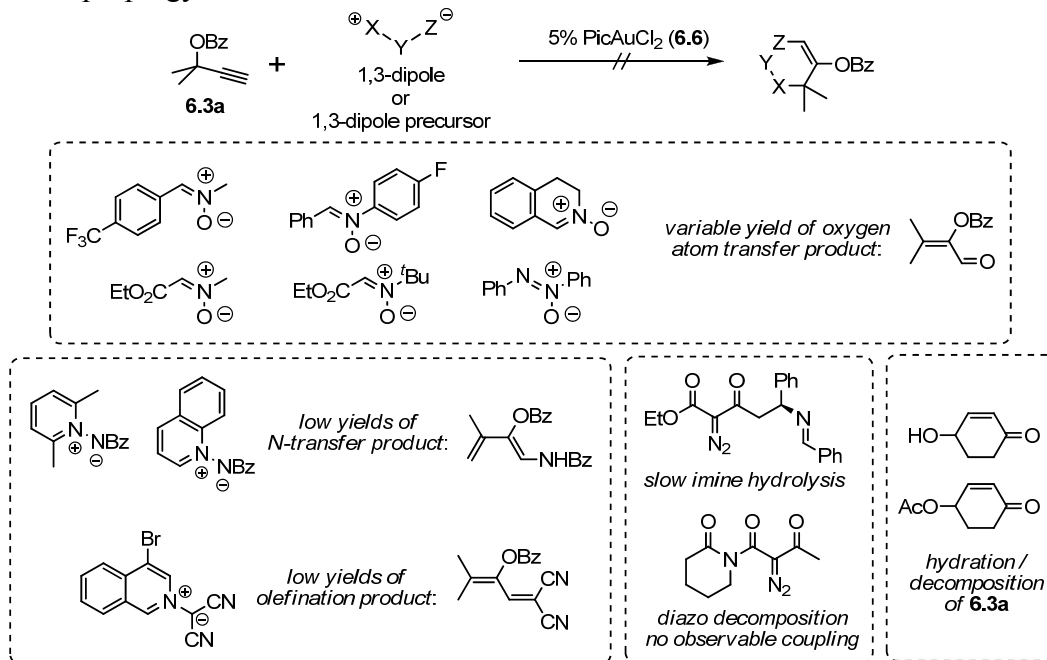


It was found that the addition of a chiral dithiophosphoric acid to the gold(III)-catalyzed annulation of **6.3a** and **6.4i** resulted in formation of the product with slight enantiomeric excess (eq 10). With one equivalent of the acid relative to the gold catalyst, moderate conversion and minimal enantioinduction was observed (~5%). Doubling the amount of acid resulted in an increase in the enantiomeric excess of the product, although under these conditions low conversion was observed. These unoptimized results are encouraging, given that gold(III)-catalyzed enantioselective reactions that proceed via π -activation are essentially unknown.¹⁹



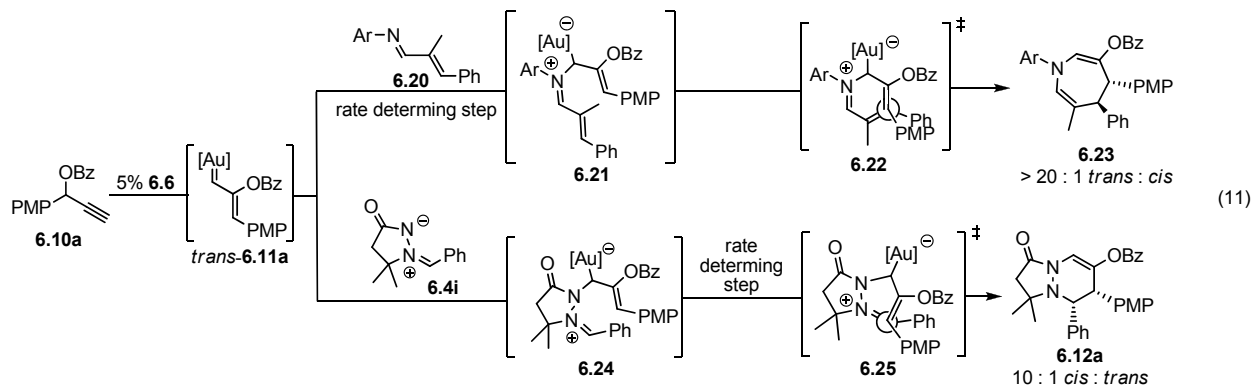
We also screened a number of other carbene precursors (propargyl acetals^{11f}, 1,6-enynes^{16,20}, diazocompounds²¹, and cyclopropenes²²) and 1,3-dipoles as additional coupling partners. However, in none of the cases investigated were any annulation products detected. Several of 1,3-dipoles are shown in Figure 1, along with a brief description of the results. In most cases, both gold(I) and gold(III) catalysts were tested. Zhang and coworkers have reported that 2-(1-alkynyl)-2-alken-1-ones and nitrones do undergo [3 + 3] annulation.²³

Figure 1. Failed attempts to annulate other 1,3-dipoles and 1,3-dipole precursors with propargyl ester **6.3a**. Results are described in italics.



Comparison to the [4 + 3] Cycloaddition of Propargyl Esters and α - β -Unsaturated Imines

In chapter 5, the gold(III)-catalyzed annulation of propargyl esters and α - β -unsaturated imines was discussed in detail. In this chapter, a similar annulation reaction has been presented. Several interesting observations can be made when these two reactions are directly compared. Both reactions are proposed to proceed via gold-carbenoid intermediate **6.11** (eq 11). Competition experiments suggest that addition of α - β -unsaturated imines to this intermediate is the rate-limiting step, whereas in the reaction with azomethine imines, cyclization of allyl-gold intermediate **6.24** is rate limiting. The diastereoselectivity of both reactions can be explained with similar transition states (**6.22** and **6.25**). Although, because the preferred imine geometries of **6.20** and **6.4i** are opposite, the reactions give opposite *cis:trans* selectivity.



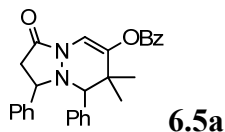
Conclusions

In conclusion, we have developed a gold(III)-catalyzed synthesis of diazabicycles from readily available starting materials. This report represents the first example of a formal cycloaddition between alkenyl metal carbenoids and 1,3-dipoles. In contrast to the previously reported cycloadditions,^{10d,11f} this reaction highlights the difference in the reactivity of alkenyl Fischer carbenes and the alkenyl Au-carbenoids generated from the rearrangement of propargyl esters.

Supporting Information

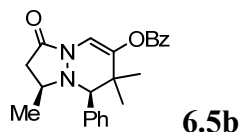
General Information. Unless otherwise noted, reagents were obtained commercially and used without further purification. Small scale reactions (< 3mL) were carried out in Fisher Scientific disposable scintillation vials. HPLC grade dichloromethane (CH₂Cl₂), ACS grade hexanes, and ACS grade ethyl acetate (EtOAc) were obtained from Fischer Scientific. TLC analysis of reaction mixtures was performed on Merck silica gel 60 F254 TLC plates using UV light and ceric ammonium molybdate stain to visualize the reaction components. Flash chromatography was carried out on ICN SiliTech 32-63 D 60 Å silica gel. ¹H and ¹³C NMR spectra were recorded with Bruker AV-300, AVB-400, AVQ-400, DRX-500, AV-500, and AV-600 spectrometers and referenced to CDCl₃ unless otherwise noted. Mass spectral and analytical data were obtained via the Micro-Mass/Analytical Facility operated by the College of Chemistry, University of California, Berkeley. X-ray structure acquisition and analysis were performed by Dr. Frederick J. Hollander of the University of California, Berkeley College of Chemistry X-ray crystallographic facility. Azomethine imines were made according to the literature.²⁴

General procedure for the gold(III)-catalyzed [3+3] reaction. To a one dram vial equipped with a magnetic stir bar, was sequentially added 4Å molecular sieves, azomethine imine (~0.2 mmol, 1 equiv), propargyl ester (1.3 equiv) and CH₂Cl₂ (0.3 M). The reaction was cooled to 0°C in an ice bath and PicAuCl₂ (0.05 equiv) was added. The vial was sealed and the resulting mixture was stirred at 0°C. After 3 hours, the mixture was allowed to warm slowly to room temperature, and monitored periodically by TLC and/or NMR. Upon consumption of the azomethine imine (2 – 8 hours in total), diastereoselectivity was determined by ¹H-NMR of an aliquot of the crude reaction mixture. Flash column chromatography on silica gel (hexanes/ethyl acetate) provided the desired bicyclic products. Reactions of achiral azomethine imines were performed at room temperature.

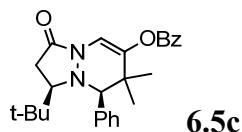


NMR analysis of the crude reaction mixture indicated a 8:1 *cis:trans* ratio. Chromatography provided first the minor *trans* diastereomer as a white foam (5.1 mg, 10% yield). ¹H NMR (600 MHz, CDCl₃) δ 8.12 (d, 2H, *J* = 7.2 Hz), 7.63-7.60 (m, 2H), 7.51-7.45 (m, 3H), 7.40-7.30 (m, 7H), 7.25 (s, 1H), 6.84 (d, 1H, *J* = 7.2 Hz), 3.81 (app t, 1H, *J* = 9.9 Hz), 3.65 (s, 1H), 2.74 (dd, 1H, *J* = 16.8, 8.4 Hz), 2.63 (dd, 1H, *J* = 16.8, 12 Hz), 1.54 (s, 3H), 0.79 (s, 3H). ¹³C NMR (150 MHz, CDCl₃) δ 165.1, 164.6, 139.9, 138.3, 134.9, 133.8, 132.5, 130.5, 130.3, 129.6, 129.5, 129.1, 129.0, 128.8, 128.7, 128.7, 128.5, 128.0, 127.9, 112.0, 69.8, 61.1, 41.3, 39.7, 22.4.

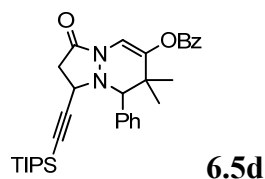
Followed by the major *cis* diastereomer as a white foam (40 mg, 79% yield). ^1H NMR (400 MHz, CDCl_3) δ 8.12 (d, 2H, $J = 7.2$ Hz), 7.62 (t, 1H, $J = 7.6$ Hz), 7.49 (t, 2H, $J = 7.6$ Hz), 7.23-7.18 (m, 1H), 7.22 (s, 1H), 7.16-7.01 (m, 5H), 6.91 (dd, 2H, $J = 7.6, 1.2$ Hz), 6.64 (d, 1H, 7.6 Hz), 6.51 (t, 1H, $J = 7.6$ Hz), 3.96 (dd, 1H, $J = 10.6, 9.2$ Hz), 3.85 (s, 1H), 2.98 (dd, 1H, $J = 17.2, 9.2$ Hz), 2.71 (dd, 1H, $J = 17.2, 10.6$ Hz), 1.24 (s, 3H), 0.91 (s, 3H). ^{13}C NMR (100 MHz, CDCl_3) δ 164.9, 163.3, 142.0, 141.3, 133.8, 132.7, 131.6, 131.4, 130.2, 129.5, 128.8, 128.4, 128.2, 127.5, 127.2, 127.1, 126.5, 110.8, 78.8, 66.2, 41.8, 41.3, 22.8, 22.1. HRMS (ESI) calc. for $[\text{C}_{28}\text{H}_{27}\text{O}_3\text{N}_2]^+$ 439.2016, found 439.2009. X-ray quality crystals of the major diastereomer were grown from ether.



NMR analysis of the crude reaction mixture indicated a 8:1 *cis:trans* ratio. Chromatography provided first a 1:1 mixture of diastereomers (9.0 mg, 24% yield), followed by the major diastereomer as a white solid (28.6 mg, 76%). ^1H NMR (500 MHz, CDCl_3) δ 8.11 (d, 2H, $J = 8.0$ Hz), 7.62 (t, 1H, $J = 7.2$ Hz), 7.57 (s, 1H), 7.51 (t, 2H, $J = 8.0$ Hz), 7.38-7.28 (bs, 3H), 7.21 (s, 1H), 7.13 (s, 1H), 3.80 (s, 1H), 3.21-3.17 (m, 1H), 2.75-2.70 (q, 1H), 2.35-2.30 (q, 1H), 1.25 (s, 3H), 0.94 (s, 3H), 0.89 (d, 3H, $J = 7.8$ Hz). ^{13}C NMR (125 MHz, CDCl_3) δ 165.2, 164.8, 140.9, 134.6, 133.7, 131.9, 130.7, 130.2, 129.5, 128.9, 128.8, 128.4, 127.5, 111.0, 57.3, 41.1, 39.2, 22.8, 22.3, 22.2. HRMS (ESI) calc. for $[\text{C}_{23}\text{H}_{25}\text{N}_2\text{O}_3]^+$ 377.1865, found 377.1865.

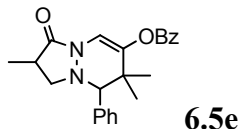


NMR analysis of the crude reaction mixture indicated a 20:1 *cis:trans* ratio. Chromatography provided the major diastereomer as a white foam (76.5 mg, 92% yield). ^1H NMR (600 MHz, CDCl_3) δ 8.09 (d, 2H, $J = 7.8$ Hz), 7.60 (t, 1H, $J = 7.2$ Hz), 7.55 (bs, 1H), 7.57 (t, 2H, $J = 7.8$ Hz), 7.36 (bs, 3H), 7.15 (s, 1H), 7.05 (s, 1H), 3.84 (s, 1H), 2.82 (d, 1H, $J = 9.0$ Hz), 2.69-2.64 (m, 1H), 2.37-2.34 (d, 1H, $J = 17.4$ Hz) 1.33 (s, 3H), 0.92 (s, 3H), 0.91 (s, 9H). ^{13}C NMR (150 MHz, CDCl_3) δ 171.4, 164.5, 143.1, 134.6, 133.7, 132.4, 130.2, 130.1, 129.6, 128.8, 128.6, 127.7, 112.3, 62.8, 42.6, 35.7, 31.4, 26.8, 22.8, 21.8. HRMS (ESI) calc. for $[\text{C}_{26}\text{H}_{31}\text{N}_2\text{O}_3]^+$ 419.2329, found 419.2328.

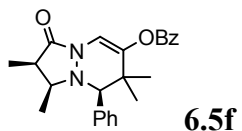


NMR analysis of the crude reaction mixture indicated a 7:1 *cis:trans* ratio. Chromatography provided first the major *cis* diastereomer as a white foam (43.7 mg, 78% yield). ^1H NMR (600 MHz, CDCl_3) δ 8.10 (d, 2H, $J = 7.2$ Hz), 7.75 (app d, 1H, $J = 7.2$ Hz), 7.61 (t, 1H, $J = 7.5$ Hz), 7.48 (d, 2H, $J = 7.8$ Hz), 7.36-7.30 (m, 3H), 7.18 (app d, 1H, $J = 6.6$ Hz), 7.11 (s, 1H), 3.80 (app t, 1H, $J = 9.6$ Hz), 3.78 (s, 1H), 2.98 (dd, 1H, $J = 17.4, 9.6$ Hz), 2.83 (dd, 1H, $J = 17.4, 9.6$ Hz), 1.23 (s, 3H), 1.14-1.00 (m, 21H), 0.93 (s, 3H). ^{13}C NMR (150 MHz, CDCl_3) δ 164.8, 163.1, 141.4, 133.8, 132.8, 131.8, 130.2, 129.4, 129.0, 128.8, 127.9, 127.7, 110.8, 105.9, 87.1, 78.4,

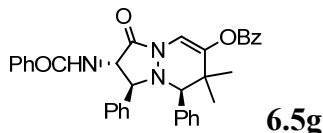
52.4, 41.5, 39.4, 22.6, 22.3, 18.8, 11.2. HRMS (ESI) calc. for $[C_{33}H_{43}O_3N_2Si]^+$ 543.3037, found 543.3030. Followed by a 1.8:1 mixture of *cis:trans* isomers (10.0 mg, 18% yield). The following peaks were distinctive for the *trans* diastereomer: 1H NMR (600 MHz, $CDCl_3$) δ 7.14 (s, 1H), 4.22 (s, 1H), 2.88 (dd, 1H, $J = 15.6, 6.9$ Hz) 2.63 (dd, 1H, $J = 15.6, 3.0$ Hz).



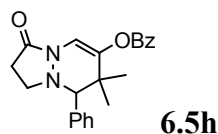
NMR analysis of the crude reaction mixture indicated a 1.3:1 mixture of diastereomers. Chromatography provided a 1.4:1 mixture as a white foam (85 mg, 94% yield). 1H NMR (600 MHz, $CDCl_3$) δ 8.12-8.09 (m, 4.8H), 7.61 (app t, 2.4H, $J = 7.5$ Hz), 7.54-7.32 (m, 14.4H), 7.20-7.16 (m, 2.4H), 7.11 (s, 1.4H), 7.10 (s, 1H), 3.63 (s, 1H), 3.60 (s, 1.4 H), 3.67 (app t, 1.4H, $J = 9.0$ Hz), 2.95 (bs, 1H), 2.81-2.73 (m, 1.4H), 2.70-2.65 (m, 2H), 2.11 (dd, 1H, $J = 12.6, 9.0$ Hz), 1.30 (bs, 3H), 1.29 (d, 4.2H, $J = 6.6$ Hz), 1.15 (s, 4.2H), 1.11 (bs, 3H), 1.06 (bs, 3H), 1.01 (s, 4.2H). ^{13}C NMR (150 MHz, $CDCl_3$) δ 168.2, 167.5, 165.0, 165.0, 140.6, 140.4, 134.7, 134.6, 133.8, 131.4, 131.3, 130.3, 130.2, 130.2, 129.5, 129.3, 129.2, 128.8, 128.6, 128.5, 128.5, 128.3, 128.2, 128.2, 128.1, 110.9, 110.9, 76.8, 58.9, 40.8, 40.7, 37.5, 37.0, 22.8, 22.7, 22.2, 15.4, 13.2. HRMS (ESI) calc. for $[C_{28}H_{27}O_3N_2]^+$ 377.1860, found 377.1854.



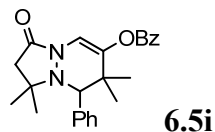
The requisite *cis*-substituted azomethine imine was selectively recrystallized from hot methanol/ether. NMR analysis of the crude reaction mixture indicated a 10:1 *cis:trans* ratio. Chromatography provided this mixture as a off-white foam (28 mg, 72% yield). The follow peaks were assigned to the major isomer: 1H NMR (400 MHz, $CDCl_3$) δ 8.10 (d, 2H, $J = 8$ Hz), 7.62-7.58 (m, 2H), 7.47 (t, 2H, $J = 7.8$ Hz), 7.39-7.34 (m, 3H), 7.21-7.11 (m, 1H), 7.10 (s, 1H), 3.70 (s, 1H), 2.61 (dq, 1H, $J = 10.8, 6$ Hz), 2.33 (dq, 1H, $J = 10.8, 7.2$ Hz), 1.29 (s, 3H), 1.15 (d, 3H, $J = 7.2$ Hz), 0.90 (s, 3H), 0.71 (d, 3H, $J = 6$ Hz). ^{13}C NMR (100 MHz, $CDCl_3$) δ 166.9, 165.0, 140.3, 134.6, 133.7, 132.0, 131.4, 130.2, 129.5, 128.9, 128.8, 128.6, 128.4, 127.3, 110.7, 78.3, 67.3, 44.6, 41.0, 23.1, 22.2, 20.3, 13.6. HRMS (ESI) calc. for $[C_{24}H_{27}O_3N_2]^+$ 391.2016, found 391.2015.



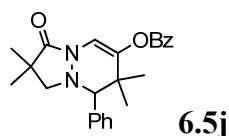
NMR analysis of the crude reaction mixture indicated the product was formed as a single diastereomer. Chromatography provided the product as a pale yellow foam (62 mg, 91% yield). 1H NMR (400 MHz, $CDCl_3$) δ 8.07 (d, 2H, $J = 8.4$ Hz), 7.56-7.52 (m, 4H), 7.44-7.28 (m, 7H), 7.08-7.00 (m, 6H), 6.85 (d, 2H, $J = 7.6$ Hz), 6.58 (d, 1H, $J = 8.0$ Hz), 6.38 (t, 1H, $J = 7.6$ Hz), 4.68 (t, 1H, $J = 9.6$ Hz), 4.05 (d, 2H, $J = 8.8$ Hz), 1.20 (d, 3H, $J = 10.4$ Hz), 0.88 (s, 3H). ^{13}C NMR (100 MHz, $CDCl_3$) δ 166.9, 164.5, 161.4, 142.2, 140.1, 133.7, 132.7, 132.0, 131.6, 131.3, 130.0, 129.3, 128.7, 128.3, 128.2, 127.9, 127.5, 127.3, 127.2, 127.1, 126.0, 110.3, 78.4, 70.9, 60.8, 41.2, 30.9, 29.7, 29.3, 22.7, 22.4, 21.8, 14.1, 14.0. HRMS (ESI) calc. for $[C_{35}H_{32}N_3O_4]^+$ 558.2387, found 558.2379



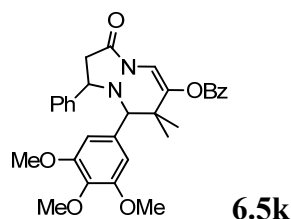
The reaction was performed at room temperature. ^1H NMR(600 MHz, CDCl_3) δ 8.12 (d, 2H, $J = 7.8$ Hz), 7.61 (t, 1H, $J = 7.8$ Hz), 7.59-7.33 (m, 6H), 7.19-7.11 (m, 1H), 6.96 (s, 1H), 3.65 (s, 1H), 3.31 (t, 1H, $J = 9.0$ Hz), 2.70-2.63 (m, 1H), 2.51-2.46 (m, 2H), 1.25 (s, 3H), 1.02 (s, 3H). ^{13}C NMR (150 MHz, CDCl_3) δ 165.0, 164.9, 140.6, 134.5, 133.8, 131.4, 130.2, 129.5, 129.1, 128.8, 128.5, 128.3, 128.2, 110.8, 50.9, 40.7, 31.5, 22.8. HRMS (ESI) calc. for $[\text{C}_{22}\text{H}_{23}\text{N}_2\text{O}_3]^+$ 363.1703, found 363.1704.



^1H NMR (500 MHz, CDCl_3) δ 8.09 (d, 2H, $J = 7.5$ Hz), 7.63-7.58 (m, 2H), 7.47 (t, 2H, $J = 7.8$ Hz), 7.36-7.31 (m, 3H), 7.23-7.19 (m, 1H), 7.15 (s, 1H), 3.98 (s, 1H), 2.58 (d, 1H, $J = 16$ Hz), 2.21 (d, 1H, $J = 16$ Hz), 1.19 (s, 3H), 1.19 (s, 3H), 0.93 (s, 3H), 0.82 (s, 3H). ^{13}C NMR (100 MHz, CDCl_3) δ 165.0, 164.7, 139.3, 135.4, 133.7, 131.9, 131.6, 130.2, 129.5, 128.8, 128.6, 128.1, 127.2, 111.0, 69.7, 63.1, 47.5, 40.6, 28.1, 23.2, 22.9, 21.4. HRMS (ESI) calc. for $[\text{C}_{24}\text{H}_{27}\text{N}_2\text{O}_3]^+$ 391.2016, found 391.2015. Enantiomeric excess was determined on a Shimadzu VP Series Chiral HPLC (Chiralcel AD-H column, 85:15 hexanes/ethanol, 1 mL/min) tr 9.9 min, 12.9 min.

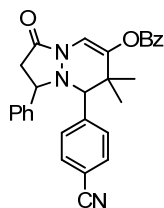


^1H NMR(600 MHz, CDCl_3) δ 8.10 (d, 2H, $J = 7.2$ Hz), 7.59 (t, 1H, $J = 6.0$ Hz), 7.52 (d, 1H, $J = 7.8$ Hz), 7.47 (t, 2H, $J = 7.8$ Hz), 7.41-7.33 (m, 3H), 7.18-7.17 (m, 1H), 7.08 (s, 1H), 3.59 (s, 1H), 3.07-3.05 (d, 1H, $J = 9.0$ Hz), 2.29-2.27 (d, 1H, $J = 9.0$ Hz), 1.27 (s, 3H), 1.15 (s, 6H), 1.02 (s, 3H). ^{13}C NMR (150 MHz, CDCl_3) δ 170.0, 165.0, 140.3, 134.6, 133.7, 131.3, 130.2, 129.5, 129.3, 128.8, 128.4, 128.2, 128.0, 110.9, 76.2, 64.6, 41.4, 40.7, 22.9, 22.7, 22.5, 22.2. HRMS (ESI) calc. for $[\text{C}_{24}\text{H}_{27}\text{N}_2\text{O}_3]^+$ 391.2016, found 391.2023.



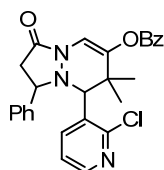
NMR analysis of the crude reaction mixture indicated a 6:1 *cis:trans* ratio. Chromatography provided first the minor *trans* diastereomer as a clear oil (8mg, ~70% purity, 8% yield). ^1H NMR (500 MHz, CDCl_3) δ 8.12 (d, 2H, $J = 8$ Hz), 7.63 (t, 1H, $J = 7.3$ Hz), 7.50-7.33 (m, 7H), 7.15 (s, 1H), 7.01 (s, 1H), 6.04 (s, 1H), 3.95 (s, 3H), 3.89 (s, 3H), 3.86 (s, 3H), 3.84-3.81 (m, 1H), 3.57 (s, 1H), 2.76 (dd, 1H, $J = 16.5, 8$ Hz), 2.62 (dd, 1H, $J = 16.5, 12$ Hz), 1.57 (s, 3H), 0.82 (s, 3H). ^{13}C NMR (150 MHz, CDCl_3) δ 165.1, 164.6, 154.3, 152.4, 139.9, 138.4, 137.8, 133.9, 133.8, 133.4, 130.4, 130.3, 130.2, 129.8, 129.3, 129.2, 129.1, 129.1, 129.0, 128.8, 128.7, 127.9, 125.4,

112.1, 109.5, 105.6, 69.9, 62.0, 61.2, 61.1, 56.6, 56.3, 41.3, 41.1, 39.5, 34.9, 31.8, 25.5, 22.9, 21.9, 14.3. Followed by the major *cis* diastereomer as a white foam (57 mg, 71% yield). ¹H NMR (400 MHz, CDCl₃) δ 8.11 (d, 2H, *J* = 7.6 Hz), 7.62 (t, 1H, *J* = 7.4 Hz), 7.50 (t, 2H, *J* = 7.8 Hz), 7.19 (s, 1H), 7.19-7.12 (m, 3H), 7.00 (dd, 1H, *J* = 7.4, 1.8 Hz), 6.40 (d, 1H, *J* = 1.6 Hz), 5.87 (d, 1H, *J* = 1.6 Hz), 4.04 (app t, 1H, *J* = 9.8 Hz) 3.88 (s, 3H), 3.76 (s, 1H) 3.70 (s, 3H), 3.18 (s, 3H), 3.02 (dd, 1H, *J* = 17.6, 9.4 Hz), 2.69 (dd, 1H, *J* = 17.6, 10.4 Hz), 1.27 (s, 3H), 0.95 (s, 3H). ¹³C NMR (100 MHz, CDCl₃) δ 164.9, 163.3, 152.3, 151.8, 142.8, 141.3, 137.9, 133.8, 130.2, 129.4, 128.8, 128.5, 128.5, 127.4, 127.0, 110.8, 109.1, 108.4, 78.8, 65.4, 60.9, 56.6, 55.1, 41.6, 41.5, 23.0, 22.3. HRMS (ESI) calc. for [C₃₁H₃₃O₆N₂]⁺ 529.2333, found 529.2329.



6.5l

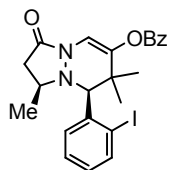
NMR analysis of the crude reaction mixture indicated a 5:1 *cis:trans* ratio. Chromatography provided first the minor *trans* diastereomer as a white foam (13.5mg, 15% yield). ¹H NMR (600 MHz, CDCl₃) δ 8.11 (d, 2H, *J* = 7.8 Hz), 7.80 (qd, 2H, *J* = 8.7, 1.5 Hz), 7.64-7.61 (m, 2H), 7.49 (t, 2H, *J* = 7.8 Hz) 7.43-7.31 (m, 5H), 7.21 (s, 1H), 6.96 (d, 1H, *J* = 7.8 Hz), 3.72 (s, 1H), 3.69 (dd, 1H, *J* = 11.4, 8.4 Hz), 2.77 (dd, 1H, *J* = 16.8, 8.4 Hz), 2.64 (dd, 1H, *J* = 16.8, 11.4 Hz), 1.55 (s, 3H), 0.74 (s, 3H). ¹³C NMR (150 MHz, CDCl₃) δ 165.2, 164.5, 140.4, 139.2, 137.4, 134.0, 133.3, 132.9, 131.7, 130.3, 130.0, 129.4, 129.2, 129.0, 128.9, 127.7, 118.6, 112.6, 112.3, 69.1, 61.6, 41.1, 39.6, 30.5 (broad) 22.2. Followed by the major *cis* diastereomer as a white foam (73.5 mg, 79% yield). ¹H NMR (600 MHz, CDCl₃) δ 8.10 (d, 2H, *J* = 7.8 Hz), 7.62 (t, 1H, *J* = 7.2 Hz), 7.52-7.47 (m, 3H), 7.28 (d, 1H, *J* = 7.8 Hz), 7.21 (s, 1H), 7.17 (t, 1H, *J* = 7.2 Hz), 7.10 (t, 2H, *J* = 7.5 Hz), 6.88 (d, 2H, *J* = 7.2 Hz), 6.76 (d, 1H, *J* = 8.4 Hz), 6.75 (d, 1H, *J* = 8.4 Hz), 3.90 (s, 1H), 3.89 (dd, 1H, *J* = 11.4, 8.4 Hz), 2.96 (dd, 1H, *J* = 17.4, 8.4 Hz), 2.75 (dd, 1H, *J* = 17.4, 11.4 Hz), 1.20 (s, 3H), 0.89 (s, 3H). ¹³C NMR (150 MHz, CDCl₃) δ 164.8, 162.8, 141.0, 140.1, 138.1, 133.9, 132.1, 131.9, 131.3, 130.2, 129.5, 129.3, 128.8, 128.6, 127.7, 127.4, 118.5, 112.0, 110.8, 78.3, 67.4, 41.6, 41.0, 22.7, 21.9. HRMS (ESI) calc. for [C₂₉H₂₆O₃N₃]⁺ 464.1969, found 464.1959.



6.5m

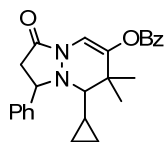
NMR analysis of the crude reaction mixture indicated a 1.7:1 *cis:trans* ratio. Chromatography provided this mixture as a pale yellow solid (123 mg, 98% yield). ¹H NMR (600 MHz, CDCl₃) δ 8.38 (d, 1H, *J* = 4.8 Hz), 8.11 (d, 3.4H, *J* = 7.8 Hz), 8.09 (d, 2H, *J* = 7.8 Hz), 8.05 (d, 1H, *J* = 7.8 Hz), 8.02 (d, 1.7H, *J* = 3.6 Hz), 7.62 (app t, 2.7H, *J* = 7.5 Hz), 7.49 (app t, 5.4H, *J* = 7.2 Hz), 7.43-7.34 (m, 6.4 Hz), 7.24 (s, 1.7H), 7.19 (s, 1H), 7.13-7.06 (m, 6.4H), 6.94 (d, 3.4H, *J* = 7.2 Hz), 6.33 (dd, 1.7 H, *J* = 7.8, 4.8 Hz), 4.70 (s, 1.7H), 4.56 (s, 1H), 3.98 (dd, 1.7H, *J* = 12, 8.7 Hz), 3.78 (dd, 1H, *J* = 11.4, 8.4 Hz), 2.95 (dd, 1.7H, *J* = 16.8, 8.7 Hz), 2.81 (dd, 1H, *J* = 16.8, 8.4 Hz), 2.74 (dd, 1.7H, *J* = 16.8, 12 Hz), 2.65 (dd, 1H, *J* = 16.8, 11.4 Hz), 1.60 (s, 3H), 1.21 (s, 5.1H), 1.21 (s, 5.1H), 0.77 (s, 3H). ¹³C NMR (150 MHz,

CDCl₃) δ 165.2, 164.8, 164.6, 162.7, 153.2, 141.9, 149.1, 149.1, 142.0, 141.0, 140.2, 140.0, 139.5, 137.9, 134.0, 133.9, 1302, 129.9, 129.3, 129.0, 129.0, 128.9, 128.8, 128.8, 127.7, 127.4, 127.4, 123.6, 120.2, 112.2, 110.8, 71.9, 67.8, 63.4, 61.3, 41.8, 41.7, 41.2, 40.0, 30.5, 22.8, 21.6, 21.1. HRMS (ESI) calc. for [C₂₇H₂₅O₃N₃Cl]⁺ 474.1579, found 474.1569.



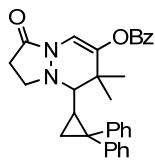
6.5n

NMR analysis of the crude reaction mixture indicated a 1.8:1 mixture of diastereomers. Chromatography provided the mixture as a white foam (31mg, 72%). ¹H NMR (500 MHz, CDCl₃) δ 8.11-8.07 (m, 5.7H), 7.96 (d, 1.8H, *J* = 8.0 Hz), 7.92 (d, 1H, *J* = 8.0 Hz), 7.61 (t, 3H, *J* = 8.5 Hz), 7.56 (m, 2H), 7.49-7.34 (m, 12.3H), 7.14 (d, 2.8H, *J* = 7.5 Hz), 7.07-7.03 (m, 1.8H), 7.01-6.98 (m, 1H), 4.62 (s, 1H), 4.50 (s, 1.7H), 3.22-3.15 (m, 1.8H), 2.92 (bs, 1H), 2.77-2.71 (q, 1.8H), 2.58-2.53 (q, 1H), 2.34-2.28 (m, 2.8H), 1.60 (s, 3H), 1.35 (d, 3.2H, *J* = 6.0 Hz), 1.27 (s, 6.7H), 1.06 (s, 5.8H), 0.84 (s, 3.2H), 0.79 (d, 5.5H, *J* = 6.0 Hz). ¹³C NMR (125 MHz, CDCl₃) δ 165.39, 165.18, 165.02, 164.8, 140.59, 140.54, 140.15, 139.5, 138.5, 137.1, 133.8, 133.7, 132.9, 130.5, 130.2, 130.1, 129.9, 129.5, 129.4, 129.3, 128.8, 127.1, 111.7, 110.9, 105.0, 104.4, 77.8, 71.5, 57.2, 52.7, 42.5, 40.3, 39.3, 39.2, 30.3, 23.1, 22.2, 22.1, 21.8, 18.5. HRMS (ESI) calc. for [C₂₃H₂₄N₂O₃I]⁺ 503.0826, found 503.0807.



6.5p

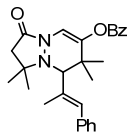
NMR analysis of the crude reaction mixture indicated a 2.8:1 *cis:trans* ratio. Chromatography provided first the major *cis* diastereomer as a clear oil (21mg, 30% yield). ¹H NMR (400 MHz, CDCl₃) δ 8.11 (d, 2H, *J* = 7.2 Hz), 7.62 (t, 1H, *J* = 7.6 Hz), 7.52-7.47 (m, 4H), 7.40-7.30 (m, 3H), 7.09 (s, 1H), 5.12 (dd, 1H, *J* = 12.4, 8 Hz), 2.93 (dd, 1H, *J* = 16.4, 8 Hz), 2.63 (dd, 1H, *J* = 16.4, 12.4 Hz), 1.92 (d, 1H, *J* = 9.6 Hz), 1.44 (s, 3H), 1.19 (s, 3H), 0.92-0.80 (m, 2H), 0.65-0.57 (m, 1H), 0.35-0.29 (m, 1H), 0.16-0.10 (m, 1H). ¹³C NMR (100 MHz, CDCl₃) δ 164.3, 164.6, 139.3, 138.6, 133.7, 130.2, 129.6, 129.2, 128.8, 128.5, 127.6, 111.3, 67.5, 60.1, 42.3, 42.2, 30.0, 23.2, 5.4, 2.6. HRMS (ESI) calc. for [C₂₅H₂₇O₃N₂]⁺ 403.2016, found 439.2025. Followed by the minor *trans* diastereomer as a clear oil (7.5 mg, 11% yield). ¹H NMR (600 MHz, CDCl₃) δ 8.12 (d, 2H, *J* = 7.2 Hz), 6.63 (t, 1H, *J* = 7.2 Hz), 7.54-7.48 (m, 4H), 7.34 (t, 2H, *J* = 7.5 Hz), 7.26 (t, 1H, *J* = 7.5 Hz), 7.09 (s, 1H), 4.54 (dd, 1H, *J* = 11.4, 9 Hz), 2.99 (dd, 1H, *J* = 17.4, 9 Hz), 2.57 (dd, 1H, *J* = 17.4, 11.4 Hz), 2.07 (d, 1H, *J* = 10.8 Hz), 1.40 (s, 3H), 1.20 (s, 3H), 0.62-0.57 (m, 1H), 0.41-0.35 (m, 2H), 0.22-0.18 (m, 1H), -0.05 - -0.10 (m, 1H).



6.5q

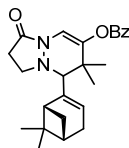
The reaction was performed at 35 °C. NMR analysis of the crude reaction mixture indicated a 2:1 *cis:trans* ratio. Chromatography provided first the major *cis* diastereomer as a clear oil (14mg, 30% yield). ¹H NMR (500 MHz, CDCl₃) δ 8.11 (d, 2H, *J* = 7 Hz), 7.62 (t, 1H, *J* = 7 Hz),

7.49 (t, 2H, $J = 7.8$ Hz), 7.41-7.34 (m, 4H), 7.31-7.18 (m, 5H), 7.00 (d, 2H, $J = 7$ Hz), 6.95 (s, 1H), 3.70 (td, 1H, $J = 7, 2$ Hz), 2.61-2.52 (m, 1H), 2.45 (d, 1H, $J = 9.5$ Hz), 2.26 (ddd, 1H, $J = 16.5, 8, 2$ Hz), 2.13-1.95 (m, 3H), 1.41 (s, 3H), 1.38-1.32 (m, 1H), 1.32 (s, 3H). Followed by the minor trans diastereomer as a clear oil (7 mg, 15% yield). $^1\text{H NMR}$ (500 MHz, CDCl_3) δ 8.03 (d, 2H, $J = 7$ Hz), 7.58 (t, 1H, 7 Hz), 7.45 (t, 2H, $J = 7.8$ Hz), 7.41 (d, 2H, $J = 7.5$ Hz), 7.35 (t, 2H, $J = 7.5$ Hz), 7.29 (t, 1H, $J = 7$ Hz), 7.21 (t, 2H, $J = 7.5$ Hz), 7.15 (t, 1H, $J = 7.5$ Hz), 7.01 (d, 2H, $J = 7.5$ Hz), 6.99 (s, 1H), 3.88 (t, 1H, $J = 8$ Hz), 3.18 (dt, 1H, $J = 12.5, 8.5$ Hz), 2.76-2.59 (m, 2H), 2.46 (d, 1H, $J = 10.5$ Hz), 2.04-1.93 (m, 2H), 1.47 (dd, 1H, $J = 9, 5$ Hz), 1.42 (s, 3H), 0.66 (s, 3H).



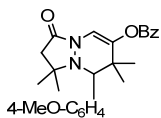
6.5w

The reaction was performed at 50 °C in 1,2-dichloroethane. Chromatography provided the desired product along with 30% of an unknown impurity (5 mg, 10% yield). $^1\text{H NMR}$ (400 MHz, CDCl_3) δ 8.11 (d, 2H, $J = 7.2$ Hz), 7.62 (t, 1H, 7.4 Hz), 7.49 (t, 2H, $J = 7.8$ Hz), 7.40-7.25 (m, 5H), 7.09 (s, 1H), 6.52 (s, 1H), 3.59 (s, 1H), 2.64 (d, 1H, $J = 16$ Hz), 2.30 (d, 1H, $J = 16$ Hz), 2.05 (s, 3H), 1.35 (s, 3H), 1.34 (s, 3H), 1.26 (s, 3H), 1.18 (s, 3H).



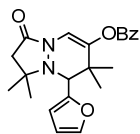
6.5x

The reaction was performed at 35 °C. NMR analysis of the crude reaction mixture indicated a 0.4:1 ratio of diastereomers. Chromatography provided this same mixture (6 mg, 15% yield). $^1\text{H NMR}$ (500 MHz, CDCl_3) δ 8.11 (d, 2.8H, $J = 7.5$ Hz), 7.61 (t, 1.4H, 7.5 Hz), 7.48 (t, 2.8H, $J = 7.5$ Hz), 7.02 (d, 0.4H, $J = 6$ Hz), 6.99 (s, 1H), 5.63-5.53 (m, 1.4H), 3.36-3.28 (m, 1H), 3.07 (d, 1H, $J = 15$ Hz), 3.00 (d, 0.4H, $J = 21$ Hz), 2.82-2.30 (m, 9H), 2.18-2.05 (m, 1.8 H), 1.35-0.85 (m, 19H). HRMS (ESI) calc. for $[\text{C}_{25}\text{H}_{31}\text{N}_2\text{O}_3]^+$ 407.2329, found 407.2326.



6.5y

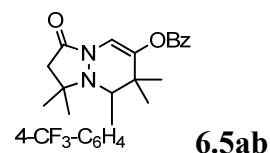
The reaction was performed at room temperature. Chromatography provided the desired product as a clear oil (4 mg, 11% yield). $^1\text{H NMR}$ (500 MHz, CDCl_3) δ 8.09 (d, 2H, $J = 7$ Hz), 7.61 (t, 1H, $J = 7.5$ Hz), 7.52-7.46 (m, 3H), 7.14 (s, 1H), 7.14-7.11 (m, 1H), 6.89-6.84 (m, 2H), 3.93 (s, 1H), 3.83 (s, 3H), 2.57 (d, 1H, $J = 16$ Hz), 2.19 (d, 1H, $J = 16$ Hz), 1.19 (s, 3H), 1.18 (s, 3H), 0.92 (s, 3H), 0.85 (s, 3H).



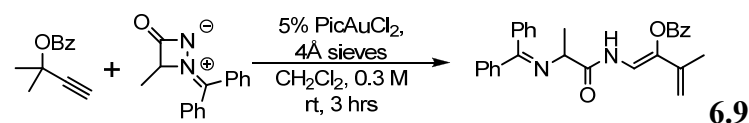
6.5z

The reaction was performed at 40°C. Chromatography provided the desired product as a clear oil (21 mg, 55% yield). $^1\text{H NMR}$ (600 MHz, CDCl_3) δ 8.08 (d, 2H, $J = 7.8$ Hz), 7.60 (t, 1H, $J = 7.8$ Hz), 7.48 (t, 2H, $J = 7.8$ Hz), 7.42 (d, 1H, $J = 1.2$ Hz), 7.13 (s, 1H), 6.40-6.36 (m, 2H), 4.03 (s,

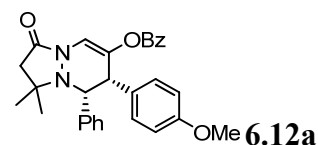
1H), 2.32 (d, 1H, $J = 16.2$ Hz), 2.22 (d, 1H, $J = 16.2$ Hz), 1.27 (s, 3H), 1.21 (s, 3H), 1.12 (s, 3H), 0.94 (s, 3H). ^{13}C NMR (100 MHz, CDCl_3) δ 166.7, 165.0, 149.9, 141.7, 139.4, 133.7, 130.2, 129.5, 128.8, 111.6, 111.2, 111.1, 62.3, 60.8, 46.3, 41.3, 25.4, 24.3, 22.5.



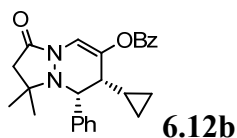
The reaction was performed at room temperature. Chromatography provided the desired product as a clear oil (35 mg, 99% yield). ^1H NMR (500 MHz, CDCl_3) δ 8.09 (d, 2H, $J = 7$ Hz), 7.76 (d, 1H, $J = 8$ Hz), 7.64-7.58 (m, 3H), 7.48 (t, 2H, $J = 8$ Hz), 7.36 (d, 1H, $J = 8$ Hz), 7.17 (s, 1H), 4.06 (s, 1H), 2.57 (d, 1H, $J = 16.5$ Hz), 2.24 (d, 1H, $J = 16.5$ Hz), 1.20 (s, 3H), 1.15 (s, 3H), 0.96 (s, 3H), 0.84 (s, 3H). ^{13}C NMR (125 MHz, CDCl_3) δ 165.3, 165.0, 140.1, 139.0, 134.1, 132.2, 132.1, 130.6, 130.5, 129.6, 129.1, 124.5, 111.5, 69.5, 63.4, 47.5, 40.8, 28.3, 23.4, 23.3, 22.1.



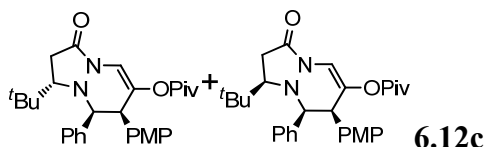
Chromatography on neutral alumina (Brockmann Activity II, 5%→25% EtOAc in hexanes) provided the product as a white foam (85 mg, 51% yield). ^1H NMR (500 MHz, CDCl_3) δ 9.12 (d, 1H, $J = 11.5$ Hz), 8.24 (d, 2H, $J = 8$ Hz), 7.72 (1H, $J = 7.5$ Hz), 7.54 (t, 2H, $J = 7.8$ Hz), 7.46-7.43 (m, 3H), 7.29 (d, 2H, $J = 7.5$ Hz), 7.19 (t, 1H, $J = 7.5$ Hz), 7.15 (d, 1H, $J = 11.5$ Hz), 7.09-7.07 (m, 2H), 6.79 (t, 2H, $J = 8$ Hz), 4.97 (s, 1H), 4.90 (s, 1H), 4.04 (q, 1H, $J = 7$ Hz), 2.03 (s, 3H), 1.31 (d, 3H, $J = 7$ Hz). ^{13}C NMR (125 MHz, CDCl_3) δ 171.8, 169.5, 164.0, 138.4, 135.6, 135.5, 135.3, 134.1, 130.6, 130.6, 129.1, 129.1, 129.0, 128.9, 128.2, 128.1, 127.4, 112.6, 111.1, 70.0, 21.0, 19.1. HRMS (ESI) calc. for $[\text{C}_{28}\text{H}_{27}\text{N}_2\text{O}_3]^+$ 439.2016, found 439.2010. The enamine geometry was assigned by NOESY.



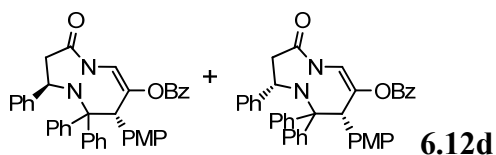
NMR analysis of the crude reaction mixture indicated a 10:1 *cis:trans* ratio. Chromatography provided this mixture as a white foam (81 mg, 87% yield). The follow peaks were assigned to the major isomer: ^1H NMR (600 MHz, CDCl_3) δ 7.89 (d, 2H, $J = 8.4$ Hz), 7.51 (t, 1H, $J = 7.5$ Hz), 7.43 (s, 1H), 7.36 (t, 2H, $J = 7.8$ Hz), 7.37-7.14 (m, 4H), 7.16 (t, 1H, $J = 7.5$ Hz), 6.87-6.20 (m, 4H), 4.60 (d, 1H, $J = 3$ Hz), 3.77 (s, 4H), 2.71 (d, 1H, $J = 16.2$ Hz), 2.28 (d, 1H, $J = 16.2$ Hz), 1.21 (s, 3H), 0.73 (s, 3H). In addition, the following peaks were distinctive for the minor diastereomer: ^1H NMR (600 MHz, CDCl_3) δ 7.70 (d, 2H, $J = 8.4$ Hz), 4.28 (d, 1H, $J = 8.4$ Hz), 3.84 (d, 1H, $J = 8.4$ Hz), 3.63 (s, 3H), 2.65 (d, 1H, $J = 16.2$ Hz), 2.30 (d, 1H, $J = 16.2$ Hz), 1.23 (s, 3H), 0.69 (s, 3H). ^{13}C NMR peaks were not assigned: ^{13}C NMR (150 MHz, CDCl_3) δ 165.4, 165.3, 164.9, 164.7, 159.1, 158.6, 138.1, 136.1, 136.1, 135.9, 133.6, 133.4, 131.8, 130.1, 129.9, 129.9, 129.7, 129.3, 129.3, 129.6, 128.5, 128.4, 128.4, 128.2, 128.2, 128.0, 127.6, 126.5, 113.6, 113.1, 112.1, 67.9, 64.4, 63.5, 62.4, 55.3, 55.2, 52.3, 50.4, 47.8, 47.6, 28.4, 27.9, 20.6, 20.6. HRMS (ESI) calc. for $[\text{C}_{29}\text{H}_{29}\text{O}_4\text{N}_2]^+$ 469.2122, found 469.2127.



NMR analysis of the crude reaction mixture indicated a 10:1 *cis:trans* ratio. Chromatography provided this mixture as an off-white foam (74 mg, 93% yield). The follow peaks were assigned to the major isomer: ^1H NMR (600 MHz, CDCl_3) δ 8.08 (d, 2H, $J = 7.8$ Hz), 7.59 (t, 1H, $J = 7.8$ Hz), 7.50-7.43 (m, 4H), 7.31-7.26 (m, 3H), 7.18 (s, 1H), 4.38 (d, 1H, $J = 4.2$ Hz), 2.55 (d, 1H, $J = 16.5$ Hz), 2.23 (d, 1H, $J = 16.5$ Hz), 2.05 (dd, 1H, $J = 9.9, 4.2$ Hz), 1.20 (s, 3H), 0.96 (s, 3H), 0.90-0.84 (m, 1H), 0.45-0.41 (m, 1H), 0.14-0.10 (m, 2H), -0.54 - -0.56 (m, 1H). ^{13}C NMR (150 MHz, CDCl_3) δ 165.4, 165.2, 137.3, 137.1, 133.7, 131.0, 130.1, 129.4, 128.8, 128.3, 127.7, 111.7, 63.2, 63.0, 48.7, 47.3, 27.8, 22.2, 11.3, 5.3, 3.8. In addition, the following peaks were distinctive for the minor diastereomer: ^1H NMR (600 MHz, CDCl_3) δ 8.09 (d, 2H, $J = 7.8$ Hz), 7.14 (d, 1H, $J = 1.8$ Hz), 3.95 (d, 1H, $J = 8.4$ Hz), 2.57 (d, 1H, $J = 16.5$ Hz), 2.25 (d, 1H, $J = 16.5$ Hz), 1.29 (s, 3H), 0.65 (s, 3H), -0.12 - -0.14 (m, 2H), -1.09 - -1.12 (m 1H). HRMS (ESI) calc. for $[\text{C}_{25}\text{H}_{27}\text{O}_3\text{N}_2]^+$ 403.2016, found 403.2021.

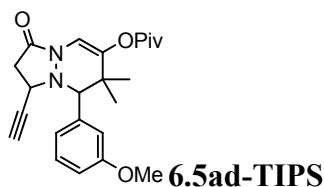


NMR analysis of the crude reaction mixture indicated a 2:1 mixture of diastereomers. Chromatography provided the mixture as a white foam (83 mg, 99% yield). The follow peaks were assigned to the major isomer: ^1H NMR (600 MHz, CDCl_3) δ 7.25-7.1 (m, 5H), 7.11 (d, 1H, $J = 2.4$ Hz), 6.73 (d, 2H, $J = 9$ Hz), 6.52 (d, 2H, $J = 9$ Hz), 4.97 (dd, 1H, $J = 6.6, 2.4$ Hz), 4.11 (d, 1H, $J = 6.6$ Hz), 3.63 (s, 3H), 2.83 (dd, 1H, $J = 11.4, 4.8$ Hz), 2.25 (dd, 1H, $J = 18, 4.8$ Hz), 2.05 (dd, 1H, $J = 18, 11.4$ Hz), 0.90 (s, 9H), 0.88 (s, 9H). The following peaks were assigned to the minor isomer: 7.9-6.0 (broad peaks, 9H), 7.19 (t, 7.5Hz), 7.07 (d, 1H, $J = 1.2$ Hz), 4.31 (d, 1H, $J = 3.3$ Hz), 3.80 (s, 3H), 3.78 (d, 1H, $J = 3.3$ Hz), 2.73 (app s, 1H), 2.73 (app q, 1H, $J = 9.4$ Hz), 2.39 (ddd, 1H, $J = 10.2, 6, 6$ Hz), 0.98 (s, 9H), 0.69 (s, 9H). ^{13}C NMR peaks were not assigned: ^{13}C NMR (150 MHz, CDCl_3) δ 176.8, 176.5, 171.2, 167.2, 159.2, 158.5, 139.6, 137.7, 135.7, 135.4, 131.3, 130.8 (broad), 128.8, 128.7 (broad), 128.5, 128.2, 127.1, 113.4, 113.1, 112.9, 72.0, 68.9, 64.6, 62.2, 55.4, 55.2, 50.0, 48.0, 39.0, 38.9, 35.6, 35.4, 32.6, 31.5, 26.9, 26.8, 26.6, 25.6. HRMS (ESI) calc. for $[\text{C}_{29}\text{H}_{37}\text{O}_4\text{N}_2]^+$ 477.2748, found 477.2747. X-ray quality crystals of the minor isomer were grown from ether/pentanes.

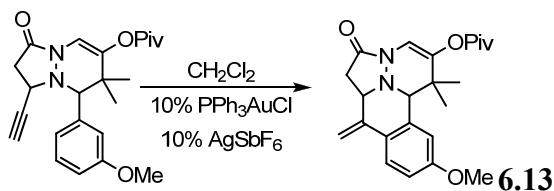


NMR analysis of the crude reaction mixture indicated a 4:1 mixture of diastereomers. Chromatography provided the mixture as a white foam (54 mg, 58% yield). The follow peaks were assigned to the major isomer: ^1H NMR (600 MHz, CDCl_3) δ 8.60 (d, 1H, $J = 7.8$ Hz), 7.84 (d, 2H, $J = 8.4$ Hz), 7.71 (dd, 1H, $J = 8.4, 1.8$ Hz), 7.58 (t, 1H, $J = 7.5$ Hz), 7.53 (t, 1H, $J = 7.5$ Hz), 7.51-7.30 (m, 11H), 7.12-7.07 (m, 1H), 6.95-6.90 (m, 2H), 6.72 (dd, 1H, $J = 8.4, 2.4$ Hz), 6.59-6.45 (m, 2H), 6.15 (dd, 1H, $J = 8.4, 2.4$ Hz), 6.09 (dd, 1H, $J = 8.4, 2.4$ Hz), 4.90 (d, 1H, $J = 10.2$ Hz), 4.35 (s, 1H), 3.62 (s, 3H), 2.21 (dd, 1H, $J = 17.4, 10.2$ Hz), 1.99 (dd, 1H, $J = 17.4, 1.2$

Hz). The following peaks were assigned to the minor isomer: 7.74 (d, 2H, $J = 8.4$ Hz), 7.55-7.30 (m, 19H), 7.23 (t, 1H, $J = 7.2$ Hz), 7.12-7.07 (m, 1H), 6.59-6.45 (m, 2H), 4.75 (d, 1H, $J = 2.4$ Hz), 4.48 (d, 1H, $J = 10.2$ Hz), 3.60 (s, 3H), 1.85 (d, 1H, $J = 17.4$ Hz), 1.41 (dd, 1H, $J = 17.4, 10.2$ Hz). ^{13}C NMR peaks were not assigned: ^{13}C NMR (150 MHz, CDCl_3) δ 39.1, 39.7, 54.6, 55.2, 55.2, 55.5, 57.6, 58.3, 58.8, 73.6, 76.8, 112.5, 112.7, 113.3, 113.9, 114.2, 114.5, 124.9, 125.8, 126.2, 126.9, 127.2, 127.4, 127.6, 127.6, 127.8, 128.0, 128.2, 128.5, 128.6, 128.8, 128.9, 129.0, 129.1, 129.2, 129.2, 129.3, 129.3, 130.0, 130.0, 130.1, 130.2, 130.3, 130.7, 131.2, 132.2, 132.7, 133.6, 133.7, 135.0, 140.2, 140.4, 140.6, 140.8, 141.1, 143.7, 144.4, 158.2, 158.7, 164.8, 165.1, 168.0. The diastereomers could not be definitively assigned by NOESY. HRMS (ESI) calc. for $[\text{C}_{39}\text{H}_{33}\text{N}_2\text{O}_4]^+$ 593.2435, found 593.2435.



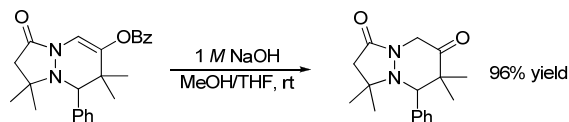
NMR analysis of the crude reaction mixture indicated a 1.6:1 *cis:trans* ratio. This crude mixture was concentrated and redissolved in THF. The solution was cooled to 0°C followed by addition of tetrabutylammonium fluoride solution (1M in THF, 0.33mL, 1.5 eq). After stirring for 30 minutes, the reaction was quenched with saturated ammonium chloride solution and extracted three times with ethyl acetate. The combined organic extracts were dried over MgSO_4 , filtered, and concentrate *in vacuo*. Chromatography (10% \rightarrow 25% EtOAc in hexanes/ CH_2Cl_2 8:2) provided the desired product as an off-white foam (63 mg, 72% yield). ^1H NMR (600 MHz, CDCl_3) δ 7.28-7.20 (m, 5.2H), 6.92-6.87 (m, 5.2H), 6.75 (d, 1.6H, $J = 7.8$ Hz), 6.70 (s, 1H), 3.81 (s, 9H), 3.74-3.70 (m, 2.6H), 3.69 (s, 1.6H), 3.63 (s, 1H), 2.91-2.86 (m, 2.6H), 2.79-2.62 (m, 2.6H), 2.20 (s, 1.6H), 2.14 (s, 1H), 2.37 (s, 23.4H), 1.18 (s, 4.8H), 1.16 (s, 3H), 0.85 (s, 7.8H). ^{13}C NMR (150 MHz, CDCl_3) δ 176.5, 162.9, 162.8, 159.1, 158.6, 141.4, 134.2, 134.1, 128.9, 128.5, 124.6, 124.2, 118.3, 117.3, 115.4, 113.4, 110.2, 82.0, 81.7, 78.3, 77.7, 73.9, 73.8, 55.4, 51.9, 51.8, 41.2, 41.2, 39.5, 38.5, 27.4, 22.7, 22.2. HRMS (ESI) calc. for $[\text{C}_{23}\text{H}_{29}\text{N}_2\text{O}_4]^+$ 397.2122, found 397.2119.



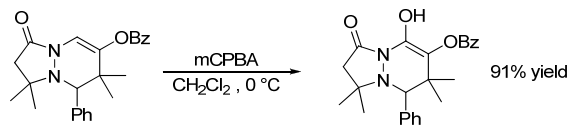
A solution of Ph_3PAuCl (5.5 mg, 0.1 equiv) and AgSbF_6 (3.8mg, 0.1 equiv) in CH_2Cl_2 (0.3 mL) was sonicated for 60 seconds. The resulting mixture was passed through a glass wool filter into a solution of the substrate (44 mg, 1 equiv) in CH_2Cl_2 (0.2 mL). This combined solution was stirred at 35°C for 24 hours in a sealed 1 dram vial. Chromatography of the crude reaction mixture provided the desired product as a white solid (34 mg, 2:1 dr). ^1H NMR (600 MHz, CDCl_3) δ 7.63 (d, 2H, $J = 8.4$ Hz), 7.29 (d, 1H, $J = 7.8$ Hz), 7.24 (t, 1H, $J = 7.8$ Hz), 7.17 (d, 2H, $J = 1.8$ Hz), 6.91-6.86 (m, 3H), 6.83 (s, 2H), 6.71 (bs, 1H), 5.96 (bs, 1H), 5.52 (d, 2H, $J = 1.2$ Hz), 5.33 (s, 1H), 4.90 (d, 2H, $J = 1.2$ Hz), 3.98 (s, 2H), 3.86 (s, 3H), 3.82 (s, 6H), 3.82-3.80 (m, 1H), 3.73-3.69 (m, 2H), 2.85-2.60 (m, 6H), 1.54 (s, 6H), 1.53 (s, 3H), 1.31 (s, 9H), 1.29 (s, 18H), 1.27 (s, 3H), 1.07 (s, 6H). ^{13}C NMR (150 MHz, CDCl_3) δ 176.9, 176.7, 164.9, 164.6, 159.4,

140.8, 140.6, 140.5, 135.8, 134.9, 128.3, 127.1, 127.0, 123.5, 119.9, 113.2, 113.0, 111.2, 111.0, 110.3, 104.7, 70.1, 62.2, 55.7, 55.5, 42.0, 39.5, 39.5, 38.5, 34.9, 27.4, 27.4, 22.1, 21.8.

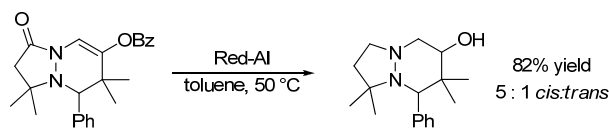
Further functionalization reactions of bicyclic products.



To a solution of benzoate **5i** (30.0 mg, 0.077 mmol) in methanol/tetrahydrofuran (2:1, 1 mL) at 0°C, was added NaOH (1M, 0.15 mL, 2 equiv). The resulting mixture was stirred at room temperature for 3 hours. After consumption of the starting material, the reaction was diluted with brine and extracted with diethyl ether (3 x 2 mL). The combined organic extracts were dried over sodium sulfate, concentrated, and subjected to flash column chromatography on silica gel (10% → 40% EtOAc in hexanes). The desired product (**6.14**) was isolated as a clear oil (21.2 mg, 96% yield). ¹H NMR (500 MHz, CDCl₃) δ 7.32-7.26 (m, 3H), 7.23-7.10 (m, 1H), 7.03-6.95 (m, 1H), 4.54 (d, 1H, *J* = 17.5 Hz), 4.19 (d, 1H, *J* = 17.5 Hz), 3.98 (s, 1H), 2.02 (d, 1H, *J* = 16 Hz), 1.73 (d, 1H, *J* = 16 Hz), 1.47 (s, 3H), 1.33 (s, 3H), 1.24 (s, 3H), 0.72 (s, 3H). ¹³C NMR (125 MHz, CDCl₃) δ 207.6, 170.4, 137.8, 128.5, 72.3, 60.7, 50.1, 49.7, 43.8, 28.8, 27.4, 24.4, 22.2. HRMS (ESI) calc. for [C₁₇H₂₃N₂O₂]⁺ 287.1754, found 287.1752.

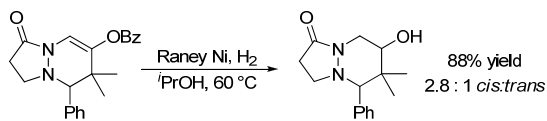


To a solution of benzoate **5i** (30.0 mg, 0.077 mmol) in wet CH₂Cl₂ (1 mL) at 0°C, was added mCPBA (21 mg, 75%, 0.091 mmol, 1.2 equiv). After consumption of the starting material (one hour), the reaction was diluted with aqueous sodium bicarbonate and extracted with CH₂Cl₂. The combined organic extracts were dried over sodium sulfate, concentrated, and subjected to flash column chromatography on silica gel (20% → 50% EtOAc in hexanes). The desired product (**S2**) was isolated as a white solid (28.4 mg, 91% yield). ¹H NMR (500 MHz, CDCl₃) δ 8.04 (d, 2H, *J* = 7.8 Hz), 7.72 (d, 1H, *J* = 7.5 Hz), 7.65 (s, 1H), 7.59 (t, 1H, *J* = 7.8 Hz), 7.44 (t, 2H, *J* = 7.8 Hz), 7.40-7.25 (m, 1H), 7.35-7.29 (m, 2H), 7.04-7.02 (m, 1H), 4.00 (s, 1H), 2.96 (d, 1H, *J* = 12.5 Hz), 2.24 (d, 1H, *J* = 12.5 Hz), 1.62 (s, 3H), 1.26 (s, 3H), 1.17 (s, 3H), 0.69 (s, 3H). ¹³C NMR (125 MHz, CDCl₃) δ 185.8, 163.4, 154.2, 136.9, 134.0, 130.3, 129.4, 129.0, 128.7, 128.5, 128.4, 128.2, 127.6, 115.2, 104.9, 71.1, 67.6, 54.8, 41.5, 28.8, 27.9, 21.0, 19.9. HRMS (ESI) calc. for [C₂₄H₂₇N₂O₄]⁺ 407.1965, found 407.1963. The regiochemistry was assigned using HMQC, HMBC, and NOESY spectra.

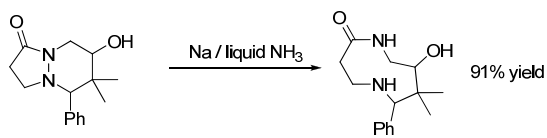


a solution of benzoate **5i** (30.0 mg, 0.077 mmol) in toluene (1 mL) at -78°C, was added a solution of Red-Al in toluene (0.2 mL, 0.63 mmol, 8 equiv). The solution was allowed to slowly warm to room temperature followed by heating at 50°C for 3 hours. The reaction was then cooled to 0°C and carefully quenched with aqueous sodium bicarbonate (0.2 mL). After stirring for a further fifteen minutes, the reaction was diluted with CH₂Cl₂, dried over sodium sulfate, filtered, and concentrated. Flash column chromatography on silica gel (CH₂Cl₂ → 15% MeOH in

CH₂Cl₂) provided the desired product (**S3**) as a white solid (17.4 mg, 82% yield, 1:0.2 *cis:trans*). ¹H NMR (500 MHz, CDCl₃) δ 7.51-7.48 (m, 1.2H), 7.26-7.15 (m, 3.6H), 7.13-7.10 (m, 1.2H), 3.68 (s, 0.2H), 3.59 (dd, 1H, *J* = 10.8, 4 Hz), 3.38 (s, 1H), 3.28 (bs, 0.2H), 3.10 (dd, 1H, *J* = 10.8, 4 Hz), 3.05-2.90 (m, 1.6H), 2.56 (app t, *J* = 10.8 Hz), 2.50-2.42 (m, 1.2 H), 1.75-1.67 (m, 2.4H), 1.05 (s, 0.6H), 1.02 (s, 3H), 0.99 (s, 3H), 0.97 (s, 0.6H), 0.72 (s, 0.6H), 0.67 (s, 3H), 0.59 (s, 3H), 0.55 (s, 0.6H). ¹³C NMR (125 MHz, CDCl₃) δ 136.9, 132.3, 132.2, 131.8, 131.3, 127.5, 127.3, 127.2, 126.4, 126.3, 74.9, 74.2, 71.9, 67.7, 62.8, 62.3, 57.2, 56.9, 52.0, 51.6, 41.7, 41.3, 39.6, 38.6, 31.5, 31.4, 24.6, 24.4, 22.8, 22.6, 22.1, 14.2. HRMS (ESI) calc. for [C₁₇H₂₇N₂O]⁺ 275.2118, found 275.2113. NOESY was used to assign the major isomer as *cis*.



A 50% aqueous solution of Raney Nickel (0.3g) was washed with *i*PrOH (3 x 2 mL). To the resulting solid, was added a solution of benzoate **5h** (32.0 mg, 0.088 mmol) in *i*PrOH (1 mL). The resulting mixture was placed under an atmosphere of hydrogen gas and stirred at 60°C for 3 hours. The reaction mixture was cooled to room temperature and filtered through celite, eluting with additional *i*PrOH (5 mL), concentrated and subjected to flash column chromatography on silica gel (CH₂Cl₂ → 15% MeOH in CH₂Cl₂). The desired product (**S4**) was isolated as a white solid (20.3 mg, 88% yield, 2.8:1 *cis:trans*). ¹H NMR (500 MHz, CDCl₃) δ 7.45-7.41 (m, 3.8H), 7.39-7.25 (m, 11.4 H), 7.12-7.11 (m, 1H), 7.11-7.10 (m, 2.8H), 4.20 (dd, 2.8H, *J* = 12.8, 5.3 Hz), 4.14 (dd, 1H, *J* = 13.8, 2.3 Hz), 3.75 (s, 1H), 3.56 (bs, 1H), 3.52-3.47 (m, 3.8H), 3.26-3.18 (m, 3.8H), 3.13 (bs, 1H), 3.11 (s, 2.8H), 3.06 (app t, 2.8H, *J* = 12 Hz), 2.93 (bs, 2.8H), 2.64-2.52 (m, 2H), 2.51-2.47 (m, 9.4H), 1.01 (s, 3H), 0.98 (s, 8.4H), 0.85 (s, 3H), 0.83 (s, 8.4H). ¹³C NMR (125 MHz, CDCl₃) δ 177.6, 169.8, 136.8, 135.9, 130.9, 130.9, 128.8, 128.7, 128.3, 128.2, 128.1, 127.9, 127.8, 79.1, 73.0, 72.7, 72.1, 49.6, 49.2, 45.0, 43.7, 40.1, 39.0, 30.7, 30.5, 24.1, 20.4, 12.9. HRMS (ESI) calc. for [C₁₅H₂₁N₂O₂]⁺ 261.1598, found 261.1600. NOESY was used to assign the major isomer as *cis*.



Following the procedure of Matsuyama *et. al.*,²⁵ approximately 10 mL of liquid ammonia was condensed at -78°C under argon in a three-necked flask equipped with a Dewar condenser cooled with dry ice/acetone. A solution of the alcohol obtained as described above (16.0 mg, 0.061 mmol) in tetrahydrofuran (2 mL) was added to the flask, followed by sodium metal (25 mg, 1.09 mmol, 18 equiv.). After 15 minutes, the cooling bath was removed and the solution was allowed to reflux for 20 minutes. The resulting dark blue solution was again cooled to -78°C and quenched with solid ammonium chloride until the blue color disappeared. At this point, both the Dewar condenser and the cooling bath were removed and the liquid ammonia was allowed to evaporate. The remaining residue was diluted with CH₂Cl₂ and filter through celite, rinsing thoroughly with CH₂Cl₂. The organic extracts were concentrated and subjected to flash column chromatography on silica gel (CH₂Cl₂ → EtOAc → 15% MeOH in EtOAc) to provided the desired product (**S5**) as a white solid (14.6 mg, 91% yield). ¹H NMR analysis of the product was complicated by the presence of *trans* and *cis*-amide bond conformers. These signals coalesced at 360K to give the same 2.8:1 ratio of diastereomers that was present in the starting material. The

^1H NMR chemical shifts of the major isomer at room temperature are given followed by the simplified spectrum at 360K.). ^1H NMR (600 MHz, CDCl_3 , room temperature) δ 7.37-7.13 (m, 5H), 6.20 (d, 1H, $J = 10.8$ Hz), 4.17 (dd, 1H, $J = 13.8, 10.8$ Hz), 3.58 (s, 1H), 3.50 (d, 1H, $J = 6$ Hz), 3.13 (dd, 1H, $J = 13.8, 6$ Hz), 3.03-2.90 (m, 1H), 2.82 (dd, 1H, $J = 12.9, 7.8$), 2.64-2.60 (m, 1H), 2.60-2.53 (m, 1H), 2.35 (ddd, 1H, $J = 11.4, 11.4, 7.8$ Hz), 2.21 (dd, 1H, $J = 11.4, 4.2$ Hz), 1.02 (s, 3H), 0.64 (s, 3H). ^1H NMR (600 MHz, CDCl_3 , 360K) δ 7.31-7.16 (m, 19H), 6.18 (bs, 2.8H), 5.82 (bs, 1H), 4.19 (bs, 2.8H), 3.94 (bs, 2H), 3.80-3.45 (m, 11.4H), 3.30-2.71 (m, 11.4H), 2.70-2.50 (m, 3.8H), 2.35-2.13 (m, 6.6H), 1.03 (s, 8.4H), 0.93 (s, 3H), 0.71 (s, 8.4H), 0.67 (s, 3H). ^{13}C NMR (150 MHz, CDCl_3 , room temperature) δ 176.6, 176.2, 139.7, 129.1, 128.8, 128.3, 128.1, 128.0, 127.8, 127.7, 127.4, 81.2, 77.7, 68.1, 65.0, 43.6, 43.4, 42.6, 42.2, 41.9, 41.3, 41.1, 39.9, 25.8, 25.6, 21.2, 20.5, 20.4. HRMS (ESI) calc. for $[\text{C}_{15}\text{H}_{23}\text{N}_2\text{O}_2]^+$ 263.1754, found 263.1756.

References

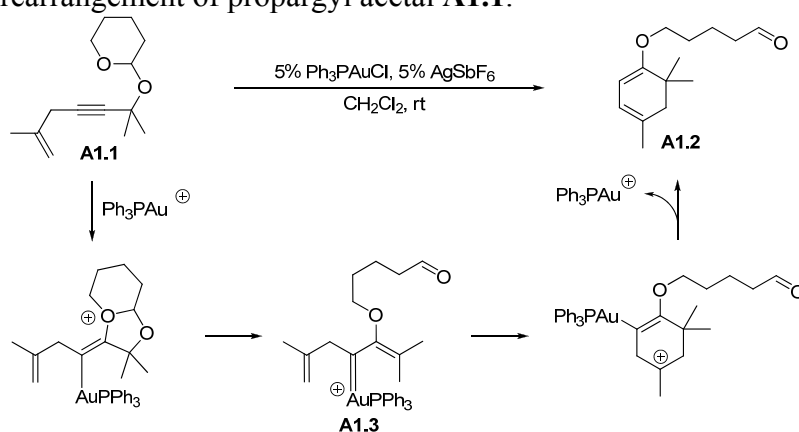
- (1) Shapiro, N. D.; Shi, Y. Toste, F. D. *J. Am. Chem. Soc.* **2009**, *131*, 11654.
- (2) (a) Barluenga, J.; Rodríguez, F.; Fañanás, F. J.; Flórez, J. *Topics Organomet. Chem.* **2004**, *13*, 59. (b) Barluenga, J.; Santamaria, J.; Tomás, M. *Chem. Rev.* **2004**, *104*, 2259. (c) Sierra, M. A., Fernández I., Cossío, F. P. *Chem. Commun.* **2008**, 4671.
- (3) (a) Davies, H. M. L.; Clark, D. M.; Alligood, D. B.; Elband, G. R. *Tetrahedron* **1987**, *43*, 4265. (b) Davies, H. M. L.; Hu, B. *Tetrahedron Lett.* **1992**, *33*, 453.
- (4) For descriptions of singlet vinylcarbene, see: (a) Hoffmann, R.; Zeiss, G. D.; Van Dine, G. W. *J. Am. Chem. Soc.* **1968**, *90*, 1485. (b) Davis, J. H.; Goddard III, W. A.; Bergman, R. G. *J. Am. Chem. Soc.* **1977**, *99*, 2427. (c) Sevin, A.; Arnaud-Danon, L. *J. Org. Chem.*, **1981**, *46*, 2346. (d) Honjou, N.; Pacansky, J.; Yoshimine, M. *J. Am. Chem. Soc.* **1985**, *107*, 5332. (e) Yoshimine, M.; Pacansky, J.; Honjou, N. *J. Am. Chem. Soc.* **1989**, *111*, 2785.
- (5) (a) Bertrand, G. Ed.; *Carbene Chemistry: From Fleeting Intermediates to Powerful Reagents*, FontisMedia: Lausanne, Dekker, New York, 2002. (b) Moss, R. A.; Platz, M. S.; Jones Jr., M. Eds.; *Reactive Intermediate Chemistry*, Wiley-Interscience: Hoboken, NJ, 2004.
- (6) Nucleophilic singlet vinylcarbenes react as 3-carbon units in cycloadditions with olefins, see: Boger, D. L.; Wysocki, R. J. *J. Org. Chem.* **1988**, *53*, 3408.
- (7) (a) Davies, H. M. L. *Curr. Org. Chem.* **1998**, *2*, 463. (b) Davies, H. M. L.; Walji, A. M. in *Modern Rhodium-Catalyzed Organic Reactions*; Evans, P. A. Ed.; Wiley-VCH: Weinheim, Germany, 2005; p 301.
- (8) For the first use of the term carbenoid as a “description of intermediates which exhibit reactions qualitatively similar to those of carbenes without necessarily being free divalent carbon species,” see: Closs, G. L.; Moss, R. A. *J. Am. Chem. Soc.* **1964**, *86*, 4042.
- (9) For examples of formal [3 + 3] cycloaddition reactions of azomethine imines, see: (a) Perreault, C.; Goudreau, S. R.; Zimmer, L. E.; Charette, A. B. *Org. Lett.* **2008**, *10*, 689. (b) Chan, A.; Scheidt, K. A. *J. Am. Chem. Soc.* **2007**, *129*, 5334. (c) Shintani, R.; Hayashi, T. *J. Am. Chem. Soc.* **2006**, *128*, 6330.
- (10) For examples of gold-catalyzed intermolecular cycloaddition reactions using propargyl esters, see: (a) Johansson, M. J.; Gorin, D. J.; Staben, S. T.; Toste, F. D. *J. Am. Chem. Soc.* **2005**, *127*, 18002. (b) Gorin, D. J.; Dubé, P.; Toste, F. D. *J. Am. Chem. Soc.* **2006**, *128*, 14480. (c) Gorin, D. J.; Watson, I. D. G.; Toste, F. D. *J. Am. Chem. Soc.* **2008**, *130*, 3736. (d) Shapiro, N. D.; Toste, F. D. *J. Am. Chem. Soc.* **2008**, *130*, 9244.
- (11) For additional examples of gold-catalyzed intermolecular cycloaddition reactions, see: (a) Ito, Y.; Sawamura, M.; Hayashi, T. *J. Am. Chem. Soc.* **1986**, *108*, 6405. (b) Asao, N.; Takahashi, K.; Lee, S.; Kasahara, T.; Yamamoto, Y. *J. Am. Chem. Soc.* **2002**, *124*, 12650. (c) Kusama, H.; Miyashita, Y.; Takaya, J.; Iwasawa, N. *Org. Lett.* **2006**, *8*, 289. (d) Melhado, A. D.; Luparia, M.; Toste, F. D. *J. Am. Chem. Soc.* **2007**, *129*, 12638. (e) Zhang, G.; Huang, X.; Li, G.; Zhang, L. *J. Am. Chem. Soc.* **2008**, *130*, 1814. (f) Zhang, G.; Zhang, L. *J. Am. Chem. Soc.* **2008**, *130*, 12598.
- (12) (a) Fürstner, A.; Davies, P. W. *Angew. Chem., Int. Ed.* **2007**, *46*, 3410. (b) Hashmi, A. S. K. *Chem. Rev.* **2007**, *107*, 3180. (c) Gorin, D. J.; Toste, F. D. *Nature* **2007**, *446*, 395. (d) Shen, H. C. *Tetrahedron* **2008**, *64*, 7847. (e) Jiménez-Núñez, E.; Echavarren, A. M. *Chem. Rev.* **2008**, *108*, 3326.

-
- (13) Similar *cis*-selectivity has been observed; see: ref 9. (a) Suárez, A.; Downey, C. W.; Fu, G. C. *J. Am. Chem. Soc.* **2005**, *127*, 11244. (b) Bonin, M.; Chauveau, A.; Micouin, L. *Synlett* **2006**, *15*, 2349.
- (14) Employing a different propargyl ester (acetate or pivalate) provided no change in selectivity.
- (15) HCl, PtCl₂, PdCl₂(PPh₃)₂, [IrCl(cod)]₂, and [RuCl₂(CO)₃]₂ failed to promote this reaction.
- (16) Witham, C. A.; Mauleón, P.; Shapiro, N. D.; Sherry, B. D.; Toste, F. D. *J. Am. Chem. Soc.* **2007**, *129*, 5838.
- (17) This substrate combination was chosen to aid in characterization of the products. Nearly identical selectivities were observed in reactions employing either **6.10a** or **6.10c**.
- (18) Nevado, C.; Echavarren, A. M. *Chem. Eur. J.* **2005**, *11*, 3155.
- (19) (a) Corma, A.; Domínguez, I.; Doménech, A.; Fornés, V.; Gómez-García, C. J.; Ródenas, T.; Sabater, M. J. *J. Catal.* **2009**, *265*, 238. (b) Chao, C.-M.; Genin, E.; Toullec, P. Y.; Genêt, J.-P.; Michelet, V. *J. Organomet. Chem.* **2009**, *694*, 538.
- (20) (a) Nieto-Oberhuber, C.; Muñoz, M. P.; Buñuel, E.; Nevado, C.; Cárdenas, D. J.; Echavarren, A. M. *Angew. Chem., Int. Ed.* **2004**, *43*, 2402. (b) López, S.; Herrero-Gómez, E.; Pérez-Galán, P.; Nieto-Oberhuber, C.; Echavarren, A. M. *Angew. Chem., Int. Ed.* **2006**, *45*, 6029.
- (21) For reviews, see: (a) Wee, A. G. H. *Curr. Org. Synth.* **2006**, *3*, 499. (b) Davies, H. M. L.; Beckwith, R. E. J. *Chem. Rev.* **2003**, *103*, 2861. (c) Davies, H. M. L.; Antoulinakis, E. G. *Org. React.* **2001**, *57*, 1. (d) Ye, T.; McKervey, M. A. *Chem. Rev.* **1994**, *94*, 1091. (e) *Modern Catalytic Methods for Organic Synthesis with Diazo Compounds*; Doyle M. P., McKervey, M. A., Ye, T., Eds.; Wiley: New York, 1998. (f) *Metal-Carbenes in Organic Synthesis*; Zaragoza-Dorwald, F., Ed.; Wiley-VCH: Weinheim, Germany, 1998. For gold-catalyzed reaction of α -diazoesters, see: (g) Fructos, M. R.; Belderrain, T. R.; de Frémont, P.; Scott, N. M.; Nolan, S. P.; Díaz-Requejo, M. M.; Pérez, P. J. *Angew. Chem., Int. Ed.* **2005**, *44*, 5284. (h) Fructos, M. R.; de Frémont, P.; Nolan, S. P.; Díaz-Requejo, M. M.; Pérez, P. J. *Organometallics* **2006**, *25*, 2237.
- (22) (a) Benitez, D.; Shapiro, N. D.; Tkatchouk, E.; Wang, Y.; Goddard, W. A. III; Toste, F. D. *Nature Chem.* **2009**, *1*, 482. (b) Seidel, G.; Mynott, R.; Fürstner, A. *Angew. Chem. Int. Ed.* **2009**, *48*, 2510. (c) Bauer, J. T.; Hadfield, M. S.; Lee, A.-L. *Chem. Commun.* **2008**, 6405.
- (23) Liu, F.; Yu, Y.; Zhang, J. *Angew. Chem. Int. Ed.* **2009**, *48*, 5505.
- (24) (a) Taylor, E. C.; Clemens, R. J.; Davies, H. M. L. *J. Org. Chem.* **1983**, *48*, 4567. (b) Perri, S. T.; Slater, S. C.; Toske, S. G.; White, J. D. *J. Org. Chem.* **1990**, *55*, 6037. (c) Svete, J.; Prešeren, A.; Stanovnik, B.; Golič, L.; Golič-Grdadolnik, S. *J. Heterocyclic Chem.* **1997**, *34*, 1323. (d) Shintani, R.; Fu, G. C. *J. Am. Chem. Soc.* **2003**, *123*, 10778. (e) Suárez, A.; Downey, W.; Fu, G. C. *J. Am. Chem. Soc.* **2005**, *127*, 11244. (f) Sibi, M. P.; Rane, D.; Stanley, L. M.; Soeta, T. *Org. Lett.* **2008**, *10*, 2971.
- (25) Matsuyama, H.; Itoh, N.; Matsumoto, A.; Ohira, N.; Hara, K.; Yoshida, M.; Iyoda, M. *J. Chem. Soc., Perkin Trans 1*, **2001**, 2924.

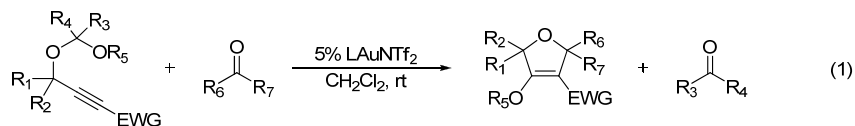
Appendix 1. Asymmetric Gold(I)-Catalyzed [3+2] Annulation of Aldehydes and Propargyl Acetals/Ketals

The rearrangement of propargyl esters has provided a platform for the development of numerous transition metal catalyzed reactions.¹ Thus, the discovery of a similar platform that might provide access to additional or complementary reactivity would be a potentially important development. It was with this goal in mind that we began investigating the reactivity of propargyl acetals and ketals.²

Scheme 1. A possible mechanism for the Au(I)-catalyzed rearrangement of propargyl acetal **A1.1**.



Some of our initial experiments suggested that this was a viable strategy. For example, the rearrangement of propargyl acetal **A1.1** to cyclohexadiene **A1.2** may proceed via Au-carbenoid **A1.3** (Scheme 1). Around the same time, Zhang and coworkers reported the Au-catalyzed intermolecular annulation of propargyl acetals and ketals with aldehydes and ketones (eq 1).³ In our minds, this report raised several mechanistic questions that were less than adequately addressed. We were also curious to find out if this transformation could be rendered asymmetric.



We began by investigating the use of chiral phosphine ligands in the annulation of alkynes **A1.4a-f** with cinnamaldehyde (Table 1). An initial experiment with (R)-BINAP(AuCl)₂ provided a promising lead (75% ee, entry 1). A subsequent ligand screen revealed that (R)-DTBM-MeO-BIPHEP provided the highest selectivity (90% ee, entry 3). A slight decrease in ee was observed when larger acetals were used (entries 4-5), while switching to a larger *tert*-butyl ester led to an increase in ee (94% ee, entry 9).

Table 1. Reaction Optimization.

entry	propargyl acetal	R	EWG	L*	dihydrofuran	yield (%) ^a	ee (%)	HPLC Conditions ^b
1	A1.4a	Et	CO ₂ Et	(R)-BINAP	A1.5a	80	75	AD 99:1 Hex: <i>i</i> PrOH (8.9, 11.9 min)
2	" "	Et	CO ₂ Et	(R)-MeO-BIPHEP	" "	80	10	" "
3	" "	Et	CO ₂ Et	(R)-DTBM-MeO-BIPHEP	" "	70	90	" "
4	A1.4b	(CH ₂) ₄ OTBS	CO ₂ Et	" "	A1.5b	70	86	AD 99.5:0.5 Hex: <i>i</i> PrOH (8.3, 9.2 min)
5	A1.4c	Cy	CO ₂ Et	" "	A1.5c	70	84	AD 99.5:0.5 Hex:EtOH (5.1, 8.6 min)
6	A1.4d	<i>t</i> Bu	CO ₂ Et	" "	A1.5d	<10	--	--
7	A1.4e	Et	CO ₂ Me	" "	A1.5e	80	89	AD 98:2 Hex: <i>i</i> PrOH (5.9, 7.3 min)
8	A1.4f	Et	CO ₂ (2,4,6-Me ₃ -C ₆ H ₂)	" "	A1.5f	80	87	AD 98:2 Hex: <i>i</i> PrOH (8.7, 10.1 min)
9	A1.4g	Et	CO ₂ <i>t</i> Bu	" "	A1.5g	50	94	OD 99.5:0.5 Hex: <i>i</i> PrOH (9.7, 10.8 min)

^a Approximate yields judged from examination of the crude ¹H NMR spectra. ^b Determined on a Shimadzu VP Series Chiral HPLC with Chiralcel AD and OD columns, 1 mL/min.

With optimal conditions in hand, we briefly explored the substrate scope of this transformation (Table 2). Several substrates with enantiomeric excesses over 80% were identified, including *p*-anisaldehyde, α -methyl-cinnamaldehyde, and β -phenyl-cinnamaldehyde. Unfortunately, the yields for many of these reactions were less than 50%. Further optimization of the reaction conditions is warranted.

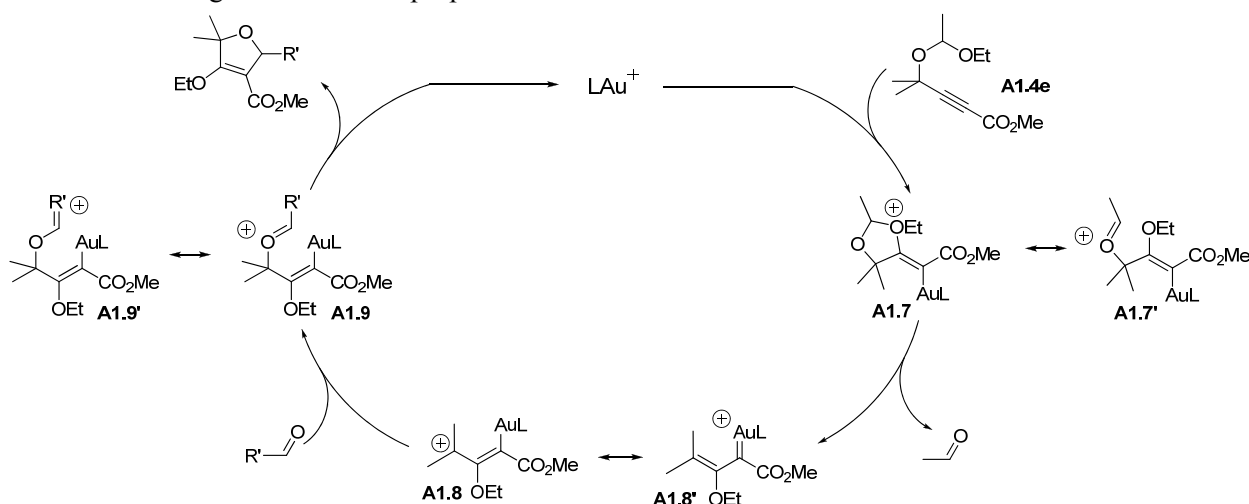
Table 2. A Brief Screen of Scope in Aldehyde.

 AD 98:2 Hex: <i>i</i> PrOH (7.0 (major), 8.8 min) 95% ee	 OD 99:1 Hex: <i>i</i> PrOH 0.5 mL/min (9.9, 11.0 min) 82% ee	 AD 98:2 Hex: <i>i</i> PrOH (5.2, 5.8 min) 87% ee	 OJ 96:04 Hex: <i>i</i> PrOH 0.5 mL/min (20.5, 25.4 min) 75% ee
 AD 95:5 Hex: <i>i</i> PrOH (9.6, 12.2 min) <10% ee, trace pdt ^a	 WH 97:3 Hex: <i>i</i> PrOH (19.4, 23.1 min) <10% ee	 WH 99:1 Hex:EtOH (6.6, 9.0 min) 79% ee, slow reaction	 none of desired pdt ^b
 none of desired pdt ^b	 none of desired pdt ^b	 none of desired pdt ^b	

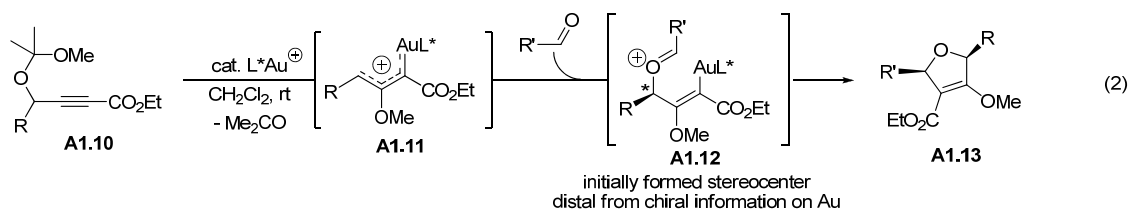
Enantiomeric excess determined on a Shimadzu VP Series Chiral HPLC with Chiralcel columns, 1 mL/min unless otherwise noted. ^a 66% ee using (R)-Cl₂MeO-BIPHEP(AuCl)₂. ^b Using rac-BINAP(AuCl)₂.

Zhang and coworkers proposed mechanism is illustrated in Scheme 2. Initial Au-promoted 1,2-migration of the propargyl acetal moiety leads to formation of cationic intermediate **A1.8**. They postulate that resonance form **A1.8** is ‘favored’ over Au-carbenoid **A1.8’**, a view that is in line with our analysis of substituent effects on the charge distribution in vinyl Au carbenoids (Chapter 2). Subsequent addition of a second aldehyde or generates oxonium **A1.9**. Noting that only electron rich aldehydes participate in this reaction, Zhang and coworkers postulate that while 5-*endo-trig* cyclizations of **A1.9** and **A1.7’** are disfavored according to Baldwin’s rules⁴, “resonance form [**A1.9’**] can undergo favored and facile 5-*exo-trig* cyclization.” The idea that an intermediate can react through a particular resonance form is ridiculous. Assuming the rest of their mechanism is more or less correct, a more reasonable explanation for this observation is that the electronics of the R’ substituent may affect the directionality of the lowest unoccupied molecular orbital in intermediate **A1.9**.⁵ Moreover, given that the rate determining step is unknown, it may be that the formation of **A1.9** is effected by the electronics of the incoming aldehyde.

Scheme 2. Zhang and coworkers proposed mechanism.



Given this proposed mechanism, we hypothesized that enantioselective annulation of secondary propargyl ketals would pose a more difficult challenge (eq 2).⁶ In this scenario, the formation of intermediate **A1.12** creates a stereocenter that is quite distant from the chiral ancillary ligand on the gold catalyst.



We were therefore pleased to find that the (R)-BINAP(AuNTf₂)₂-catalyzed annulation of propargyl ketal **A1.10a** with cinnamaldehyde provided dihydrofuran **A1.13a** with moderate enantiomeric excess (50% ee, Table 2, entry 1). A subsequent screen of ancillary ligands again revealed that (R)-DTBM-MeO-BIPHEP provided the highest selectivity (65% ee, entry 3). Unfortunately the yield of this reaction was moderate (51%). Furthermore, increasing the bulk of

the propargyl substituent from methyl to cyclohexyl or iso-propyl (entries 9-10), resulted in a further decrease in yield with no associated increase in enantiomeric excess. Little to no increase in selectivity and yield was observed when *p*-anisaldehyde was used in place of cinnamaldehyde. Nevertheless, it may be possible to increase the selectivity and yield for these substrates with additional screening of ligands and reaction conditions.

Table 2. Annulation of Secondary Propargyl Ketals.

entry	propargyl acetal	R	dihydrofuran	L*	yield (%) ^a	<i>cis</i> : <i>trans</i>	ee (%) ^b	HPLC Conditions
1	A1.10a	Me	A1.13a	(R)-BINAP	79	7 : 1	-50	AD 98:2 Hex: <i>i</i> PrOH (11.6, 12.4 min) ^b
2	↓	↓	↓	(S)-H ₈ -BINAP	76	8 : 1	+58	
3	↓	↓	↓	(S)-Difluorophos	50	5 : 1	+40	
4	↓	↓	↓	(S)-Cy-SEGPHOS	75	3 : 1	+27	
5	↓	↓	↓	(R)-tol-SDP	73	7 : 1	+25	
6	↓	↓	↓	(R)-BIPHEP	58	5 : 1	-10	
7	↓	↓	↓	(R)-Cl,MeO-BIPHEP	74	7 : 1	-10	
8	↓	↓	↓	(R)-DTBM-MeO-BIPHEP	51	3 : 1	+65	
9	A1.10b	Cyclohexyl	A1.13b	""	32	8 : 1	40	AD 99:1 Hex: <i>i</i> PrOH (16.9, 22.6 min) ^b
10	A1.10c	<i>i</i> Pr	A1.13c	""	35	>10 : 1	65	WH 99:1 Hex: <i>i</i> PrOH (13.7, 18.7 min) ^b

^a Yields determined by ¹H NMR versus an internal standard. ^b For the major *cis* isomer.

We briefly explored other nucleophilic components for this reaction including olefins, imines, epoxides, isocyanides, isocyanates, isothiocyanates, and 1,3-dipoles. Unfortunately, no productive formal cycloaddition was observed for these classes of compounds.

In conclusion, we have shown that the gold-catalyzed formal cycloaddition of propargyl acetals and ketals with aldehydes can be rendered asymmetric. The substrate scope is quite broad for the aldehyde component, while further for on expanding the scope in propargyl acetal/ketal is warranted. In addition, several mechanistic questions remain unanswered. ¹⁸O-labelling experiments would confirm the origin of the dihydrofuran oxygen⁷, while calculations could support the formation of cationic intermediates **A1.8** and **A1.11** and aide in the development of a stereochemical model.

References

- (1) (a) Ohe, K. *Bull. Korean Chem. Soc.* **2007**, *28*, 2153. (b) Gorin, D. J.; Sherry, B. D.; Toste, F. D. *Chem. Rev.* **2008**, *108*, 3351. (c) Jiménez-Núñez, E.; Echavarren, A. M. *Chem. Rev.* **2008**, *108*, 3326.
- (2) This work was performed in collaboration with Maurizio Bernasconi.
- (3) Zhang, G.; Zhang, L. *J. Am. Chem. Soc.* **2008**, *130*, 12598.
- (4) (a) Baldwin, J. E. *J. Chem. Soc., Chem. Commun.* **1976**, 734. (b) Baldwin, J. E.; Thomas, R. C.; Kruse, L. I.; Silberman, L. *J. Org. Chem.* **1977**, *42*, 3846.
- (5) Johnson, C. D. *Acc. Chem. Res.* **1993**, *26*, 476.
- (6) Yields are highest for secondary propargyl ketals and tertiary propargyl acetals. Secondary propargyl acetals give poor yields, while tertiary propargyl ketals are difficult to synthesize.
- (7) In a possible alternative mechanism the dihydrofuran oxygen would originate from the propargyl acetal oxygen. Attack of the aldehyde on intermediate **A1.7**, followed by cyclization, and gold/acid-catalyzed cleavage of the resulting acetal would provide the observed product.

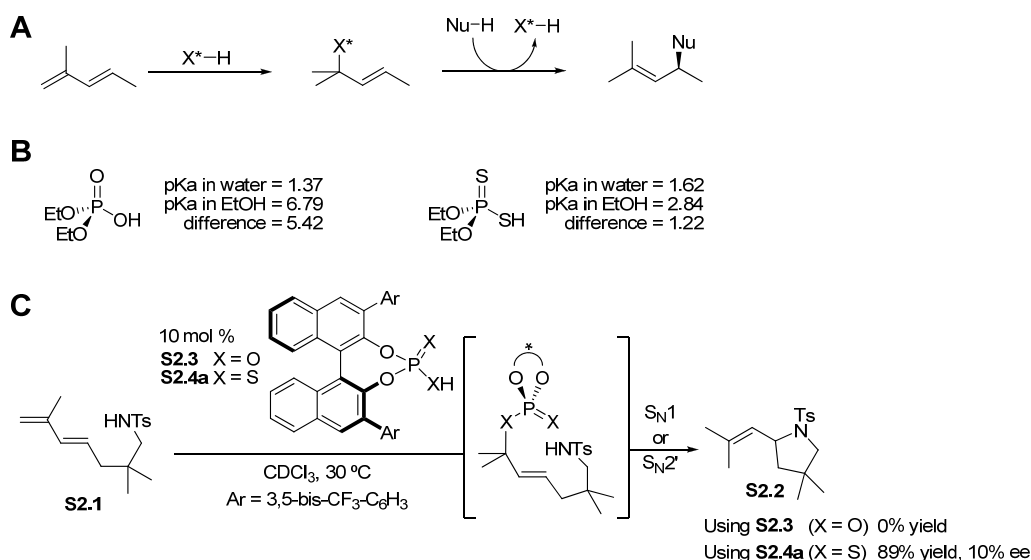
Appendix 2. Brønsted Acid-Catalyzed Asymmetric Hydroamination of Dienes

The observation that strong acids will catalyze the addition of protic nucleophiles to olefins was made more than a century ago. The ability to predict the regioselectivity of these reactions is taught in every introductory chemistry class as Markovnikov's rule. More recently, great progress has been made towards also rendering these reactions enantioselective. However, to date, and without exception, achieving high selectivity in these reactions has required the use of a metal catalyst. The development of a purely organic catalyst for such a transformation would represent not only a potential practical improvement, but also a significant expansion of the scope of enantioselective organocatalytic transformations.¹

Typically, very strong Brønsted acids (i.e. triflic acid, pK_a ~ -15) are required to promote the hydroamination of unactivated olefins.^{2,3} This poses several problems towards the development of efficient chiral analogs.^{4,5,6} Firstly, by their very nature these acids are highly dissociated in solution, resulting in increased separation between the acidic proton and the potentially chiral anion. Any even slightly basic functionality in the substrate or reaction media will exacerbate this problem. Secondly, assuming that an efficient chiral acid can be developed, acid-catalyzed racemization of the resulting products may become problematic.⁷ Finally, many functional groups are incompatible with such strongly acidic conditions.

To overcome these problems we considered the advantages of a nucleophilic⁸ and acidic catalyst. Upon protonation of an olefin, the anion (X⁻) of such a catalyst would be liable to intercept the resulting carbocation (Figure 1A). Because this mechanistic scenario results in the formation of a C-X bond, it necessarily decreases the distance the resulting carbon-based and the chiral information on X.

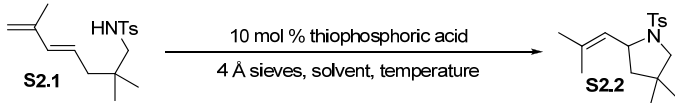
Figure 1. (A) Regioselective addition of an X-H bond across a diene followed by S_N2' displacement. (B) Thiophosphoric acids exhibit similar acidity in water and nonaqueous media. (C) Thiophosphoric acids catalyze the hydroamination of allenes under mild conditions.

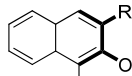
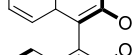
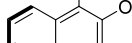
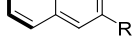
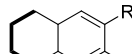
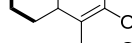
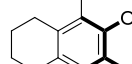
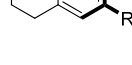
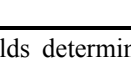


The search for a nucleophilic Brønsted acid led us to consider dithiophosphoric acids.^{9,10,11,12} While their oxygenated analogs, phosphoric acids, can be considered strong acids in water, they are actually quite weak in organic solvents.¹³ In contrast, dithiophosphoric acids maintain much of their acidity even in organic solvents (Figure 1B).^{14,15} This difference may be attributed to the increased polarizability of sulfur (2.90) versus oxygen (0.802), which also results in significantly enhanced nucleophilicity. Under radical-free conditions, the addition of achiral mono- and dithiophosphoric acids to unactivated dienes is known to proceed with Markovnikov regioselectivity.¹⁶ Combining these ideas, we were pleased to find that while phosphoric acid **S2.3** left diene **S2.1** untouched, dithiophosphoric **S2.4a** catalyzed the desired hydroamination reaction (10% ee, Figure 1C).

With a proof of concept in hand, we set about to further optimize the catalyst (Table 1). We quickly discovered that aryl substituents in the 9 and 9' positions were significantly better than aliphatic substituents (entries 1-2 vs. 3-4). A further increase in enantioselectivity was observed on going to the reduced, H₈-BINOL-derived catalyst **S2.5a** (62% ee, entry 5). Further optimization revealed that running the reaction in fluorobenzene at slightly reduced temperatures resulted in a significant increase in selectivity (77% ee, entry 6). Based on the proposed S_N2'-type mechanism, we hypothesized that further extension of the catalyst away from the acidic moiety might further improve the selectivity. To our delight, placing a phenyl substituent in the 10-position of the anthracene improved the enantioselectivity to 94% ee (entry 7). Further increasing the bulk of this phenyl substituent resulted in slight changes in enantioselectivity, with catalyst **S2.5d** providing the highest selectivity (entry 9).

Table 1. Catalyst Optimization.



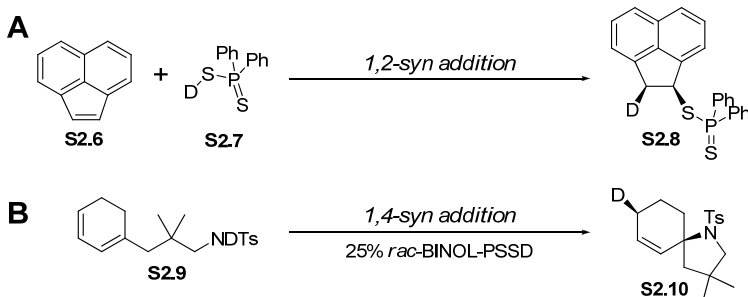
entry	catalyst	Solvent, Temp	% yield ^a	% ee
1	 S2.4b R = Adamantyl	CDCl ₃ , 30 °C	TBD	~10
2	 S2.4c R = SiPh ₃		TBD	~5
3	 S2.4d R = 1-naphthyl		TBD	~41
4	 S2.4e R = 9-anthracenyl		TBD	~56
5	 S2.5a R = 9-anthracenyl	FC ₆ H ₅ , 15 °C	98	62
6	 S2.5b R = 10-Ph-9-anthracenyl		91	77
7	 S2.5c R = 10-(3,5-bis-CF ₃ -C ₆ H ₃)-9-anthracenyl		92	94
8	 S2.5d R = 10-(3,5-bis- <i>t</i> -Bu-C ₆ H ₃)-9-anthracenyl		95	92
9	 S2.5d R = 10-(3,5-bis- <i>t</i> -Bu-C ₆ H ₃)-9-anthracenyl		96 ^b	96

^a Yields determined by ¹H NMR versus an internal standard. ^b The major enantiomer has (*R*) absolute stereochemistry.

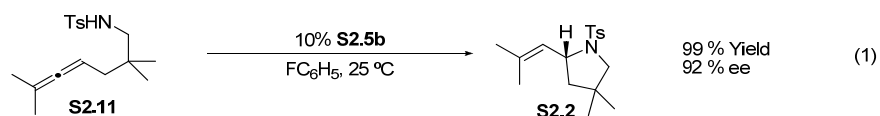
With optimal conditions in hand, we have begun to examine the substrate scope. Initial investigations suggest that the olefin and sulfonyl groups can be varied considerably with little effect on enantioselectivity or yield. Several interesting mechanistic observations were also made (Figure 2). Addition of a stoichiometric quantity of thioacid **S2.7** to acenaphthylene resulted in exclusive formation of *syn* addition adduct **S2.8**. Furthermore, thiophosphoric acid catalyzed

cyclization of deuterio-diene **S2.9** resulted in formation of **S2.10**, with deuterium incorporation *cis* to the amine. Taken together, these experiments suggest a mechanism consisting of *syn* addition of the thiophosphoric across the distal olefin, followed by *syn* addition of the amine. Initial calculations suggest that depending on the solvent polarity, addition of the amine may occur via an S_N2' or S_N1-type mechanism.

Figure 2. Mechanistic experiments.



We postulated that hydrothiolation of allene **8a** would lead to the same intermediate thioester, and should therefore also be a viable substrate for this reaction. In accord with this mechanistic hypothesis, this substrate was indeed converted to pyrrolidine **4a** with nearly identical enantiomeric excess (eq 1). Whether starting from diene **S2.1** or allene **S2.11**, the major enantiomer of the product has (*R*) absolute stereochemistry. This is opposite to that obtained in the (*S*)-phosphate controlled enantioselective Au-catalyzed cyclization of **S2.11**.¹⁷

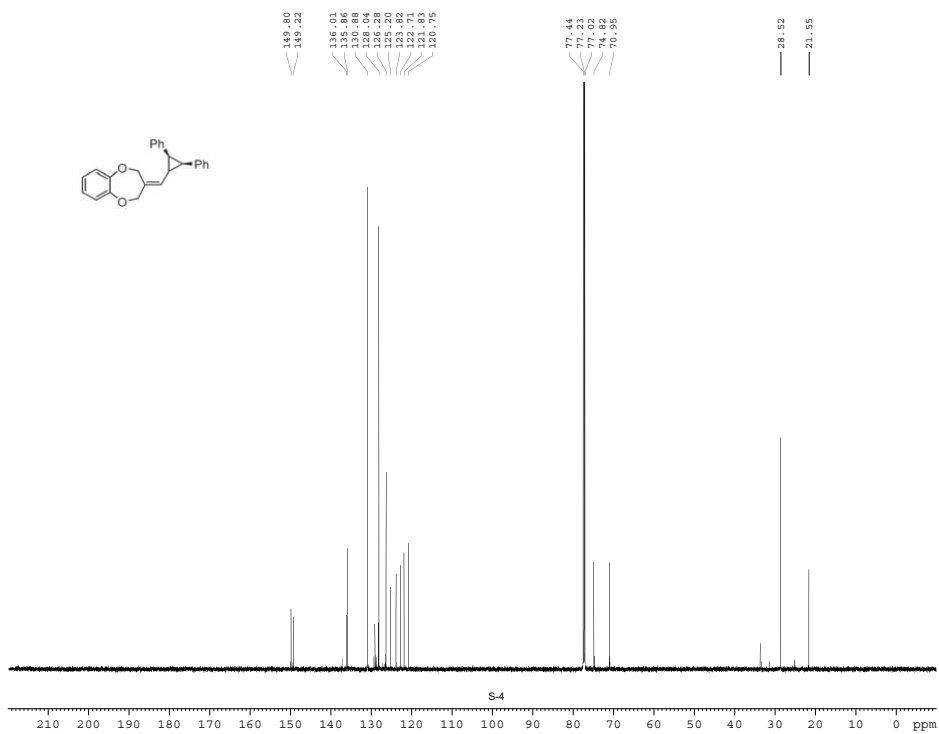
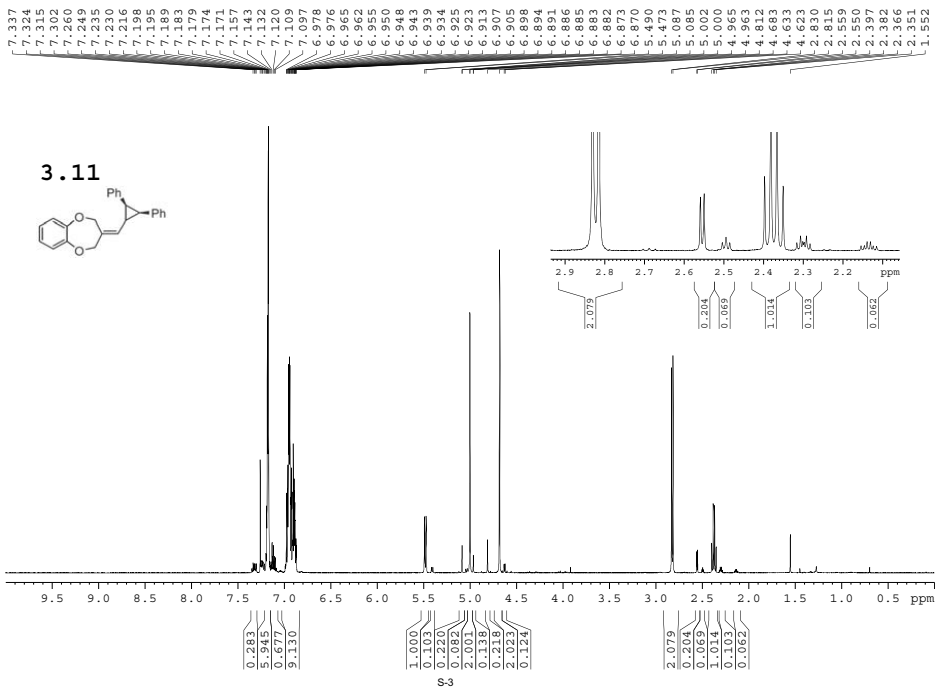


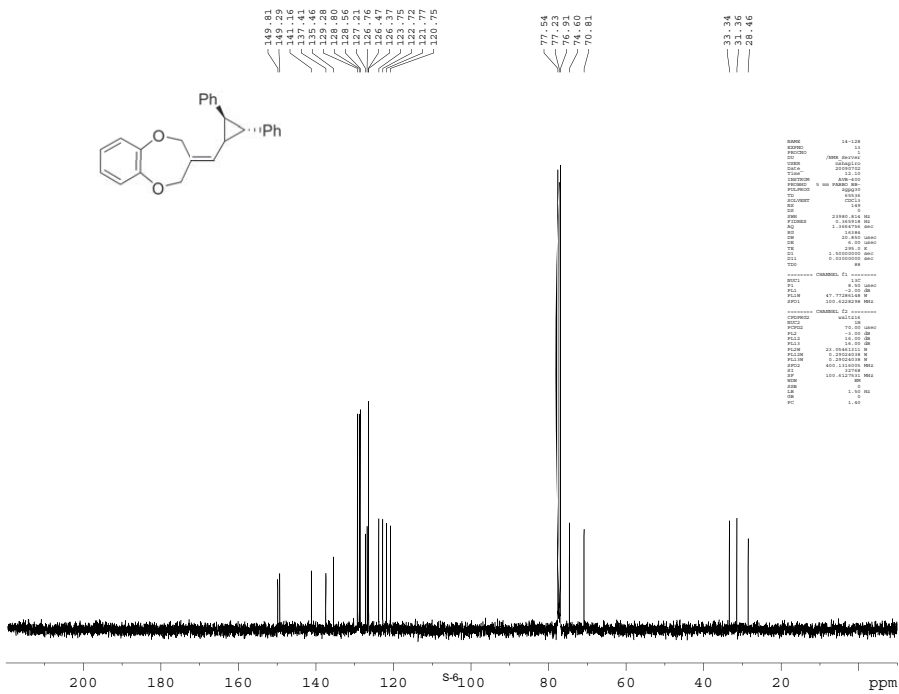
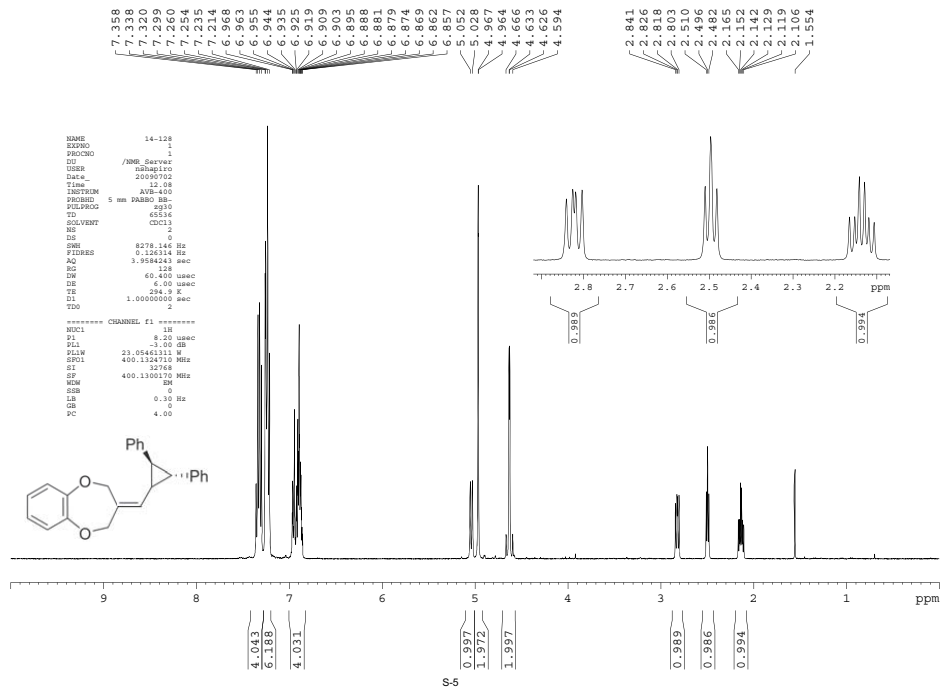
In conclusion, this work represents the first highly enantioselective Brønsted acid-catalyzed hydroamination of unactivated olefins. Efforts to expand the substrate scope by further optimizing the catalyst structure are ongoing.

References

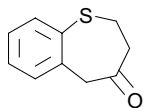
- (1) This work was carried out in collaboration with Vivek Rauniyar, Gregory Hamilton, and Jeffrey Wu.
- (2) Li, Z.; Zhang, J.; Brouwer, C.; Yang, C.-G.; Reich, N. W.; He, C. *Org. Lett.* **8**, 4175 (2006).
- (3) Rosenfeld, D. C.; Shekhar, S.; Takemiya, A.; Utsunomiya, M.; Hartwig, J. F. *Org. Lett.* **8**, 4179 (2006).
- (4) T. Akiyama, *Chem. Rev.* **107**, 5744 (2007).
- (5) D. Nakashima, H. Yamamoto, *J. Am. Chem. Soc.* **128**, 9626 (2006).
- (6) P. García-García, F. Lay, P. García-García, C. Rabalakos, B. List, *Angew. Chem. Int. Ed.* **48**, 4363 (2009).
- (7) Pawlas, J., Nakao, Y., Kawatsura, M., Hartwig, J. F. *J. Am. Chem. Soc.* **124**, 3669 (2002).
- (8) Leavitt, C. M.; Gresham, G. L.; Benson, M. T.; Gaumet, J.-J.; Peterman, D. R.; Klaehn, J. R.; Moser, M.; Aubriet, F.; Van Stipdonk, M. J.; Groenewold, G. S. *Inorg. Chem.* **47**, 3056 (2008).
- (9) G. R. Norman, W. M. LeSuer, T. W. Mastin, *J. Am. Chem. Soc.* **124**, 3669 (1952).
- (10) A. A. Oswald, K. Griesbaum, B. E. Hudson Jr., *J. Org. Chem.* **28**, 1262 (1963).
- (11) C. H. Cheon, H. Yamamoto, *J. Am. Chem. Soc.* **130**, 9246 (2008)
- (12) G. Pousse, A. Devineau, V. Dalla, L. Humphreys, M.-C. Lasne, J. Rouden, J. Blanchet, *Tetrahedron* **65**, 10617 (2009).
- (13) A. A. Kryuchkov, A. G. Matveeva¹, A. A. Grigoreva¹, E. K. Kuznetsova¹, E. I. Matrosov, M. I. Kabachnik, *Russ. Chem. Bul.* **36**, 1145 (1987).
- (14) M. I. Kabachnik, T. A. Mastrukova, A. E. Shipov, T. A. Melentyeva, *Tetrahedron* **9**, 10 (1960).
- (15) T. A. Mastryukova, L. L. Spivak, A. A. Grigoreva, E. K. Urzhuntseva, M. I. Kabachnik, *Zh. Obshch. Khim.* **41**, 1953 (1971).
- (16) (a) W. H. Mueller, A. A. Oswald *J. Org. Chem.* **31**, 1894 (1966).
- (17) G. L. Hamilton, E. J. Kang, E. J.; M. Mba; F. D. Toste, *Science* **317**, 496 (2007).

Appendix 3. Additional Supporting Information for Chapter 3

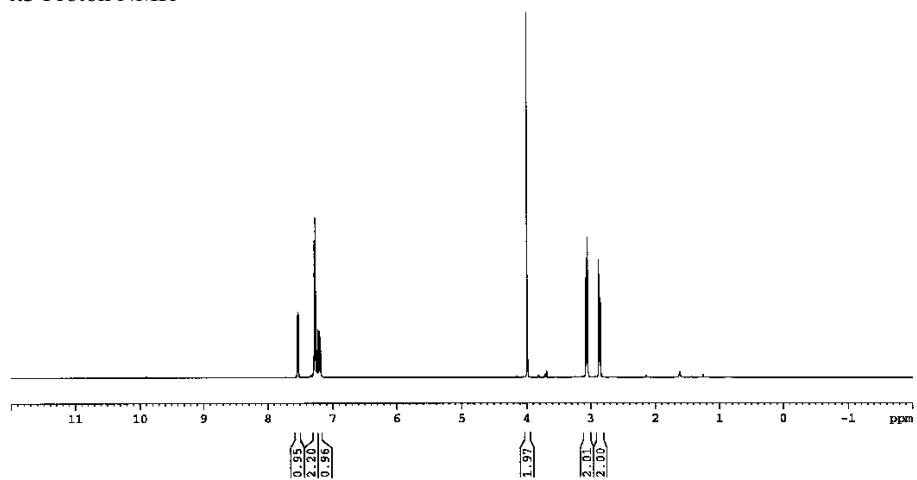




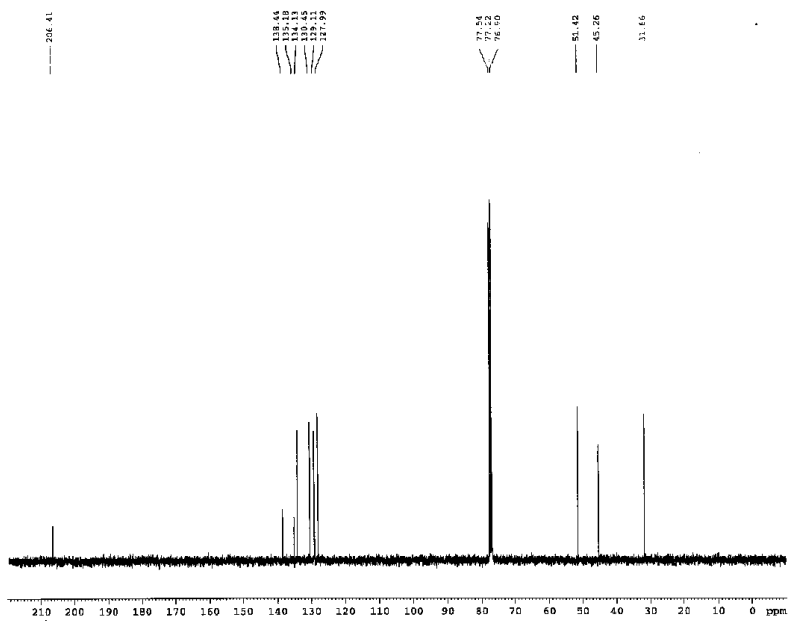
Appendix 4. Additional Supporting Information for Chapter 4

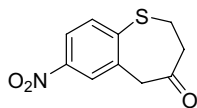


4.3 Proton NMR

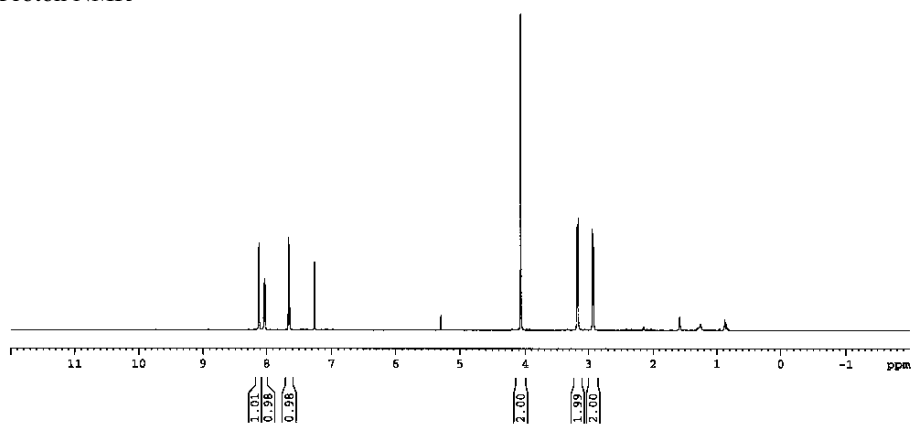


4.3 Carbon NMR

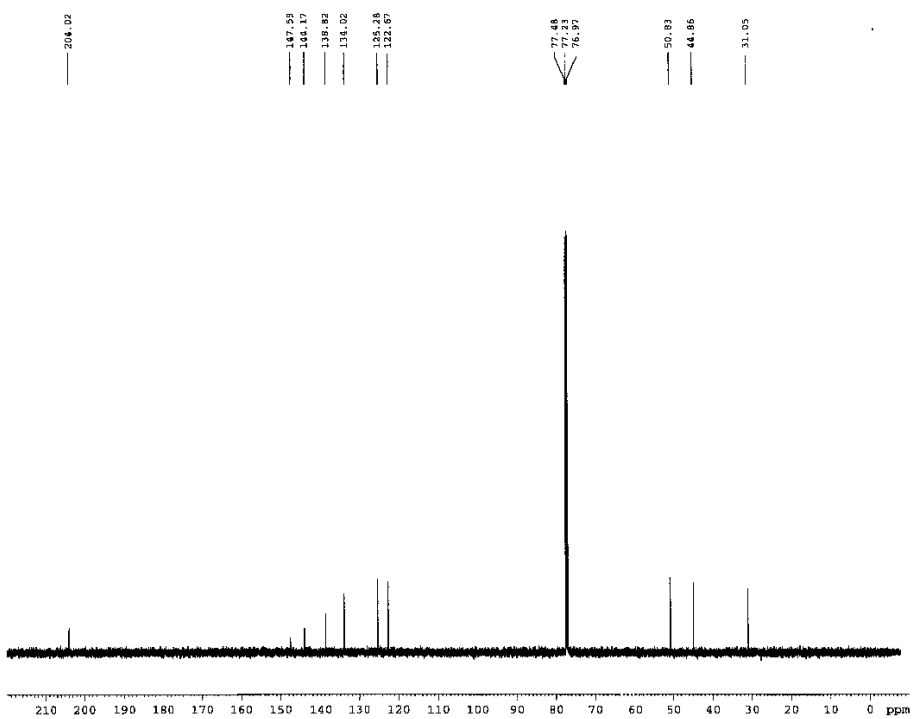


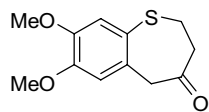


4.5 Proton NMR

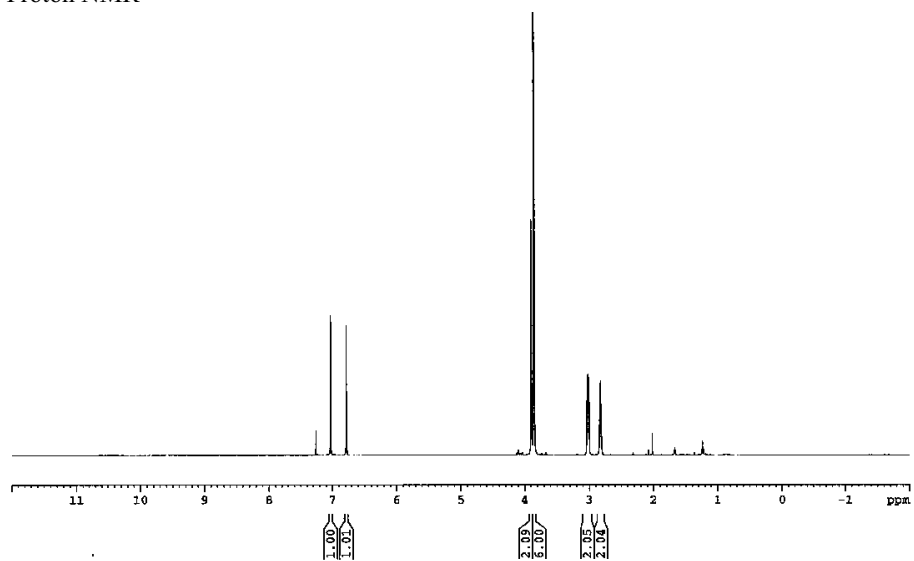


4.5 Carbon NMR

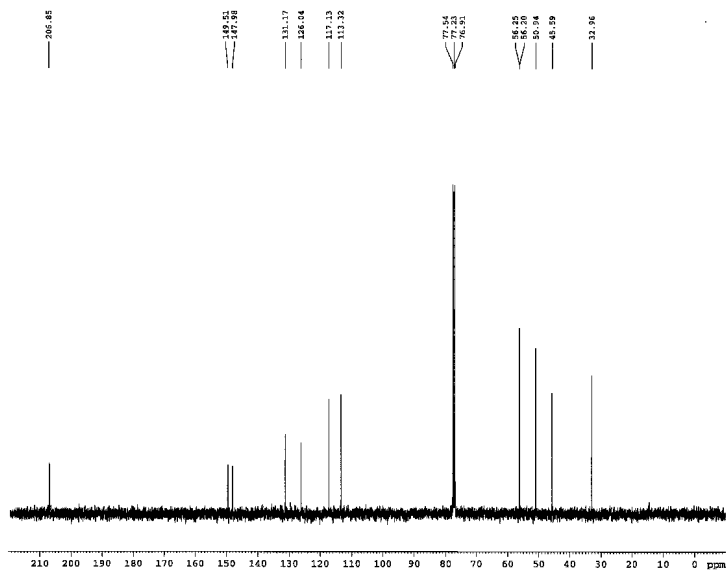


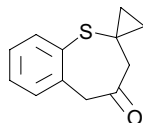


4.7 Proton NMR

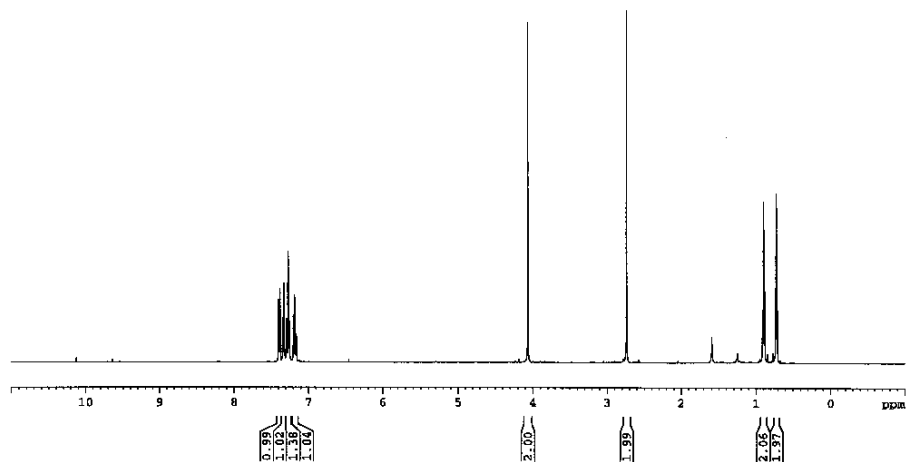


4.7 Carbon NMR

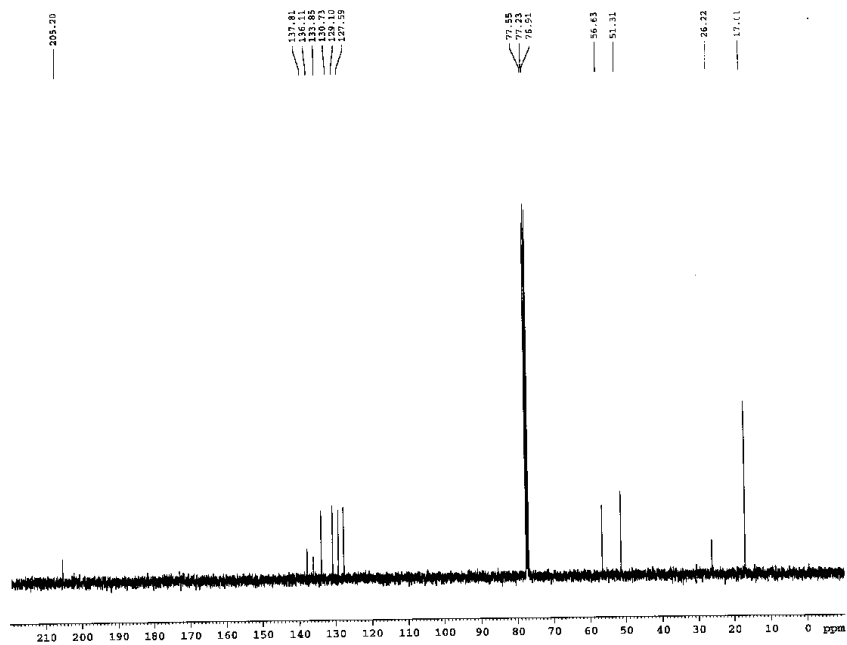


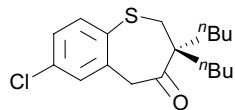


4.9 Proton NMR

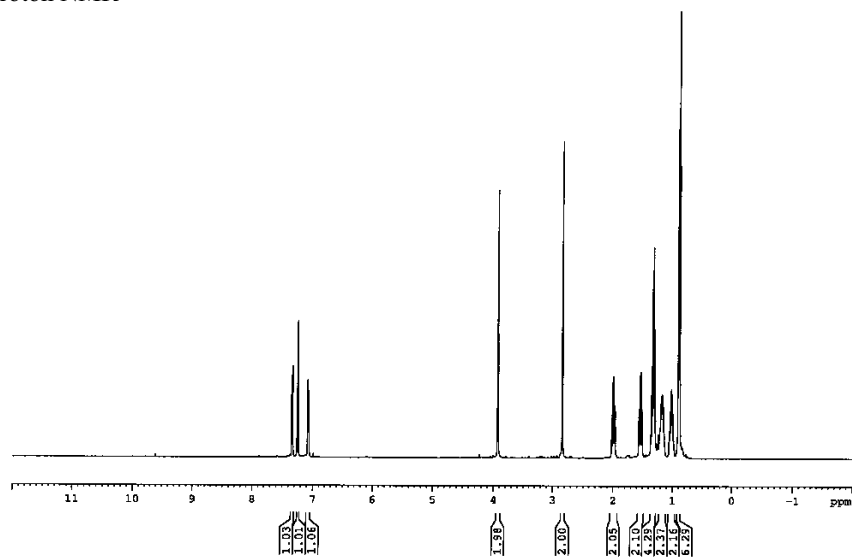


4.9 Carbon NMR

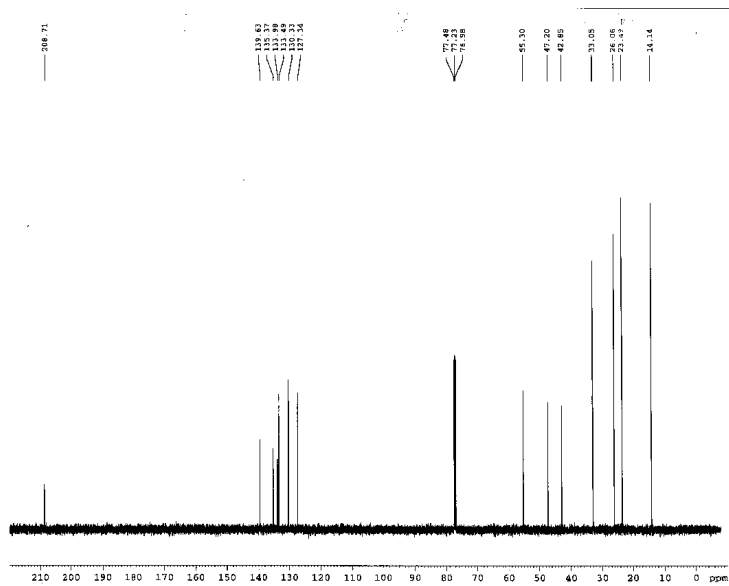


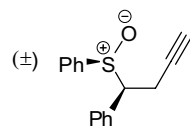


4.11 Proton NMR

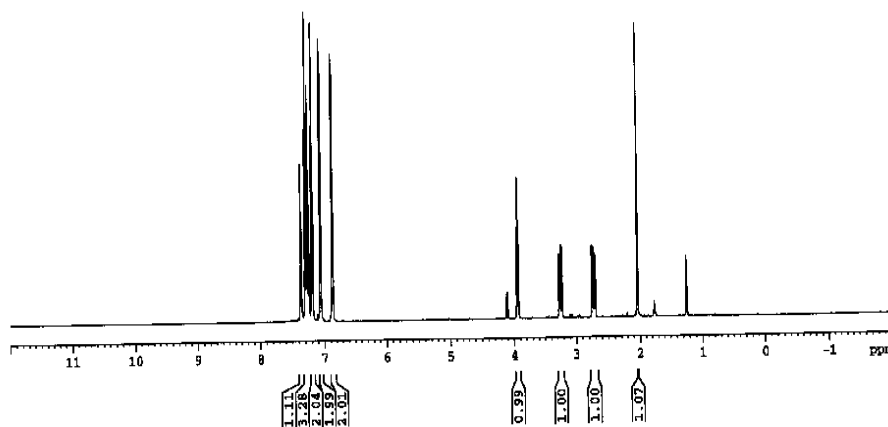


4.11 Carbon NMR

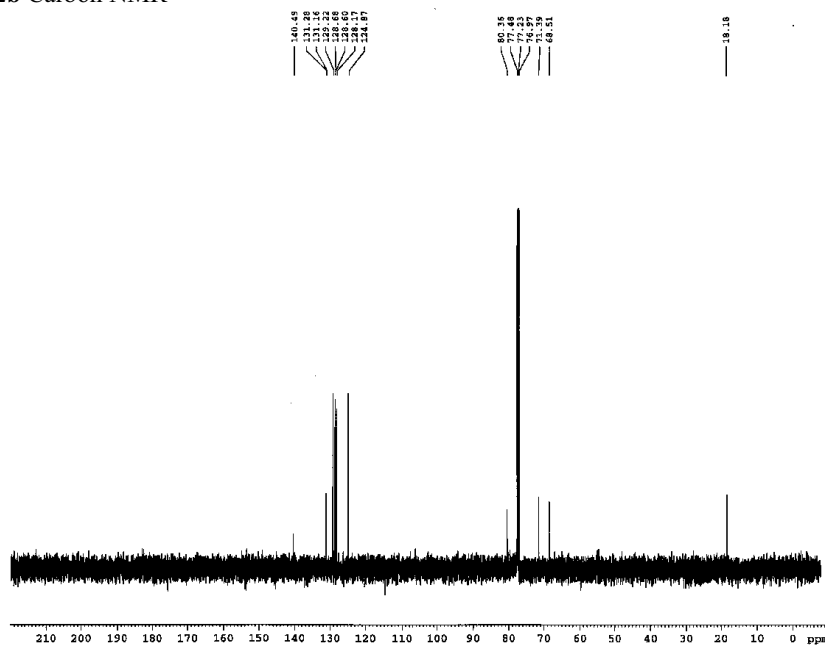


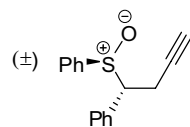


(±)-4.12b (less polar diastereomer) Proton NMR

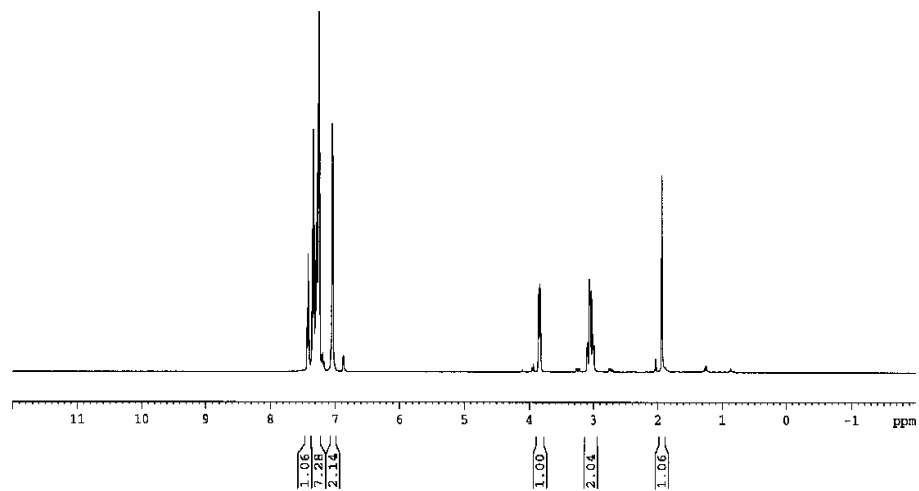


(±)-4.12b Carbon NMR

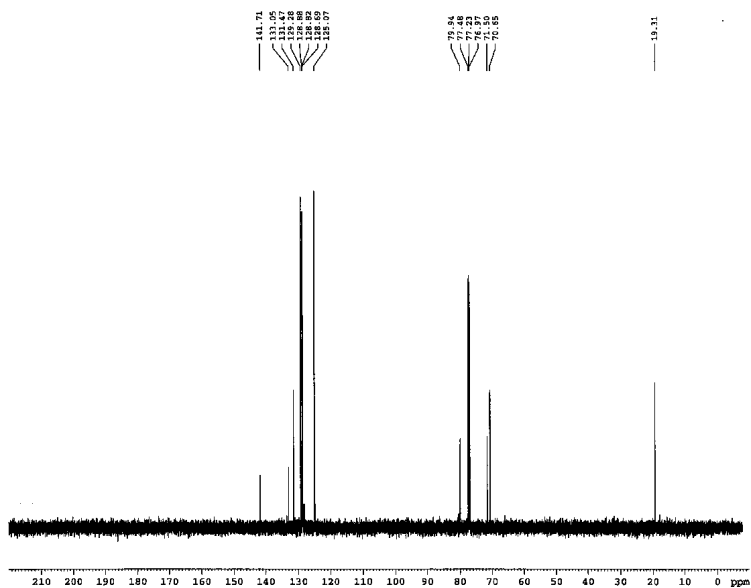


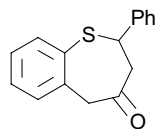


(±)-4.12 (more polar diastereomer) Proton NMR

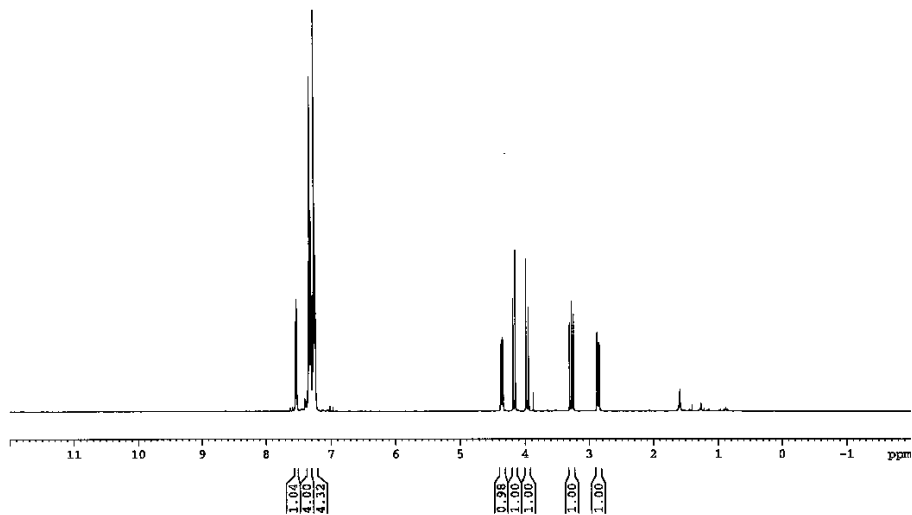


(±)-4.12 Carbon NMR

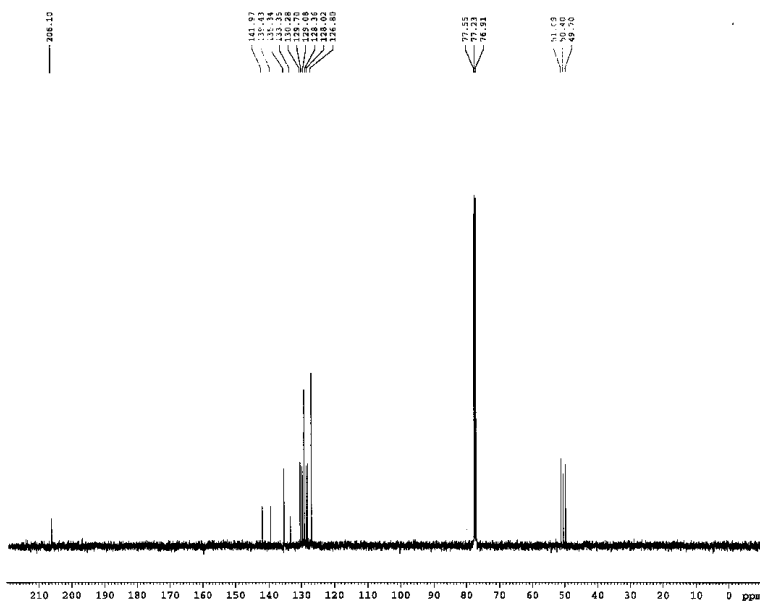


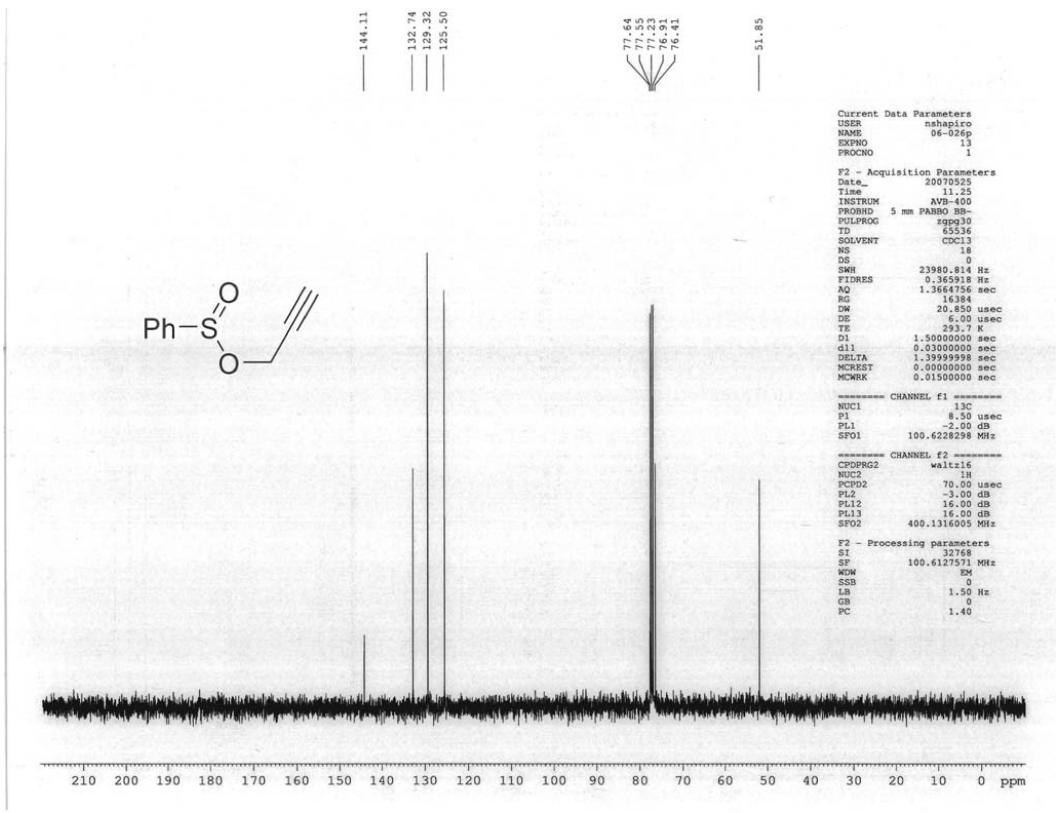
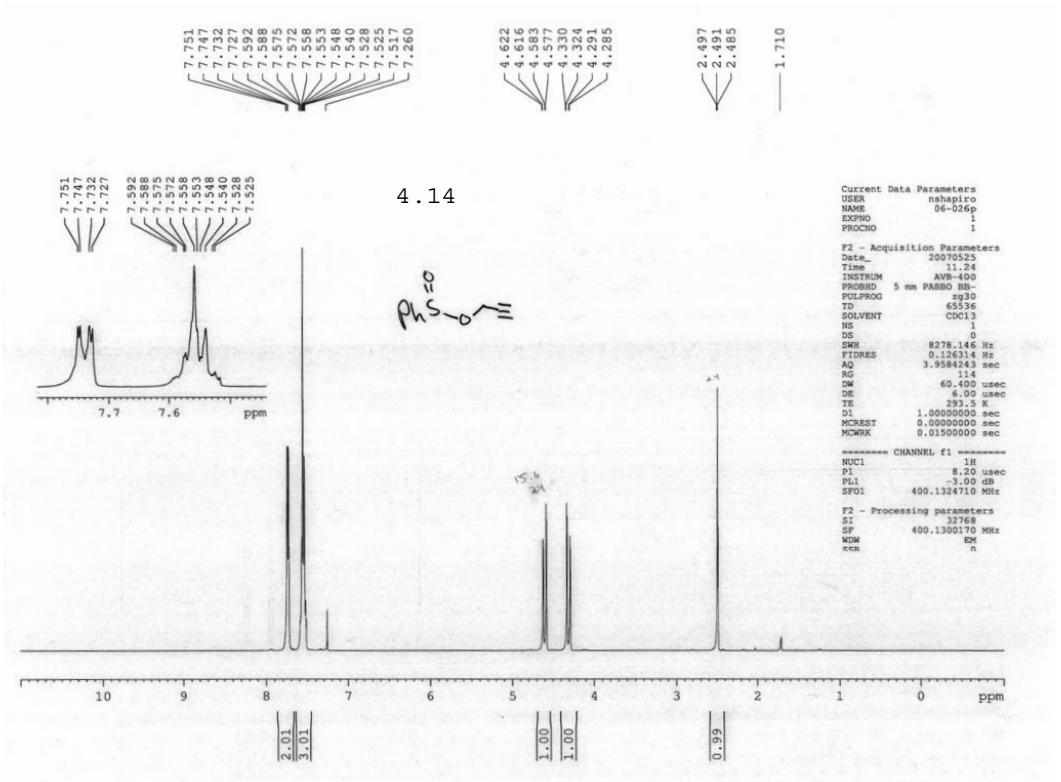


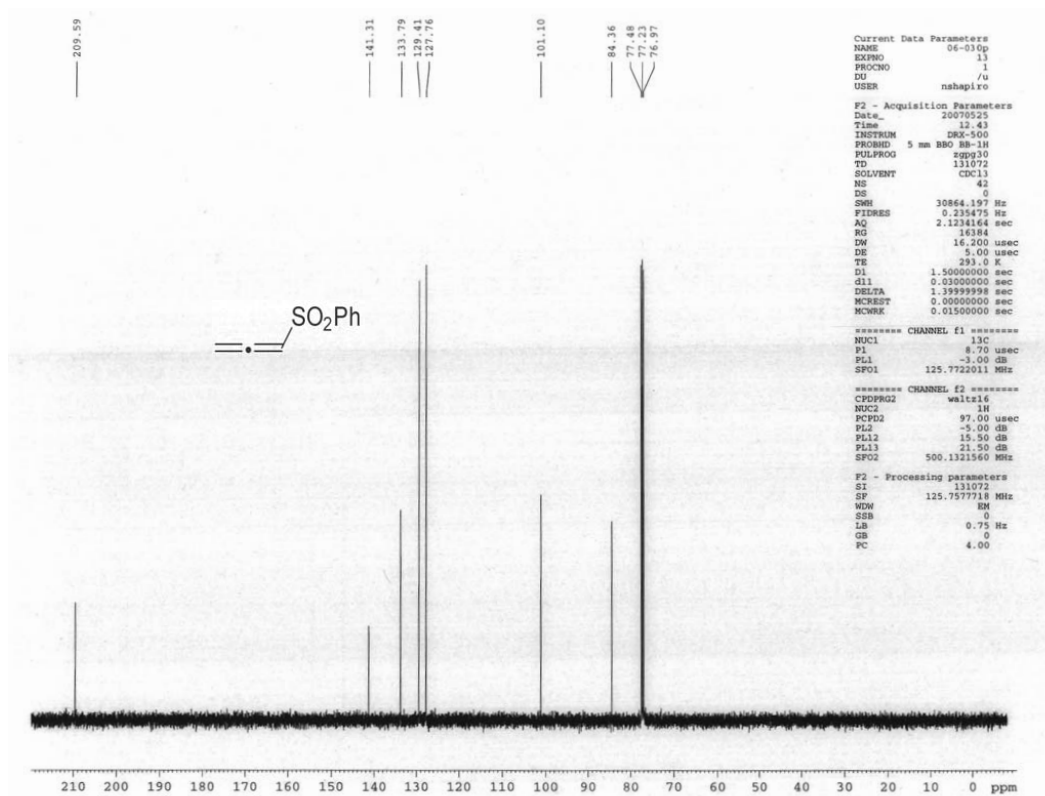
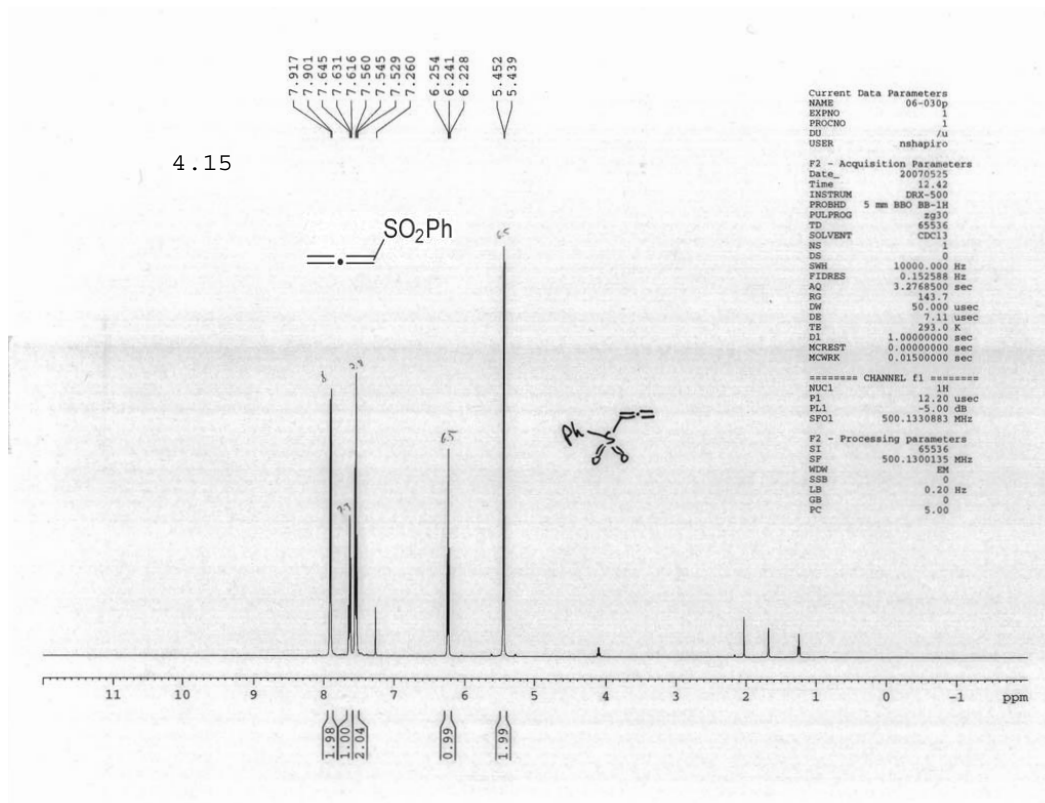
4.13 Proton NMR

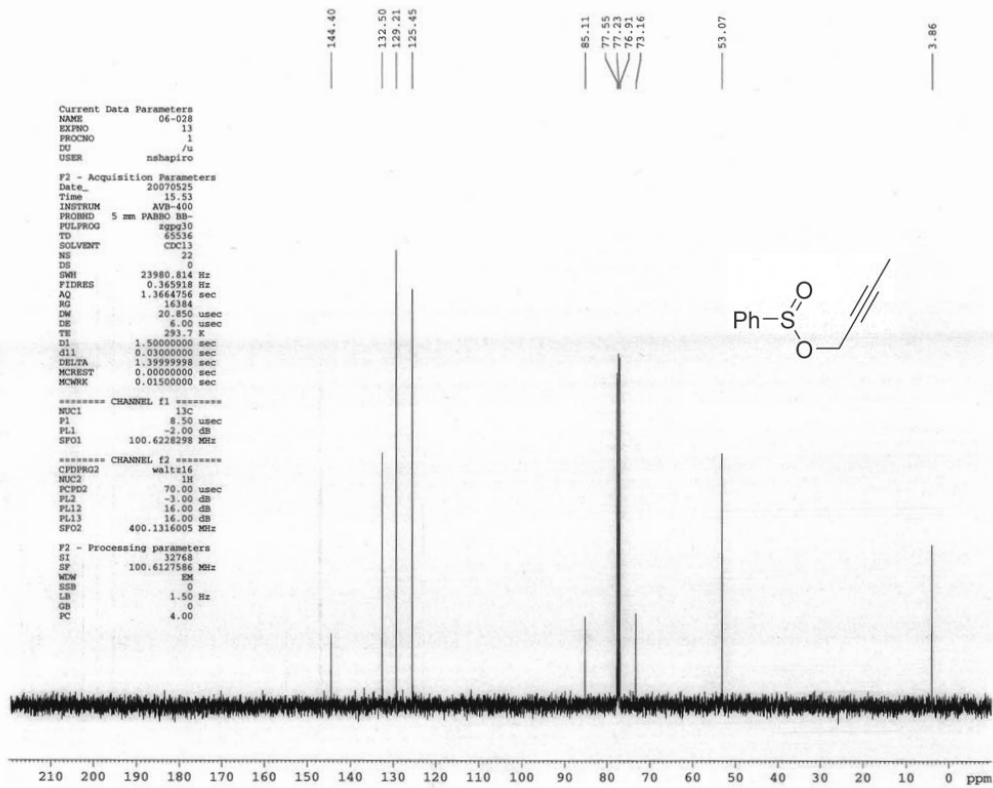
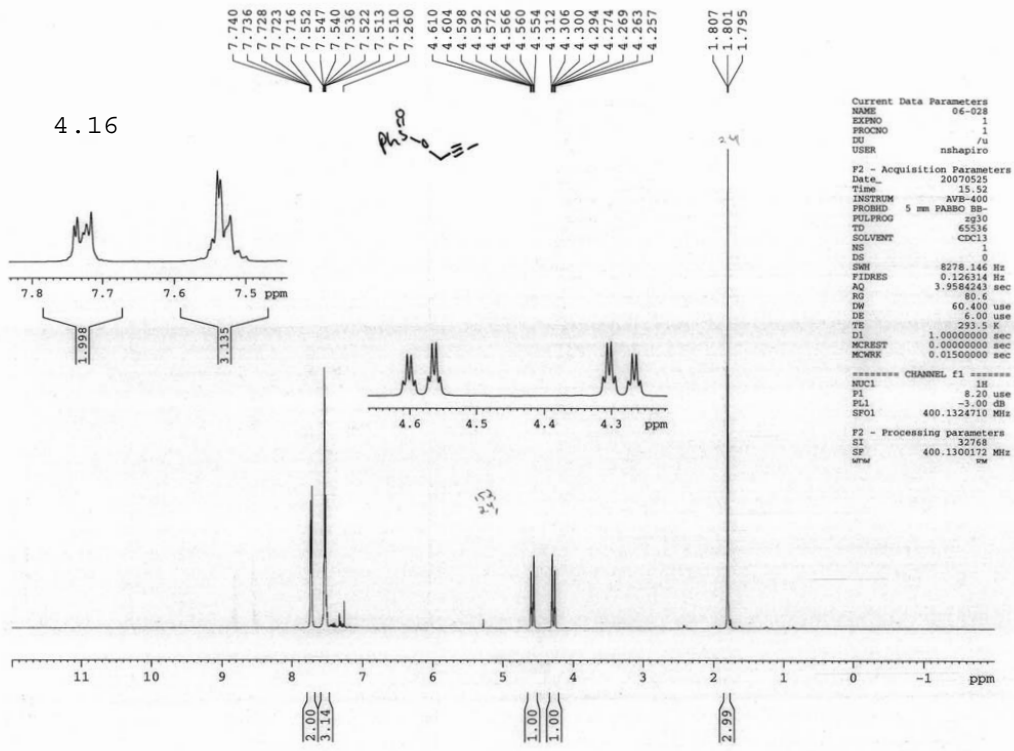


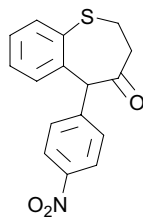
4.13 Carbon NMR



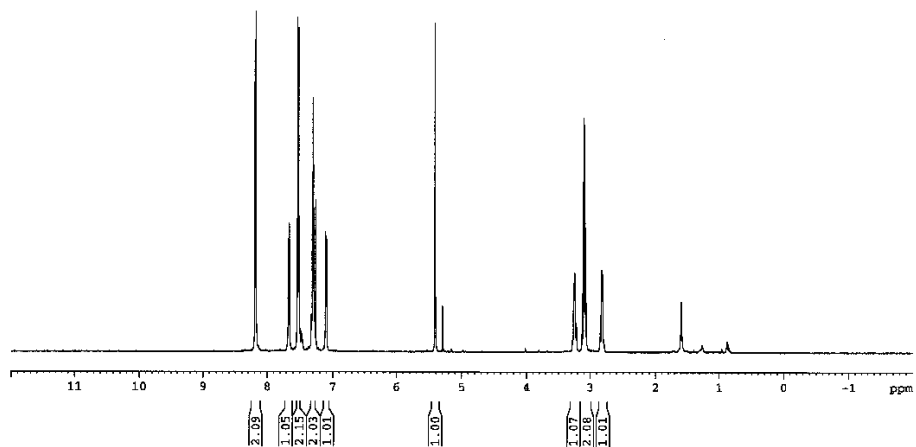




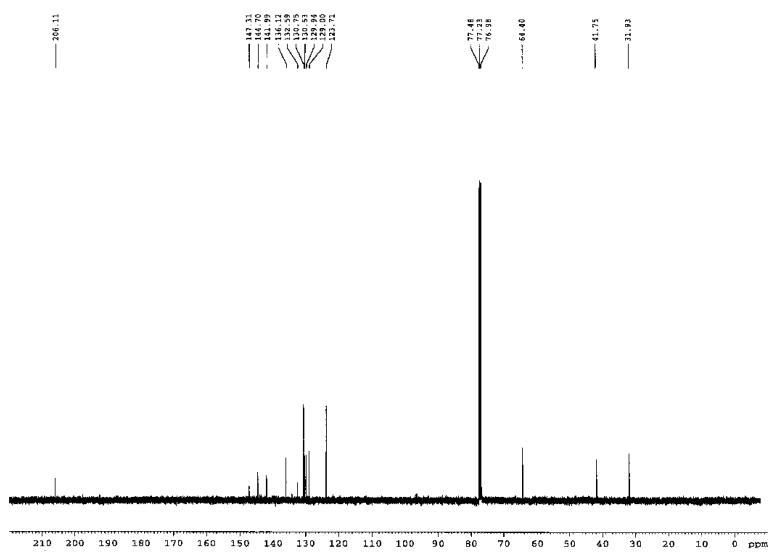


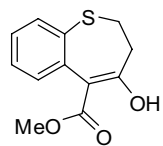


4.19 Proton NMR

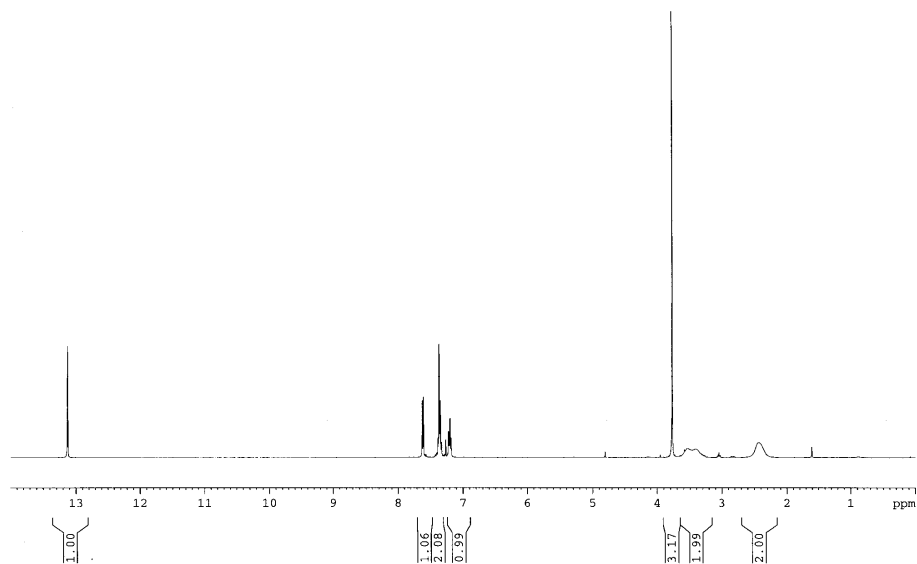


4.19 Carbon NMR

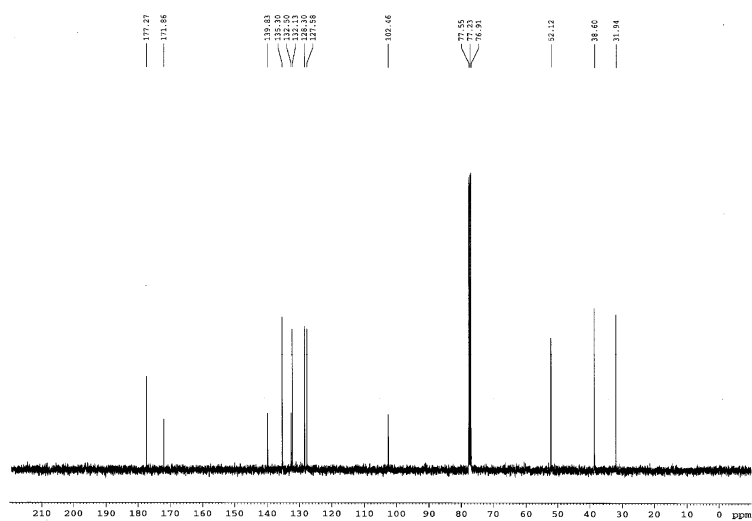


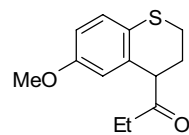


4.21 Proton NMR

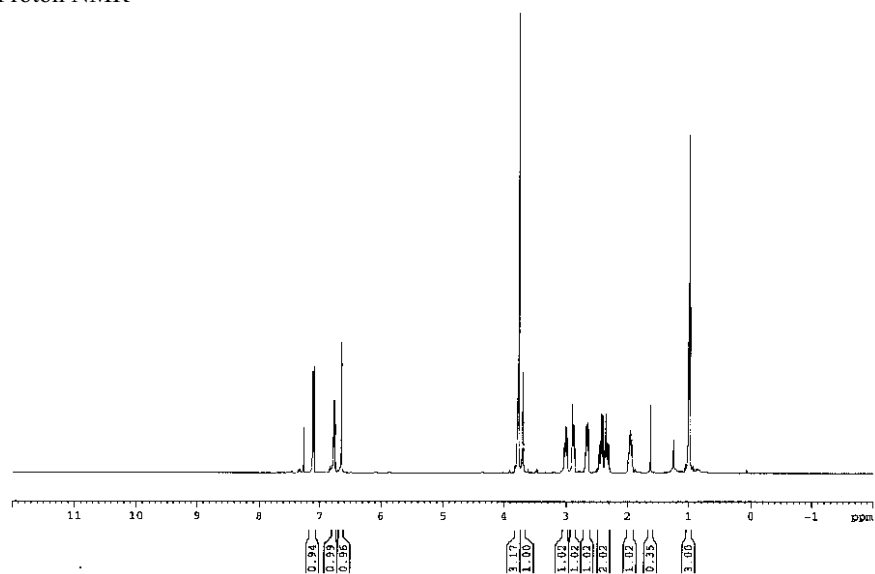


4.21 Carbon NMR

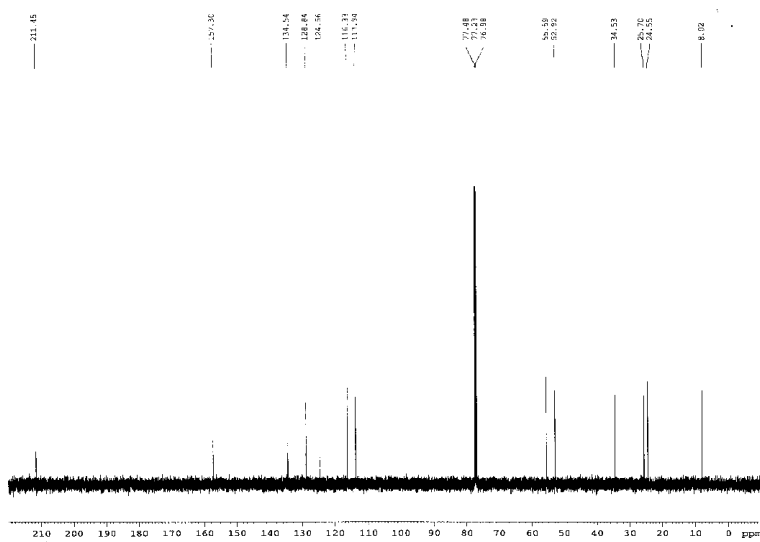


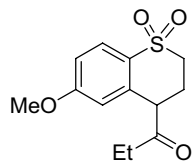


4.23 Proton NMR

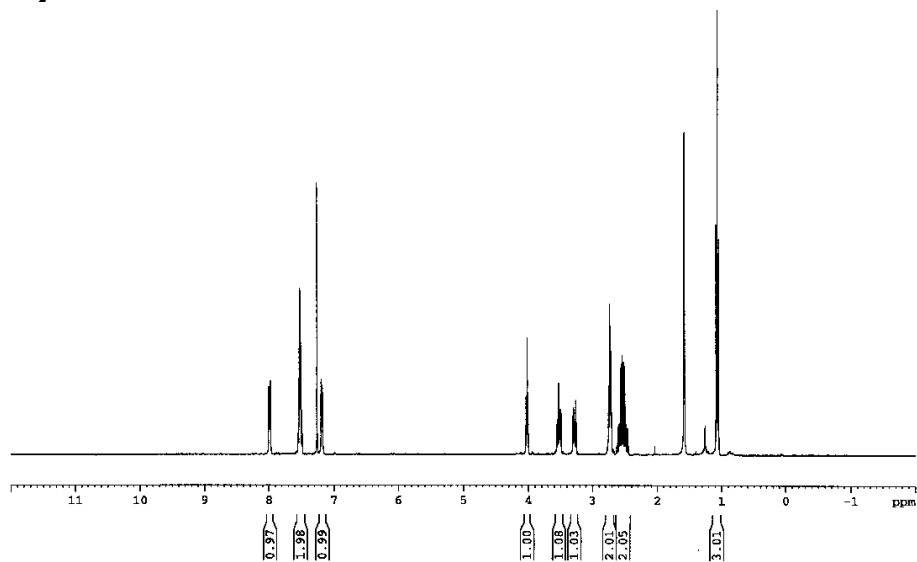


4.23 Carbon NMR

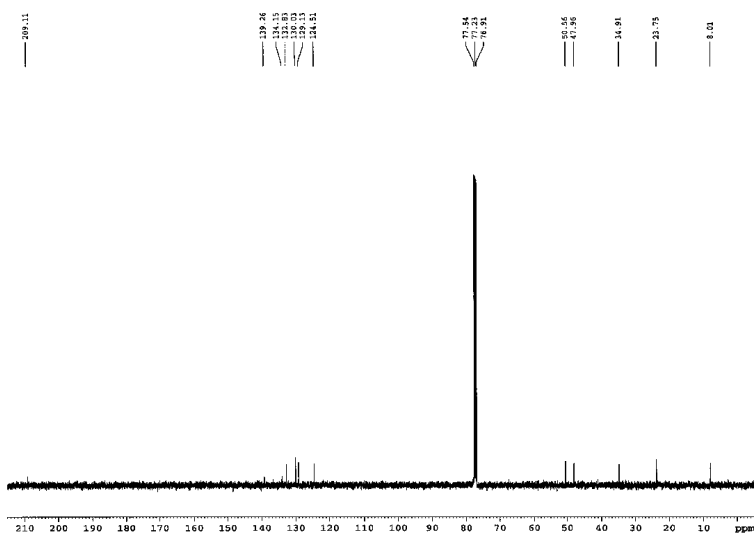


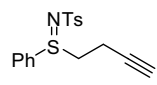


4.23-O₂ Proton NMR

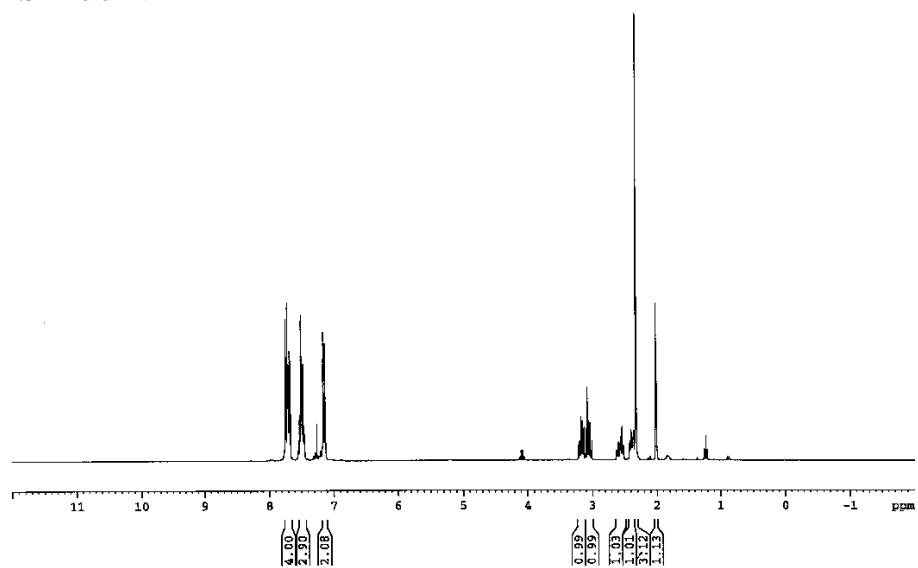


4.23-O₂ Carbon NMR

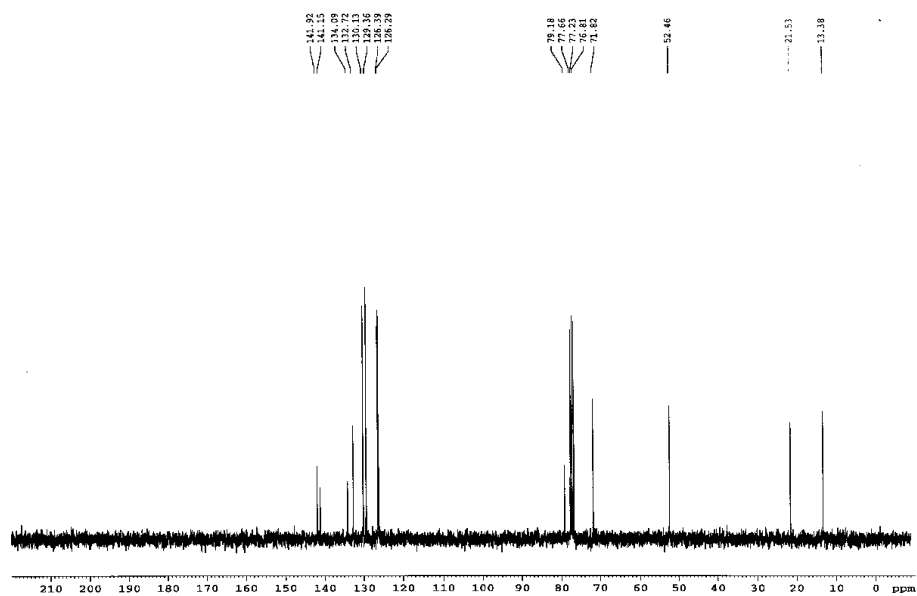


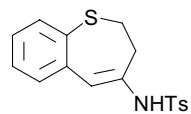


4.31 Proton NMR

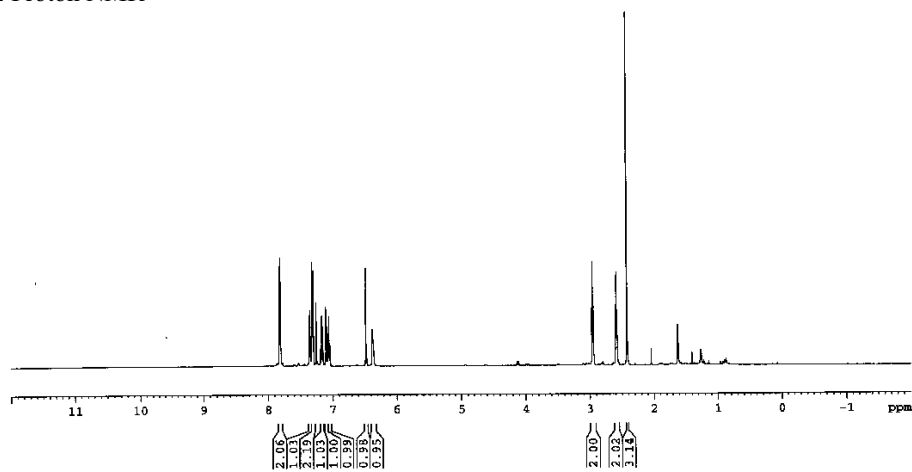


4.31 Carbon NMR

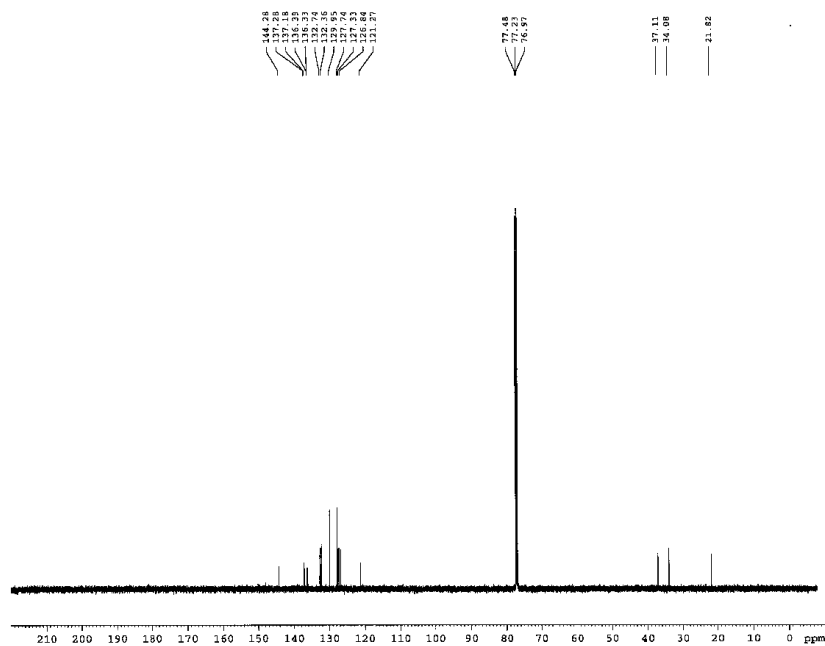


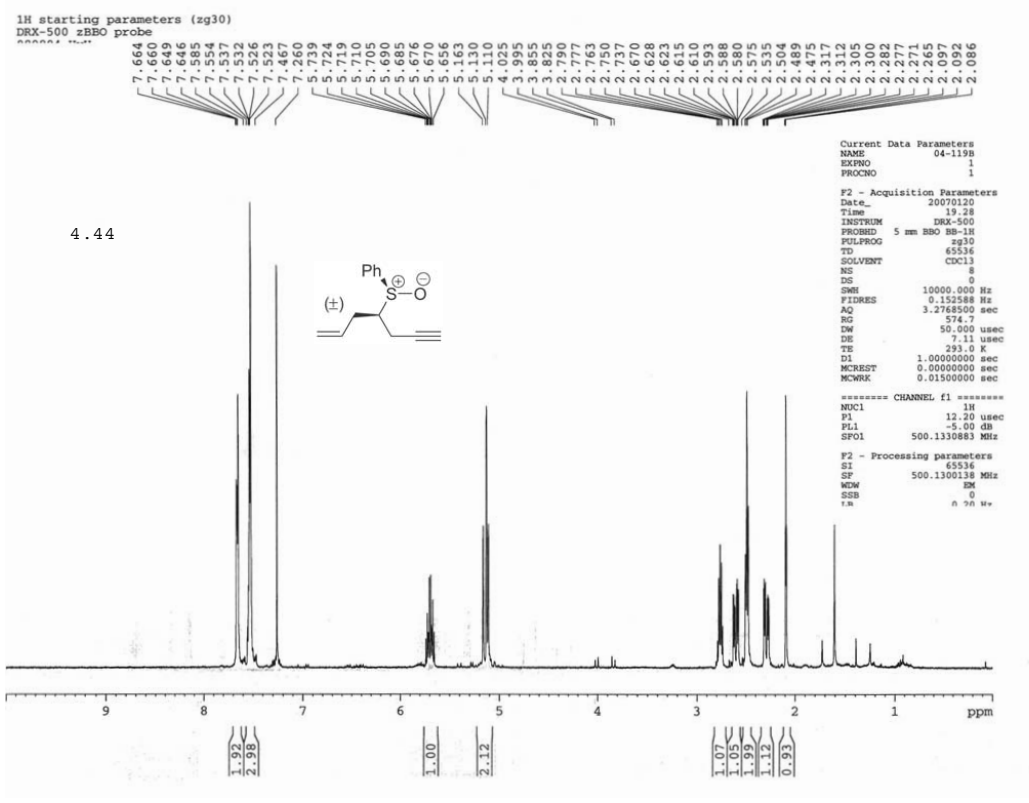
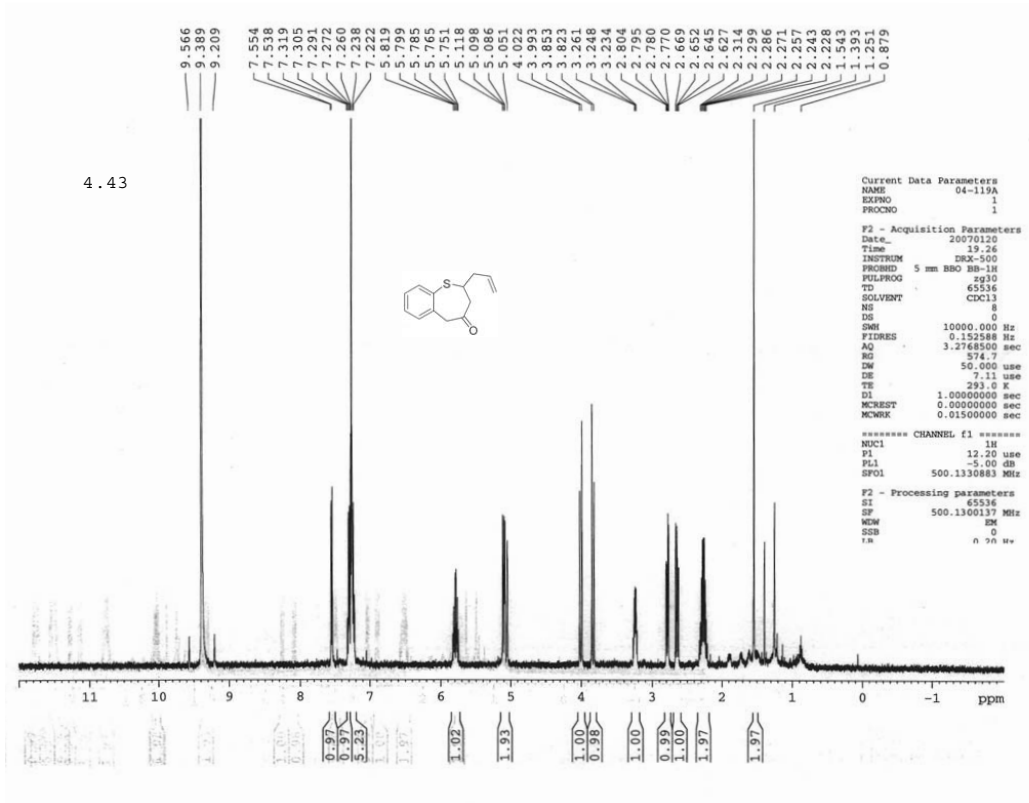


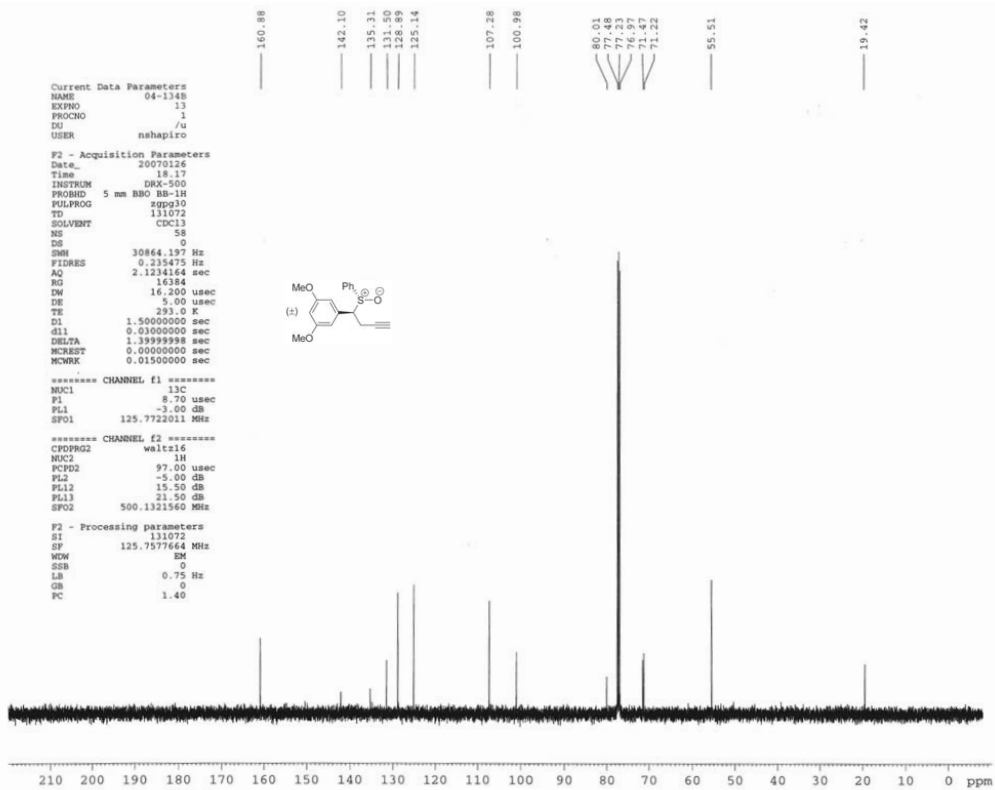
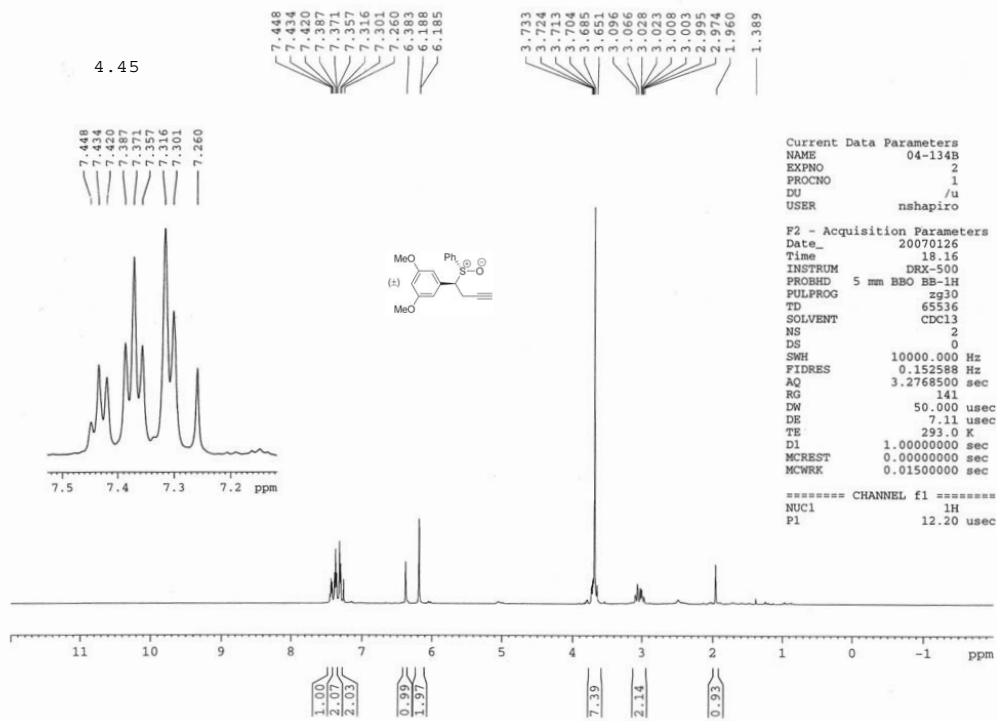
4.32 Proton NMR



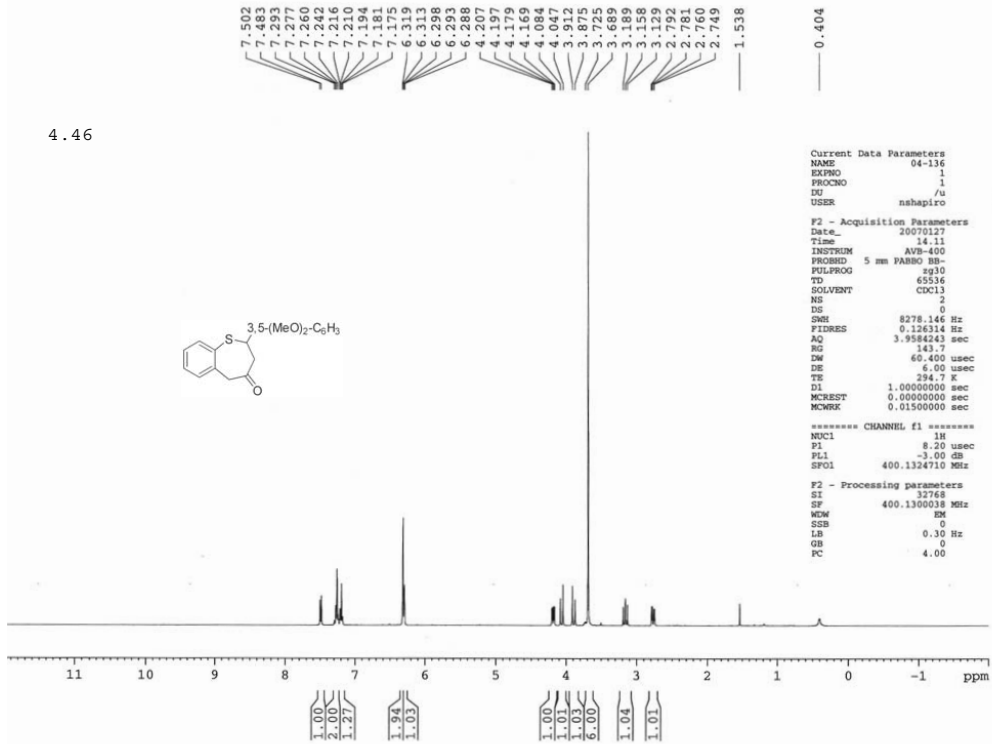
4.32 Carbon NMR







4.46



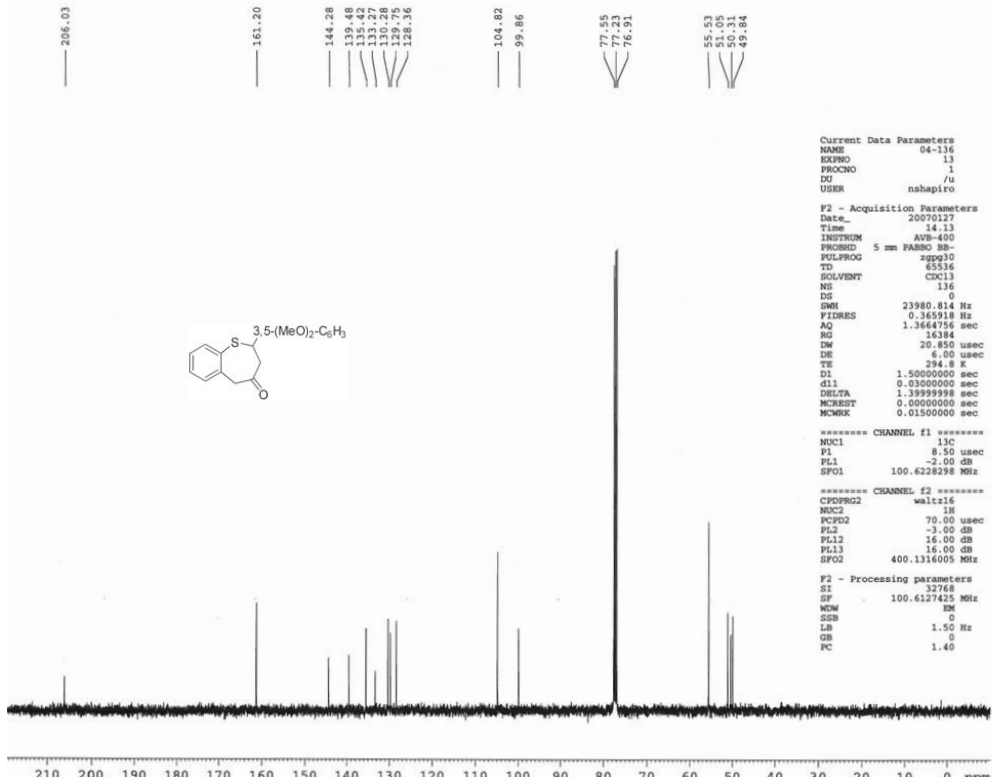
```

Current Data Parameters
NAME      04-136
EXPNO    1
PROCNO   1
DU       /u
USER     nshapiro

F2 - Acquisition Parameters
Date_    20070127
Time     14.11
INSTRUM  AVB-400
PROBHD   5 mm PABBO BB-
PULPROG  zg30
TD        65536
SOLVENT  CDCl3
NS        2
DS        0
SWH       8278.146 Hz
FIDRES   0.126314 Hz
AQ        3.958443 sec
RG        143.7
DW        60.400 usec
DE        6.00 usec
TE        294.7 K
D1        1.0000000 sec
MCREST   0.0000000 sec
MCMRST   0.0150000 sec

***** CHANNEL f1 *****
NUC1      1H
P1        8.20 usec
PL1       -3.00 dB
SFO1      400.1324710 MHz

F2 - Processing parameters
SI        32768
SF        400.1300038 MHz
WDW       EM
SSB       0
LB        0.30 Hz
GB        0
PC        4.00
  
```



```

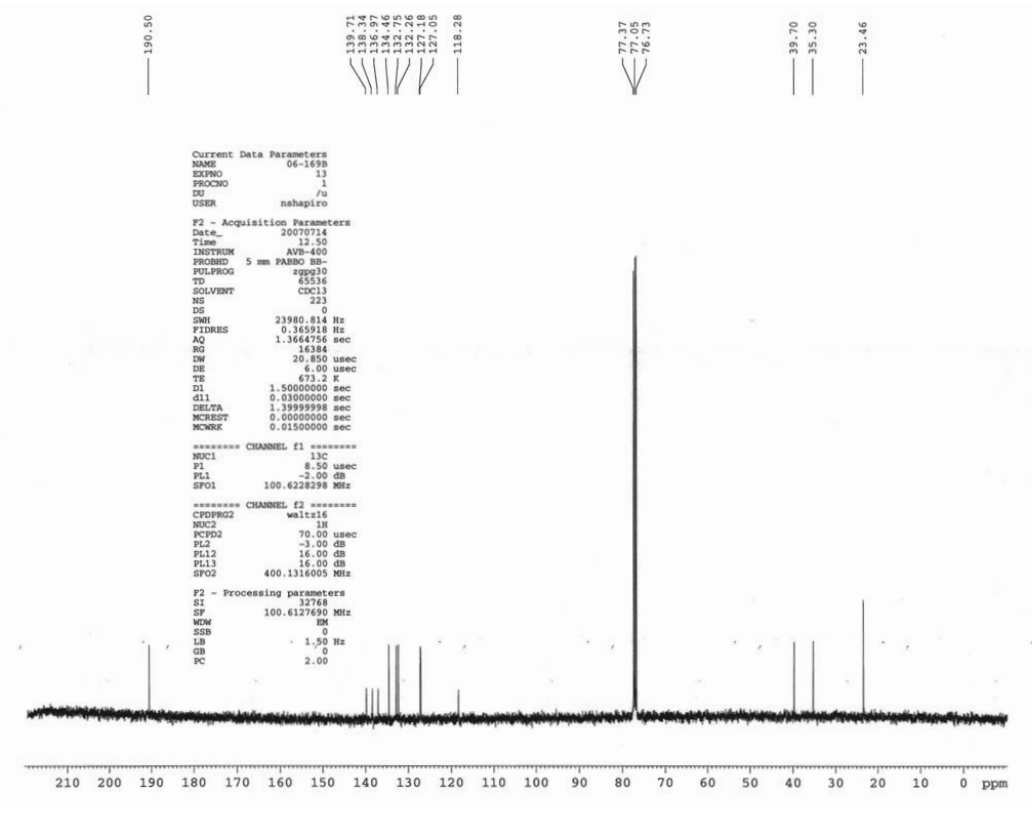
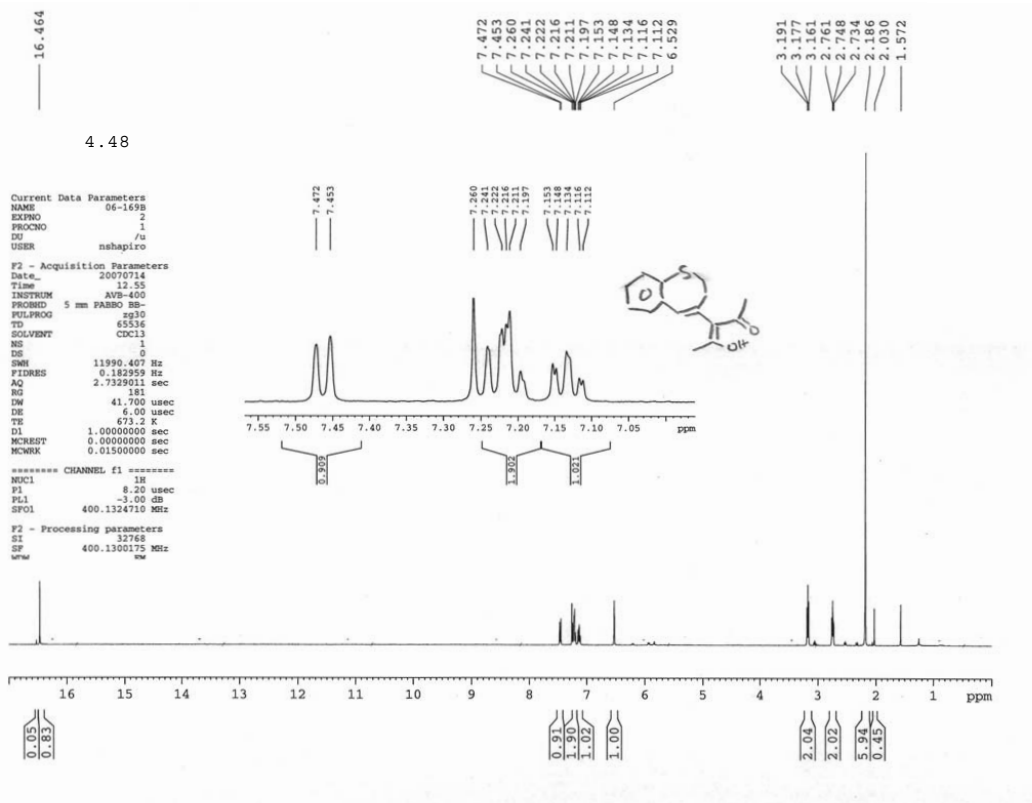
Current Data Parameters
NAME      04-136
EXPNO    13
PROCNO   1
DU       /u
USER     nshapiro

F2 - Acquisition Parameters
Date_    20070127
Time     14.13
INSTRUM  AVB-400
PROBHD   5 mm PABBO BB-
PULPROG  zgpg30
TD        65536
SOLVENT  CDCl3
NS        136
DS        0
SWH      23980.814 Hz
FIDRES   0.365918 Hz
AQ        1.3644756 sec
RG        16384
DW        20.850 usec
DE        6.00 usec
TE        294.8 K
D1        1.5000000 sec
d11      0.0300000 sec
DELTA    1.3999998 sec
MCREST   0.0000000 sec
MCMRST   0.0150000 sec

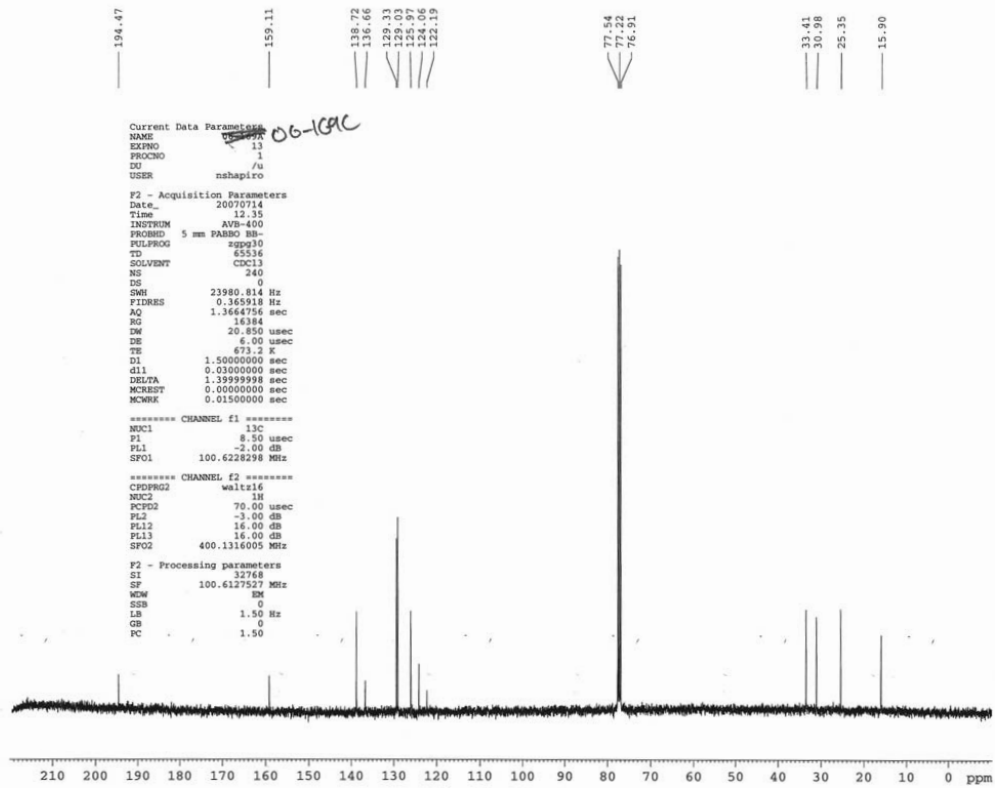
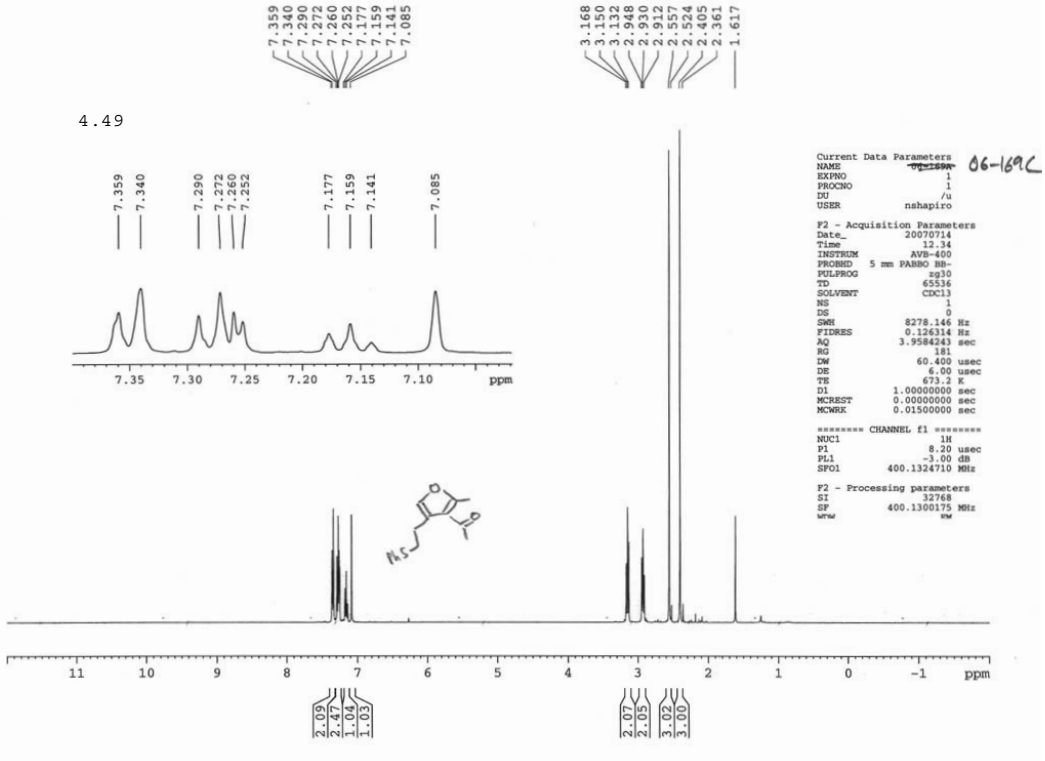
***** CHANNEL f1 *****
NUC1      13C
P1        8.50 usec
PL1       -2.00 dB
SFO1      100.628298 MHz

***** CHANNEL f2 *****
CPDPRG2  waltz16
NUC2      1H
PCPD2    70.00 usec
PL2       -3.00 dB
PL12     16.00 dB
PL13     16.00 dB
SFO2      400.1316005 MHz

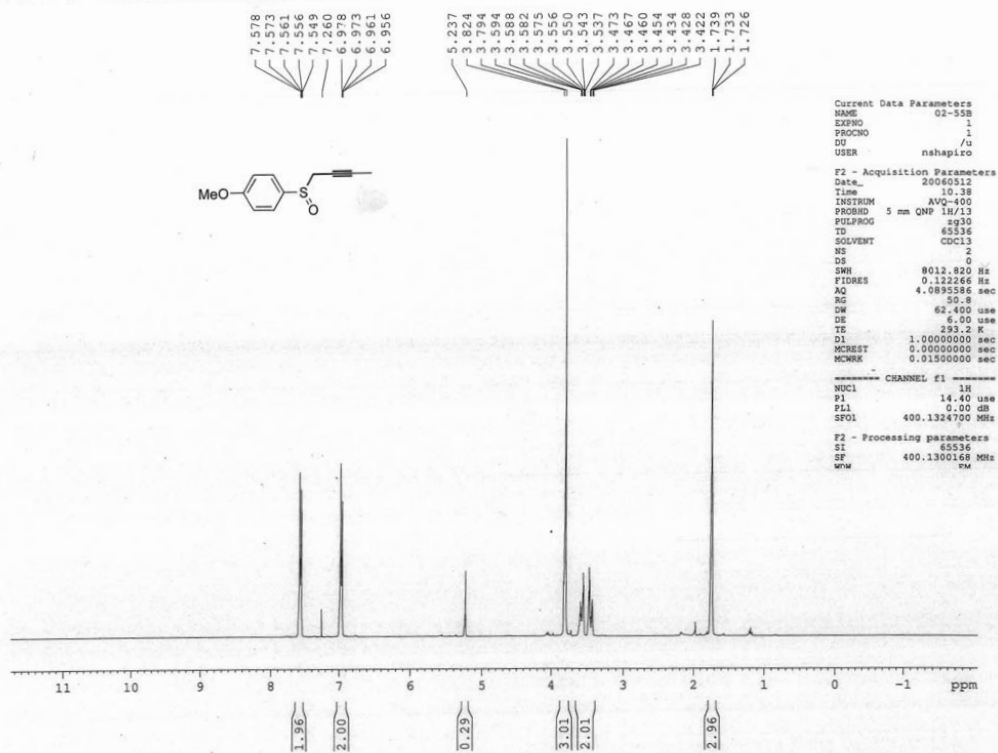
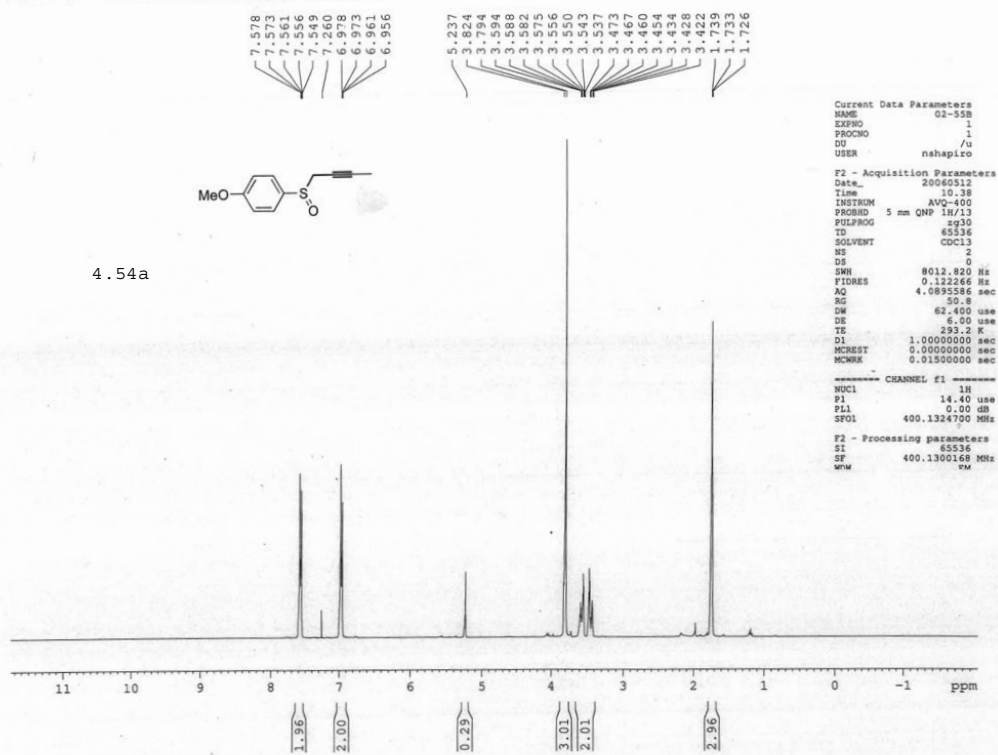
F2 - Processing parameters
SI        32768
SF        100.6127425 MHz
WDW       EM
SSB       0
LB        1.50 Hz
GB        0
PC        1.40
  
```



4.49



4.54a



DRX-500 zBb robe
080804 HVH

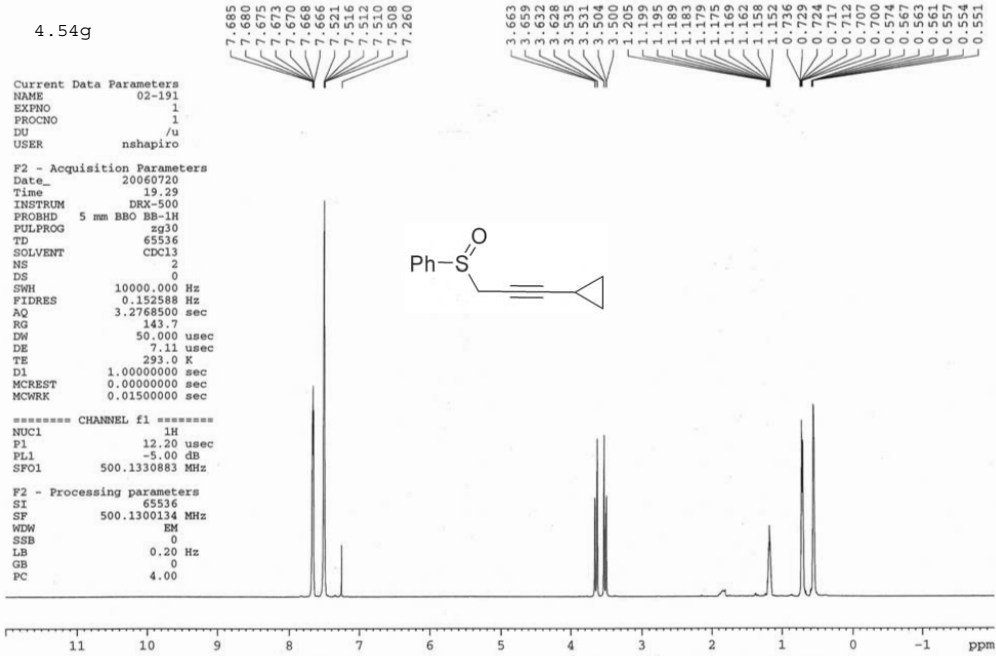
4.54g

Current Data Parameters
NAME 02-191
EXPNO 1
PROCNO 1
DU /u
USER nshapiro

F2 - Acquisition Parameters
Date_ 20060720
Time 19.29
INSTRUM DRX-500
PROBHD 5 mm BBO BB-1H
PULPROG zg30
TD 65536
SOLVENT CDCl3
NS 2
DS 0
SWH 10000.000 Hz
FIDRES 0.152588 Hz
AQ 3.2768500 sec
RG 143.7
DM 50.000 usec
DE 7.11 usec
TE 293.0 K
D1 1.00000000 sec
MCREST 0.00000000 sec
MCWRK 0.01500000 sec

***** CHANNEL f1 *****
NUC1 1H
P1 12.20 usec
PL1 -5.00 dB
SFO1 500.1330883 MHz

F2 - Processing parameters
SI 65536
SF 500.1300134 MHz
WDW EM
SSB 0
LB 0.20 Hz
GB 0
PC 4.00



13C DRX-500 a ZBBO probe
starting parameters with zgpg30 (waltz16)
uses n*tdo
012504 HVH

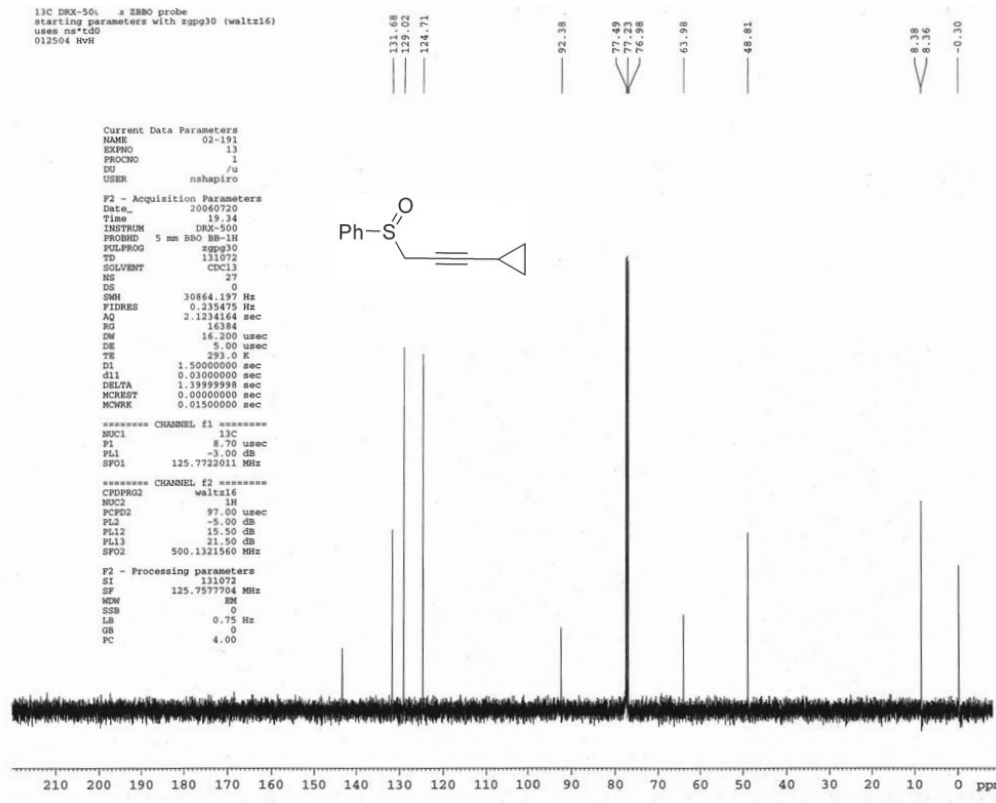
Current Data Parameters
NAME 02-191
EXPNO 13
PROCNO 1
DU /u
USER nshapiro

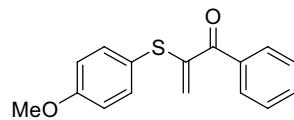
F2 - Acquisition Parameters
Date_ 20060720
Time 19.34
INSTRUM DRX-500
PROBHD 5 mm BBO BB-1H
PULPROG zgpg30
TD 131072
SOLVENT CDCl3
NS 27
DS 0
SWH 30864.197 Hz
FIDRES 0.235475 Hz
AQ 2.1234164 sec
RG 16384
DM 16.200 usec
DE 5.00 usec
TE 293.0 K
D1 1.50000000 sec
d11 0.03000000 sec
DELTA 1.39899998 sec
MCREST 0.00000000 sec
MCWRK 0.01500000 sec

***** CHANNEL f1 *****
NUC1 13C
P1 8.70 usec
PL1 -3.00 dB
SFO1 125.7722011 MHz

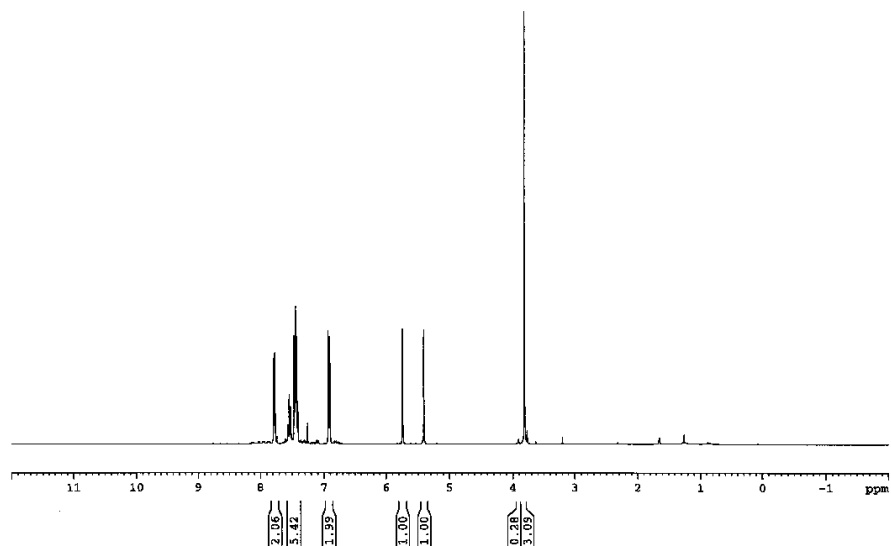
***** CHANNEL f2 *****
CPROG2 waltz16
NUC2 1H
PCPD2 97.00 usec
PL2 -5.00 dB
PL12 15.50 dB
PL13 21.50 dB
SFO2 500.1321560 MHz

F2 - Processing parameters
SI 131072
SF 125.7577704 MHz
WDW EM
SSB 0
LB 0.75 Hz
GB 0
PC 4.00

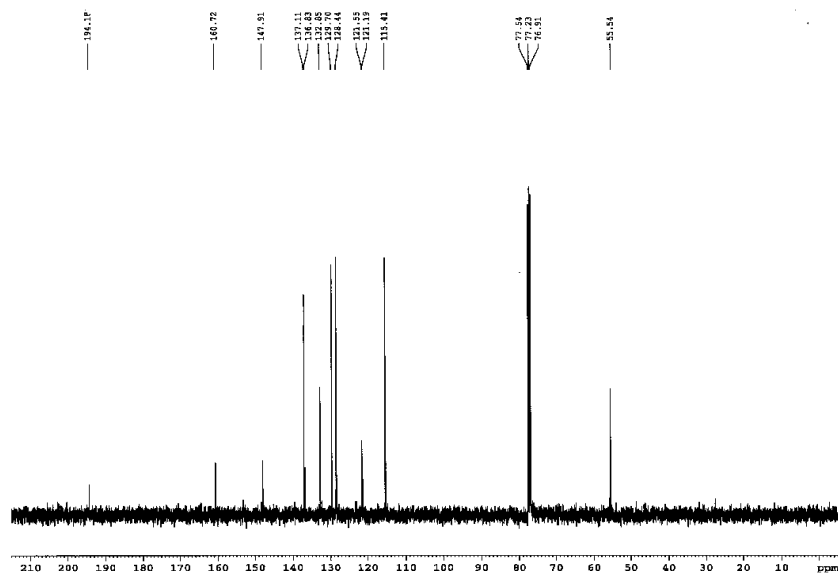


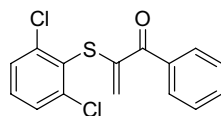


4.56a Proton NMR

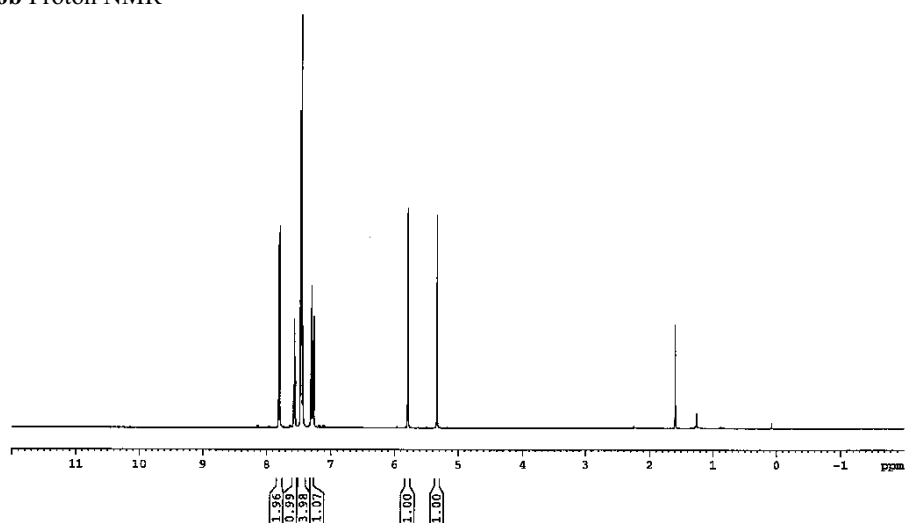


4.56a Carbon NMR

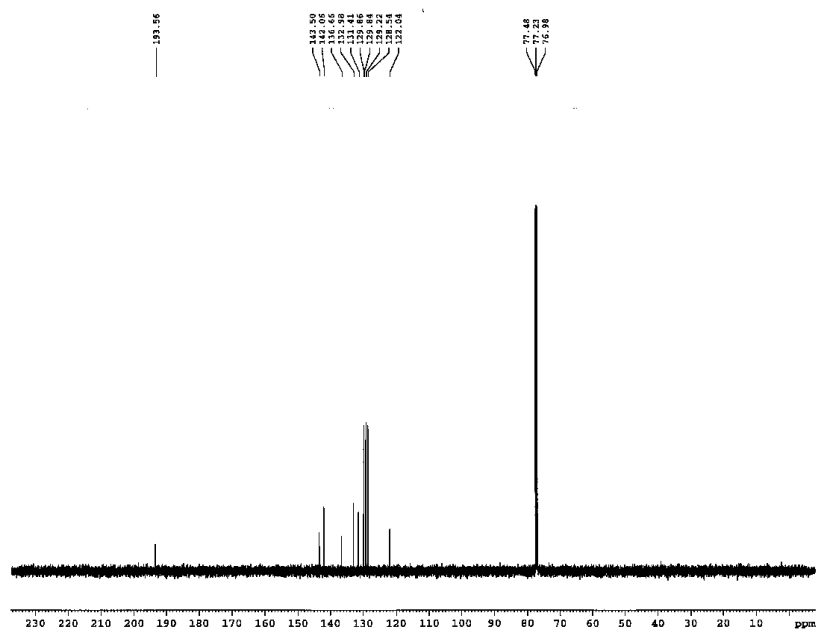


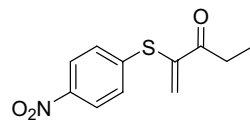


4.56b Proton NMR

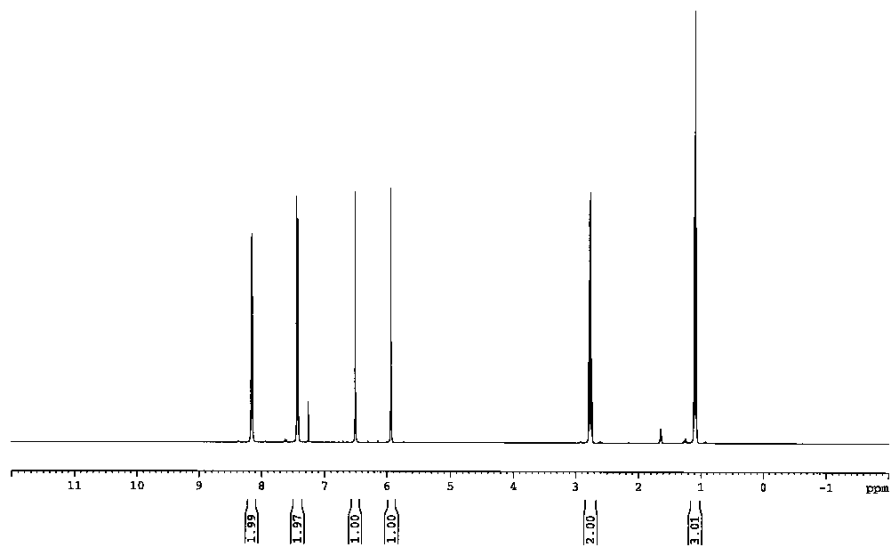


4.56b Carbon NMR

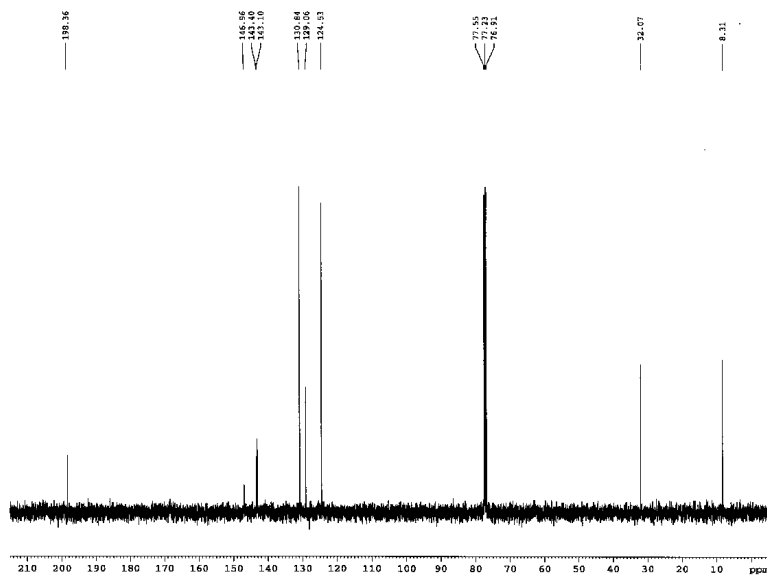


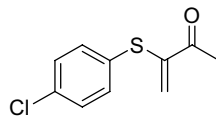


4.56c Proton NMR

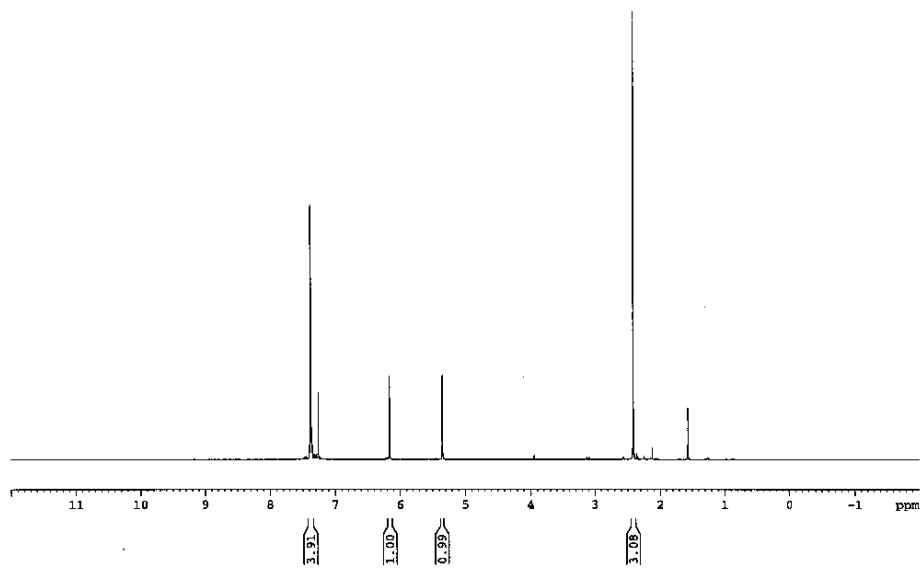


4.56c Carbon NMR

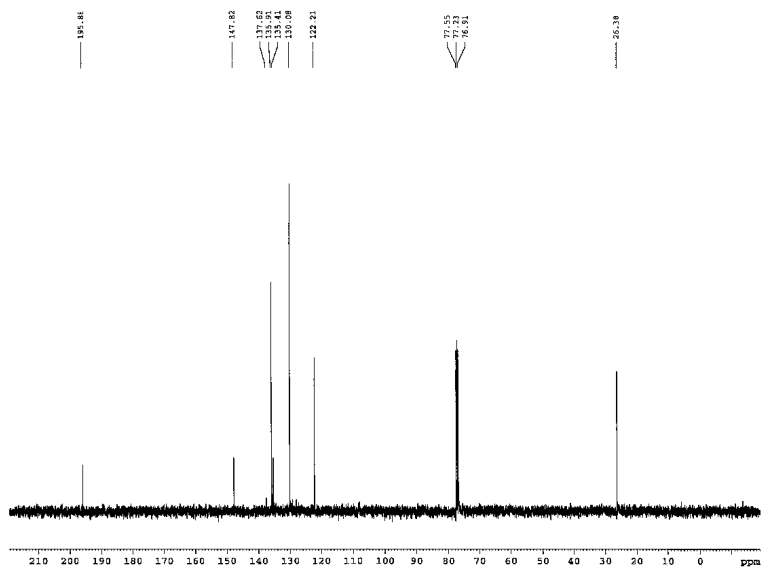


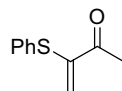


4.56d Proton NMR

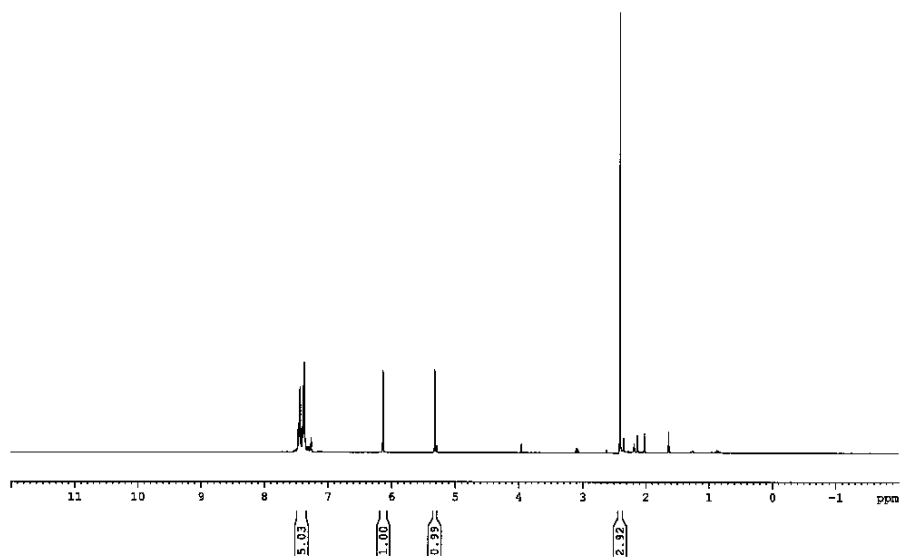


4.56d Carbon NMR

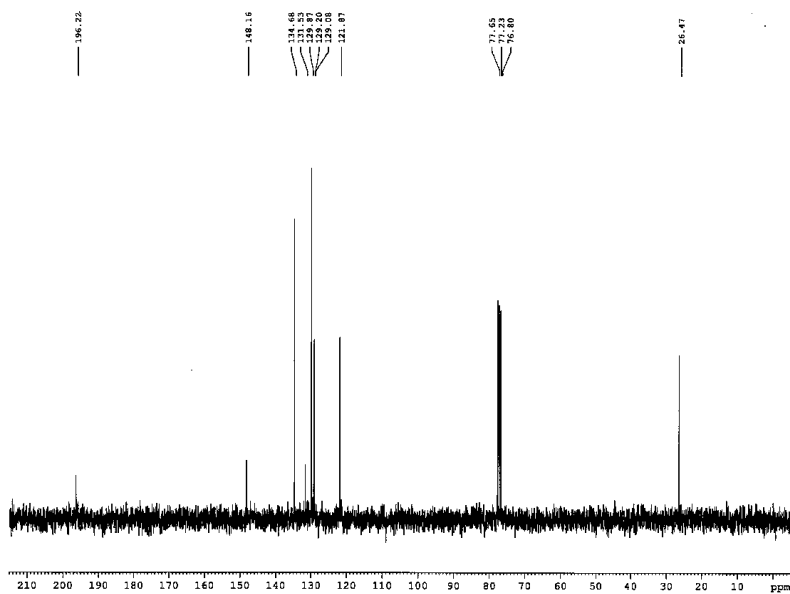


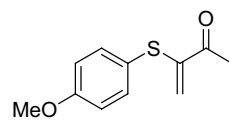


4.56e Proton NMR

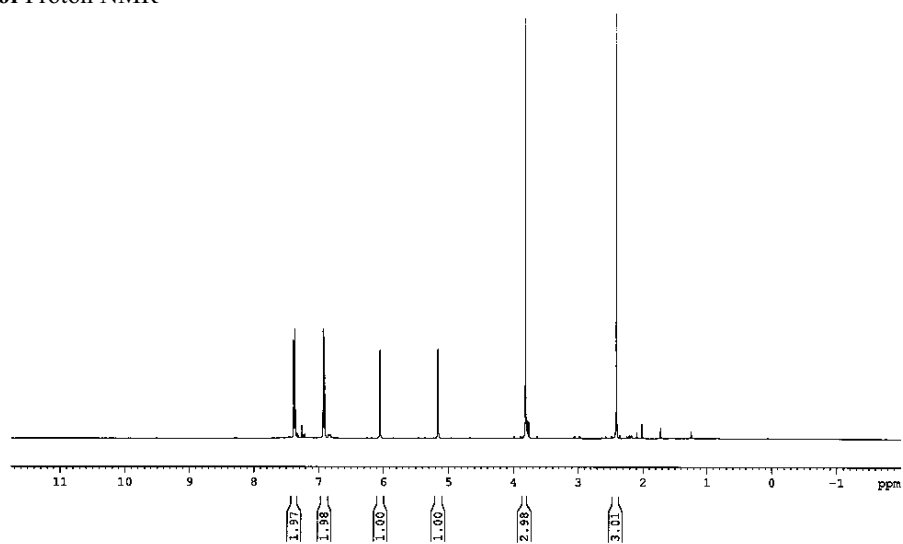


4.56e Carbon NMR

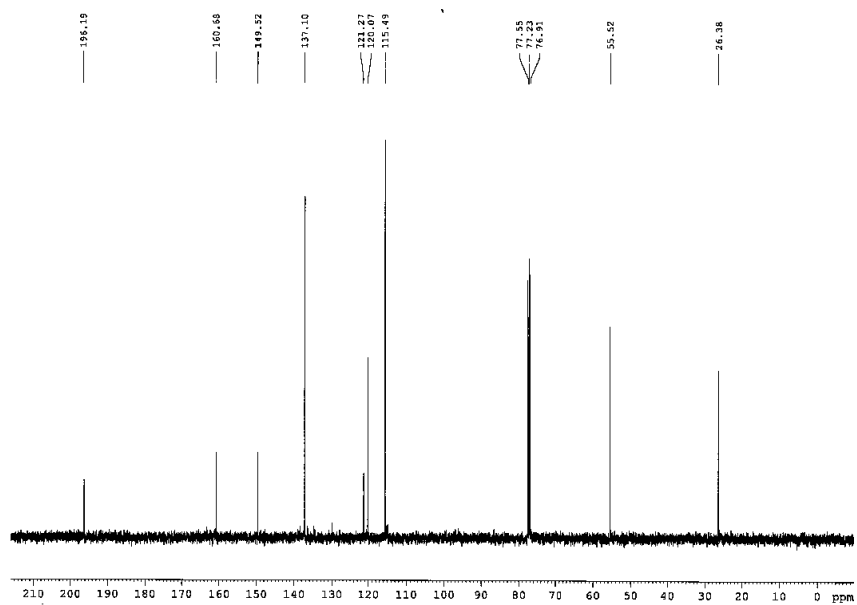


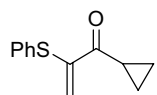


4.56f Proton NMR

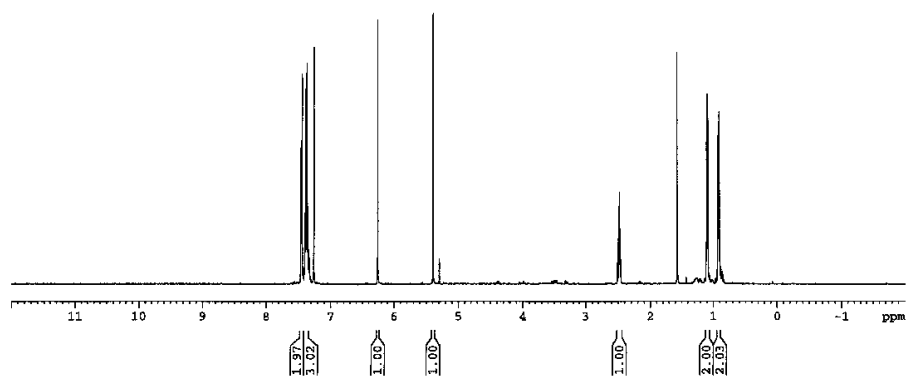


4.56f Carbon NMR

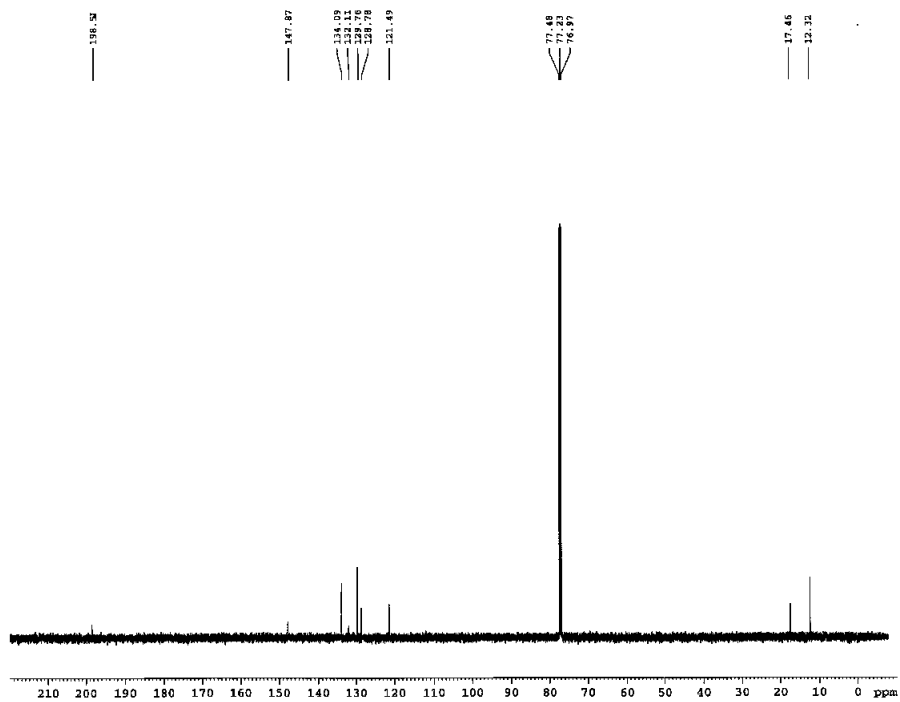


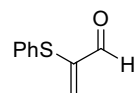


4.56g Proton NMR

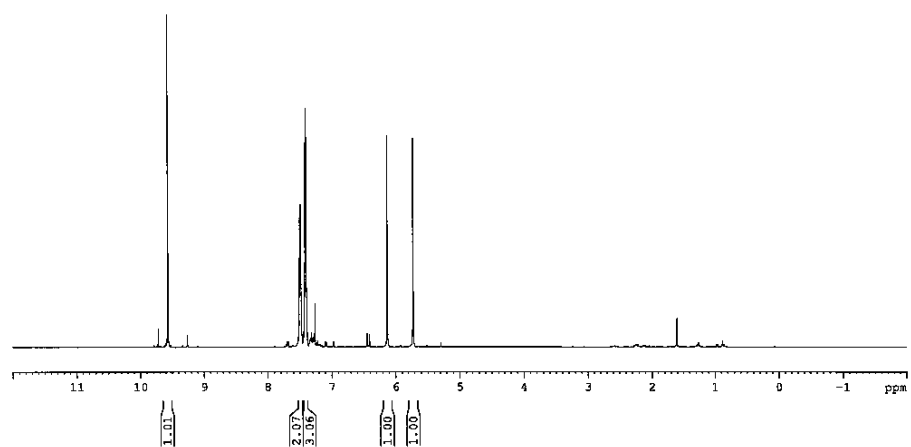


4.56g Carbon NMR

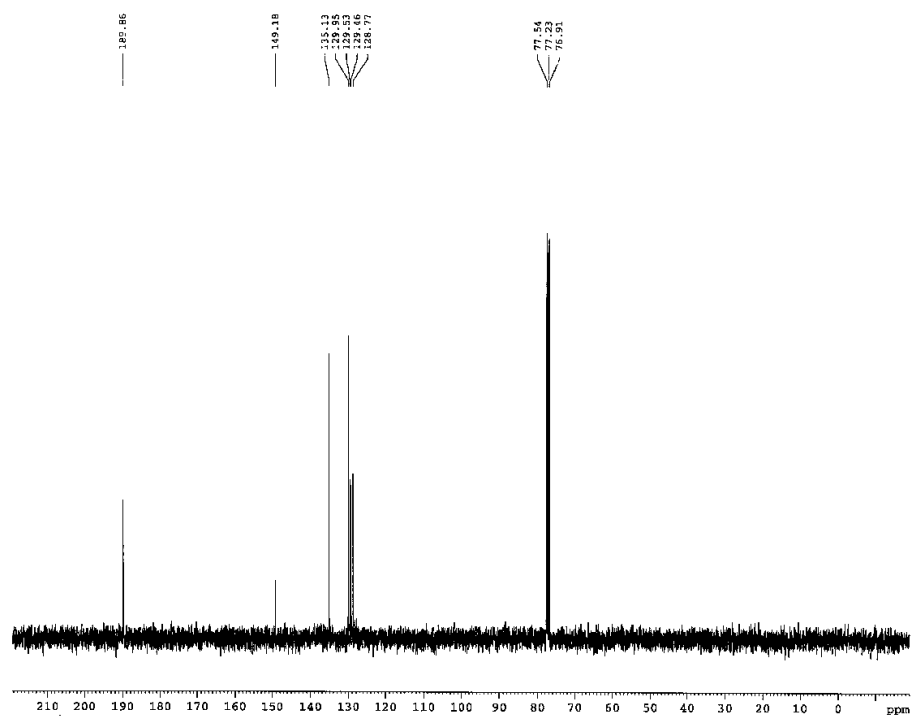


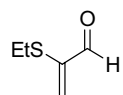


4.56h Proton NMR

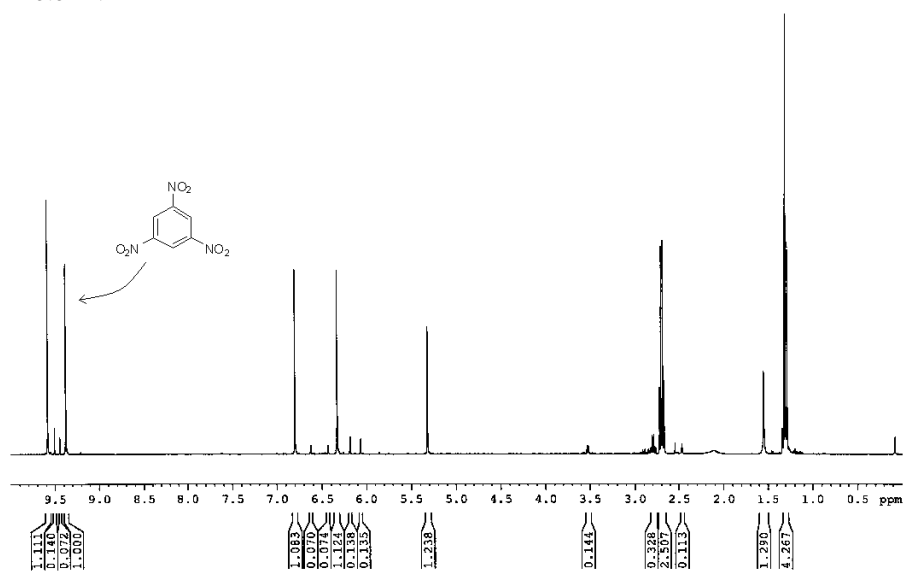


4.56h Carbon NMR

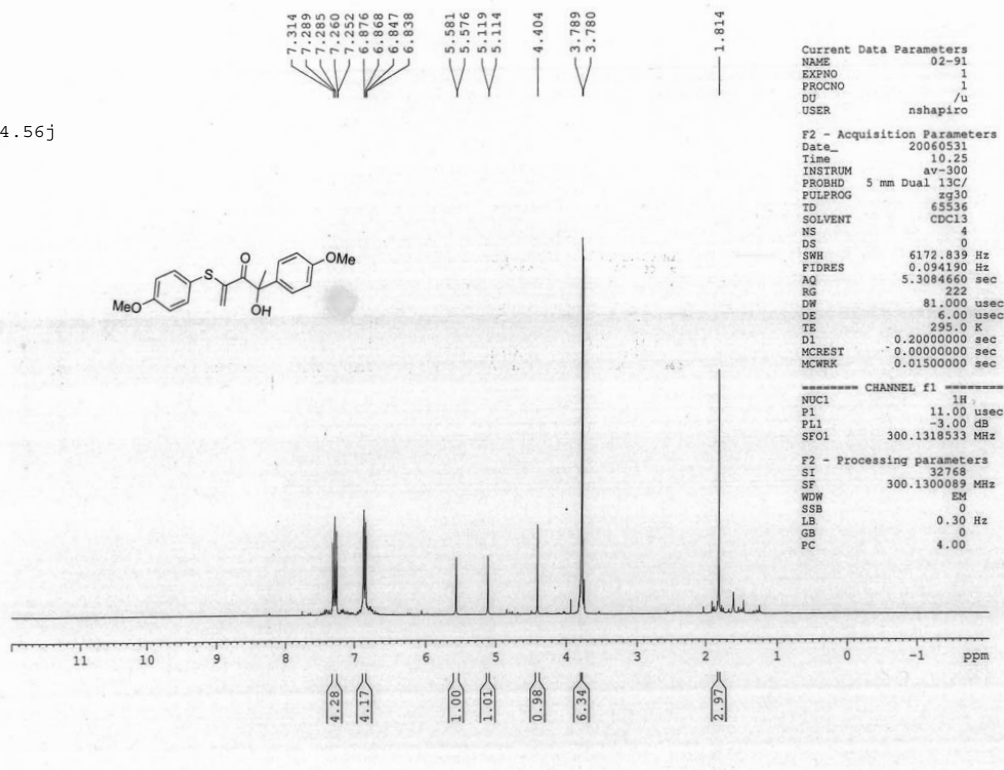
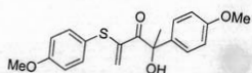


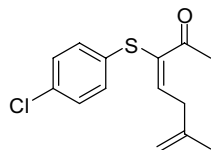


4.56i Proton NMR

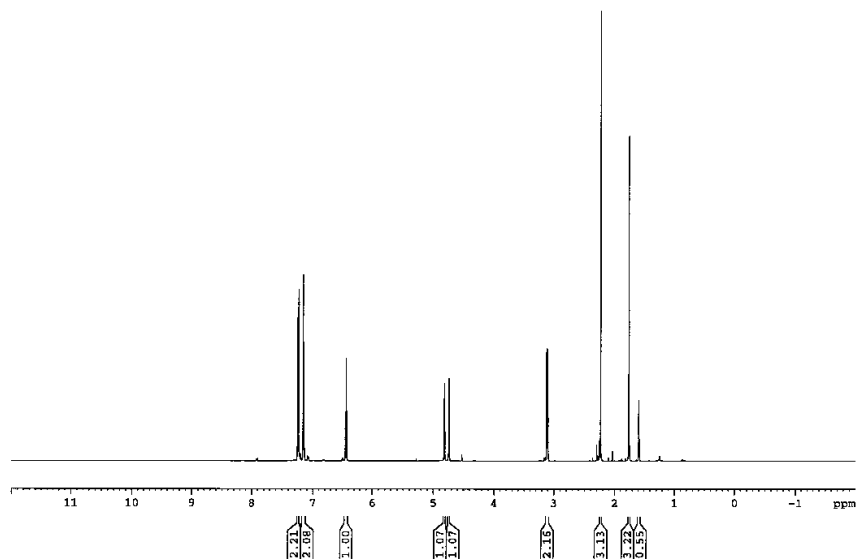


4.56j

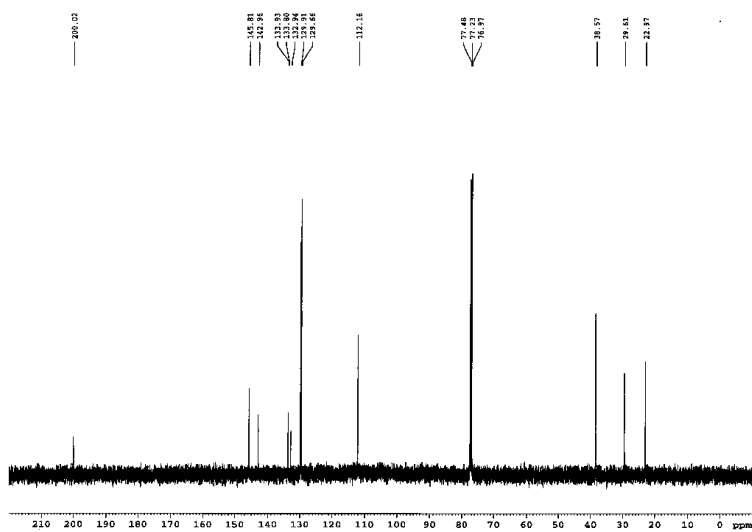


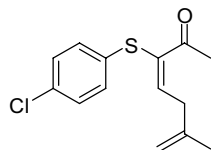


4.58-*E* Proton NMR

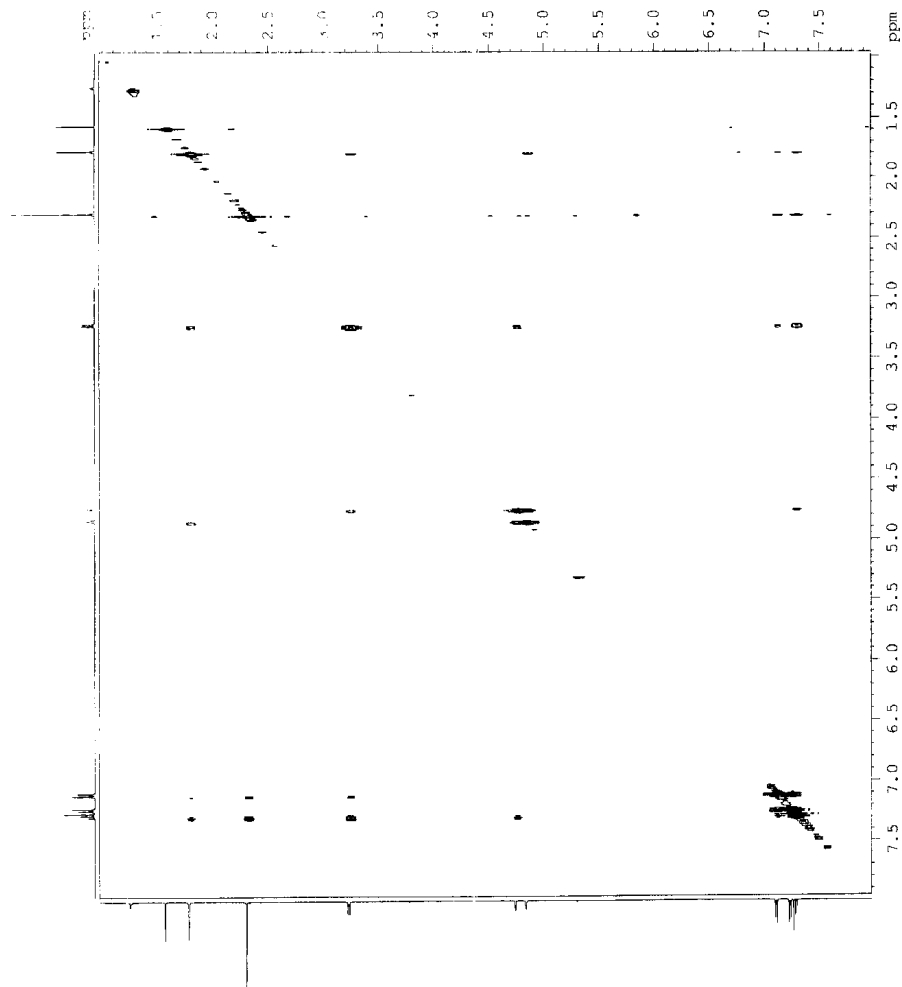


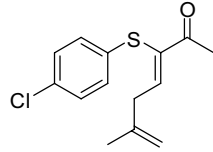
4.58-*E* Carbon NMR



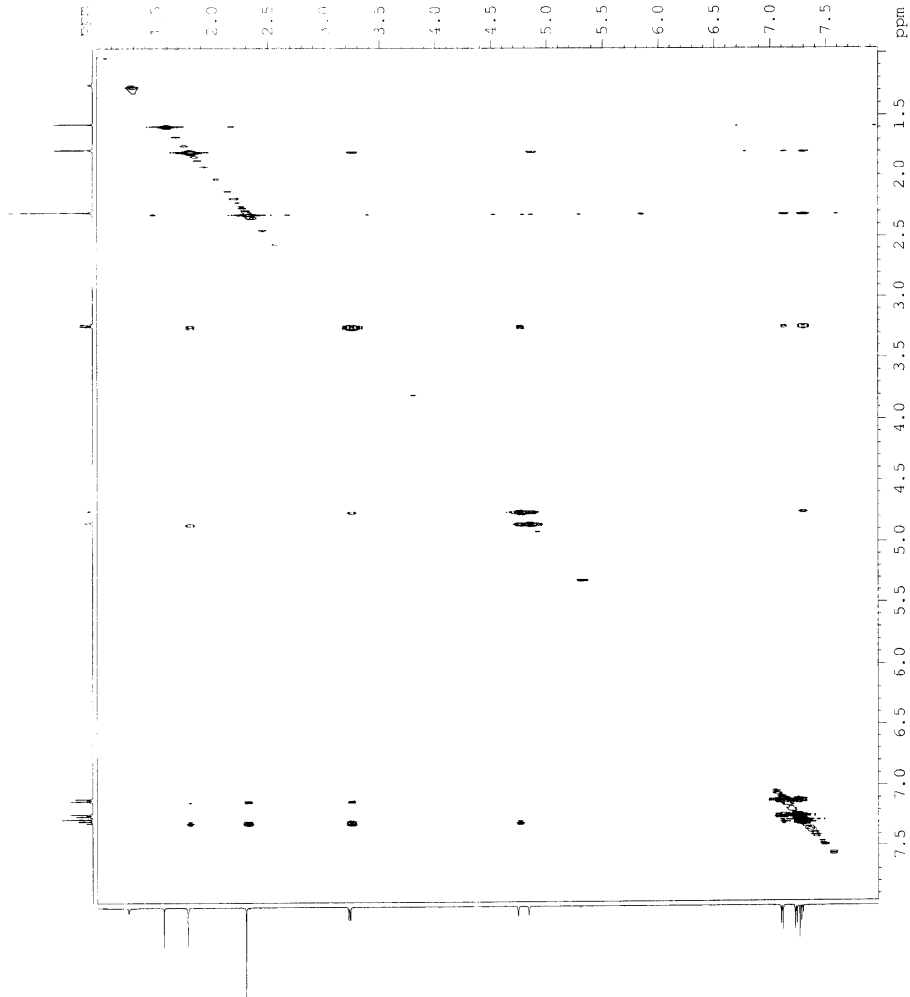


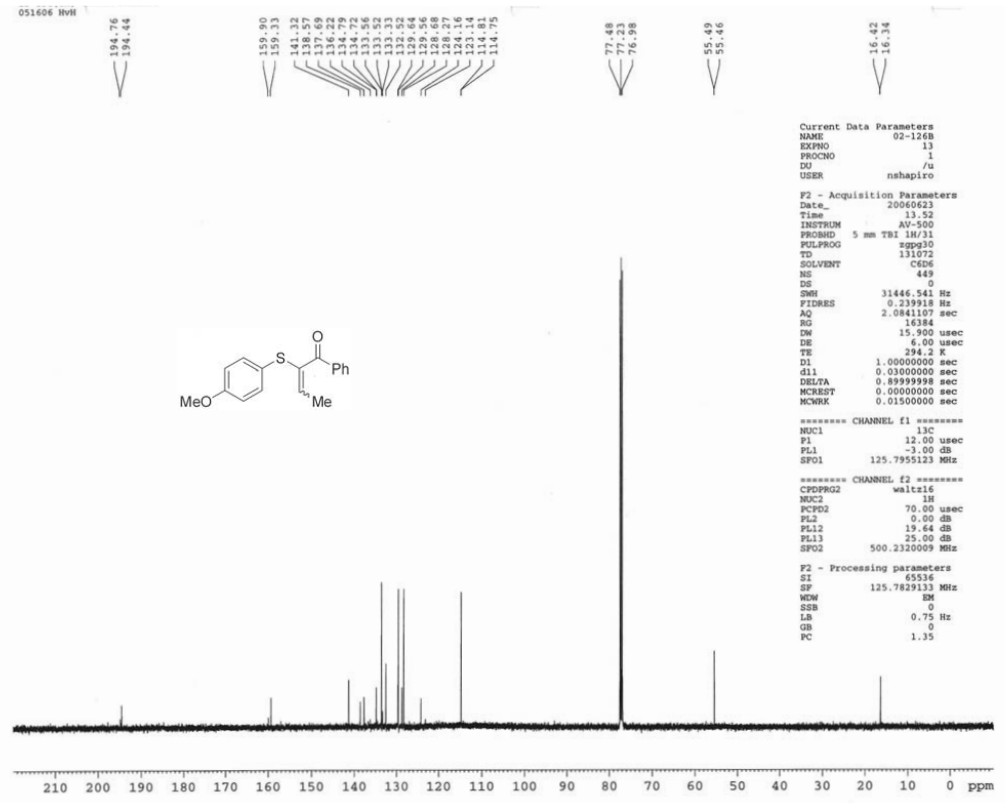
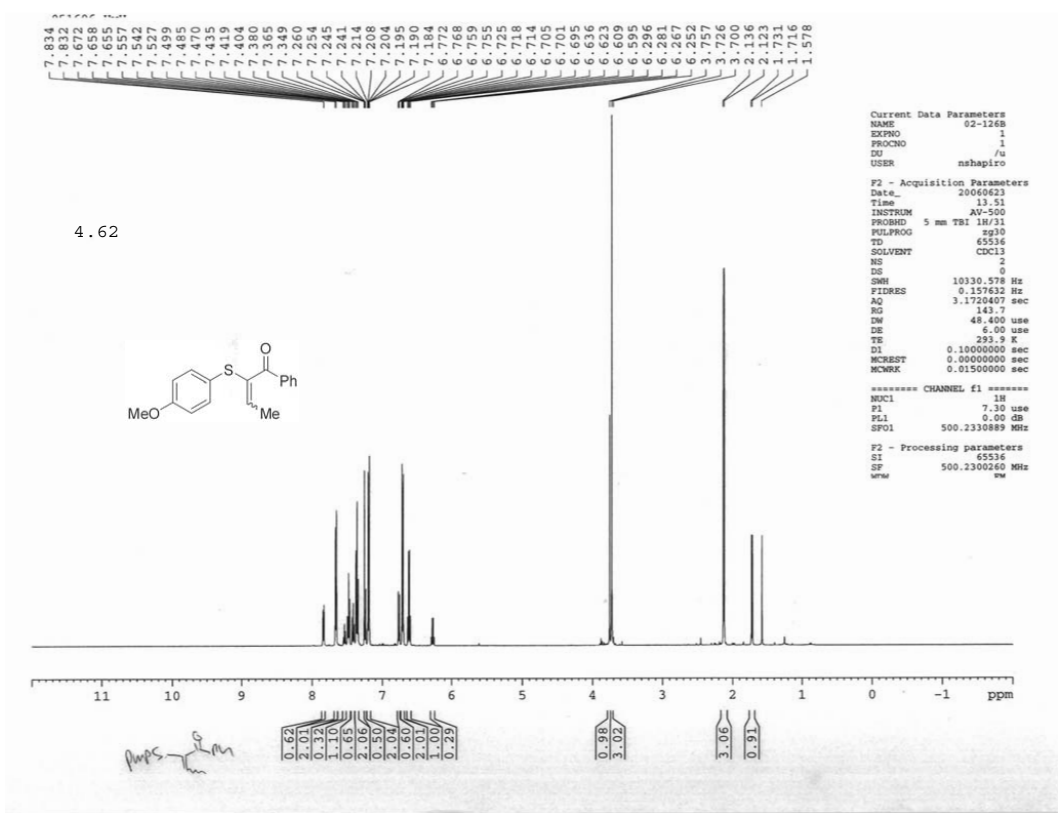
4.58-*E* nOesy NMR

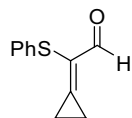




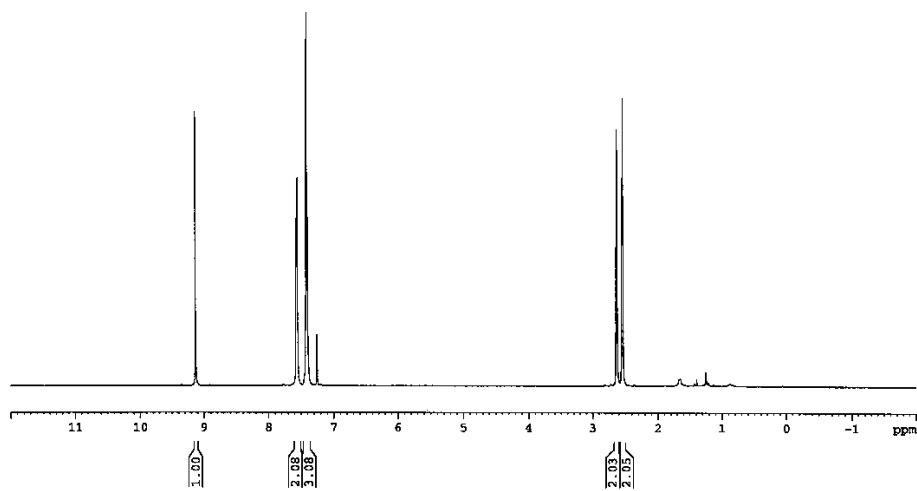
4.58-Z nOesy NMR



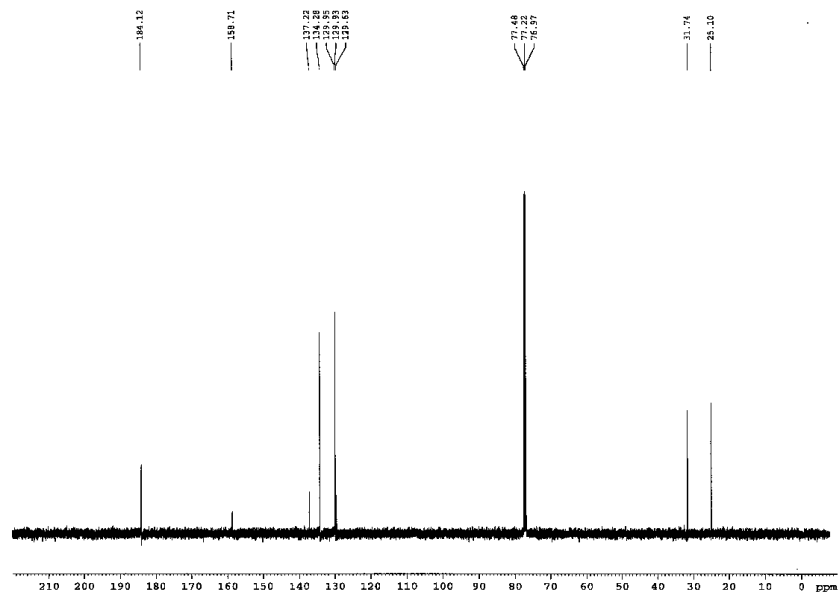




4.64 Proton NMR



4.64 Carbon NMR

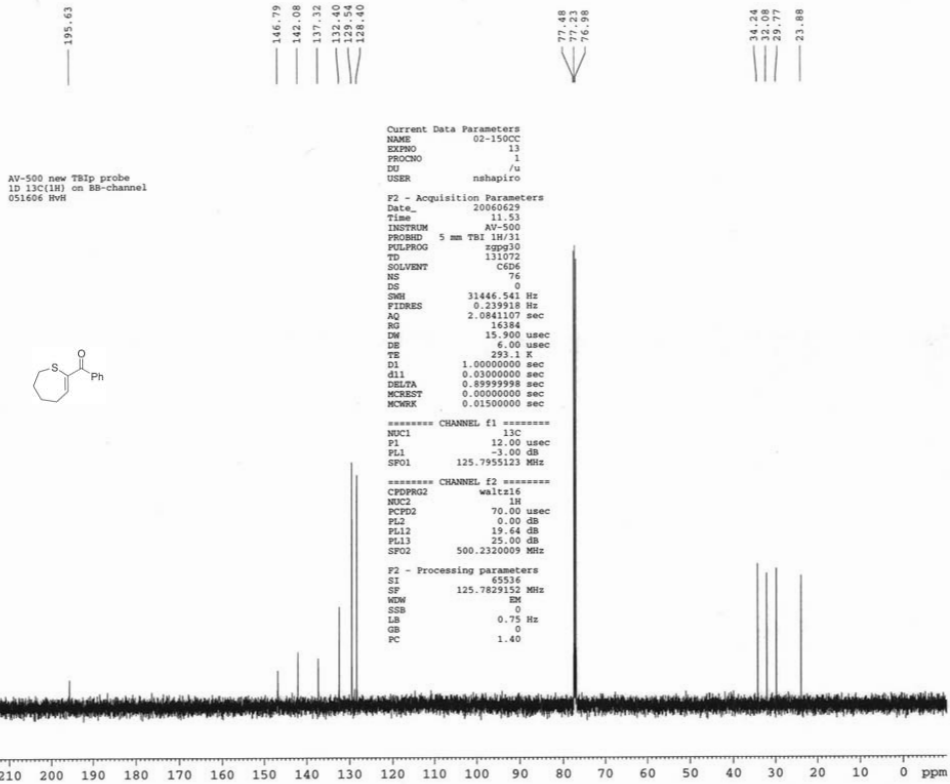
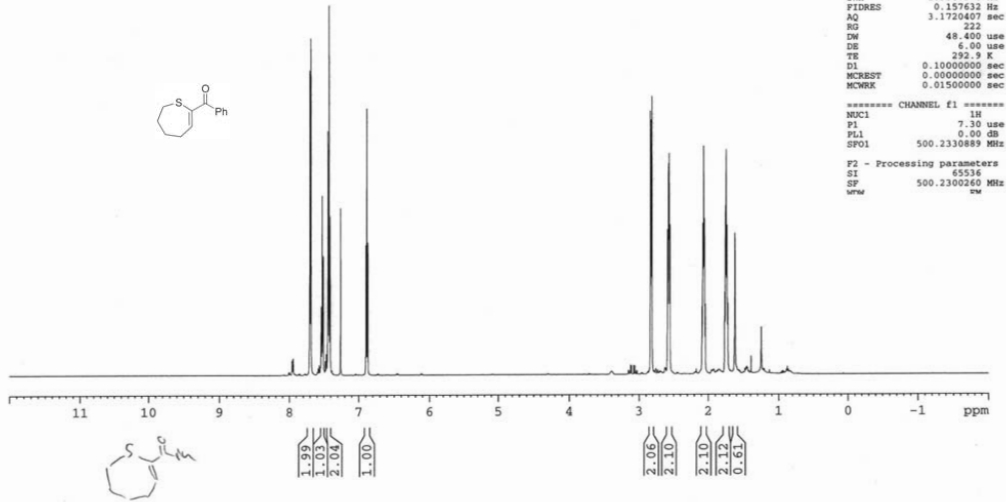


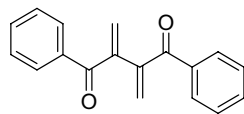
AV-500 r. TBI (HXP) probe
1D 1H starting parameters

7.961
7.946
7.705
7.690
7.567
7.540
7.525
7.510
7.469
7.463
7.441
7.426
7.411
7.260
6.885
6.872

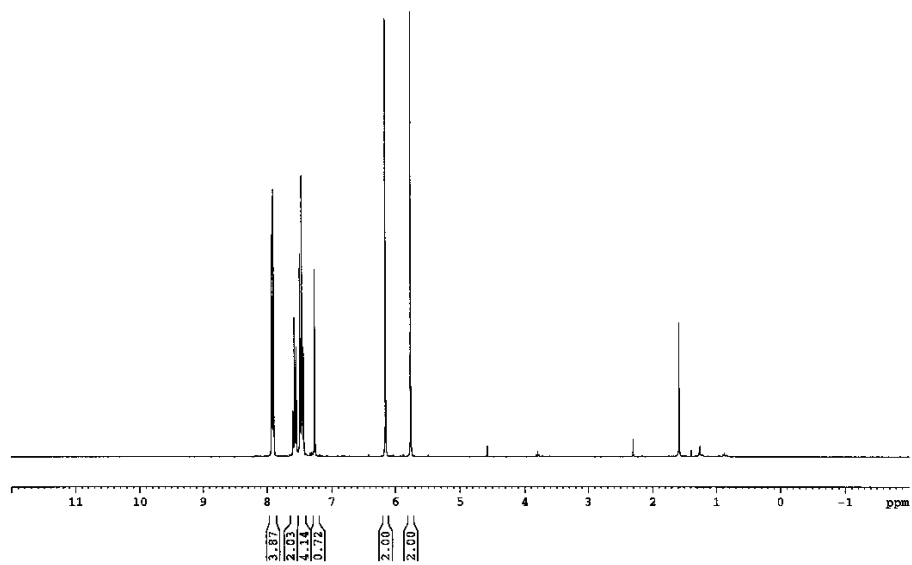
2.838
2.831
2.826
2.821
2.814
2.588
2.575
2.566
2.091
2.079
2.074
2.068
2.061
2.056
2.044
1.768
1.756
1.745
1.735
1.722
1.620
1.591
1.248

4.66

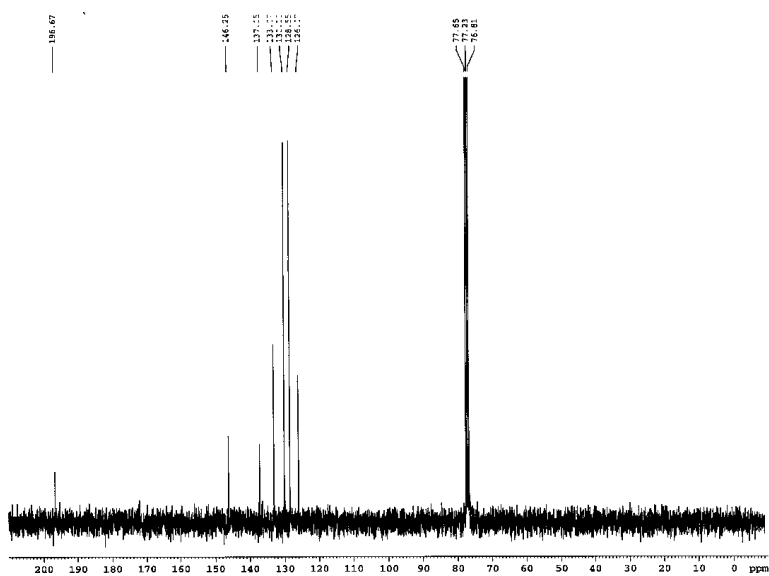




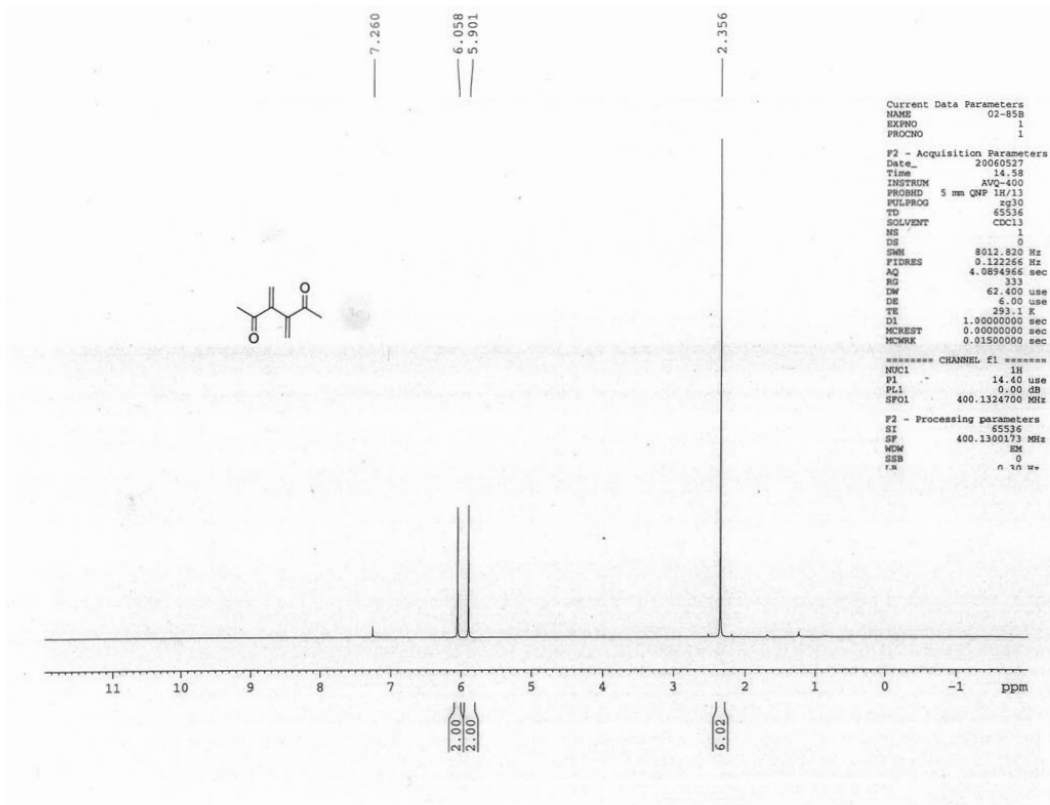
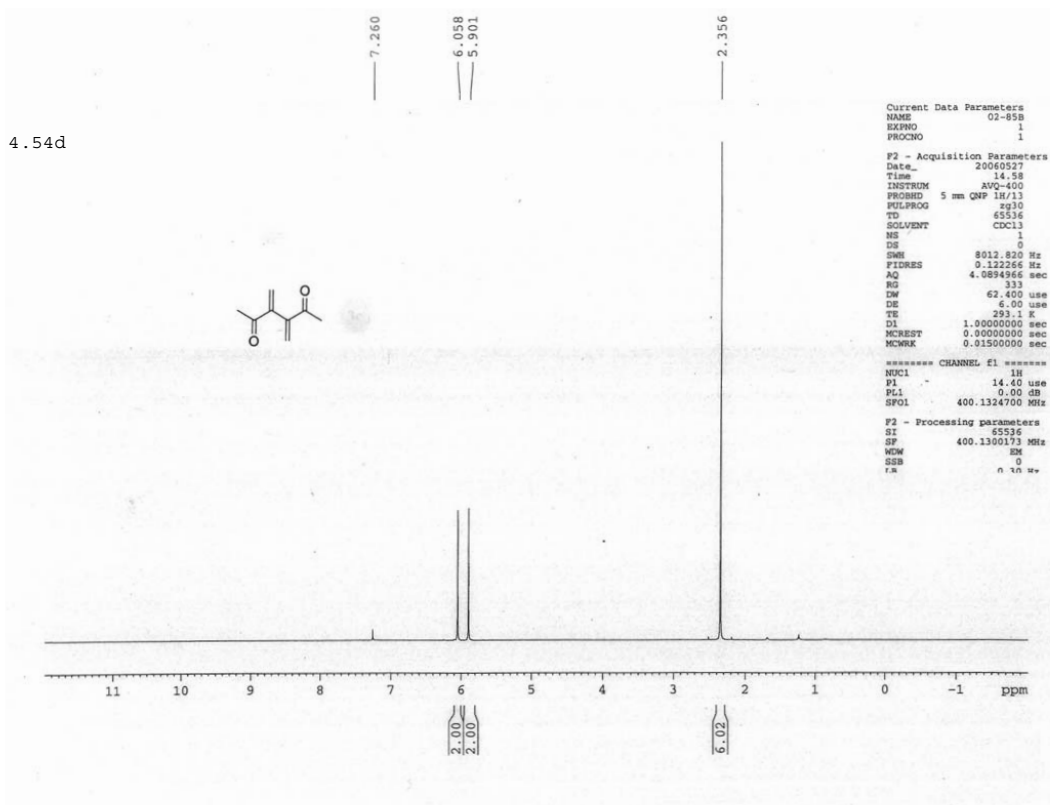
4.67a Proton NMR



4.67a Carbon NMR

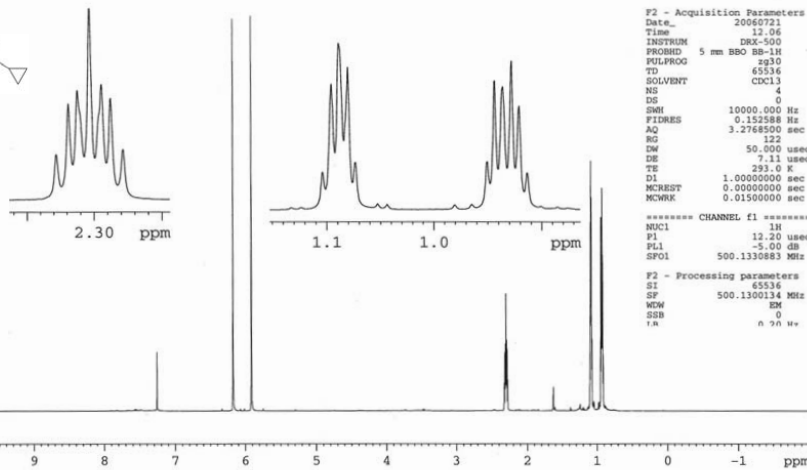
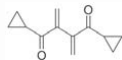


4.54d



DRX-500 zBBu probe

4.54g

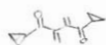


Current Data Parameters
 NAME 02-192C
 EXPNO 1
 PROCNO 1

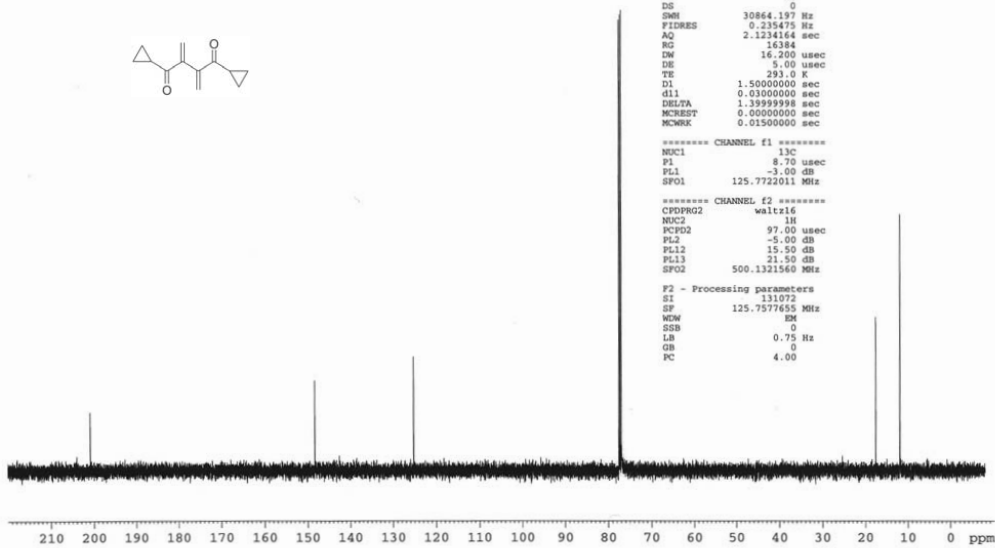
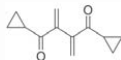
F2 - Acquisition Parameters
 Date_ 20060721
 Time 12.06
 INSTRUM DRX-500
 PROBHD 5 mm BBO BB-1H
 PULPROG zg30
 TD 6536
 SOLVENT CDCl3
 NS 4
 DS 0
 SWH 10000.000 Hz
 FIDRES 0.152588 Hz
 AQ 3.276800 sec
 RG 122
 DW 50.000 usec
 DE 7.11 usec
 TE 293.0 K
 D1 1.0000000 sec
 MCREST 0.0000000 sec
 MCWRR 0.0150000 sec

***** CHANNEL f1 *****
 NUC1 1H
 P1 12.20 usec
 PL1 -5.00 dB
 SFO1 500.1330883 MHz

F2 - Processing parameters
 SI 6536
 SF 500.1300114 MHz
 WF 0
 SSB 0
 GB 0
 PC 0.90 W



200.86, 148.37, 125.24, 77.18, 77.23, 76.97, 17.63, 11.91



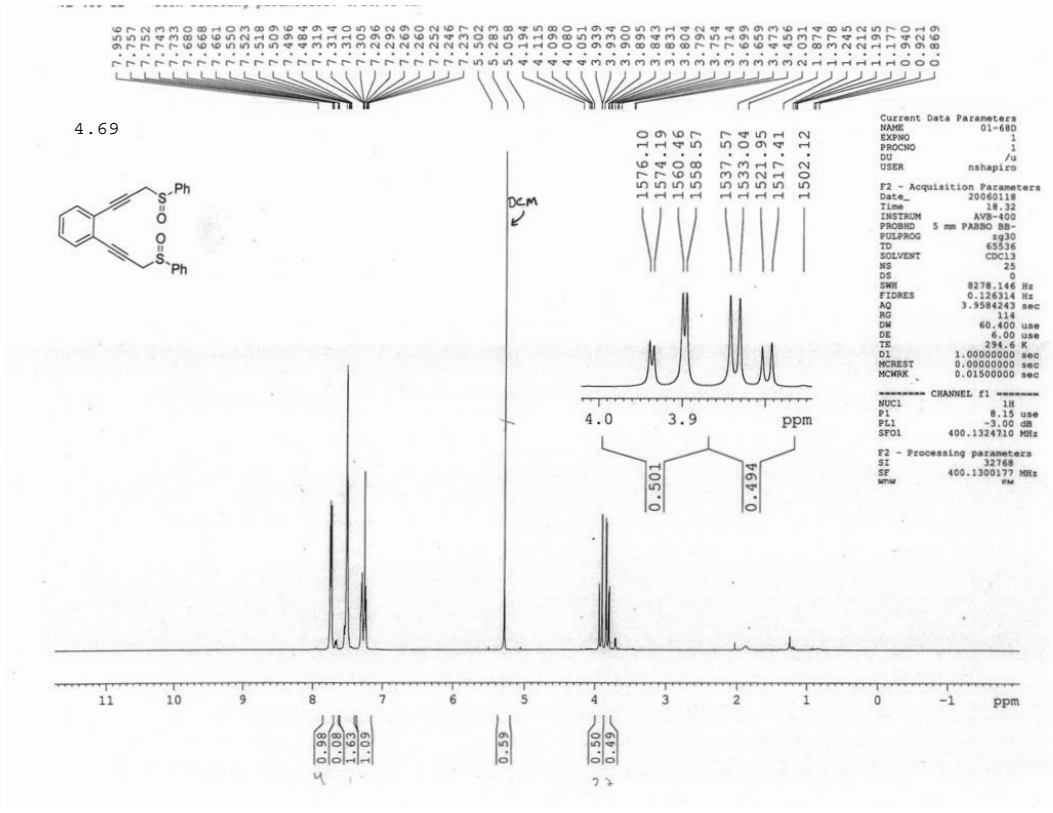
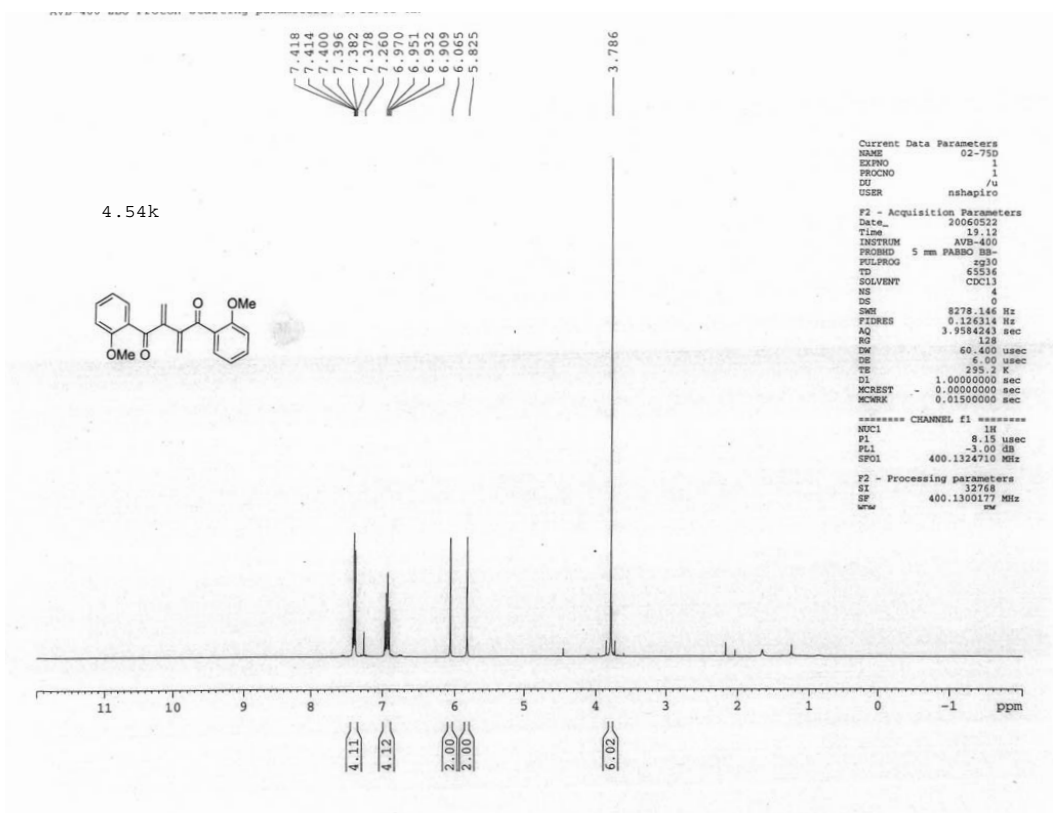
Current Data Parameters
 NAME 02-192C
 EXPNO 13
 PROCNO 1

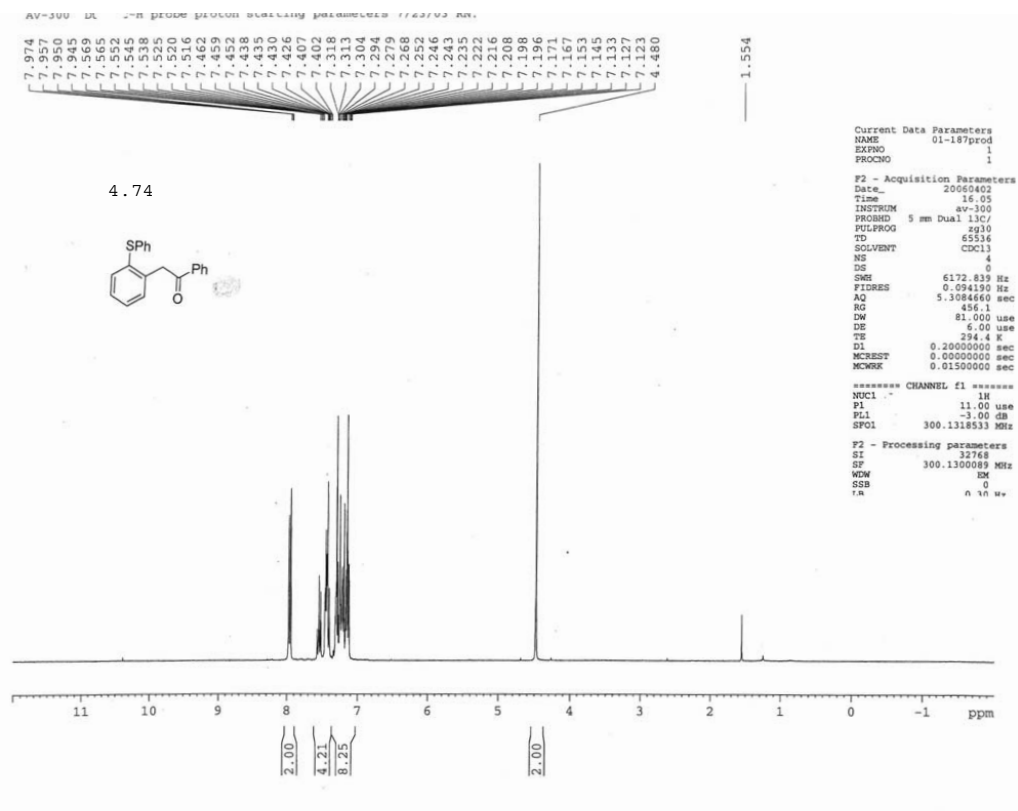
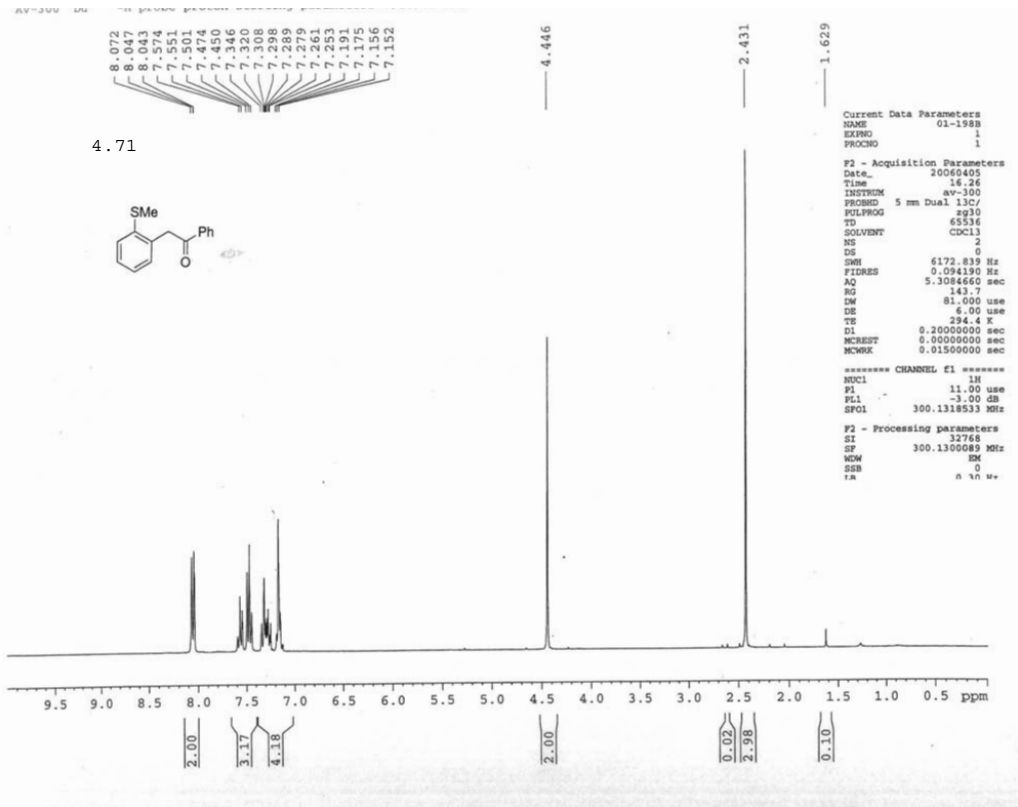
F2 - Acquisition Parameters
 Date_ 20060721
 Time 12.08
 INSTRUM DRX-500
 PROBHD 5 mm BBO BB-1H
 PULPROG zgpg30
 TD 13102
 SOLVENT CDCl3
 NS 28
 DS 0
 SWH 30864.197 Hz
 FIDRES 0.23475 Hz
 AQ 2.1234164 sec
 RG 16384
 DW 16.200 usec
 DE 5.00 usec
 TE 293.0 K
 D1 1.5000000 sec
 d11 0.0300000 sec
 DELTA 1.3999998 sec
 MCREST 0.0000000 sec
 MCWRR 0.0150000 sec

***** CHANNEL f1 *****
 NUC1 13C
 P1 8.70 usec
 PL1 -3.00 dB
 SFO1 125.7722011 MHz

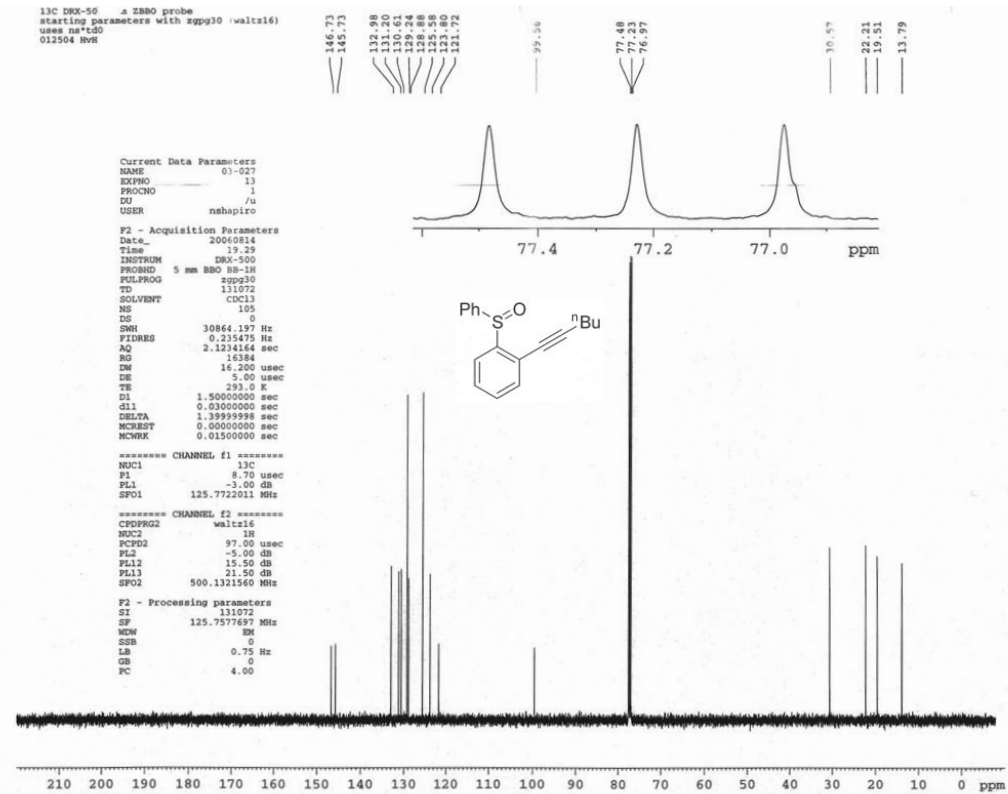
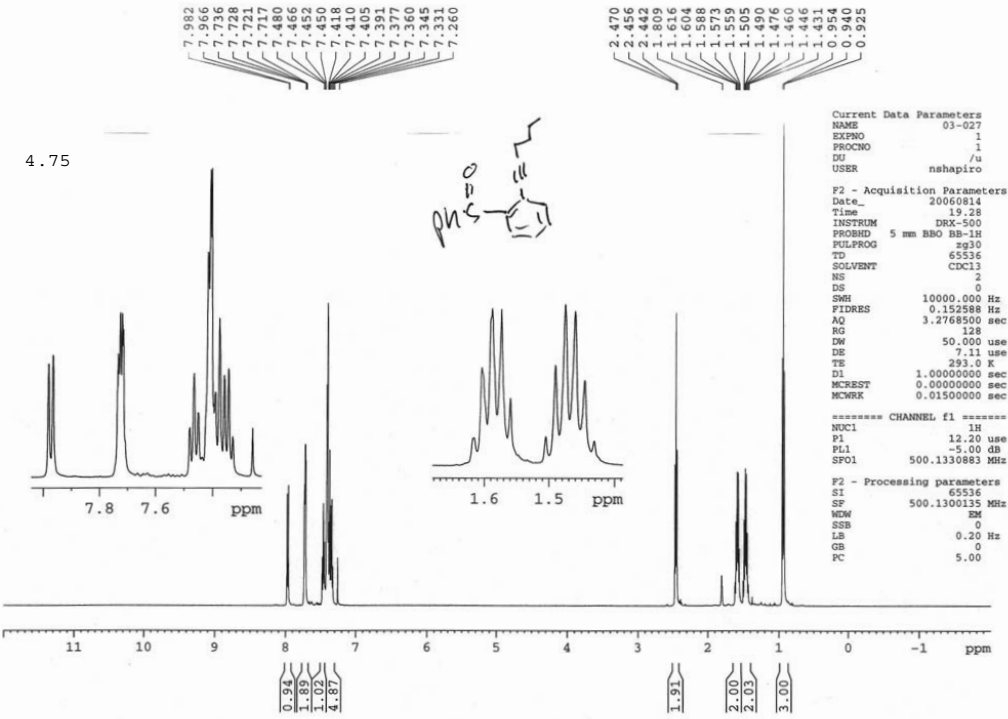
***** CHANNEL f2 *****
 CPDPRG2 waltz16
 NUC2 1H
 PCPD2 97.00 usec
 PL2 -5.00 dB
 PL12 15.50 dB
 PL13 21.50 dB
 SFO2 500.1321560 MHz

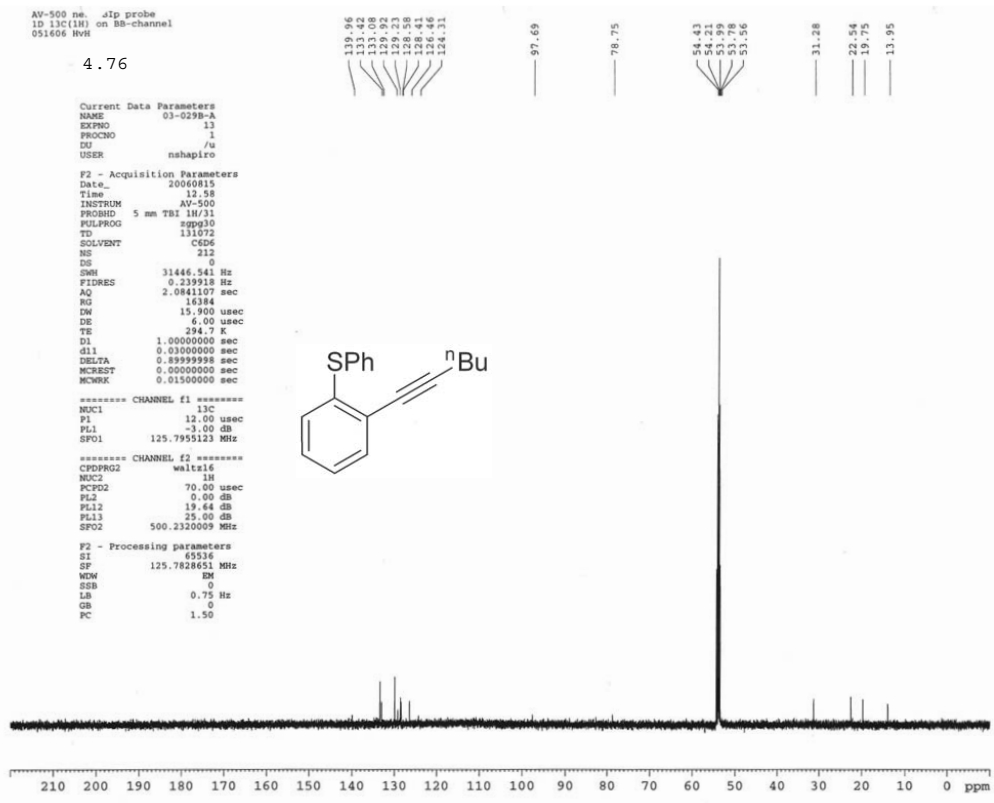
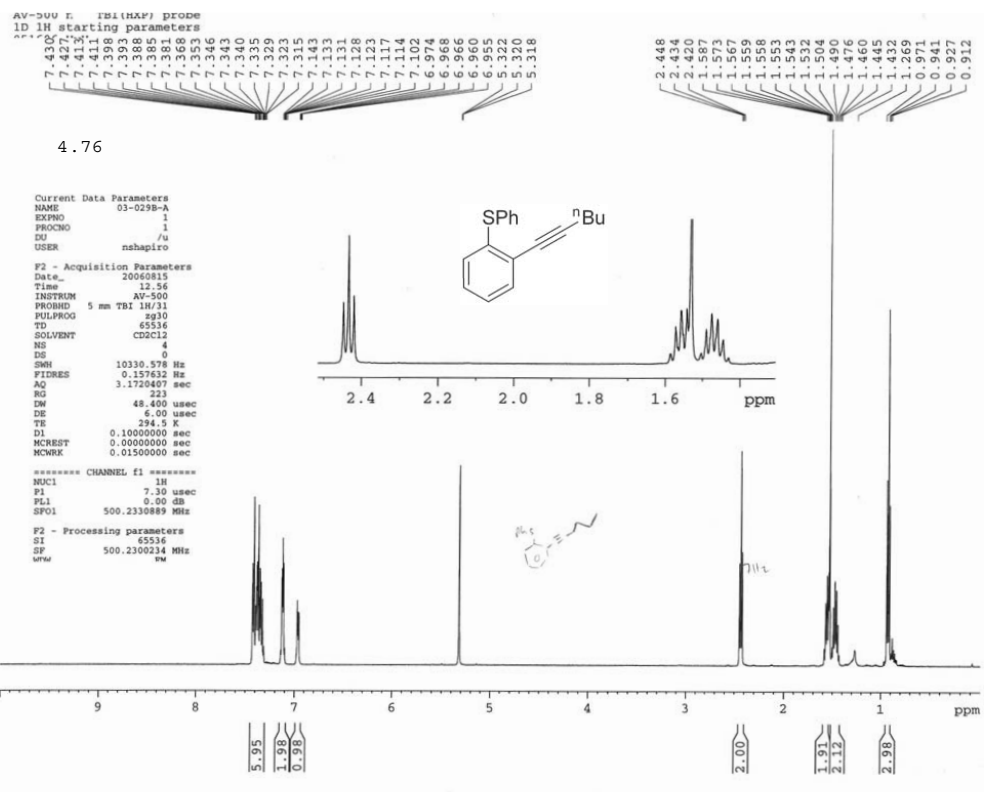
F2 - Processing parameters
 SI 13102
 SF 125.7577655 MHz
 WF 0
 SSB 0
 LB 0.75 Hz
 GB 0
 PC 4.00

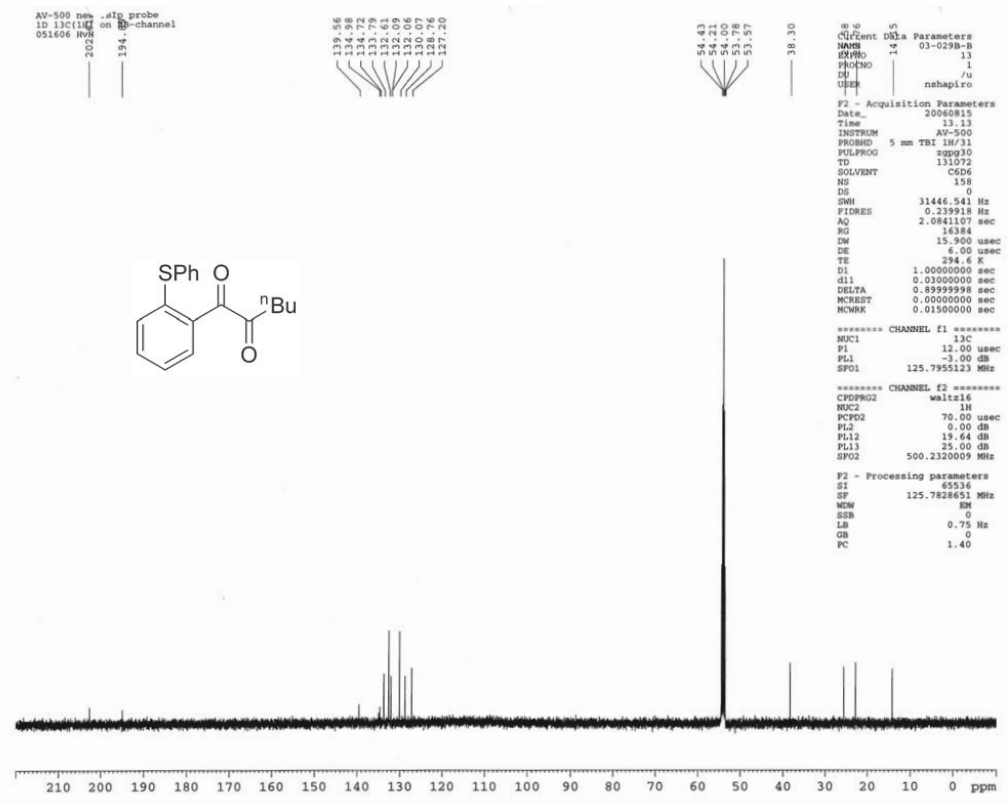
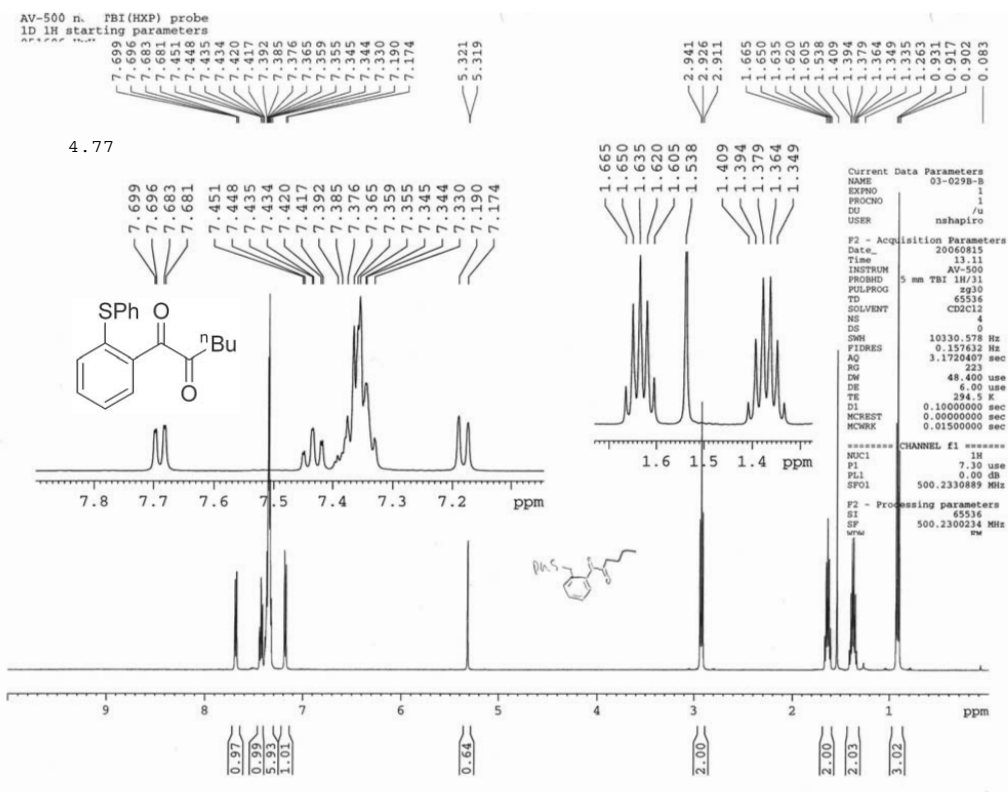


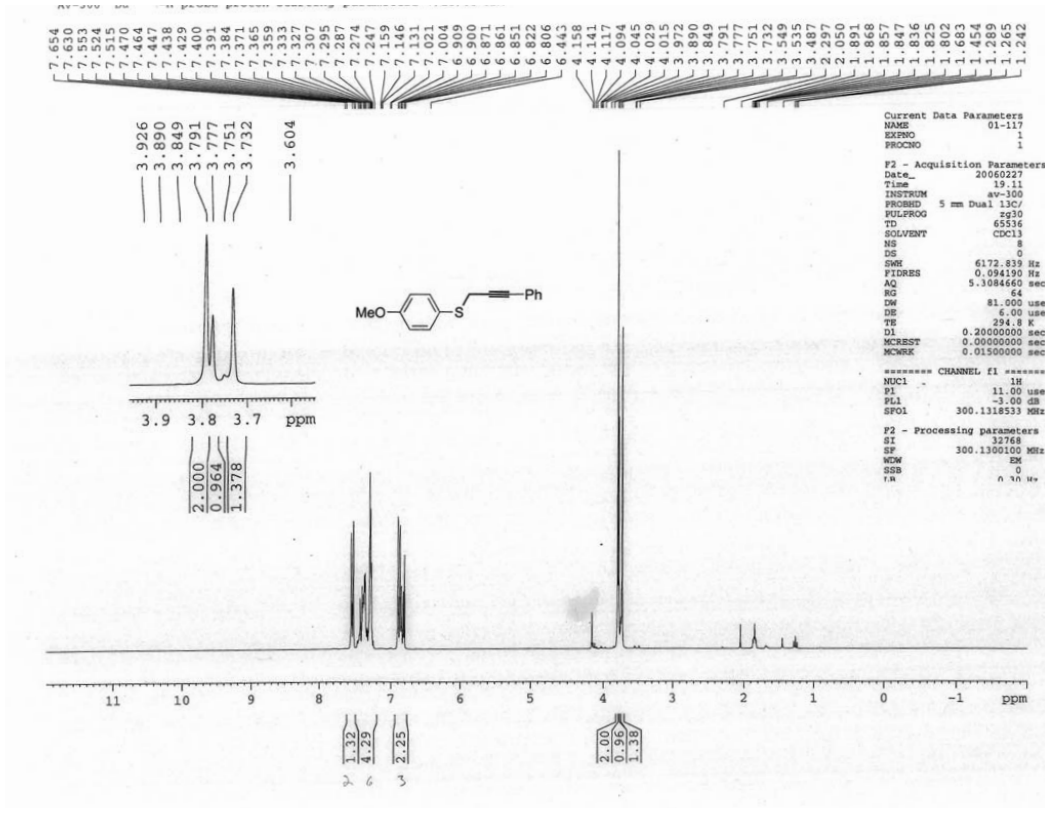
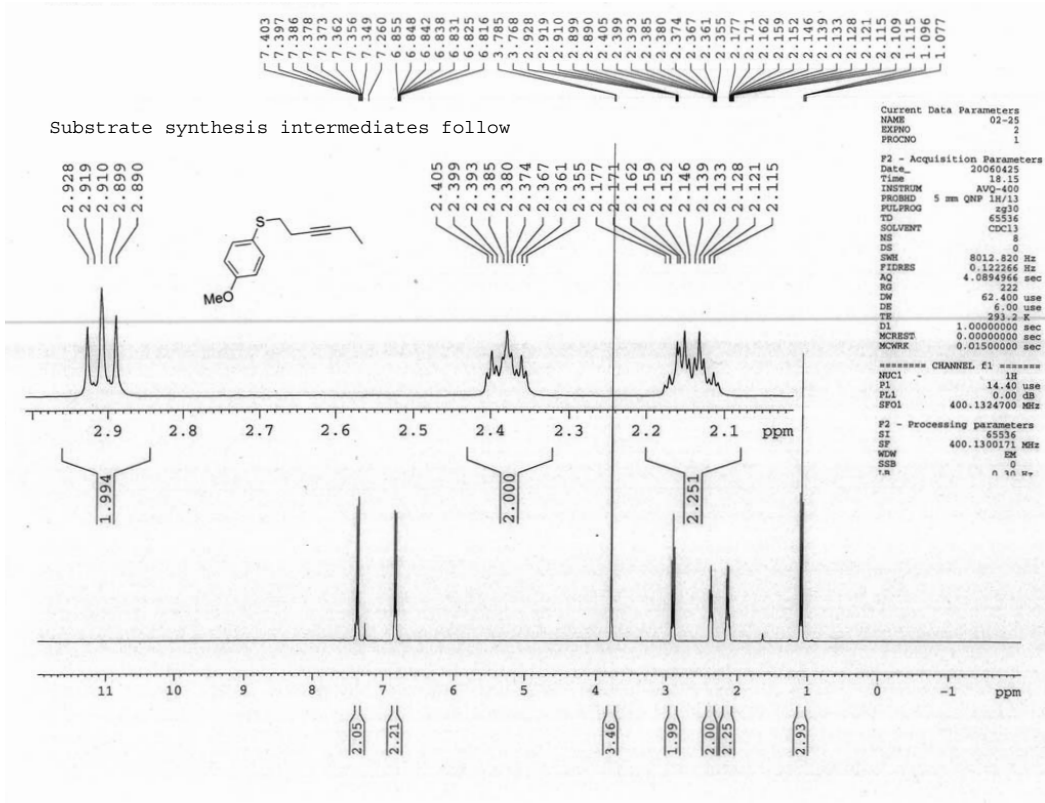


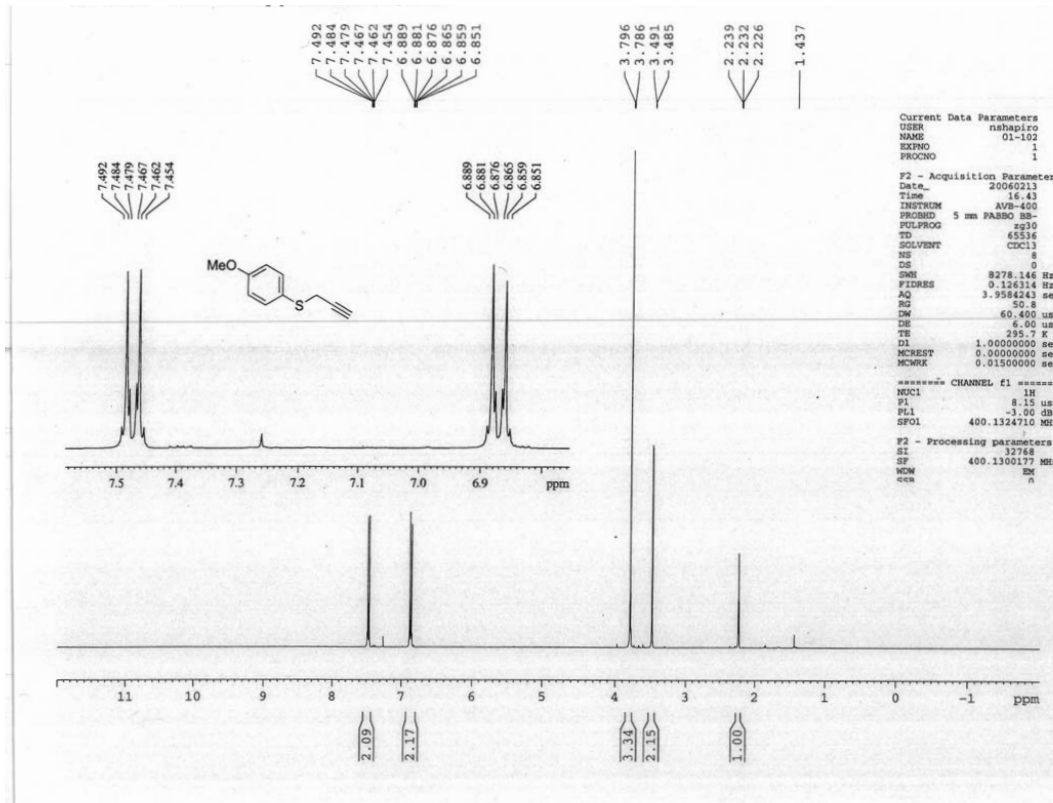
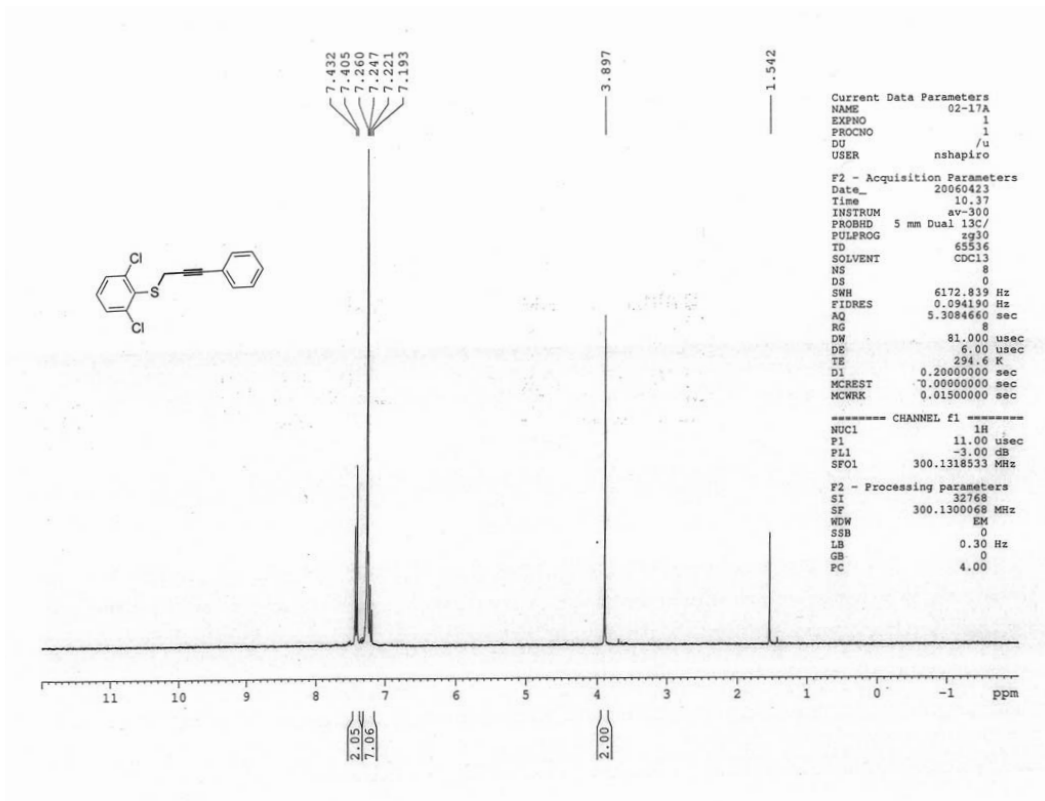
DRX-500 zBl ,probe
080804 HvH

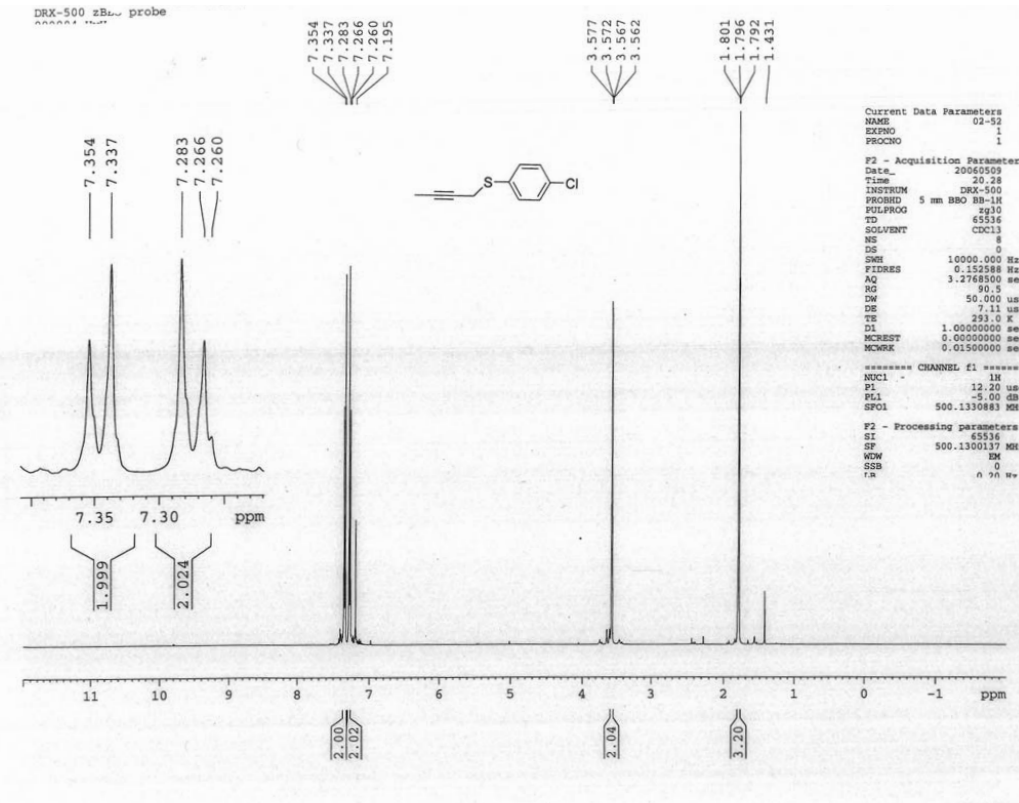
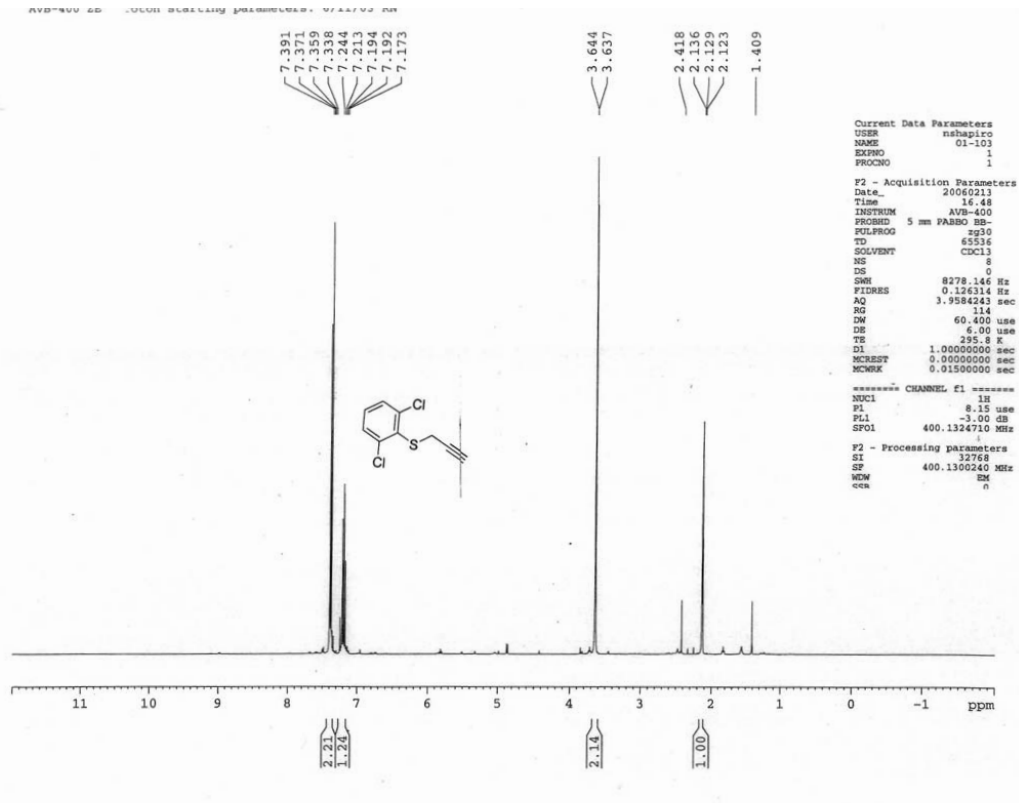




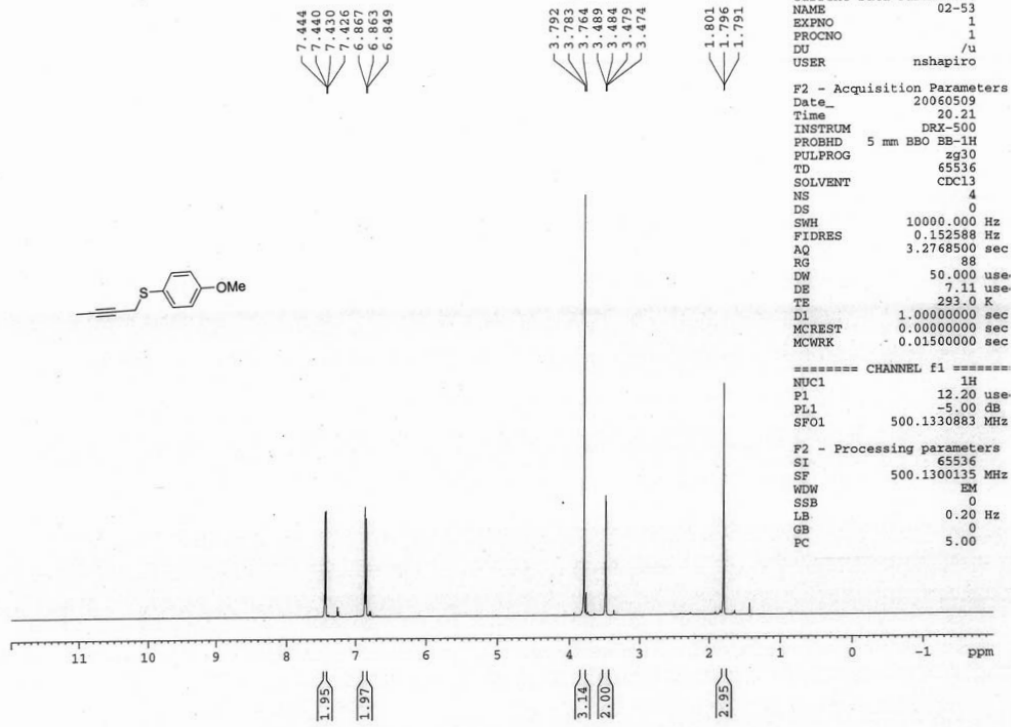




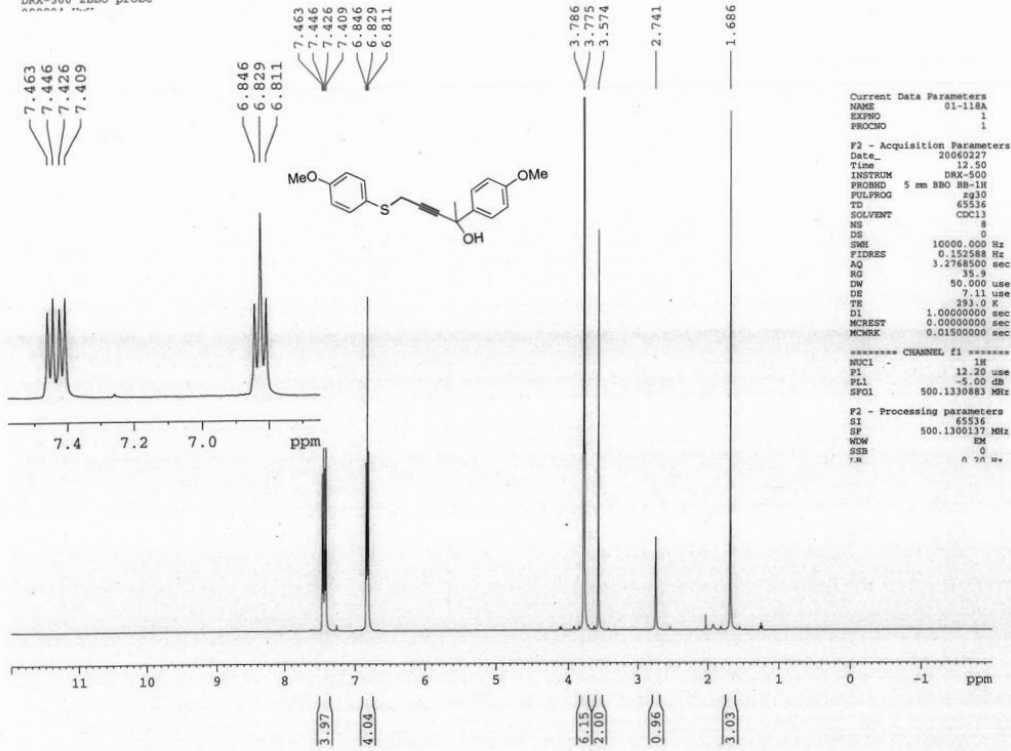




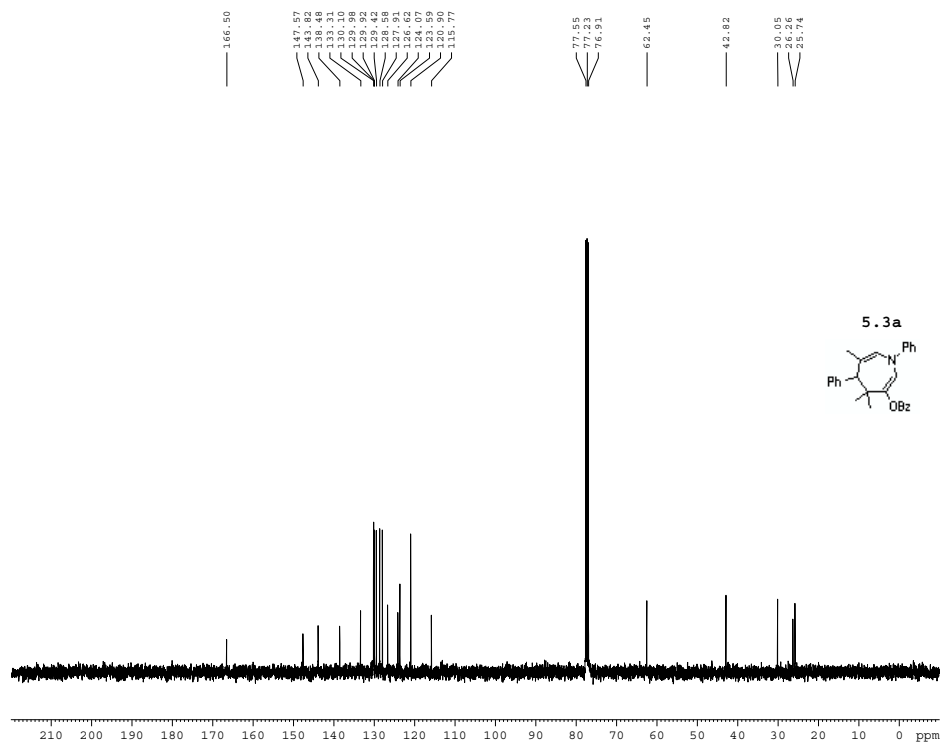
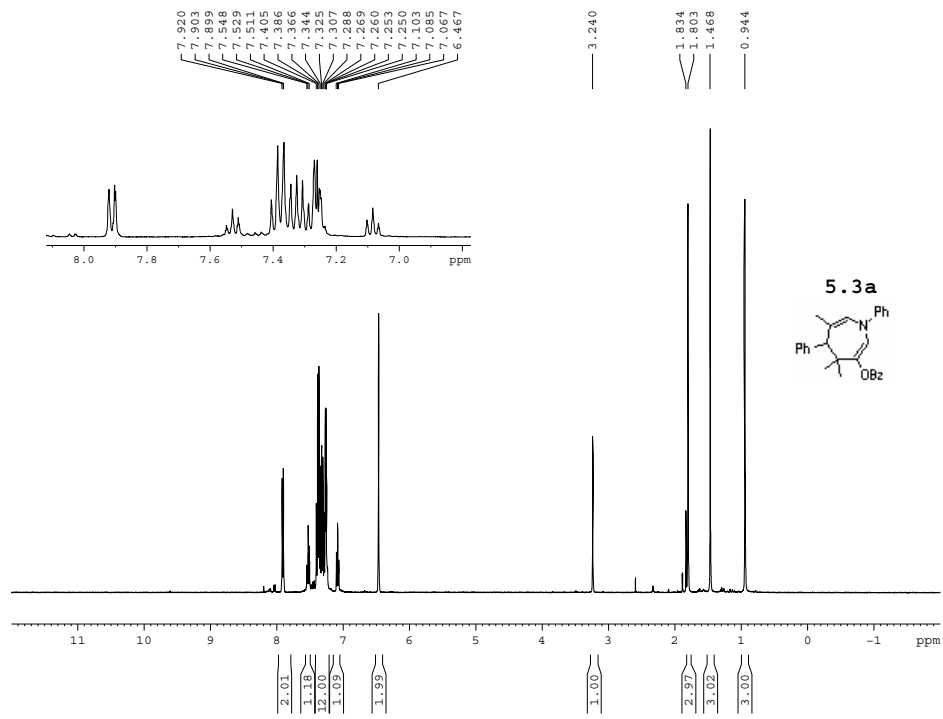
080804 HvH

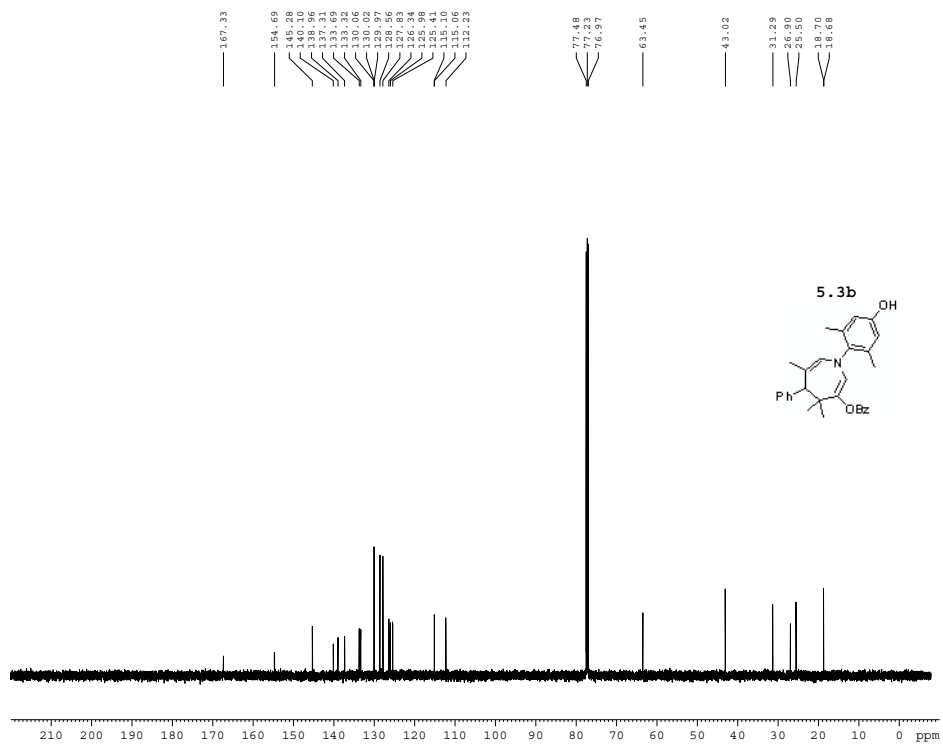
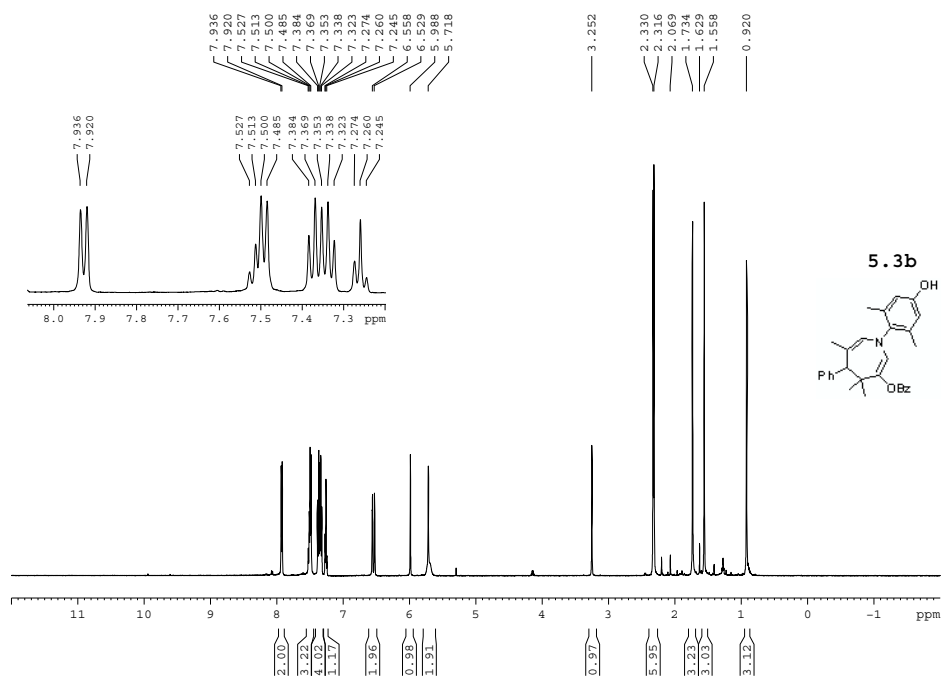


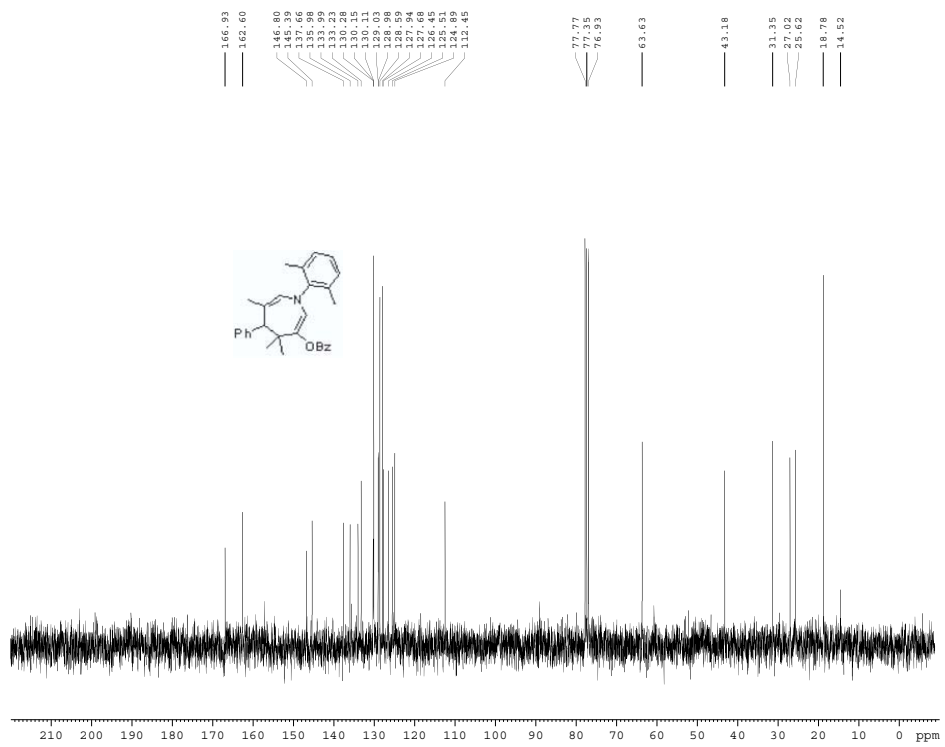
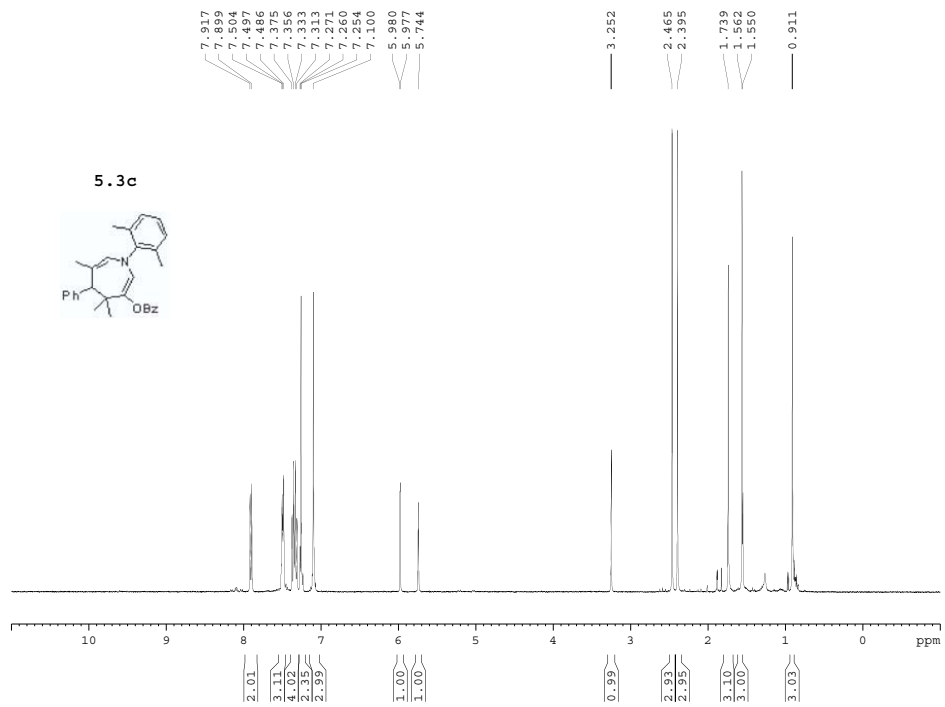
DRX-500 zBb probe

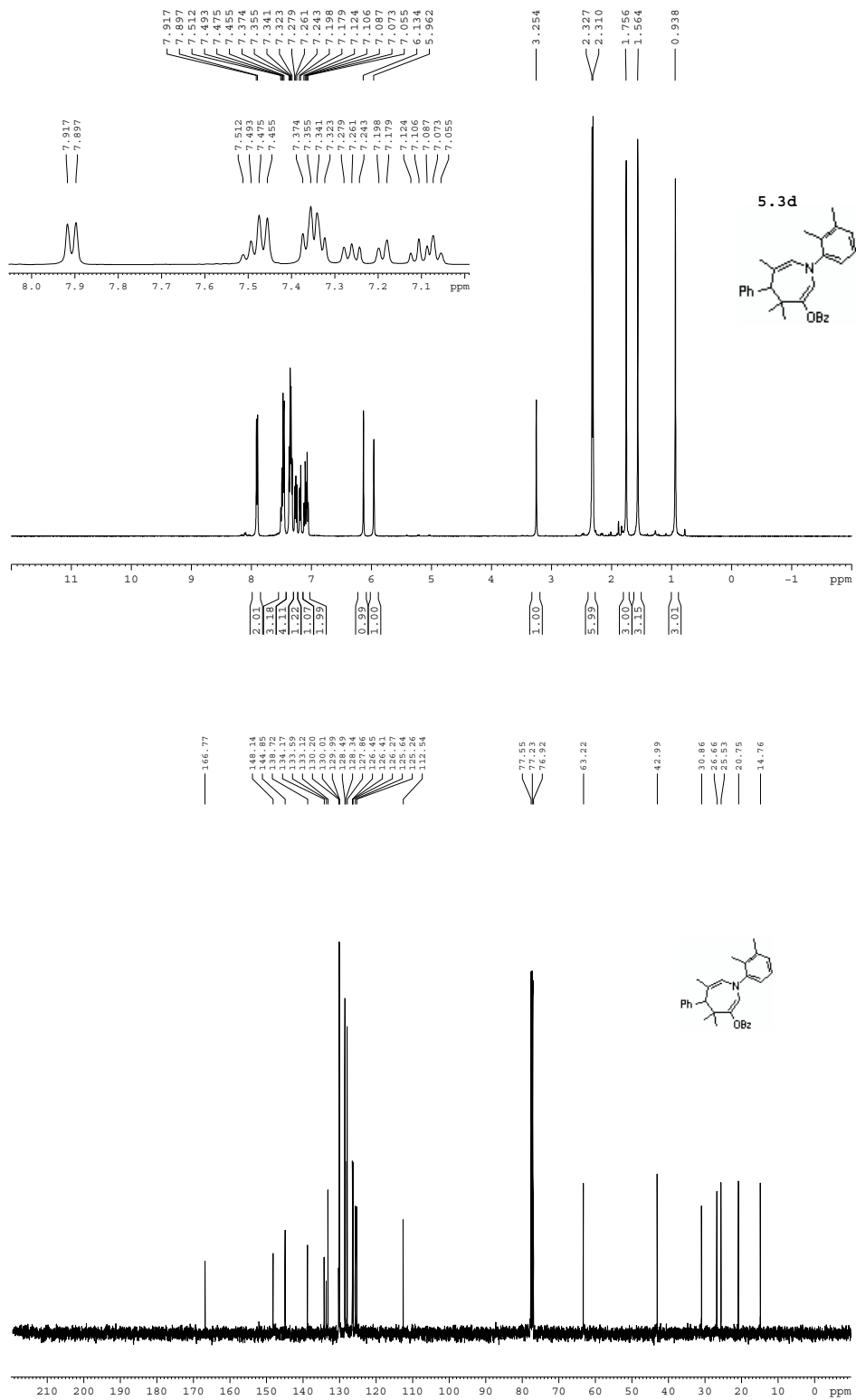


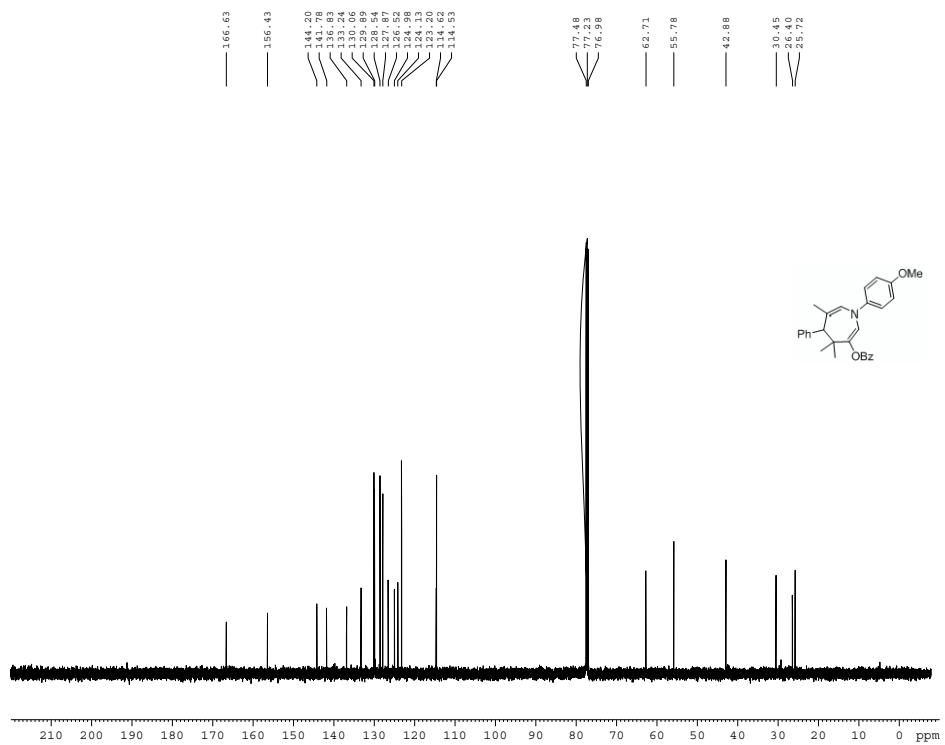
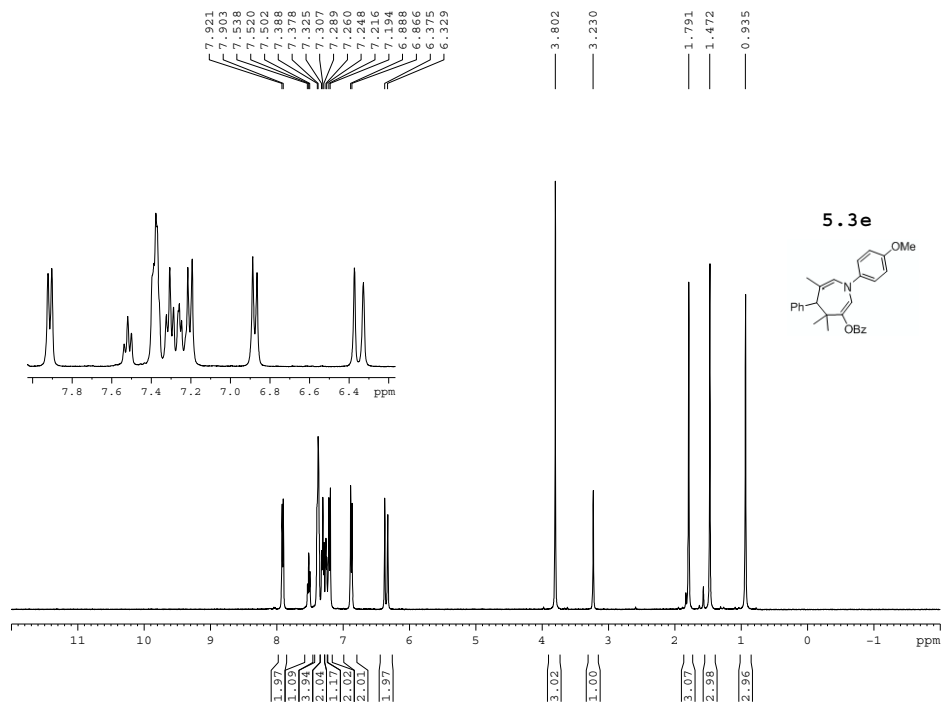
Appendix 5. Additional Supporting Information for Chapter 5

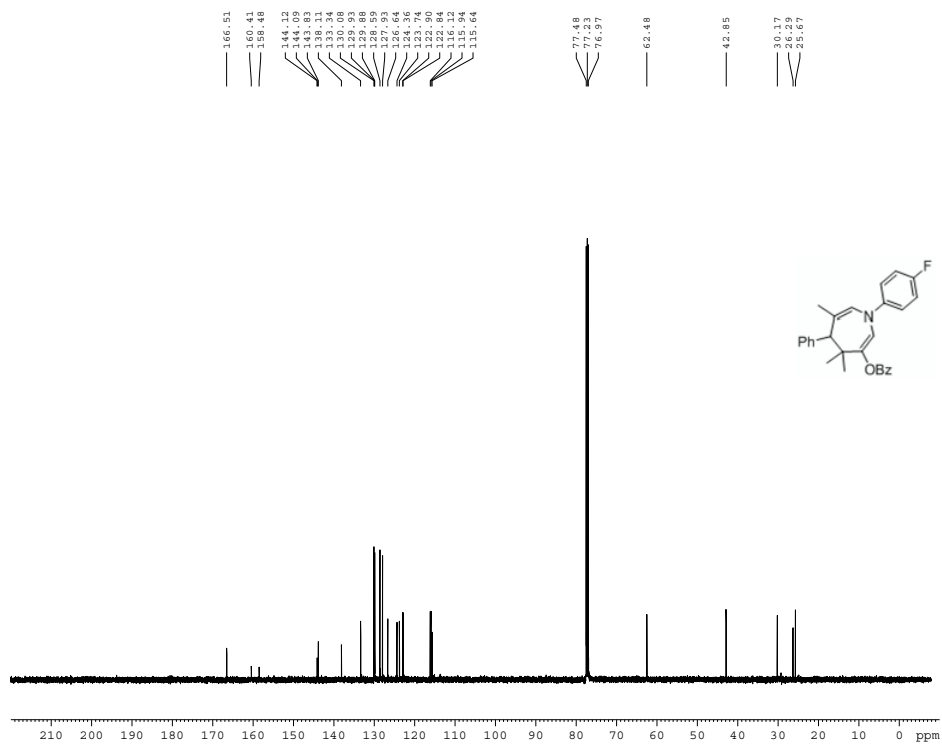
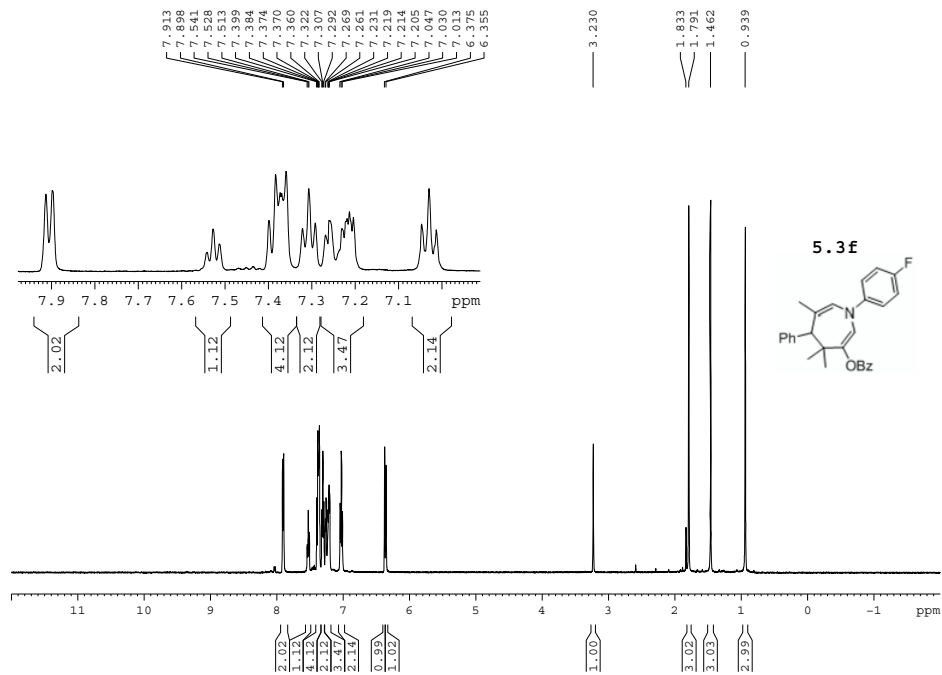


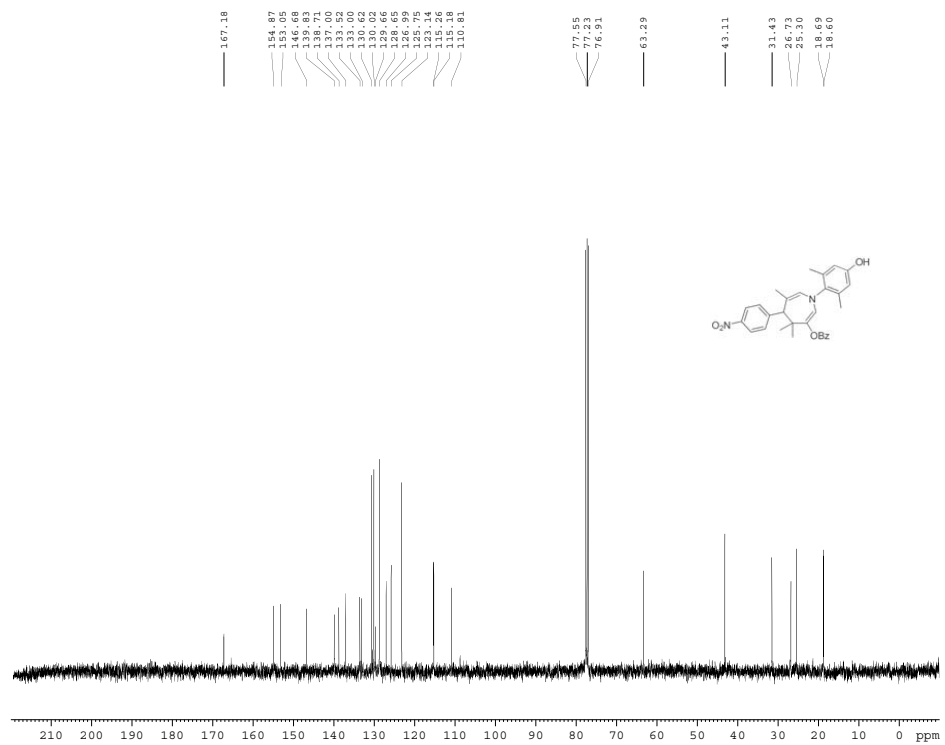
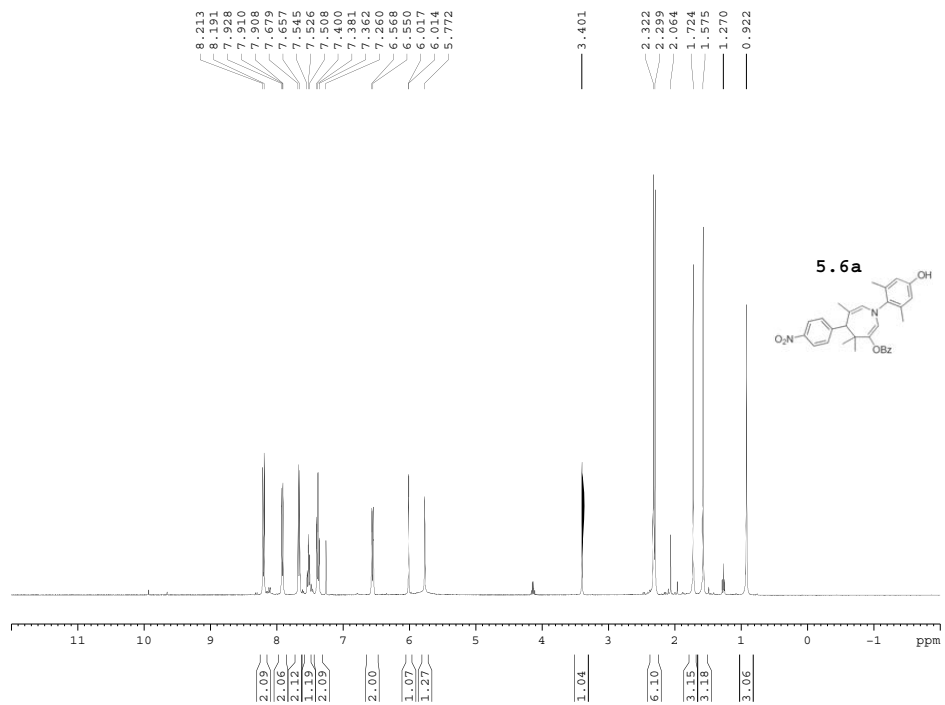


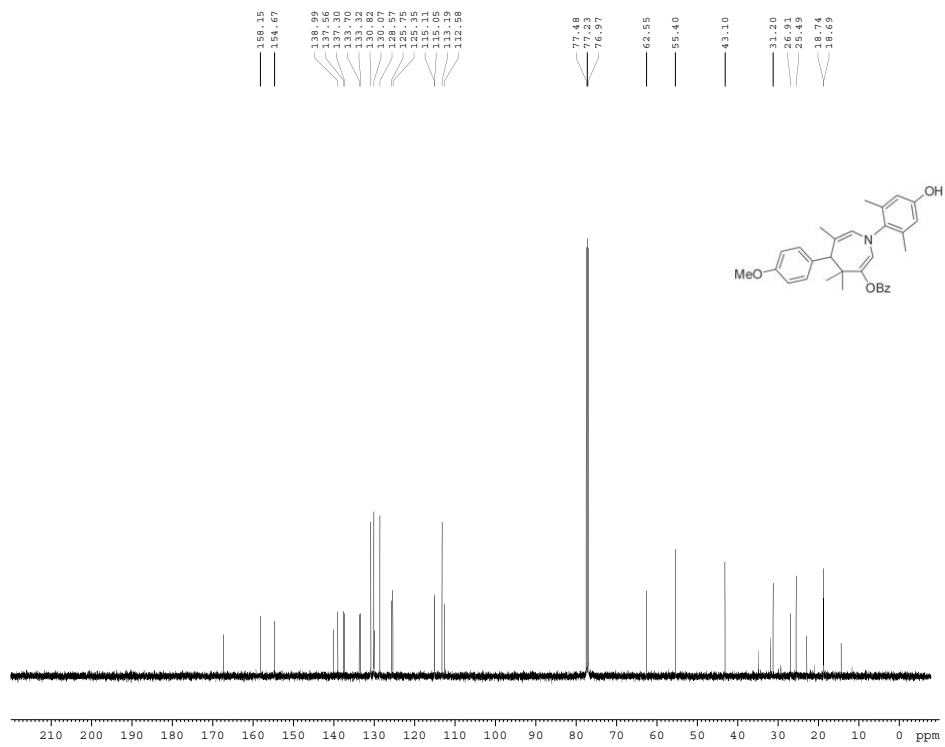
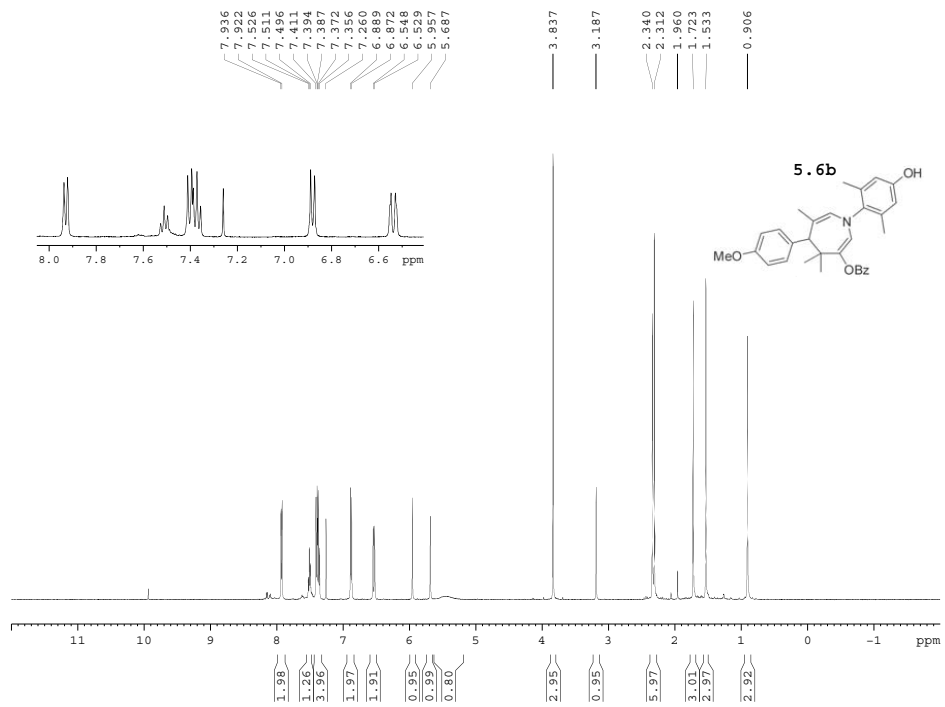


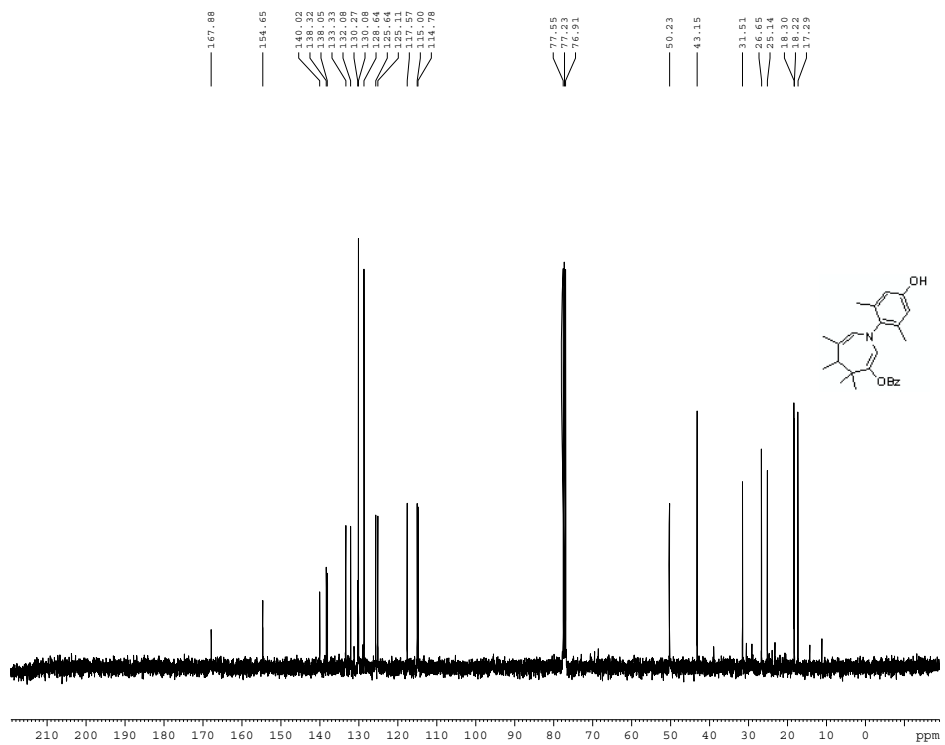
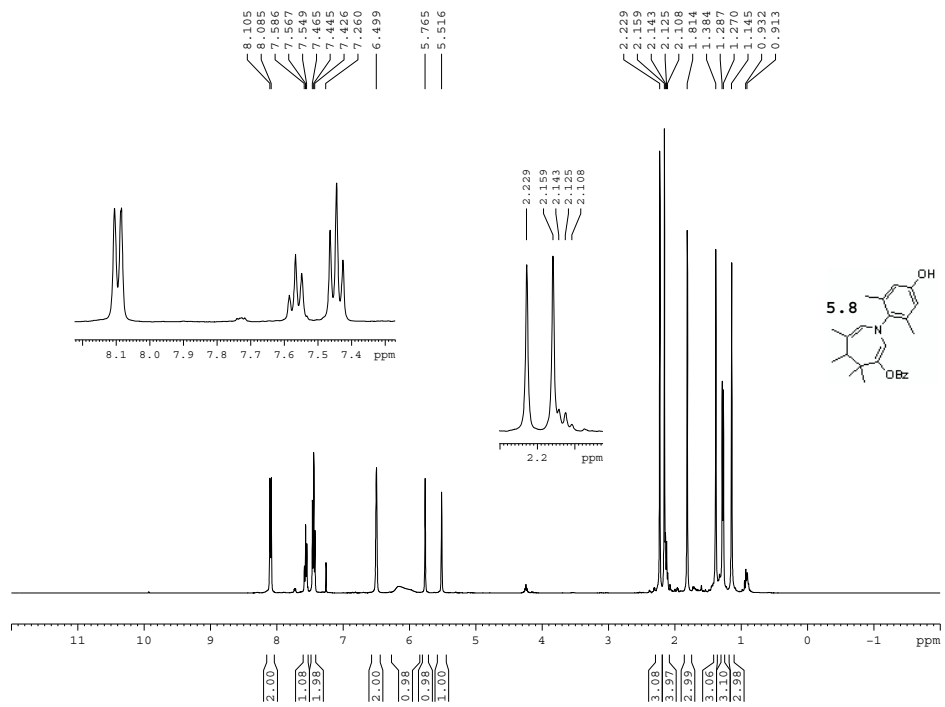


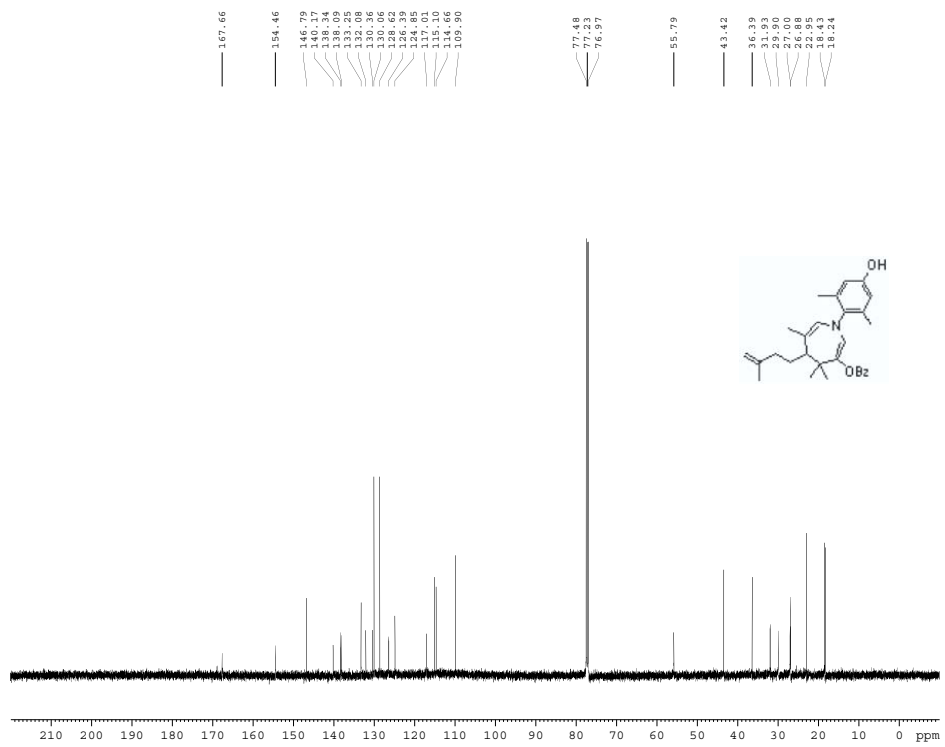
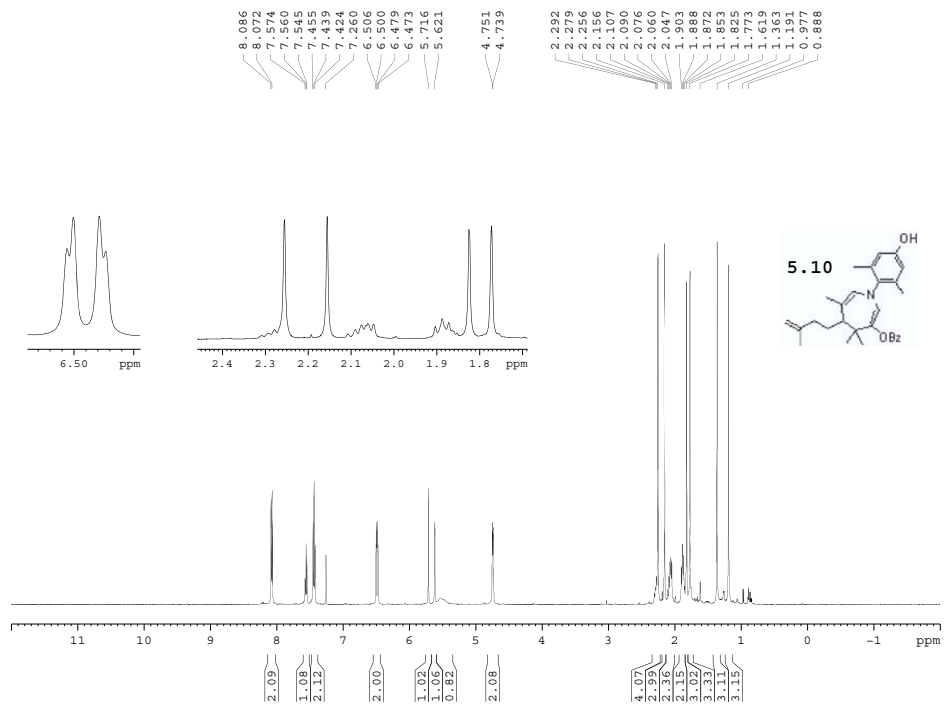


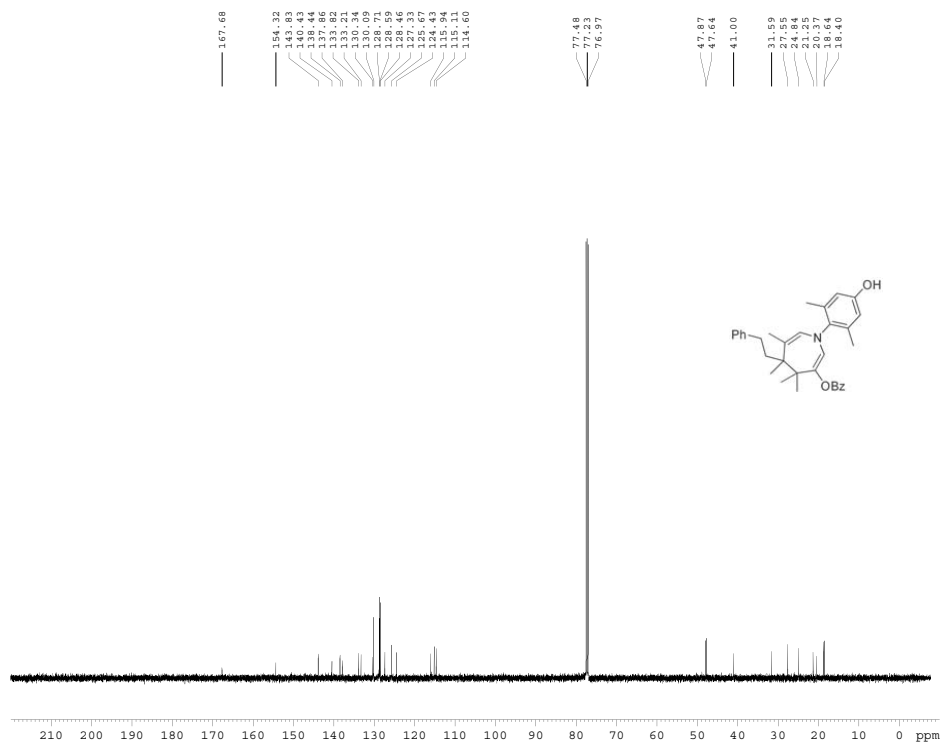
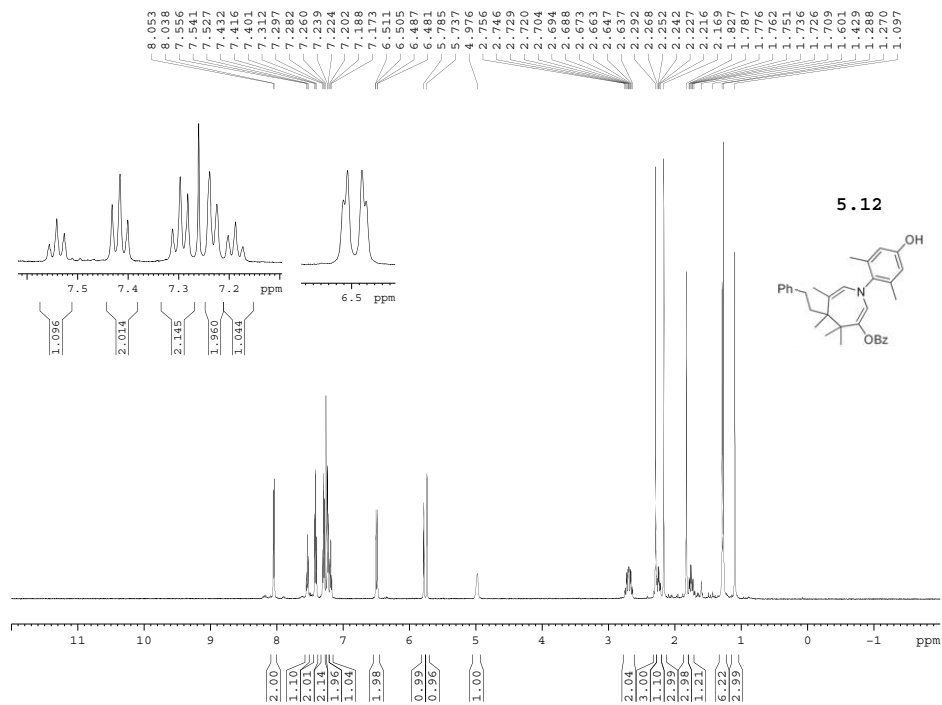


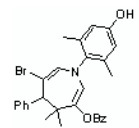
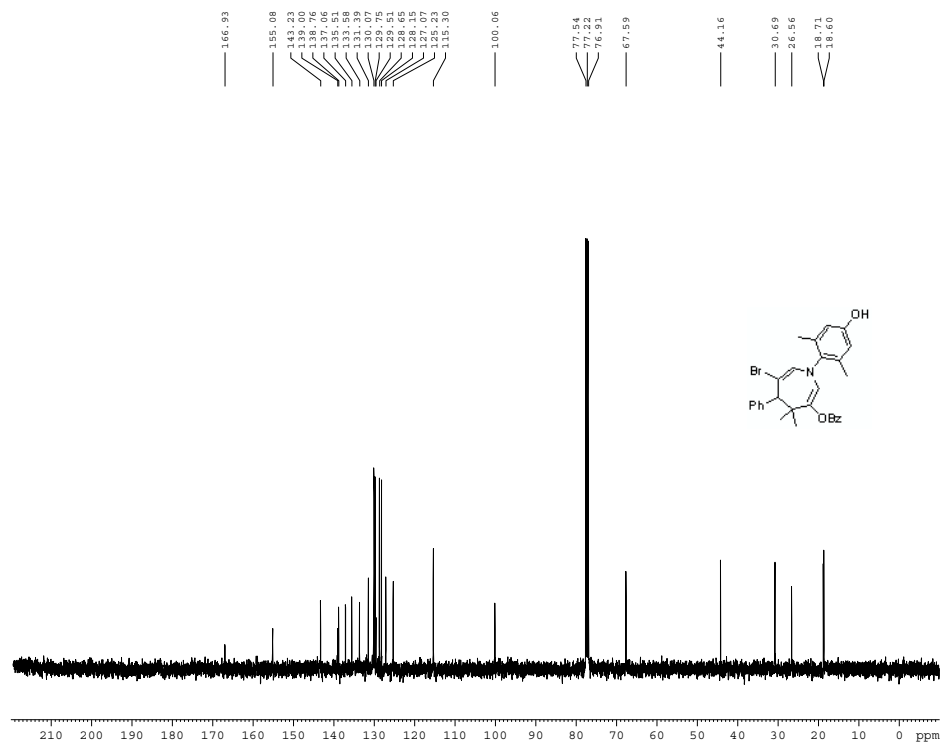
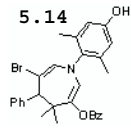
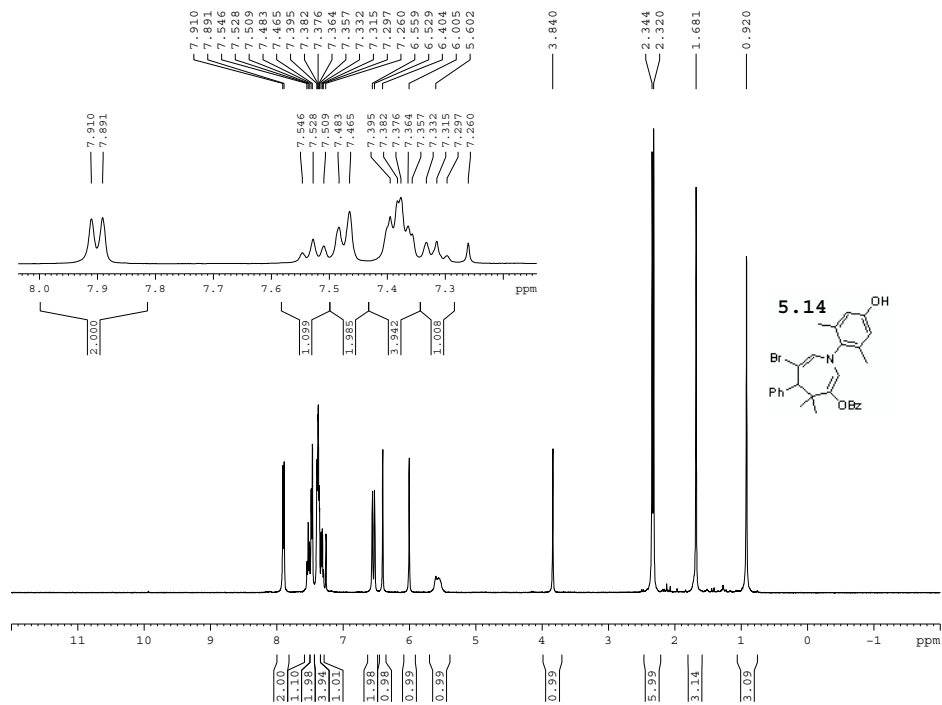


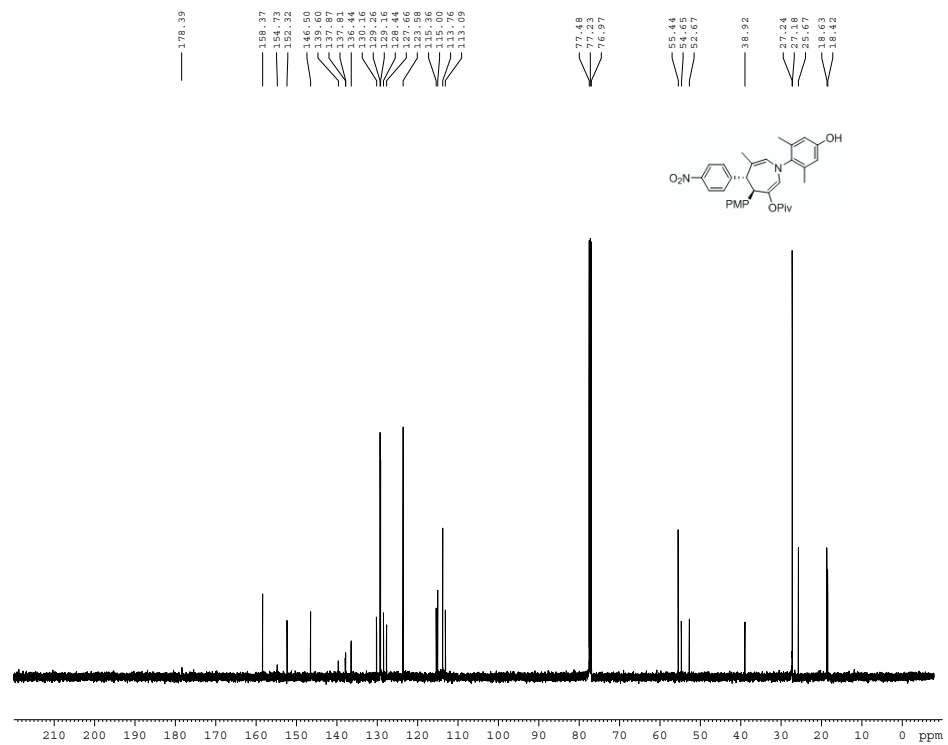
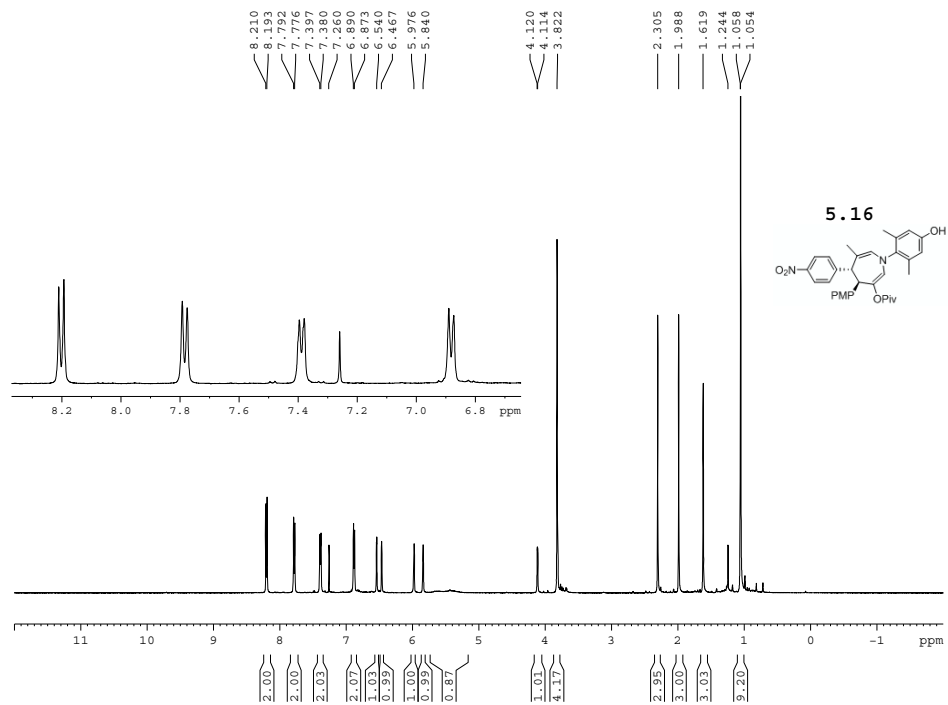


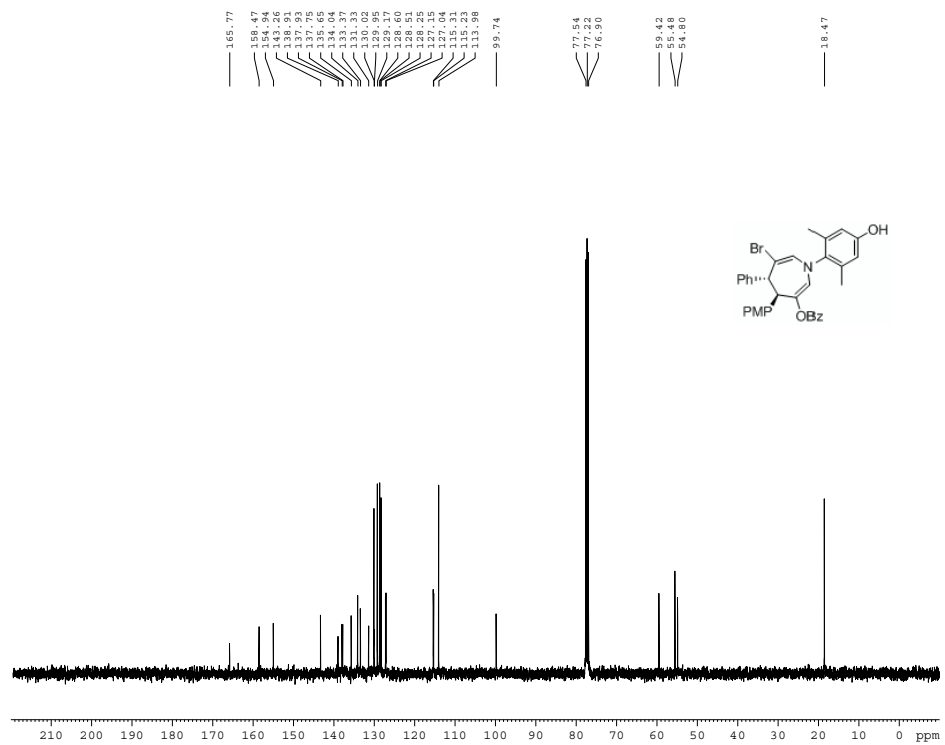
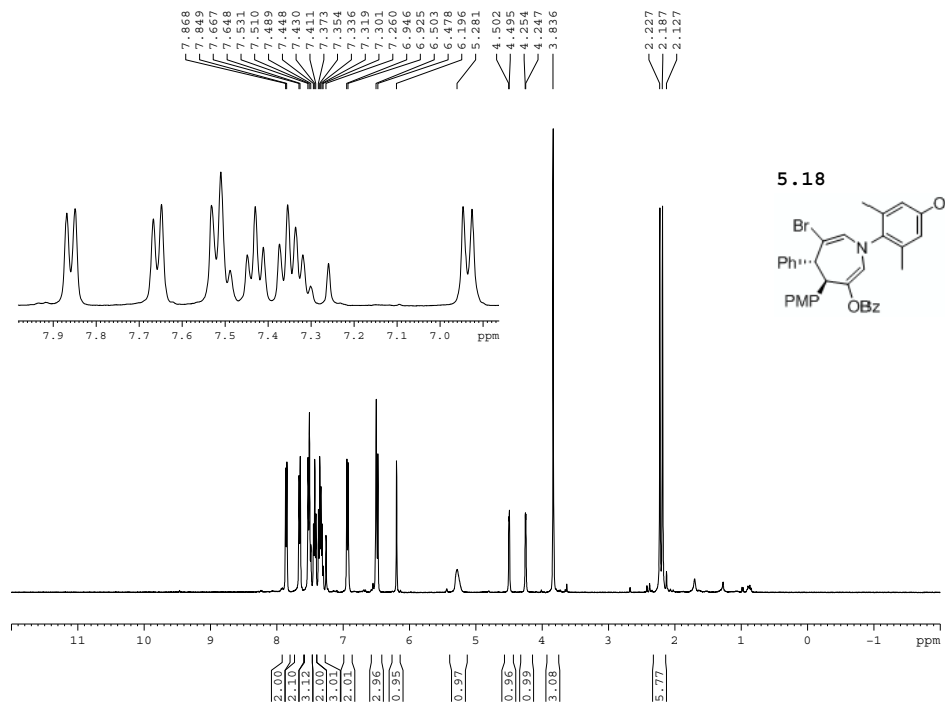


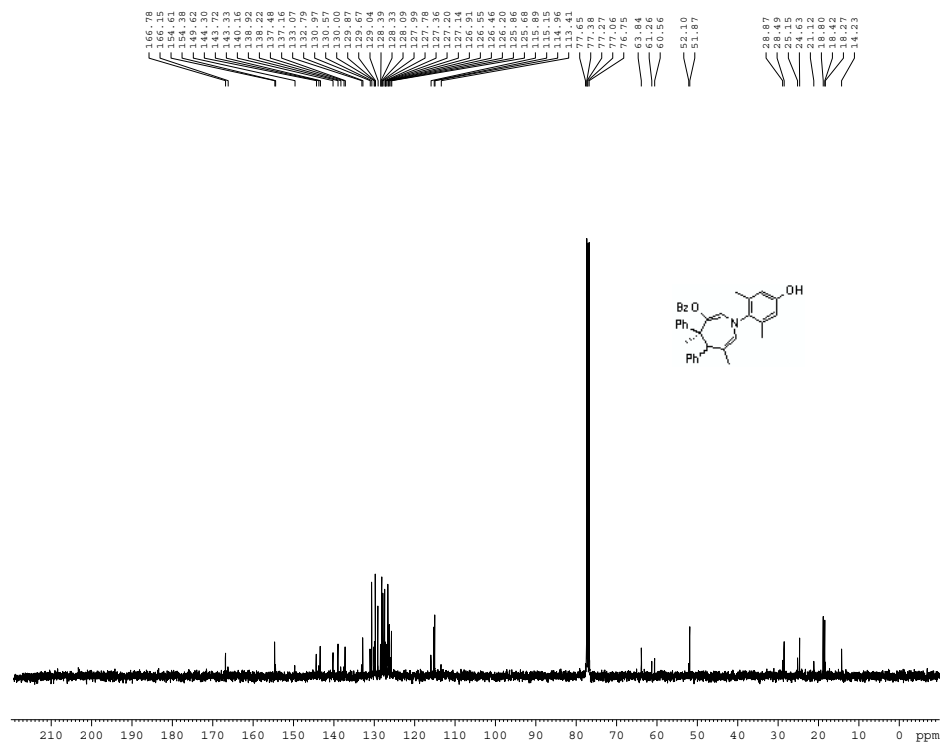
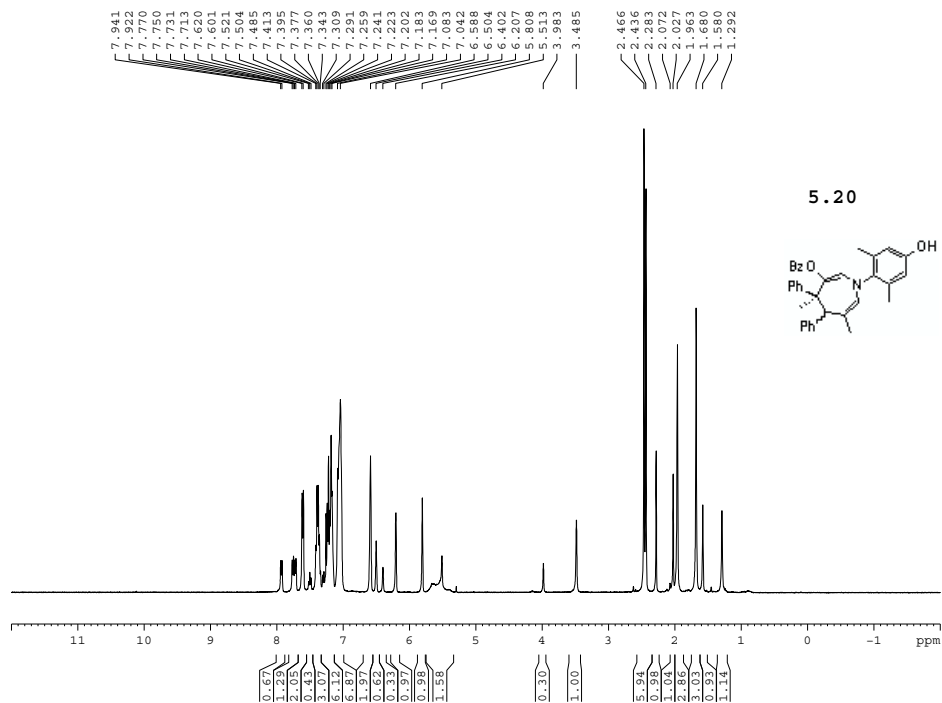


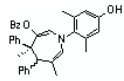




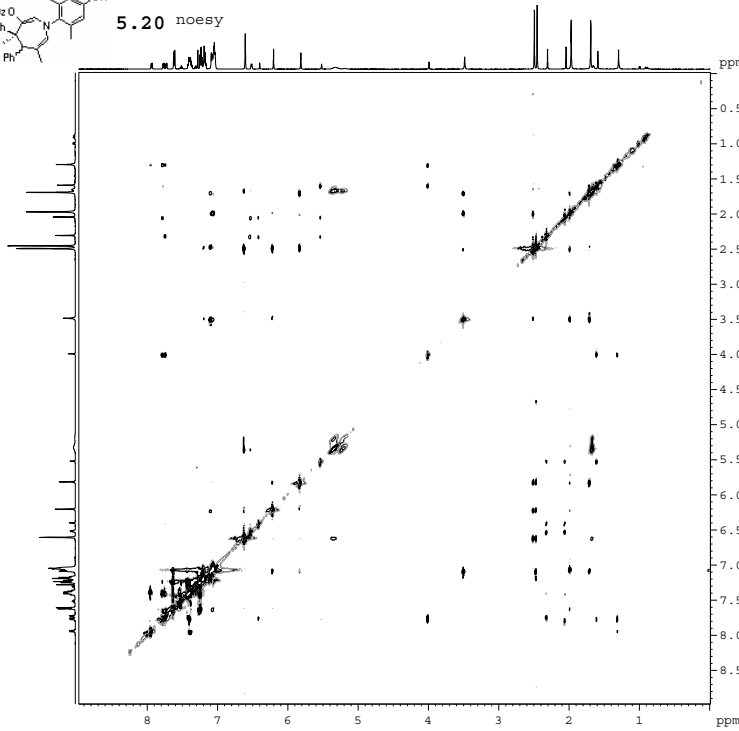








5.20 noesy



Current Data Parameters
 USER nshapiro
 NAME 09-129-noesy-2
 EXPNO 11
 PROCNO 1

F2 - Acquisition Parameters
 Date 20080907
 Time 19.35
 INSTRUM AV-500
 PROCNO 5 mm TBI 1H/31
 PULPROG noesypph
 TD 4096
 SOLVENT CDCl3
 NS 2
 DS 4
 SWH 4496.403 Hz
 FIDRES 1.097755 Hz
 AQ 0.458325 sec
 RG 88
 DW 111.200 usec
 DE 7.11 usec
 TE 300.2 K
 D0 0.0001038 sec
 D1 4.0000000 sec
 D8 0.6500000 sec
 D16 0.0001000 sec
 IM0 0.0002231 sec
 MCREST 0.0000000 sec
 MCKK 4.0000000 sec
 TAU 0.32890001 sec

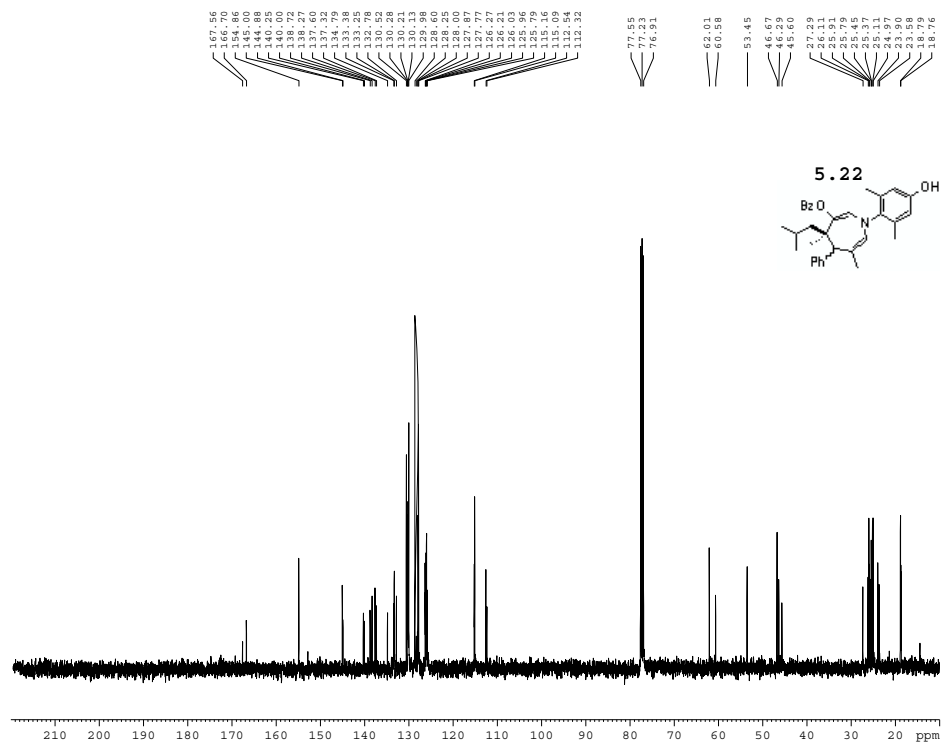
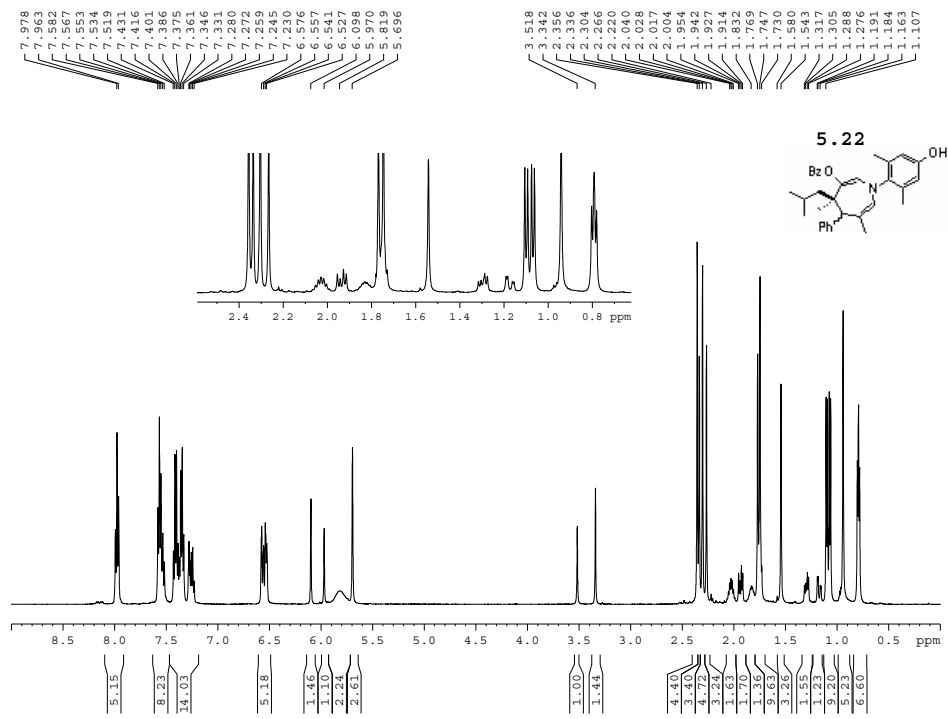
----- CHANNEL f1 -----
 NUCL 1H
 P1 7.60 usec
 P2 15.20 usec
 P11 0.00 dB
 SFO1 500.2322510 MHz

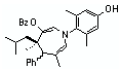
----- GRADIENT CHANNEL -----
 GPRAM1 SINE.100
 GPRAM2 SINE.100
 GPC1 0.00 %
 GPC2 0.00 %
 GPF1 0.00 %
 GPF2 0.00 %
 GPZ1 40.00 %
 GPZ2 40.00 %
 P16 1000.00 usec

F1 - Acquisition parameters
 ND0 1
 TD 128
 SFO1 500.2323 MHz
 FIDRES 35.171638 Hz
 SW 9.000 ppm
 PRMODE TPP1

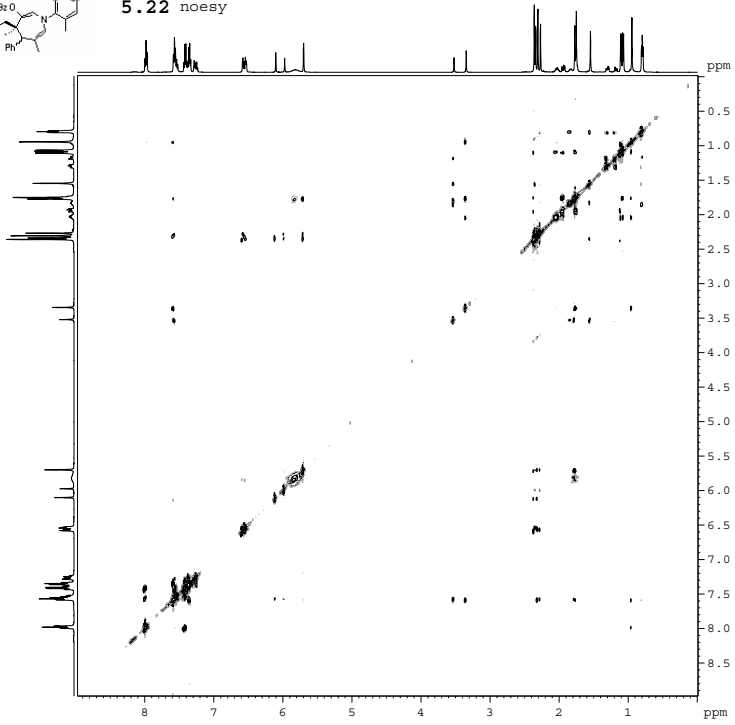
F2 - Processing parameters
 SI 2048
 SF 500.2300104 MHz
 WDW GSIK
 SSB 2
 LB 0.00 Hz
 GB 0
 PC 4.00

F1 - Processing parameters
 SI 2048
 SF 500.2300104 MHz
 WDW GSIK
 SSB 2
 LB 0.00 Hz
 GB 0





5.22 noesy



```

Current Data Parameters
NAME      09-076-noesy
EXPNO    11
PROCNO   1
DU       /4
USER     nshapiro

F2 - Acquisition Parameters
Date_    20080307
Time     19.05
INSTRUM  AV-500
PROBHD   5 mm TBI 1H/31
PULPROG  noesyppm
TD       4096
SOLVENT  CDCl3
NS       2
DS       4
SWH      4496.403 Hz
FIDRES   1.097755 Hz
AQ       0.4556364 sec
RG       88
SM       111.200 use
DE       7.11 use
TE       300.0 K
AQ       0.00010138 sec
D1       5.00000000 sec
DS       0.32889997 sec
D16      0.00010000 sec
SFO1     0.00022313 sec
MCREST   0.00000000 sec
MCMRXX   5.00000000 sec
TAU      0.26389998 sec

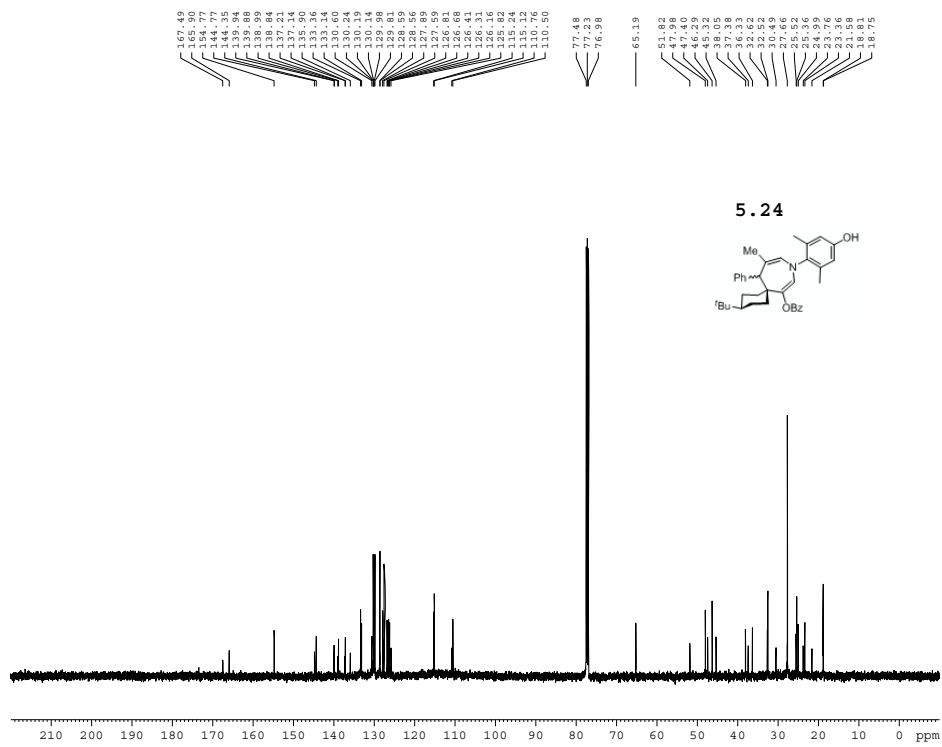
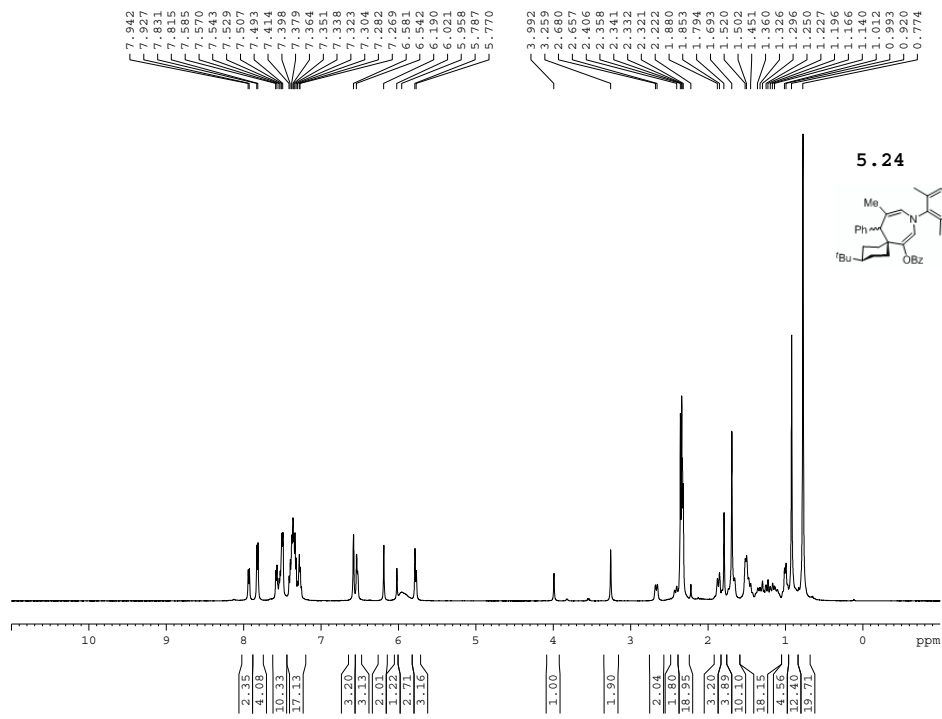
----- CHANNEL f1 -----
NUC1     1H
P1       7.60 use
P2       15.20 use
PC1      0.00 GB
SFO1     500.2322510 MHz

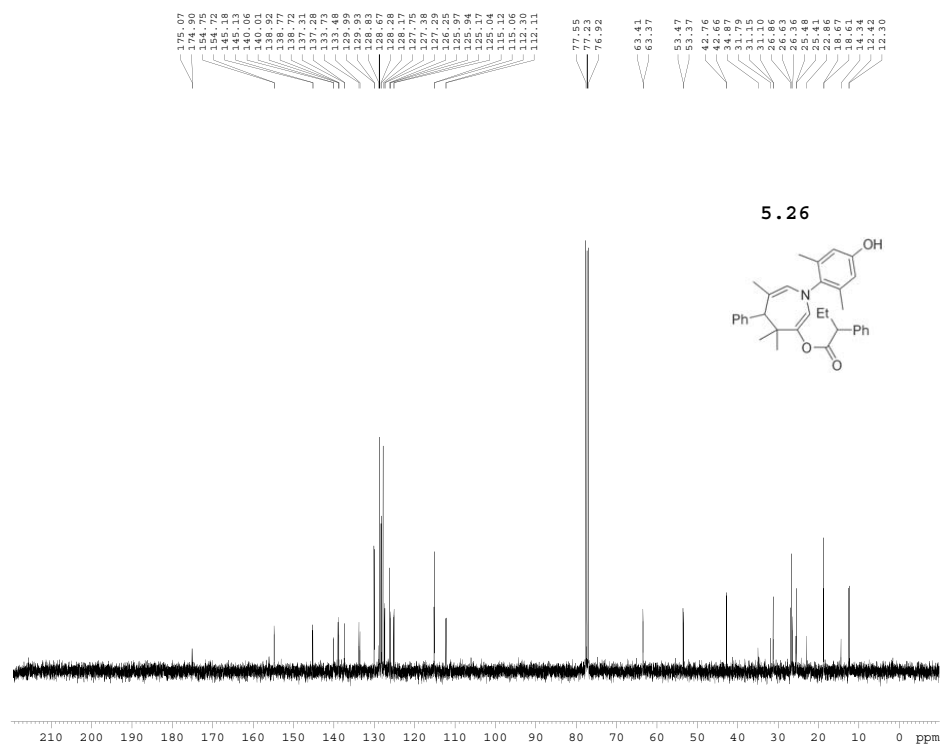
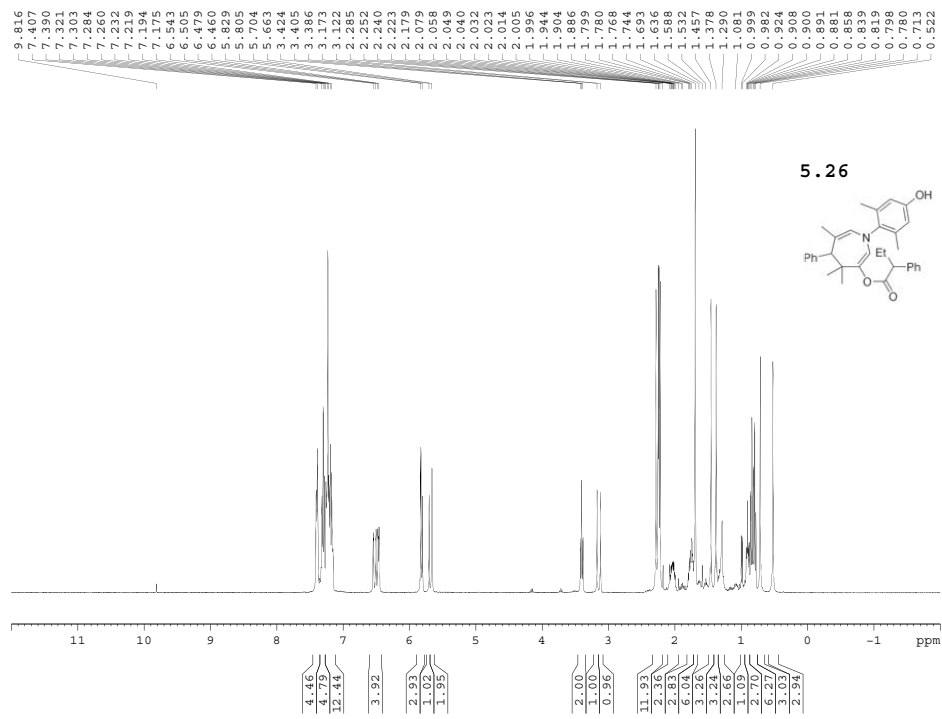
----- GRADIENT CHANNEL ---
GPMAG1   SINE.100
GPMAG2   SINE.100
GP11     0.00 %
GP12     0.00 %
GP13     0.00 %
GP14     0.00 %
GP15     40.00 %
GP16     -40.00 %
P16      1000.00 use

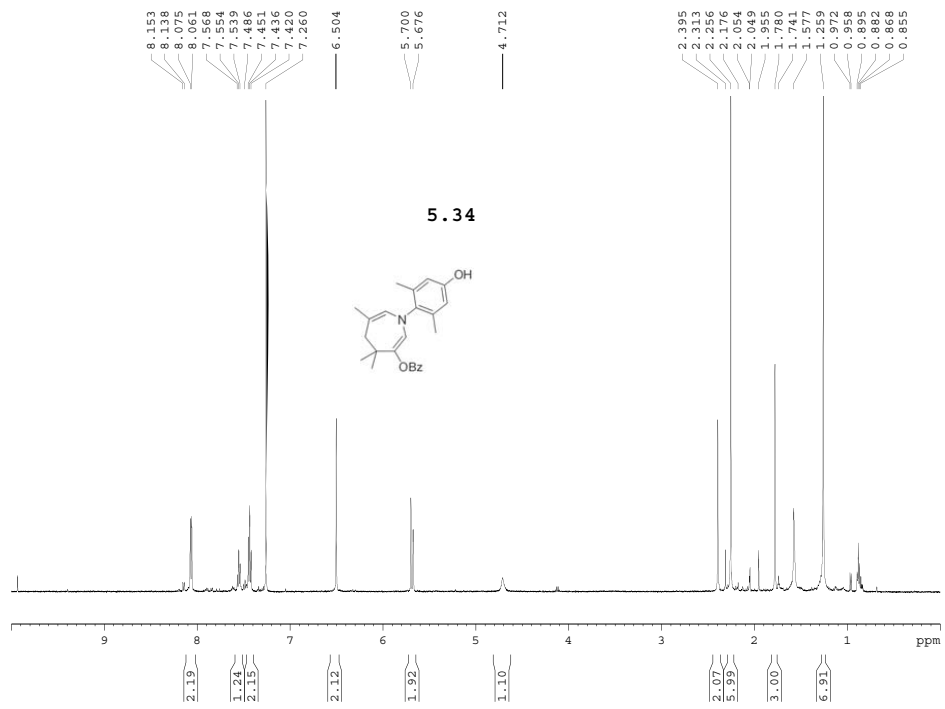
F1 - Acquisition parameters
MD0      1
TD        128
SFO1     500.2323 MHz
FIDRES   35.174638 Hz
SM       9.000 ppm
P0MODE   TBP1

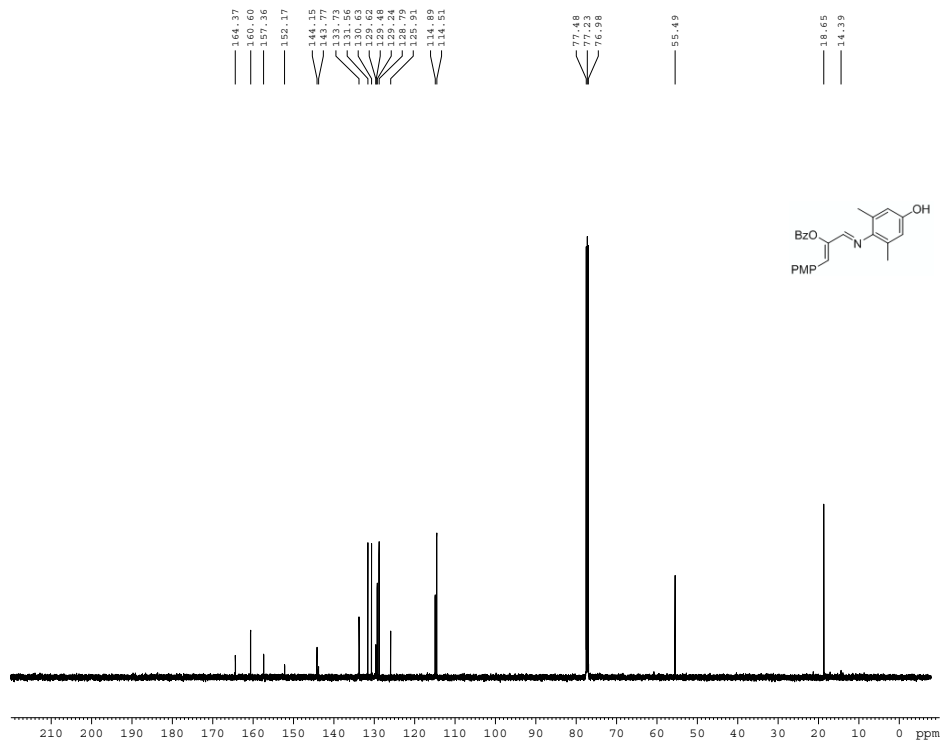
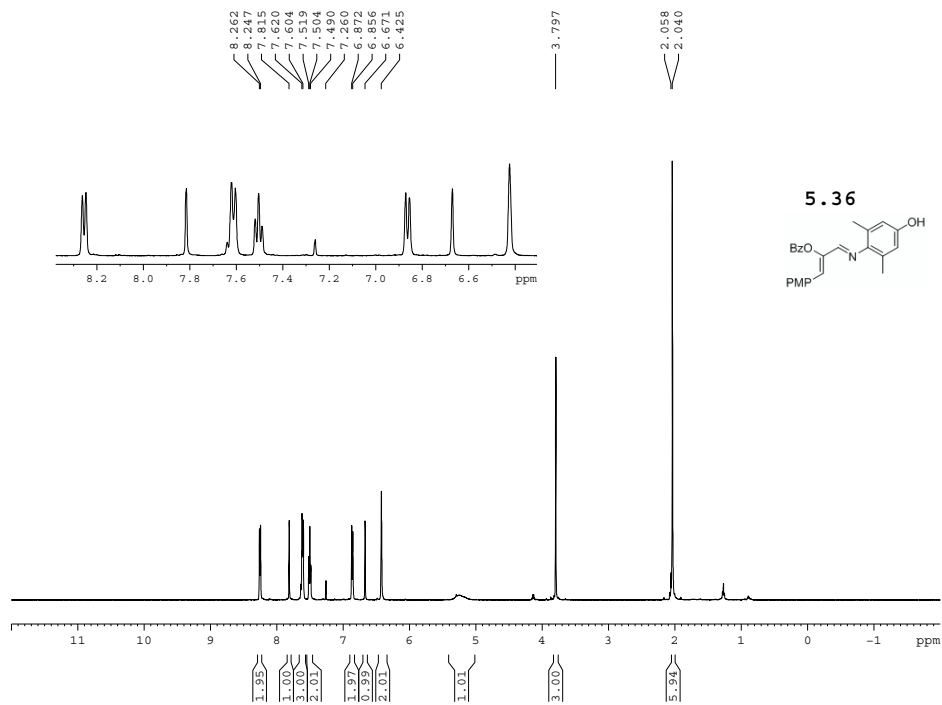
F2 - Processing parameters
SI       2048
SF       500.2300104 MHz
WDW      QSINE
SSB      0
LB       0.00 Hz
GB       0
PC       4.00

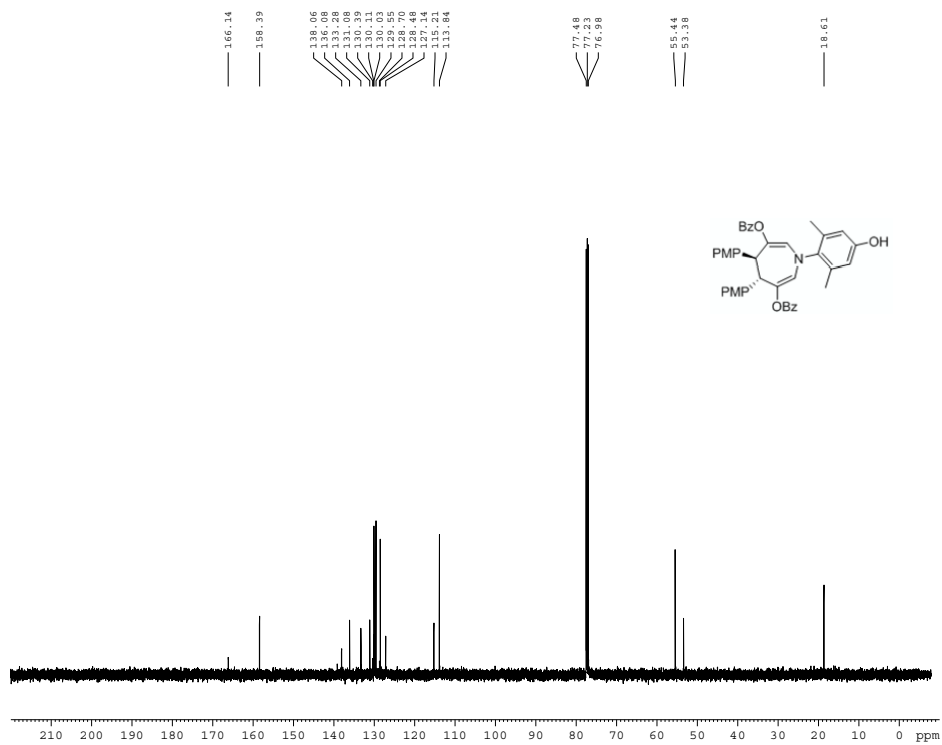
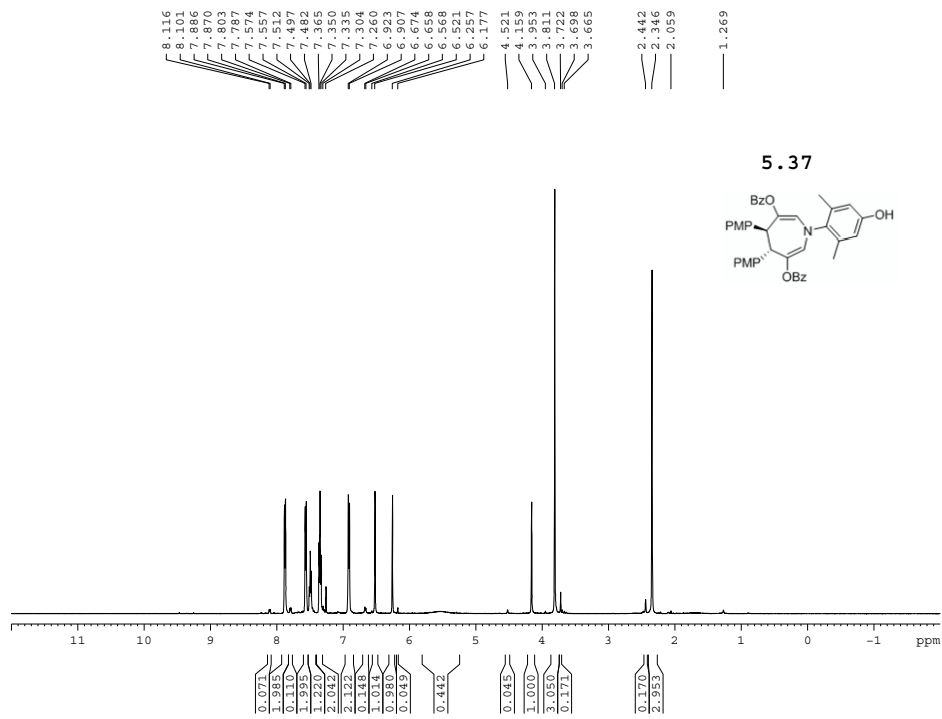
F1 - Processing parameters
SI       2048
WDW      TBP1
SF       500.2300104 MHz
WDW      QSINE
SSB      2
LB       0.00 Hz
GB       0
  
```

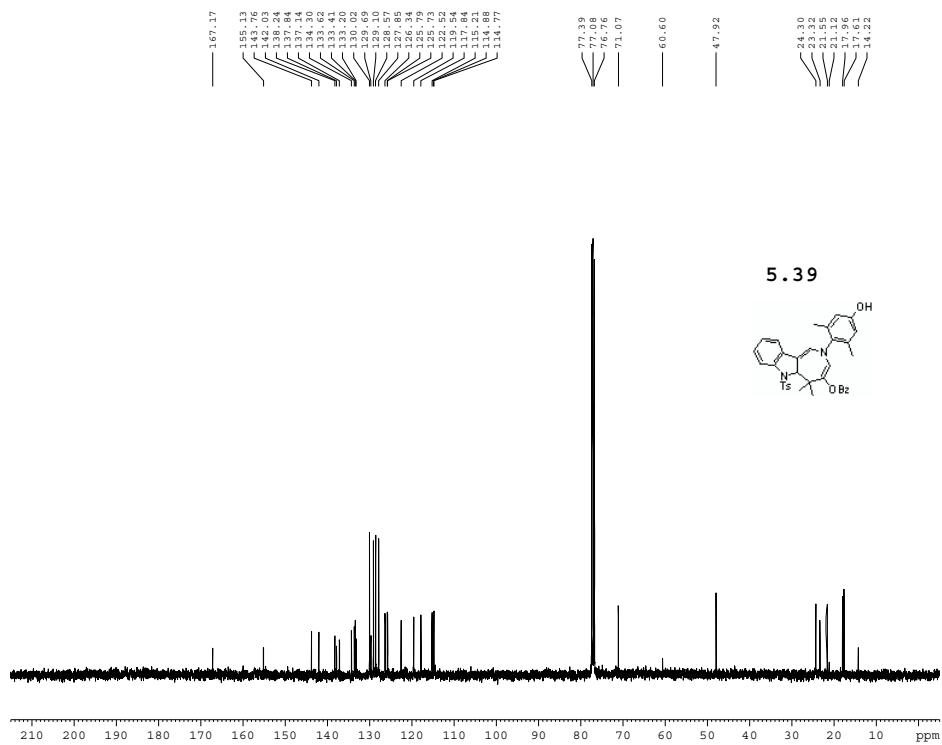
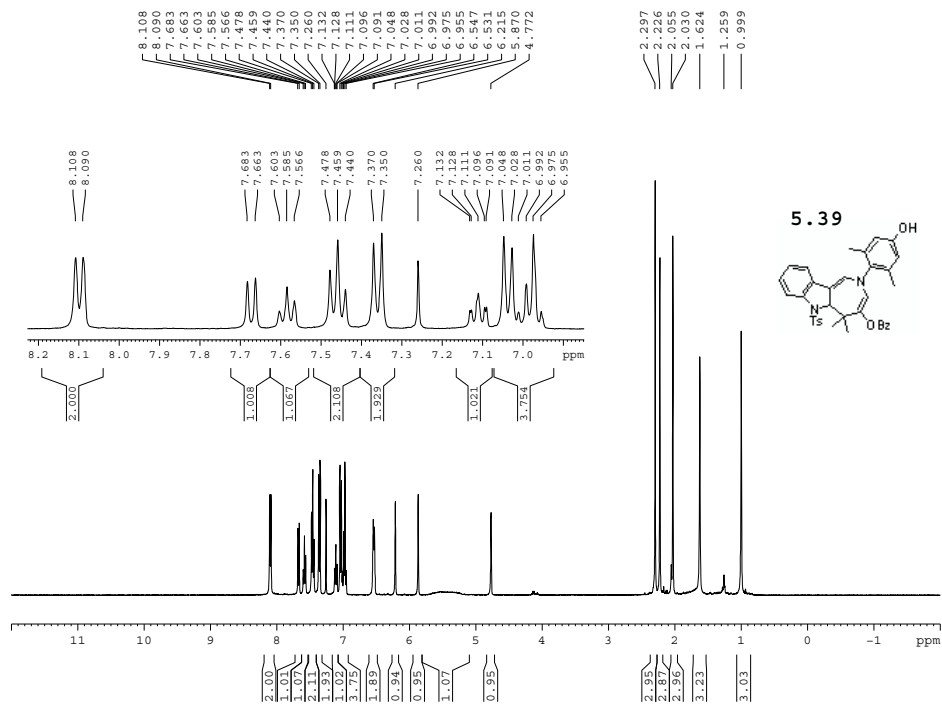



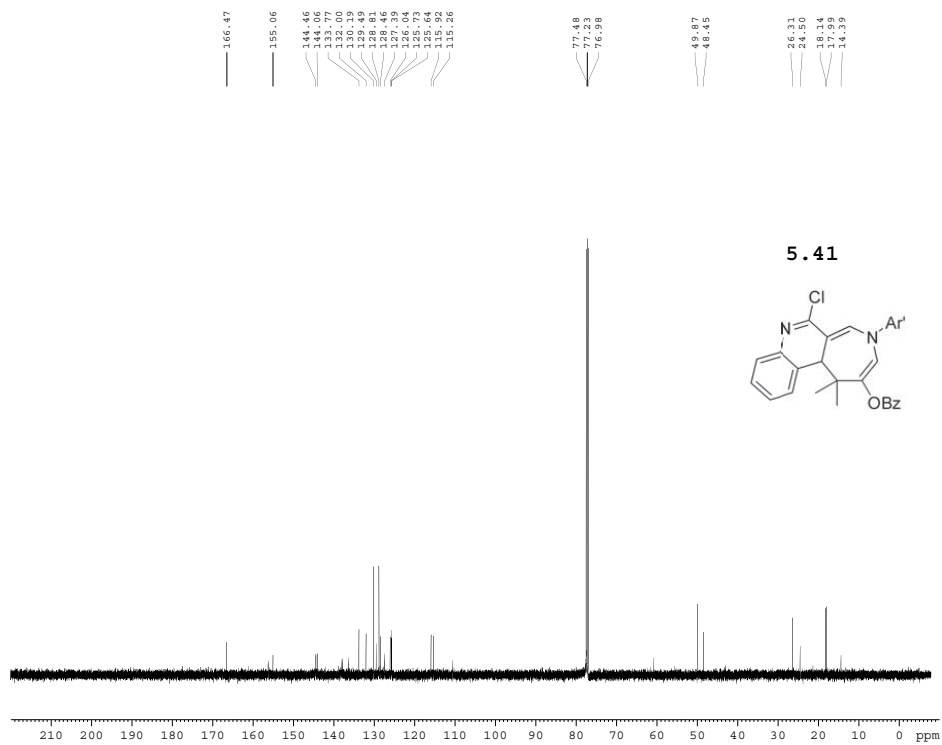
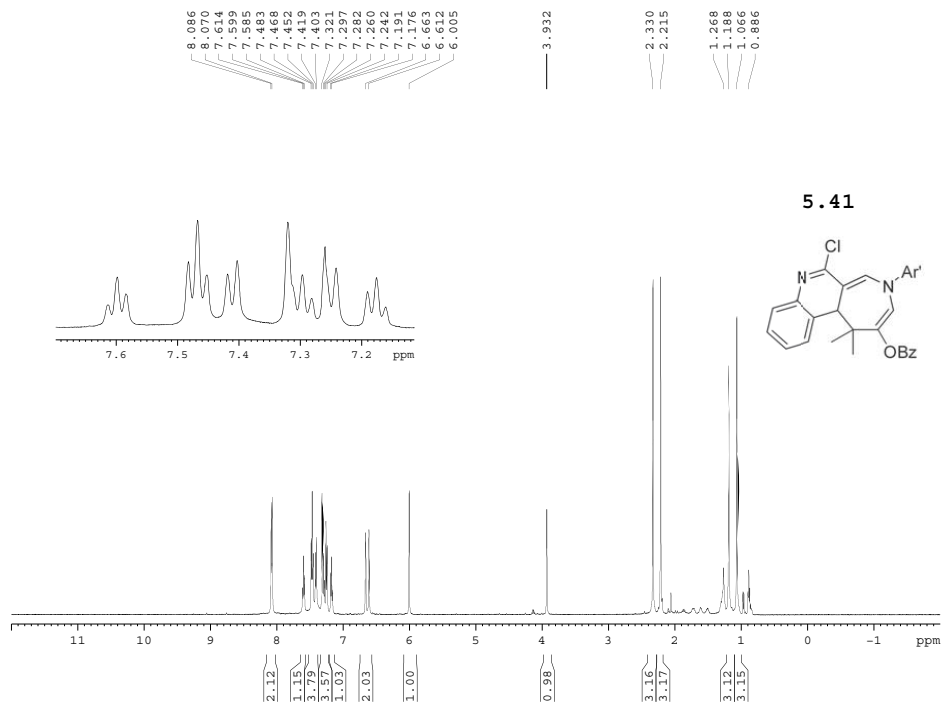


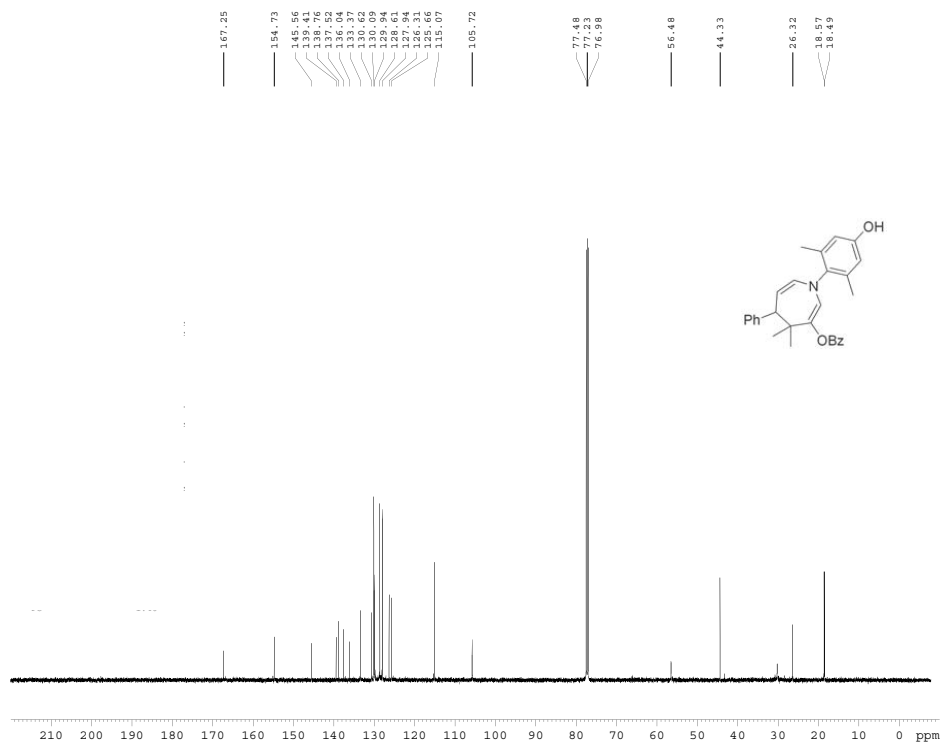
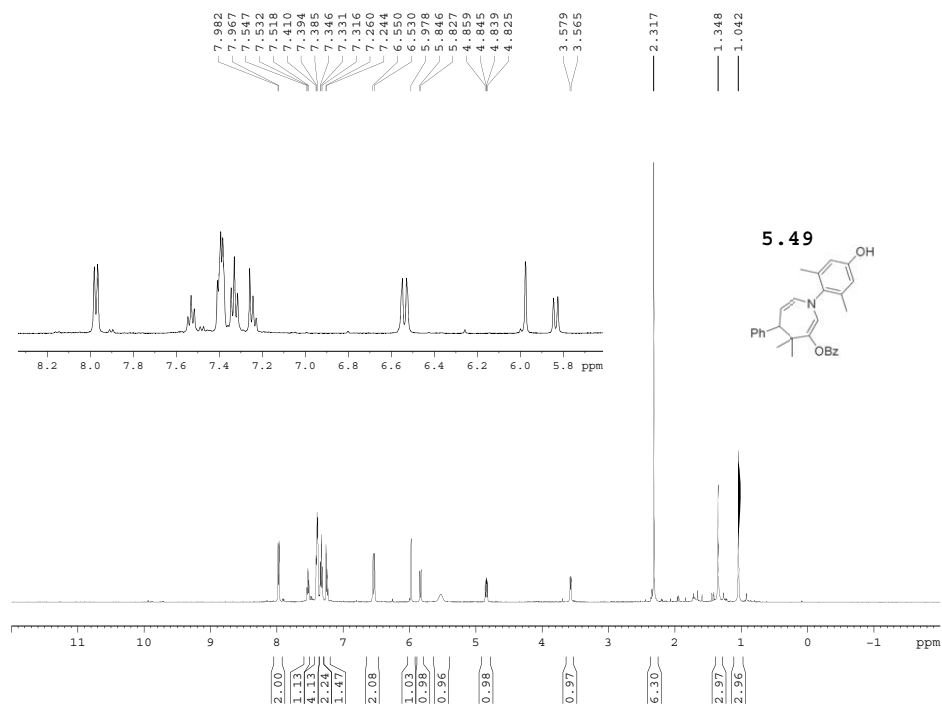


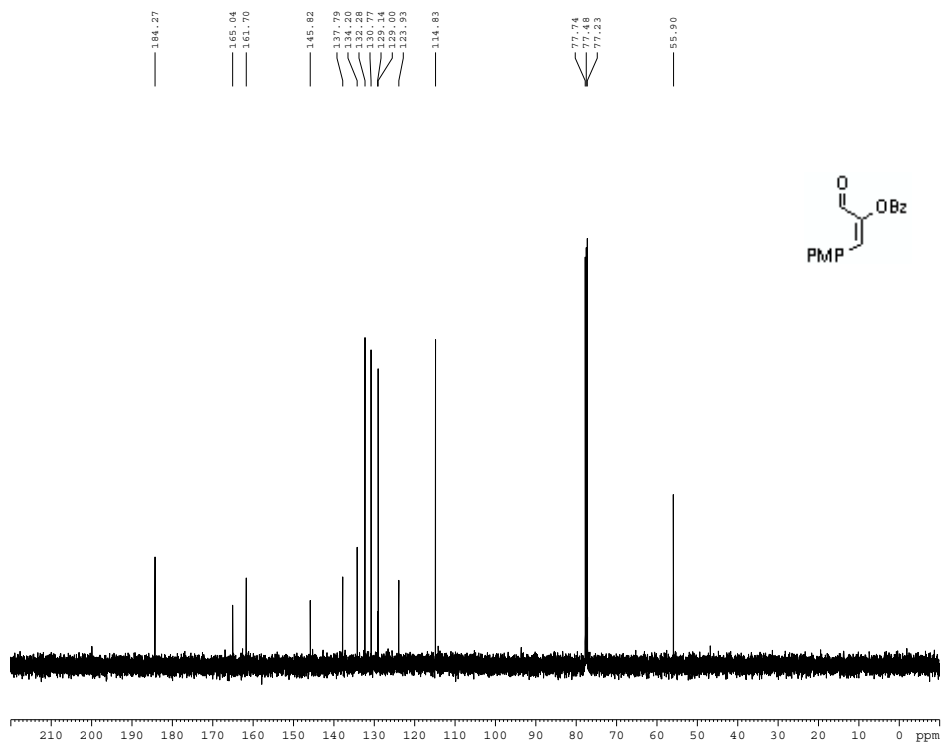
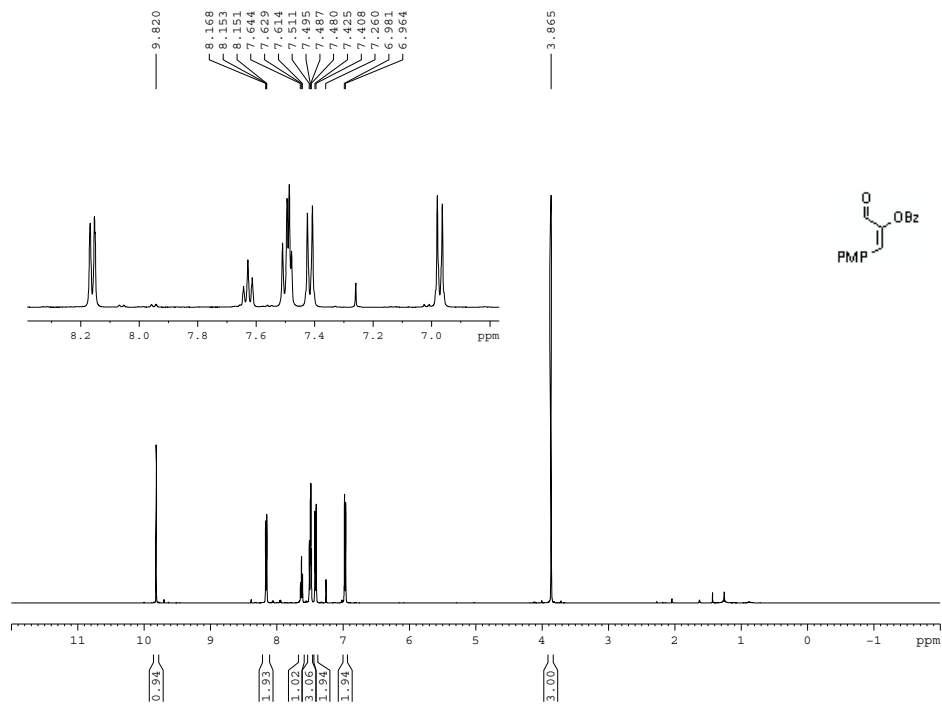


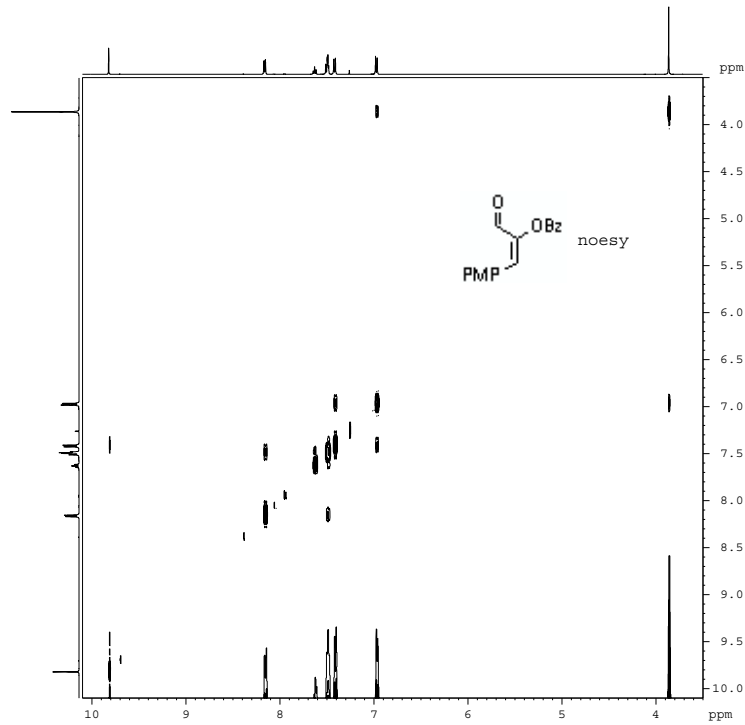












```

Current Data Parameters
NAME      09-1496
EXPNO    11
PROCNO   1
DU       /u
USER     nbapiro

F2 - Acquisition Parameters
Date      20080601
Time      13.22
INSTRUM   AV-500
PROBHD    5 mm TBI 1H/31
PULPROG   noesyppg3
TD         4096
SOLVENT   CDCl3
NS         1
DS         1
SWH        3591.954 Hz
FIDRES     0.876942 Hz
AQ         0.3703824 sec
RG         60
DM         139.200 usec
DE         7.11 usec
TE         300.2 K
d0         0.00012915 sec
D1         5.00000000 sec
D8         2.09999990 sec
D16        0.00010000 sec
IRF        0.00027765 sec
MCREST     0.00000000 sec
MORPH      0.00000000 sec
TAU        1.04890001 sec

----- CHANNEL f1 -----
NUC1       1H
P1         7.60 usec
PC         15.20 usec
PL1        0.00 dB
SFO1       500.233515 MHz

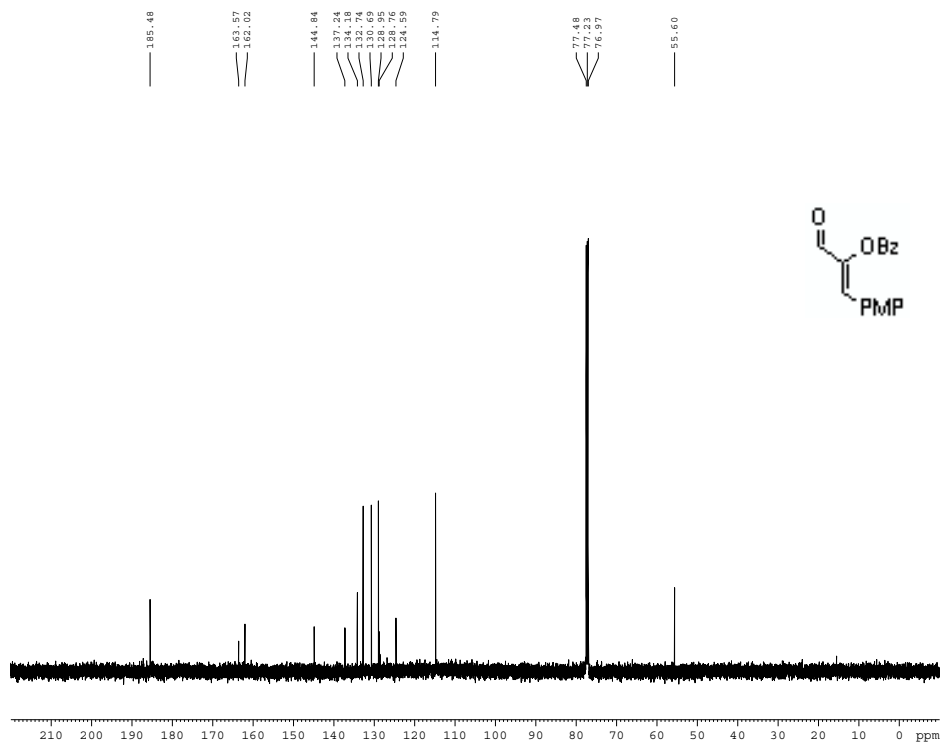
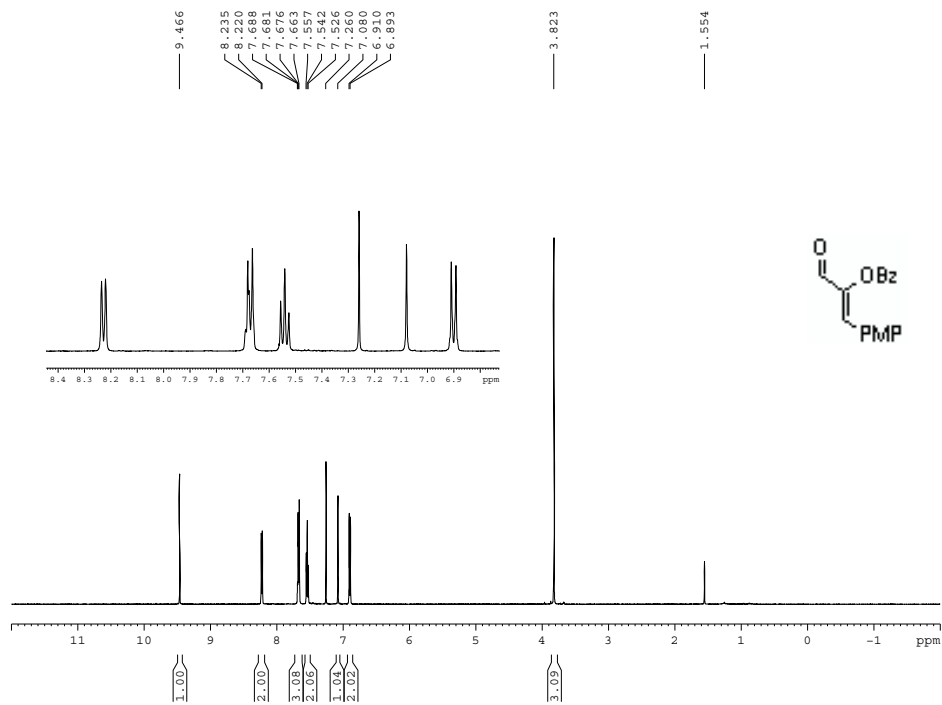
----- GRADIENT CHANNEL -----
GPRAM1     SINE 100
GPRAM2     SINE 100
GPX1       0.00 %
GPX2       0.00 %
GPF1       0.00 %
GPF2       0.00 %
GPE1       40.00 %
GPE2       +40.00 %
P16        1000.00 usec

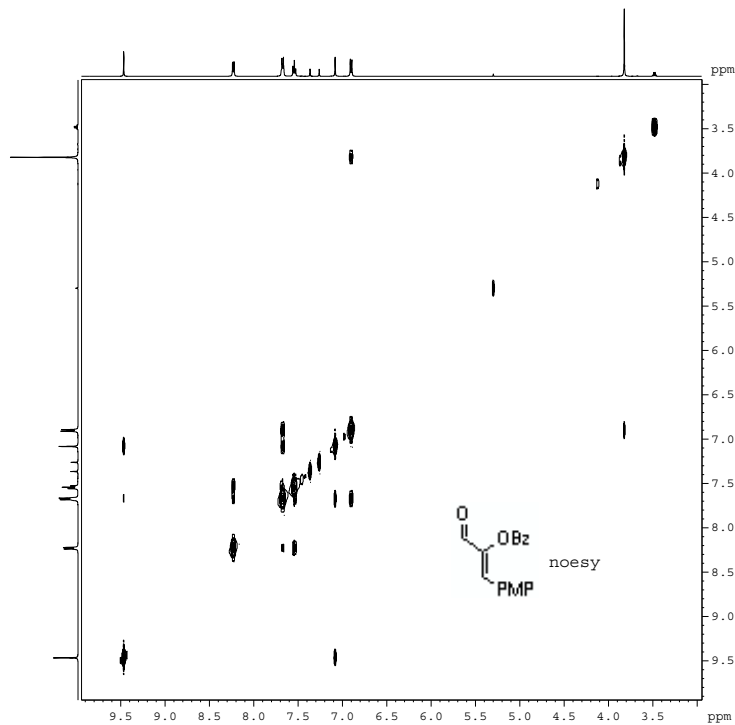
F1 - Acquisition parameters
RG         128
SFO1       500.2334 MHz
FIDRES     28.137943 Hz
SW         7.200 ppm
PULPROG   zgpg30

F2 - Processing parameters
SI         2048
SF         500.2300104 MHz
WDW        COSINE
SSB        0
LB         0.00 Hz
GB         0
PC         4.00

F1 - Processing parameters
SI         2048
WDW        zgpg30
SF         500.2300104 MHz
WDW        COSINE
SSB        0
LB         0.00 Hz
GB         0

```





```

Current Data Parameters
NAME      U9-149C-2
EXPRO    11
PROCNO   1
SU       1
USER     nshapiro

F2 - Acquisition Parameters
Date_    20080501
Time     12.43
INSTRUM  AV-500
PROBHD   5 mm TBI 1H/31
PULPROG  noesypph
TD       4096
SOLVENT  CDCl3
NS       2
DS       8
SWH      1501.401 Hz
FIDRES   0.854834 Hz
AQ       0.5851016 sec
RG       222
DM       142.800 usec
DE       7.11 usec
TE       300.0 K
CO       0.0013132 sec
D1       5.0000000 sec
D8       2.0000000 sec
D16      0.00010000 sec
IND      0.00028559 sec
MCREST   0.0000000 sec
MCMRG    5.0000001 sec
TAU      1.0489001 sec

----- CHANNEL f1 -----
NUC1     1H
P1       7.60 usec
P2       15.20 usec
PL1      0.00 dB
SFO1     500.232515 MHz

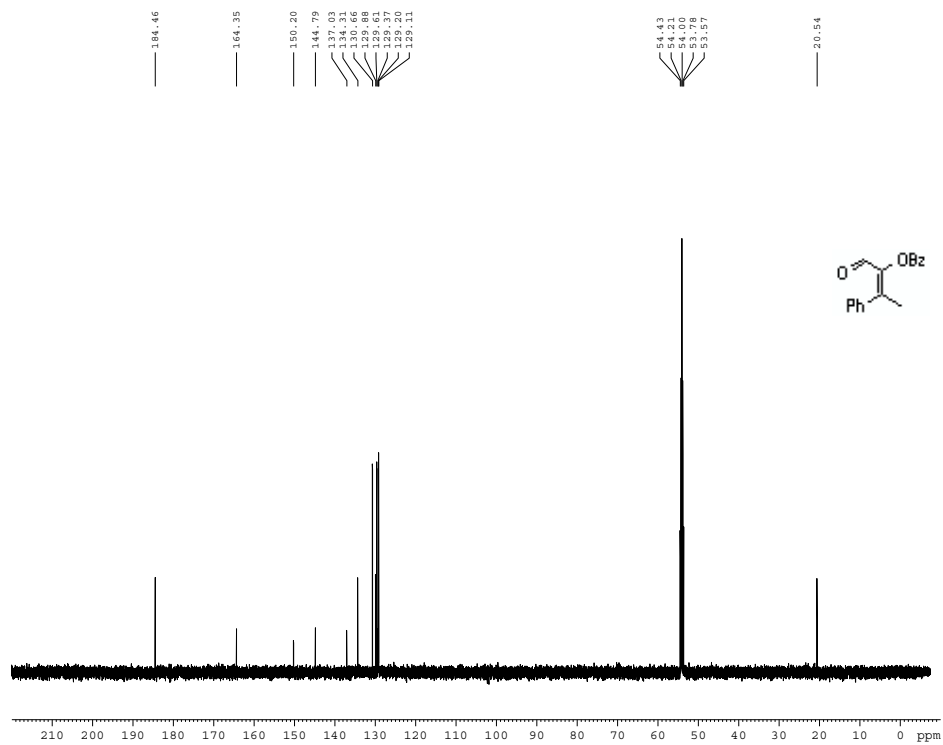
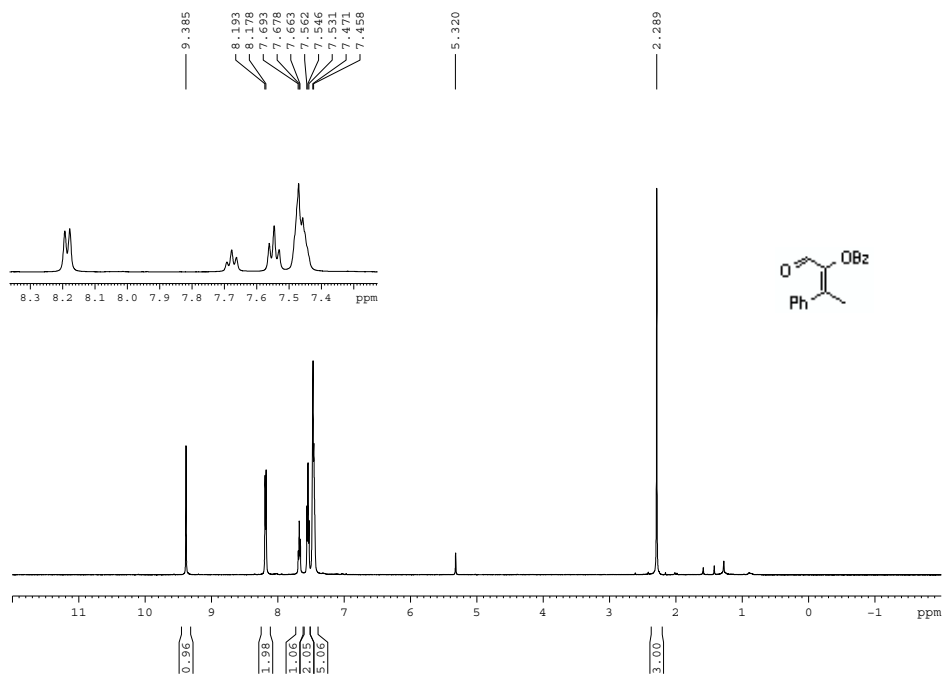
----- GRADIENT CHANNEL -----
GPRAM1   SINE.100
GPRAM2   SINE.100
GPF1     0.00 %
GPF2     0.00 %
GPF3     0.00 %
GPF4     0.00 %
GPF5     40.00 %
GPF6     40.00 %
P16      1000.00 usec

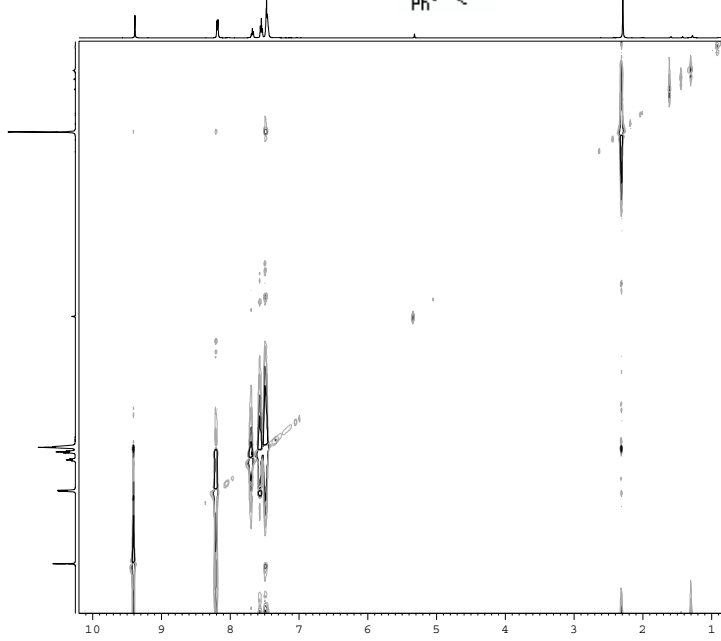
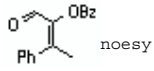
F1 - Acquisition parameters
ND0      1
TD       1
SFO1     500.2333 MHz
FIDRES   27.193888 Hz
SW       7.000 ppm
FREQCEN  TMR1

F2 - Processing parameters
SI       2048
SF       500.2300289 MHz
WDW      Q91NF
SSB      2
LB       0.00 Hz
GB       0
FC       4.00

F1 - Processing parameters
SI       2048
MC2      TMR1
SF       500.2300288 MHz
WDW      Q91NF
SSB      2
LB       0.00 Hz
GB       0

```





```

Current Data Parameters
NAME          09-112A
EXPNO        11
PROCNO       1
F2           fu
USER         rshapiro

PPM F2 - Acquisition Parameters
Date_        20080427
Time         10.21
INSTRUM      DRX-500
PROBHD       5 mm BBO BB-1H
PULPROG      noesyzgpg3
TD           2048
SOLVENT      CDCl3
NS           1
DS           4
SWH          5000.000 Hz
FIDRES       2.441406 Hz
AQ           0.2048500 sec
RG           128
AQ           100.000 usec
DE           7.11 usec
TE           293.0 K
CO           0.0008444 sec
C1           6.0000000 sec
C2           2.7300000 sec
C3           0.0002000 sec
C4           0.0019995 sec
MCREST       0.0000000 sec
MCMXK        6.0000000 sec
TAU          1.36380005 sec

4.5 ----- CHANNEL f1 -----
NUC1         1H
P1           12.20 usec
P2           24.40 usec
PL1          -5.00 dB
SFO1         500.1327507 MHz

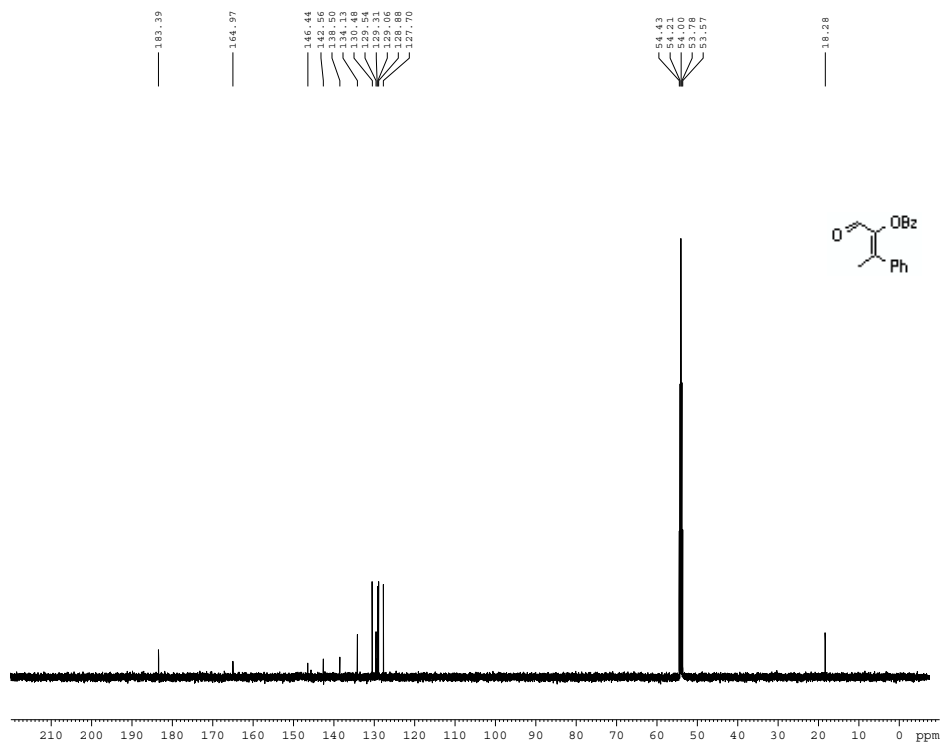
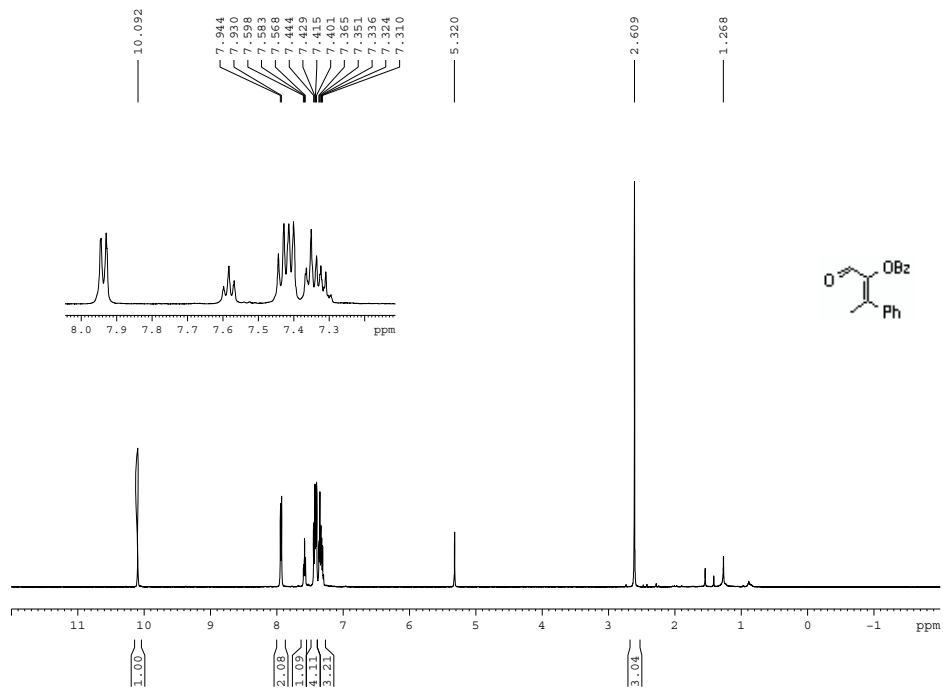
5.5 ----- GRADIENT CHANNEL -----
GPRAMP1     SINE.100
GPRAMP2     SINE.100
GPF1        0.00 V
GPF2        0.00 V
GPF3        0.00 V
GPF4        40.00 V
GPF5        -40.00 V
P16         1000.00 usec

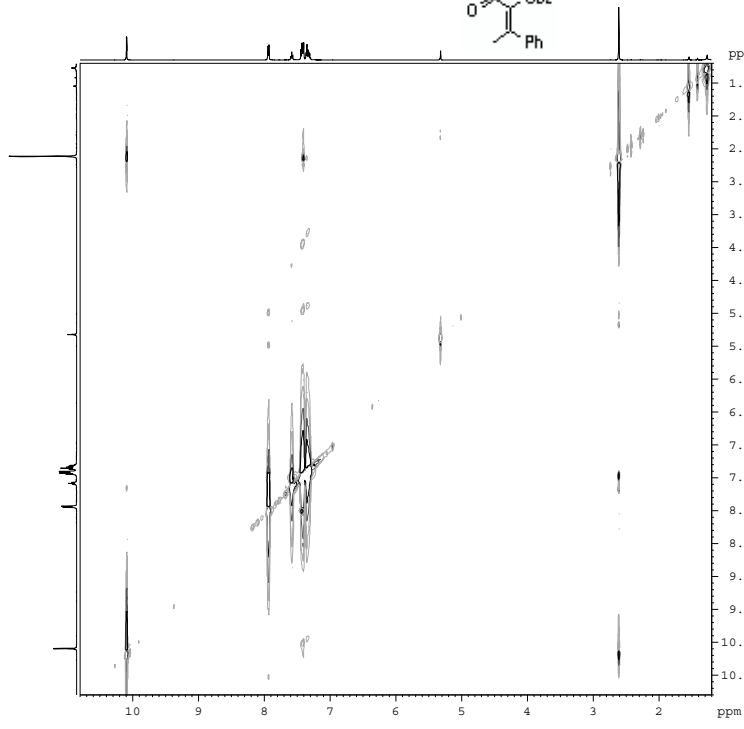
7.0 F1 - Acquisition parameters
NUC1         1
TD           256
SFO1         500.130128 MHz
FIDRES       19.536135 Hz
SF           10.000 ppm
F2MODE       TQF1

8.0 F2 - Processing parameters
SI           1024
SF           500.1300128 MHz
MSWB        QSINE
SUB         2
LB           0.00 Hz
GB           0
PC           5.00

9.5 F1 - Processing parameters
SI           256
NUC1         1H
SF           500.1300128 MHz
MSWB        QSINE
SUB         2
LB           0.00 Hz
GB           0

```





```

Current Data Parameters
NAME          09-128
EXPNO         1
PROCNO        1
DU            /s
USER          nabapiro

F2 - Acquisition Parameters
Date_         20080427
Time          11.13
INSTRUM      DRX-500
PROBHD       5 mm BBO BB-1H
PULPROG      zgpg30
TD            2048
SOLVENT      CDCl3
NS            2
DS            4
SWH           5000.000 Hz
FIDRES       2.441406 Hz
AQ           0.2048500 sec
RG            128
SW           100.000 use
DE           7.11 use
TE           293.0 K
D0           0.0000844 sec
D1           4.0000000 sec
D8           2.1199989 sec
D16          0.0002000 sec
IN0           0.0001999 sec
MCREST       0.0000000 sec
MCRMK        4.0000000 sec
TAU          1.0587999 sec

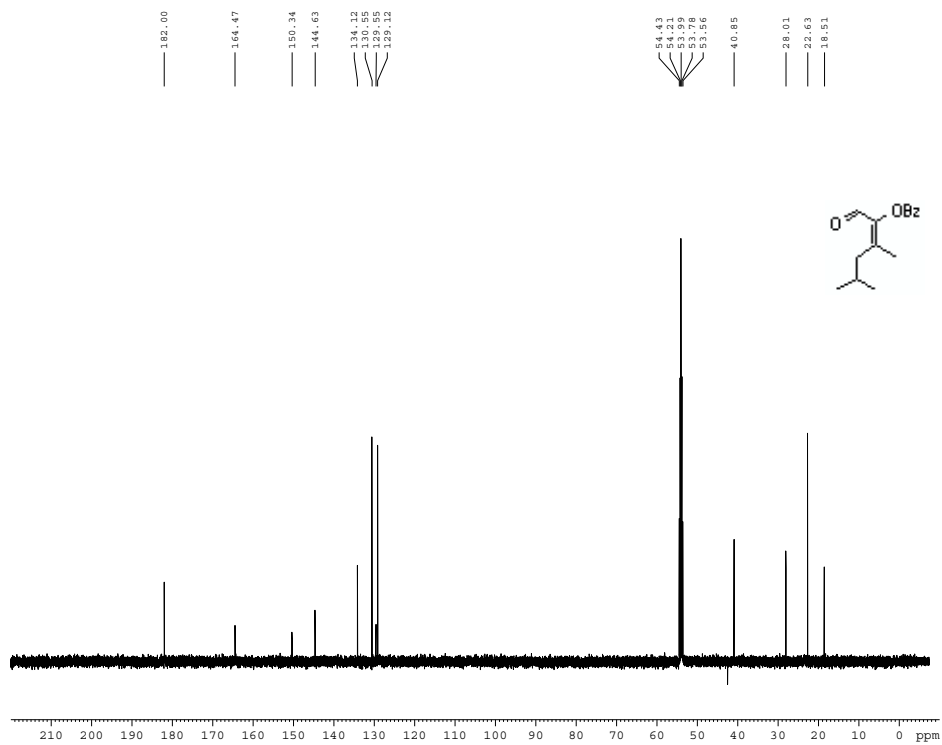
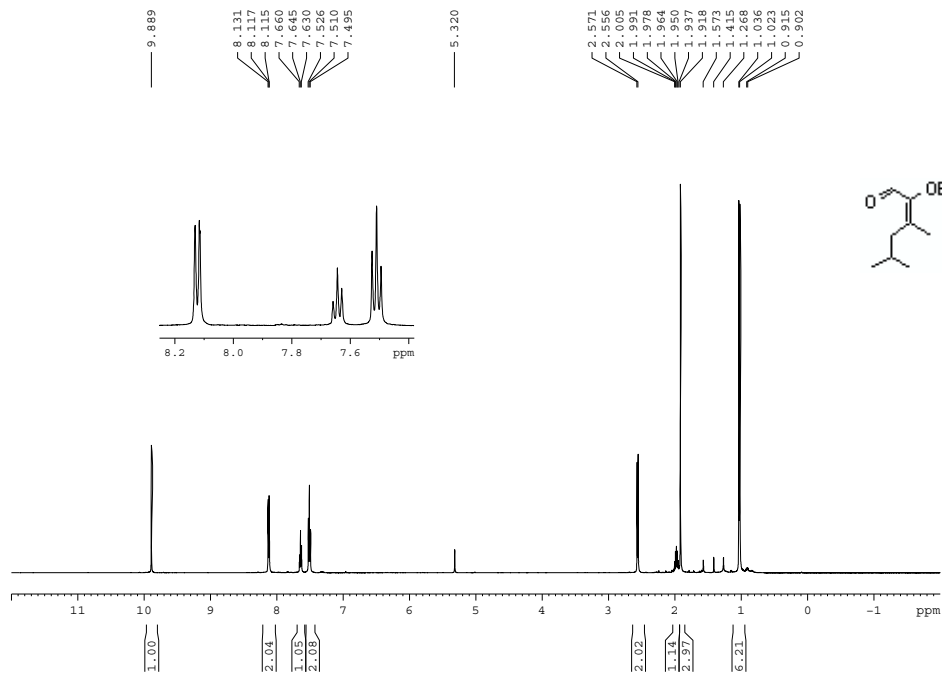
----- CHANNEL f1 -----
NUC1          1H
P1            12.20 use
P2            24.40 use
PL1           -5.00 dB
SFO1          500.1330008 MHz

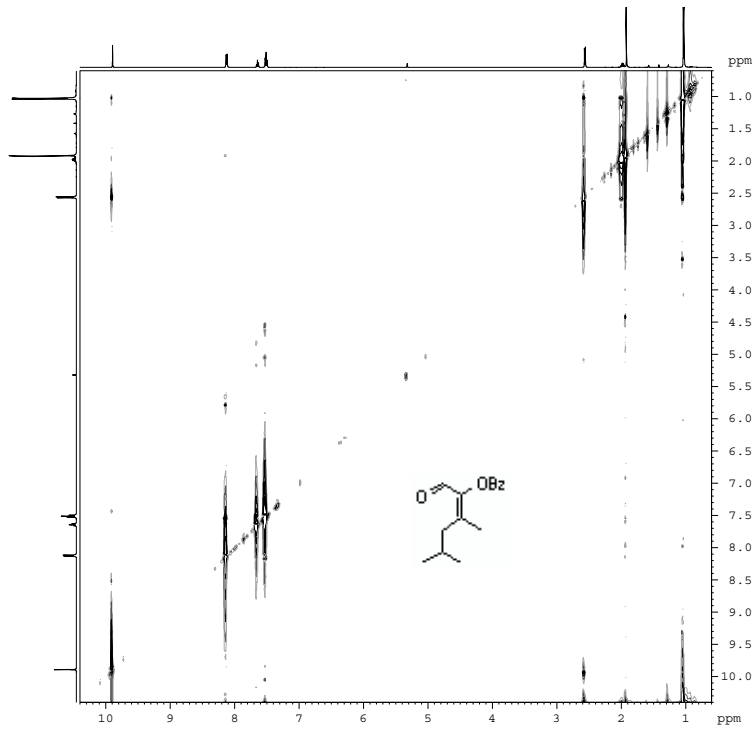
----- GRADIENT CHANNEL ---
GPRAM1       SINE 100
GPRAM2       SINE 100
GPF1         0.00 %
GPF2         0.00 %
GPF3         0.00 %
GPF4         0.00 %
GPF5         40.00 %
GPF6        -40.00 %
P16          1000.00 use

F1 - Acquisition parameters
NUC          1
TD            256
SFO1         500.133 MHz
FIDRES       19.536135 Hz
SW           10.000 ppm
P1MODE       TPP1

F2 - Processing parameters
SI            1024
SF           500.1300127 MHz
WDW          QSINE
SSB           2
LB            0.00 Hz
GB            0
PC            5.00

F1 - Processing parameters
SI            256
NUC          TPP1
SF           500.1300128 MHz
WDW          QSINE
SSB           2
LB            0.00 Hz
GB            0
  
```

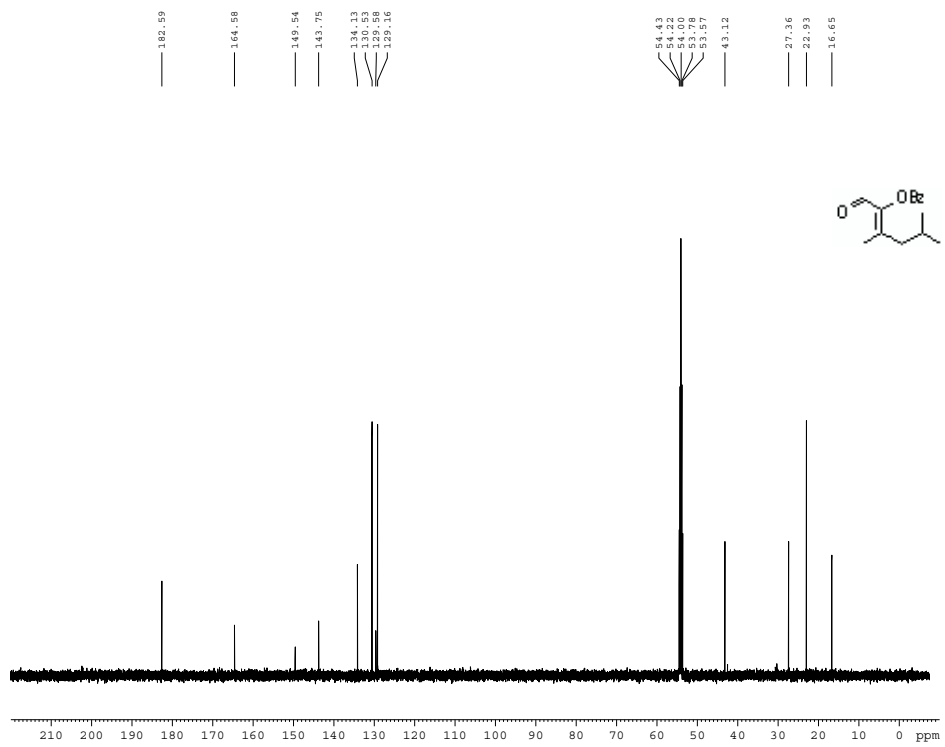
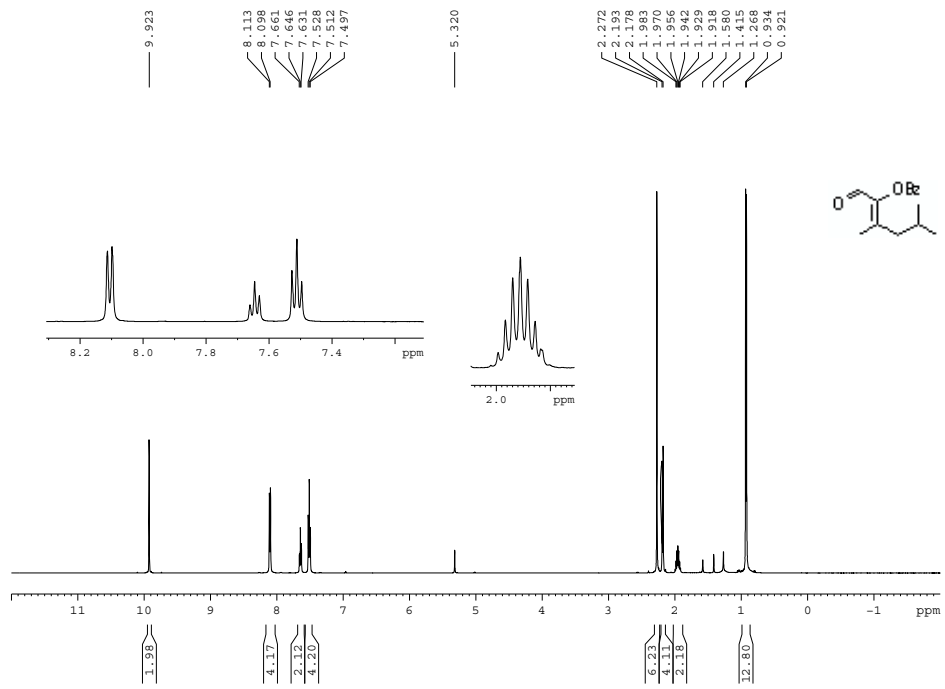



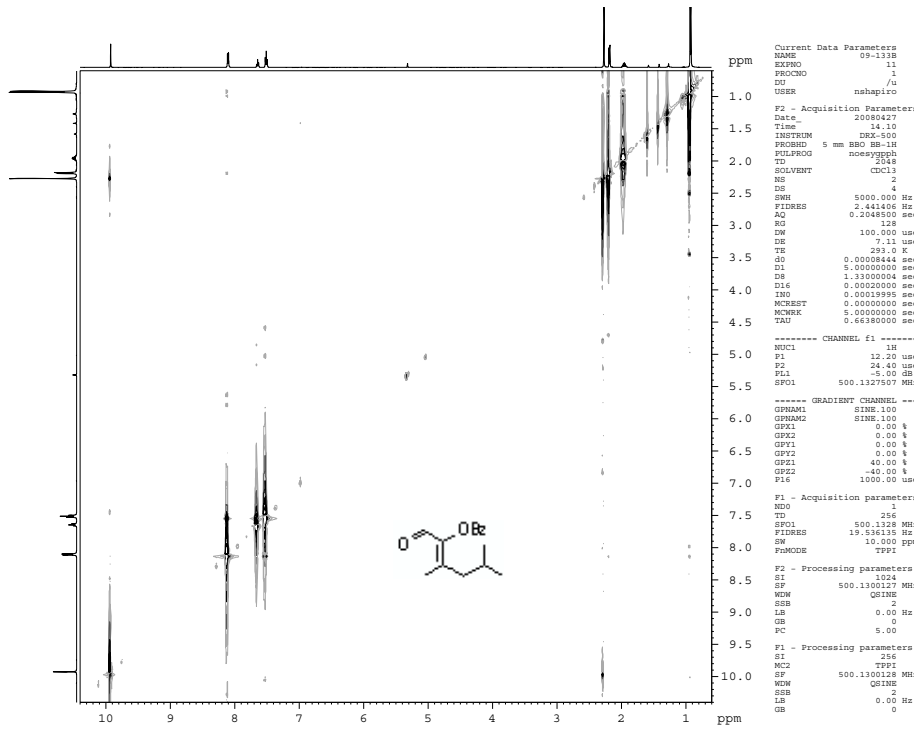


```

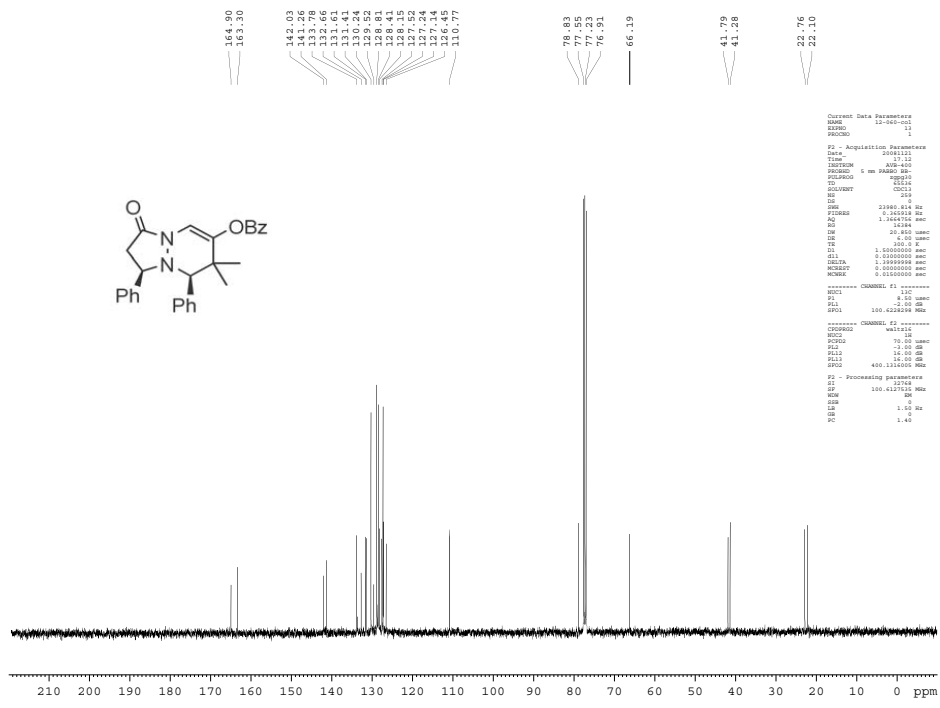
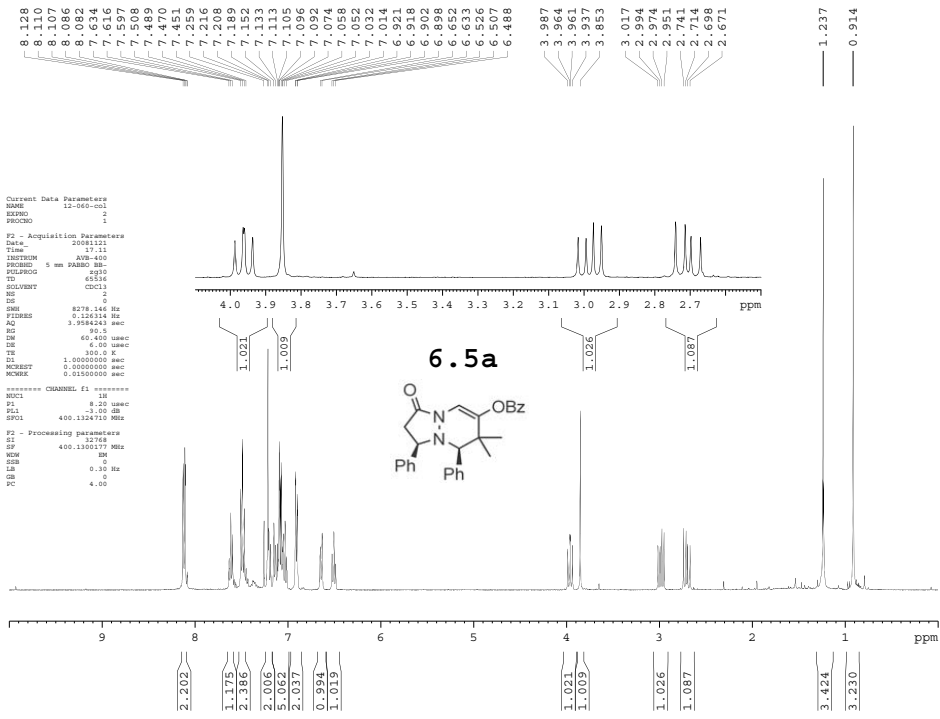
Current Data Parameters
NAME      09-1116
EXPNO    11
PROCNO   11
DO       subsp /0
=====
F2 - Acquisition Parameters
Date_    20080427
Time     22.22
INSTRUM  DR3-500
PROBHD   5 mm BBO MM-1H
PULPROG  zgpg30
TD       2648
SOLVENT  CDCl3
NS       1
DS       4
SWH      500.000 Hz
FIDRES   0.441400 Hz
AQ       0.204800 sec
RG       328
DE       100.000 usec
DE2      7.15 usec
TE       293.0 K
CO       0.0000000 sec
D1       1.2000000 sec
D11      0.0000000 sec
D12      0.0000000 sec
D13      0.0000000 sec
D14      0.0000000 sec
D15      0.0000000 sec
D16      0.0000000 sec
D17      0.0000000 sec
D18      0.0000000 sec
D19      0.0000000 sec
D20      0.0000000 sec
D21      0.0000000 sec
D22      0.0000000 sec
D23      0.0000000 sec
D24      0.0000000 sec
D25      0.0000000 sec
D26      0.0000000 sec
D27      0.0000000 sec
D28      0.0000000 sec
D29      0.0000000 sec
D30      0.0000000 sec
===== CHANNEL f1 =====
NUC1     13C
P1       12.00 usec
P2       24.40 usec
PC1      25.00 dB
SFO1     500.1327507 MHz
===== GRADIENT CHANNEL =====
GPMAX1   2.00 usec
GPMAX2   2.00 usec
GPR1     0.00 %
GPR2     0.00 %
GPR3     0.00 %
GPR4     0.00 %
GPR5     0.00 %
GPR6     0.00 %
GPR7     0.00 %
GPR8     0.00 %
GPR9     0.00 %
GPR10    0.00 %
GPR11    0.00 %
GPR12    0.00 %
GPR13    0.00 %
GPR14    0.00 %
GPR15    0.00 %
GPR16    0.00 %
=====
F1 - Acquisition parameters
NUC1     13C
P1       12.00 usec
P2       24.40 usec
PC1      25.00 dB
SFO1     500.1327507 MHz
=====
F2 - Processing parameters
SI       32768
SF       500.1301275 MHz
WDW      EM
SSB      0
LB       0.00 Hz
GB       0
PC       5.00
=====
F1 - Processing parameters
SI       32768
SF       500.1301275 MHz
WDW      EM
SSB      0
LB       0.00 Hz
GB       0

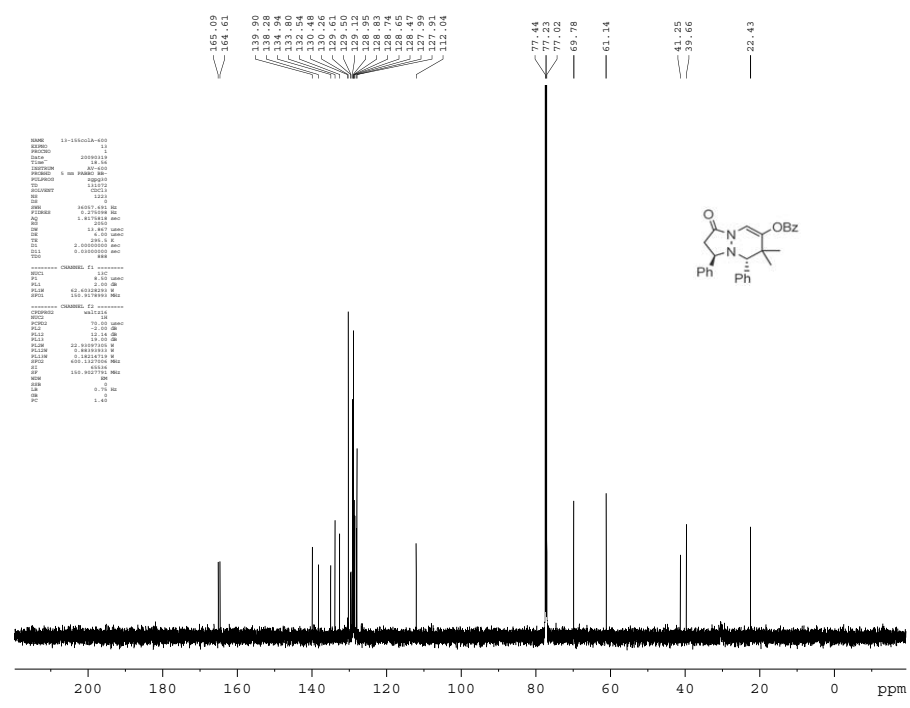
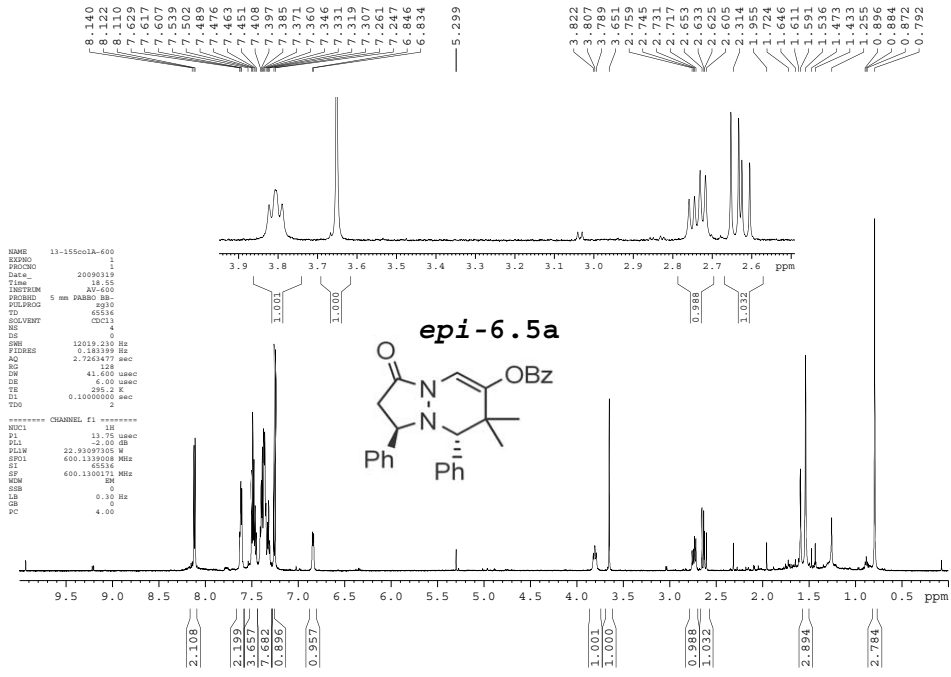
```

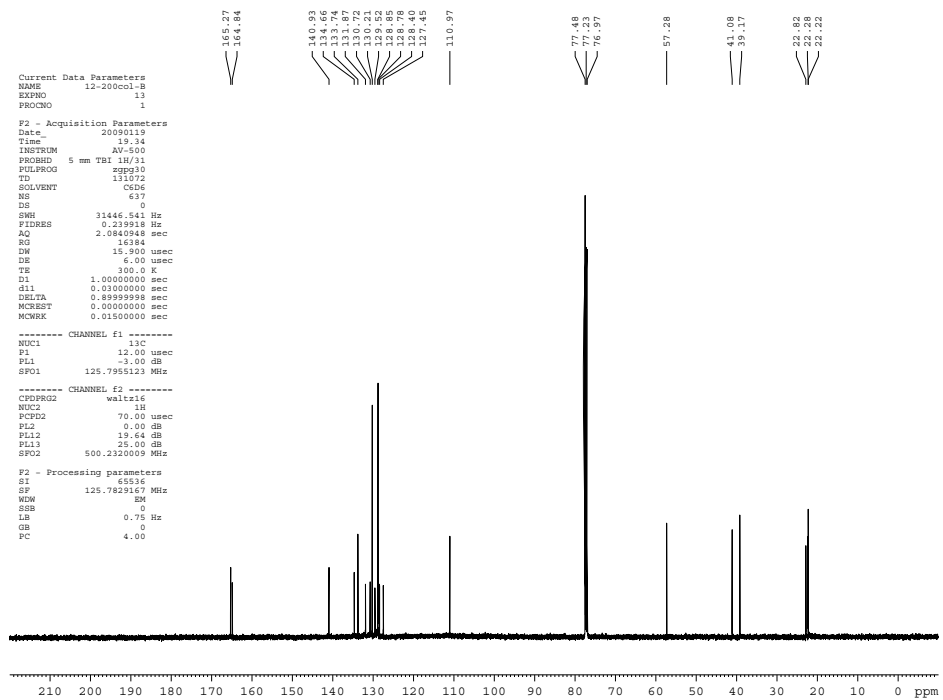
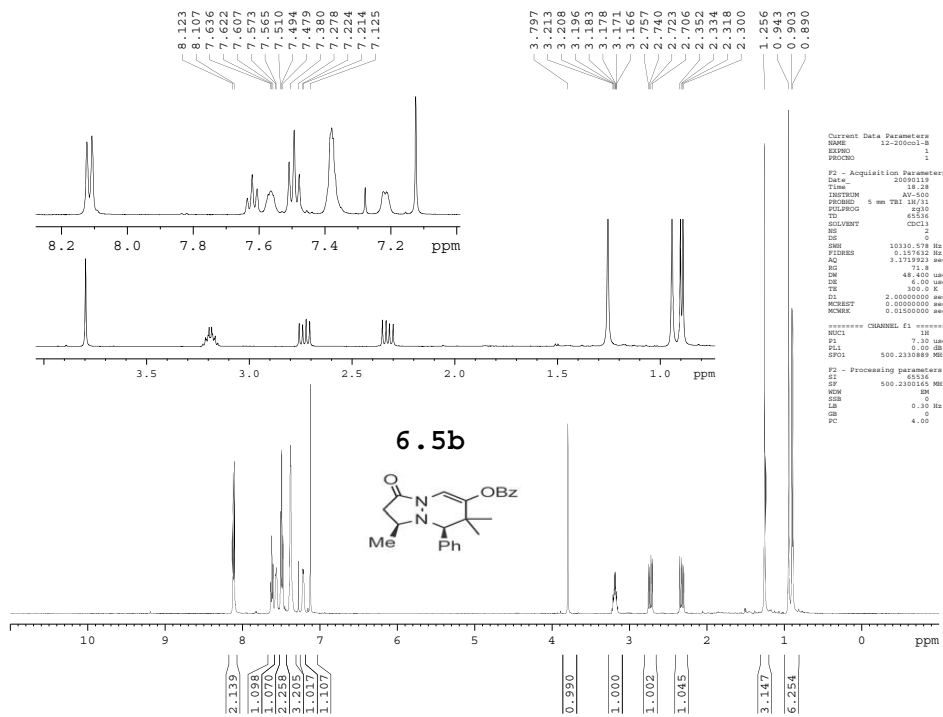




Appendix 6. Additional Supporting Information for Chapter 6







```

Current Data Parameters
NAME 12-20001-B
EXPNO 1
PROCNO 1

F2 - Acquisition Parameters
Date_ 20090119
Time 18.28
INSTRUM AV-500
PROBHD 5 mm TBI 1H/13
PULPROG zgpg30
TD 65536
SOLVENT CDCl3
NS 2
DS 2
SM 10330.578 Hz
FIDRES 0.105612 Hz
AQ 3.1719223 sec
RG 71.4
DE 48.400 usec
TE 300.0 K
D1 2.0000000 sec
MCREST 0.0000000 sec
MCWRR 0.0150000 sec

***** CHANNEL f1 *****
NUC1 13C
P1 7.00 usec
PL1 0.00 dB
SFO1 500.2320009 MHz

F2 - Processing parameters
SI 65536
SF 500.2320145 MHz
WDW EM
SSB 0
LB 0.75 Hz
GB 0
PC 4.00
  
```

```

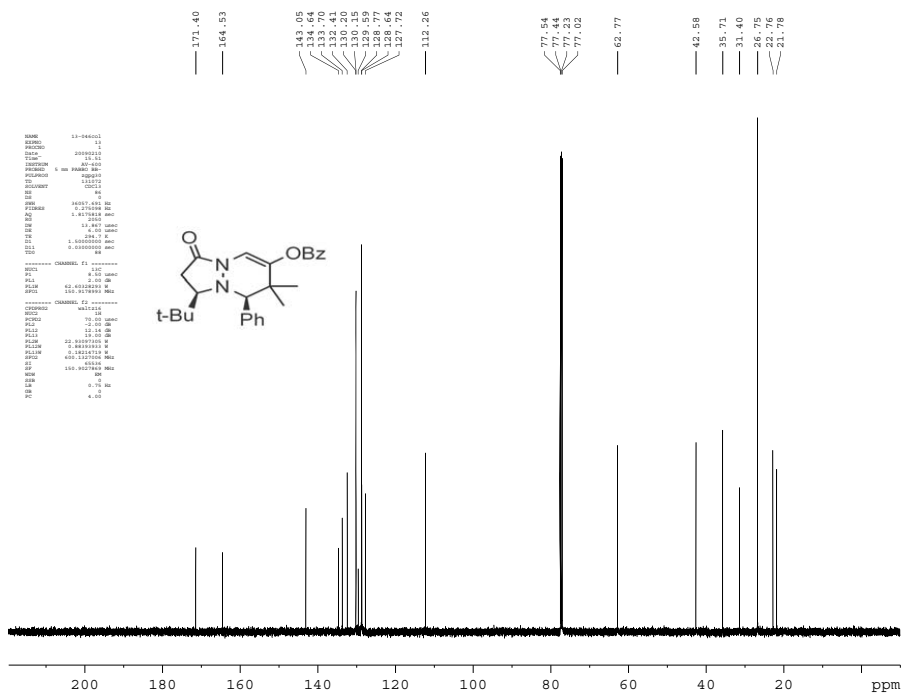
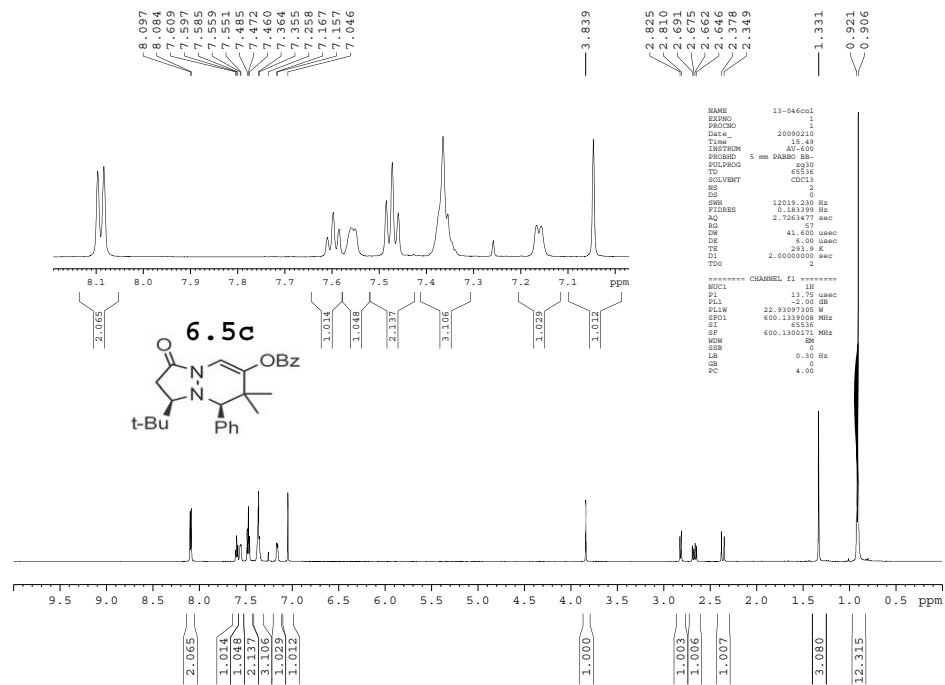
Current Data Parameters
NAME 12-20001-B
EXPNO 13
PROCNO 1

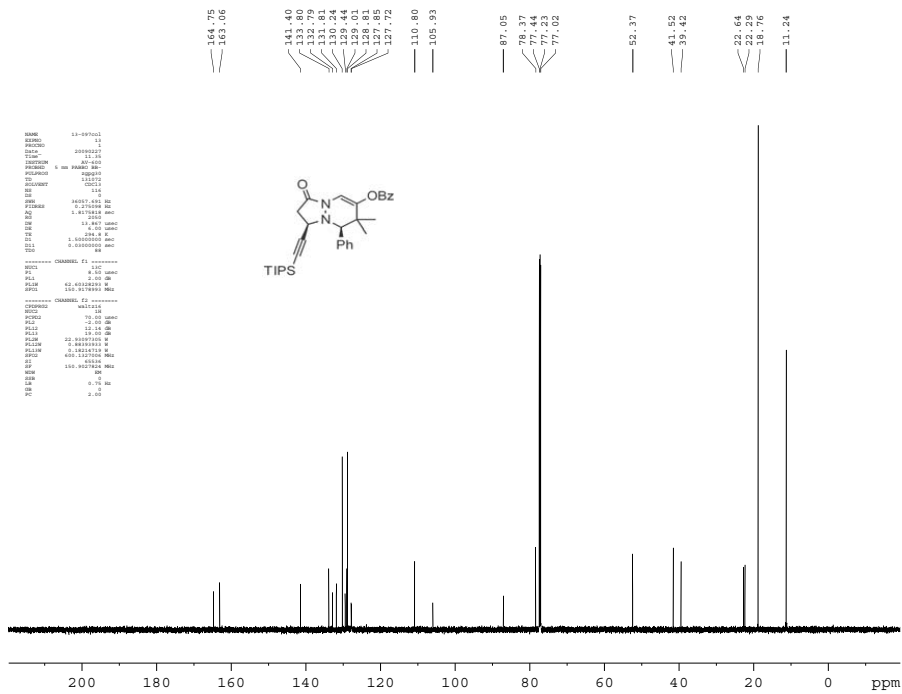
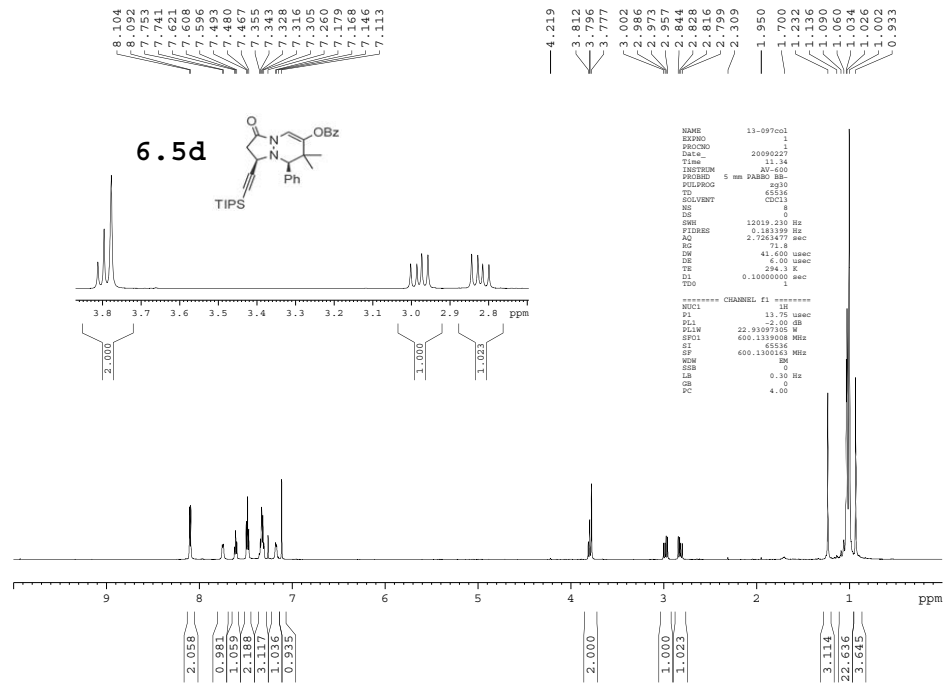
F2 - Acquisition Parameters
Date_ 20090119
Time 19.34
INSTRUM AV-500
PROBHD 5 mm TBI 1H/13
PULPROG zgpg30
TD 131072
SOLVENT CDCl3
NS 637
DS 0
SM 31446.541 Hz
FIDRES 0.239918 Hz
AQ 2.0840348 sec
RG 16384
DE 15.900 usec
TE 300.0 K
D1 1.0000000 sec
d11 0.0300000 sec
DELTA 0.8999998 sec
MCREST 0.0000000 sec
MCWRR 0.0150000 sec

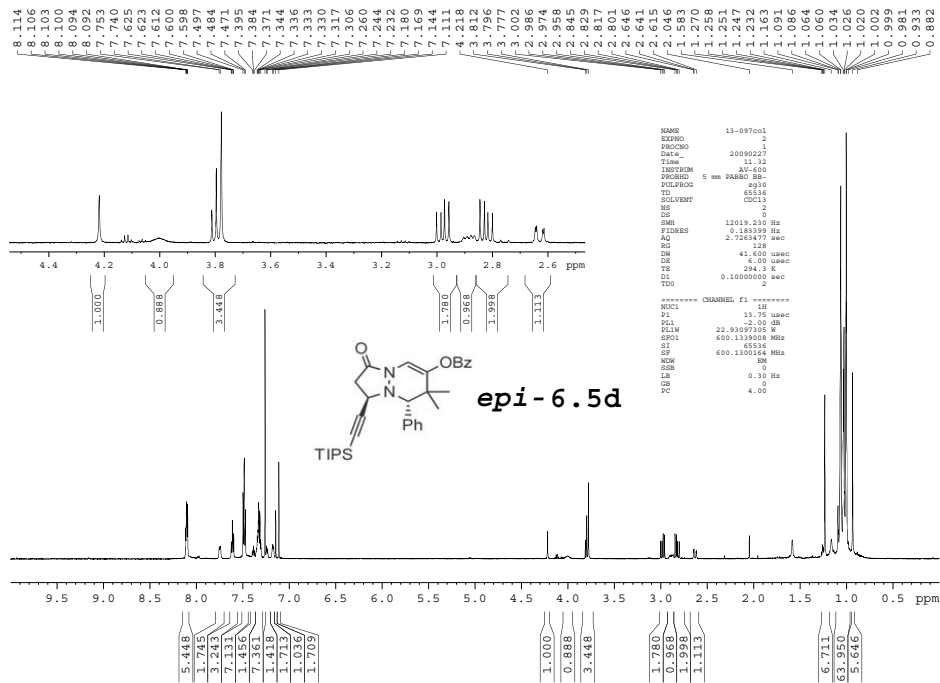
***** CHANNEL f1 *****
NUC1 13C
P1 12.00 usec
PL1 -1.00 dB
SFO1 125.7955123 MHz

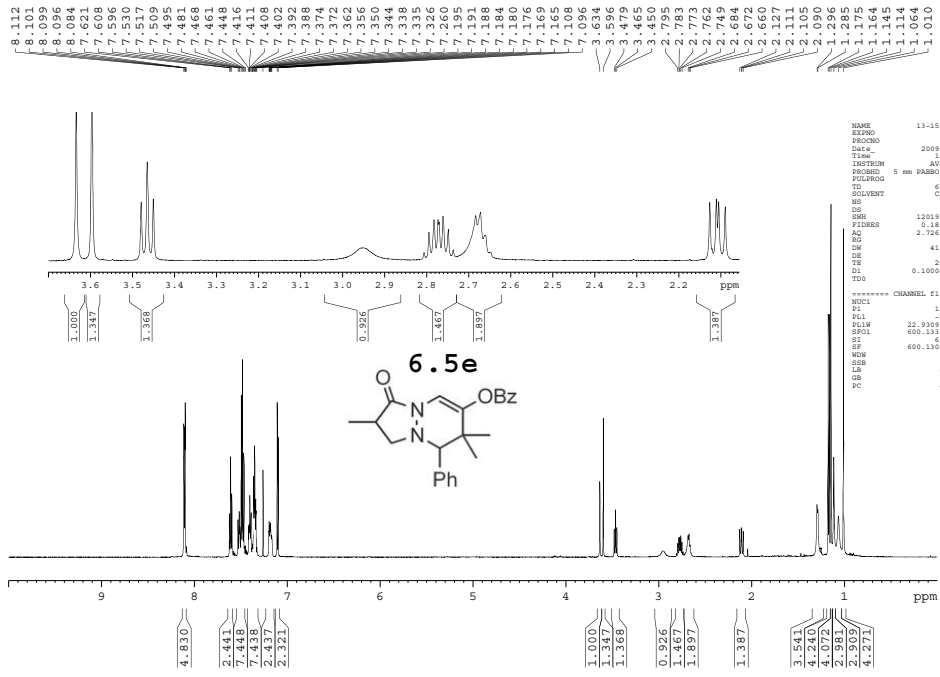
***** CHANNEL f2 *****
CPDPRG2 waltz16
NUC2 1H
PCPD2 70.00 usec
PL2 0.00 dB
PL12 19.64 dB
PL13 25.00 dB
SFO2 500.2320009 MHz

F2 - Processing parameters
SI 65536
SF 125.7429167 MHz
WDW EM
SSB 0
LB 0.75 Hz
GB 0
PC 4.00
  
```

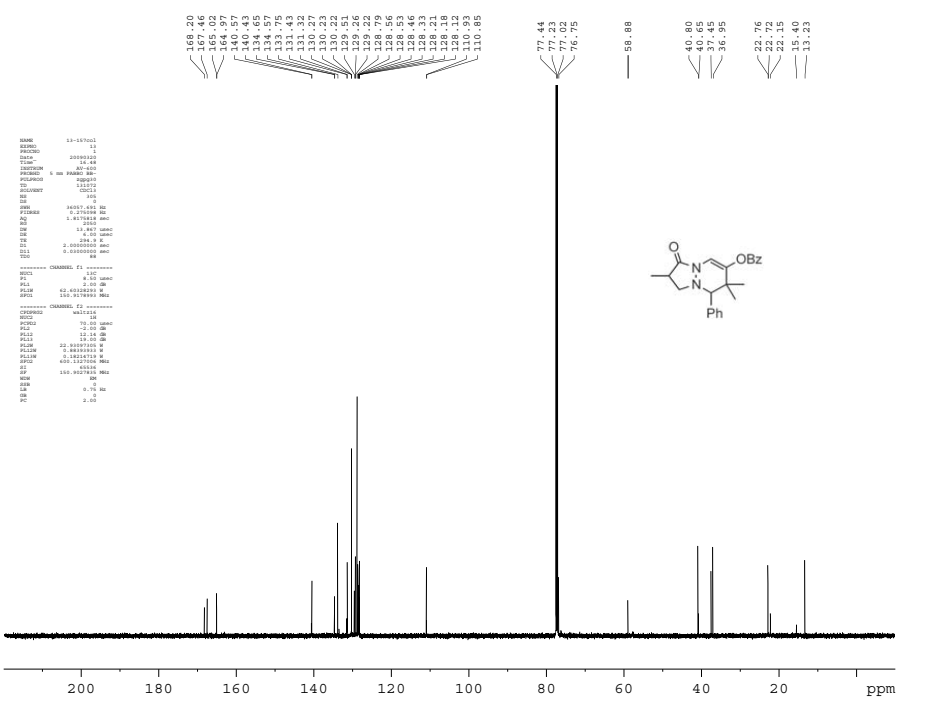






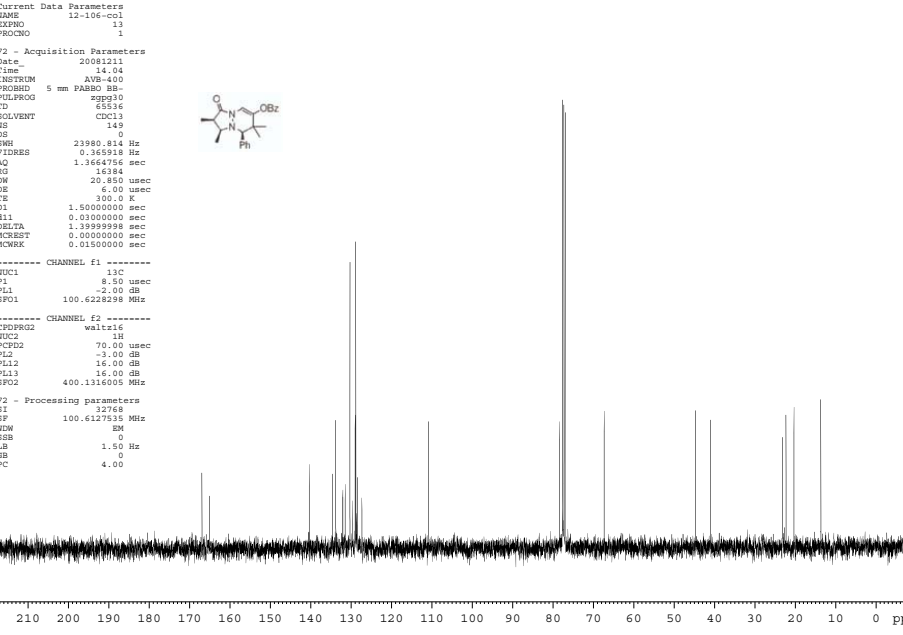
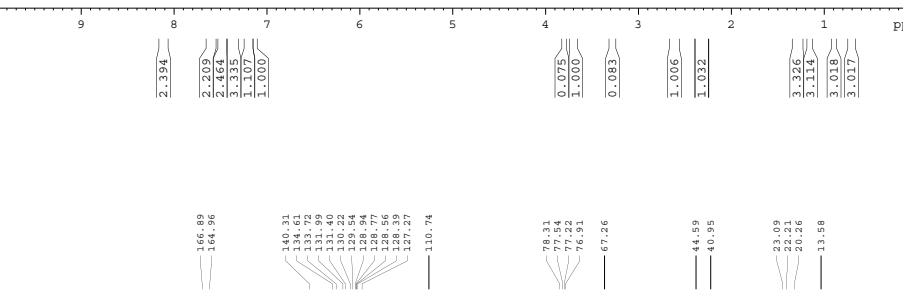
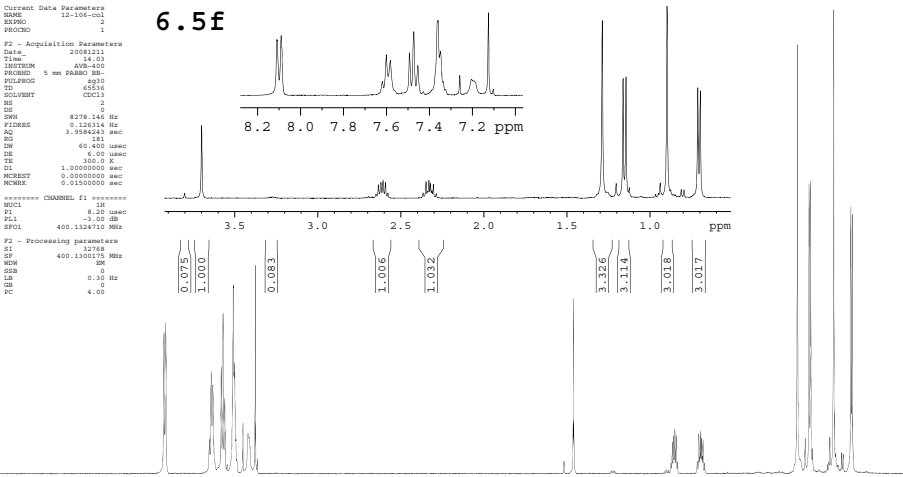
```

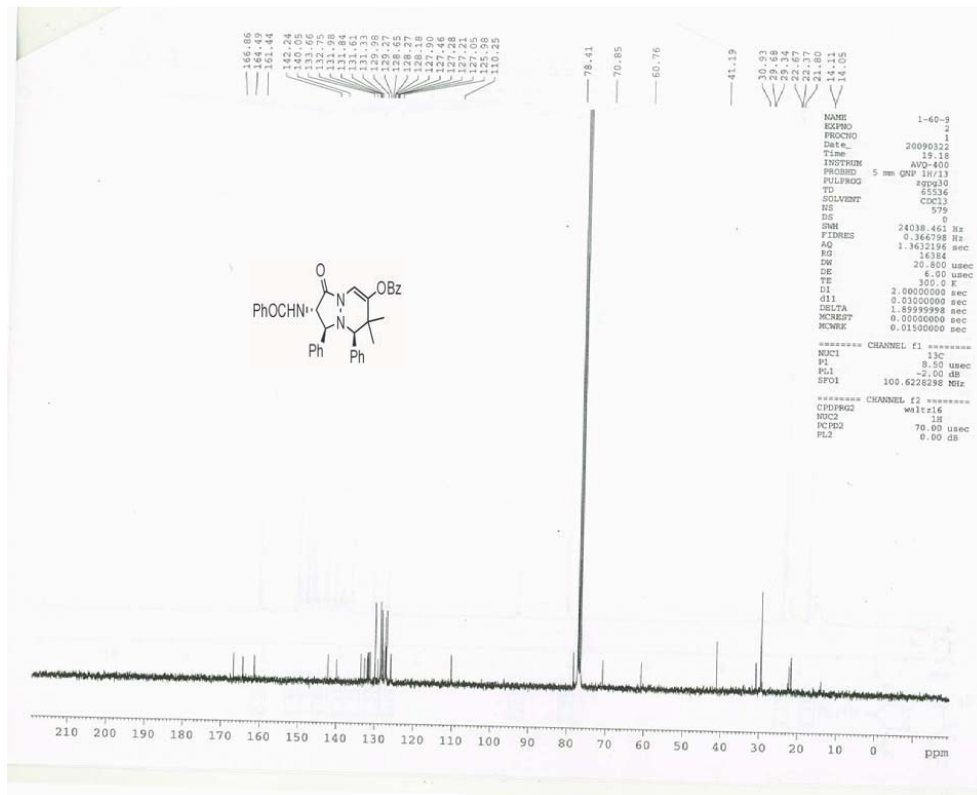
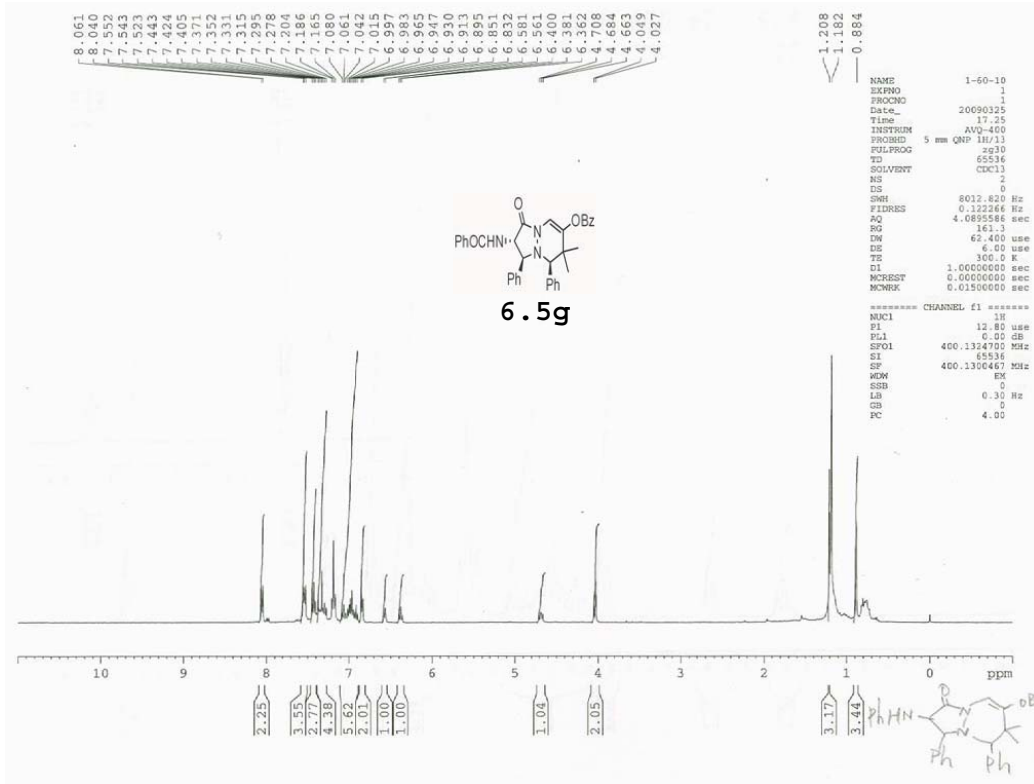
NAME      13-157001
EXPNO    1
PROCNO   1
Date_    20090120
Time     16.47
INSTRUM  AV-400
PROBHD   5 mm DABBO BB-
PULPROG  zg30
TD        65536
SOLVENT  CDCl3
NS        2
DS        2
SFO       100.626130 MHz
AQ        0.183399 sec
RG         2.0263477
SR         320
SWH        41.600 MHz
FIDRES    0.1000000
TE        294.2 K
TD0        0.1000000
===== CHANNEL f1 =====
NUC1      13
P1        13.75 usec
PL1       -2.00 dB
RG1       22.9197705 MHz
SFO1      100.626130 MHz
SI         32768
SF         600.136020 MHz
WDW        EM
SSB        0
LB         0.30 MHz
GB         0
PC         4.00
  
```

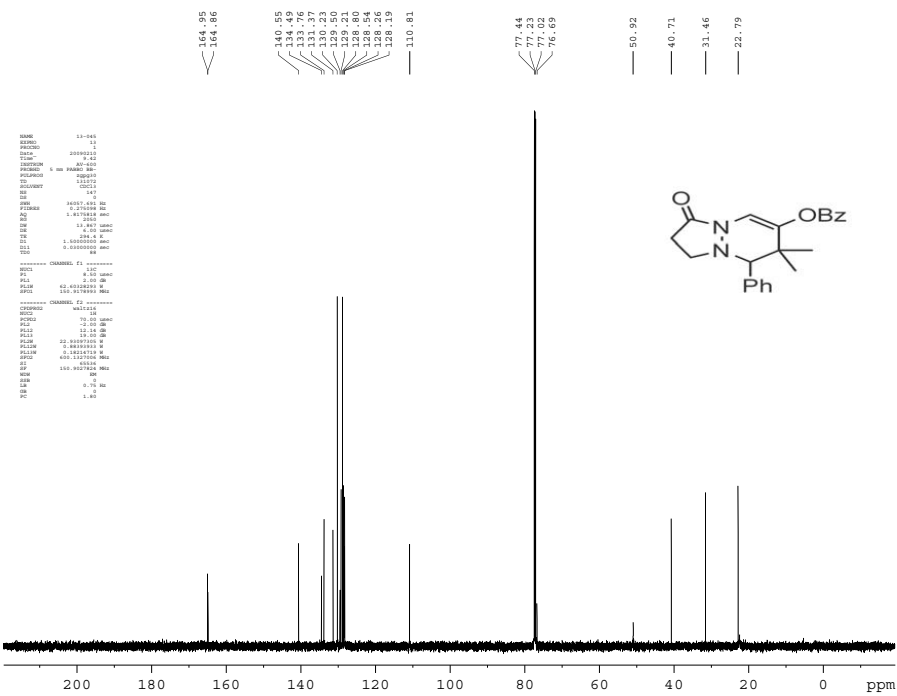
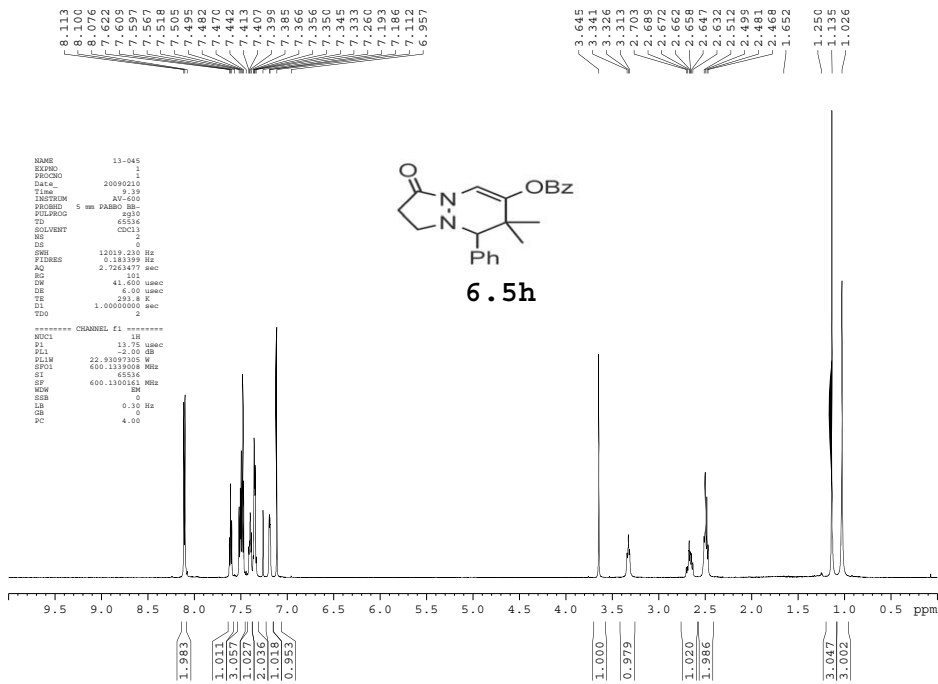


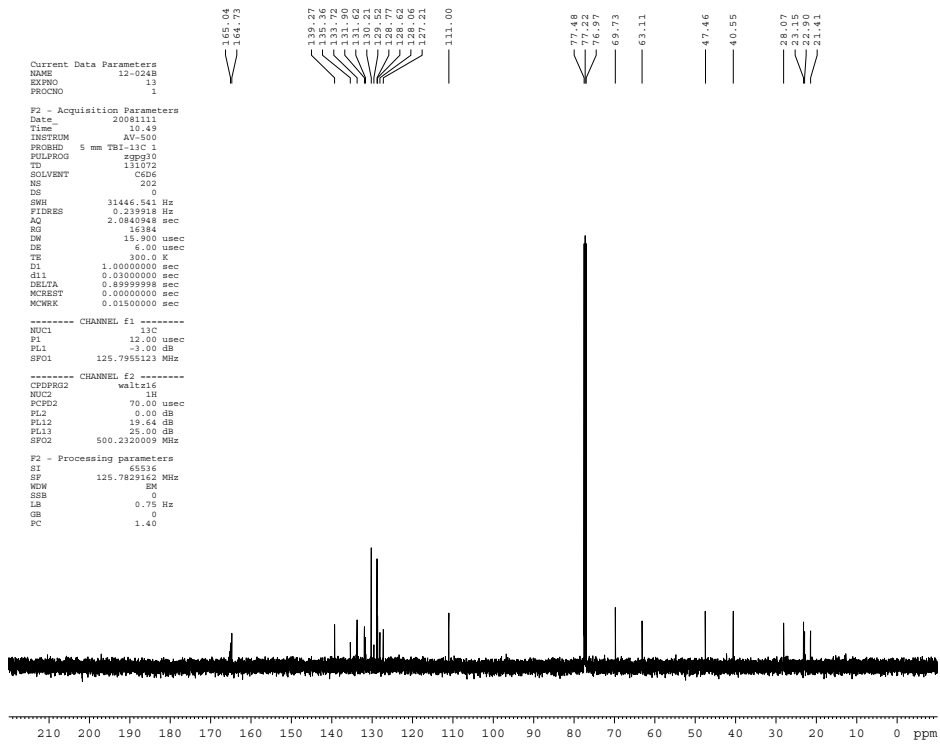
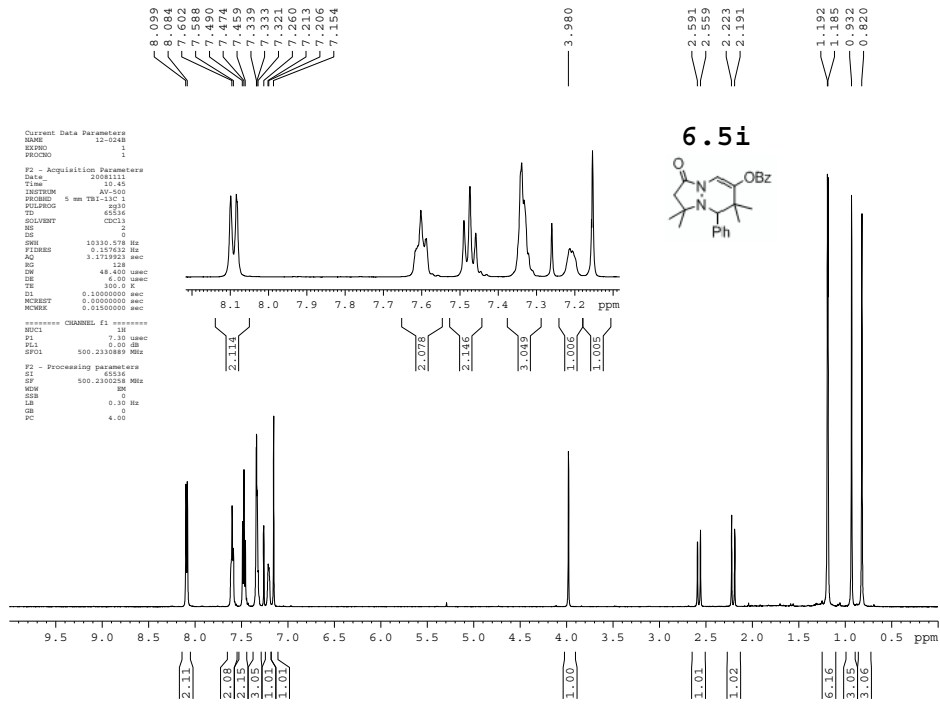
```

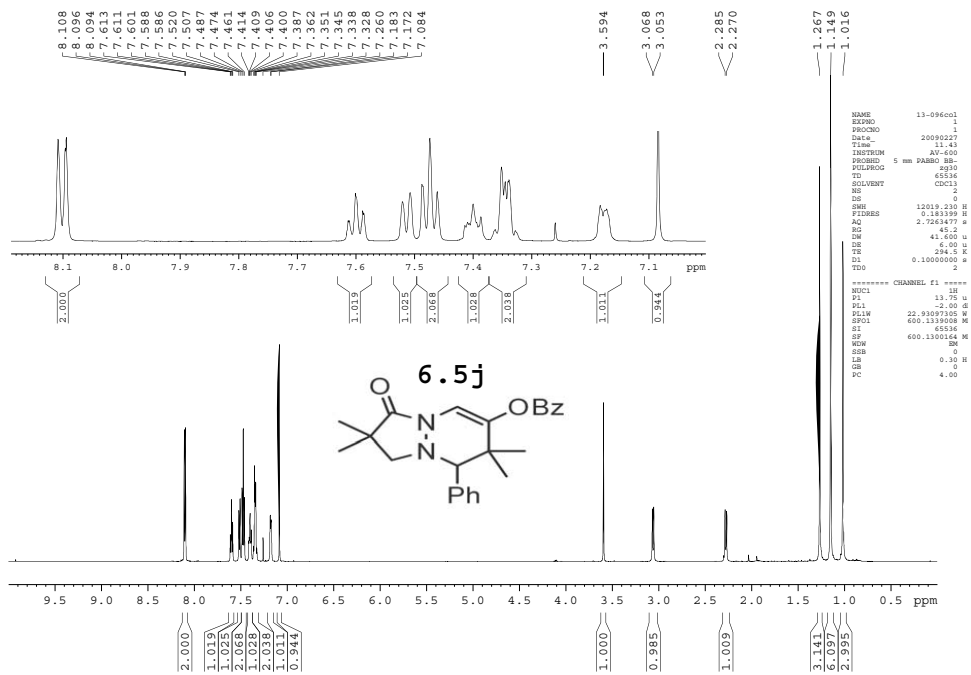
NAME      13-157001
EXPNO    1
PROCNO   1
Date_    20090120
Time     16.47
INSTRUM  AV-400
PROBHD   5 mm DABBO BB-
PULPROG  zg30
TD        65536
SOLVENT  CDCl3
NS        2
DS        2
SFO       100.626130 MHz
AQ        0.183399 sec
RG         2.0263477
SR         320
SWH        41.600 MHz
FIDRES    0.1000000
TE        294.2 K
TD0        0.1000000
===== CHANNEL f1 =====
NUC1      13
P1        13.75 usec
PL1       -2.00 dB
RG1       22.9197705 MHz
SFO1      100.626130 MHz
SI         32768
SF         600.136020 MHz
WDW        EM
SSB        0
LB         0.30 MHz
GB         0
PC         4.00
===== CHANNEL f2 =====
NAME      waltz16
EXPNO    1
PROCNO   1
Date_    20090120
Time     16.47
INSTRUM  AV-400
PROBHD   5 mm DABBO BB-
PULPROG  zgpg30
TD        65536
SOLVENT  CDCl3
NS        2
DS        2
SFO       100.626130 MHz
AQ        0.183399 sec
RG         2.0263477
SR         320
SWH        41.600 MHz
FIDRES    0.1000000
TE        294.2 K
TD0        0.1000000
===== CHANNEL f3 =====
NAME      waltz16
EXPNO    1
PROCNO   1
Date_    20090120
Time     16.47
INSTRUM  AV-400
PROBHD   5 mm DABBO BB-
PULPROG  zgpg30
TD        65536
SOLVENT  CDCl3
NS        2
DS        2
SFO       100.626130 MHz
AQ        0.183399 sec
RG         2.0263477
SR         320
SWH        41.600 MHz
FIDRES    0.1000000
TE        294.2 K
TD0        0.1000000
  
```





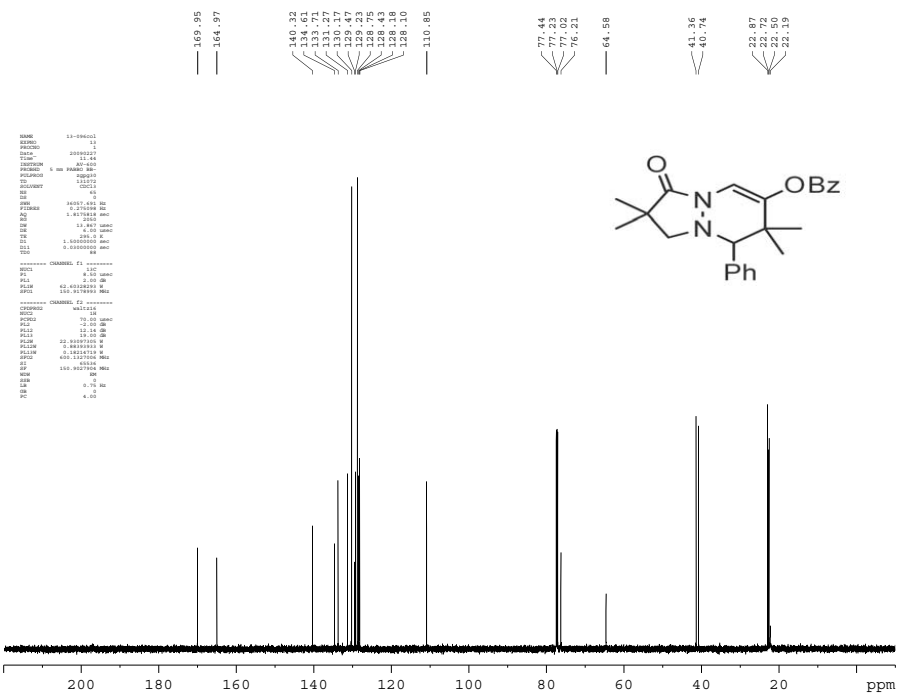






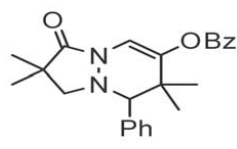
```

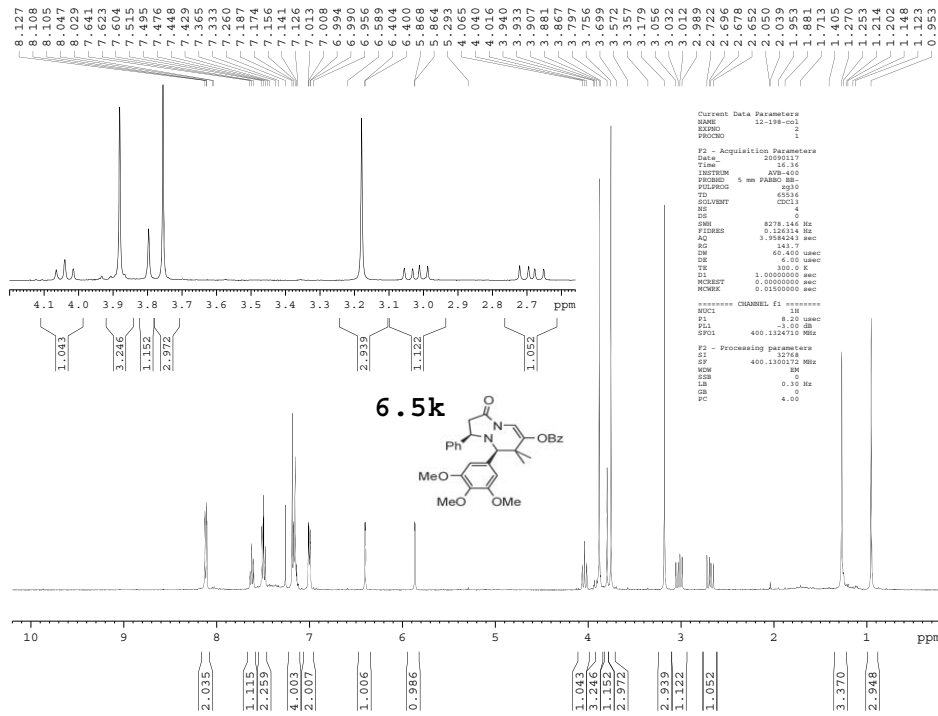
NAME      13-096001
EXPNO     1
PROCNO    1
Date_     20090227
Time      11.43
INSTRUM   AV-600
PROBHD    5 mm DABBO BB-
PULPROG   zg30
TD         65536
SOLVENT   CDCl3
NS         2
DS         0
F2         12019.230 H
FIDRES    0.183199 H
AQ         2.7584877 s
RG         65.2
SM         41.500 u
SF         600.131008 M
TE         294.5 K
TS         0.1000000 s
TQ         2
===== CHANNEL f1 =====
NUC1       13C
P1         19.75 u
PC1        -2.00 dB
PL1W      22.91097105 W
SFO1       600.131008 M
WDW        EM
SSB        0
LB         0.30 H
GB         0
PC         4.00
  
```



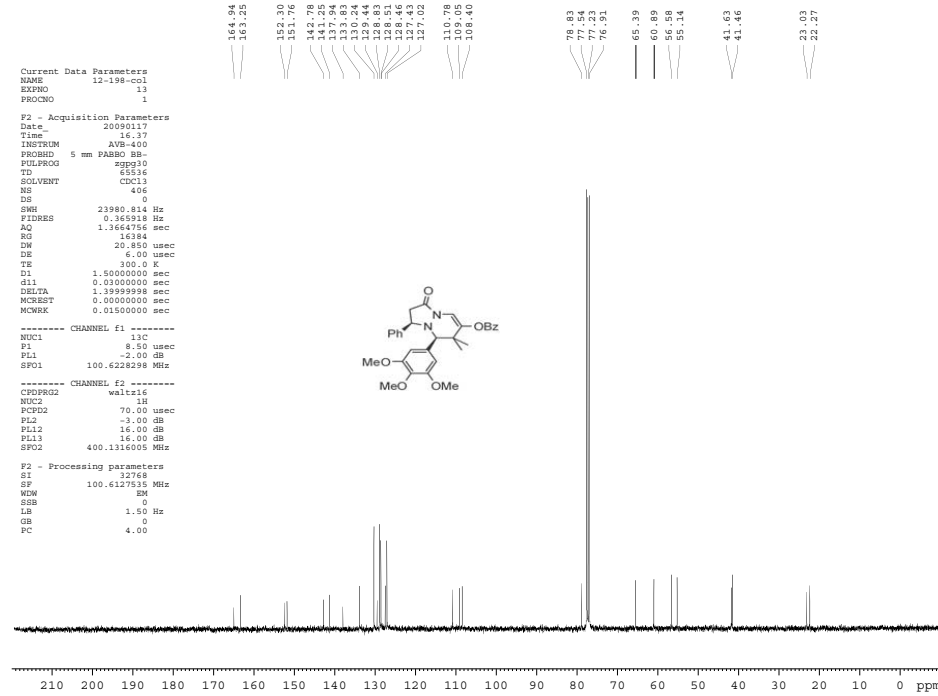
```

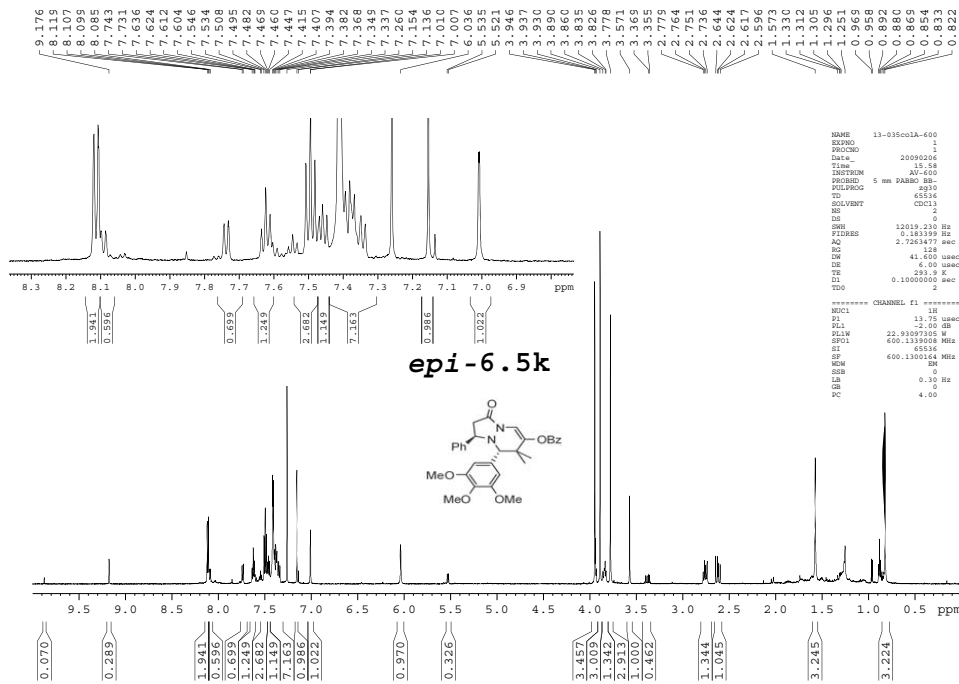
NAME      13-096001
EXPNO     1
PROCNO    1
Date_     20090227
Time      11.43
INSTRUM   AV-600
PROBHD    5 mm DABBO BB-
PULPROG   zgpg30
TD         65536
SOLVENT   CDCl3
NS         2
DS         0
F2         12019.230 H
FIDRES    0.183199 H
AQ         2.7584877 s
RG         65.2
SM         41.500 u
SF         600.131008 M
TE         294.5 K
TS         0.1000000 s
TQ         2
===== CHANNEL f1 =====
NUC1       13C
P1         19.75 u
PC1        -2.00 dB
PL1W      22.91097105 W
SFO1       600.131008 M
WDW        EM
SSB        0
LB         0.30 H
GB         0
PC         4.00
===== CHANNEL f2 =====
NAME      waltz16
EXPNO     1
PROCNO    1
Date_     20090227
Time      11.43
INSTRUM   AV-600
PROBHD    5 mm DABBO BB-
PULPROG   zgpg30
TD         65536
SOLVENT   CDCl3
NS         2
DS         0
F2         12019.230 H
FIDRES    0.183199 H
AQ         2.7584877 s
RG         65.2
SM         41.500 u
SF         600.131008 M
TE         294.5 K
TS         0.1000000 s
TQ         2
===== CHANNEL f3 =====
NAME      waltz16
EXPNO     1
PROCNO    1
Date_     20090227
Time      11.43
INSTRUM   AV-600
PROBHD    5 mm DABBO BB-
PULPROG   zgpg30
TD         65536
SOLVENT   CDCl3
NS         2
DS         0
F2         12019.230 H
FIDRES    0.183199 H
AQ         2.7584877 s
RG         65.2
SM         41.500 u
SF         600.131008 M
TE         294.5 K
TS         0.1000000 s
TQ         2
  
```





corresponds to expt 2 (major diastereomer)





```

NAME 13-035001A-600
EXPNO 1
PROCNO 1
Date_ 20090404
Time 15.58
INSTRUM spect
PROBHD 5 mm DABBO BB-
PULPROG zgpg30
TD 65536
SOLVENT CDCl3
NS 2
DS 2
SWH 12019.230 Hz
F2IDEB 0.181339 Hz
AQ 2.7263477 sec
RG 128
DM 41.600 usec
DE 6.00 usec
TE 293.9 K
SI 0.1000000 sec
TDO 2

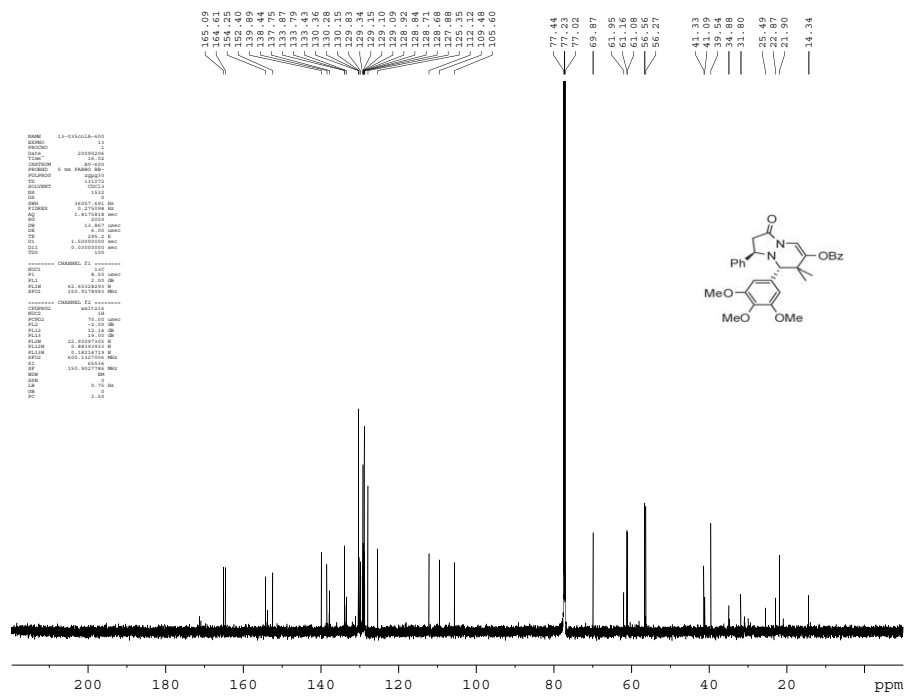
```

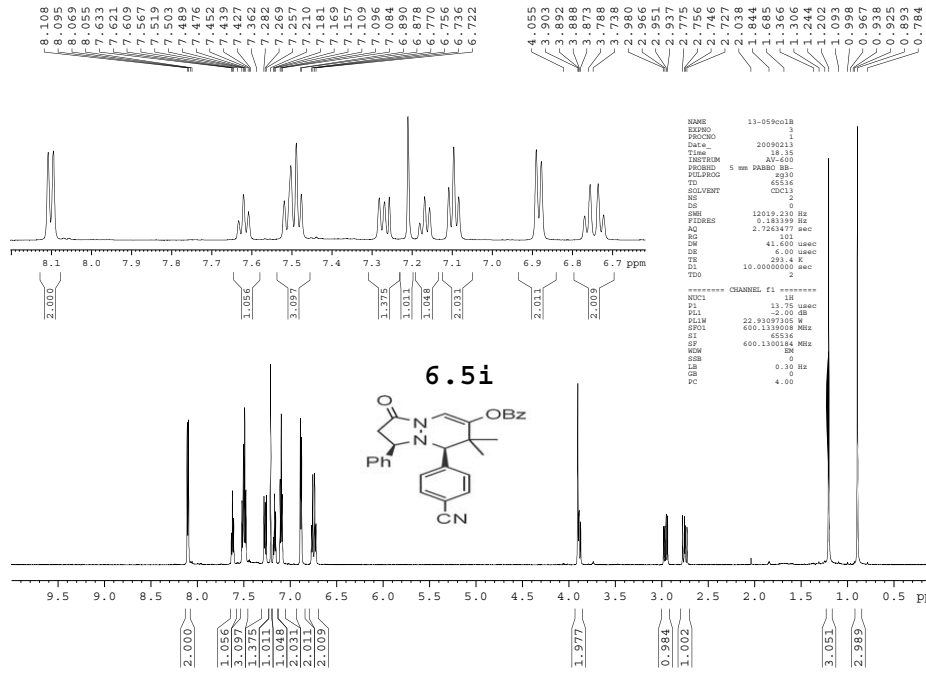
***** CHANNEL f1 *****

```

NUC1 13
P1 13.76 usec
PL1 0.00 dB
SFO1 400.1338000 MHz
SF02 600.1300164 MHz
SSB 0
GB 0
PC 4.00

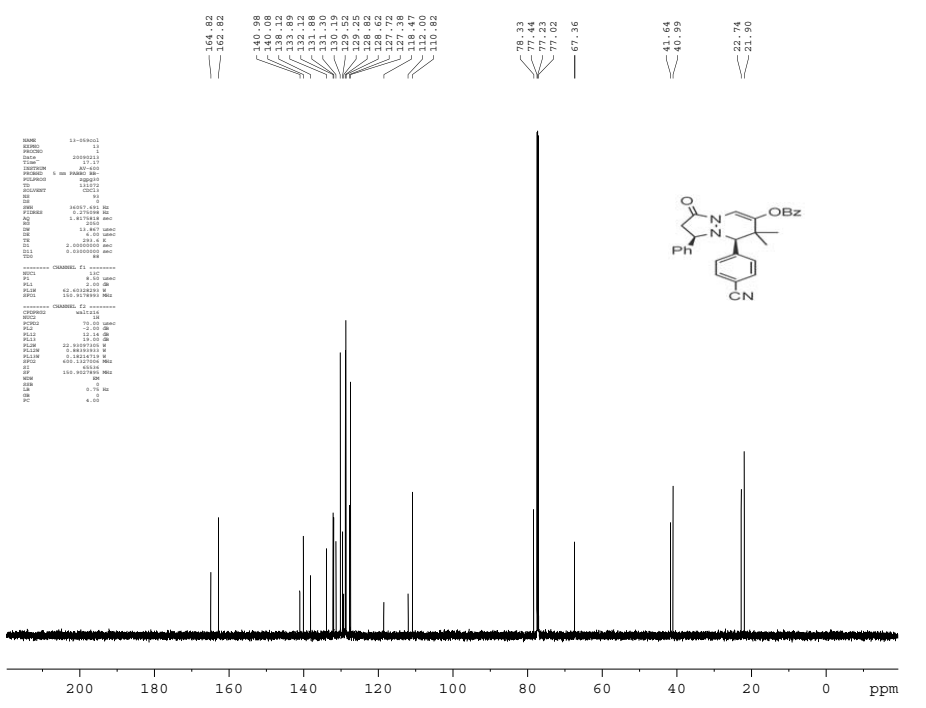
```





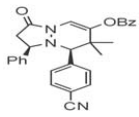
```

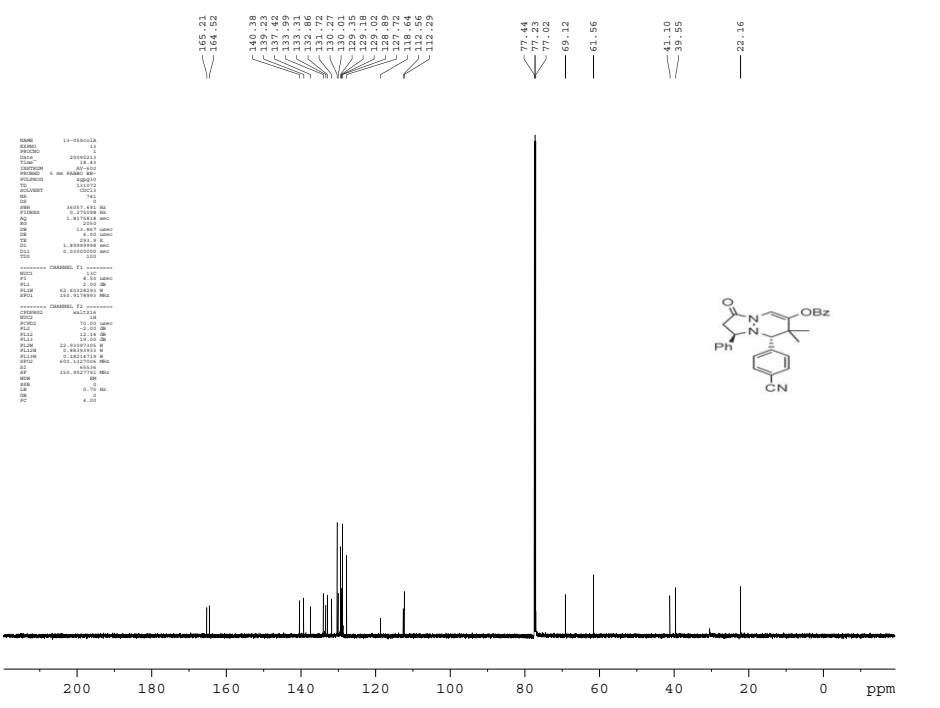
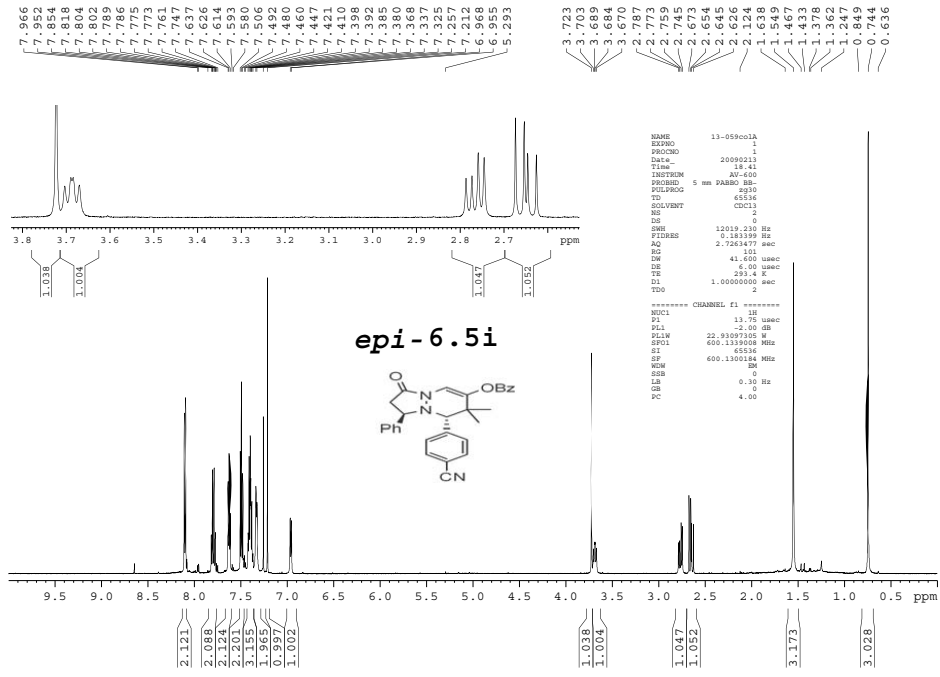
NAME      13-05801B
EXPNO    1
PROCNO   1
Date_    20090211
Time     18.15
INSTRUM  AG-400
PROBHD   5 mm PABBO BB-
PULPROG  zg30
TD        65536
SOLVENT  CDCl3
NS        2
DS        0
SFR       12019.230 Hz
FIDRES   0.183398 Hz
AQ        2.7283477 sec
RG         512
DR         41.600 usec
DE         6.400 usec
TE        293.4 K
DQ         10.0000000 sec
TD0       2
***** CHANNEL f1 *****
NUC1      13
P1        12.00 usec
PL1       0.00 dB
NUC2      13
P2        12.00 usec
PL2       0.00 dB
SFO1      600.1360000 MHz
SFO2      600.1360000 MHz
SF        600.1360184 MHz
WDW       EM
SSB       0
GB        0
CB        0.38 Hz
PC        0
GC        4.00
  
```



```

NAME      13-05801B
EXPNO    1
PROCNO   1
Date_    20090211
Time     18.15
INSTRUM  AG-400
PROBHD   5 mm PABBO BB-
PULPROG  zgpg30
TD        65536
SOLVENT  CDCl3
NS        2
DS        0
SFR       12019.230 Hz
FIDRES   0.183398 Hz
AQ        2.7283477 sec
RG         512
DR         41.600 usec
DE         6.400 usec
TE        293.4 K
DQ         10.0000000 sec
TD0       2
***** CHANNEL f1 *****
NUC1      13
P1        12.00 usec
PL1       0.00 dB
SFO1      600.1360000 MHz
SFO2      600.1360000 MHz
SF        600.1360184 MHz
WDW       EM
SSB       0
GB        0
CB        0.38 Hz
PC        0
GC        4.00
***** CHANNEL f2 *****
NUC2      13
P2        12.00 usec
PL2       0.00 dB
SFO3      600.1360000 MHz
SFO4      600.1360000 MHz
SF        600.1360184 MHz
WDW       EM
SSB       0
GB        0
CB        0.38 Hz
PC        0
GC        4.00
  
```



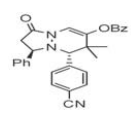


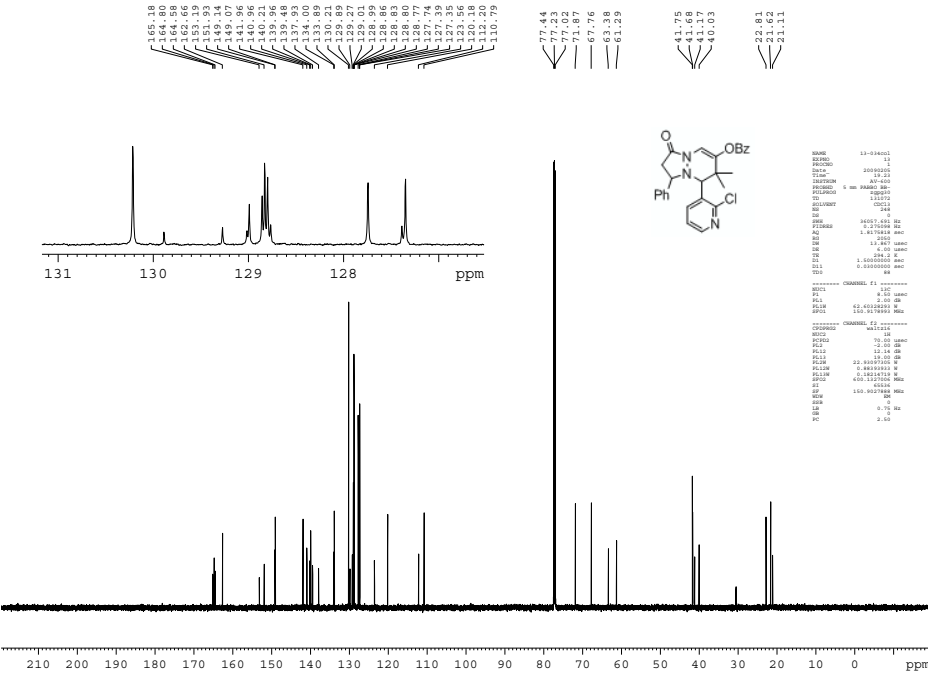
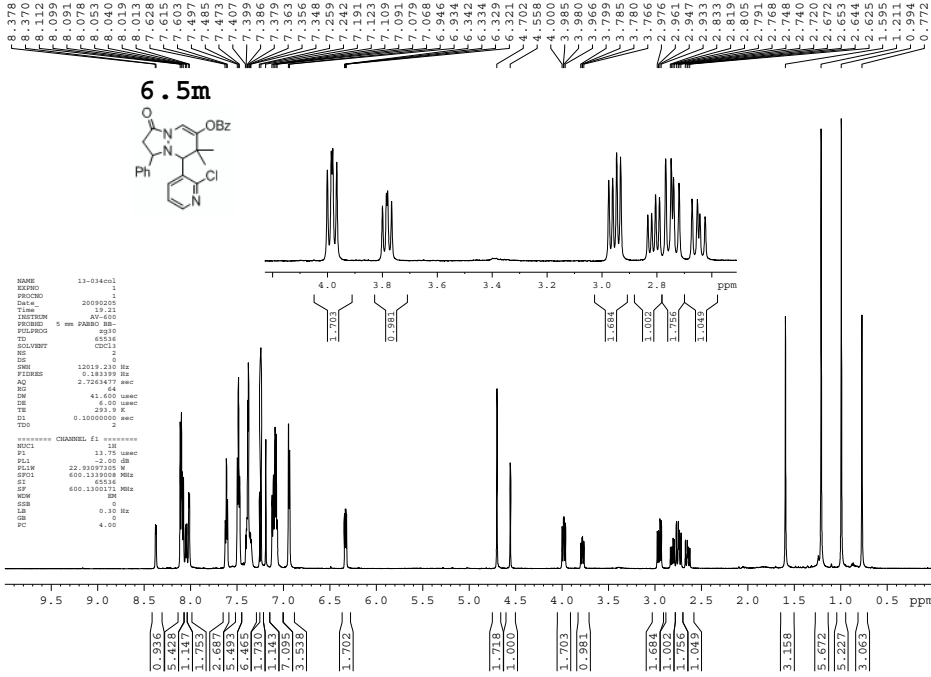
```

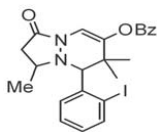
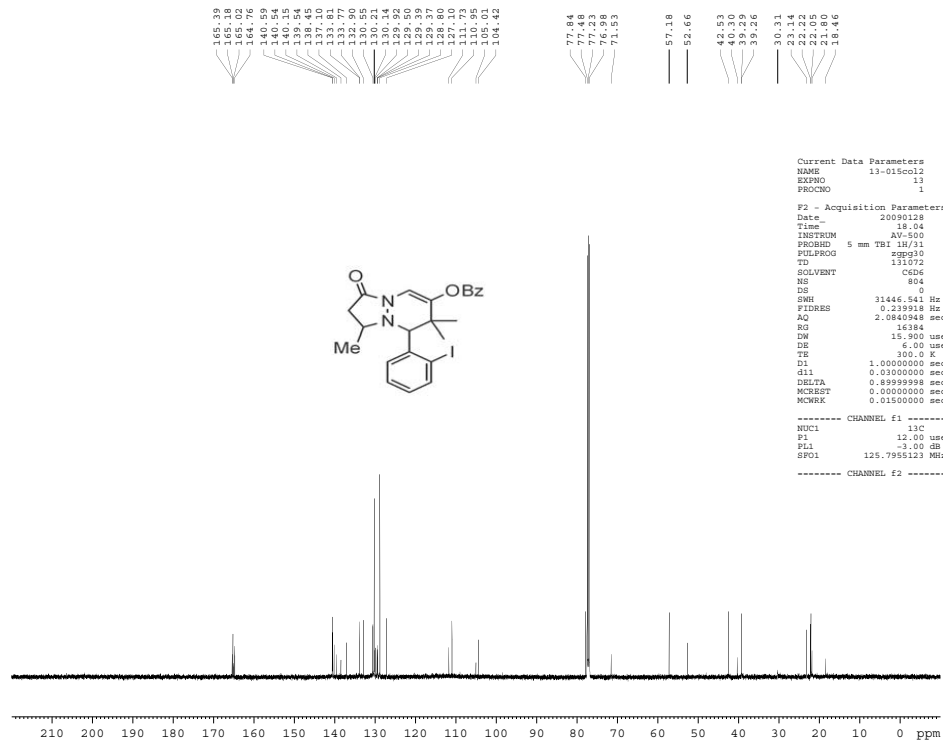
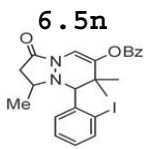
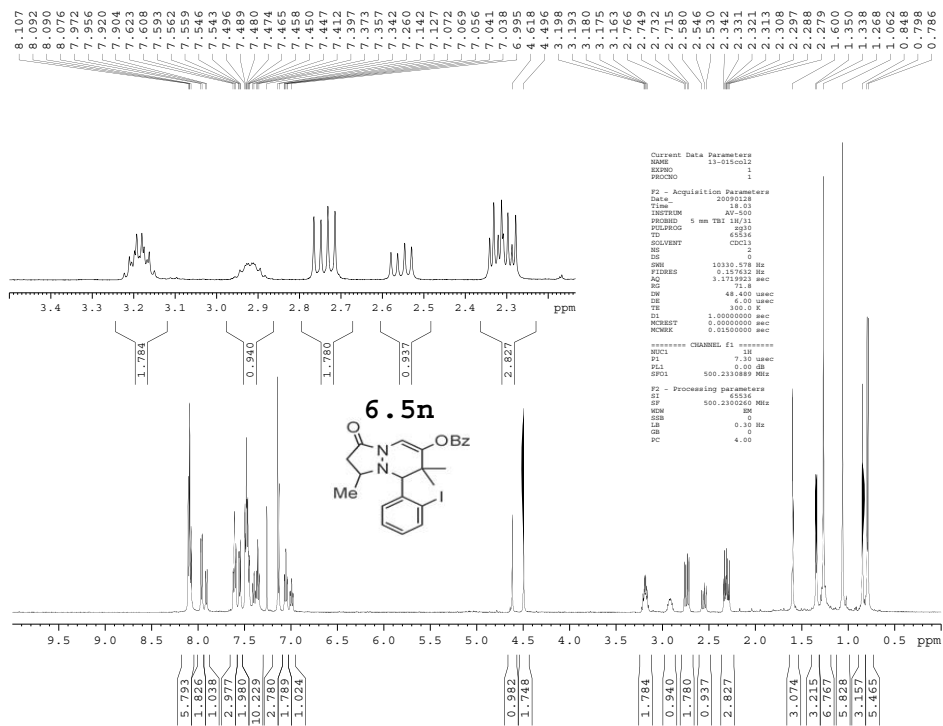
NAME      13-059001A
EXPNO    1
PROCNO    1
F2      20090211
TIME     18.41
INSTRUM   MS-400
PROBHD    5 mm PABBO BB-
PULPROG   zgpg30
TD        65536
SOLVENT   CDCl3
NS        2
DS        4
SWH       12019.330 Hz
FIDRES    0.183399 Hz
AQ        2.7263477 sec
RG         512
DELTA     100
EN        41.400 usec
TE        293.4 K
DELTA2    1.0000000 sec
TD0       2
----- CHANNEL f1 -----
NUC1      13
P1        12.00 usec
PL1       -2.00 dB
SFO1      101.625375 MHz
SF        600.1300000 MHz
WDW       EM
SSB       0
GB        0.10 Hz
PC        4.00
  
```

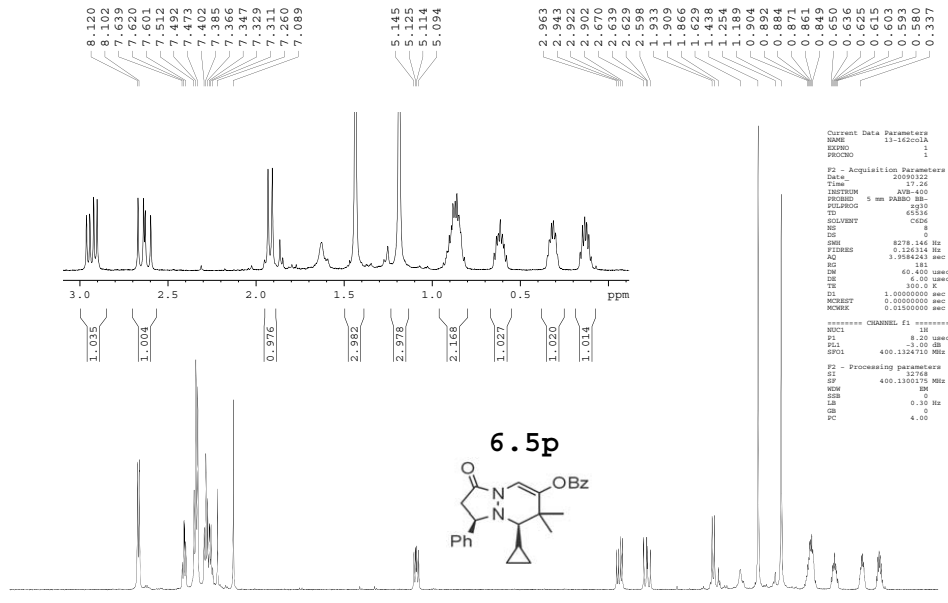
```

NAME      13-059001A
EXPNO    1
PROCNO    1
F2      20090211
TIME     18.41
INSTRUM   MS-400
PROBHD    5 mm PABBO BB-
PULPROG   zgpg30
TD        65536
SOLVENT   CDCl3
NS        2
DS        4
SWH       12019.330 Hz
FIDRES    0.183399 Hz
AQ        2.7263477 sec
RG         512
DELTA     100
EN        41.400 usec
TE        293.4 K
DELTA2    1.0000000 sec
TD0       2
----- CHANNEL f1 -----
NUC1      13
P1        12.00 usec
PL1       -2.00 dB
SFO1      101.625375 MHz
SF        600.1300000 MHz
WDW       EM
SSB       0
GB        0.10 Hz
PC        4.00
  
```









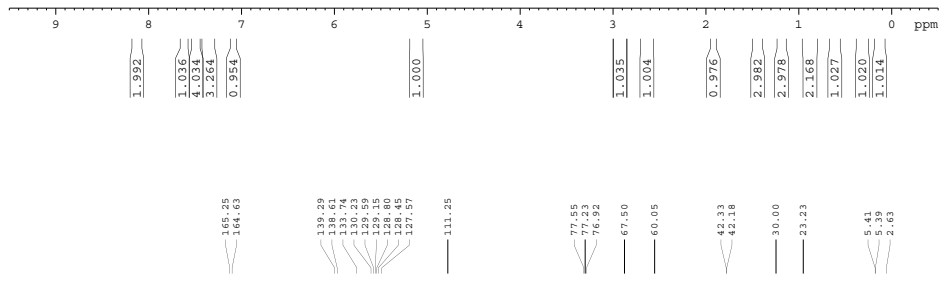
```

Current Data Parameters
NAME 13-162001A
EXPNO 13
PROCNO 1

F2 - Acquisition Parameters
Date_ 20090322
Time 17.29
INSTRUM ATR-400
PROBHD 5 mm PABBO BB-
PULPROG zgpg30
TD 65536
SOLVENT CDCl3
NS 185
DS 0
SWH 23280.914 Hz
FIDRES 0.365918 Hz
AQ 1.3664786 sec
RG 16384
DM 20.850 usec
DE 6.00 usec
TE 300.0 K
D1 1.50000000 sec
d11 0.03000000 sec
DELTA 1.19999998 sec
MCKEY 0.03000000 sec
MCKWK 0.01500000 sec

----- CHANNEL f1 -----
NUC1 13C
P1 8.50 usec
PL1 -2.00 dB
SFO1 100.628388 MHz

F2 - Processing parameters
SI 32768
SF 400.1300175 MHz
WDW EM
SSB 0
LB 0.30 Hz
GB 0
PC 4.00
  
```



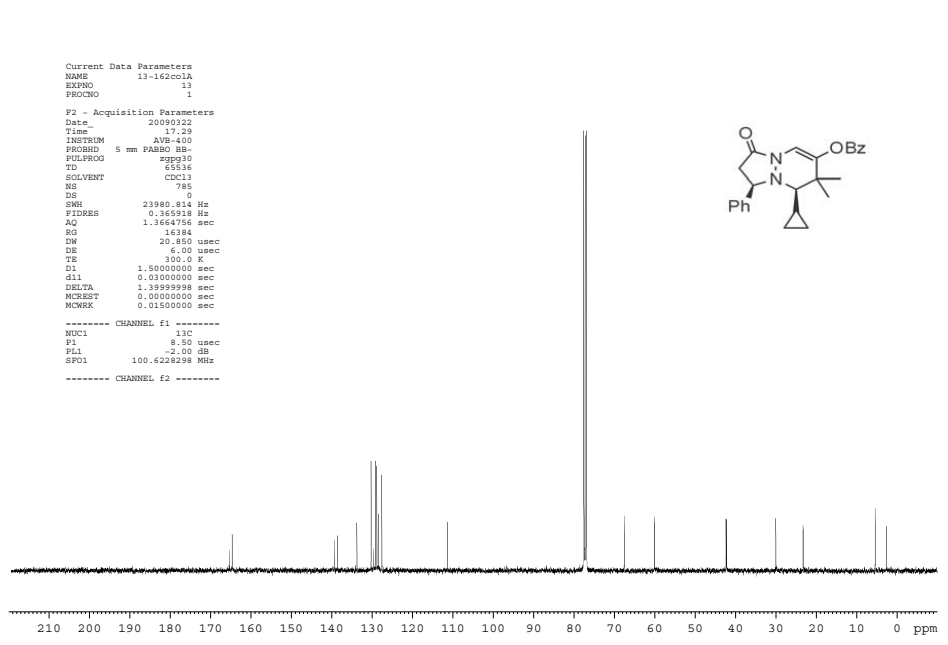
```

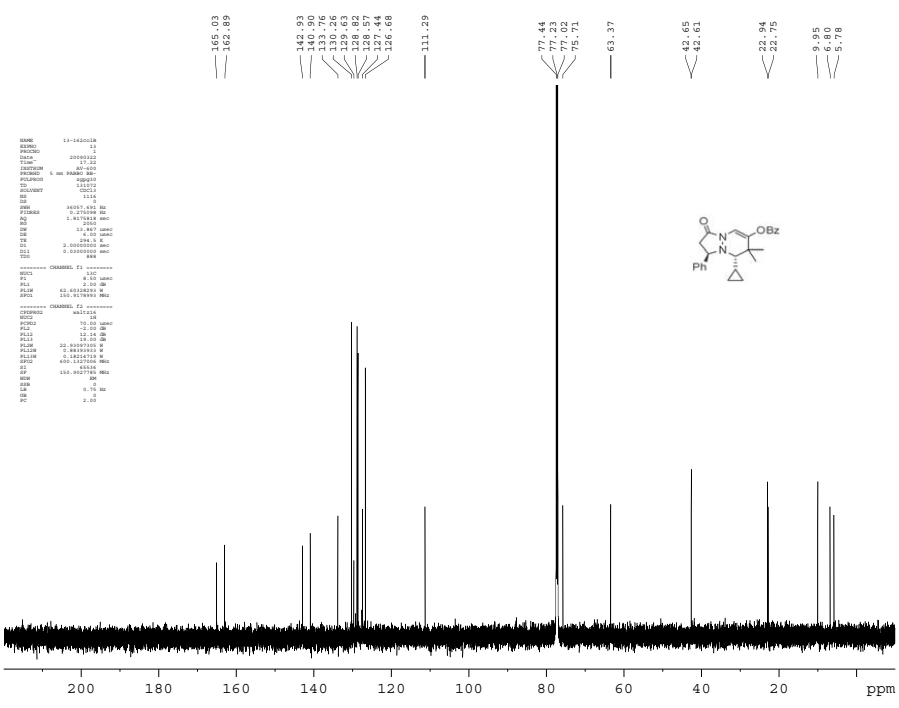
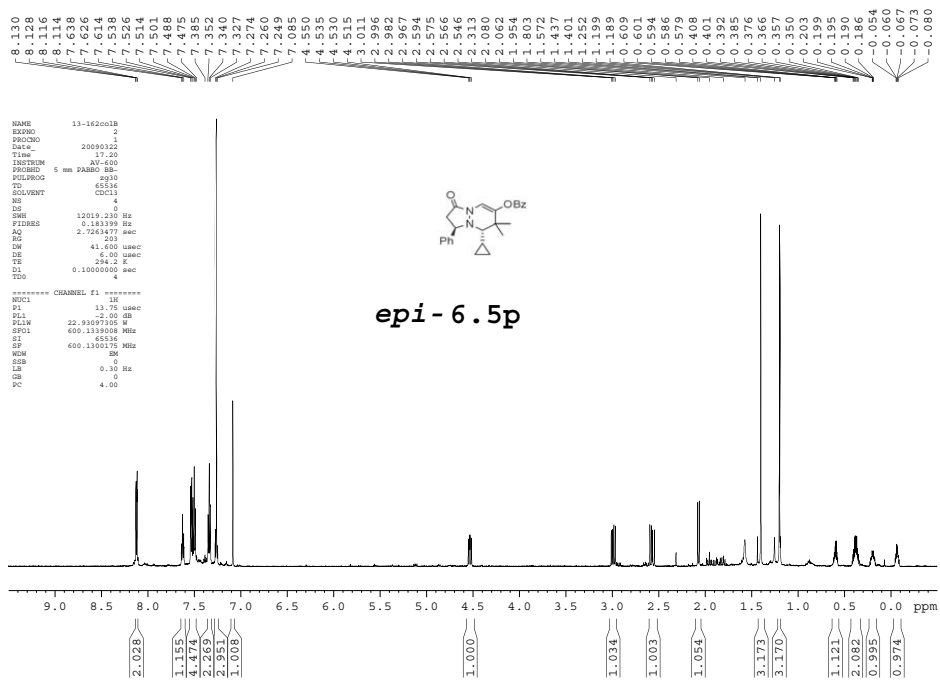
Current Data Parameters
NAME 13-162001A
EXPNO 13
PROCNO 1

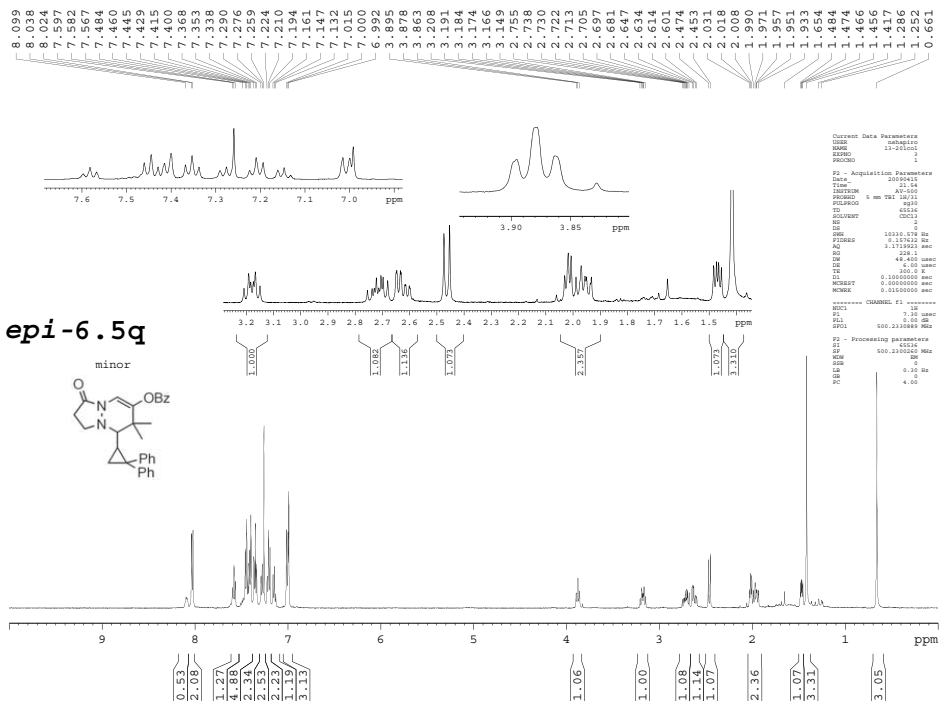
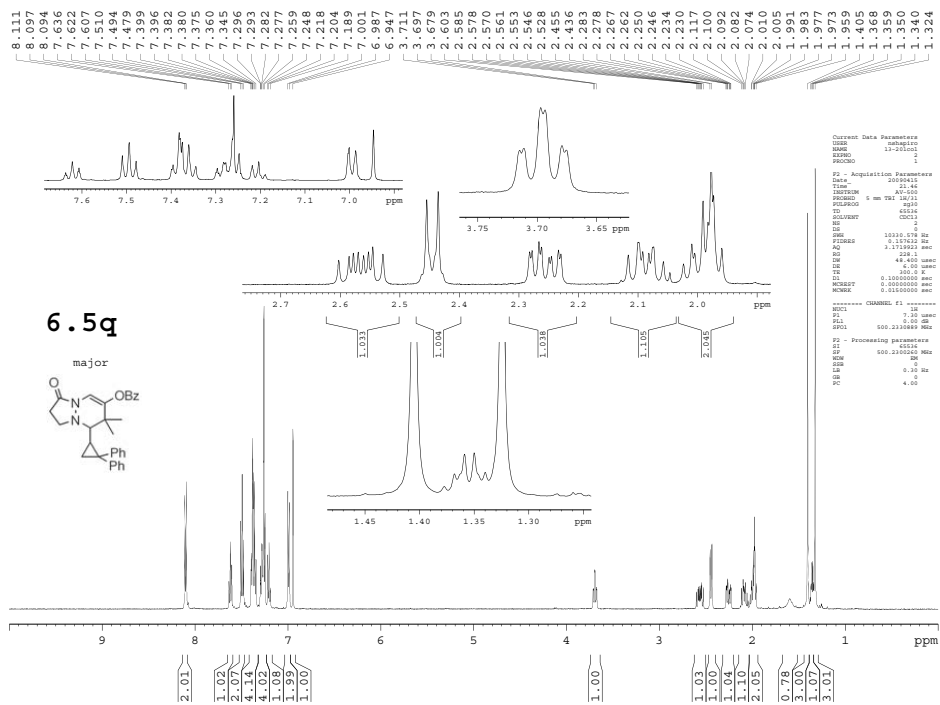
F2 - Acquisition Parameters
Date_ 20090322
Time 17.29
INSTRUM ATR-400
PROBHD 5 mm PABBO BB-
PULPROG zgpg30
TD 65536
SOLVENT CDCl3
NS 185
DS 0
SWH 23280.914 Hz
FIDRES 0.365918 Hz
AQ 1.3664786 sec
RG 16384
DM 20.850 usec
DE 6.00 usec
TE 300.0 K
D1 1.50000000 sec
d11 0.03000000 sec
DELTA 1.19999998 sec
MCKEY 0.03000000 sec
MCKWK 0.01500000 sec

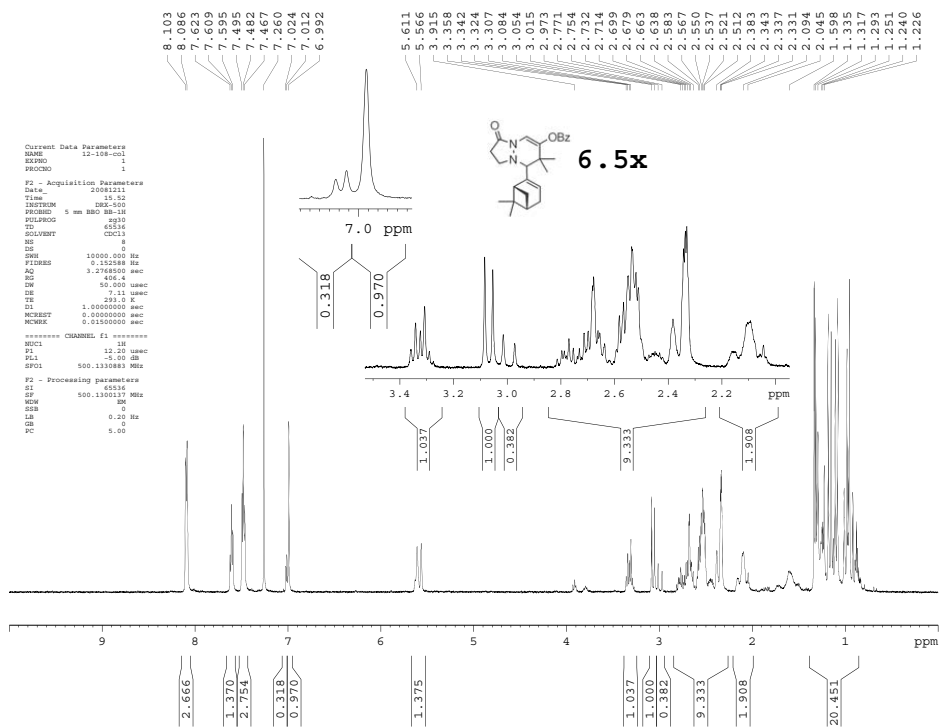
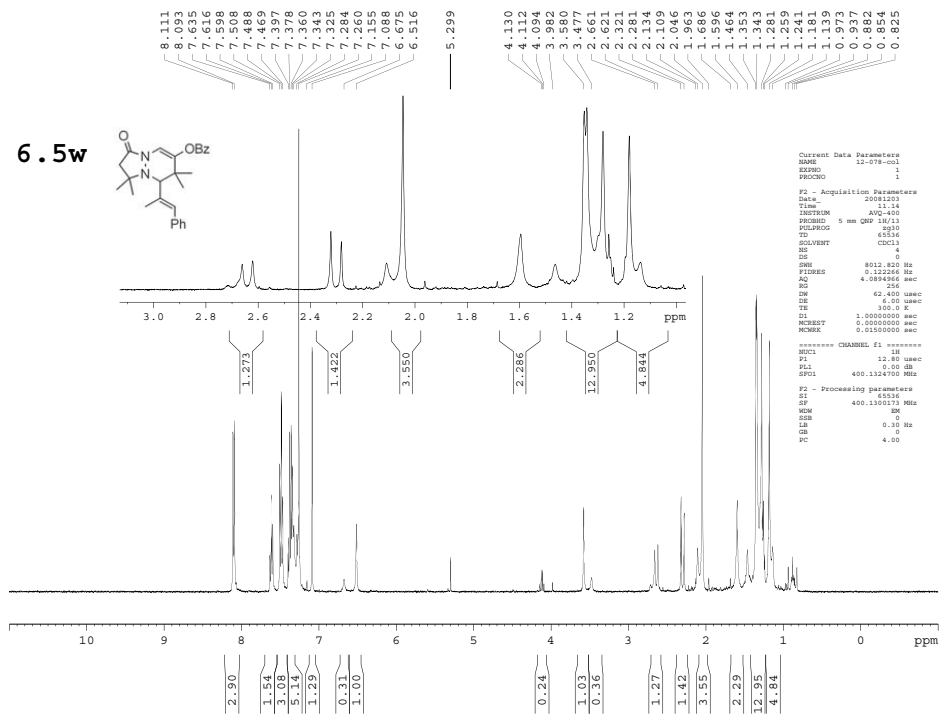
----- CHANNEL f1 -----
NUC1 13C
P1 8.50 usec
PL1 -2.00 dB
SFO1 100.628388 MHz

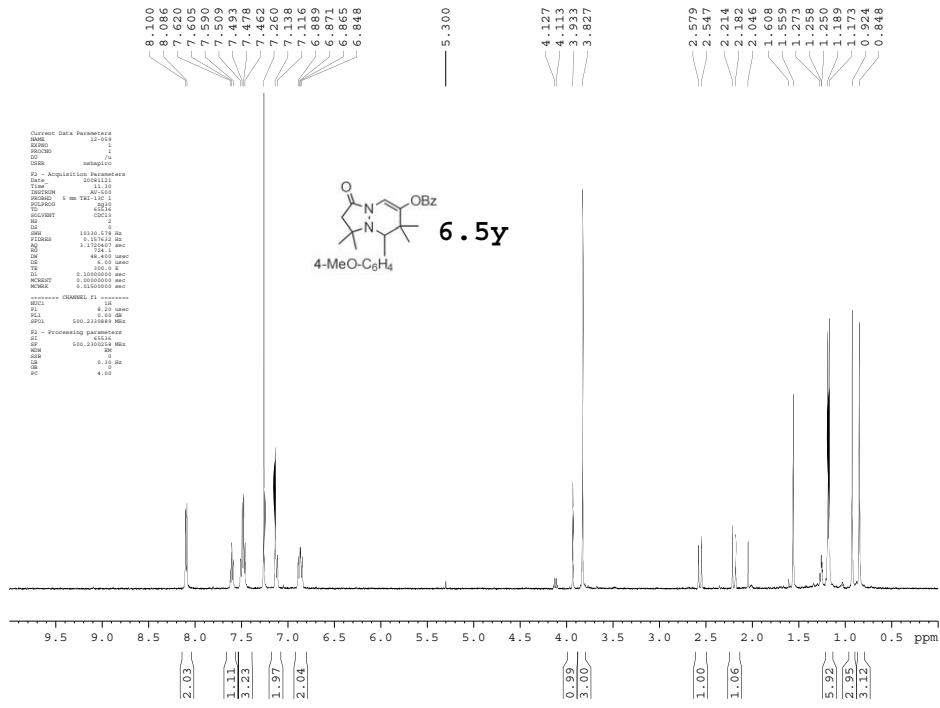
----- CHANNEL f2 -----
  
```

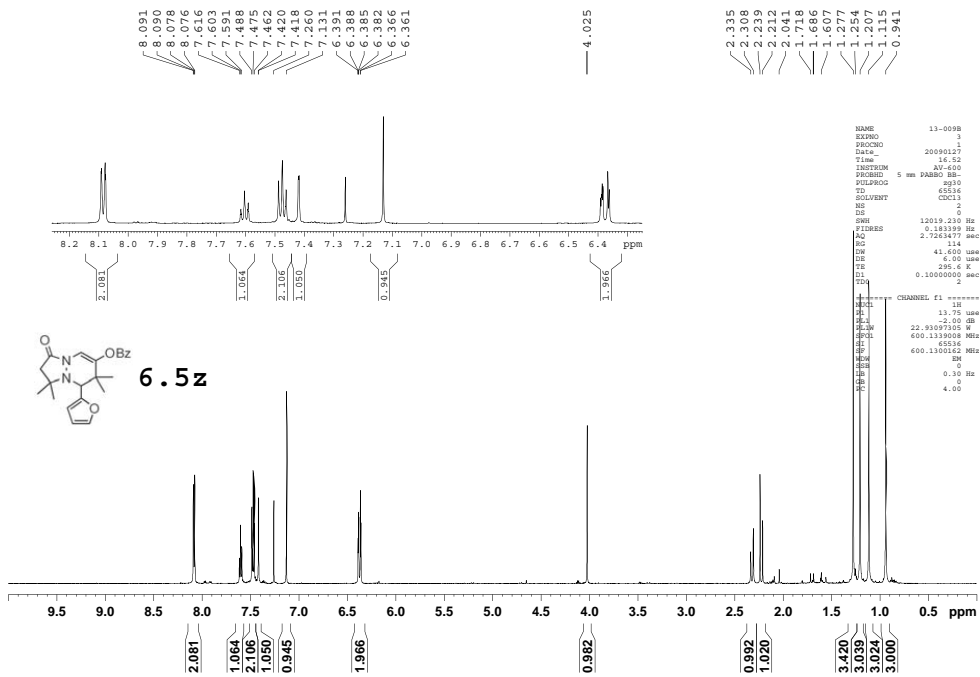








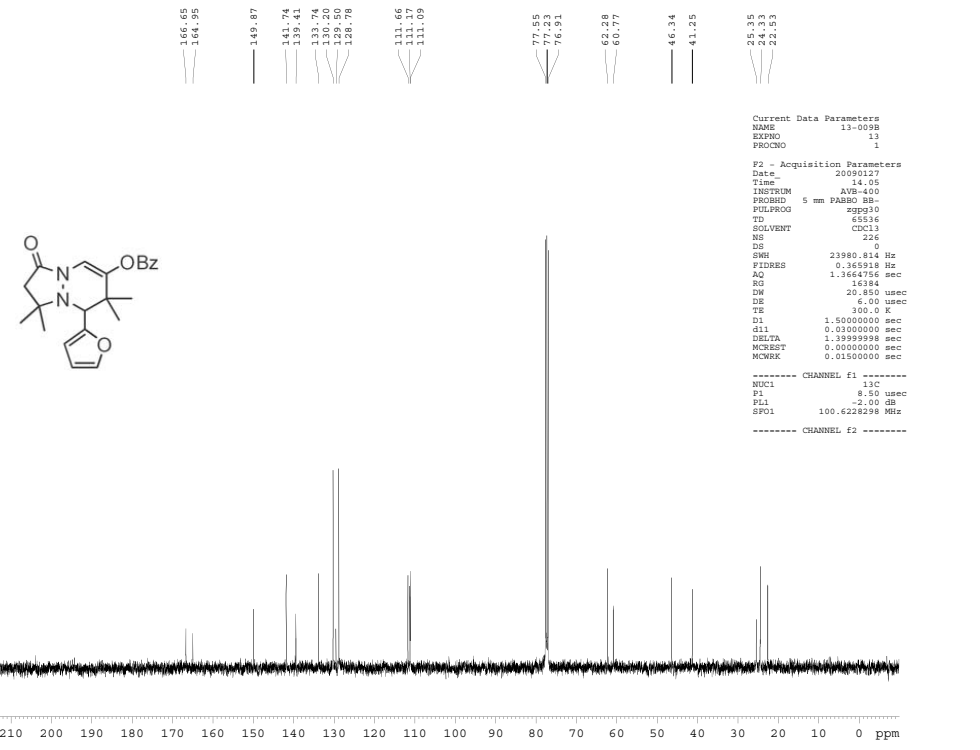


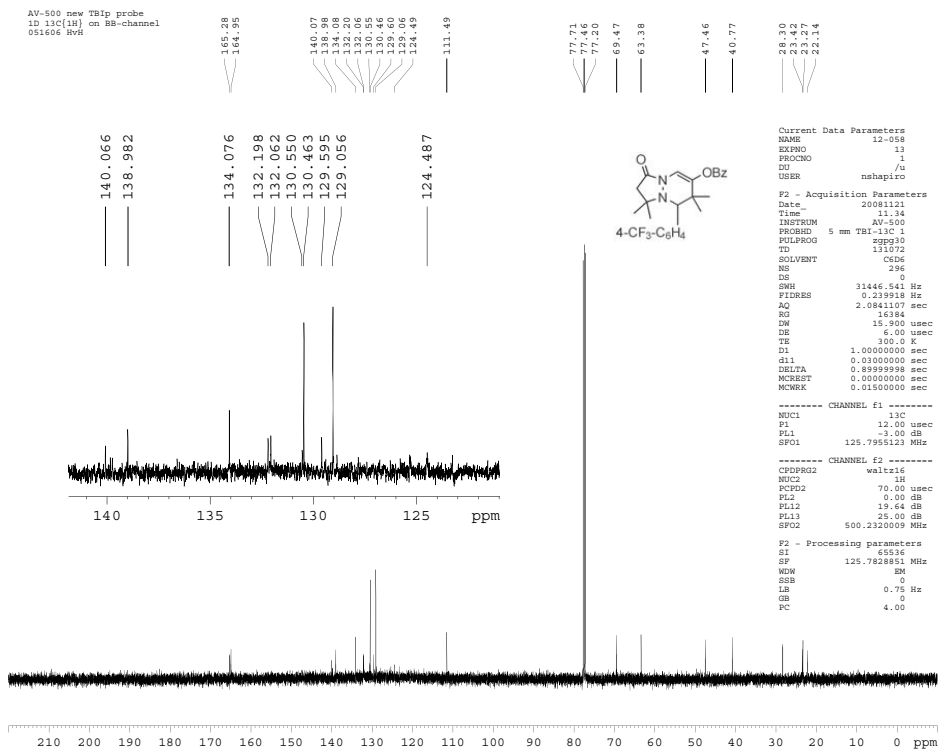
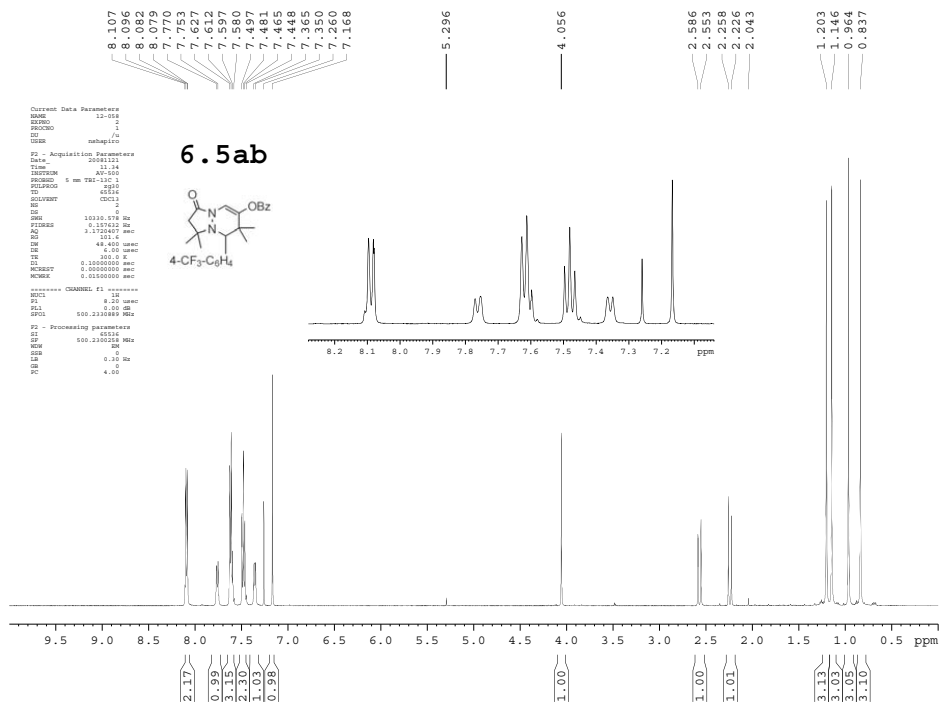


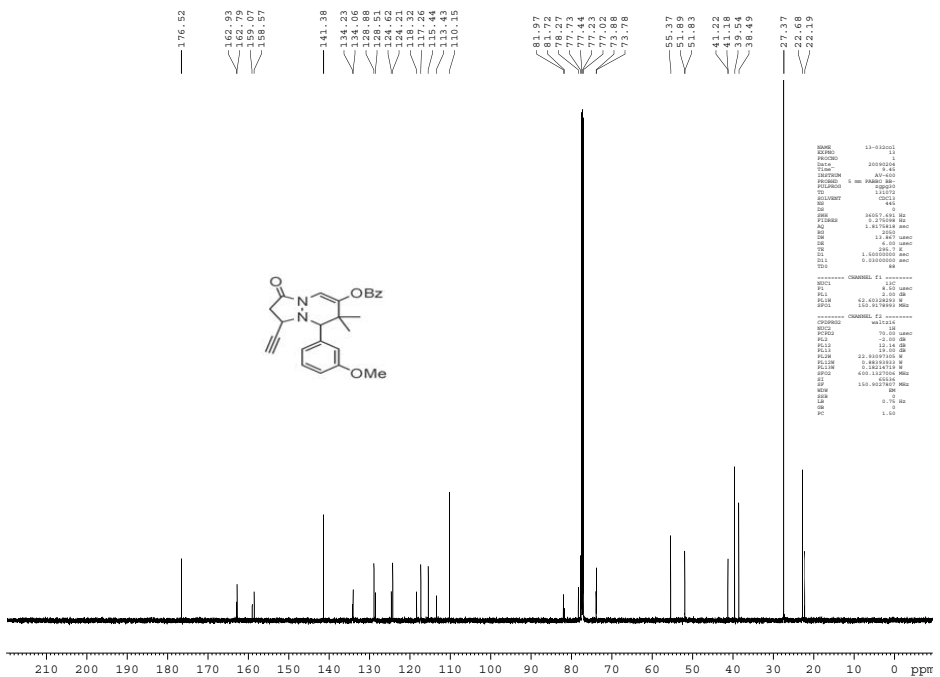
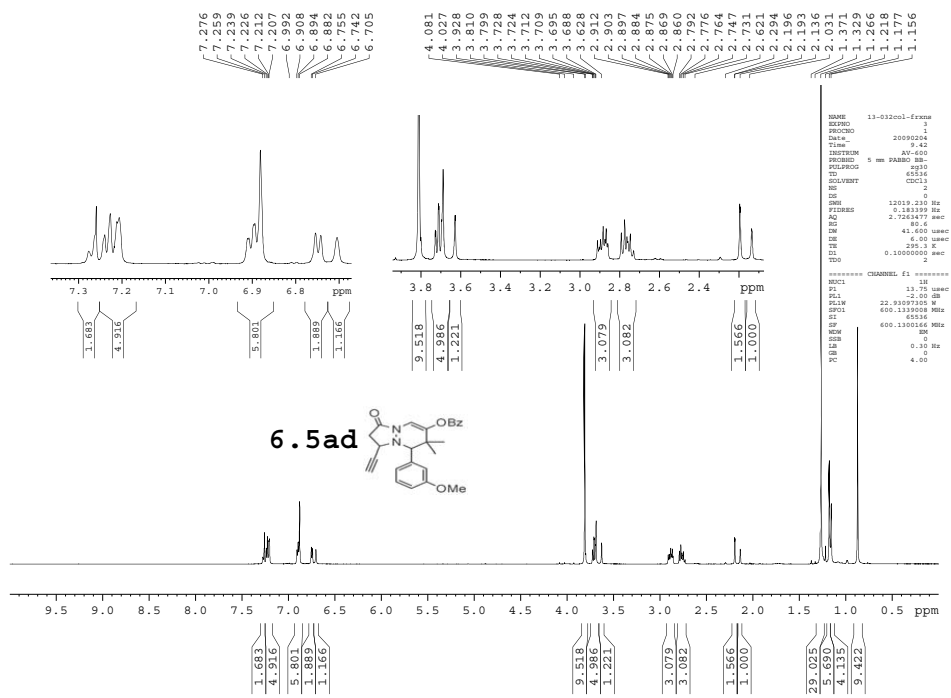
```

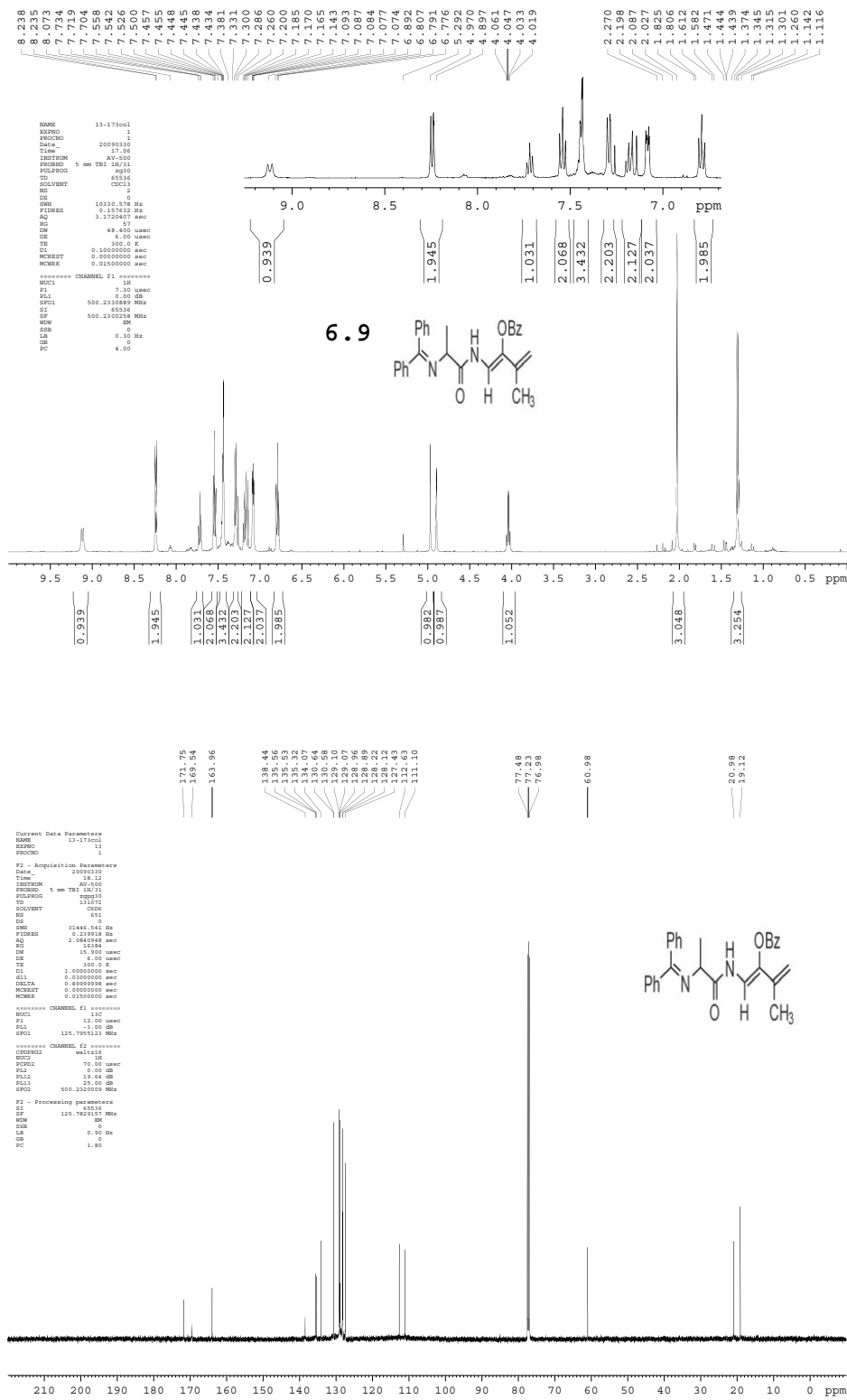
NAME      13-009B
EXPNO     1
PROCNO    1
Date_     20090127
Time      14.05
INSTRUM   AVB-400
PROBHD    5 mm PABBO BB-
PULPROG   zgpg30
TD         65536
SOLVENT   CDCl3
NS         2
DS         0
SWH        12019.230 Hz
FIDRES     0.183399 Hz
AQ         2.7243477 sec
RG         114
RW         41.600 usec
DE         6.00 usec
TE         298.2 K
D1         0.10000000 sec
----- CHANNEL f1 -----
NUC1       13C
PI         13.75 usec
PL1        -2.00 dB
SFO1       100.6262998 MHz
----- CHANNEL f2 -----
NUC1       1H
PI         11.75 usec
PL1        -2.00 dB
SFO1       400.1330000 MHz
----- CHANNEL f3 -----
NUC1       1H
PI         11.75 usec
PL1        -2.00 dB
SFO1       400.1330000 MHz
DE         0.30 Hz
TE         0.00 usec

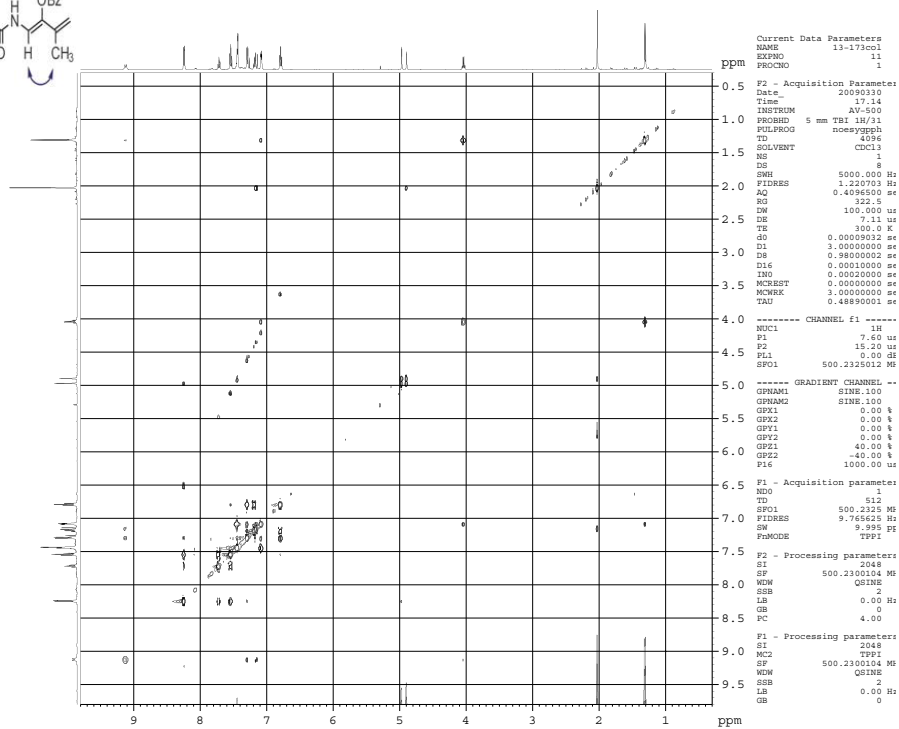
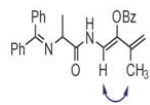
```











```

Current Data Parameters
NAME      13-173col
EXPNO    1
PROCNO   1

F2 - Acquisition Parameters
Date_    20090330
Time     17.14
INSTRUM  AV-500
PROBHD   5 mm TBI 1H/31
PULPROG  noesypph
TD        4096
SOLVENT  CDCl3
NS        1
DS        8
SWH       5000.000 MHz
FIDRES   1.220703 MHz
AQ        0.4096500 sec
RG        327.5
DW        100.000000 us
DE        7.11 us
TE        300.0 K
SFO       0.00000000 sec
D1        3.00000000 sec
D8        0.98000002 sec
D15       0.09010000 sec
RG        0.00020000 sec
MCHRES   0.00000000 sec
TAS       3.00000000 sec
TAU       0.48890001 sec

----- CHANNEL f1 -----
NUC1      1H
P1        7.40 us
P2        15.20 us
PL1       0.00 dB
PL2       0.00 dB
SFO1      500.232612 MHz

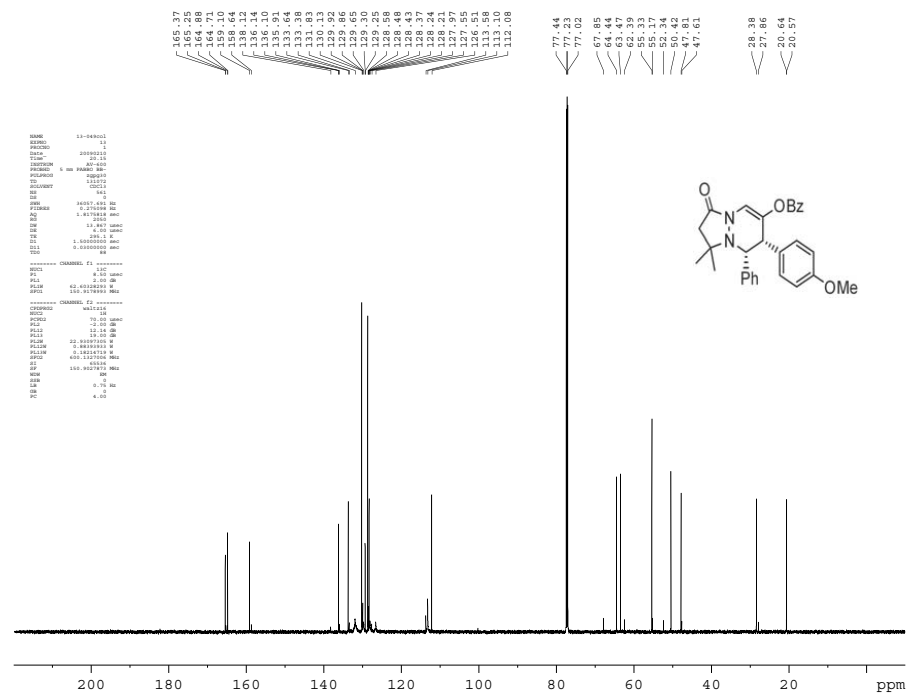
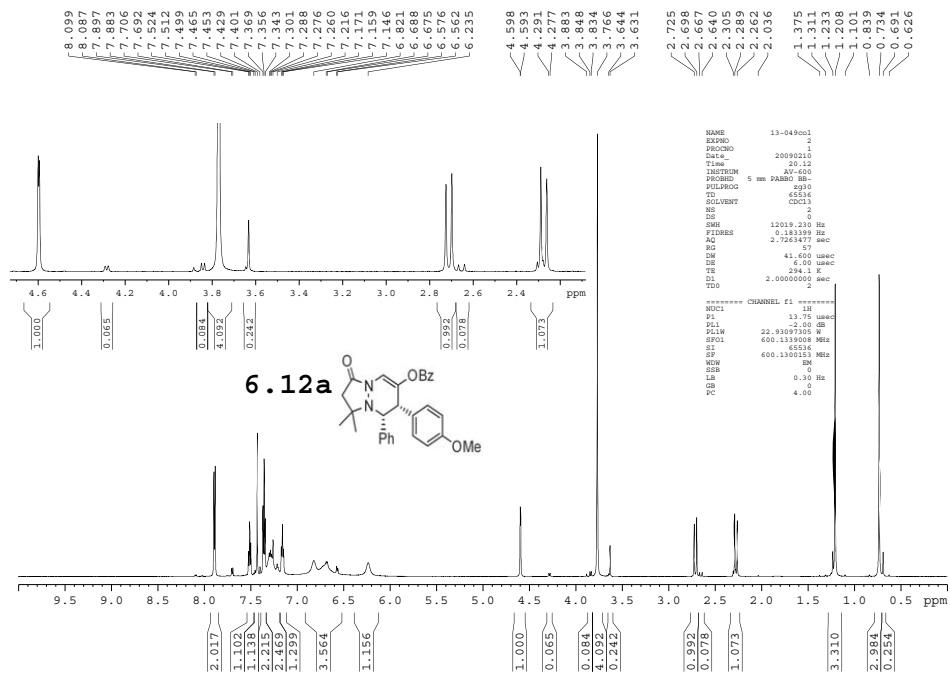
----- GRADIENT CHANNEL -----
GPNAM1    SINE.100
GPNAM2    SINE.100
GP1       0.00 %
GP2       0.00 %
GP3       0.00 %
GP4       0.00 %
GP5       40.00 %
GP6       -40.00 %
P16       1000.00 us

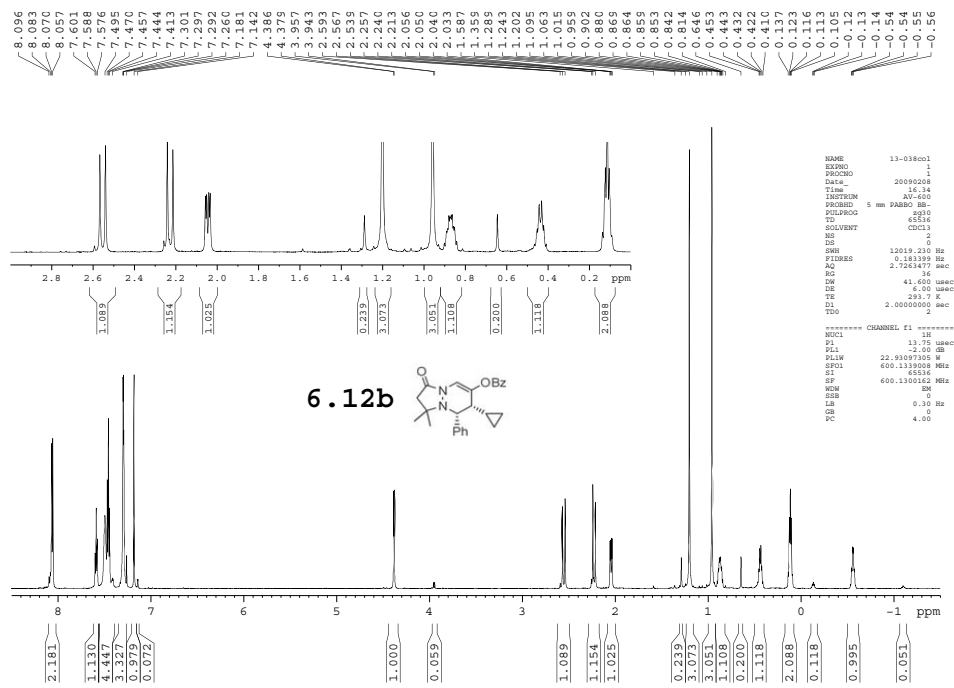
F1 - Acquisition parameters
ND0        1
TD         512
SFO1      500.23225 MHz
FIDRES    9.765625 MHz
SW        9.995 MHz
P1MODE    TPP1

F2 - Processing parameters
SI         2048
SF        500.2300104 MHz
SBS       2
GB        0
PC        4.00

P1 - Processing parameters
SI         2048
MC1       TPP1
SF        500.2300104 MHz
SBS       2
GB        0.00 MHz
PC        0
  
```

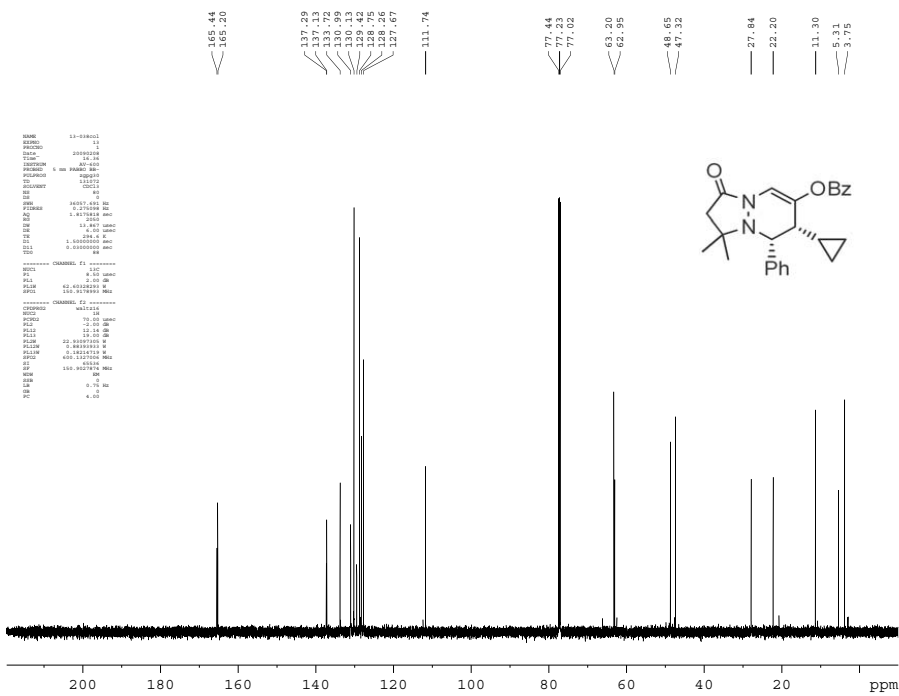
6.9





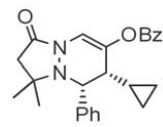
```

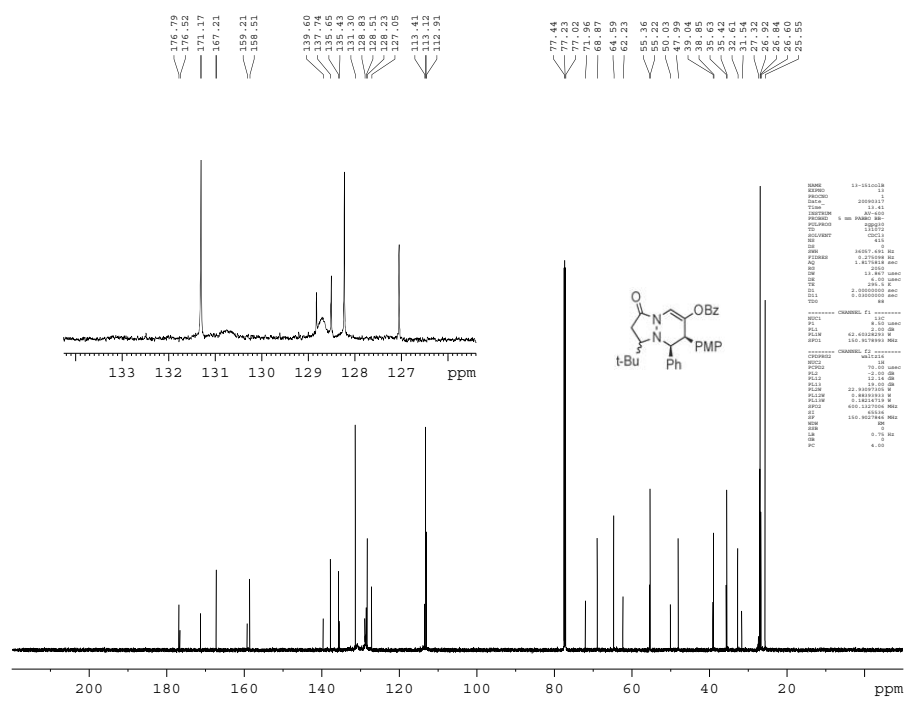
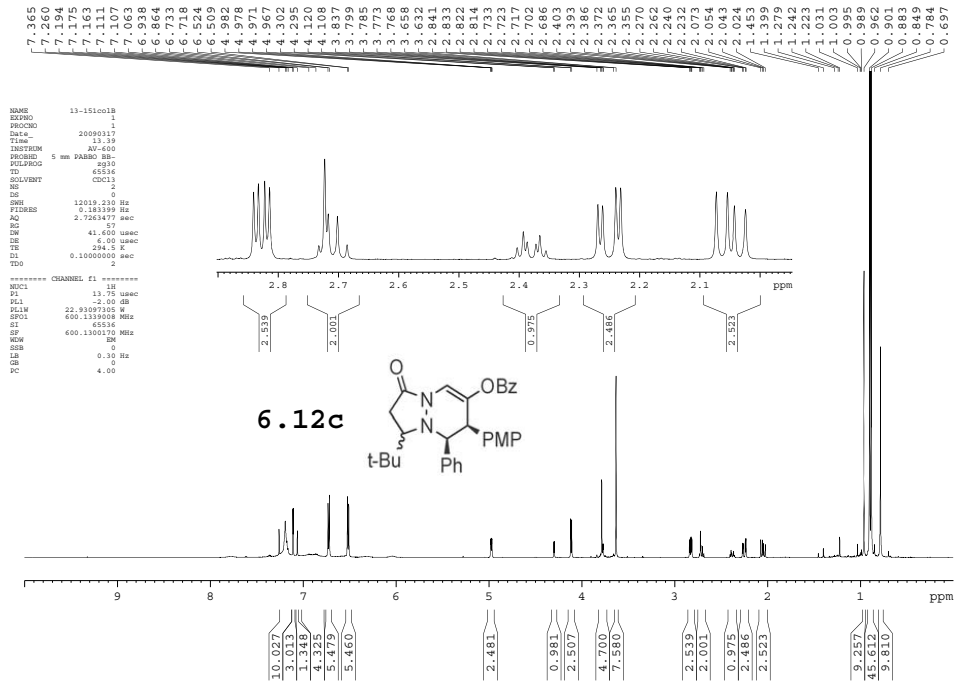
NAME      13-038001
EXPNO     1
PROCNO    1
Date_     20090208
Time      16.14
INSTRUM   AV-600
PROBHD    5 mm DABBO 1H-
PULPROG   zgpg
TD         65536
SOLVENT    CDCl3
NS         2
DS         0
SB         12019.210 Hz
FIDRES    0.183399 Hz
AQ         2.1623477 sec
RG         36
DE         41.600 usec
EM         6.00 usec
TE         293.7 K
D1         2.00000000 sec
T10
===== CHANNEL f1 =====
NUC1       13
P1         13.75 usec
PL1        22.91097305 W
SFO1       600.133005 MHz
SI         65536
SF         600.133005 MHz
WDW        EM
SSB        0
LB         0.30 Hz
GB         0
PC         4.00
  
```



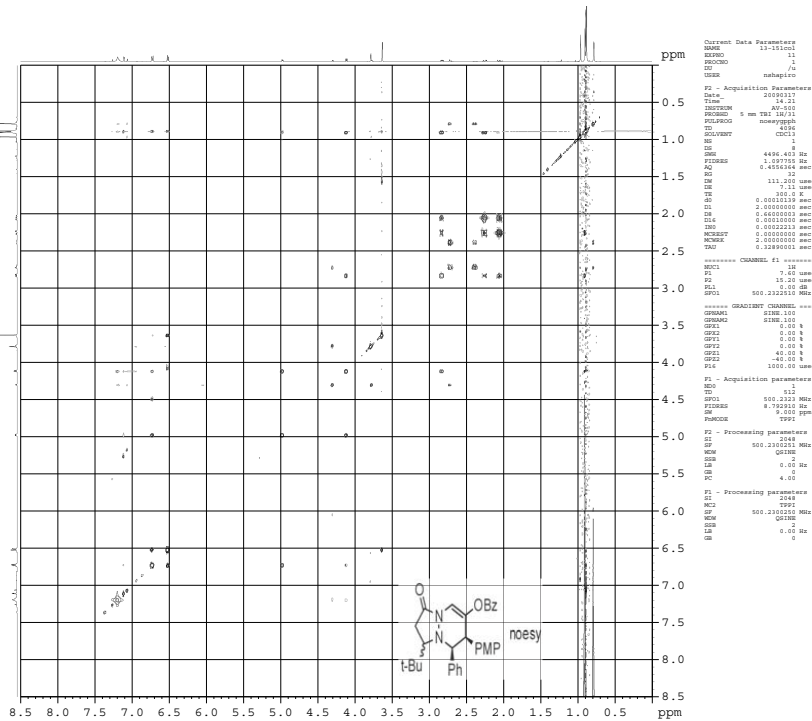
```

NAME      13-038001
EXPNO     1
PROCNO    1
Date_     20090218
Time      16.14
INSTRUM   AV-600
PROBHD    5 mm DABBO 1H-
PULPROG   zgpg
TD         65536
SOLVENT    CDCl3
NS         2
DS         0
SB         12019.210 Hz
FIDRES    0.183399 Hz
AQ         2.1623477 sec
RG         36
DE         41.600 usec
EM         6.00 usec
TE         293.7 K
D1         2.00000000 sec
T10
===== CHANNEL f1 =====
NUC1       13
P1         13.75 usec
PL1        22.91097305 W
SFO1       600.133005 MHz
SI         65536
SF         600.133005 MHz
WDW        EM
SSB        0
LB         0.30 Hz
GB         0
PC         4.00
===== CHANNEL f2 =====
NAME      13-038001
EXPNO     1
PROCNO    1
Date_     20090218
Time      16.14
INSTRUM   AV-600
PROBHD    5 mm DABBO 1H-
PULPROG   zgpg
TD         65536
SOLVENT    CDCl3
NS         2
DS         0
SB         12019.210 Hz
FIDRES    0.183399 Hz
AQ         2.1623477 sec
RG         36
DE         41.600 usec
EM         6.00 usec
TE         293.7 K
D1         2.00000000 sec
T10
===== CHANNEL f2 =====
  
```





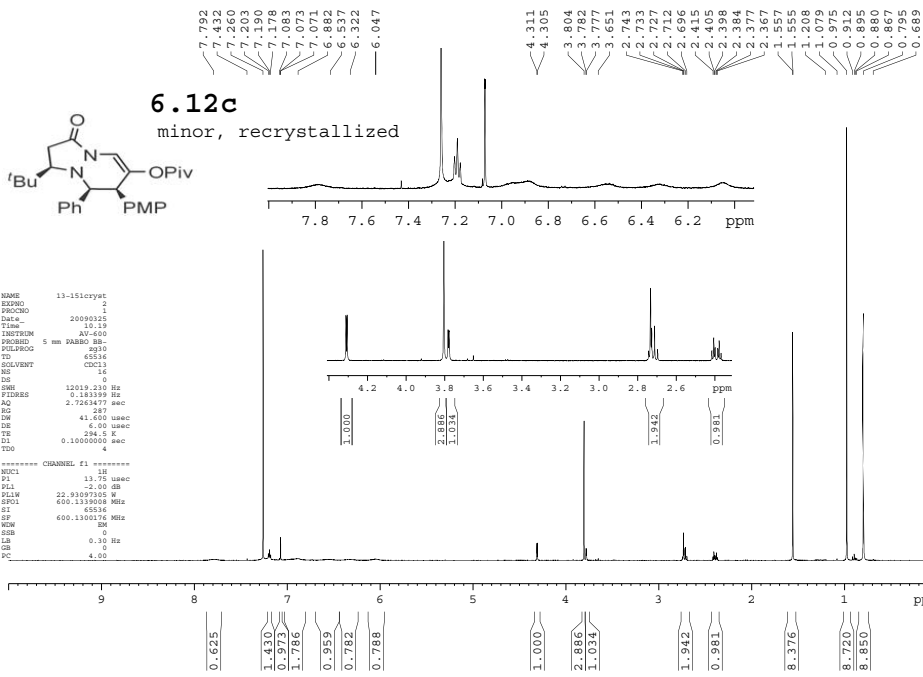
6.12c
noesy

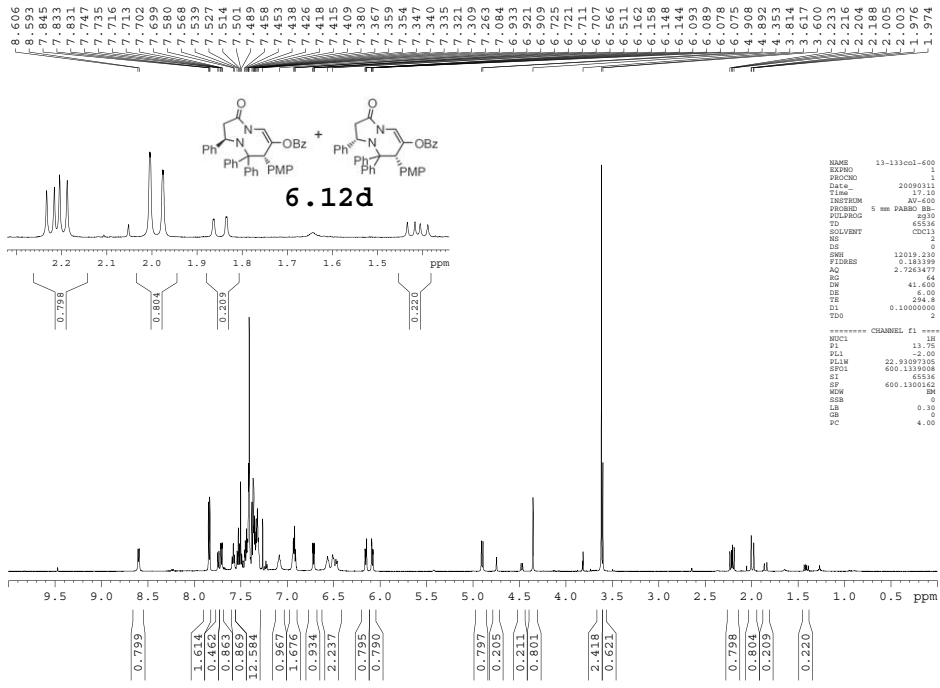


```

Current Data Parameters
NAME      13-151cryst
EXPNO    2
PROCNO   1
Date_    20090317
Time     07:23
INSTRUM  AV-600
PROBHD   5 mm TBI ZH/1
PULPROG  zgpg30
TD        65536
SOLVENT  CDCl3
NS        16
DS        4
SWH       4490.615 Hz
FIDRES   0.189795 Hz
AQ        0.487614 sec
RG         320
AQ        111.1111111 sec
TE        300.2 K
DE        0.0012118 sec
DI        2.0000000 sec
DE        0.0010000 sec
DI        0.0010000 sec
SFO       600.1380000 MHz
NUC1      13C
NUC2      15N
===== CHANNEL f1 =====
NUC1      13C
P1        13.75 usec
PL1       -2.00 dB
SFO1      101.6261260 MHz
===== GRADIENT CHANNEL =====
GPM1      SINE 100
GPM2      SINE 100
GPM3      SINE 100
GPM4      SINE 100
GPM5      SINE 100
GPM6      SINE 100
GPM7      SINE 100
GPM8      SINE 100
GPM9      SINE 100
GPM10     SINE 100
===== Acquisition parameters =====
SI        1
SF         600.1380000 MHz
WDW        EM
SSB         0
LB          0.00 Hz
GB          0.00 Hz
PC          4.00
===== Processing parameters =====
SI        1
SF         600.1380000 MHz
WDW        EM
SSB         0
LB          0.00 Hz
GB          0.00 Hz
PC          4.00
===== Acquisition parameters =====
SI        1
SF         600.1380000 MHz
WDW        EM
SSB         0
LB          0.00 Hz
GB          0.00 Hz
PC          4.00
===== Processing parameters =====
SI        1
SF         600.1380000 MHz
WDW        EM
SSB         0
LB          0.00 Hz
GB          0.00 Hz
PC          4.00

```

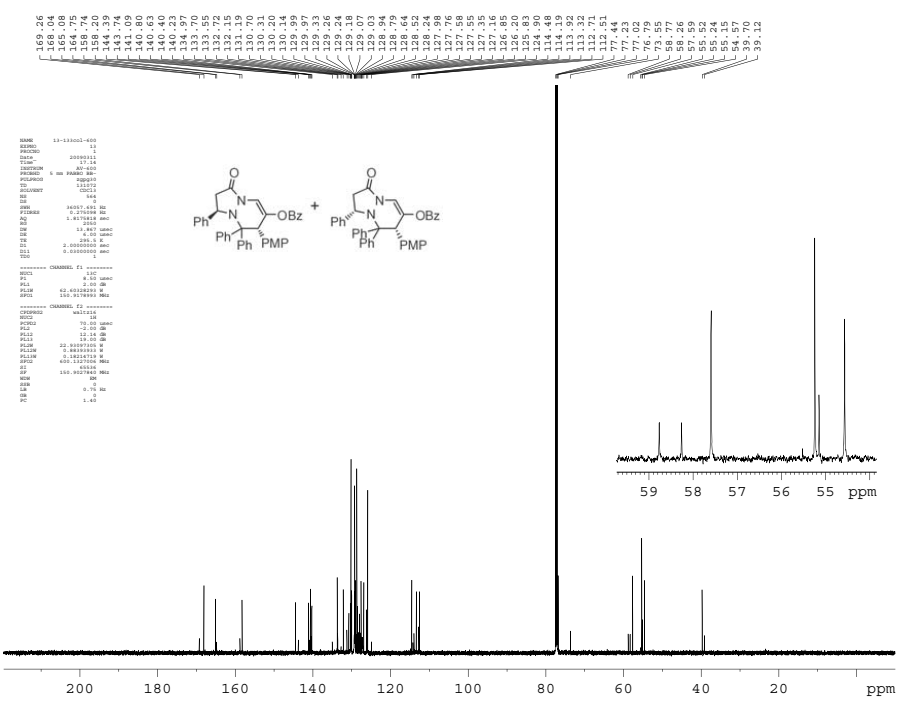




```

NAME 13-133eol-600
EXPNO 1
PROCNO 1
DATE_ 20090311
TIME 17:13
INSTRUM AV-600
PROBHD 5 mm PABBO BB
PULPROG zgpg30
TD 65536
SOLVENT cdc13
SI 2
SF 12013.230 MHz
AQ 0.181399 Hz
RG 2.72618470 umc
DE 41.664
TE 304.2 K
DL 0.100000000 sacc
TSD 2
===== CHANNEL f1 =====
NUC1 13.26 umsc
P1 2.00 dB
PL1 22.9307700 dB
SFO1 600.1300000 MHz
SI 45536
SF 600.1300000 MHz
WDW EM
SSB 0
LB 0.30 Hz
GB 0
PC 4.00

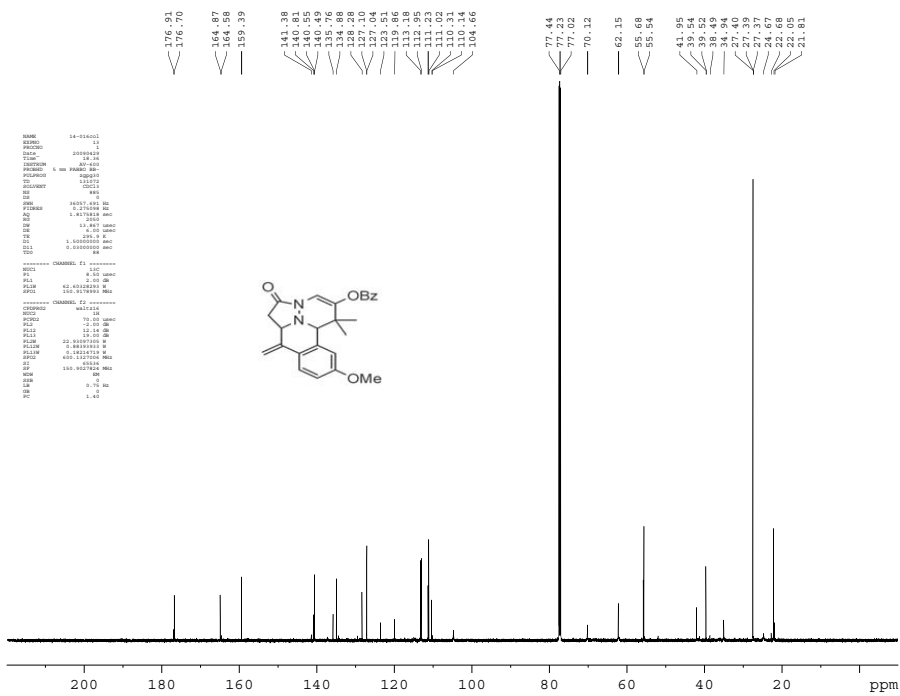
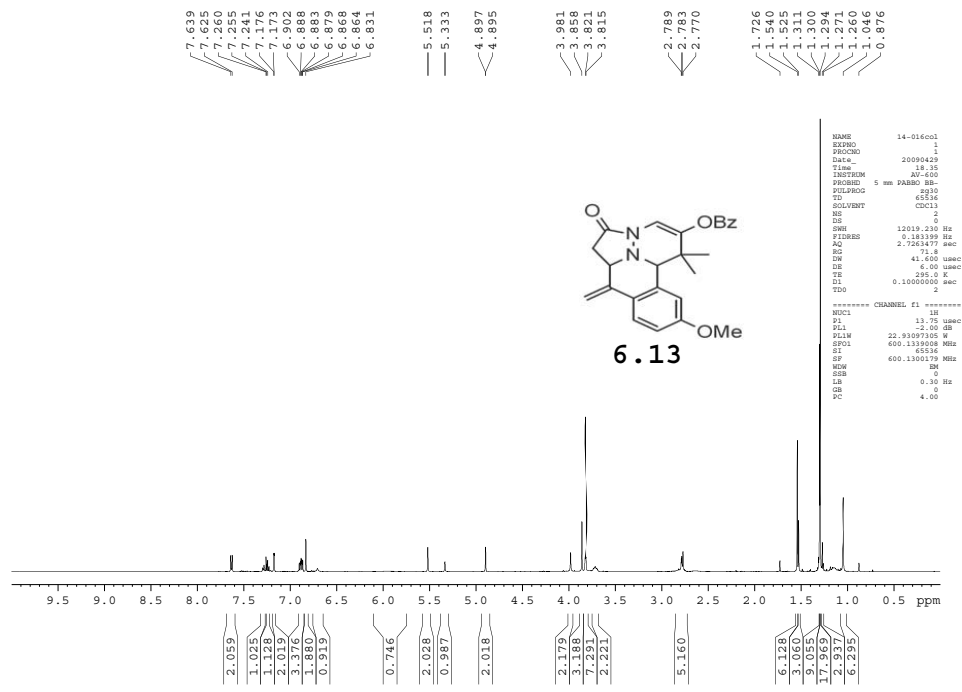
```

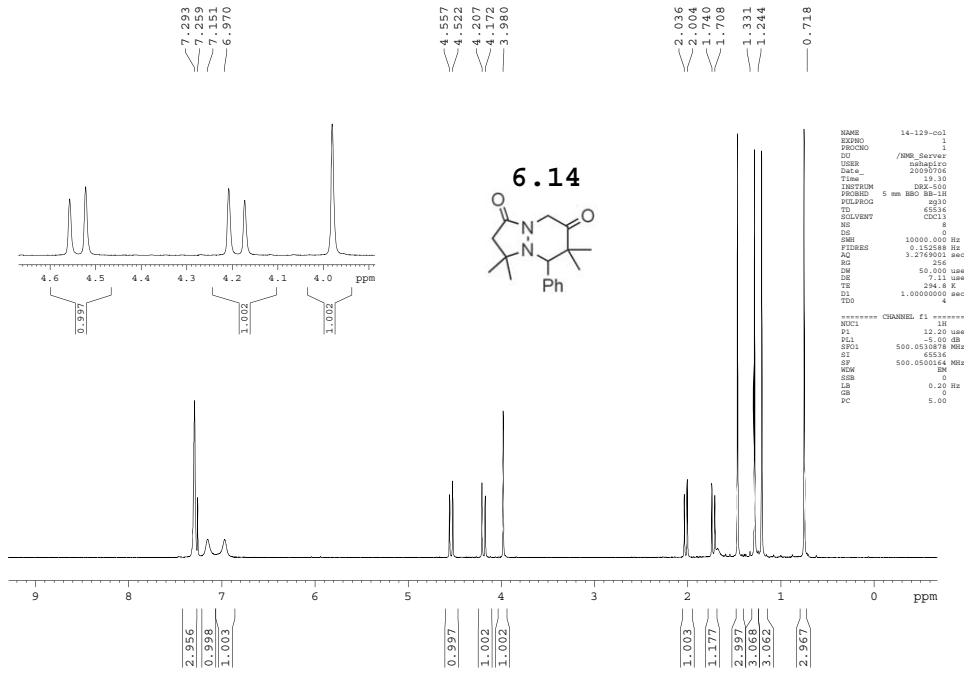


```

NAME 13-133eol-600
EXPNO 1
PROCNO 1
DATE_ 20090311
TIME 17:13
INSTRUM AV-600
PROBHD 5 mm PABBO BB
PULPROG zgpg30
TD 65536
SOLVENT cdc13
SI 2
SF 12013.230 MHz
AQ 0.181399 Hz
RG 2.72618470 umc
DE 41.664
TE 304.2 K
DL 0.100000000 sacc
TSD 2
===== CHANNEL f1 =====
NUC1 13.26 umsc
P1 2.00 dB
PL1 22.9307700 dB
SFO1 600.1300000 MHz
SI 45536
SF 600.1300000 MHz
WDW EM
SSB 0
LB 0.30 Hz
GB 0
PC 4.00
===== CHANNEL f2 =====
NAME 13-133eol-600
EXPNO 1
PROCNO 1
DATE_ 20090311
TIME 17:13
INSTRUM AV-600
PROBHD 5 mm PABBO BB
PULPROG zgpg30
TD 65536
SOLVENT cdc13
SI 2
SF 12013.230 MHz
AQ 0.181399 Hz
RG 2.72618470 umc
DE 41.664
TE 304.2 K
DL 0.100000000 sacc
TSD 2
===== CHANNEL f3 =====
NAME 13-133eol-600
EXPNO 1
PROCNO 1
DATE_ 20090311
TIME 17:13
INSTRUM AV-600
PROBHD 5 mm PABBO BB
PULPROG zgpg30
TD 65536
SOLVENT cdc13
SI 2
SF 12013.230 MHz
AQ 0.181399 Hz
RG 2.72618470 umc
DE 41.664
TE 304.2 K
DL 0.100000000 sacc
TSD 2

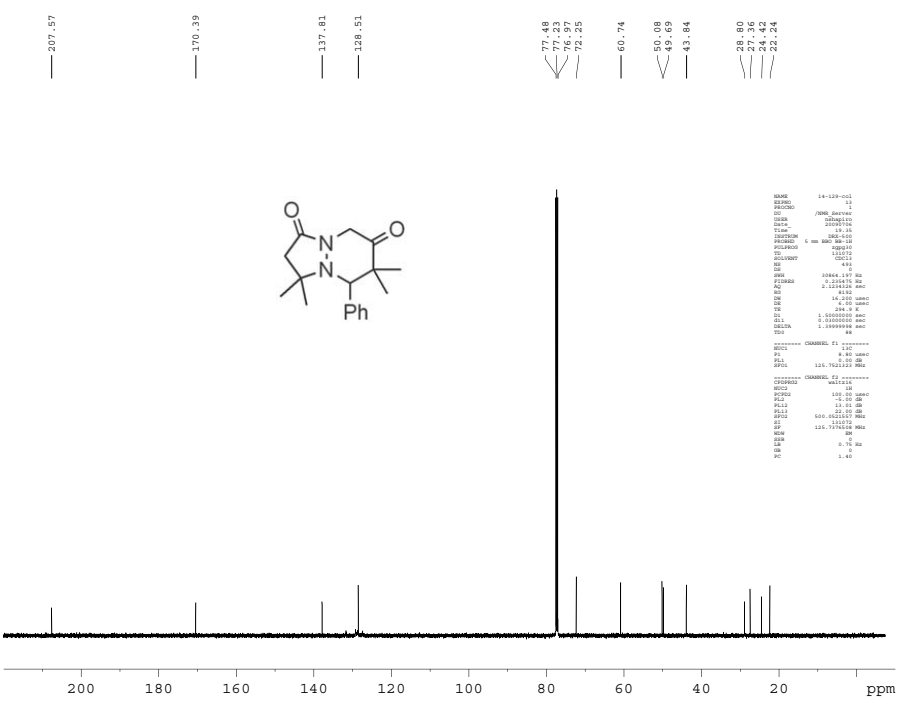
```





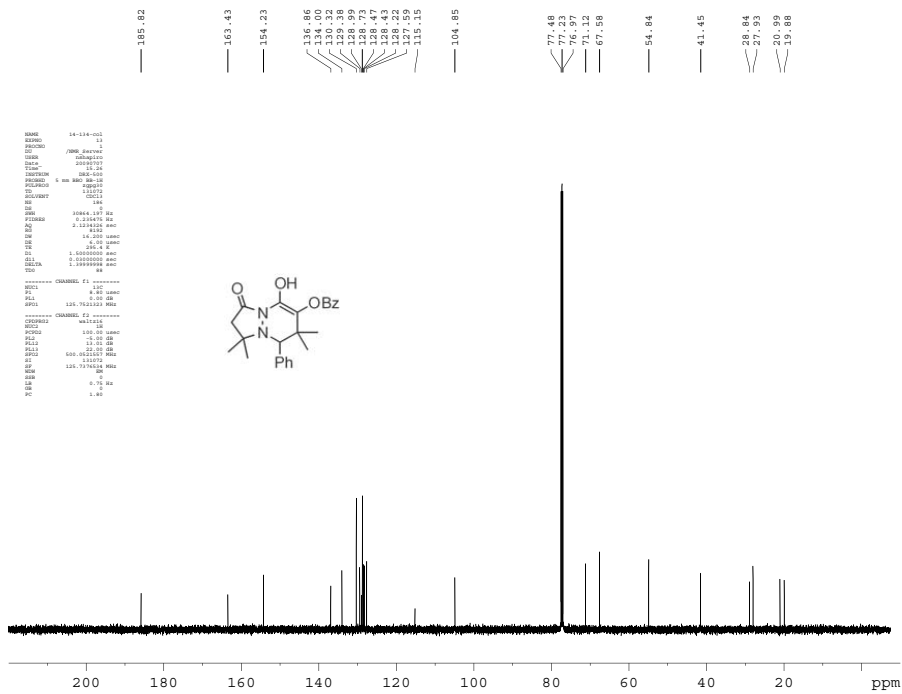
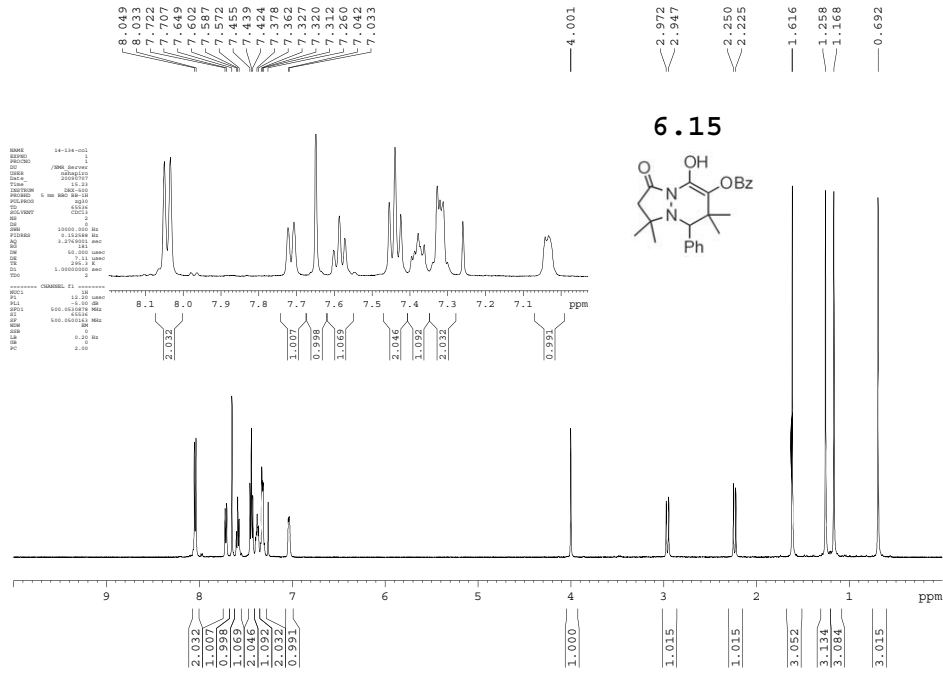
```

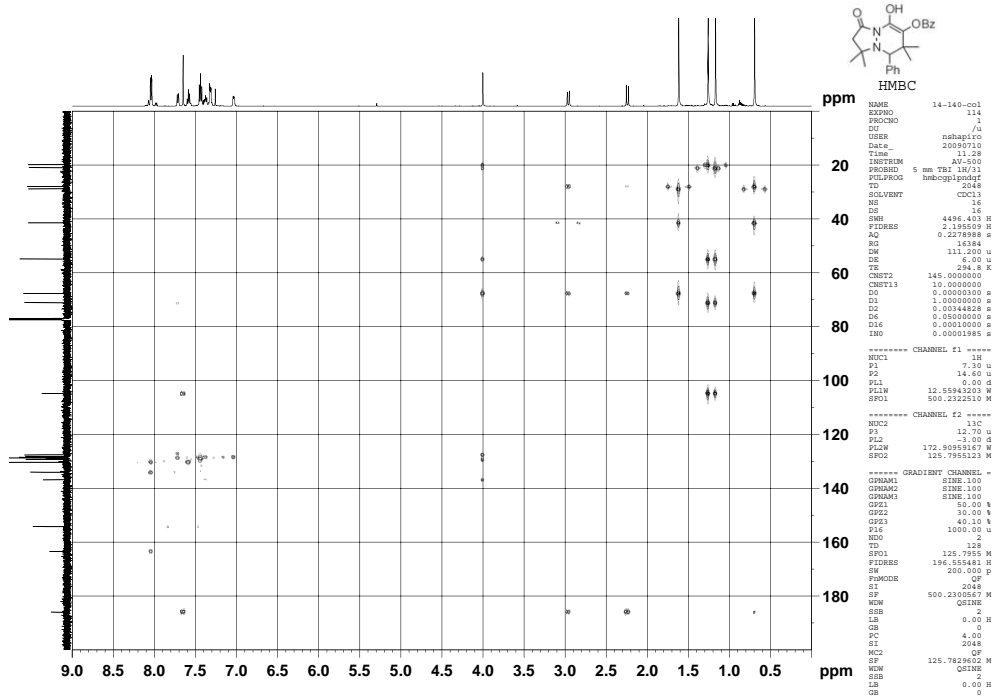
NAME      14-129-001
EXPNO     1
PROCNO    1
INSTRUM   /NMG_Server
USER      nabapiro
Date_     20090704
Time      19.30
INSTRUM   300-500
PROBHD    5 mm BBO BB-1H
PULPROG   zgpg30
TD         65536
SOLVENT   CDCl3
NS         4
DS         0
SWH        10000.000 Hz
FIDRES     0.152588 Hz
AQ         3.2705001 sec
RG         256
SM         50.000 usec
DE         2.11 usec
TE         298.2 K
D1         1.00000000 sec
TD0        4
===== CHANNEL f1 =====
NUC1       1H
P1         12.00 usec
PL1        0.00 dB
SFO1       500.638078 MHz
SI         65536
SF         500.638078 MHz
WDW        EM
SSB        0
GB         0.20 Hz
PC         5.00
  
```



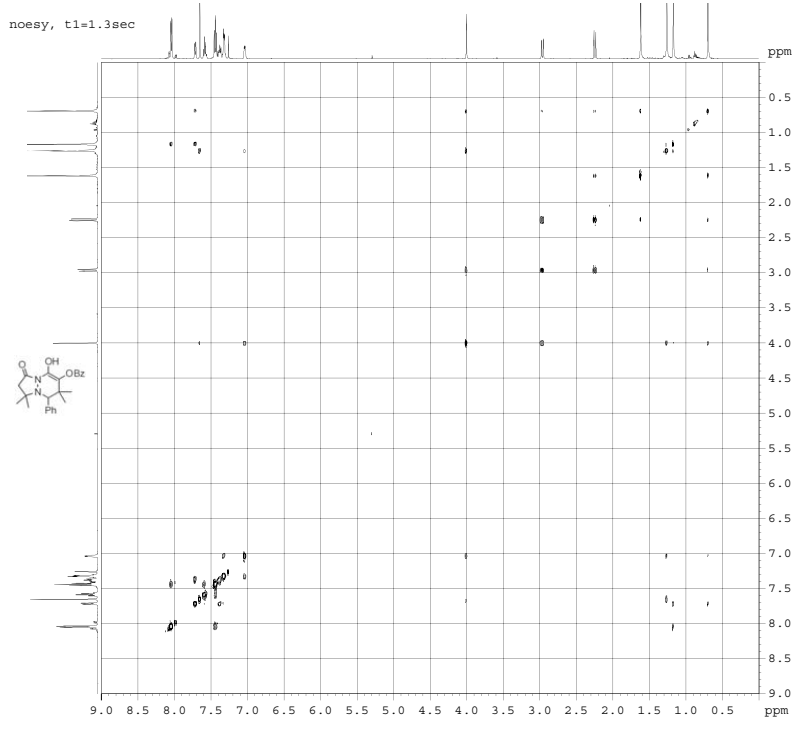
```

NAME      14-129-001
EXPNO     1
PROCNO    1
INSTRUM   /NMG_Server
USER      nabapiro
Date_     20090704
Time      19.31
INSTRUM   300-500
PROBHD    5 mm BBO BB-1H
PULPROG   zgpg30
TD         65536
SOLVENT   CDCl3
NS         4
DS         0
SWH        10000.000 Hz
FIDRES     0.152588 Hz
AQ         3.2705001 sec
RG         256
SM         50.000 usec
DE         2.11 usec
TE         298.2 K
D1         1.00000000 sec
TD0        4
===== CHANNEL f1 =====
NUC1       13C
P1         12.00 usec
PL1        0.00 dB
SFO1       125.761354 MHz
===== CHANNEL f2 =====
NAME      14-129-001
EXPNO     1
PROCNO    1
INSTRUM   /NMG_Server
USER      nabapiro
Date_     20090704
Time      19.31
INSTRUM   300-500
PROBHD    5 mm BBO BB-1H
PULPROG   zgpg30
TD         65536
SOLVENT   CDCl3
NS         4
DS         0
SWH        10000.000 Hz
FIDRES     0.152588 Hz
AQ         3.2705001 sec
RG         256
SM         50.000 usec
DE         2.11 usec
TE         298.2 K
D1         1.00000000 sec
TD0        4
===== CHANNEL f2 =====
NUC1       13C
P1         12.00 usec
PL1        0.00 dB
SFO1       125.761354 MHz
PC         1.40
  
```

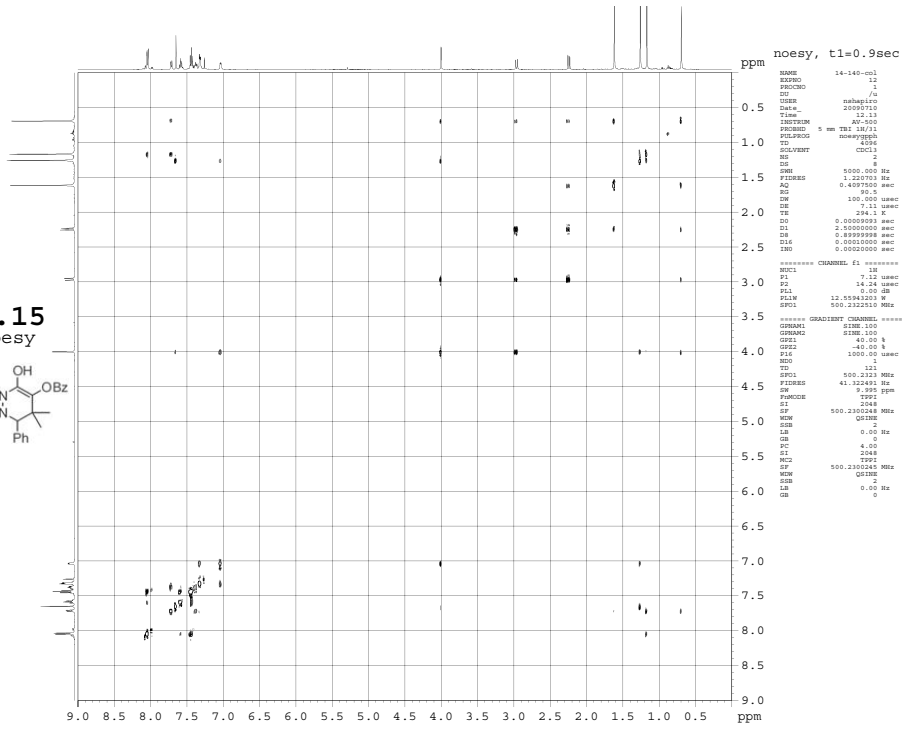





6.15



6.15
noesy



noesy, t1=0.9sec

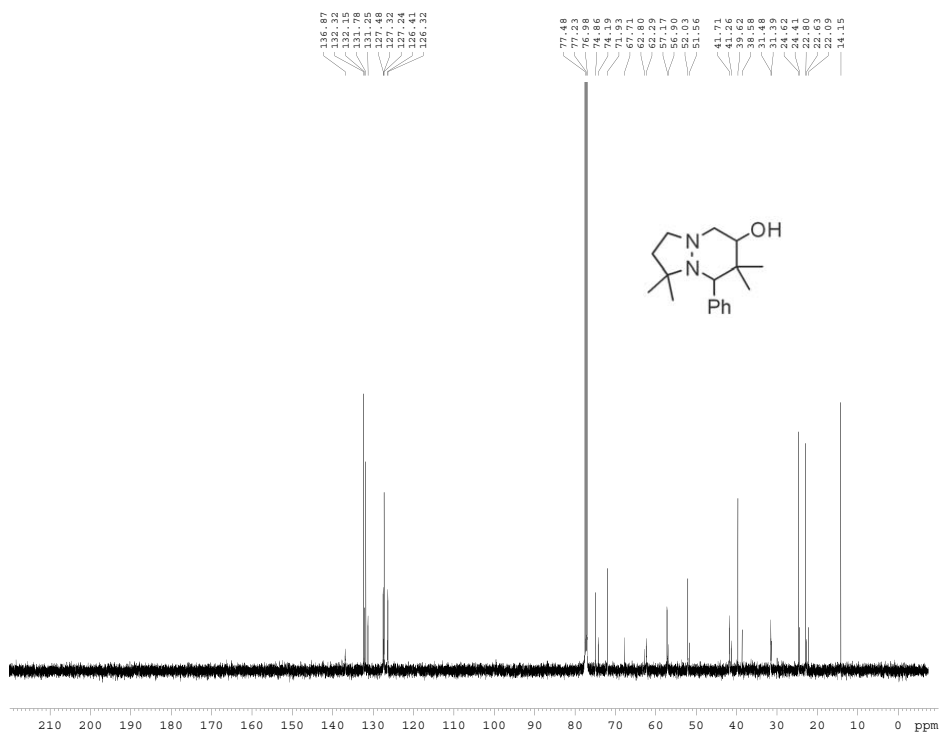
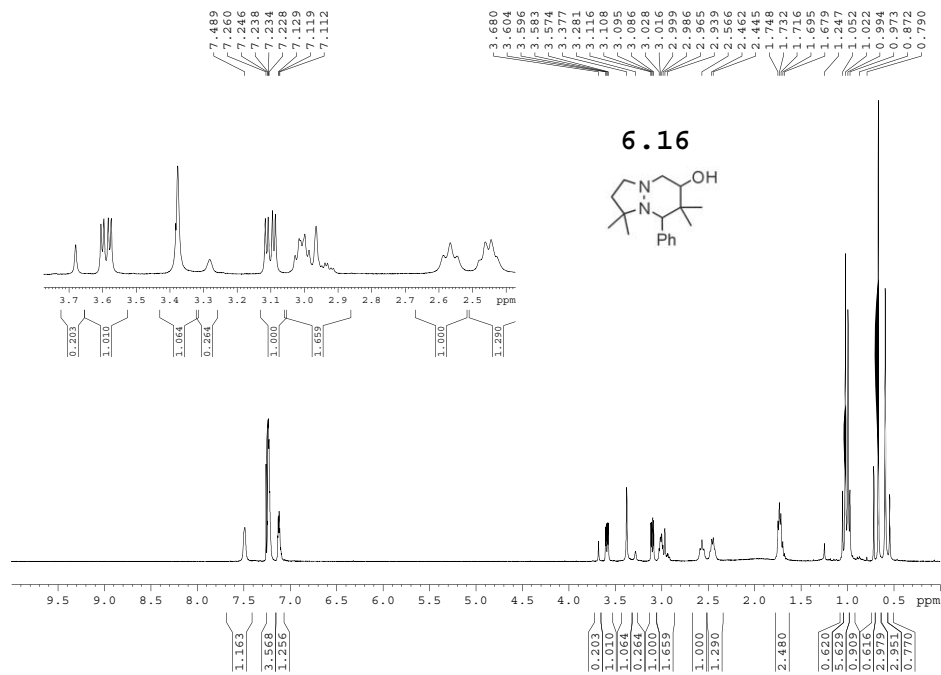
```

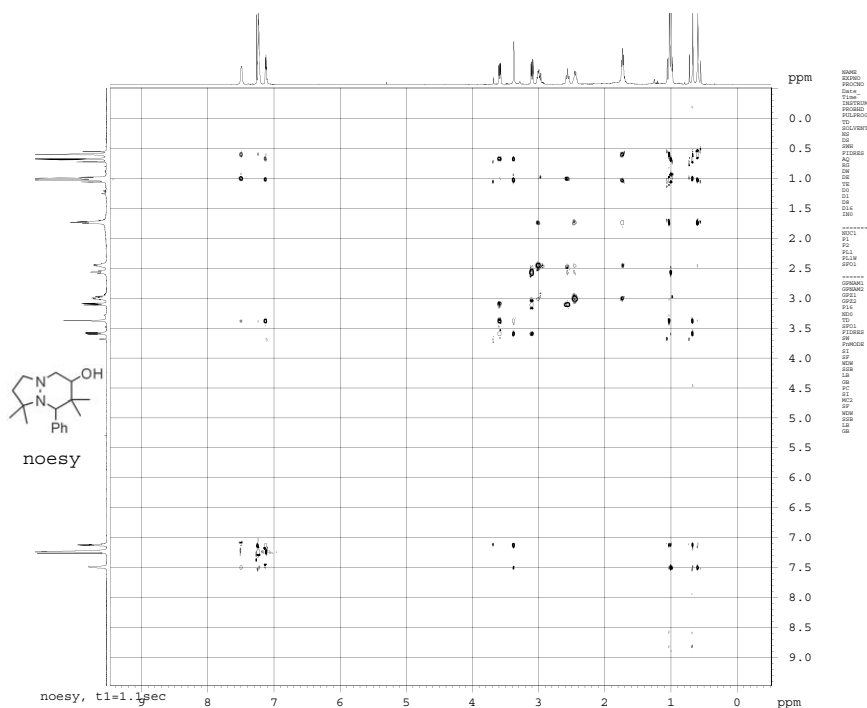
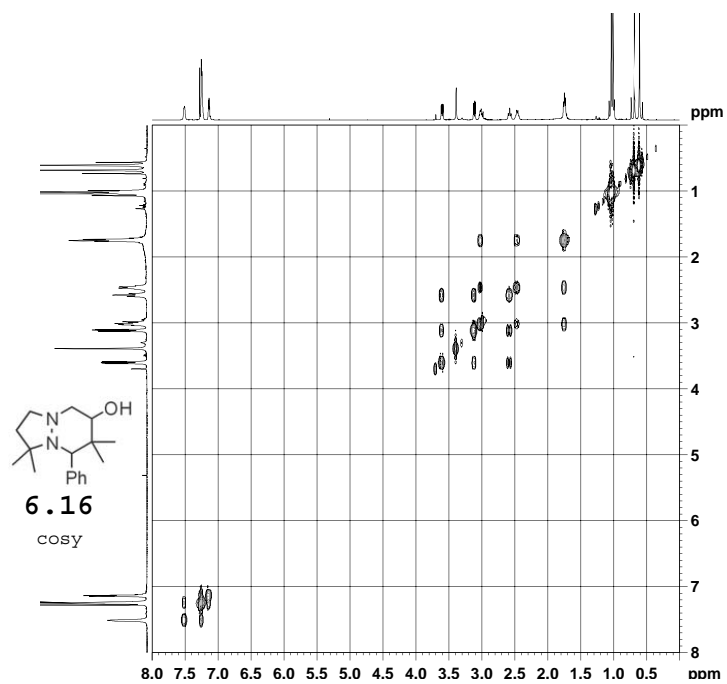
NAME      14-140-001
EXPNO     12
PROCNO    1
CG         /o
NAME      nabap10
Date_     20090710
Time      12.13
INSTRUM   spect
PROBHD    5 mm TR 1H/13
PULPROG   noesygph0
TD         4096
SOLVENT   CDCl3
NS         2
DS         2
SWH        500.000 MHz
FIDRES    1.220703 Hz
AQ         0.490700 sec
RG         650.5
DE         100.000 usec
TE         294.1 K
DQ         7.11 usec
DD         0.0000000 sec
DE         2.0000000 sec
DM         0.0000000 sec
CL6        0.00010000 sec
LSD        0.00010000 sec
LSD0       0.00020000 sec

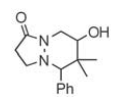
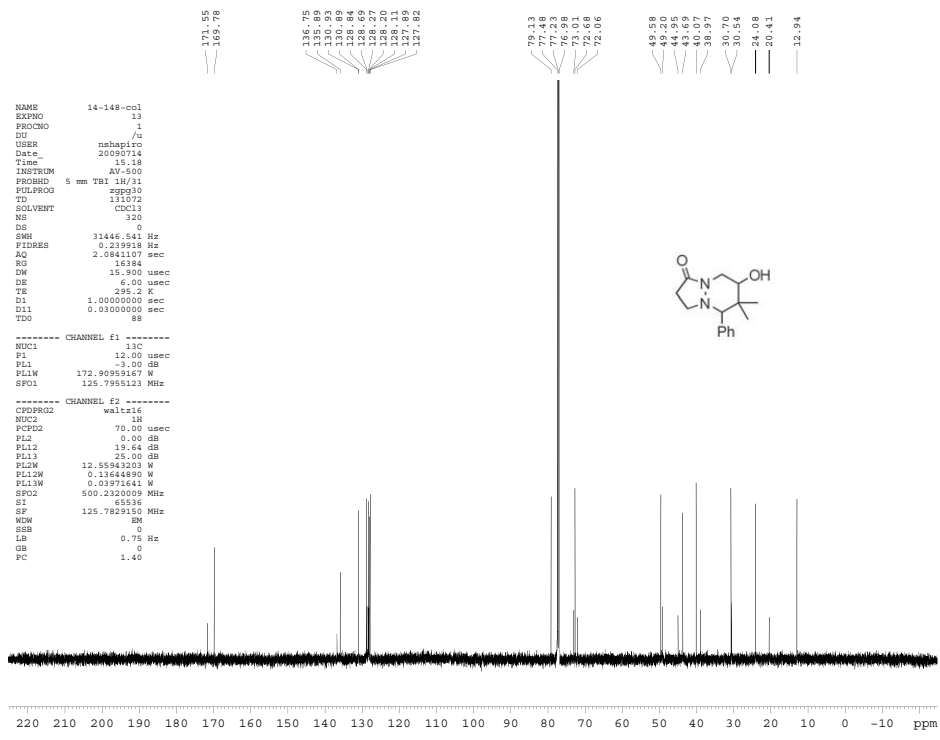
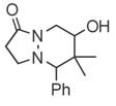
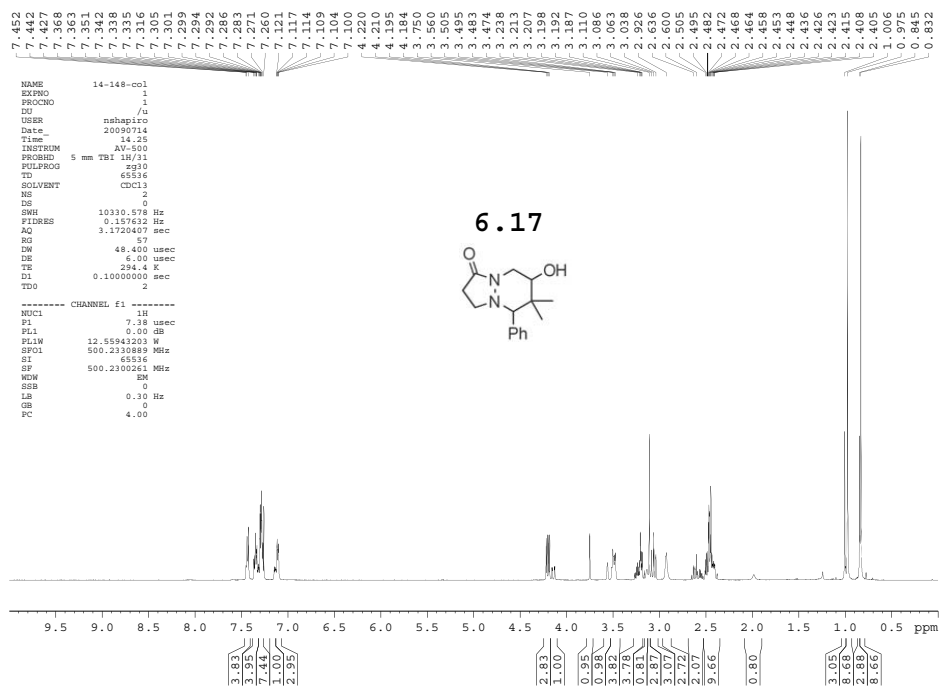
***** CHANNEL f1 *****
NUC1       13C
PC         7.10 usec
PL         14.24 usec
PT1        0.00 dB
PULSE1    12.0000000 usec
SFO1       500.232210 MHz

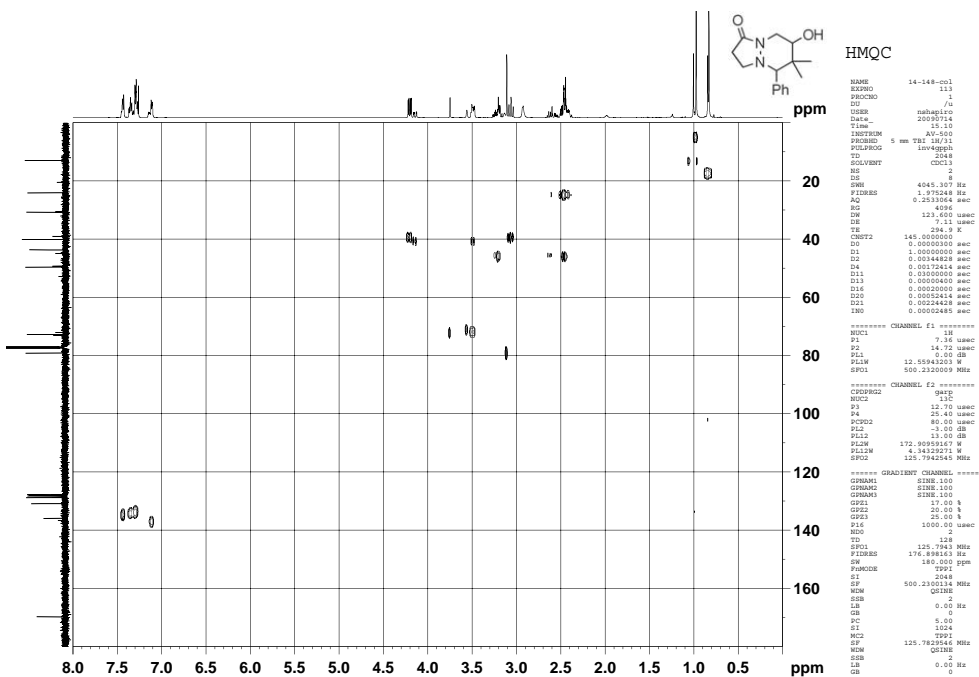
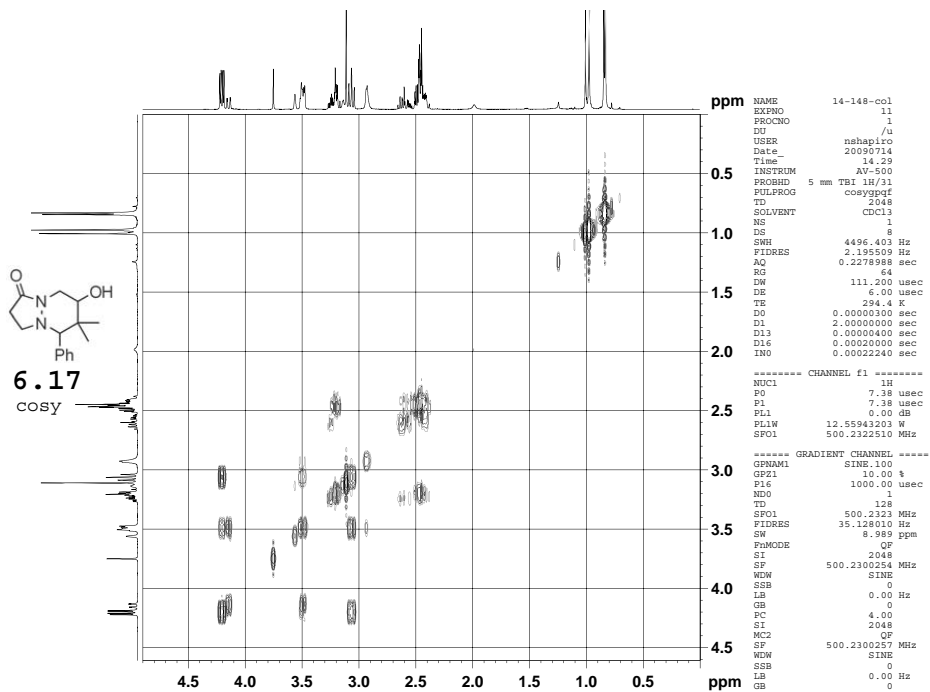
***** GRABUNT CHANNEL *****
GRAB1      SINE 100
GRAB2      SINE 100
GRAB3      SINE 100
GRAB4      SINE 100
GRAB5      SINE 100
GRAB6      SINE 100
GRAB7      SINE 100
GRAB8      SINE 100
GRAB9      SINE 100
GRAB10     SINE 100
GRAB11     SINE 100
GRAB12     SINE 100
GRAB13     SINE 100
GRAB14     SINE 100
GRAB15     SINE 100
GRAB16     SINE 100
GRAB17     SINE 100
GRAB18     SINE 100
GRAB19     SINE 100
GRAB20     SINE 100
GRAB21     SINE 100
GRAB22     SINE 100
GRAB23     SINE 100
GRAB24     SINE 100
GRAB25     SINE 100
GRAB26     SINE 100
GRAB27     SINE 100
GRAB28     SINE 100
GRAB29     SINE 100
GRAB30     SINE 100
GRAB31     SINE 100
GRAB32     SINE 100
GRAB33     SINE 100
GRAB34     SINE 100
GRAB35     SINE 100
GRAB36     SINE 100
GRAB37     SINE 100
GRAB38     SINE 100
GRAB39     SINE 100
GRAB40     SINE 100
GRAB41     SINE 100
GRAB42     SINE 100
GRAB43     SINE 100
GRAB44     SINE 100
GRAB45     SINE 100
GRAB46     SINE 100
GRAB47     SINE 100
GRAB48     SINE 100
GRAB49     SINE 100
GRAB50     SINE 100
GRAB51     SINE 100
GRAB52     SINE 100
GRAB53     SINE 100
GRAB54     SINE 100
GRAB55     SINE 100
GRAB56     SINE 100
GRAB57     SINE 100
GRAB58     SINE 100
GRAB59     SINE 100
GRAB60     SINE 100
GRAB61     SINE 100
GRAB62     SINE 100
GRAB63     SINE 100
GRAB64     SINE 100
GRAB65     SINE 100
GRAB66     SINE 100
GRAB67     SINE 100
GRAB68     SINE 100
GRAB69     SINE 100
GRAB70     SINE 100
GRAB71     SINE 100
GRAB72     SINE 100
GRAB73     SINE 100
GRAB74     SINE 100
GRAB75     SINE 100
GRAB76     SINE 100
GRAB77     SINE 100
GRAB78     SINE 100
GRAB79     SINE 100
GRAB80     SINE 100
GRAB81     SINE 100
GRAB82     SINE 100
GRAB83     SINE 100
GRAB84     SINE 100
GRAB85     SINE 100
GRAB86     SINE 100
GRAB87     SINE 100
GRAB88     SINE 100
GRAB89     SINE 100
GRAB90     SINE 100
GRAB91     SINE 100
GRAB92     SINE 100
GRAB93     SINE 100
GRAB94     SINE 100
GRAB95     SINE 100
GRAB96     SINE 100
GRAB97     SINE 100
GRAB98     SINE 100
GRAB99     SINE 100
GRAB100    SINE 100

```

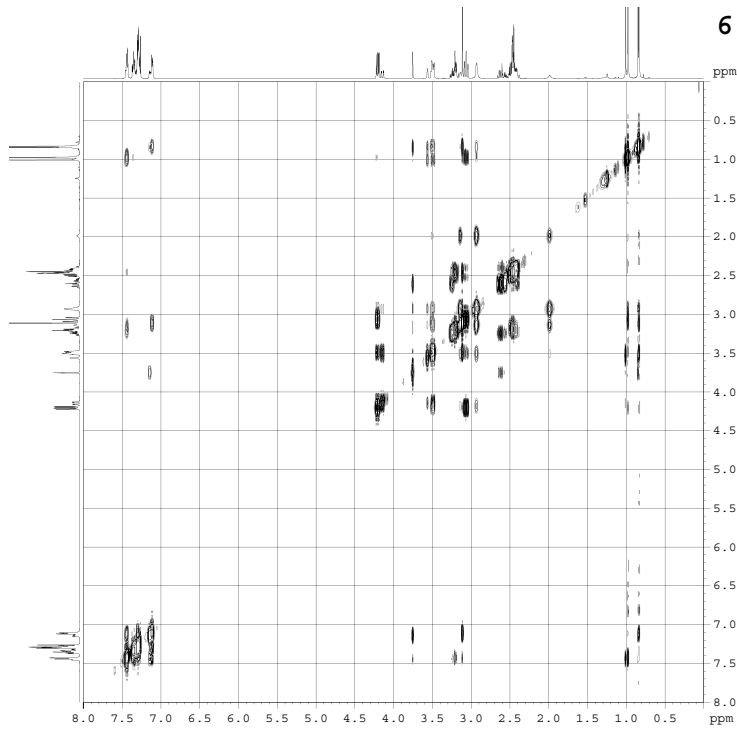
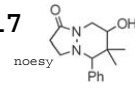








6.17

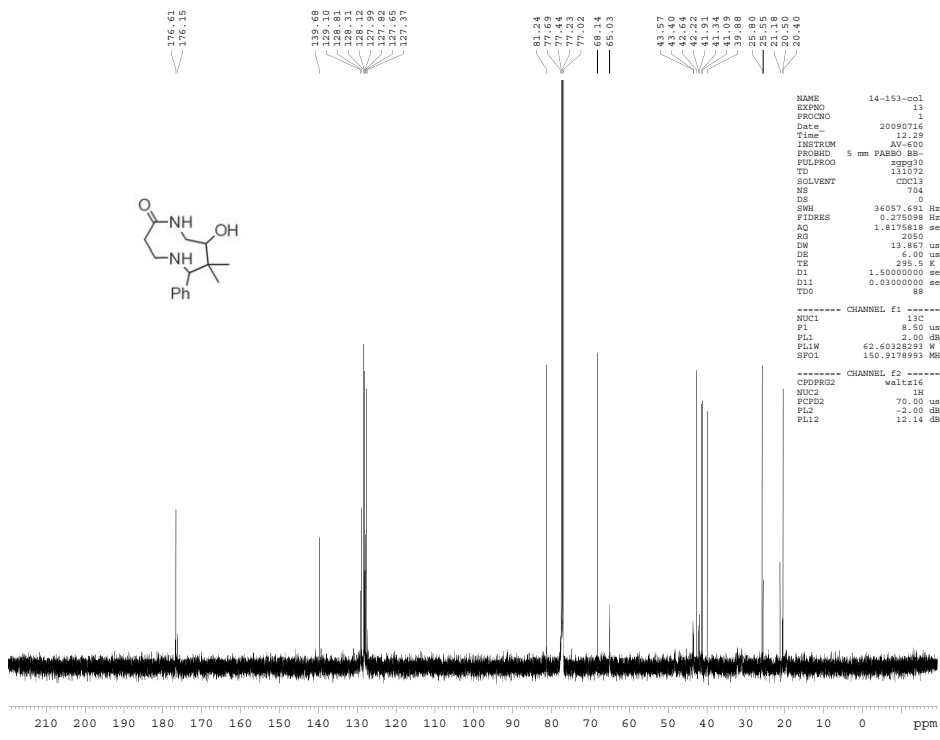
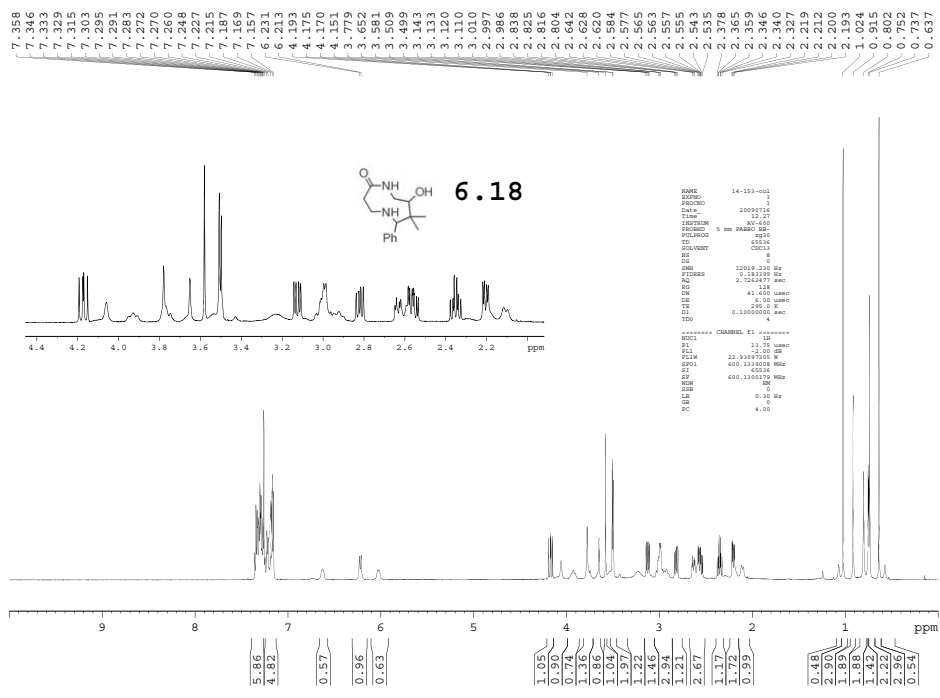


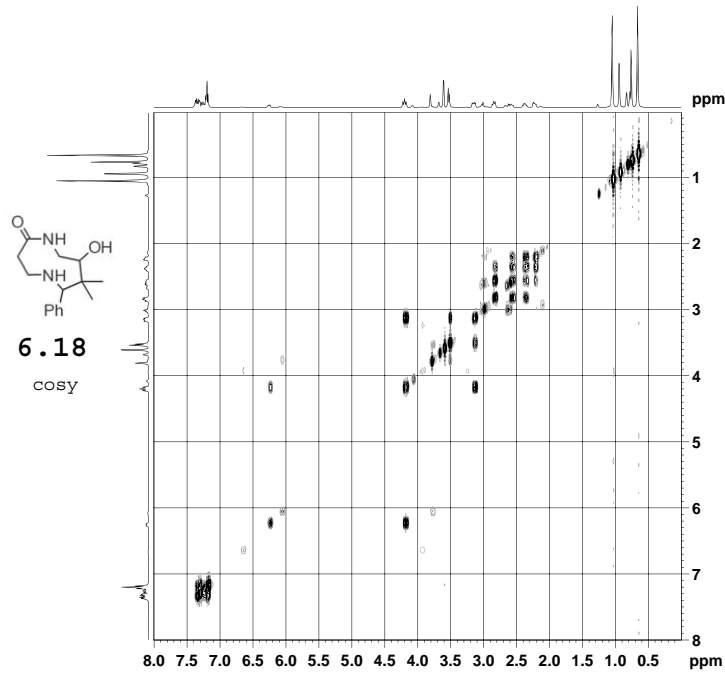
```

NAME          14-148-col
EXPNO         12
PROCNO        1
DS             4
USER          nshapiro
Date_         20090714
Time         14.34
INSTRUM       5 mm TBI 1H/1
PROBHD        AV-500
PULPROG       noesypph
TD            4096
SOLVENT       CDCl3
NS            4
DS            8
SWH           4045.307 Hz
FIDRES       0.987624 Hz
AQ           0.5064392 sec
RG            71.8
DM           123.600 usec
DE           7.11 usec
TE           294.4 K
D0           0.00011400 sec
D1           2.50000000 sec
D8           1.04999995 sec
D16          0.00010000 sec
IN0          0.00024800 sec

----- CHANNEL f1 -----
NUC1          1H
P1            7.18 usec
P2            14.76 usec
PL1           0.00 dB
PL1W          12.55943023 W
SFO1          500.2320009 Mhz

----- GRADIENT CHANNEL -----
GENAM1       SINE.100
GENAM2       SINE.100
GPR21        40.00 V
GPR22        -40.00 V
P16          1000.00 usec
WDW          1
TD           128
SFO2         500.232 Mhz
FIDRES       11.655306 Hz
SM           8.100 ppm
P1M0DE       TPPI
SI           2048
SF           500.2300104 Mhz
WDW          QBINE
SSB          2
LB           0.00 Hz
GB           0
PC           5.00
SI           2048
WDW          TPPI
SF           500.2300104 Mhz
WDW          QBINE
SSB          2
LB           0.00 Hz
GB           0
    
```



```

NAME      14-153-c01-vt
EXPNO    111
PROCNO   1
USER     /NMR_Server
Date_    mhaapico
Date_    20090716
Time     15.42
INSTRUM  DRX-500
PROBHD   5 mm BBO BB-1H
PULPROG  cosyppgaf
TD        2648
SOLVENT  CDCl3
NS        1
DS        8
SH        4005.410 Hz
FIDRES   1.956255 Hz
AQ        0.2557652 sec
RG        128
DW        124.800 usec
DE        6.00 usec
TE        300.0 K
d0        0.0000360 sec
d1        2.0000000 sec
d11       0.0000400 sec
d14       0.0002000 sec
INO       0.00024995 sec

----- CHANNEL f1 -----
NUC1      1H
PQ        12.20 usec
P1        12.20 usec
P11       5.00 dB
SFO1      500.0520002 MHz

----- GRADIENT CHANNEL -----
GPRAM1    SINE 100
GPRAM2    SINE 100
GPZ1      10.00 %
GPZ2      10.00 %
F14       1000.00 usec
ND0       1
TD        128
SFO1      500.052 MHz
FIDRES    31.256250 Hz
SW        8.001 ppm
PQMODE    QP
SI        1024
SP        500.0500000 MHz
WDW       SINE
SSB       0
LB        0.00 Hz
GB        0
PC        5.00
SI        512
WC2       QP
SP        500.0500000 MHz
WDW       SINE
SSB       0
LB        0.00 Hz
GB        0
  
```

